

ISBN 978-4-908553-67-7

Guideline of Ocean Observations

Volumes 1-10

Fourth Edition

The Oceanographic Society of Japan
April 2020



This page left intentionally blank.

Foreword for the 4th edition

In recent years, climate change has emerged with serious consequences in many regions of the world. Materials released into the ocean by human activities are diversifying, and the abundance in the ocean continues to increase. In such a changing marine environment, technological innovations in oceanographic observation are progressing rapidly. On the other hand, it is required to share these technologies properly in the community and provide data that guarantees traceability and comparability. It is also essential to hand down these technologies and the basic knowledges to the oceanographers of the next generation.

The Oceanographic Society of Japan (JOS) has established an editorial committee for Guideline of Ocean Observations to capture the latest trends in ocean observation and provide the community with state-of-the-art guidelines. JOS decided to make this guideline both in Japanese and English, so that not only ocean scientists in Japan but in other countries can share those knowledges.

The first edition of Guideline of Ocean Observations was published in September 2015 with an overview of oceanographic observations and the latest oceanographic and analytical methods. After that, two revisions were made, and by April 2018, a total of 10 volumes and 40-chapter guidelines were arranged.

In this 4th edition, 12 chapters are newly added, and the contents of almost all chapters are satisfied. In addition, two chapters have been updated in this edition. For this guidelines, 44 authors working on a broad area of oceanography are involved in the writing.

We hope that these guidelines will be used by many researchers around the world and contribute to the advancement of oceanography.

Editor in chief for 4th edition

Guideline of Ocean Observations

Shigeyoshi Ootosaka

This page left intentionally blank.

Foreword for the 3rd edition

Under the academic/social needs to cope with global environmental problem such as climate changes and ocean acidification, technical innovation on ocean observations have been progressed rapidly in recent years. Progresses are also ongoing in the field of world-wide organization of ocean observation by using common observation procedures and standard/reference materials because it is obviously vital to publish data that guarantees traceability and comparability with appropriate reference materials or certified reference materials and that is clear about its uncertainties. Aiming to catch up such year-to-year progress in the ocean observations field, and to provide state-of-the-art guideline of ocean observations to the communities, the Oceanographic Society of Japan (JOS) has established the editorial committee of Guideline of Ocean Observations in 2015, and published the Guideline of Ocean Observations describing the most up-to-date oceanographic observation methods and analytical techniques. The first edition of this Guideline of Ocean Observations were published in September 2015.

In the 2nd edition, several improvements had made in the table-of-contents page, reflecting the addition of authors and reviewers in some chapters. Some descriptions regarding sea ice observations (Vol.7, Chap.5) had updated reflecting the changes in terminology of sea ice by WMO Sea-Ice Nomenclature (2014). Also, link address of “Guide to best practice for ocean CO₂ measurements” in Vol.3 had changed from Carbon Dioxide Information Analysis Center (CDIAC) to the Ocean Carbon Data System located within the NOAA National Centers for Environmental Information (NOAA-OCADS). Several chapters in sediment observation (Vol.5) and natural/artificial radioactivity (Vol.9) are also added.

In this 3rd edition, several improvements had also made in the table-of-contents page, reflecting the addition of authors and reviewers in some chapters. We hope that these guidelines will be used by many researchers worldwide and will contribute to the advance of oceanography.

Thereafter this Guideline in English version will be renewed under the review of the editorial committee, updating description corresponding to technical progresses as well as adding new observation items if necessary.

Editor in chief for 3rd edition
Guideline of Ocean Observations
Tsuneo Ono

This page left intentionally blank.

Foreword for the 2nd edition

Under the academic/social needs to cope with global environmental problem such as climate changes and ocean acidification, technical innovation on ocean observations have been progressed rapidly in recent years. Progresses are also ongoing in the field of world-wide organization of ocean observation by using common observation procedures and standard/reference materials because it is obviously vital to publish data that guarantees traceability and comparability with appropriate reference materials or certified reference materials and that is clear about its uncertainties. Aiming to catch up such year-to-year progress in the ocean observations field, and to provide state-of-the-art guideline of ocean observations to the communities, the Oceanographic Society of Japan (JOS) has established the editorial committee of Guideline of Ocean Observations in 2015, and published the Guideline of Ocean Observations describing the most up-to-date oceanographic observation methods and analytical techniques. The first edition of this Guideline of Ocean Observations was published in December 2016. Thereafter this Guideline is renewed every year under the review of the editorial committee, updating description corresponding to technical progresses as well as adding new observation items if necessary.

In this 2nd edition, some descriptions regarding sea ice observations (Vol.7, Chap.5) had updated reflecting the changes in terminology of sea ice by WMO Sea-Ice Nomenclature (2014). Also, link address of “Guide to best practice for ocean CO₂ measurements” in Vol.3 had changed from CDIAC to NOAA-OCADS.

Several chapters in Sediment Analysis (Vol.5) and Natural and artificial radioactivity (Vol.9) are added as well as other small additions.

We hope that these guidelines will be used by many researchers worldwide and will contribute to the advance of oceanography.

Editor in chief for 2nd edition

Guideline of Ocean Observations

Tsuneo Ono

This page left intentionally blank.

Foreword

Measures to mitigate and adapt to climate change are urgently needed; the importance of understanding the state of climate change in the oceans is rising. In monitoring environmental changes at the global scale, it is obviously vital to publish data that guarantees traceability and comparability with appropriate reference materials or certified reference materials and that is clear about its uncertainties.

In recent years we have been building our knowledge of changes within the oceans through international cooperation and collaboration, for example, by re-occupation of World Ocean Circulation Experiment (WOCE); our findings were cited in the Fifth Assessment Report from the IPCC. To implement plans to make all measurement values used in climate change research completely SI-traceable, the General Conference on Weights and Measures has been providing advice to relevant institutions. Through measures such as promulgating the use of standard materials for nutrients, we are making progress in comparability of data, research that depends on this comparability, and R&D on standard materials.

However, the guidelines used for measurement and analysis do not seem to be keeping up with this progress. The Oceanographic Observation Guidelines published by the Japan Meteorological Agency in 1999 are relatively widely used in Japan, but their content is not always completely up-to-date and the Guidelines are now quite hard to obtain. In 2010, the WOCE Manual was revised and published as the GO-SHIP Oceanographic Observation Manual (IOCCP Report No.14, 2010), but this is principally for repeat hydrography in the open ocean; it was not intended to guide a wide range of users. There are a number of other manuals and guidelines available but some of them are only written in Japanese, whereas others are only written in English; moreover, they mix together up-to-date content and less up-to-date content.

In this context, the Oceanographic Society of Japan (JOS) has decided to set up an editorial committee for oceanographic observation guidelines, to review and collate the various existing guidelines, and to incorporate necessary revisions and fill in any gaps. We will publish Oceanographic Observation Guidelines describing the most up-to-date

oceanographic observation methods and analytical techniques, and we will make these new guidelines available through the JOS website.

We intend to continuously update these guidelines so that the most up-to-date methods are always accessible. We hope that these guidelines will be used by many researchers worldwide and will contribute to the advance of oceanography.

Editor in chief

Oceanographic observation guidelines

Takeshi Kawano

List of the authors at the time of writing

Michio AOYAMA	Japan Agency for Marine-Earth Science and Technology/ Institute of Environmental Radioactivity, Fukushima University (for Vol.1 Chap.1; Vol.3 Chap.2; Vol.9 Chap.1) Japan Agency for Marine-Earth Science and Technology/ University of Tsukuba (for Vol.1 Chap.2; Vol.1 Chap.4; Vol.3 Chap.2 rev)
Takafumi ARAMAKI	National Institute for Environmental Studies
Sanae CHIBA	Japan Agency for Marine-Earth Science and Technology
Fuminori HASHIHAMA	Tokyo University of Marine Science and Technology
Kazuhiko HAYASHI	Japan Meteorological Agency
Masao ISHII	Meteorological Research Institute, JMA
Hideki KAERIYAMA	Japan Fisheries Research and Education Agency
Kenichi KATAYAMA	Marine Works Japan Ltd.
Takeshi KAWANO	Japan Agency for Marine-earth Science and Technology
Hiroshi KOBAYASHI	University of Yamanashi
Shigeaki KOJIMA	Graduate School of Frontier Sciences / Atmosphere and Ocean Research Institute, The University of Tokyo
Naohiro KOSUGI	Meteorological Research Institute, JMA
Shinya KOUKETSU	Japan Agency for Marine-Earth Science and Technology
Yuichiro KUMAMOTO	Japan Agency for Marine-Earth Science and Technology
Hideaki MAKI	National Institute for Environmental Studies
Keitaro MATSUMOTO	Marine Works Japan Ltd.
Hiroshi MATSUNAGA	Marine Works Japan Ltd.
Yutaka MICHIDA	Atmosphere and Ocean Research Institute, the University of Tokyo
Takashi MIYAO	Japan Meteorological Agency
Akihiko MURATA	Japan Agency for Marine-Earth Science and Technology
Toshiya NAKANO	Japan Meteorological Agency
Shin-ichiro NAKAOKA	National Institute for Environmental Studies
Hisashi NARITA	Tokai University
Hajime OBATA	Atmosphere and Ocean Research Institute, the University of Tokyo
Hiroshi OGAWA	Atmosphere and Ocean Research Institute, the University of Tokyo
Shigeyoshi OTOSAKA	Japan Atomic Energy Agency (for Vol.5 Chapt.1; Vol.5 Chapt.2; Vol.5 Chapt.3; Vol.5 Chapt.4; Vol.5 Chapt.6; Vol.9 Chapt.2) The University of Tokyo (for Vol.5 Chapt.5)
Satoshi OZAWA	Marine Works Japan Ltd.
Hiroaki SAITO	Atmosphere and Ocean Research Institute, the University of Tokyo
Daisuke SASANO	Japan Meteorological Agency
Hironori SATO	Marine Works Japan Ltd.
Mitsuhide SATO	Graduate School of Agricultural and Life Sciences, the University of Tokyo
Souichiro SUEYOSHI	Nippon Marine Enterprises, Ltd.
Toshio SUGA	Graduate School of Science and Faculty of Science, Tohoku University
Koji SUZUKI	Hokkaido University
Toru SUZUKI	Marine Information Research Center, Japan Hydrographic Association
Mitsuhiro TORATANI	Tokai University
Takenobu TOYOTA	Hokkaido University
Hiroshi UCHIDA	Japan Agency for Marine-Earth Science and Technology
Yu UMEZAWA	Tokyo University of Agriculture and Technology
Taichi YOKOKAWA	Japan Agency for Marine-Earth Science and Technology
Takeshi YOSHIMURA	Central Research Institute of Electric Power Industry

This page left intentionally blank.

List of the reviewers at the time of review work

Kentaro ANDO	Japan Agency for Marine-Earth Science and Technology
Michio AOYAMA	Japan Agency for Marine-Earth Science and Technology/ Institute of Environmental Radioactivity, Fukushima University
Hideki FUKUDA	Atmosphere and Ocean Research Institute, the University of Tokyo
Koichi GOTO	KANSO Co. Ltd.
Ken IKEHARA	National Institute of Advanced Industrial Science and Technology
Joji ISHIZAKA	Nagoya University
Hideki KAERIYAMA	Japan Fisheries Research and Education Agency
Yohei KAYUKAWA	National Institute of Advanced Industrial Science and Technology
Naohiro KOSUGI	Meteorological Research Institute, JMA
Atsushi KUBO	Shizuoka University
Yuichiro KUMAMOTO	Japan Agency for Marine-earth Science and Technology
Masashi KUSAKABE	Marine Ecology Research Institute
Tsuyoshi MATSUMOTO	University of the Ryukyus
Akihiko MURATA	Japan Agency for Marine-earth Science and Technology
Toshiya NAKANO	Japan Meteorological Agency
Ayako NISHINA	Kagoshima University
Kazuhiro NORISUE	Niigata University
Jun NISHIOKA	Hokkaido University
Hajime OBATA	Atmosphere and Ocean Research Institute, the University of Tokyo
Stephen OBROCHTA	Akita University
Takashi OTA	Ishinomaki Senshu University
Shigeyoshi OTOSAKA	Japan Atomic Energy Agency
Daisuke SASANO	Meteorological Research Institute
Mitsuhide SATO	Nagasaki University
Koji SEIKE	National Institute of Advanced Industrial Science and Technology
Yugo SHIMIZU	Japan Fisheries Research and Education Agency
Toshio SUGA	Graduate School of Science and Faculty of Science, Tohoku University
Koji SUZUKI	Hokkaido University
James SWIFT	Scripps Institution of Oceanography, UC San Diego
Shigenobu TAKEDA	Nagasaki University
Hiroyuki TANAKA	National Research Institute of Fisheries and Environment of Inland Sea, Japan Fisheries Research and Education Agency
Atsushi TSUDA	Atmosphere and Ocean Research Institute, the University of Tokyo
Hiroshi UCHIDA	Japan Agency for Marine-Earth Science and Technology
Kazuyuki UEHARA	Tokai University
Yu UMEZAWA	Graduate School of Fisheries and Environment Sciences, Nagasaki University
Shuki USHIO	National Institute of Polar Research
Hisayuki YOSHIKAWA	Hokkaido University
Takeshi YOSHIMURA	Hokkaido University

This page left intentionally blank.

Table of Contents

Foreword for the 4th edition

Foreword for the 3rd edition

Foreword for the 2nd edition

Foreword

List of the authors

List of the reviewers

Vol. 1 Quality Control and Standard Materials

Chap. 1	Ocean Variables and the International System of Units (SI)	G101EN:001-006	Michio AOYAMA
Chap. 2	Device for measurement and measurement standard (Etalons)	G102EN:001-012	Michio AOYAMA Hiroshi UCHIDA Akihiko MURATA Kazuhiko HAYASHI
Chap. 3	Essential Ocean Variables (EOVs) of GOOS	G103EN:001	Masao ISHII Toshio SUGA Sanae CHIBA
Chap. 4	Quality control by comparison with standards, control charts, duplicated measurements, and property-property characteristics, and the report of metadata	G104EN:001-134	Michio AOYAMA Hiroshi UCHIDA Daisuke SASANO Hajime OBATA
Chap. 5	Data Publication and International Exchange	G105EN:001-008	Toru SUZUKI Yutaka MICHIDA
Chap. 6	Calculation of the Thermophysical Properties of Seawater (2010)	G106EN:001	

Vol. 2 Physical Observation

Chap. 1	Water Sampling	G201EN:001-019	Toshiya NAKANO Hajime OBATA Kenichi KATAYAMA Satoshi OZAWA Hiroshi MATSUNAGA
Chap. 2	Water Temperature	G202EN:001-002	Toshiya NAKANO
Chap. 3	Salinity	G203EN:001	Takeshi KAWANO
Chap. 4	Density of Seawater	G204EN:001-002	Hiroshi UCHIDA
Chap. 5	Transparency	G205EN:001	Toshiya NAKANO

Vol. 3 Seawater Analysis I (Dissolved Substances)

Chap. 1	Dissolved Oxygen	G301EN:001-033	Yuichiro KUMAMOTO Daisuke SASANO Hironori SATO Keitaro MATSUMOTO
Chap. 2	The precise and accurate determination of dissolved inorganic nutrients in seawater, using Continuous Flow Analysis methods	G302ENr1:001	Michio AOYAMA
Chap. 3	Trace Metals	G303EN:001-005	Hajime OBATA

Chap. 4	Determination of total dissolved inorganic carbon in sea water	G304EN:001	
Chap. 5	Determination of total alkalinity in sea water by spectrophotometry	G305EN:001-012	Masao ISHII Naohiro KOSUGI
Chap. 6	Determination of the pH of sea water	G306EN:001	
Chap. 7	Determination of $p(\text{CO}_2)$ in air that is in equilibrium with a discrete sample of sea water	G307EN:001	
Chap. 8	Chlorofluorocarbons and Sulfur Hexafluoride	G308EN:001	
Chap. 9	Carbon isotopic ratios ($\Delta^{14}\text{C}$, $\delta^{13}\text{C}$) of dissolved inorganic carbon	G309EN:001-019	Yuichiro KUMAMOTO Takafumi ARAMAKI
Chap. 10	Dissolved organic carbon (DOC), nitrogen (DON), and phosphorus (DOP)	G310EN:001	Hiroshi OGAWA
Vol. 4 Seawater Analysis II (Particulate Substances)			
Chap. 1	Particulate organic carbon (POC), particulate nitrogen (PN), and particulate phosphorus (PP)	G401EN:001-006	Takeshi YOSHIMURA
Chap. 2	Biogenic Silica	G402EN:001-003	Fuminori HASHIHAMA
Chap. 3	Carbon and Nitrogen Stable Isotopes in Particulate Organic Matter	G403ENr1:001-009	Yu UMEZAWA
Chap. 4	Algal pigments	G404EN:001-005	Koji SUZUKI
Chap. 5	Prokaryote and Heterotrophic Nanoflagellates		
Chap. 5-1	Direct Counting Methods of Prokaryote and Heterotrophic Nanoflagellates by Epifluorescence Microscopy	G4051EN:001-006	Taichi YOKOKAWA
Chap. 5-2	Enumeration of prokaryotes by flow cytometry	G4052EN:001-004	Mitsuhide SATO
Chap. 6	Determination of Micro Zooplankton	under writing	
Chap. 7	Primary Production	G407EN:001-003	Koji SUZUKI
Vol. 5 Sediment Analysis			
Chap. 1	Seabed sediment sampling	G501EN:001-003	Hisashi NARITA Shigeyoshi OTOSAKA
Chap. 2	Physical properties of sediment (water content, bulk density and porosity)	G502EN:001-013	Hisashi NARITA Shigeyoshi OTOSAKA
Chap. 3	Loss on ignition	G503EN:001-003	Hisashi NARITA Shigeyoshi OTOSAKA
Chap. 4	Grain size distribution	G504EN:001-020	Hisashi NARITA Shigeyoshi OTOSAKA
Chap. 5	Major Component	G505EN:001-018	Hisashi NARITA Shigeyoshi OTOSAKA
Chap. 6	Pore Water	G506EN:001-006	Hisashi NARITA Shigeyoshi OTOSAKA
Vol. 6 Plankton and Benthos			
Chap. 1	Plankton Net	G601EN:001-009	Hiroaki SAITO
Chap. 2	Benthos	G602EN:001-006	Shigeaki KOJIMA

Vol. 7	Underway		
Chap. 1	Determination of $p(\text{CO}_2)$ in air that is in equilibrium with a continuous stream of sea water	G701ENr1:001-003	Daisuke SASANO Shin-ichiro NAKAOKA
Chap. 2	Acoustic Doppler Current Profilers	G702EN:001-005	Shinya KOUKETSU
Chap. 3	Bathymetry	G703EN:001-009	Hiroshi UCHIDA Souichiro SUEYOSHI
Chap. 4	Weather Observations	G704EN:001-085	Toshiya NAKANO
Chap. 5	Sea Ice	G705ENr1:001-047	Takenobu TOYOTA
Chap. 6	Indirect radiation and aerosol optical thickness	G706EN:001-007	Mitsuhiro TORATANI Hiroshi KOBAYASHI
Vol. 8	Measurements by Sensors		
Chap. 1	TSG	under writing	
Chap. 2	XBT/XCTD	under writing	
Chap. 3	Conductivity-Temperature-Depth profiler (CTD) (Blue-water measurements)	G803EN:001	
Chap. 4	Conductivity-Temperature-Depth profiler (CTD) (coastal-water measurements)	under writing	
Chap. 5	CTD Oxygen Sensor Calibration Procedures	G805EN:001	
Chap. 6	Fluorometer	under writing	
Chap. 7	Turbidity Sensor and Transmissometer	under writing	
Chap. 8	Light fields and optical properties	under writing	
Chap. 9	Lowered Acoustic Doppler Current Profiler (LADCP)	G809EN:001-007	Shinya KOUKETSU
Vol. 9	Natural and Artificial Radioactivity		
Chap. 1	Radiometric Determination of Anthropogenic Radionuclides in Seawater samples	G901ENr1:001-014	Michio AOYAMA
Chap. 2	Seabed sediment	G902EN:001-008	Shigeyoshi OTOSAKA Hisashi NARITA
Chap. 3	Intentionally blank chapter.		
Chap. 4	Plankton and Benthos	G904EN:001-005	Hideki KAERIYAMA
Vol. 10	Marine Pollutant Observation		
Chap. 1	Intentionally blank chapter.		
Chap. 2	Petroleum and Hydrocarbons	G1002EN:001-019	Hideaki MAKI
Chap. 3	Microplastics (Surface Water Trawl Surveys for Small Debris Items)	G1003EN:001-009	Takashi MIYAO
Chap. 4	Floating Marine Pollutants (Shipboard Sighting Surveys for Macro-Debris Items)	G1004EN:001-009	Takashi MIYAO
Chap. 5	Persistent Organic Pollutants	under writing	

List of editors of each volume

This page left intentionally blank.

Ocean variables and the International system of units (SI)

○Michio AOYAMA (Research and Development Center for Global Change (RCGC) Japan Agency for Marine-Earth Science and Technology/ Institute of Environmental Radioactivity, Fukushima University)

1. Introduction

The International System of Units (SI) consists of seven base units for length, mass, time, electric current, thermodynamic temperature, amount of a substance, and luminous intensity. The corresponding and clearly defined units (and their symbols) are the meter (m), kilogram (kg), second (s), ampere (A), kelvin (K), mole (mol), and candela (cd).

An instrument is calibrated with a working standard, and the working standard is calibrated with a reference standard that is more precise (smaller uncertainty) than the working standard. If there is an unbroken chain of calibration that reaches the International System of Units (SI), the result of a measurement with the instrument is said to be traceable to the SI.

Instruments used for all ocean observations should, in principle, be explicitly traceable to the SI. For each instrument there should be a system chart traceable to the SI. For example, Figure 1 shows a traceability system chart for mass at a research institution that would be relevant if a scientist were performing certification work with reference material for nutrient concentrations in seawater. As shown in Figure 1, all of the instruments used to measure weight, temperature, pressure, and the ambient humidity in the room containing the electronic balance must have a certificate that is traceable to the SI.

The word "uncertainty" has been used since the early 1990s to characterize the reliability of measurement data. Conventionally, concepts such as "error" and "accuracy" have been used to characterize the reliability of a measurement. The terminology, however, has varied among scientific fields and between countries. The Certificate in Investment Performance Measurement Program has tried to unify the methods used to assess and express the reliability of measurement data. The result has been a publication by the Joint Committee for Guides in Metrology (JCGM) that reflects the opinions of the seven major international organizations involved in scientific measurements: "Evaluation of measurement data—Guide to the expression of uncertainty in measurement" (JCGM 100, 2008).

This document is often referred to as the Guide to Uncertainty in Measurement or GUM. The GUM describes in detail the procedure for the quantitative assessment of the uncertainty of a measurement, i.e., the degree of ambiguity of the knowledge obtained from a measurement. The basic idea is to allocate the uncertainty to two components. Type A uncertainty is associated with conventional statistical analysis and is quantified by calculating the standard deviation of the data. Type B uncertainty is estimated from various sources of information other than the information used to calculate the type A uncertainty. The combination of the type A and type B uncertainty is the whole uncertainty. It is important to consider various metrics of the technical reliability of the measurement data. These metrics are then adapted for use in academic publications. An assessment of uncertainty is also required in the ISO 9000 document (Quality management systems—Fundamentals and vocabulary) of the International Organization for Standardization and the ISO 17025 document (General requirements for competence

of calibration and testing laboratories).

In section 2, ocean variables in this Guideline are described in the context of the seven SI metrics of length, mass, time, electric current, thermodynamic temperature, amount of substance, and luminous intensity. Section 2 discusses the relationship between the international system of measurement and certified reference materials. Section 3 provides an example of a comprehensive traceability system of mass at an institute.

2. Relationship between the observed ocean variables and the SI

Table 1 shows the relationships between ocean variables and the SI described in Volumes 2, 3, and 9 of this guideline. When certified reference materials are obtained and associated methods of measurement for each ocean variable are used to calibrate measurement instruments, comparability of the results of measurements of ocean variables can be obtained. However, for a standard reference material such as the number of moles of a substance, it has been difficult in practice to ensure comparability of observed amounts. In addition, because receiving a calibration certificate is relatively expensive, full traceability cannot always be achieved.

However, an effort should be made to have measurements of ocean variables traceable to the SI. An exception is the liter, a non-SI metric of volume. In SI units, 1 liter should be 1 dm³ or 10⁻³ m³. Although a liter is not an SI unit, it is acceptable to continue to use liter as a metric of volume in an appropriate context (BIPM, 2006). However, the conversion from volume of water to mass of water requires knowledge of the density of the water. Therefore, a report of a quantity per liter should be accompanied by the temperature and salinity of the seawater at the time of the measurement.

Table1. Relationship between ocean variables and the SI

Observables	Reported volume unit	Alternative units	global standard	Standard instrument or standard substance	Basic quantity Symbol	Length L	Mass M	Time T	Electric current I	Temperature theta	Amount of substance N	Luminous intensity J
					Unit Symbol	meter m	Kilogram kg	Second s	ampere A	Kelvin K	mole mol	Candela cd
Time and Location												
Time	y/m/d/min/second/degree		UTC									
Location			WGS-84									
Physical observation												
Water temperature	Degree.C		ITS-90	SPRT							1	
Salinity			TEOS-10	IAPSO Standard seawater			1,-1					
Density	kg m-3		TEOS-10			-3		1				
Pressure	Pa					-1		1	-2			
Transparency	m					1						
Water sampling analysis (Dissolved state)												
Dissolved oxygen	mol kg-1			NMIJ KIO3								Amount of substance
Nutrient	mol kg-1			SCOR, NMIJ and KANSO CRM				-1				1
Trace metal	nM							-1				1
DIC	mol kg-1					-3						1
Talk	mol kg-1			SIO CRM				-1				1
pH	µatm											
pCO2	µatm							1				
CFC, SF6	mol kg-1							-1				1
C-13	%			VPDB								1,-1
C-14	%			"1890 wood"								1,-1
DOC/DON/DOP	mol kg-1							-1				1
natural radioactivity and artificial radioactivity												
Sea water	Bq m-3											Amount of substance
Marine sediment	Bq kg-1	Bq kg-1										1
Large organisms	Bq kg-1							-1				1
Plankton benthos	Bq kg-1							-1				1
Universal Time, Coordinated												
UTC												

3. An example of a complete traceability system

All observed ocean variables should, in general, be explicitly traceable to the SI. In the case of an instrument that measures mass, the traceability system chart should be available to facilitate traceability to the SI. As an example, Figure 1 shows the traceability system chart for mass measurements at a research institution that would be used to authenticate the certification of a reference material for nutrients in seawater. All weights and the balance to be used (Figure 1) as well as all the equipment for measuring room temperature, air pressure, and humidity must have a valid calibration certificate. This requirement implies that it is possible to calculate the whole uncertainty of the mass measurement. Table 2 shows the results of the calculation of the whole uncertainty associated with preparation of a certain solution. The results show that the uncertainties due to the weight and balance are small. However, the uncertainties due to the water temperature at the time of calibrating the volumetric flask and the room temperature at the time of making the buoyancy correction are relatively large. Thus, by estimating the magnitude of the uncertainty for each individual factor, it is possible to estimate the magnitude of the uncertainty of ocean variables, and it becomes possible to formulate a procedure to reduce the uncertainties of those variables.

Figure 1. An example of a complete traceability system chart for mass

International System of Units (SI)		National Institute of Standards and Technology (NIST)		Sato Co. Ltd		IA Japan (ILAC)		National Institute of Advanced Industrial Science and Technology (AIST)	
Weight	Ms-AMH-38-VAC	2188	1694248	Digital thermometer	mirror cooling dew-point meter	7563-02	DewStar S-1S-8	Model: TT12 precision temperature indicator	Weight
				52WJ0008	002E12			model number or capacity	specified secondary standard instrument
				Digital multi-thermometer	Precision humidity generator	TR2114	SRH-IR135 (ADR)	Implement number	Identification symbol C
				73430473	0105-301/0901-404/0901-406			Certificate number	1mg~20kg
barometer	RPMA4BA10 OKs	1453	9154F	Data Logger				Working standard platinum resistance thermometer	
				SK-L200TH αD + SK-LTH α-2				WS-IPRT	
				main body: 004870 sensor: 18294				Implement number	
Implement No.				M18751				Certificate number	
Certificate No. Inspectors									
				Electronic balance	Electronic balance	Electronic balance	Electronic balance	Thermometer	Weight
				BP210D	LP620S	CPA6202S	CPA6202S	PT sensor	100g
				60506238	90608659	26907790	26907790	MODS002-01-PT-01	200g
				T-1402009	T-1402013	T-1402015	T-1402015	ST 2820057	11425455
								MT12928010	11725362
								14-10522-000	141740
								Thermometer	141741
								PT sensor	Weight
								MODS002-01-PT-01	500g
								K-320	1000g
								ST 2017002	11525550
								MT12928014	31429430
								14-10523-000	141743
								Weight	141624
								200mg ~	Weight
								30307406	20g
								141739	30307406

Table 2. An example of an uncertainty budget for mass

		equipment	Type of uncertainty	Value
Weight g	Mass	100	Type A	100 g
	Mass	200	Type A	200 g
Non-linearity of the balance	Mass	BP210D 210g	Type B	200 g
Precision of the balance	Mass	200	Type A (10 times repeated)	199.99959 g
Buoyancy correction	room temperature		Type B (rectangle)	20 °C
	Atmospheric pressure		Type B (rectangle)	1013.25 hPa
	Humidity		Type B (rectangle)	50 %
Water temperature	Water temperature		Type B (rectangle)	20 °C

		Uncertainty	Divisor (probability distribution)		Sensitivity coefficient	standard uncertainty relative value(%)
Weight g	Mass	0.000045 g	2	2	1	0.0000225
	Mass	0.0001 g	2	2	1	0.000025
Non-linearity of the balance	Mass	0.0002	$\sqrt{3}$	1.732050808	1	0.0000577
Precision of the balance	Mass	5.67646E-05 g	1	1	1	0.0000284
Buoyancy correction	room temperature	0.5 °C	$\sqrt{3}$	1.732050808	3.87E-06 ml·ml ⁻¹ ·K ⁻¹	0.00000559
	Atmospheric pressure	0.081 hPa	$\sqrt{3}$	1.732050808	1.04E-06 ml·ml ⁻¹ ·hPa ⁻¹	4.82E-09
	Humidity	3 %	$\sqrt{3}$	1.732050808	9.26E-08 ml·ml ⁻¹ ·% ⁻¹	0.000000321
Water temperature	Water temperature	0.04 °C	2	2	0.000118 ml·ml ⁻¹ ·K ⁻¹	0.0000118

References

BIPM (Bureau international des poids et mesures). 2006. The International system of units (SI), 8th edition.

JCGM (Joint Committee for Guides in Metrology) 100. 2008. Evaluation of measurement data – Guide to the expression of uncertainty in measurement, 1st edition.

Acronym

UTC	Universal Time, Coordinated
WGS-84	World Geodetic System, WGS1984
ITS-90	The International Temperature Scale 1990
TEOS-10	Thermodynamic Equation Of Seawater - 2010 (TEOS-10)

Device for measurement and measurement standard (Etalons)

○ Michio AOYAMA (Japan Agency for Marine-Earth Science and Technology, and University of Tsukuba)

Hiroshi UCHIDA (Japan Agency for Marine-Earth Science and Technology)

Akihiko MURATA (Japan Agency for Marine-Earth Science and Technology)

Kazuhiko HAYASHI (Japan Meteorological Agency)

1. Introduction

Ensuring that there are procedures over measurements of ocean variables requires reliable and stable measuring instruments, correct measurement methods, and measurement standards. A measurement standard is frequently used as a reference in establishing values of measured quantities and determining associated measurement uncertainties for other quantities of the same kind. In this way, metrological traceability is established through calibration of other measurement standards, measuring instruments, or measuring systems [International Vocabulary of Metrology, VIM, ISO/IEC Guide 99:2007, [https://isotc.iso.org/livelink/livelink/fetch/2000/2122/4230450/8389141/ISO IEC Guide 99 2007 %28Bilingual%29 %2D International vocabulary of metrology %2D%2D Basic and general concepts and associated terms %28VIM%29.pdf?nodeid=8389169&vernum=-2](https://isotc.iso.org/livelink/livelink/fetch/2000/2122/4230450/8389141/ISO_IEC_Guide_99_2007_%28Bilingual%29_%2D_International_vocabulary_of_metrology_%2D%2D_Basic_and_general_concepts_and_associated_terms_%28VIM%29.pdf?nodeid=8389169&vernum=-2) accessed on 5 March 2020]. Determining the value indicated by a measuring instrument or the value of an actual measuring instrument and its uncertainty based on a measurement standard is called calibration. Comparability of measurements of ocean variables can be secured through calibration.

Section 2 of this chapter defines key terms related to standards based on VIM. In section 3 we outline device for measurement and measurement standard (Etalons). Then we present procedures for measurement of temperature, pressure, salinity, oxygen, nutrients, total dissolved inorganic carbon, alkalinity, pH and density. Eight of 9 parameters are common parameters in hydrographic observations and these are listed as level 1 data of GO-SHIP cruises (Core Measurements, Categories and Submission Timelines ; <https://www.go-ship.org/DatReq.html> accessed on 5 March 2020) and defined as that level 1 data are of highest priority to fulfill the scientific objectives of the GO-SHIP cruises. We also describe density in this chapter because direct measurement of density might become an important parameter in hydrographic observations when we consider a link between salinity and density.

2. Terms related to standards

Terms related to standards are defined as part of the VIM. Definitions of the main terms related to this chapter are as follows.

RM (Reference Material): material, sufficiently homogeneous and stable with reference to

specified properties, which has been established to be fit for its intended use in measurement or in examination of nominal properties

CRM (Certified Reference Material): reference material, accompanied by documentation issued by an authoritative body and providing one or more specified property values with associated uncertainties and traceabilities, using valid procedures

Primary standard: measurement standard established using a primary reference measurement procedure, or created as an artifact, chosen by convention

Secondary standard: measurement standard established through calibration with respect to a primary measurement standard for a quantity of the same kind

Uncertainty: non-negative parameter characterizing the dispersion of the quantity values being attributed to a measurand, based on the information used

Calibration: operation that, under specified conditions, in a first step, establishes a relation between the quantity values with measurement uncertainties provided by measurement standards and corresponding indications with associated measurement uncertainties and, in a second step, uses this information to establish a relation for obtaining a measurement result from an indication

Traceability: property of a measurement result whereby the result can be related to a reference through a documented unbroken chain of calibrations, each contributing to the measurement uncertainty

Metrological comparability: comparability of measurement results, for quantities of a given kind, that are metrologically traceable to the same reference

3. Device for measurement and measurement standard (Etalons) for ocean observations

Table 1 summarizes the device for measurement and measurement standard (Etalons) for basic ocean observations. Table 1 outlines the standard instrument, reference material and measuring instrument for 9 variables. In addition, Table 2 shows the accuracy and/or measurement uncertainties targeted by high-quality ocean observations based on Hood (2010) and stated accuracy/uncertainty in Essential Ocean Variables, EOVS, identified by the GOOS Expert Panels for oxygen, nutrients and carbonate system parameters (https://www.goosocean.org/index.php?option=com_content&view=article&id=14&Itemid=114, accessed on 5 March 2020). For details, please refer to the corresponding chapters of this Guideline of Ocean Observations.

Table 1. Device for measurement and measurement standard (Etalons) for basic ocean observations

Variables	Standard instrument	Reference material	Measuring instrument	Remarks
Temperature	Standard Platinum Resistance Thermometer		Temperature sensor	ITS-90.
				A standard thermometer for deep sea that does not depend on pressure can be used for in situ calibration of temperature sensors.
Pressure	Dead weight piston gauge		Pressure sensor	
Salinity		IAPSO ^a seawater standard	Salinometer, conductivity sensor	Calculated from TEOS-10 from temperature and electrical conductivity values.
Oxygen		NMIJ ^b CRM (KIO ₃ solution)	Titration device, oxygen sensor	The amount of dissolved oxygen is obtained indirectly by titrating produced iodine corresponding to the amount of dissolved oxygen with a sodium thiosulfate solution.
Nutrients		NMIJ ^b CRM KANSO ^c CRM	Gas-segmented continuous flow analyzer	
		SCOR-JAMSTEC ^d CRM		
Total dissolved inorganic carbon		SIO ^e CRM	Coulometer	
Alkalinity		SIO CRM	Titration device	
pH			Spectrophotometer	Calculated from the absorption spectrum of the indicator chemical.
Density		Pure water	Vibrating-tube density meter	Measure density difference between pure water and seawater samples.

^a International Association for the Physical Sciences of the Oceans

^b National Meteorology Institute of Japan

^c KANSO Company, Ltd.

^d Scientific Committee on Ocean Research–Japan Agency for Marine-Earth Science and Technology

^e Scripps Institute of Oceanography

Table 2. Accuracy and/or measurement uncertainties for high-quality ocean observations. Hood (2010) does not use the concept of uncertainty but considers accuracy as an expanded uncertainty.

Variables	Uncertainty	Remarks
Thermometer	0.002 °C	Hood (2010)
Conductivity sensor	0.002 g kg ⁻¹	Hood (2010)
Pressure sensor	3 dbar	Hood (2010)
Oxygen sensor	1%	Hood (2010)
Practical salinity	0.001	Hood (2010)
Oxygen	0.5 µmol kg ⁻¹	EOV: ship-based repeat hydrography
Nitrate	0.03 µmol kg ⁻¹	EOV: ship-based repeat hydrography
Phosphate	0.005 µmol kg ⁻¹	EOV: ship-based repeat hydrography
Silicate	0.1 µmol kg ⁻¹	EOV: ship-based repeat hydrography
Total dissolved inorganic carbon	2 µmol kg ⁻¹	EOV: ship-based repeat hydrography
Alkalinity	2 µmol kg ⁻¹	EOV: ship-based repeat hydrography
pH	0.005	EOV: ship-based repeat hydrography
Density	0.002 kg m ⁻³	Wolf et al. (in prep.)

3.1 Temperature

The current temperature standard is the International Temperature Scale of 1990 (ITS-90). In ITS-90, the temperature scale is defined by fixed points, an interpolation instrument, and an interpolation formula divided into several temperature regions. In the temperature range for actual ocean observations, temperature scales are defined based on two fixed points—the triple point of water (0.01 °C) and the melting point of gallium (29.7646 °C)—and the Standard Platinum Resistance Thermometer (SPRT).

The traceability system of temperature to *Le Système international d'unités* (SI) is based on ITS-90. By calibrating with a SPRT, traceability to the SI of the thermometer is ensured. SI traceable thermometers are available, and SI traceable calibration is available in Japan as well as in many other countries.

In practice, the temperature of the seawater (water temperature) is measured when the thermometer indicates the temperature of the seawater after thermodynamic equilibrium is

established between the seawater and thermometer. Determining the time required for equilibrium requires consideration of the time constant associated with the heat capacity of the thermometer.

The temperature sensor (SBE 3plus) of the conductivity-temperature-depth (CTD) instrument (SBE 9plus) is manufactured by Sea-Bird Electronics, a company whose instruments are widely used for observations in the open ocean. The sensor can be calibrated by the manufacturer to within an uncertainty of about 0.001 °C. However, some CTD temperature sensors have a pressure dependence (up to 0.002 °C per 6000 dbar, Uchida et al., 2015), so care is needed when measuring the water temperature at depths greater than 2000 dbar. By comparing and calibrating the CTD temperature sensor based on the deep ocean standard thermometer (SBE 35) manufactured by Sea-Bird Electronics in the deep ocean, the water temperature in the deep ocean can be measured with an uncertainty of 0.0007 °C (Uchida et al., 2015). For both the CTD temperature sensor and the deep ocean standard thermometer, it is necessary to ascertain the temporal changes of the sensor characteristics from the history of calibration by the manufacturer in the laboratory, etc., and to use the instrument calibrated periodically in consideration of the required accuracy.

3.2 Salinity

Salinity is defined by the International Thermodynamic Equation of Seawater 2010 (TEOS-10), and the IAPSO (International Association for the Physical Sciences of the Ocean) standard seawater is the de facto standard of measurement. TEOS-10 estimates the absolute salinity (unit: g kg^{-1}) from the measured value of practical salinity (no units, Practical Salinity Scale of 1978: PSS-78) defined by the electrical conductivity ratio.

3.2.1 Salinometer and IAPSO standard seawater

Practical salinity is measured with an electrical conductivity salinometer (for example, the AUTOSAL 8400B manufactured by Guildline Instruments is widely used). Calibration of the electrical conductivity salinometer should be conducted by measuring the conductivity of IAPSO standard seawater with an assigned value of the electrical conductivity ratio. In practice, the salinity of seawater is determined from electrical conductivity by introducing seawater into the cell inside the equipment. Alternatively, the electrical conductivity is measured by inserting an electrical conductivity sensor into the target seawater, and the conductivity is then converted to practical salinity. Temperature has a large effect on the measurement of electrical conductivity. For precise salinity measurements, the precision of the temperature measurement must be controlled so that it is consistent with the degree of uncertainty required for the salinity measurement. Specifically, when the set temperature of the electrical conductivity salinometer is T °C, it is important to ensure that the ambient temperature is in the range between T °C and T minus 2 °C.

IAPSO standard seawater is surface seawater collected in the eastern North Atlantic Ocean. The water is filtered, the organic matter decomposed, the electrical conductivity adjusted, etc. The water is then stored in a glass bottle. The electrical conductivity ratio at 15 °C and 1 atm for PSS-78 potassium chloride solution is then assigned (Bacon et al., 2007). However, it has been pointed out that there is an uncertainty of about 0.001 in terms of practical salinity in the K15 value that is assigned (Kawano et al., 2006). To study changes of salinity in the deep ocean, care must therefore be taken. During a cruise, it is important to calibrate the conductivity salinometer using a single batch of IAPSO standard seawater and to report the batch number of the IAPSO standard seawater used for the salinity measurement.

3.2.2 conductivity sensor

In general, the output value of the electrical conductivity sensor is more likely than the output value of the temperature sensor or pressure sensor to shift suddenly because of a physical impact or to shift slowly because of contamination of the cell. For the conductivity sensor, there is also a pressure dependence that cannot be evaluated by laboratory calibration. To correct for this pressure dependence, it is necessary to compare and calibrate the CTD electrical conductivity sensor by using salinity data measured for in situ water samples for high-quality ocean observations. The salinity uncertainty associated with the CTD conductivity sensor therefore depends on the uncertainty of the salinity of the seawater sample and the sensor calibration method.

3.2.3 Practical salinity calculation

Calculating practical salinity from the conductivity ratio of the electrical conductivity sensor requires knowing the ratio of the electrical conductivity to the electrical conductivity at a practical salinity of 35, temperature of 15 °C (the International Practical Temperature Scale 1968: IPTS-68), and pressure of 0 dbar. For the value of the above electrical conductivity ratio, TEOS-10 adopts the value of 4.29140 S/m reported by Culkin and Smith (1980). This value is also used in the calibration of electrical conductivity sensors at Sea-Bird Electronics, but different values may be used, depending on the manufacturer. For example, 4.2896 S/m is used for Tsurumi Seiki XCTD. These different values are not a problem when using the software provided by the manufacturer to calculate salinity, but care must be taken when the user is calculating the salinity using homemade software.

3.3 Pressure

For pressure, a system of standard mass has been established by the Metre Convention, and a dead weight piston gauge is used as the primary standard for pressure. The SI traceability of the pressure is ensured by comparing and calibrating with the piston gage. Alternatively, piston gauges can be calibrated as SI traceable. In recent years, high-precision digital pressure gauges with excellent stability (for example, quartz vibration type pressure gauges manufactured by

Paroscientific, Inc.) have been available, and they can be incorporated into standard pressure systems (Kobata et al., 2011). Such gauges have also been used as digital pressure calibrators (for example, the E-DWT manufactured by Fluke) to ensure SI traceability.

The quartz crystal resonator pressure gauge available from the Paroscientific, Inc. is also used in the Sea-Bird Electronics CTD (SBE 9plus) pressure sensor, which is widely used for observations in the open ocean. Quartz crystal resonator pressure gauges have lower hysteresis (the characteristic of outputting different values when pressure is increasing and when pressure is decreasing) and are very stable. Proper calibration of the pressure sensor before a cruise ensures that the pressure can be measured to within an uncertainty of about 0.02%, and there is generally no need to correct measured data. The temporal drift and shift of the CTD pressure sensor can be monitored using values of atmospheric pressure (deviation from standard atmospheric pressure) measured on the deck before and after making CTD observations. If the difference between the values measured on the deck before and after a CTD observation is large (for example, about 1 dbar), there is presumably a problem with the correction of the temperature characteristics. In that case, calibration, including the temperature characteristics, must be performed. Normally, calibration is performed only at room temperature, except for the manufacturer's calibration when the sensor is shipped to users. It is important to use a CTD pressure sensor that has been calibrated periodically to ensure the required accuracy and to ascertain the time-dependent characteristics of the sensor from the history of calibration in the laboratory by the manufacturer and the user.

3.4 Oxygen

3.4.1 Titration

The method for determining the dissolved oxygen concentration in seawater is generally the Carpenter method (Carpenter, 1965), which is an improvement of the Winkler method, but is hereafter simply referred to as the Winkler method. In this Winkler method, manganese hydroxide “fixes” dissolved oxygen under alkaline conditions, and the “fixed” dissolved oxygen quantitatively oxidizes iodine ions to free iodine under acidic conditions. Titrating the free iodine with a sodium thiosulfate solution of known concentration indirectly quantifies the dissolved oxygen concentration.

The sodium thiosulfate solution concentration is determined by titration of a potassium iodate solution of known concentration. In Japan, SI-traceable certified reference potassium iodate standards are supplied by the National Meteorology Institute of Japan, National Institute of Advanced Industrial Science and Technology (NMIJ). However, the dissolved oxygen concentration determined by the Winkler method includes the concentration of interfering substances in the seawater sample. Therefore, strictly speaking, the dissolved oxygen concentration obtained by the Winkler method is not SI traceable unless the concentrations of the interfering substances are also quantified at the same time for each seawater sample.

The Winkler method with an automatic titrator can measure dissolved oxygen to within a standard uncertainty of about $0.14 \mu\text{mol kg}^{-1}$ when the concentration is $250 \mu\text{mol kg}^{-1}$

(Kumamoto et al., 2015). The measurement, however, does not include the effects of the seawater blank (the total effect of the substances in the seawater sample that interfere with the Winkler method). With the exception of anoxic seawater, the seawater blank concentration in the open ocean is equivalent to a dissolved oxygen concentration of $1 \mu\text{mol kg}^{-1}$ or less, but the blank cannot be ignored in high-precision observations, for which the target uncertainty might be $0.5 \mu\text{mol kg}^{-1}$. Assuming that the seawater blank is $0.5 \pm 0.5 \mu\text{mol kg}^{-1}$, the overall uncertainty of the measured dissolved oxygen concentration, including the effect of the seawater blank, is estimated to be $0.6 \mu\text{mol kg}^{-1}$ when the true concentration is $250 \mu\text{mol kg}^{-1}$. In such a case, however, it must be clearly stated that the reported concentration has been corrected for the effect of the seawater blank ($0.5 \mu\text{mol kg}^{-1}$).

3.4.2 Oxygen sensor

It is also common to measure the dissolved oxygen concentration continuously by attaching an oxygen sensor to the CTD. In general, the output of an oxygen sensor is likely to shift because of contamination or deterioration of the oxygen detection membrane. There is also a dependence on pressure that cannot be evaluated by laboratory calibration. For the oxygen sensor of a CTD used in high-precision ocean observations, it is therefore necessary to calibrate the oxygen sensor based on the dissolved oxygen concentration of the seawater sample determined by the Winkler method in a manner analogous to the way an electrical conductivity sensor is calibrated by salinity of the seawater sample measured by salinometer. The uncertainty of the dissolved oxygen concentration determined by the CTD oxygen sensor therefore depends on the uncertainty of the dissolved oxygen concentration of the seawater sample and the method by which the sensor is calibrated.

3.5 Nutrients

The NMIJ has supplied SI traceable CRM for nutrients in seawater since June 2014. The NMIJ CRM locates top of traceability and is primary standard. In addition, since June 2015, an SI traceable CRM has been supplied by the KANSO Company, Ltd. (KANSO). The KANSO CRM is secondary standard.

Nitrate, phosphate, and silicate concentrations of NMIJ CRM have been certified by three analytical methods, including the colorimetric methods commonly used while those of KANSO CRM are certified by colorimetric methods only (Aoyama, 2016).

In the NMIJ certification document, the mass fractions of nitrate ions and phosphate ions are shown directly, and the mass fraction of silicon is shown as the mass fraction of dissolved silica. In addition, the seawater density at $25 \text{ }^\circ\text{C}$ is shown as reference information. For conversion to mol kg^{-1} , the units normally used, it is necessary to convert from mass fraction to molar concentration using the latest atomic weights at the time of issuance of the certificate.

Nutrient concentrations in seawater samples are assayed by adding reagents that produce a color reaction, and the concentrations are determined quantitatively via a colorimetric method that calculates the concentration from the absorbance. At present, colorimetric analysis is

performed mainly by continuous flow analysis (CFA) equipment (for example, the Auto Analyzer manufactured by BL TEC K.K.).

When performing nutrient analysis by any method, it is necessary to explicitly measure CRMs to ensure metrological comparability, hereafter comparability, and traceability. In addition, the solution (CRM, inhouse standard solution, or deep-sea water as tracking standard, etc.) should have a concentration close to the maximum concentration of the analytical sample. It is also essential to repeat the analysis a number of times so that a statistically significant value is obtained (for example, the analysis may be repeated nine or more times) and to evaluate and describe the repeatability of the analysis at roughly that maximum concentration (expressed as the standard deviation of the obtained value). In addition, the uncertainty of the analysis depends on the concentration, and the uncertainty of the analysis increases at low concentrations. It is therefore desirable to evaluate the uncertainty of the analysis at different concentrations covering the full range of sample concentrations. When analyzed by a well-trained analytical engineer using finely tuned analytical instruments, the reproducibility of nitrate, phosphate, and silicate analyses (standard deviation of single assays) in the Pacific Ocean is less than 0.2% of the concentration of which ranges were around 35-40 $\mu\text{mol kg}^{-1}$, 2.5-2.9 $\mu\text{mol kg}^{-1}$ 120-140 $\mu\text{mol kg}^{-1}$ for nitrate, phosphate, and silicate (N = 16).

3.6 Total dissolved inorganic carbon, alkalinity, and pH

For the measurement of total dissolved inorganic carbon and alkalinity, a CRM is available from Prof. A. G. Dickson's laboratory at the Scripps Institute of Oceanography (SIO), University of California. The CRM is widely used for quality control of data. For the measurement of pH, there is currently no CRM.

The widely used methods for high-precision measurements of total dissolved inorganic carbon, alkalinity, and pH (Bockmon and Dickson, 2015) are described below. For total dissolved inorganic carbon, a coulometric titration method using a coulometer is widely used. This is a method in which dissolved inorganic carbon in a seawater sample is extracted as carbon dioxide, absorbed in the cathode solution of an electrolytic cell, and accurately titrated using a coulometer with hydroxide ions generated via electrolysis of water (Ishii et al., 2000). For alkalinity, potentiometric acid titration using an open cell is widely used. This method is published as international standard ISO 22719:2008 (Water quality – Determination of total alkalinity in sea water using high precision potentiometric titration). A colorimetric method using an indicator dye (*m*-cresol purple) and a spectrophotometer is widely used for pH measurements. This method is also published as international standard ISO 18191:2015 (Water quality – Determination of pH in sea water – Method using the indicator dye *m*-cresol purple). Increasing the purity of the indicator by an appropriate technique makes it in principle unnecessary to use a standard material, and the pH of seawater can be accurately measured.

Recently, 59 laboratories from around the world have participated in an inter-laboratory

comparison experiment for measuring total dissolved inorganic carbon, alkalinity, and pH (Bockmon and Dickson, 2015). For total dissolved inorganic carbon and alkalinity, a CRM is used in almost all laboratories, and about half of the laboratories agree to within $5 \mu\text{mol kg}^{-1}$. About 20–25% of the laboratories have high-precision instrumentation, and their uncertainty is less than $2 \mu\text{mol kg}^{-1}$. In other laboratories, when the concentration of a sample is close to the CRM concentration, the reported concentrations are consistent with one another, but for samples with concentrations higher than the CRM, the reported values have shown greater dispersion. The indication is that CRMs with higher concentrations are needed. In the case of pH, there are large variations in measured values because there is no standard for pH, but the measured values of seven laboratories using indicators with increased purity showed similar values within 0.004, and they were close to the target uncertainty (0.003) for high-precision observation.

3.7 Density

In Japan, a traceability system for density has been established with silicon single-crystals at the top of traceability (Fujii, 2009). The density of seawater is usually measured with a vibrating-tube density meter (the Anton-Paar DMATM 5000M is widely used in the field of density measurements). Vibrating-tube density meters are usually calibrated with air and water, and pure water standard solutions for calibration of SI-traceable density meters are commercially available. However, the uncertainty of the density assigned to the pure water standard solution is large (about 0.01 kg m^{-3}) and cannot be used for precise measurements of seawater density. The differences between the measured density values of pure water from ultrapure water production equipment and that of seawater samples should therefore be determined first. The values obtained by calculation from the equation of state of water (IAPWS-95: the IAPWS Formulation 1995 for the Thermodynamic Properties of Ordinary Water Substance for General and Scientific Use, Wagner and Pruss, 2002) are then added to the density of pure water to obtain the density of seawater (so called “substitution method”; Wolf, 2008). However, because this equation of state is defined by the isotopic composition of Standard Mean Ocean Water (SMOW), the density difference due to the deviation of the stable isotope ratio ($\delta^{18}\text{O}$ and δD) of pure water used for measurement from SMOW should be corrected.

Recently, the NMIJ has developed a hydrostatic weighing device (primary standard) for seawater density measurements using silicon single-crystals as a sinker. The SI-traceable calibration of the density of standard seawater with that device has an uncertainty of 0.002 kg m^{-3} . At present, there is no standard seawater for measuring seawater density, but in order to ensure comparability of measurements of the densities of seawater samples, the density of IAPSO standard seawater, etc. should be measured together with the seawater samples in order to compare the result with the calibrated density determined by the NMIJ. However, it should

be noted that the density of IAPSO standard seawater increases with time due to dissolution of silicon from glass containers (0.0004 kg m^{-3} per year, Uchida et al., 2011).

References

- Aoyama, M. (2016): Determination of dissolved nutrients (N, P, SI) in seawater with high precision and inter-comparability using gas-segmented continuous flow analyzers. *Guideline of Ocean Observations*, vol. 3, chap. 2, G302EN:001–095.
- Bacon, S., F. Culkin, N. Higgs and P. Ridout (2007): IAPSO Standard Seawater: Definition of the uncertainty in the calibration procedure, and stability of recent batches. *J. Atmos. Oceanic Technol.*, 24, 1785–1799.
- Bockmon, E. E. and A. G. Dickson (2015): An inter-laboratory comparison assessing the quality of seawater carbon dioxide measurements. *Marine Chemistry*, 171, 36–43.
- Carpenter, J.H. (1965): The Chesapeake Bay Institute technique for the Winkler dissolved oxygen method. *Limnology and Oceanography*, 10, 141–143.
- Culkin, F. and N. Smith (1980): Determination of the concentration of potassium chloride solution having the same electrical conductivity, at 15°C and infinite frequency, as standard seawater of salinity 35.0000‰ (chlorinity 19.37394‰), *IEEE J. Oceanic Eng.*, 5, 22–23.
- Fujii, K. (2009): A new density standard replaced from water – Using silicon single-crystals as the top of traceability in density measurement –. *Synthesiology English edition*, 3, 187–198.
- Hood, E. M. (2010): Introduction to the collection of expert reports and guidelines. *The GO-SHIP Repeat Hydrography Manual: A Collection of Expert Reports and Guidelines*, IOCCP Report No. 14, ICPO Publication Series No. 134, Version 1.
- Ishii, M., H. Y. Inoue and H. Matsueda (2000): Coulometric precise analysis of total inorganic carbon in seawater. Technical Reports of the Meteorological Research Institute No. 41 doi:10.11483/mritechrepo.41 (in Japanese with English abstract)
- Kawano, T., M. Aoyama, T. Joyce, H. Uchida, Y. Takatsuki and M. Fukasawa (2006): The latest batch-to-batch difference table of standard seawater and its application to the WOCE onetime sections. *J. Oceanogr.*, 62, 777–792.
- Kumamoto, Y., Y. Takatani, T. Miyao, H. Sato and K. Matsumoto (2015): Dissolved oxygen. *Guideline of Ocean Observations*, vol. 3, chap. 1, G301JP:001–029 (English edition is in prep.)
- Kobata, T. M., Kojima and H. Kajikawa (2011): Improvement of reliability in pressure measurements and international mutual recognition – Incorporation of industrial digital pressure gauges to the national metrology system –. *Synthesiology*, 4, 209–221. (in Japanese with English abstract)
- Uchida, H., T. Kawano, M. Aoyama and A. Murata (2011): Absolute salinity measurements of standard seawaters for conductivity and nutrients. *La mer*, 49, 119–126.
- Uchida, H., T. Nakano, J. Tamba, J. Widiatmo, K. Yamazawa, S. Ozawa and T. Kawano (2015): Deep ocean temperature measurement with an uncertainty of 0.7 mK. *J. Atmos. Oceanic. Guideline of Ocean Observation Vol.1 Chap.2 Quality control with standard equipment and materials*
© Michio Aoyama, Hiroshi Uchida, Akihiko Murata, Kazuhiko Hayashi 2019 G102EN:001-012

Technol., 32(11), 2199–2210.

Wagner, W. and A. Pruss,(2002): "[The IAPWS Formulation 1995 for the Thermodynamic Properties of Ordinary Water Substance for General and Scientific Use.](#)" *J. Phys. Chem. Ref. Data*, **31**, 387-535.

Wolf, H. (2008): Determination of water density: limitations at the uncertainty level of 1×10^{-6} . *Accred. Qual. Assur.*, 13, 587–591.

Wolf, H., S. Weinreben, H. Uchida and R. Pawlowicz: Best practice guide for the measurement of seawater density (in preparation under the activity of the Joint Committee on the Properties of Seawater, <http://www.teos-10.org/JCS.htm>)

Essential Ocean Variables (EOVs) of GOOS

Masao ISHII

(Oceanography and Geochemistry Research Department, Meteorological Research Institute)

Toshio SUGA

(Graduate School of Science and Faculty of Science, Tohoku University)

Sanae CHIBA

(Research and Development Center for Global Change,

Japan Agency for Marine-Earth Science and Technology)

The Global Ocean Observing System (GOOS), being sponsored by UNESCO/IOC, WMO, UNEP, and ICSU, is a programme to coordinate observations around the global ocean for climate, ocean health, and real-time services. In accordance with the "Framework for Ocean Observing", GOOS defines Essential Ocean Variables (EOVs) of physics, biogeochemistry, biology and ecosystems, the methods of many of these measurements being guided in this Guideline.

The latest information and the list of GOOS EOVs are available with their specification sheets at the following web site.

http://goosocean.org/index.php?option=com_content&view=article&id=14&Itemid=114

This page left intentionally blank.

Quality control by comparison with standards, control charts, duplicated measurements, and property-property characteristics, and the report of metadata

○Michio AOYAMA^{1,2}, Hiroshi UCHIDA¹, Daisuke SASANO³, and Hajime OBATA⁴

¹Research Institute for Global Change (RIGC), Japan Agency for Marine-Earth Science and Technology (JAMSTEC)

²Center for Research in Isotopes and Environmental Dynamics (CRiED), University of Tsukuba

³Japan Meteorological Agency (JMA)

⁴Atmosphere and Ocean Research Institute (AORI), University of Tokyo

Abstract

High-quality data from observations in the ocean and the comparability and traceability of observational data with stated uncertainty are important requirements for oceanographic research. Now we are able to obtain high-quality observational data that is comparable and traceable to the International System of Units (*Système International d'Unités*, SI) with stated uncertainty for many of the variables discussed in Volume 1, Chapter 2 of this guideline. This chapter describes 1) quality control procedures necessary to obtain SI-traceable data with stated uncertainty, 2) metadata reporting, 3) best practices for quality control implemented on a few cruises, 4) an introduction to software such as Ocean data view and 2D/3D property-property plot for quality control, 5) improvement of data quality obtained along 137°E from 10°–24°N (section P9) by the Japan Meteorological Agency since 1967 and some other examples of improvement of obtained data.

List of acronyms used in this chapter

Acronym	Meaning
AIC	Akaike Information Criterion
AORI	Atmosphere and Ocean Research Institute
Chl. <i>a</i>	Chlorophyll <i>a</i>
CRiED	Center for Research in Isotopes and Environmental Dynamics
CRM	Certified Reference Material
CSK	Cooperative Study of the Kuroshio and Adjacent Regions
CSR	Cruise summary report
CTD	Conductivity-temperature-depth
dbar	Decibar
DIC	Dissolved inorganic carbon
EEPROM	Electrically erasable programmable read-only memory
FS	Full scale
GaMP	Melting point of gallium
GLODAP	GLobal Ocean Data Analysis Project
GO	General Oceanics
hPa	Hectopascal = 100 Pascals
IAPSO	International Association for the Physical Sciences of the Oceans
ICES	International Council for the Exploration of the Sea
IOC	International Oceanographic Commission
IOCCP	International Ocean Carbon Coordination Project
ITS-90	International Temperature Scale of 1990
JAMSTEC	Japan Agency for Marine-Earth Science and Technology
JCSS	Japan Calibration Service System
JFE	JFE Advantech Co., Ltd.
JMA	Japan Meteorological Agency
K	Kelvin degree

LAN	Local area network
NIST	National Institute of Standards and Technology
NMIJ	National Metrology Institute of Japan
Num	Number of measurements
ODV	Ocean Data View
Pa	Pascal (unit of pressure)
PACIFICA	Pacific ocean interior Carbon (the name of a dataset)
psia	Pounds per square inch absolute
QC	Quality control
RCGC	Research and Development Center for Global Change
RIGC	Research Institute for Global Change
RM	Reference material
ROSCOP	Report of Observations/Samples collected by Oceanographic Programmes
S	Siemens
SBE	Sea-Bird Electronics
SCOR	Scientific Committee on Oceanic Research
SEASOFT	Software Engineering of America software
SI	<i>Système International d'Unités</i> (The International System of Units)
SIO	Scripps Institute of Oceanography
S/N	Serial number
SPRT	Standard Platinum Resistance Thermometer
TA	Total alkalinity
TB	Teledyne Benthos
TC	Temperature-conductivity
TPW	Triple point of water
TSG	Thermosalinograph
WHP	WOCE Hydrographic Programme
WHPO	WOCE Hydrographic Program Office
WOCE	World Ocean Circulation Experiment

Table of contents

1. Introduction.....	5
2. Quality control procedures to obtain SI-traceable data with stated uncertainty	6
2-1. Unbroken chain of comparison that can produce the best SI-traceable instruments/materials.....	6
2-2. Pre- and post-cruise calibration of sensors and water sample measurements.....	7
3. Metadata report and access to data by Intergovernmental Oceanographic Commission (IOC) recommendations.....	8
3-1. Cruise Summary Reports and metadata of the cruise.....	8
3-2. Metadata and examples of metadata of several cruises.....	10
4. Best practices of quality control procedures for sensors in the case of the MR15-05 cruise by JAMSTEC and the RF16-06 cruise by the JMA.....	12
4-1. Quality control and calibration of sensors in the case of the MR15-05 cruise (JAMSTEC).....	12
4-2. Quality control and calibration of sensors in the case of the RF16-06 cruise (JMA)	32
5. Best practices for quality control of bottle salinity, oxygen concentration, nutrient concentrations, and carbonate system parameters.....	48
5-1. Quality control for bottle sampling parameters in the case of the MR15-05 cruise (JAMSTEC).....	48
5-2. Quality control for bottle sampling parameters in the case of the RF16-06 cruise (JMA)	58
5-3. Quality control for trace metals in seawater during the R.V. Hakuho Maru KH-09-5 cruise (AORI, University of Tokyo)	96
5-4. General procedure of quality control flag assignment.....	99
6. Quality control by 2D/3D property/property plots by Ocean Data View.....	100
6-1. Recommended softwares.....	100
6-2. 2D/3D property/property plot by ODV.....	100
7. History of a region, 32°–35°S and 178°–170°W, in the South Pacific Ocean: evidence of improvement of data quality by different organizations.....	103
8. History along the P09 section: evidence of improvement of quality of data collected by the same organization.....	105
8.1 Comparability among stations.....	105
8.2 Comparability among cruises.....	106
8.3 Use of nutrient CRMs.....	108
Acknowledgements.....	109
References.....	109
Appendix.....	113
I IOC data policy 2003.....	114
II-1 Cruise summary report of KH-09-5.....	117
II-2 Post cruise metadata of the cruise KH-09-05.....	118
II-3 Cruise summary report, expanded version by R/V Ryofu Maru.....	121

1 **1. Introduction**

2 High-quality data from observations in the ocean and the comparability and traceability of
3 observational data with stated uncertainties are important requirements for oceanographic research. The
4 purpose of this Guideline of Ocean Observation, published by the Oceanographic Society of Japan, is
5 to articulate how those requirements are to be met.

6 It is important and customary to share data obtained by various types of ocean observations, not only
7 for scientific research but also for a wide variety of other purposes, including the prediction of weather
8 and climate, the operational forecasting of the marine environment, the preservation of life, the
9 mitigation of adverse anthropogenic impacts on the marine and coastal environment, and the
10 advancement of scientific understanding that makes application of this information possible. The timely,
11 free, and unrestricted international exchange of oceanographic data requires that the data be
12 accompanied by metadata (i.e., data about data).

13 The long history of quality control of observational hydrographic data by the oceanographic
14 community reflects the need to obtain high-quality data as much as possible. The World Ocean
15 Circulation Experiment (WOCE) era was the first period of time when systematic quality control of
16 observational hydrographic data was done by the data originator and by reviewers. Examples include
17 the article review system, which was organized by the WOCE Hydrographic Program Office (WHPO).
18 Data originators submitted their cruise reports with data and its quality flag following
19 “REQUIREMENTS FOR WOCE HYDROGRAPHIC PROGRAMME DATA REPORTING” (WOCE
20 Report 67/91, Joyce and Corry, 1994). Reviewers investigated all reported data by using MATLAB
21 scripts and/or graphic software written by collaborators of the WHPO activity. There is also good
22 guidance in the document titled “REFERENCE-QUALITY WATER SAMPLE DATA Notes on
23 Acquisition, Record Keeping, and Evaluation” ([https://cchdo.github.io/hdo-
24 assets/documentation/policies/Data_Evaluation_reference.pdf](https://cchdo.github.io/hdo-assets/documentation/policies/Data_Evaluation_reference.pdf), accessed 30 March 2020) by J. Swift at
25 the Scripps Institute of Oceanography (Swift, 2010).

26 Today, we are able to have high-quality observational data that are comparable and traceable to the
27 Système Internationale (SI) with stated uncertainty for many parameters, as stated in Volume 1, Chapter
28 2 of this guideline.

29 This chapter 4 of volume 1 covers the following topics: 1) description of quality control procedures
30 needed to obtain SI-traceable accuracy with stated uncertainty, 2) metadata reports, 3) examples of best
31 practices of quality control conducted on a few cruises, 4) introduction of quality control software such
32 as Ocean Data View and 2D/3D property-property plots for quality control, 5) improvement of the
33 quality of data obtained on cruises along 137°E from 10°–24°N (section P9) by the Japan Meteorological
34 Agency since 1967 and some other examples of improvement of obtained data.

35
36

37 2. Quality control procedures to obtain SI-traceable data with stated uncertainty

38 *2-1. Unbroken chain of comparison that can produce the best SI-traceable instruments/materials*

39 We show basic quality control procedures for sensors and water sample measurements in sections 4
40 and 5, respectively. One of the basic goals of quality control is to ensure comparability and traceability
41 to the SI with stated uncertainty, as described in Vol 1, Chap 1 (Aoyama, 2016) and Vol 1, Chap 2
42 entitled “Device for measurement and measurement standard (Etalons) “ (Aoyama et al., 2019) in this
43 guideline.

44 Based on the SI traceability system, an unbroken chain of comparison is needed to achieve the best
45 SI-traceable instruments/materials, e.g., a temperature primary standard based on the International
46 Temperature Scale of 1990 (ITS-90) for seawater temperature measurements and a silicon mass primary
47 standard of mass for silicate concentration measurements. Our oceanographic community and
48 metrology community, through the national metrology institutes in each country, have traditionally
49 provided primary measurement standards to underpin a wide range of physical and chemical
50 measurements. Temperature measurements are based on ITS-90 (traceable to SI using a standard
51 platinum resistance thermometer, SPRT). Comparability of salinity measurements has been ensured
52 using the International Association for the Physical Sciences of the Oceans (IAPSO) salinity standard
53 seawater provided by Ocean Scientific International, UK. Comparability and traceability of the
54 carbonate system parameter measurements has been ensured using certified reference materials (CRMs)
55 provided by the laboratory of A. G. Dickson, Scripps Institute of Oceanography (SIO), USA (Dickson,
56 2003; 2010). Comparability and traceability of nutrient concentration measurements has been ensured
57 using CRMs provided by the National Metrology Institute of Japan (NMIJ) and SCOR-JAMSTEC and
58 KANSO CRMs provided by the KANSO Co. Ltd. (Sato et al., 2010; Aoyama et al., 2012). For these
59 community-accepted standards such as salinity standard solution, carbonate CRM, and nutrient CRMs,
60 continual monitoring and readily available documentation are essential to keep the consistency and long-
61 term quality of those standards through studies such as batch to batch comparison studies of salinity
62 standard solution (Mantyla, 1987; Aoyama et al., 2002; Kawano et al., 2006), inter-laboratory
63 comparison exercises of carbonate system CRM (Bockmon and Dickson, 2015) and inter-laboratory
64 comparison exercises (Aoyama et al., 2006, 2007, 2008, 2012, 2016, 2018).

65 It is also possible to use some standard instruments and high-quality data obtained by
66 physical/chemical measurements to calibrate raw data from sensors/instruments onboard.

67 Duplicate/replicate measurements may also be made on water samples for quality control and for
68 determination of the magnitude of reproducibility of the measurements. Multiple measurements of the
69 same sample may also be made. The number of such measurements might be 7–9 or more. A good
70 example to get comparability among the measurements at multiple stations is also to use deep-sea water
71 as tracking standard instead of CRMs. In this case, only comparability can be ensured but can not be
72 ensured for SI traceability.

73 If CRMs or SI-traceable measurements/instruments were involved, there is a need to conduct further
74 data quality control to discover inconsistencies and other anomalies in the data as well as to perform
75 data-cleansing activities (e.g., removing outliers, flagging data as questionable or bad) to improve the
Guideline of Ocean Observation Vol.1 Chap.4 Quality control by comparison with standards, control charts,
duplicated measurements, and property-property characteristics, and the report of metadata ©Michio Aoyama,
Hiroshi Uchida, Daisuke Sasano, Hajime Obata 2019 G104EN:001-134

76 data quality. Inconsistencies and outliers may occur for several reasons, including simple/complex
77 human errors, mechanical malfunctions of instruments/sensors, and communication problems between
78 sensors and the host computer.

79 After quality control is carried out via an unbroken chain of comparisons with standards, a control
80 chart, and duplicate measurements, the quality control of property-property characteristics described in
81 this chapter may be performed during the onboard measurements and may be performed after a dataset
82 that includes all parameters has been completed.

83 ***2-2. Pre- and post-cruise calibration of sensors and water sample measurements***

84 Best practices for pre- and post-cruise calibration of conductivity-temperature-depth (CTD) systems
85 and underway measurements are the main part of the quality control procedures described in section 4.

86 For water sample measurements, the best practices for bottle salinity, oxygen concentrations,
87 nutrient concentrations, carbonate system parameters, and chlorophyll *a* (Chl. *a*) concentrations are
88 described in section 5.

89

90

91 **3. Metadata report and access to data by Intergovernmental Oceanographic Commission (IOC)**
92 **recommendations**

93 ***3-1. Cruise Summary Reports and metadata of the cruise***

94 A Cruise Summary Report (CSR) is used to provide metadata for scientists, data managers, and
95 program managers who need information about measurements and samples collected at ocean, namely,
96 who has collected what, when, and where. Historically parameters were defined using the Report of
97 Observations/Samples collected by Oceanographic Programmes (ROSCOP) parameter codes. The
98 ROSCOP was conceived by IOC/IODE in the late 1960s in order to provide a low level inventory for
99 tracking oceanographic data collected on research vessels. The ROSCOP form was extensively revised
100 in 1990, and was re-named the CSR. Most marine disciplines are represented in the CSR, including
101 physical, chemical, and biological oceanography, marine geology and geophysics, fisheries, marine
102 contaminants, and marine meteorology. Traditionally, it is the chief scientist's obligation to submit a
103 CSR to his/her National Oceanographic Data Centre (NODC) within two to three weeks after the cruise
104 (Rickards and Nast, IOC/IODE-XIX/ 12, 2007).

105 The CSR is intended to fill the gap between the first announcement of an oceanographic program
106 and the eventual catalogue of data available to users. As timely inventories of data to ensure prompt
107 exchange, the CSR contains such information as ocean area where the investigation was carried out,
108 track chart of the cruise, person who holds the data, name and volume of the data written in the IOC's
109 CSR form.

110 Currently, the CSRs directory covers cruises from 1873 till today from more than 2.000 research
111 vessels: a total of nearly 58.000 cruises, in all European waters and global oceans. This also includes
112 historic CSRs from European countries that have been loaded from the ICES database from 1960
113 onwards. (<https://www.seadatanet.org/Standards/Metadata-formats/CSR> accessed on 19 March 2020)

114 In Japan, we can submit CSRs online to Japan Oceanographic Data Center (JODC) at
115 https://www.jodc.go.jp/jodcweb/aboutInfo_j.html (accessed on 19 March 2020).

116

117 In 2003, the IOC Oceanographic Data Exchange Policy (Appendix I) was established for the
118 efficient acquisition, integration, and use of ocean observations gathered by the countries of the world
119 for a wide variety of purposes, including the prediction of weather and climate, operational forecasting
120 of the marine environment, the preservation of life, the mitigation of adverse anthropogenic impacts on
121 the marine and coastal environment, as well as for the advancement of scientific understanding that
122 makes application of this information possible. For these purposes, an appropriate data report and
123 metadata report are essential and recommended.

124 In the IOC Oceanographic Data Exchange Policy (Appendix I), data and metadata are defined as
125 follows:

126 **'Data'** consist of oceanographic observation data, derived data, and gridded fields.

127 **'Metadata'**¹ are 'data about data'. They describe the content, quality, condition, and other characteristics
128 of data.

129

130

131

132

133

134

135

136

137

138

139

140

141

142

143

144

145

146

147

148

149

150 ¹ It is easy to find information on the source of "metadata": the word was formed by combining "data"
151 with "meta-," which means "transcending" and is often used to describe a new but related discipline
152 designed to deal critically with the original one. "Meta-" was first used in that way in "metaphysics" and
153 has been extended to a number of other disciplines, giving us such words as "metapsychology" and
154 "metamathematics." "Metadata" takes the "transcending" aspect a step further and applies it to the
155 concept of pure information instead of a discipline. "Metadata" is a fairly new word (it appeared in the
156 latter half of the 20th century), whereas "data" can be traced back to the middle of the 17th century. The
157 first known use of metadata was in 1983. (<https://www.merriam-webster.com/dictionary/metadata>
158 accessed on 2 November 2019).

159 Guideline of Ocean Observation Vol.1 Chap.4 Quality control by comparison with standards, control charts,
duplicated measurements, and property-property characteristics, and the report of metadata ©Michio Aoyama,
Hiroshi Uchida, Daisuke Sasano, Hajime Obata 2019 G104EN:001-134

160 **3-2. Metadata and examples of metadata of several cruises**

161 In this section, we show various examples of metadata, simple cruise summary report, based on
 162 ROSCOP coding system and update. We also show a form for GEOTRACES cruises by AORI and
 163 expanded version of metadata by JMA (Appendix II).

164 Metadata may contain as shown below (A Guide to Submitting CTD/Hydrographic/Tracer Data and
 165 Associated Documentation to the CLIVAR and Carbon Hydrographic Data Office,
 166 https://cchdo.github.io/hdo-assets/documentation/policies/CCHDO_DataSubmitGuide.pdf).

167 **1. Highlights**

- 168 a. Cruise designation (cruise name) (e.g., "AIS01" for Amery Ice Shelf 1) [or, for a repeated WOCE-
 169 era section, the section designation(s), for example A11, IR04, etc. Include all sections covered on
 170 cruise].
- 171 b. EXPOCODE. Each leg has a unique EXPOCODE.
- 172 c. Chief scientist for each leg, including postal and electronic addresses.
- 173 d. Ship name.
- 174 e. Ports of call. Port(s) where cruise begins and ends plus any stops during the cruise.
- 175 f. Cruise dates (Official ship's log date of departure & return, port to port, for each leg).

176 **2. Cruise Summary Information**

- 177 a. Written description of the survey's geographic boundaries.
- 178 b. Cruise track showing each station with different symbols used to indicate station type.
- 179 b. Total number of stations occupied for each section, broken down by type of station and parameters
 180 sampled at each station.
- 181 c. Detailed list of each parameter measured on the cruise.
- 182 d. Floats and drifters deployed (type, identification number, location, and time).
- 183 e. Moorings deployed or recovered (type, identification, location, and time).

184 **3. List of Principal Investigators for All Measurements**

- 185 a. Name (please spell out).
- 186 b. Measurement responsibility.
- 187 c. Institution or affiliation (abbreviations should be defined).
- 188 d. Postal and electronic addresses.

189 **4. Scientific Program and Methods**

- 190 a. Narrative.
- 191 b. Interlaboratory comparisons made (if any) or comparisons with previous cruise data.
- 192 c. (Optional) Vertical sections along the ship's track showing the bottle depth distributions, and plots
 193 of property vs. property relationships.

194 **5. Major Problems and Goals Not Achieved**

195 **6. Other Incidents of Note**

196 **7. List of Cruise Participants**

- 197 a. Name (please spell out).
 198 b. Responsibility on cruise.
 199 c. Institution or affiliation (abbreviations should be defined).
 200 d. postal and electronic addresses.

201
 202 There are also applicable to add more information into CRS when the items added are appropriate.
 203 An example of cruise summary report is shown below and a few examples are in appendix II.

204 **Example of cruise summary report**

205 Reference No. : 20090040
 206 Ship Name : RYOFU MARU
 207 Ship Type : Research Vessel
 208 Cruise No./Name : 08-09
 209 Cruise Period : 2008/09/24 to 2008/10/24
 210 Responsible Laboratory :
 211 Global Environment and Marine Department, JMA
 212 Chief Scientist(s) : NAKANO, Toshiya (Leg 1) SAKURAI, Keizo (Leg 2)
 213 General Ocean Area(s) : North Pacific Ocean
 214 Geographic Coverage : 131
 215 Project Name : JCOMM(former IGOSS), WESTPAC, MARPOLMON
 216 Coordinating Body : IOC
 217 Principal Investigators : A;MINATO, S. :
 218 Global Environment and Marine Department JMA
 219 :B;HAYASHI, K. :
 220 Global Environment and Marine Department JMA
 221 :C;Senior Scientific Officer: Seismological and
 222 Volcanological Department JMA
 223 :D;HIRATA, K. : Seismological and Volcanological Research
 224 Department MRI

225 Objectives and Brief Narrative of Cruise:

226 A routine oceanographic observation (physical)
 227 Recovery of Ocean Bottom Seismographs(JMA, MRI)
 228 Maritime meteorological observations.

229 Moorings, Bottom Mounted Gear and Drifting Systems:

230	PI	LAT.	LON.	DATATYPE	DESCRIPTION
231	D	32-20.3	134-40.5	G90	Recovered:J07 3612m 2008/09/27

232 Summary of Measurements and Samples Taken:

233	PI	NO	UNITS	DATATYPE	DESCRIPTION
234	A	29	Stations	D71	Current Profiler
235	A	1051	NM	H71	Surface measurements underway (T)
236	B	60	Times	M06	Routine standard measurements

237

238

239 **4. Best practices of quality control procedures for sensors in the case of the MR15-05 cruise by**
 240 **JAMSTEC and the RF16-06 cruise by the JMA**

241 Best practices for the main quality control procedures used for pre- and post-cruise calibration of a
 242 CTD system and underway measurements are described herein.

243 Original cruise report of MR15-05 is available at
 244 http://www.godac.jamstec.go.jp/catalog/data/doc_catalog/media/MR15-05_leg1_all.pdf (accessed
 245 on 19 March 2020) and that of RF16-06 is available at <https://cchdo.ucsd.edu/cruise/49UP20160703>
 246 (accessed on 23 March 2020). In the following sections 4 and 5 we use many materials from the
 247 cruise reports and revised them to fit for this guideline.

248 ***4-1 Quality control and calibrations for sensors in the case of the MR15-05 cruise (JAMSTEC)***

249 Overview of the CTD equipment is described in (4-1-1), and the CTD system is summarized in (4-
 250 1-2). Pre-cruise calibration for sensors is the first step of quality control of data that can be obtained
 251 with sensors (4-1-3). Post-cruise calibration of sensors is the next step (4-1-4). Pre- and post-cruise
 252 calibration of the underway measurement system is also described in (4-1-5). Actual procedures are
 253 described in this chapter.

254 ***4-1-1. Summary of the CTD system used in this cruise***

255 The CTD system was a SBE 911plus system (Sea-Bird Electronics, Inc., Bellevue, Washington,
 256 USA). The SBE 911plus system controls a 36-position SBE 32 Carousel Water Sampler. The Carousel
 257 accepts 12-litre Niskin-X water sample bottles (General Oceanics, Inc., Miami, Florida, USA). The SBE
 258 9plus was mounted horizontally on a 36-position carousel frame. SBE's temperature (SBE 3) and
 259 conductivity (SBE 4) sensor modules were used with the SBE 911plus underwater unit. The pressure
 260 sensor was mounted in the main housing of the underwater unit and was ported to outside through an
 261 oil-filled plastic capillary tube. A modular unit of the underwater housing pump (SBE 5T) flushed water
 262 through the sensor tubing at a constant rate independent of the CTD's motion, and the pumping rate
 263 (3000 rpm) remained nearly constant over the entire input voltage range of 12–18 volts DC. Flow speed
 264 of the pumped water in the standard TC duct was about 2.4 m/s. Two sets of temperature and
 265 conductivity modules were used. An SBE dissolved oxygen sensor (SBE 43) was placed between the
 266 primary conductivity sensor and the pump module. Auxiliary sensors, a Deep Ocean Standards
 267 Thermometer (SBE 35), an altimeter (PSA-916T; Teledyne Benthos, Inc., North Falmouth,
 268 Massachusetts, USA), and an oxygen optode sensor (RINKO-III; JFE Advantech Co., Ltd, Kobe Hyogo,
 269 Japan) were also used with the SBE 9plus underwater unit. To minimize rotation of the CTD package,
 270 a heavy stainless-steel frame (total weight of the CTD package without seawater in the bottles was about
 271 1000 kg) was used with an aluminium plate (54 × 90 cm). To minimize attitude motion of the CTD
 272 package (rotation, pitching, and rolling) and twist of the armoured cable, a slip ring swivel was inserted
 273 between the armoured cable and the CTD package (Uchida et al., 2018).

274 ***4-1-2. Pre-cruise calibration of sensors***

275 *i. Pressure*

276 The Paroscientific series 4000 Digiquartz high-pressure transducer (Model 415K: Paroscientific,
 277 Inc., Redmond, Washington, USA) uses a quartz crystal resonator, whose frequency of oscillation varies
 278 with pressure-induced stress. The resolution is 0.01 parts per million of full scale over the absolute
 279 pressure range of 0 to 15,000 psia (0 to 10,332 dbar). Also, a quartz crystal temperature signal was used
 280 to compensate for a wide range of temperature changes at the time of an observation. The pressure
 281 sensor had a nominal accuracy of 0.015% FS (1.5 dbar), typical stability of 0.0015% FS/month (0.15
 282 dbar/month), and resolution of 0.001% FS (0.1 dbar). Because the pressure sensor measures absolute
 283 pressure, it inherently includes atmospheric pressure (about 14.7 psi). SEASOFT subtracts 14.7 psi from
 284 the computed pressure automatically.

285 Pre-cruise sensor calibrations for linearization were performed at SBE, Inc. The temporal drift of
 286 the pressure sensor was adjusted by periodic recertification corrections against a dead-weight piston
 287 gauge (Model 480DA, S/N 23906; Piston unit, S/N 079K; Weight set, S/N 3070; Bundenberg Gauge
 288 Co. Ltd., Irlam, Manchester, UK). The corrections were performed at JAMSTEC, Yokosuka, Kanagawa,
 289 Japan by Marine Works Japan, Ltd. (MWJ), Yokohama, Kanagawa, Japan, usually once per year to
 290 monitor sensor temporal drift and linearity.

291 S/N 0786, 13 July 2015

292 slope = 0.99980434

293 offset = -0.13013

294 *ii. Temperature (SBE 3)*

295 The temperature-sensing element was a glass-coated thermistor bead in a stainless-steel tube. This
 296 sensor provided pressure-free measurements at depths up to 10,500 (6800) m in its titanium (aluminium)
 297 housing. The SBE 3 thermometer has a nominal accuracy of 1 mK, typical stability of 0.2 mK/month,
 298 and resolution of 0.2 mK at 24 samples per second. The premium temperature sensor, SBE 3plus, is a
 299 more rigorously tested and calibrated version of the standard temperature sensor (SBE 3).

300 Pre-cruise sensor calibrations were performed at SBE, Inc.

301 S/N 03P4815, 16 April 2015

302 S/N 031525, 28 July 2015

303 Pressure sensitivities of the SBE 3s were corrected in accord with the method of Uchida et al.
 304 (2007), for the following sensor:

305 S/N 03P4815, -3.4597×10^{-7} (K/dbar)

306 *iii. Conductivity (SBE 4)*

307 The flow-through conductivity sensing element was a glass tube (cell) with three platinum electrodes
308 to provide in-situ measurements at depths up to 10,500 (6800) m in a titanium (aluminium) housing.
309 The SBE 4 has a nominal accuracy of 0.0003 S/m, typical stability of 0.0003 S/m/month, and resolution
310 of 0.00004 S/m at 24 samples per second. The conductivity cells have been replaced to newer style cells
311 for deep ocean measurements.

312 Pre-cruise sensor calibrations were performed at SBE, Inc.

313 S/N 042435, 1 May 2015

314 S/N 042854, 1 May 2014

315 The value of the conductivity at a salinity of 35, temperature of 15°C (IPTS-68), and pressure of
316 0 dbar was 4.2914 S/m.

317 *iv. Oxygen (SBE 43)*

318 The SBE 43 oxygen sensor uses a Clark polarographic element to provide in-situ measurements at
319 depths up to 7000 m. The range for dissolved oxygen is 120% of surface saturation in all natural waters;
320 nominal accuracy is 2% of saturation; and typical stability is 2% per 1000 hours.

321 Pre-cruise sensor calibration was performed at SBE, Inc.

322 S/N 430330, 10 May 2015

323 Note: Factory/manufacturer's calibrations of the conductivity and oxygen sensors will not provide
324 adequate quality data for WOCE-like work, and that application of data from analyses of water
325 samples at sea will be required as described in section 5.

326 *v. Deep-Ocean Standard Thermometer*

327 The deep-ocean standard thermometer (SBE 35) was an accurate, ocean-range temperature sensor
328 that could be standardized against the Triple Point of Water and Gallium Melt Point cells and was also
329 capable of measuring temperature in the ocean to depths of 6800 m. The SBE 35 was used to calibrate
330 the SBE 3 temperature sensors in situ (Uchida et al., 2007).

331 Pre-cruise sensor linearization was performed at SBE, Inc.

332 S/N 0022, 4 March 2009

333 The SBE 35 was then certified by measurements in thermodynamic fixed-point cells of the TPW
334 (0.01°C) and GaMP (29.7646°C). The slow time drift of the SBE 35 was adjusted by periodic
335 recertification corrections. Pre-cruise sensor calibration was performed at SBE, Inc. Since 2014, fixed-
336 point cells traceable to NIST temperature standards have been directly used in the manufacturer's
337 calibration of the SBE 35 (Uchida et al., 2015a).

338 S/N 0022, 4 February 2015 (slope and offset correction)

339 Slope = 1.000007

340 Offset = 0.000246

341 The time required per sample = $1.1 \times \text{NCYCLES} + 2.7$ seconds. The time of 1.1 seconds is the total
 342 time per acquisition cycle. NCYCLES is the number of acquisition cycles per sample and was set to 4.
 343 A time of 2.7 seconds is required for converting the measured values to temperature and storing the
 344 average in EEPROM.

345 *vi. Oxygen optode (RINKO)*

346 The RINKO® (JFE Alec Co., Ltd.) sensor, a fast-response optical oxygen sensor, takes advantage of
 347 the ability of selected substances to act as dynamic fluorescence quenchers. The RINKO model III is
 348 designed for use with a CTD system that will accept an auxiliary analog sensor and is designed to operate
 349 down to 7000 m.

350 Data from the RINKO can be corrected for time-dependent, pressure-induced effects by means of
 351 the same method as that developed for the SBE 43 (Edwards et al., 2010). The calibration coefficients,
 352 H1 (amplitude of hysteresis correction), H2 (curvature function for hysteresis), and H3 (time constant
 353 for hysteresis) were determined empirically as follows:

354 $H1 = 0.0055$ (for S/N 0024)

355 $H2 = 5000$

356 $\text{dbar } H3 = 2000$ seconds

357 The outputs from RINKO are the raw phase-shift data. The RINKO can be calibrated by the modified
 358 Stern-Volmer equation slightly modified from a method by Uchida et al. (2010):

359
$$\text{O}_2 (\mu\text{mol/l}) = [(V_0 / V)^E - 1] / K_{sv}$$

360 where V is voltage, V_0 is the voltage in the absence of oxygen, and K_{sv} is the Stern-Volmer constant.
 361 The coefficient E corrects for nonlinearity of the Stern-Volmer equation. The V_0 and the K_{sv} are assumed
 362 functions of temperature as follows:

363
$$K_{sv} = C_0 + C_1 \times T + C_2 \times T^2$$

364
$$V_0 = 1 + C_3 \times T$$

365
$$V = C_4 + C_5 \times V_b$$

366 where T is the CTD temperature ($^{\circ}\text{C}$) and V_b is the raw output (volts). V_0 and V are normalized by the
 367 output in the absence of oxygen at 0°C .

368 The oxygen concentration is calculated using accurate temperature data from the CTD temperature
 369 sensor instead of temperature data from the RINKO. The pressure-compensated oxygen concentration
 370 O_{2c} can be calculated as follows.

$$371 \quad O_{2c} = O_2 (1 + C_p p / 1000)$$

372 where p is the CTD pressure (dbar) and C_p is the compensation coefficient. Because the sensing foil of
 373 the optode is permeable to only gas and not to water, the optode oxygen must be corrected for salinity.
 374 The salinity-compensated oxygen can be calculated by multiplying O_{2c} by a factor to correct for the
 375 effect of salt on the oxygen solubility (Garcia and Gordon, 1992).

376 Pre-cruise sensor calibrations were performed at RCGC/JAMSTEC.

377 S/N 0024, 10 May 2015

378 *4-1-3. Post-cruise calibration of CTD sensors*

379 *i. Pressure*

380 The CTD pressure sensor offset during the cruise was estimated from the pressure readings on the
 381 ship deck. For best results, the Paroscientific sensor was powered on for at least 20 minutes before the
 382 operation. In order to get the calibration data for the pre- and post-cast pressure sensor drift, the CTD
 383 deck pressure was averaged over the first and last minute, respectively. Then the atmospheric pressure
 384 deviation from standard atmospheric pressure (14.7 psi) was subtracted from the CTD deck pressure to
 385 check for temporal drift of the pressure sensor. Atmospheric pressure was measured at the captain deck
 386 (20 m above the baseline) and at one-minute intervals.

387 The pre- and post-cast deck pressure data revealed a temperature dependence of the pressure sensor
 388 (Figure 4.1.1). To correct for the temperature dependence, the manufacturer's calibration coefficients
 389 were modified slightly on board as follows:

$$390 \quad T1 = 29.88499$$

$$391 \quad T2 = -2.565740 \times 10^{-4}$$

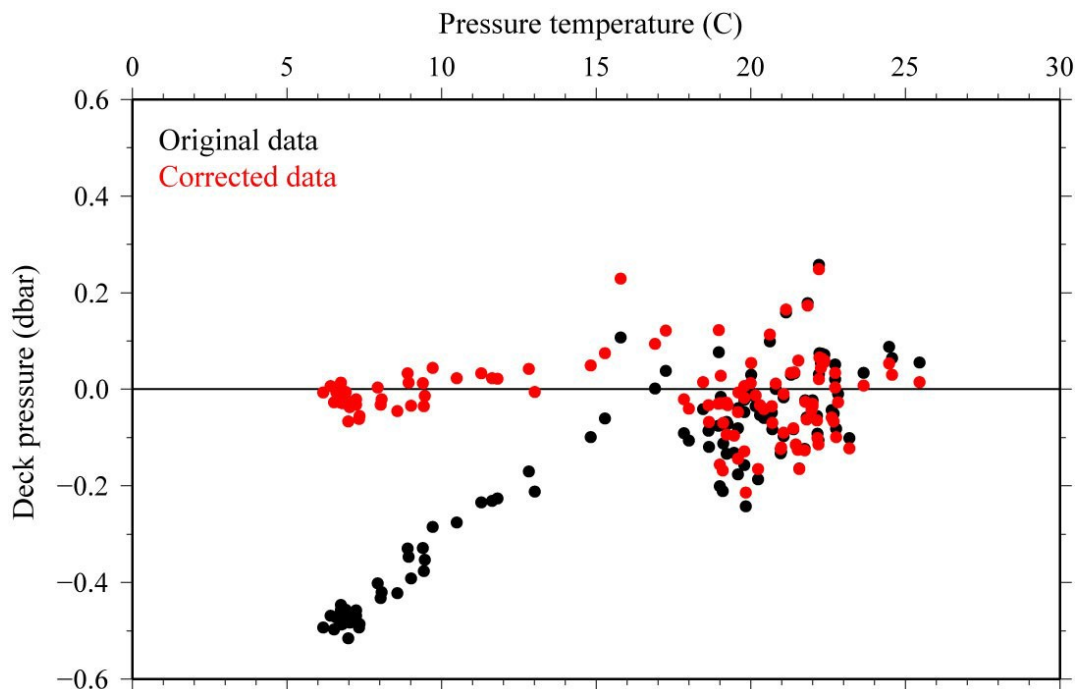
$$392 \quad T3 = 4.799030 \times 10^{-6}$$

$$393 \quad \text{Offset} = 0.0$$

394 Figure 4.1.2 shows a time series of the CTD deck pressure. The CTD pressure sensor offset was
 395 estimated from the deck pressure. The mean of the pre- and the post-cast data over the whole period
 396 provided an estimation of the pressure sensor offset (-0.01 dbar) from the pre-cruise calibration. A post-
 397 cruise correction of the pressure data was not deemed necessary for the pressure sensor.

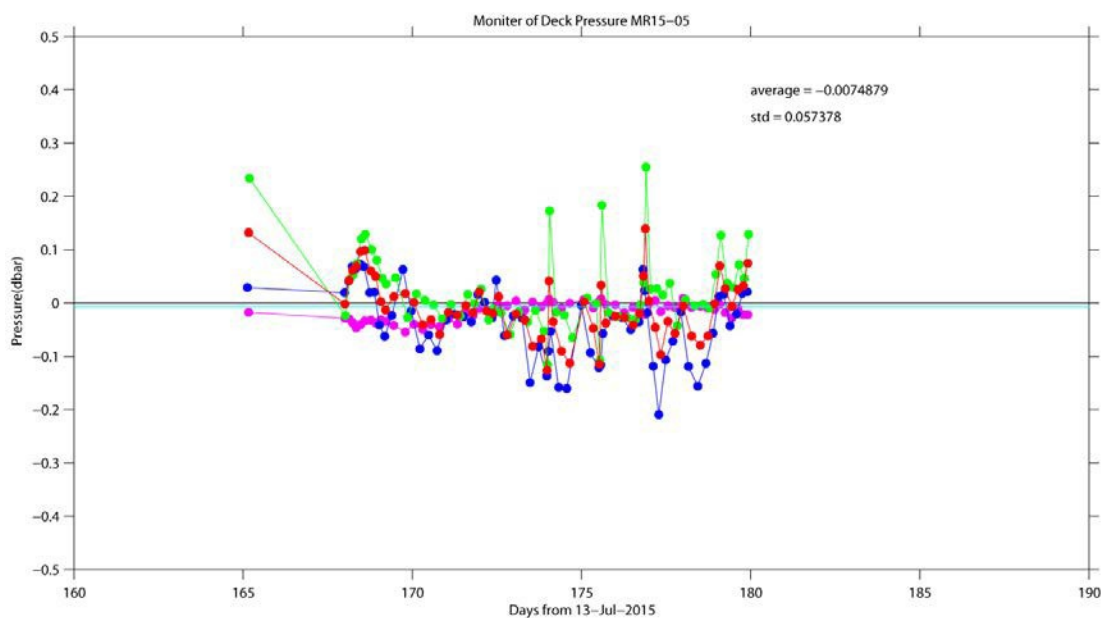
398

399



400
401
402
403
404
405

Figure 4.1.1 Pre- and post-cast CTD deck pressure. Atmospheric pressure deviation from a standard atmospheric pressure was subtracted from the CTD deck pressure. Black dots show the original data, and red dots show the data corrected for the temperature dependence of the sensor.



406
407
408
409
410

Figure 4.1.2 Time series of the CTD deck pressure. Atmospheric pressure deviation (magenta dots) from a standard atmospheric pressure was subtracted from the CTD deck pressure. Blue and green dots indicate pre- and post-cast deck pressures, respectively. Red dots indicate averages of the pre- and the post-cast deck pressures.

411 *ii. Temperature*

412 The CTD temperature sensors (SBE 3) were calibrated with the SBE 35 in accord with the method
 413 of Uchida et al. (2007) on the assumption that discrepancies between SBE 3 and SBE 35 data were due
 414 to pressure sensitivity, the viscous heating effect, and temporal drift of the SBE 3.

415 Post-cruise sensor calibration of the SBE 35 was performed in 2016 at SBE, Inc.

416

417 The CTD temperature data were preliminarily calibrated as follows:

418
$$\text{Calibrated temperature} = T - (c_0 \times P + c_1 \times t + c_2)$$

419 where T is the CTD temperature in °C, P is pressure in dbar, t is time in days from the pre-cruise
 420 calibration date of the CTD temperature, and c₀, c₁, and c₂ are calibration coefficients. The coefficients
 421 were determined using the data for depths corresponding to pressures greater than 1950 dbar. The
 422 coefficient c₁ was set to zero for this cruise.

423

424 The primary temperature data were used for the post-cruise calibration. The secondary temperature
 425 sensor was also calibrated and used instead of the primary temperature data when the quality of the
 426 primary temperature data was bad. The calibration coefficients are listed in Table 4.1.1. The results of
 427 the post-cruise calibration for the CTD temperature are summarized in Table 4.1.2 and are shown in
 428 Figure 4.1.3.

429

Table 4.1.1 Calibration coefficients for the CTD temperature sensors.

430

Serial number	c ₀ (°C/dbar)	c ₁ (°C/day)	c ₂ (°C)
3P4815	-4.79962×10^{-8}	0.0	-0.0007

434

435

436 Table 4.1.2 Difference between the CTD temperature and the SBE 35 temperature after the post-cruise
 437 calibration. Mean and standard deviation (Sdev) were calculated for data collected at pressures below
 438 and above 1950 dbar. Number is the number of data used in the calculations.

Serial number	Pressure \geq 1950 dbar			Pressure < 1950 dbar		
	Number	Mean (mK)	Sdev (mK)	Number	Mean (mK)	Sdev (mK)
3P4815	467	0.0	0.2	854	-0.0	6.8

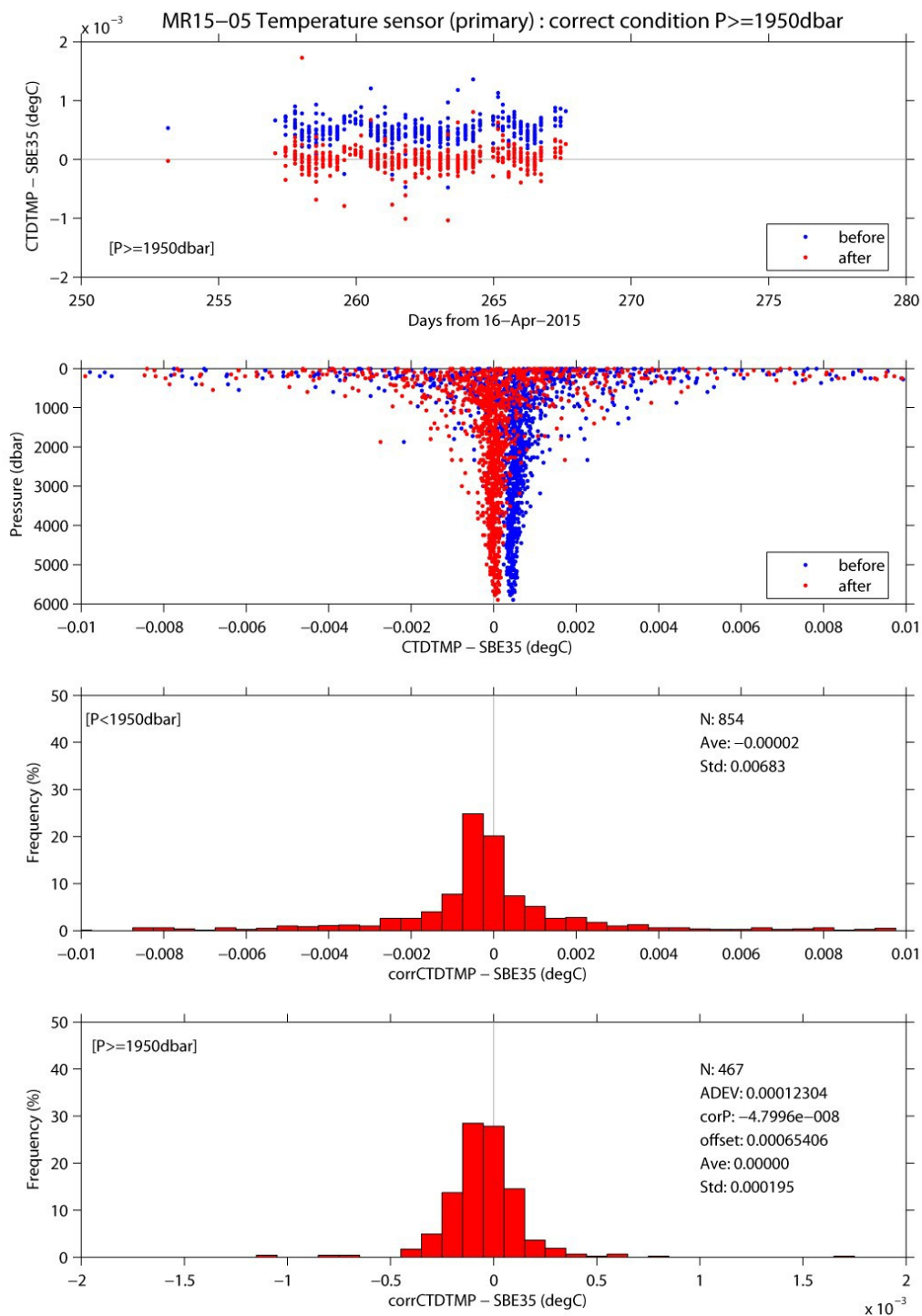


Figure 4.1.3 Difference between the CTD temperature (primary) and the SBE 35 temperature. Blue and red dots indicate before and after the post-cruise calibration using the SBE 35 data, respectively. Lower two panels show histograms of the differences after the calibration.

iii. Salinity

The discrepancy between the CTD conductivity and the conductivity calculated from the bottle salinity data with the CTD temperature and pressure data was considered to be a function of conductivity, pressure, and time. The CTD conductivity was calibrated as follows:

$$\text{Calibrated conductivity} = c_0 \times C + c_1 \times P + c_2 \times C \times P + c_3 \times C^2 + c_4 \times t + c_5$$

where C is CTD conductivity in S/m, P is pressure in dbar, t is time in days, and c0, c1, c2, c3, c4, and c5 are calibration coefficients. The best fit sets of coefficients were determined by a least squares technique to minimize the deviations from the conductivities calculated from the bottle salinity data. The coefficient c4 was set to zero for this cruise.

The primary conductivity data created by the software module ROSSUM were used after the post-cruise calibration for the temperature data. Table 4.1.3 lists the calibration coefficients. The results of the post-cruise calibration for the CTD salinity are summarized in Table 4.1.4 and shown in Figure 4.1.4.

Table 4.1.3 Calibration coefficients for the CTD conductivity sensors.

Serial number	c0	c1 S/(m dbar)	c2 1/dbar	c3 1/(S/m)	c4 S/m
042435	-1.51687×10^{-4}	1.09232×10^{-7}	-3.67361×10^{-8}	4.72348×10^{-12}	5.09192×10^{-4}

Table 4.1.4 Difference between the CTD salinity and the bottle salinity after the post-cruise calibration. Mean and standard deviation (Sdev) (in 10^{-3}) are calculated for the data collected from pressures below and above 1950 dbar. Number is the number of data used.

Serial number	Pressure \geq 1950 dbar			Pressure $<$ 1950 dbar		
	Number	Mean	Sdev	Number	Mean	Sdev
042435	493	-0.0	0.4	861	0.2	4.5

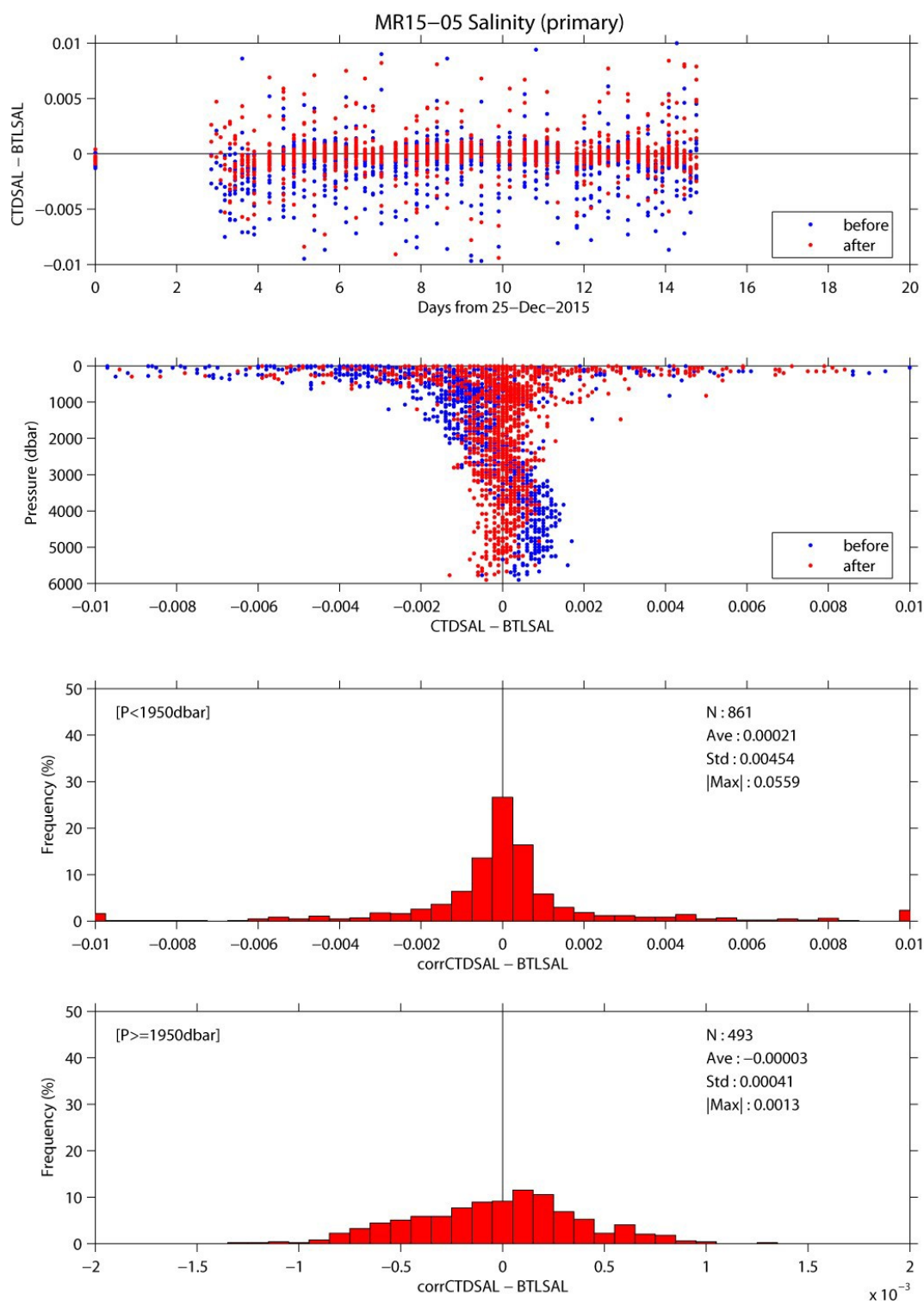


Figure 4.1.4 Difference between the CTD salinity (primary) and the bottle salinity. Blue and red dots indicate before and after the post-cruise calibration, respectively. Lower two panels show histograms of the differences after the calibration.

iv. Oxygen

The RINKO oxygen optode (S/N 0024) was calibrated and used instead of the CTD oxygen data, because the RINKO has a fast response time. The pressure-hysteresis corrected RINKO data were calibrated by the modified Stern-Volmer equation, basically in accord with Uchida et al. (2010) with slight modification:

$$[\text{O}_2] (\mu\text{mol/l}) = [(V_0 / V)^{1.5} - 1] / K_{\text{sv}}$$

and

$$K_{\text{sv}} = C_0 + C_1 \times T + C_2 \times T^2$$

$$V_0 = 1 + C_3 \times T$$

$$V = C_4 + C_5 \times V_b + C_6 \times t + C_7 \times t \times V_b$$

where V_b is the RINKO output (voltage), V_0 is the voltage in the absence of oxygen, T is temperature in °C, and t is the exciting time (days) integrated from the first CTD cast. Temporal drift of the RINKO output was corrected. The calibration coefficients were determined by minimizing the sum of the absolute deviations and also include weight from the bottle oxygen data. The revised quasi-Newton method (DMINF1) was used to determine the sets of coefficients.

The post-cruise calibrated temperature and salinity data were used for the calibration. Table 4.1.5 lists the calibration coefficients. The results of the post-cruise calibration for the RINKO oxygen are summarized in Table 4.1.6 and are shown in Figure 4.1.5.

Table 4.1.5 Calibration coefficients for the RINKO oxygen sensors.

Coefficient	S/N 0024
c0	5.56160×10^{-3}
c1	2.16834×10^{-4}
c2	2.72251×10^{-6}
c3	-1.03972×10^{-3}
c4	-2.07308×10^{-2}
c5	0.326691
c6	1.52604×10^{-4}
c7	1.29920×10^{-5}
Cp	0.015

Table 4.1.6 Difference between the RINKO oxygen and the bottle oxygen after the post-cruise calibration. Mean and standard deviation (Sdev) are calculated for the data collected from below and above a pressure of 1950 dbar. Number is the number of data used.

Serial number	Pressure \geq 1950 dbar			Pressure < 1950 dbar		
	Number	Mean ($\mu\text{mol/kg}$)	Sdev	Number	Mean ($\mu\text{mol/kg}$)	Sdev
0024	502	0.11	0.39	859	0.02	0.57

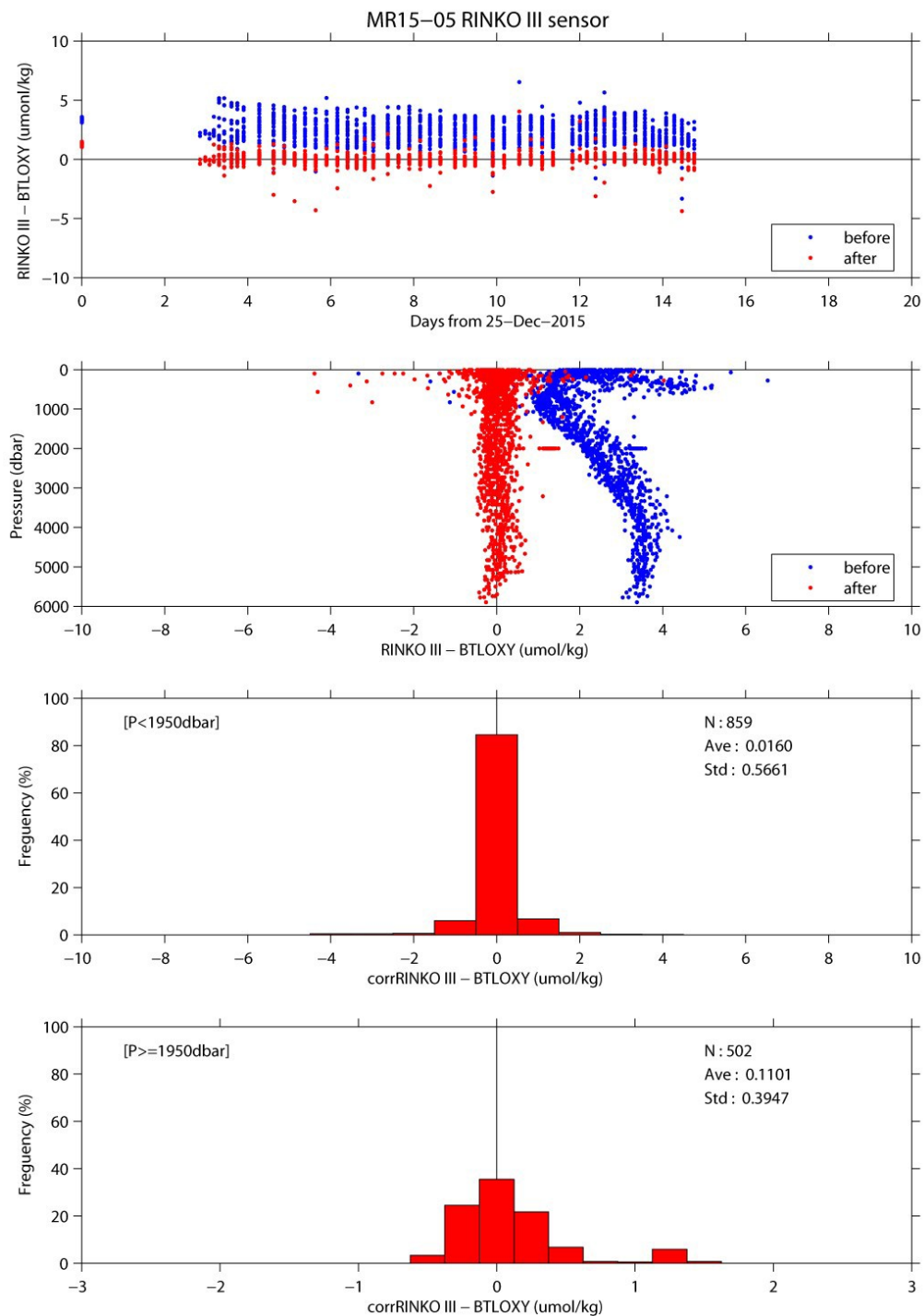


Figure 4.1.5 Difference between the CTD oxygen and the bottle oxygen. Blue and red dots indicate before and after the post-cruise calibration, respectively. Lower two panels show histograms of the differences after the calibration.

4-1-5. Underway measurements with sensors

(1) Materials and methods

The Continuous Sea Surface Water Monitoring System (Marine Works Japan Co, Ltd.) has seven sensors and automatically measures salinity, temperature, dissolved oxygen, fluorescence, and turbidity in sea surface water every minute. The system was in the sea-surface-monitoring laboratory with an intake on the bottom of the ship and was connected to a shipboard LAN system. Measured data along with time and location of the ship are displayed on a monitor and stored in a desktop computer. Sea surface water was continuously pumped up to the laboratory from a depth of about 5 m and routed to the system through a vinyl-chloride pipe. One thermometer was located just before the sea water pump in the bottom of the ship. The flow rate of the surface seawater was maintained at about 1.2 L/min. Periods of measurement, maintenance, and problems are listed in Table 4.1.7.

Software and sensors used in this system are listed below.

i. Software

Seamoni-kun Ver.1.50

ii. Sensors

Temperature and conductivity sensor

Model: SBE 45, Sea-Bird Electronics, Inc.

Serial number: 4552788-0264

Pre-cruise calibration: 30 August 2014, Sea-Bird Electronics, Inc.

Bottom of ship thermometer

Model: SBE 38, Sea-Bird Electronics, Inc.

Serial number: 3852788-0457

Pre-cruise calibration: 31 October 2014, Sea-Bird Electronics, Inc.

Dissolved oxygen sensor

Model: RINKO-II, JFE Adantech Co. Ltd.

Serial number: 0013

Pre-cruise calibration: 10 May 2015, JAMSTEC

Table 4.1.7. Log of events of the Continuous Sea-Surface-Water-Monitoring System operation.

System date	System time	Event
[UTC]	[UTC]	
2015/12/23	19:00	Logging for leg 1 start
2015/12/24	05:23–06:07	Flow rate for RINKO and optode small, though both data seem to be normal.
2015/12/29	10:11	Logging stop for C3/filter cleaning
2015/12/29	11:23	Logging restart
2016/1/5	11:27	Logging stop for C3/filter cleaning
2016/1/5	13:05	Logging restart
2016/1/5	13:05–13:25	Optode unstable.
2016/1/11	22:00	Logging for leg 1 end
2016/1/17	13:35	Logging for leg 2 start
2016/1/23	6:23	Logging for leg 2 end

(2) Pre-cruise calibration

Pre-cruise sensor calibrations for the SBE 45 and SBE 38 were performed at Sea-Bird Electronics, Inc.

Pre-cruise sensor calibrations for the oxygen sensors were performed at JAMSTEC. The oxygen sensors were immersed in freshwater in a 1-L semi-closed glass vessel, which was immersed in a temperature-controlled water bath. Temperature of the water bath was set to 1, 10, 20, or 29°C. Temperature of the freshwater in the vessel was measured by a thermistor thermometer (expanded uncertainty less than 0.01°C, ARO-PR, JFE Advantech, Co., Ltd.). At each temperature, the freshwater in the vessel was bubbled with standard gases (4, 10, 17, or 25% oxygen in an oxygen-nitrogen mixture, whose relative expanded uncertainty was 0.5%) for more than 30 minutes to ensure saturation. Absolute pressure of the vessel headspace was measured by a reference quartz crystal barometer (expanded uncertainty 0.01% of reading) and ranged from about 1040 to 1070 hPa. The data were averaged over three minutes at each calibration point (a matrix of 24 points). As a reference, the oxygen concentration of the freshwater in the calibration vessel was calculated from the oxygen concentration of the gases, temperature, and absolute pressure at the water depth (about 8 cm) of the sensor's sensing foil as follows:

$$O_2 (\mu\text{mol/L}) = \{1000 \times c(T) \times (A_p - p_{H_2O})\} / \{C \times 22.3916 \times (1013.25 - p_{H_2O})\}$$

where $c(T)$ is the oxygen solubility, A_p is absolute pressure (hPa), p_{H_2O} is the water vapour pressure (hPa), and C is the mole fraction of oxygen in the gas ($C = 0.20946$ for air).

The RINKO was calibrated by the modified Stern-Volmer equation with slight modification from the method of Uchida et al. (2010):

$$O_2 (\mu\text{mol/L}) = [(V_0 / V)^E - 1] / K_{sv}$$

where V is the raw phase difference, V_0 is the raw phase difference in the absence of oxygen, and K_{sv} is the Stern-Volmer constant. The coefficient E corrects for nonlinearity of the Stern-Volmer equation. The coefficients V_0 and the K_{sv} are assumed to be functions of temperature as follows.

$$K_{sv} = C_0 + C_1 \times T + C_2 \times T^2$$

$$V_0 = 1 + C_3 \times T$$

$$V = C_4 + C_5 \times V_b$$

where T is the CTD temperature ($^{\circ}\text{C}$), and V_b is raw output of the sensor. The oxygen concentration was calculated using accurate temperature data from the SBE 45 instead of temperature data from the RINKO. The calibration coefficients were as follows:

$$C_0 = 5.048509438066593 \times 10^{-3}$$

$$C_1 = 2.212851808960770 \times 10^{-4}$$

$$C_2 = 3.735982971782336 \times 10^{-6}$$

$$C_3 = -7.847113805097885 \times 10^{-4}$$

$$C_4 = 3.011495646664952 \times 10^{-2}$$

$$C_5 = 0.1926948014214438$$

$$E = 1.5$$

(3) Data processing and post-cruise calibration

Data from the Continuous Sea Surface Water Monitoring System were obtained at 1-minute intervals. Data from the nitrate sensor were obtained at 2-minute intervals and linearly interpolated at 1-minute intervals.

These data were processed as follows. Spikes in the temperature and salinity data were removed using a median filter with a window of 3 scans (3 minutes) when the difference between the original data and the median filtered data exceeded 0.1°C for temperature and 0.5 for salinity. Data gaps were linearly interpolated when the gap was ≤ 13 minutes. Raw data from the RINKO oxygen sensor were low-pass filtered using a Hamming filter with a window of 15 scans (15 minutes).

Salinity (g/kg) and dissolved oxygen (O_2 [$\mu\text{mol/kg}$]) data were corrected using the data from the water samples. Corrected salinity (S_{cor}) and dissolved oxygen (O_{cor}) were calculated from the following equations

$$S_{\text{cor}} = c_0 + c_1 S + c_2 t$$

$$\text{O}_{\text{cor}} [\mu \text{ mol/kg}] = c_0 + c_1 O + c_2 T + c_3 t$$

where S is salinity, t is days from a reference time (2015/12/23 19:00 [UTC]), and T is temperature in $^{\circ}\text{C}$. The best fit sets of calibration coefficients (c_0 – c_3) were determined by a least squares technique to minimize the deviations from the water-sample data. Table 4.1.8 lists the calibration coefficients.

Comparisons between the Continuous Sea Surface Water Monitoring System data and sampled water data are shown in Figures 4.1.6 and 4.1.7.

Table 4.1.8. Calibration coefficients for salinity and dissolved oxygen.

Parameter	c_0	c_1	c_2	c_3
Salinity	9.031385×10^{-2}	0.9976929	1.379279×10^{-4}	
Dissolved oxygen	9.359068	0.9362957	0.0	-8.934918×10^{-3}

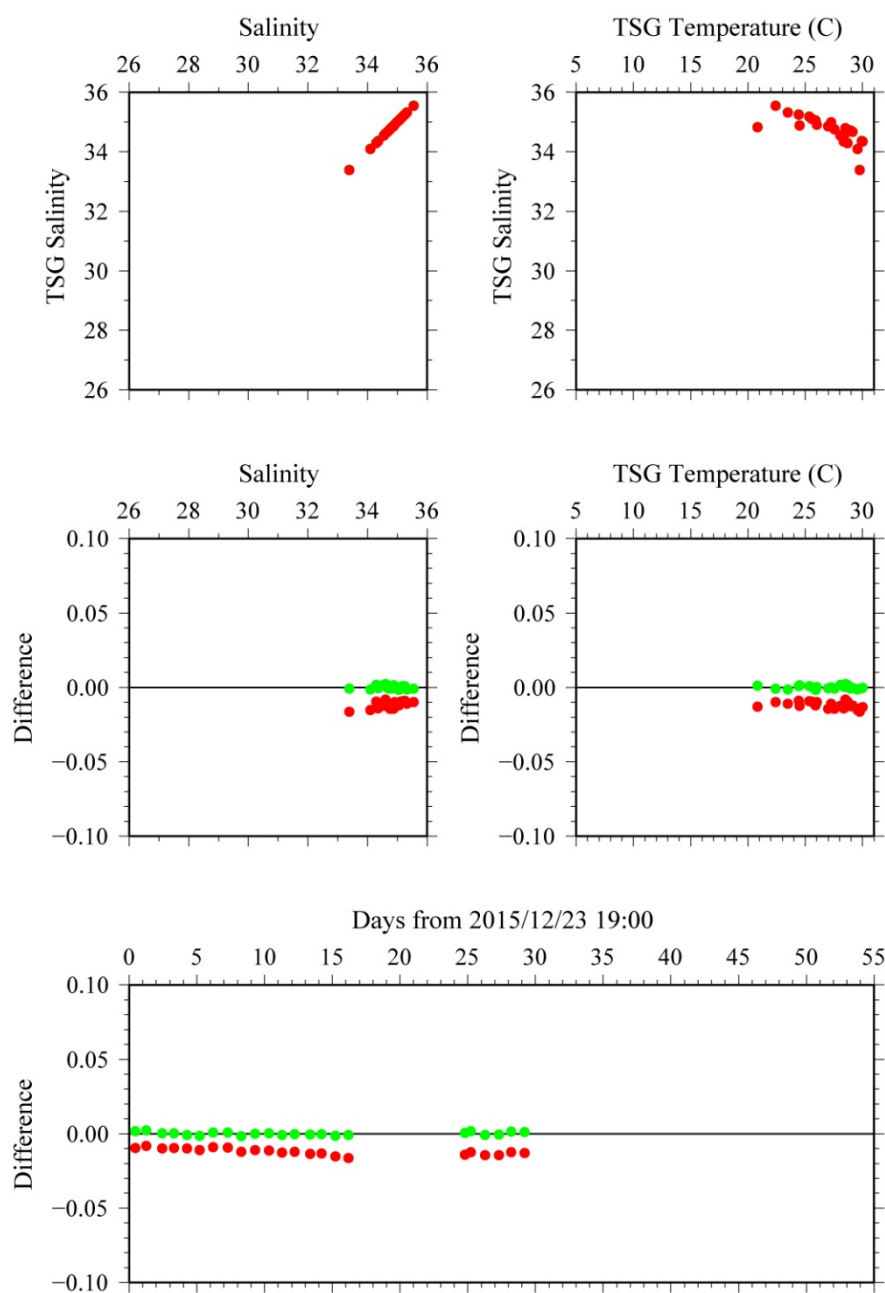


Figure 4.1.6. Comparison between TSG salinity (red: before correction, green: after correction) and sampled salinity.

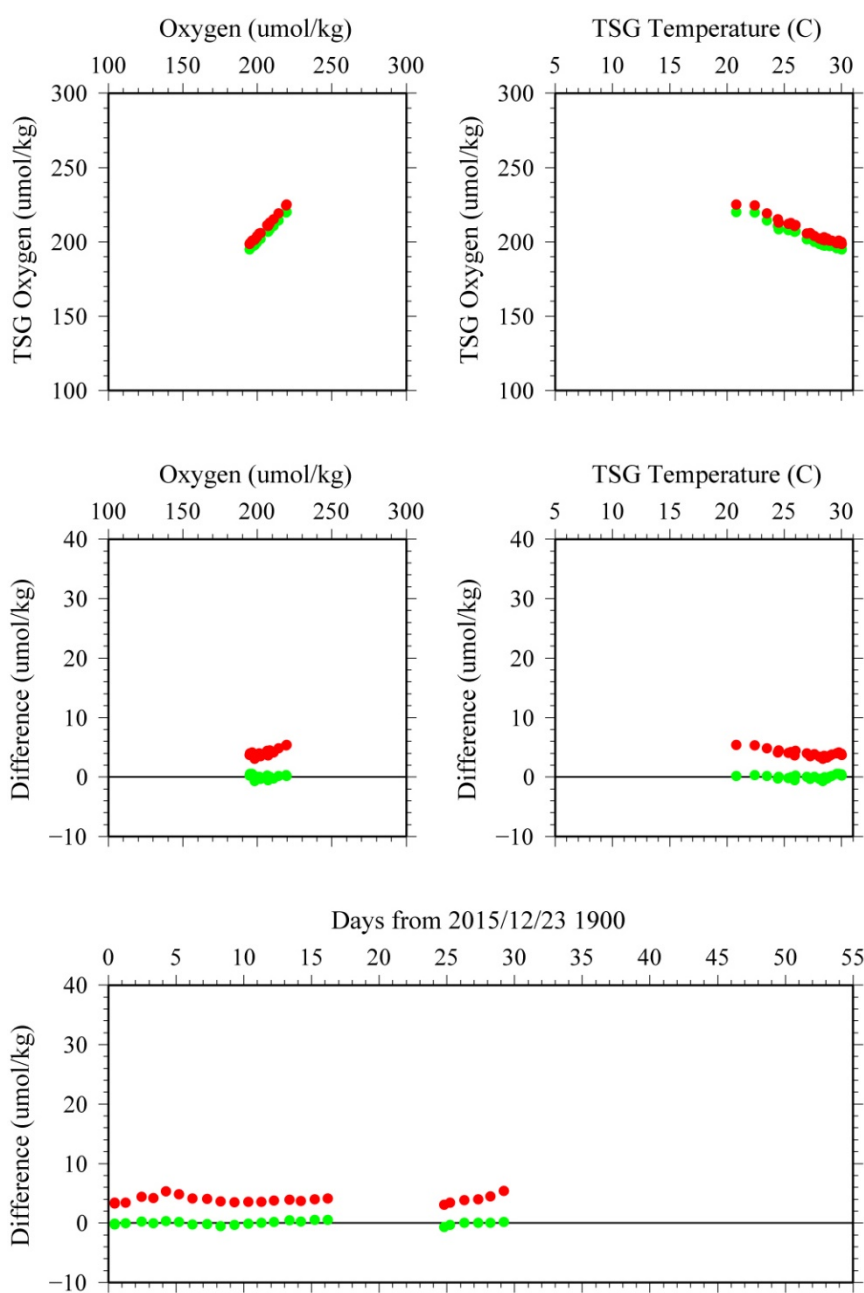


Figure 4.1.7. Comparison between TSG oxygen (red: before correction, green: after correction) and sampled oxygen.

4-2. Quality control and calibrations of sensors in the case of the RF16-06 cruise (JMA)

4-2-1. CTD O₂ measurement system

<i>Deck unit</i>	<i>Serial number</i>	<i>Station</i>
SBE 11plus (SBE)	0683	RF5802 – 5893
<i>Underwater unit</i>	<i>Serial number</i>	<i>Station</i>
SBE 9plus (SBE)	35560 (Pressure: 0764)	RF5802 – 5893
<i>Temperature</i>	<i>Serial number</i>	<i>Station</i>
SBE 3plus (SBE)	4321 (primary)	RF5802 – 5893
	4437 (secondary)	RF5802 – 5893
SBE 35 (SBE)	0062	RF5802 – 5893
<i>Conductivity</i>	<i>Serial number</i>	<i>Station</i>
SBE 4C (SBE)	2842 (primary)	RF5802 – 5893
	4316 (secondary)	RF5802 – 5893
<i>Pump</i>	<i>Serial number</i>	<i>Station</i>
SBE 5T (SBE)	7752 (primary)	RF5802 – 5893
	5501 (secondary)	RF5802 – 5893
<i>Oxygen</i>	<i>Serial number</i>	<i>Station</i>
RINKO III (JFE)	026 (foil number:144601B)	RF5802 – 5893
	008 (foil number:141304B)	RF5802 – 5893
<i>Water sampler (36 position)</i>	<i>Serial number</i>	<i>Station</i>
SBE 32 (SBE)	0734	RF5802 – 5893
<i>Altimeter</i>	<i>Serial number</i>	<i>Station</i>
PSA-916D (TB)	68640	RF5802 – 5893
<i>Water sampling bottle</i>	<i>Station</i>	
Niskin Bottle (GO)	RF5802 – 5893	

4-2-2. Pre-cruise calibration

a. Pressure

S/N 0764, 29 Sep. 2015

$$\begin{array}{llll}
 c_1 & = & -4.318853 \times 10^4 & t_1 & = & 3.005385 \times 10^1 \\
 c_2 & = & -4.853949 \times 10^{-1} & t_2 & = & -4.407111 \times 10^{-4} \\
 c_3 & = & 1.294200 \times 10^{-2} & t_3 & = & 4.098190 \times 10^{-6} \\
 d_1 & = & 3.706500 \times 10^{-2} & t_4 & = & 1.662250 \times 10^{-9} \\
 d_2 & = & 0.000000 & t_5 & = & 0.000000
 \end{array}$$

Formulae:

$$c = c_1 + c_2 \times U + c_3 \times U^2$$

$$d = d_1 + d_2 \times U$$

$$t_0 = t_1 + t_2 \times U + t_3 \times U^2 + t_4 \times U^3 + t_5 \times U^4$$

$$U \text{ (degrees Celsius)} = M \times (12\text{-bit pressure temperature compensation word}) + B$$

U: temperature in degrees Celsius

S/N 0764 coefficients in SEASOFT (configuration sheet dated on 29 Sep. 2015)

$$M = 1.289080 \times 10^{-2}, B = -8.282450$$

Finally, pressure is computed as

$$P(\text{psi}) = c \times (1 - t_0^2/t^2) \times \{1 - d \times (1 - t_0^2/t^2)\}$$

t: pressure period (μsec)

The drift-corrected pressure is computed as

$$\text{Drift corrected pressure (dbar)} = \text{slope} \times (\text{computed pressure in dbar}) + \text{offset}$$

$$\text{Slope} = 0.999960, \text{Offset} = 6.40070$$

b. Temperature (ITS-90): SBE 3plus*S/N 4321(primary), 06 May 2016*

$$\begin{aligned}
 g &= 4.39129096 \times 10^{-3} & j &= 1.99204111 \times 10^{-6} \\
 h &= 6.47616701 \times 10^{-4} & f_0 &= 1000.000 \\
 i &= 2.32416022 \times 10^{-5}
 \end{aligned}$$

S/N 4437(secondary), 06 May 2016

$$\begin{aligned}
 g &= 4.33413999 \times 10^{-3} & j &= 1.83139021 \times 10^{-6} \\
 h &= 6.37288356 \times 10^{-4} & f_0 &= 1000.000 \\
 i &= 2.11324800 \times 10^{-5}
 \end{aligned}$$

Formula:

$$\text{Temperature(ITS-90)} = \frac{1}{g + h \times \ln(f_0/f) + i \times \ln^2(f_0/f) + j \times \ln^3(f_0/f)} - 273.15$$

f: Instrument freq.[Hz]**c. Deep Ocean Standards Thermometer Temperature (ITS-90): SBE 35***S/N 0062, 25 Mar. 2006*

$$\begin{aligned}
 a_0 &= 4.41977256 \times 10^{-3} & a_3 &= -1.01508095 \times 10^{-5} \\
 a_1 &= -1.19652517 \times 10^{-3} & a_4 &= 2.17345047 \times 10^{-7} \\
 a_2 &= 1.82077469 \times 10^{-4}
 \end{aligned}$$

Formula:

$$\text{Linearized temperature(ITS-90)} = 1/\{a_0 + a_1 \times \ln^2(n) + a_3 \times \ln^3(n) + a_4 \times \ln^4(n)\} - 273.15$$

n: instrument output

The slow time drift of the SBE 35

S/N 0062, 11 Apr. 2016 (2nd step: fixed point calibration)

$$\text{Slope} = 1.000010, \text{Offset} = -0.001106$$

Formula:

$$\text{Temperature(ITS-90)} = \text{slope} \times (\text{Linearized temperature}) + \text{offset}$$

d. Conductivity: SBE 4C*S/N 2842(primary), 10 May 2016**(new cell preventing a stress concentration)*

$$\begin{array}{ll}
 g & = -1.01280649 \times 10^1 & j & = 2.70164000 \times 10^{-5} \\
 h & = 1.38834906 & CP_{cor} & = -9.57 \times 10^{-8} \\
 i & = 5.51057500 \times 10^{-4} & CT_{cor} & = 3.25 \times 10^{-6}
 \end{array}$$

S/N 4316(secondary), 16 Oct. 2015

$$\begin{array}{ll}
 g & = -9.87076057 & j & = 2.45401575 \times 10^{-4} \\
 h & = 1.29126815 & CP_{cor} & = -9.57 \times 10^{-8} \\
 i & = -2.63568263 \times 10^{-3} & CT_{cor} & = 3.25 \times 10^{-6}
 \end{array}$$

Conductivity of a fluid in the cell is expressed as:

$$C(S/m) = (g + h \times f^2 + i \times f^3 + j \times f^4) / \{10 \times (1 + CT_{cor} \times t + CP_{cor} \times p)\}$$

f: instrument frequency (kHz)

t: water temperature (degrees Celsius)

p: water pressure (dbar).

e. Oxygen (RINKO III)

The RINKO III (JFE Advantech Co., Ltd., Japan) sensor is based on the ability of a selected substance to act as a dynamic fluorescence quencher. The RINKO III model is designed to be used with a CTD system that accepts an auxiliary analog sensor, and it is designed to operate down to 7000 m. The RINKO III output is expressed in voltage from 0 to 5 V.

4-2-3. Quality control and data correction during the cruise**a. Temporal change of deck pressure**

The post-cruise drift-corrected pressure was computed as follows:

$$\text{Drift corrected pressure(dbar)} = \text{slope} \times (\text{computed pressure in dbar}) + \text{offset}$$

S/N 0764, 08 Nov. 2016

$$\text{Slope} = 0.999960, \quad \text{Offset} = 8.19890$$

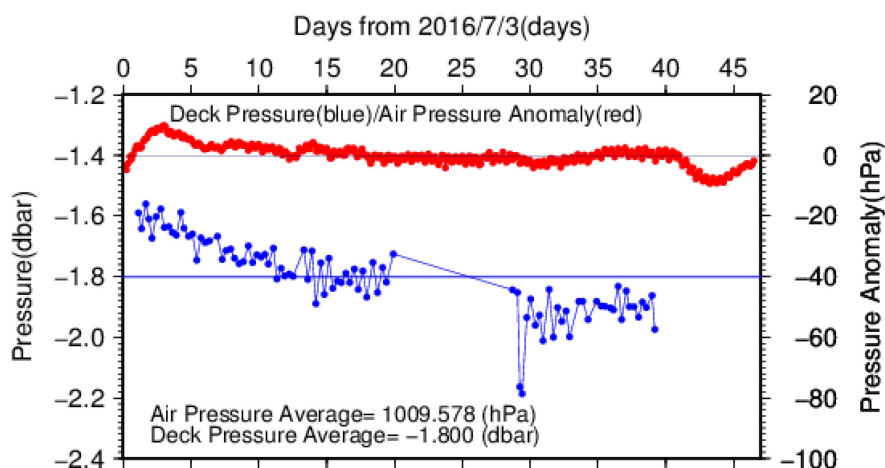


Figure 4.2.1 Time series of the CTD deck pressure. Red line indicates atmospheric pressure anomaly. Blue line and dots indicate pre-cast deck pressure and average.

b. Temperature sensor (SBE 3plus)

The practical corrections for the CTD temperature data can be made by using a SBE 35 and correcting the SBE 3plus so that it agrees with the SBE 35 (McTaggart et al., 2010; Uchida et al., 2007).

CTD temperature is corrected as follows:

$$\text{Corrected temperature} = T - (c_0 + c_1 \times P + c_2 \times P^2)$$

T : CTD temperature (degrees Celsius), P : pressure (dbar), and c_0, c_1, c_2 : coefficients

Table 4.2.1. Temperature correction summary (pressure ≥ 2000 dbar). (Bold: accepted sensor)

<i>S/N</i>	<i>Num</i>	c_0 (K)	c_1 (K/dbar)	c_2 (K/dbar ²)	<i>Stations</i>
4321	707	2.3323330×10^{-4}	1.1254432×10^{-7}	0.0000000	RF5802 – 5860
4321	327	3.6978161×10^{-4}	$-6.5882684 \times 10^{-8}$	3.1757133×10^{-7}	RF5861 – 5892
4437	707	7.8778043×10^{-4}	2.0218373×10^{-7}	0.0000000	RF5802 – 5860
4437	327	6.9565103×10^{-4}	1.9079349×10^{-7}	0.0000000	RF5861 – 5892

Table 4.2.2. Temperature correction summary for S/N 4321.

Stations	Pressure < 2000 dbar			Pressure ≥ 2000 dbar		
	Num	Average	Std	Num	Average	Std
		(K)	(K)		(K)	(K)
RF5802 – 5860	1326	-0.0004	0.0116	707	0	0.0003
RF5861 – 5892	793	-0.0004	0.0112	327	0	0.0002

Table 4.2.3. Temperature correction summary for S/N 4437.

Stations	Pressure < 2000 dbar			Pressure \geq 2000 dbar		
	Num	Average	Std	Num	Average	Std
		(K)	(K)		(K)	(K)
RF5802 – 5860	1326	-0.0002	0.0138	707	0	0.0002
RF5861 – 5892	793	-0.0036	0.0226	327	0	0.0002

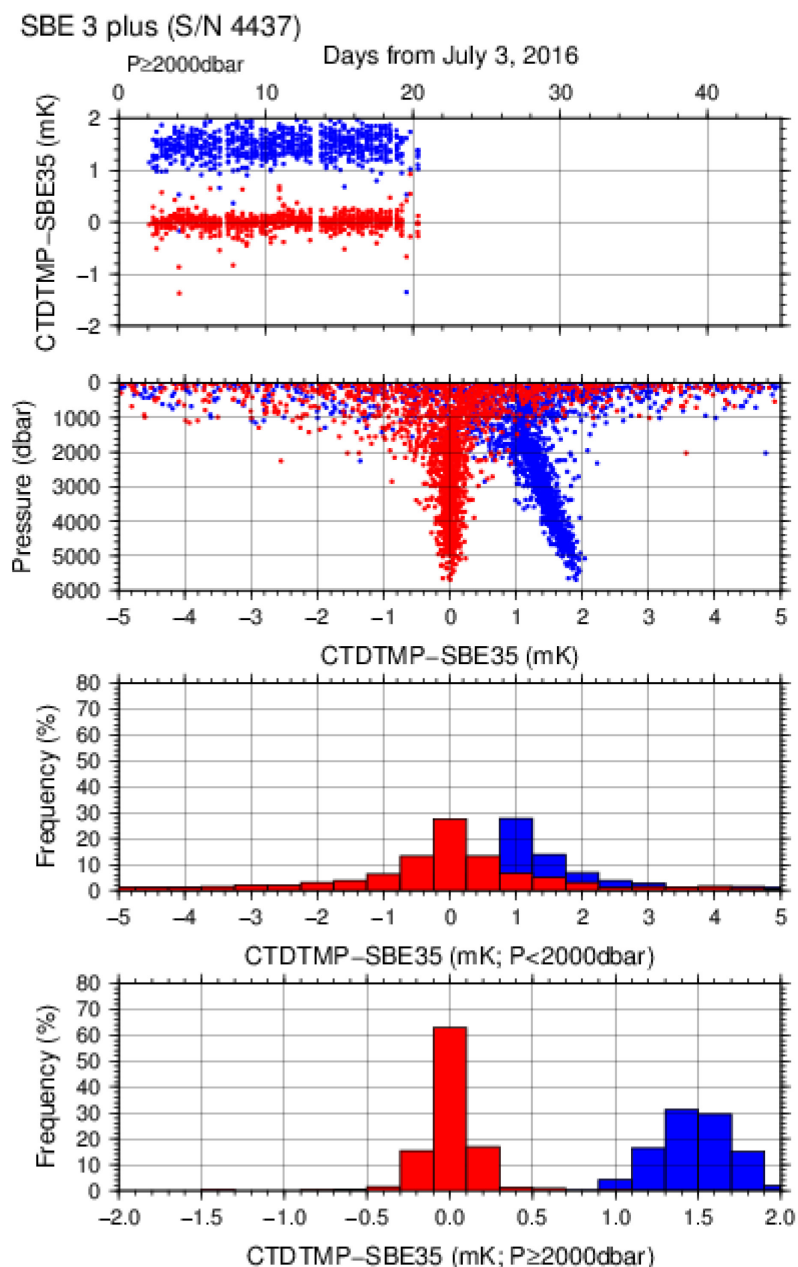


Figure 4.2.2. Difference between the CTD temperature (S/N 4437) and the Deep Ocean Standards thermometer (SBE 35) on Leg 1. Blue and red dots indicate before and after the correction using SBE 35 data, respectively. Lower two panels show histograms of the differences after correction.

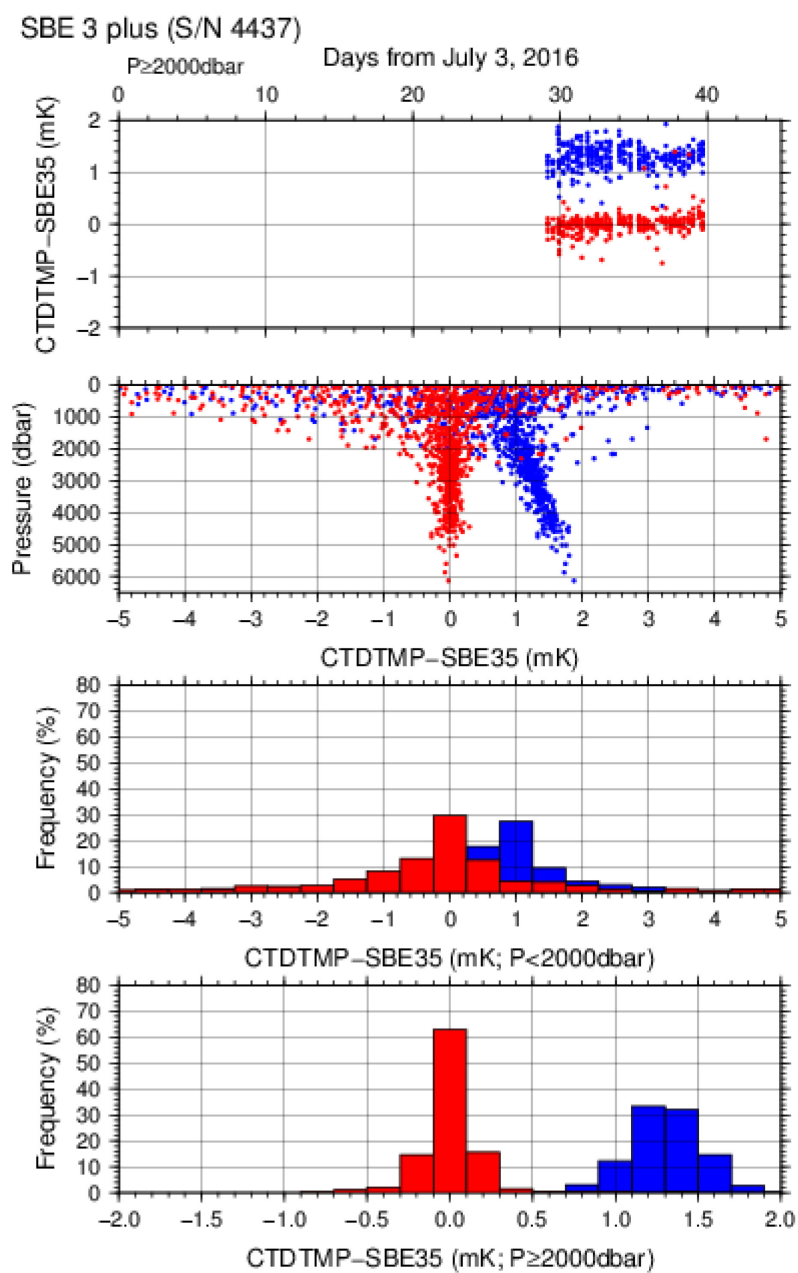


Figure 4.2.3. Difference between the CTD temperature (*S/N 4437*) and the Deep Ocean Standards thermometer (SBE 35) on Leg 2. Blue and red dots indicate before and after the correction using SBE 35 data, respectively. Lower two panels show histograms of the differences after correction.

c. Conductivity sensor (SBE 4C)

The practical corrections for CTD conductivity data can be made by using bottle salinity data to correct the SBE 4C to agree with measured conductivity (McTaggart et al., 2010).

CTD conductivity was corrected as follows:

$$\text{Corrected Conductivity} = C - \left(\sum_{i=0}^I c_i \times C^i + \sum_{j=1}^J p_j \times P^j \right)$$

C : CTD conductivity, c_i and p_j : calibration coefficients

i, j : determined by use of the AIC (Akaike, 1974). In accord with McTaggart et al. (2010), the maximum of I and J were 2.

Table 4.2.4. Conductivity correction coefficient summary. (Bold: accepted sensor)

S/N	Num	$c_0(S/m)$	c_1	$c_2(m/S)$	$p_1(S/m/dbar)$	$p_2(S/m/dbar^2)$	$Stations$
2842	2118	2.5716×10^{-4}	0.0000	0.0000	3.3558×10^{-8}	-2.7075×10^{-13}	RF5802 – 5860
2842	1130	-6.0610×10^{-5}	2.4453×10^{-4}	0.0000	1.0413×10^{-7}	-1.0413×10^{-11}	RF5861 – 5892
4316	2116	-1.1809×10^{-4}	5.9318×10^{-5}	0.0000	1.2606×10^{-7}	-1.0385×10^{-11}	RF5802 – 5860
4316	1130	-5.9158×10^{-5}	5.7968×10^{-5}	0.0000	1.0559×10^{-7}	-6.2355×10^{-12}	RF5861 – 5892

Table 4.2.5. Conductivity correction and salinity correction summary for S/N 2842.

Stations	Num	Conductivity		Num	Salinity	
		Average (S/m)	Std (S/m)		Average	Std
				Pressure < 1900 dbar		
RF5802 – 5860	1314	0.0000	0.0003	1314	0.0000	0.0022
RF5861 – 5892	754	0.0000	0.0003	754	0.0000	0.0022
				Pressure ≥ 1900 dbar		
RF5802 – 5860	804	0.0000	0.0000	804	0.0000	0.0005
RF5861 – 5892	376	0.0000	0.0001	376	0.0000	0.0006

Table 4.2.6. Conductivity correction and salinity correction summary for S/N 4316.

Stations	Num	Conductivity		Num	Salinity	
		Average (S/m)	Std (S/m)		Average	Std
				Pressure < 1900 dbar		
RF5802 – 5860	1306	0.0000	0.0002	1306	0	0.0019
RF5861 – 5892	766	0.0000	0.0003	766	0	0.0024
				Pressure ≥ 1900 dbar		
RF5802 – 5860	810	0.0000	0	810	0.0000	0.0004
RF5861 – 5892	364	0.0000	0	364	0.0000	0.0005

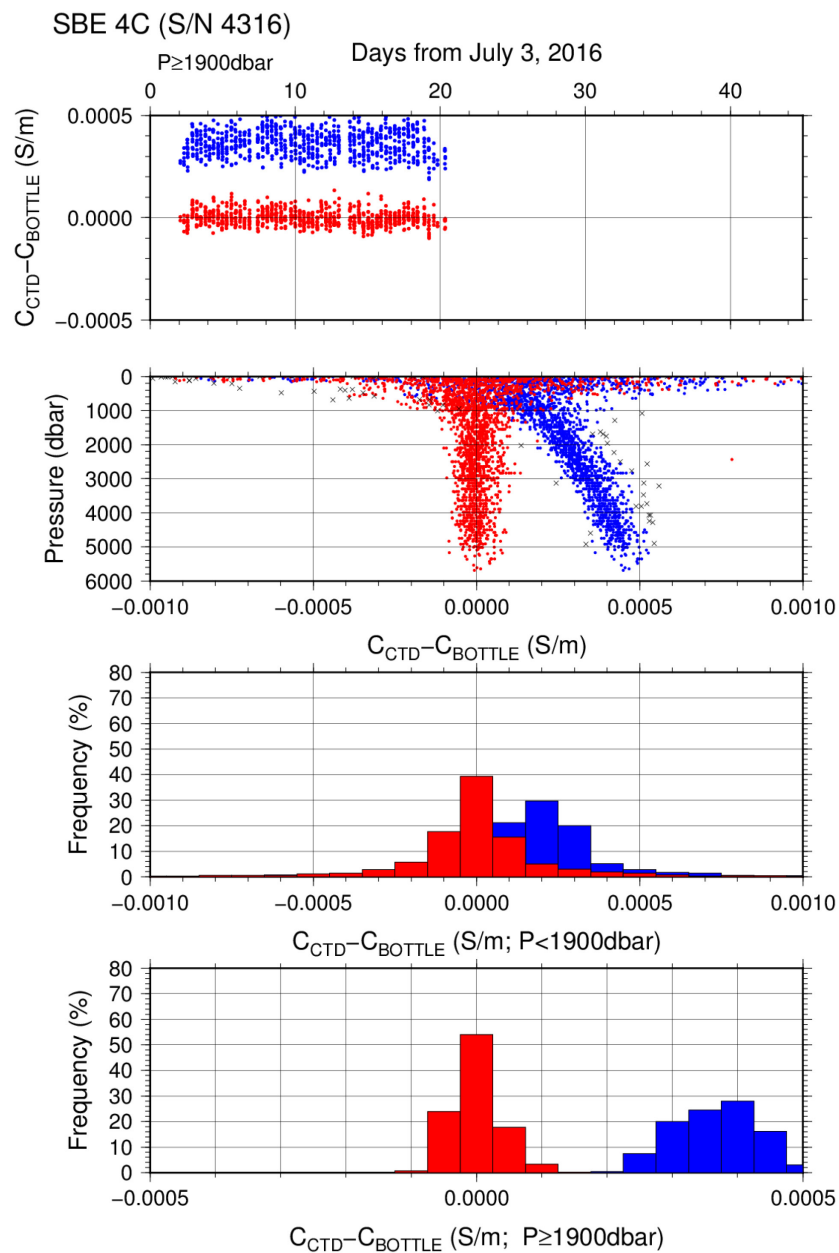


Figure 4.2.4. Difference between the CTD conductivity (*S/N 4316*) and the bottle conductivity on Leg 1. Blue and red dots indicate before and after the calibration using bottle data, respectively. Lower two panels show histograms of the differences before and after calibration.

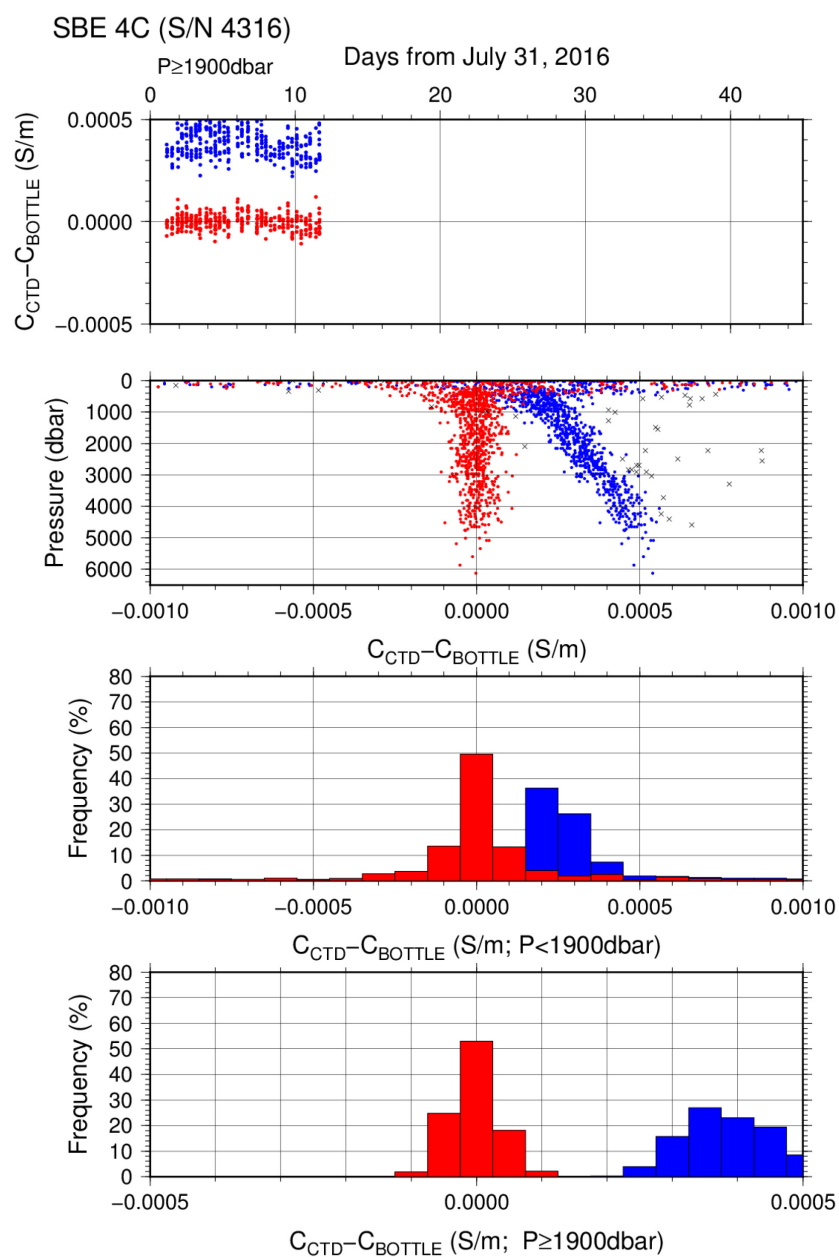


Figure 4.2.5. Difference between the CTD conductivity (*S/N 4316*) and the bottle conductivity on Leg 2. Blue and red dots indicate before and after the calibration using bottle data, respectively. Lower two panels show histograms of the differences before and after calibration.

d. Oxygen sensor (RINKO III)

The CTD oxygen concentration was calculated using the RINKO III output (voltage) with the Stern-Volmer equation in accord with the method of Uchida et al. (2008) and Uchida et al. (2010). The pressure hysteresis for the RINKO III output (voltage) was corrected in accord with Sea-Bird Electronics (2009) and Uchida et al. (2010). The equations were as follows:

$$P_0 = 1.0 + c_4 \times t$$

$$P_c = c_5 + c_6 \times v + c_7 \times T + c_8 \times T \times v$$

$$K_{sv} = c_1 + c_2 \times t + c_3 \times t^2$$

$$coef = (1.0 + c_9 \times P/1000)^{1/3}$$

$$[O_2] = O_2^{\text{sat}} \times \{(P_0/P_c - 1.0)/K_{sv} \times coef\}$$

P : pressure (dbar), t : potential temperature, v : RINKO output voltage (volt)

T : elapsed time of the sensor from the beginning of first station in calculation group in days

O_2^{sat} : dissolved oxygen saturation by Garcia and Gordon (1992) ($\mu\text{mol/kg}$)

$[O_2]$: dissolved oxygen concentration ($\mu\text{mol/kg}$)

c_1 – c_9 : determined by minimizing differences between CTD oxygen and bottle dissolved oxygen by quasi-newton method (Shanno, 1970).

Table 4.2.7. Dissolved oxygen correction coefficient summary. (Bold: accepted sensor)

S/N	26	26	8	8
$Stations$	RF5802 – 5860	RF5861 – 5892	RF5802 – 5860	RF5861 – 5892
c_1	1.73006	1.72453	1.67527	1.6871
c_2	2.51830×10^{-2}	2.08129×10^{-2}	2.37825×10^{-2}	2.24579×10^{-2}
c_3	1.27010×10^{-4}	1.24172×10^{-4}	1.39559×10^{-4}	1.46657×10^{-4}
c_4	-6.36633×10^{-4}	-1.47249×10^{-3}	-5.43750×10^{-4}	-8.87988×10^{-4}
c_5	-1.37504×10^{-1}	-1.25650×10^{-1}	-1.26993×10^{-1}	-1.23317×10^{-1}
c_6	3.10461×10^{-1}	3.06680×10^{-1}	3.03342×10^{-1}	3.01840×10^{-1}
c_7	-3.17909×10^{-4}	-3.78316×10^{-4}	3.51648×10^{-4}	-2.87248×10^{-4}
c_8	2.31975×10^{-4}	4.41860×10^{-4}	2.68911×10^{-4}	4.32304×10^{-4}
c_9	8.01352×10^{-2}	8.30326×10^{-2}	8.52965×10^{-2}	8.68856×10^{-2}

Table 4.2.8. Dissolved oxygen correction summary for S/N 026.

Stations	Pressure < 950 dbar			Pressure \geq 950 dbar		
	Num	Average	Std	Num	Average	Std
		($\mu\text{mol/kg}$)	($\mu\text{mol/kg}$)		($\mu\text{mol/kg}$)	($\mu\text{mol/kg}$)
RF5802 – 5860	1003	0.02	0.89	1010	0.00	0.26
RF5861 – 5892	608	0.00	1.1	508	0.00	0.25

Table 4.2.9. Dissolved oxygen correction summary for S/N 008.

Stations	Pressure < 950 dbar			Pressure \geq 950 dbar		
	Num	Average	Std	Num	Average	Std
		($\mu\text{mol/kg}$)	($\mu\text{mol/kg}$)		($\mu\text{mol/kg}$)	($\mu\text{mol/kg}$)
RF5802 – 5860	1003	-0.01	0.92	1010	0.00	0.28
RF5861 – 5892	608	-0.01	1.1	508	0.00	0.25

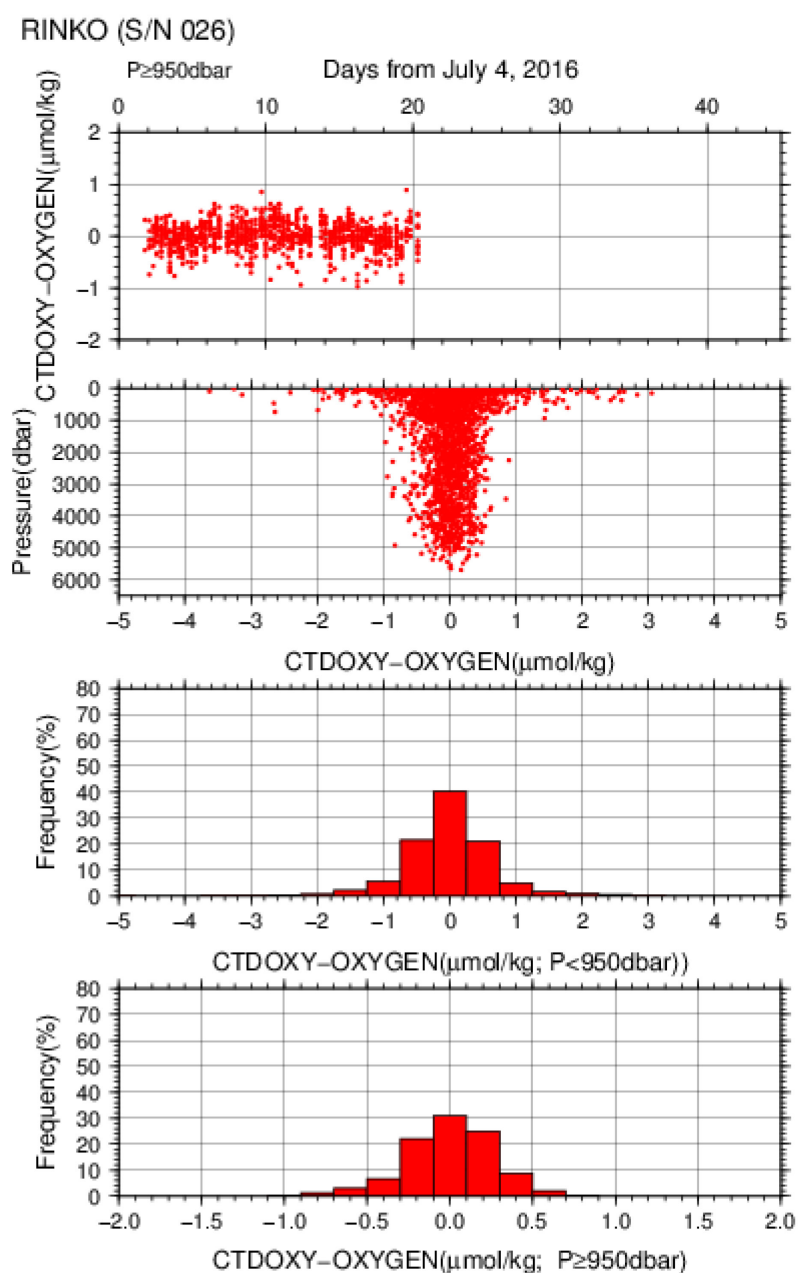


Figure 4.2.6. Difference between the CTD oxygen (S/N 026) and bottle dissolved oxygen on Leg 1. Red dots in upper two panels indicate the result of calibration. Lower two panels show histograms of the differences between calibrated oxygen and bottle oxygen.

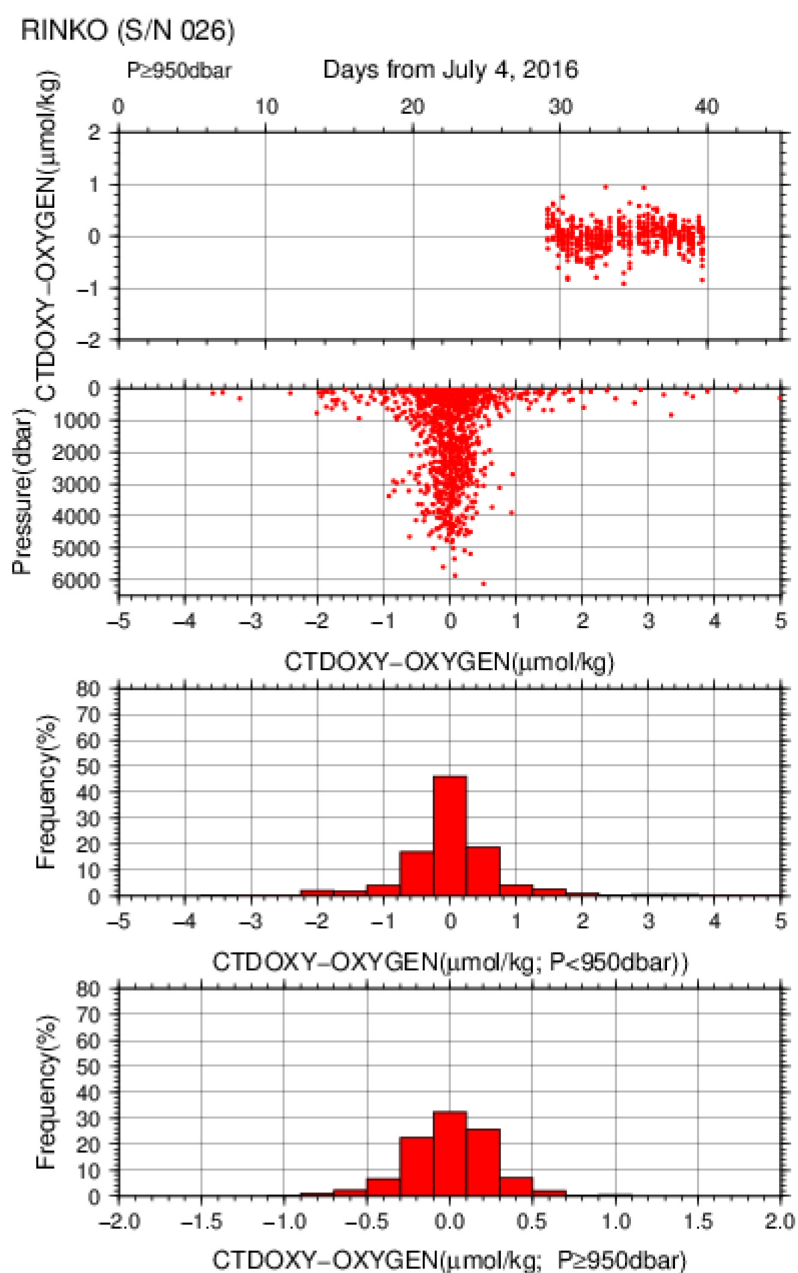


Figure 4.2.7. Difference between the CTD oxygen (S/N 026) and bottle dissolved oxygen on Leg 2. Red dots in upper two panels indicate the results of calibration. Lower two panels show histograms of the differences between calibrated oxygen and bottle oxygen.

4-2-4. Post-cruise calibration

After the cruise, post-cruise calibration of sensors was performed by the manufacturer, as shown below. We confirmed that the calibration of these sensors did not change significantly during the cruise.

a. Temperature (ITS-90): SBE 3plus

Post-cruise sensor calibration of the SBE 3plus

S/N 4321(primary), 19 Sep. 2016

$$\begin{aligned} g &= 4.39116016 \times 10^{-3} & j &= 1.95929821 \times 10^{-6} \\ h &= 6.47366452 \times 10^{-4} & f_0 &= 1000.000 \\ i &= 2.30828080 \times 10^{-5} \end{aligned}$$

S/N 4437(secondary), 19 Sep. 2016

$$\begin{aligned} g &= 4.33401810 \times 10^{-3} & j &= 1.79907757 \times 10^{-6} \\ h &= 6.37045349 \times 10^{-4} & f_0 &= 1000.000 \\ i &= 2.09767140 \times 10^{-5} \end{aligned}$$

b. Deep Ocean Standards Thermometer Temperature (ITS-90): SBE 35

Post-cruise sensor calibration of the SBE 35

S/N 0062, 09 Feb. 2017 (2nd step: fixed point calibration)

$$\text{Slope} = 1.000008, \text{Offset} = -0.001087$$

c. Conductivity: SBE 4C

Post-cruise sensor calibration for the SBE 4C

S/N 2842(primary), 06 Oct. 2016

$$\begin{aligned} g &= -1.01302170 & j &= 4.07480188 \times 10^{-5} \\ h &= 1.38907873 & CP_{cor} &= -9.57 \times 10^{-8} \\ i &= 3.47775107 \times 10^{-4} & CT_{cor} &= 3.25 \times 10^{-6} \end{aligned}$$

S/N 4316(secondary), 06 Oct. 2016

$$\begin{aligned} g &= -9.87043982 & j &= 2.44022577 \times 10^{-4} \\ h &= 1.291116243 & CP_{cor} &= -9.57 \times 10^{-8} \\ i &= -2.61078862 \times 10^{-3} & CT_{cor} &= 3.25 \times 10^{-6} \end{aligned}$$

5. Best practices for quality control of bottle salinity, oxygen concentration, nutrient concentrations, and carbonate system parameters

This section describes best practices for water sampling and quality control of measurements of bottle salinity, oxygen concentrations, nutrient concentrations, carbonate system parameters, Chl. a concentrations, and trace metal concentrations.

Original cruise report of MR15-05 is available at

http://www.godac.jamstec.go.jp/catalog/data/doc_catalog/media/MR15-05_leg1_all.pdf (accessed on 19 March 2020) and that of RF16-06 is available at <https://cchdo.ucsd.edu/cruise/49UP20160703> (accessed on 23 March 2020). In this section 5, we use many materials from the cruise reports and revised them to fit for this guideline.

5-1. Quality control for bottle sampling parameters in the case of the MR15-05 cruise (JAMSTEC)

5-1-1. Bottle salinity

i. Standard Seawater

We set salinometer as appropriately based on an GO-SHIP manual of salinity measurements (Kawano 2010). In case of MR15-05 cruises, standardization control was set to 715 and the value of STANDBY was 5216 ± 0001 and that of ZERO was 0.00000 or ± 0.00001 . We used IAPSO Standard Seawater batch P157, whose conductivity ratio is 0.99985 (the double conductivity ratio is 1.99970) as the standard for salinity measurement. We measured the salinity of 66 bottles of the Standard Seawater during the cruise. Figure 3.2.1 shows the history of the double conductivity ratio measurements of the Standard Seawater.

Temporal drift of the salinometer was corrected by using the Standard Seawater measurements. Linear temporal drift of the salinometer was estimated from the Standard Seawater measurements by using the least squares method (thin black line in Figure 5.2.1). No remarkable temporal drift was detected from the Standard Seawater measurements. The average of the double conductivity ratio was 1.99968; the standard deviation, 0.00001, was equivalent to a salinity of 0.0002.

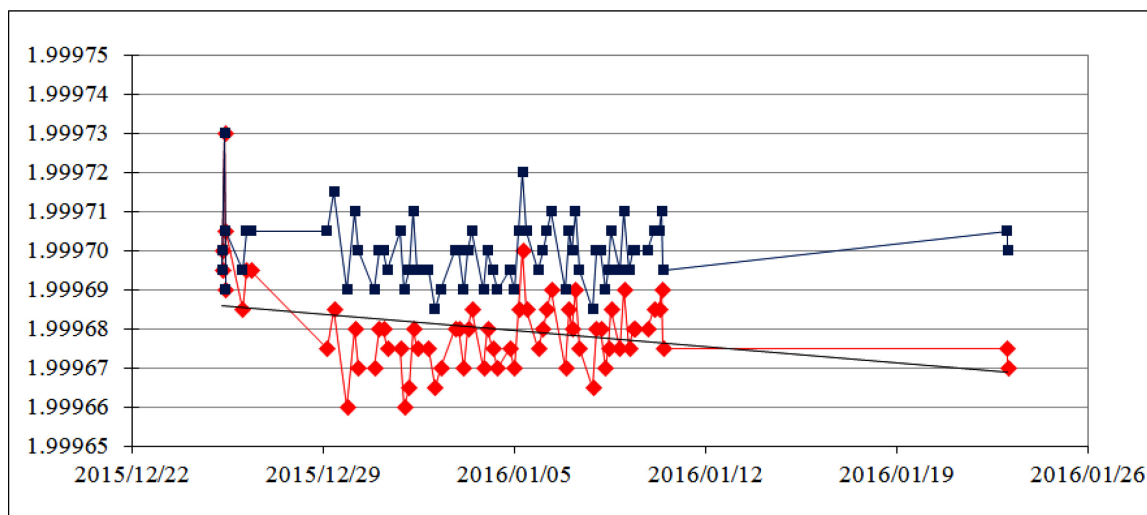


Figure 5.2.1. History of double conductivity ratio measurements of Standard Seawater (P157). Horizontal and vertical axes indicate the date and double conductivity ratio, respectively. Red dots indicate raw data, and blue dots indicate corrected data.

ii. Sub-Standard Seawater

We also used sub-standard seawater, which was deep-sea water filtered through a filter with a pore size of 0.45 μm and stored in a 20-liter cubitainer made of polyethylene and stirred for at least 24 hours before measuring. The salinity was measured every 6–8 samples to check for possible sudden drift of the salinometer. Throughout the measurements, there was no detectable sudden drift of the salinometer.

We took 257 pairs of duplicate samples collected from the same Niskin bottle. Figure 5.2.2 shows a histogram of the absolute difference between replicate samples. The root-mean-square error for 256 pairs of replicate samples, 0.0002, was acceptable from the standpoint of data quality.

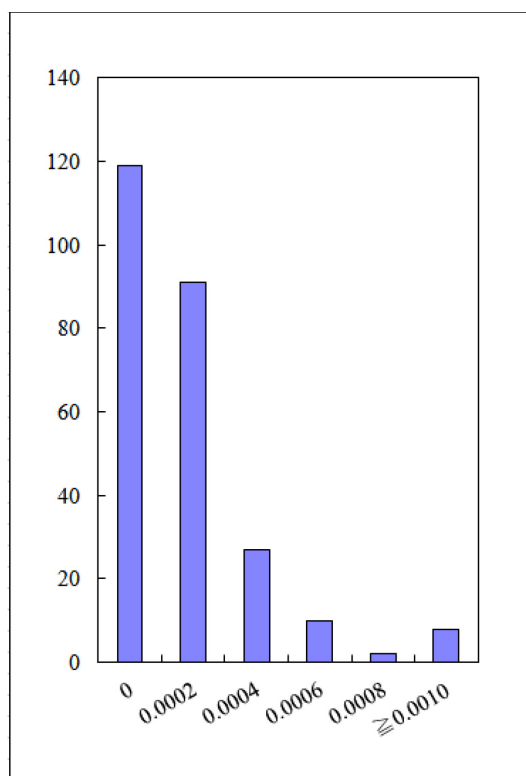


Figure 5.2.2. Histogram of the absolute differences between replicate samples. Horizontal axis is absolute difference of salinity, and vertical axis is frequency.

iv. Duplicate Samples

In this cruise, we took 36 samples at station 900 collected from different Niskin bottles at the same pressure (2000 dbar) instead of taking duplicate samples. The average salinity \pm standard deviation was 34.7300 ± 0.0002 .

5-1-2. Bottle oxygen

Standardization

The concentration of sodium thiosulfate titrant (ca. 0.025 M) was determined with a potassium iodate solution. Pure potassium iodate was dried in an oven at 130°C. Then 1.7835 g of potassium iodate that was weighed out accurately was dissolved in deionized water and diluted to a final volume of 5 liters in a calibrated volumetric flask (0.001667 M). Next, 10 cm³ of the standard potassium iodate solution was added to a flask using a volume-calibrated dispenser. Then, 90 cm³ of deionized water, 1 cm³ of sulfuric acid solution, and 0.5 cm³ of pickling reagent solution II and I were added into the flask in that order. The volume of the sodium thiosulfate titrant (usually the average of 5 measurements) equaled the molarity of the sodium thiosulfate titrant. Table 3.4.1 shows the result of the standardization during this cruise. The coefficient of variation (C.V.) for the standardizations was $0.016 \pm 0.005\%$ (standard deviation, $n = 16$), corresponds to c.a. 0.05 $\mu\text{mol kg}^{-1}$ of dissolved oxygen concentration.

Determination of the blank

The oxygen in the pickling reagents I (0.5 cm³) and II (0.5 cm³) was assumed to be 3.8×10^{-8} mol (Murray *et al.*, 1968). The blank from the presence of redox species apart from oxygen in the reagents (pickling reagents I, II, and the sulfuric acid solution) was determined as follows. Aliquots of 1 and 2 cm³ of the potassium iodate solution were added to two separate flasks, respectively. Then 100 cm³ of deionized water, 1 cm³ of sulfuric acid solution, and 0.5 cm³ of pickling reagent solution II and I each were added to the two flasks, in that order. The blank was equated to the difference between twice the first (1 cm³ of KIO₃) titrated volume of sodium thiosulfate and the second (2 cm³ of KIO₃) titrated volume. The results of triplicate blank determinations were averaged (Table 5.2.1). The average blank values for standard iodate solutions DOT-6 and DOT-8 were 0.002 ± 0.002 (standard deviation, n = 8) and 0.000 ± 0.002 (standard deviation, n = 8) cm³, respectively.

Table 5.2.1 Results of the standardization (end point, E.P.) and the blank determinations (cm³) for standard iodate solutions DOT-6 and DOT-8.

Date (UTC)	KIO ₃ No.	Na ₂ S ₂ O ₃ No.	DOT-6		DOT-8		Stations
			E.P.	Blank	E.P.	Blank	
2015/12/27	K1504E02	T1505A	3.962	0.002	3.963	0.000	001-015
2015/12/30	K1504E03	T1505A	3.965	0.003	3.965	0.001	016-026
2016/1/3	K1504E04	T1505B	3.957	0.000	3.959	0.001	027-041
2016/1/6	K1504E05	T1505B	3.957	0.002	3.958	0.000	042-052

Replicate sample measurements

From the routine CTD casts at all the stations, duplicate samples were collected at pressures of 50, 400, 1800, and 3500 dbars. The total number of duplicate sample pairs that were satisfactory for measurement purposes (flagged as 2) was 170 (Figure 5.2.3). The standard deviation of the replicate measurements, calculated by procedure SOP23 in DOE (1994), was $0.06 \mu\text{mol O}_2 \text{ kg}^{-1}$.

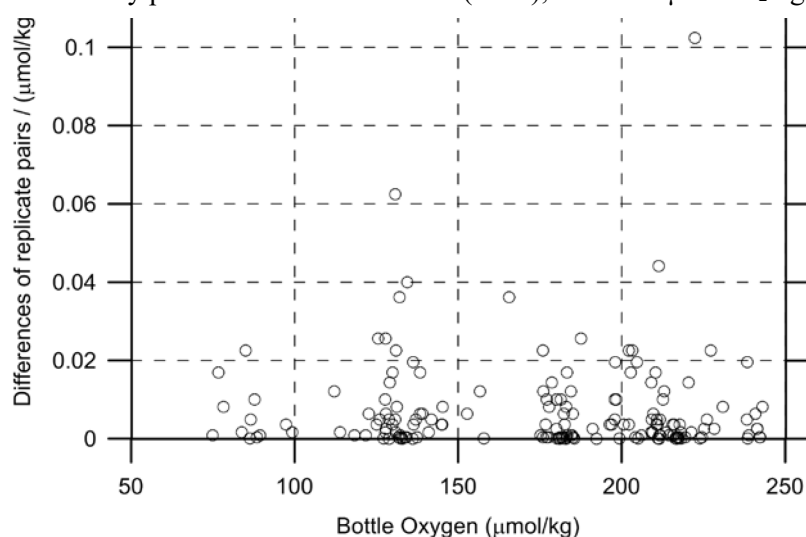


Figure 5.2.3 Magnitude of difference of oxygen concentrations between duplicate samples versus oxygen concentration.

Duplicate sample measurements

At Station 900 (test), duplicate samples were taken at 2000 dbar from all the Niskin bottles (36 bottles, Table 5.2.2) The standard deviation of the duplicate measurements was calculated to be $0.09 \mu\text{mol kg}^{-1}$, which was nearly equivalent to that of the replicate sample measurements ($0.06 \mu\text{mol kg}^{-1}$).

Table 5.2.2 Results of duplicate sample measurements.

Duplicated Niskin #	Niskin	Pressure (db)	Oxygen ($\mu\text{mol kg}^{-1}$)
1	X12J01	2000	139.67
2	X12J02	2000	139.74
3	X12J03	2001	139.73
4	X12J04	2001	139.91
5	X12J05	2000	139.78
6	X12J06	2000	139.91
7	X12J07	2000	139.85
8	X12J08	2000	139.93
9	X12J09	2000	139.87
10	X12J10	2000	139.85
11	X12J11	2001	139.96
12	X12J12	2001	139.87
13	X12J13	2001	140.02
14	X12J14	2001	139.86
15	X12J15	2001	139.89
16	X12J16	2001	139.92
17	X12J17	2000	139.97
18	X12J18	1999	139.86
19	X12J19	2000	139.97
20	X12J20	1999	139.99
21	X12J21	2000	139.94
22	X12J22	2001	139.90
23	X12J23	2001	139.97
24	X12J24	2001	139.98
25	X12J25	2000	139.91
26	X12J26	2001	139.94
27	X12J27	2000	139.93
28	X12J28	2001	139.70
29	X12J29	2001	139.89
30	X12J30	2001	139.78
31	X12J31	2001	139.88
32	X12J32	2001	139.79
33	X12J33	2001	140.02
34	X12J34	2001	139.92
35	X12J35	2000	139.77
36	X12J36	2000	139.85

CSK standard measurements

The CSK standard is a commercial potassium iodate solution (0.0100 N) for analysis of dissolved oxygen. We titrated the CSK standard solution (Lot KPG6393) against our KIO_3 standard solution (Lot K1504E01) before the cruise on 25 Dec. 2016. The normalities of our KIO_3 standard solutions were calculated to be 0.010006 ± 0.000002 N and 0.010006 ± 0.000002 N for DOT-6 and DOT-8, respectively.

Quality control flag assignment

Quality flag values were assigned to oxygen measurements using the code defined in Table 0.2 of the WOCE Hydrographic Program Office Report WHPO 91-1 Rev.2 section 4.5.2 (Joyce *et al.*, 1994). Measurement flags of 2 (good), 3 (questionable), 4 (bad), and 5 (missing) were assigned (Table 3.4.3). To distinguish between flags of 2, 3, and 4, we followed the flagging procedure as below:

- a. Bottle oxygen concentration at the sampling layer was plotted against sampling pressure. Any points not lying on a generally smooth trend were noted.
- b. The difference between bottle oxygen and CTD oxygen was then plotted against sampling pressure. If a datum deviated from a group of plots, it was flagged 3.
- c. Vertical sections against pressure and potential density were drawn. If a datum was anomalous on the section plots, the datum flag was degraded from 2 to 3, or from 3 to 4.
- d. If there was a problem in the measurement, the datum was flagged 4.
- e. If the bottle flag was 4 (did not trip correctly), the datum was flagged 4 (bad). In case the bottle flag was 3 (leaking) or 5 (unknown problem), the datum was flagged based on steps a, b, c, and d.

Table 5.2.3 Summary of number of assigned quality control flags.

Flag	Definition	Number*
2	Good	1363
3	Questionable	0
4	Bad	0
5	Not report (missing)	0
Total		1363

*Replicate samples (n = 170) were not included.

In this chapter 4, we will discuss about quality control flag assignment more general in section 5-4.

5-1-3. Nutrient measurements and estimated uncertainty using CRM

To obtain accurate and high-quality nutrient concentrations, large numbers of bottles of nutrients in seawater CRM have been prepared and used during previous cruises. In the previous worldwide expeditions, such as WOCE cruises, high reproducibility and precision of nutrient measurements were required (Joyce and Corry, 1994). Because no standards were available for the measurement of nutrients in seawater at that time, the requirements were described in terms of precision. The required precision was 1%, 1–2%, 1–3% for nitrate, phosphate and silicate, respectively. Although nutrient data from the WOCE one-time survey was of unprecedented quality and coverage because of the great care taken in sampling and measurements, differences of nutrient concentrations at crossover points were still found among the expeditions (Aoyama and Joyce, 1996, Mordy et al., 2000, Gouretski and Jancke, 2001, Aoyama, 2019). For instance, the mean offset of nitrate concentrations in deep waters was $0.5 \mu\text{mol kg}^{-1}$ for 345 crossovers in the world oceans, though the maximum was $1.7 \mu\text{mol kg}^{-1}$ (Gouretski and Jancke, 2001). At the 31 crossover points in the Pacific WHP one-time lines, the WOCE standard of reproducibility for nitrate of 1% was fulfilled at about half of the crossover points, and the maximum difference was 7% at deeper layers below 1.6°C in potential temperature (Aoyama and Joyce, 1996). In the MR1505 cruises, we used 6 lots of CRM (lots BY, BU, CA, BW, BV, and BZ) to ensure comparability and traceability to SI. Because we did duplicate measurements for all samples, we could look at uncertainty based on differences between results of duplicate samples.

Precision of nitrate analyses during this cruise

The precision of nitrate analyses during this cruise was evaluated based on 7–11 measurements of highest concentration solution of inhouse standard, eg. C-6, that were made every 8 to 13 samples. The precision for nitrate was better than 0.2% (Figure 5.2.4) and was generally good considering that the median analytical precisions during the R/V Mirai cruises conducted in 2009–2014 was 0.11% for nitrate.

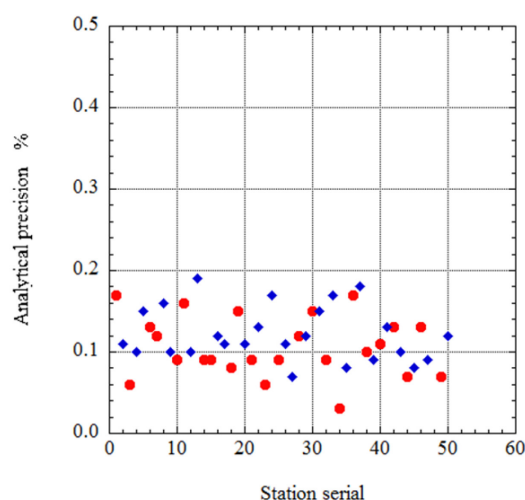


Figure 5.2.4 Time series of precision of nitrate during MR1505. Red circles indicate unit 1 of analyzer, and blue diamonds indicate unit 2 of analyzer.

Control chart: CRM lot BV measurement during this cruise

CRM lot BV was measured every run to monitor the comparability among runs. The results of lot BV during this cruise are shown as Figure 5.2.5. Error bars represent analytical precision in Figure 5.2.4. As shown in Fig. 5.2.5, the measured concentrations of CRM lot BV were well within the uncertainty of the certified value of lot BV.

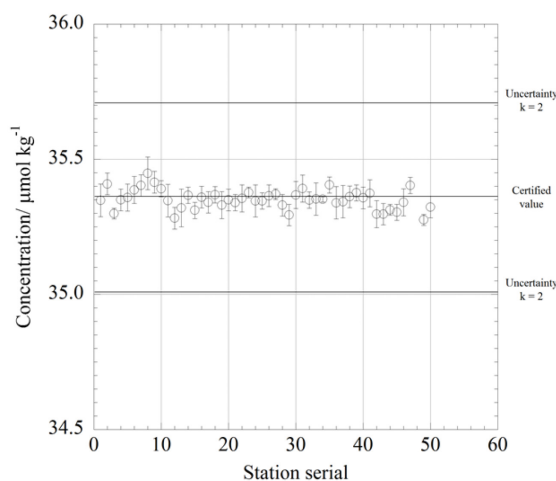


Figure 5.2.5 Control chart of CRM lot BV nitrate concentrations measured during the MR1505 cruise.

Carryover

We can also summarize the magnitudes of carryover throughout the cruise. These were within acceptable limits, as shown in Figure 5.2.6. The carryover of the nitrate measurement had a bias that was equipment-specific. The mean carryover was 0.06% at Unit 2 of analyzer and 0.17% at Unit 1 of analyzer. We carried out the maintenance for Unit 1 by replacing the glass coils with new glass coils and installing a new transmission tube before station 22. This maintenance solved the bias problem.

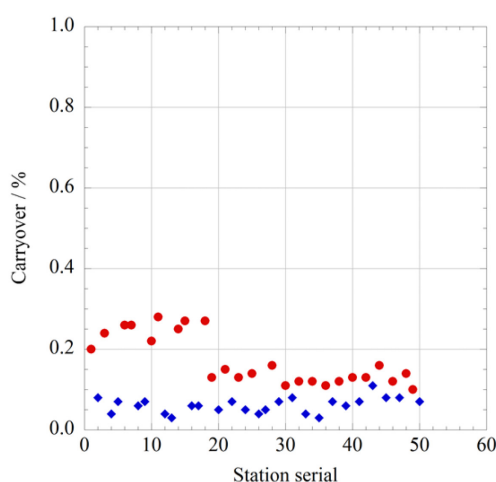


Figure 5.2.6 Time series of carryover of nitrate during MR1505. Red circles indicate unit 1, and blue diamonds indicate unit 2.

Improvement of reduction rate during nitrate measurements

When we reduced the sample flow rate, we achieved a stable and high rate of nitrate reduction to nitrite. The mean rate for 50 runs was 99.7% (± 0.4 – 0.7%) during this cruise, as shown in Figure 5.2.7.

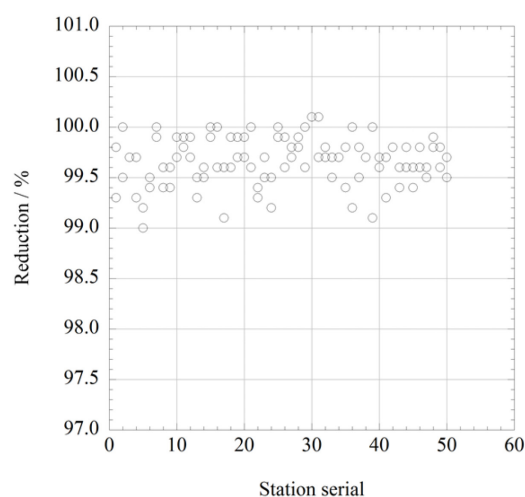


Figure 5.2.7 Time series of reduction of nitrate during MR1505

Estimation of uncertainty of nitrate concentrations

An empirical equation, to estimate the uncertainty of the measurement of nitrate was based on measurements of 24 sets of CRMs during this cruise, as shown in Figure 5.2.8.

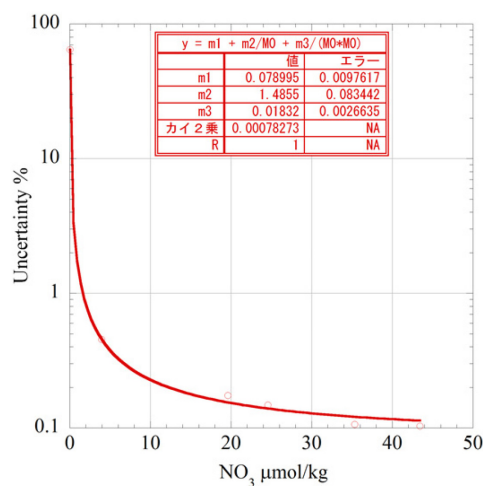


Figure 5.2.8 Estimation of uncertainty for nitrate during MR1505.

An empirical equation to estimate the uncertainty of nitrate measurements was based on measurements of 24 sets of CRMs during this cruise.

Nitrate Concentration (C_{no3}) in $\mu\text{mol kg}^{-1}$:

Uncertainty of measurement of nitrate (%) = $0.08 + 1.49 * (1 / C_{\text{no3}}) + 0.02 * (1 / C_{\text{no3}}) * (1 / C_{\text{no3}})$

where C_{no3} is the nitrate concentration of the sample.

5-1-4. Chlorophyll a

Because there is no established quality control method for Chl. a, a quality check can be done as follows.

Are there any mistakes in the filtration and measurement methods of the collected water sample?

Are the results of replicate samples too far apart?

Is it far from the shape of the vertical profile of the CTD fluorescence sensor?

(K. Sasaok, personal communication)

5-2. Quality control for bottle sampling parameters in the case of the RF16-06 cruise (JMA)

5-2-1. Bottle salinity

a. Instrument

Salinometer: AUTOSAL 8400B (S/N72103; Guildline Instruments Ltd., Canada)

Thermometer: Guildline platinum thermometers model 9450 (to monitor ambient temperature and bath temperature)

b. Sampling and measurement

The measurement system was almost the same as the system described by Kawano (2010).

Algorithm for the Practical Salinity Scale, 1978 (PSS-78; UNESCO, 1981) was employed to convert the conductivity ratios to salinities.

c. Ambient temperature, bath temperature, and surface seawater measurements

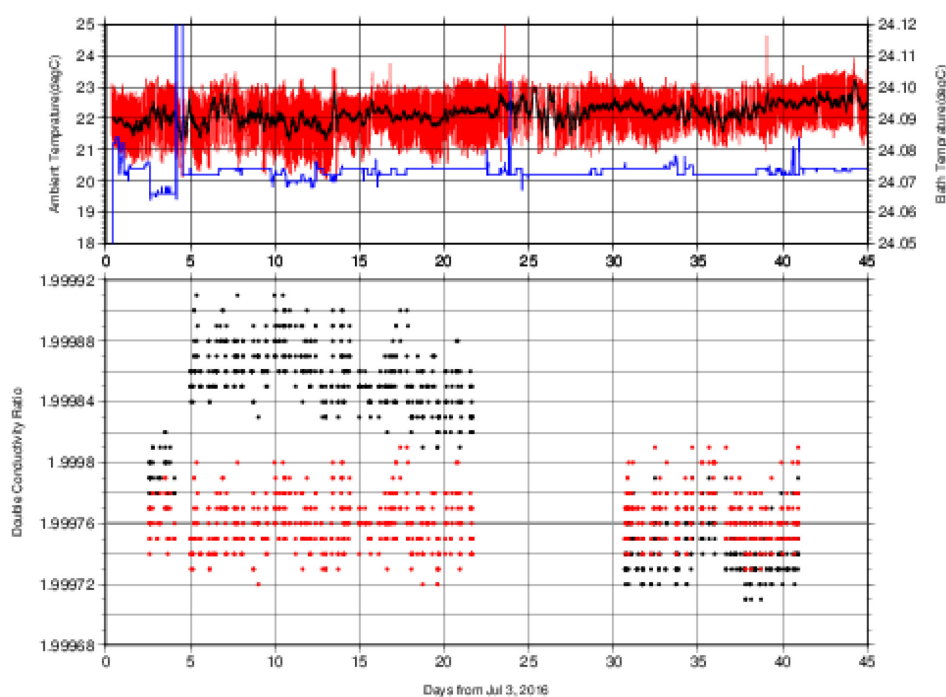


Figure 5.2.1. The upper panel, red line, black line, and blue line indicate time-series of ambient temperature, average ambient temperature, and bath temperature during the cruise. The lower panel, black dots, and red dots indicate raw and corrected time-series of the duplicate conductivity ratios of the standard seawater (IAPSO Standard Sea Water: P159 ($K_{15}=0.99998$)).

d. Replicate and duplicate samples

We took replicate (pair of water samples taken from a single Niskin bottle) and duplicate (pair of water samples taken from different Niskin bottles closed at the same depth) samples for bottle salinity throughout the cruise. Table 5.2.1 summarizes the results of the analyses. Figure 5.2.2 shows details of the results. The calculation of the standard deviation from the difference of sets was based on a procedure (SOP 23) in DOE (1994).

Table 5.2.1. Summary of replicate and duplicate salinity analyses.

Measurement	Average difference \pm S.D.
Replicate	0.0003 ± 0.0003 (N = 327)
Duplicate	0.0007 ± 0.0008 (N = 137)

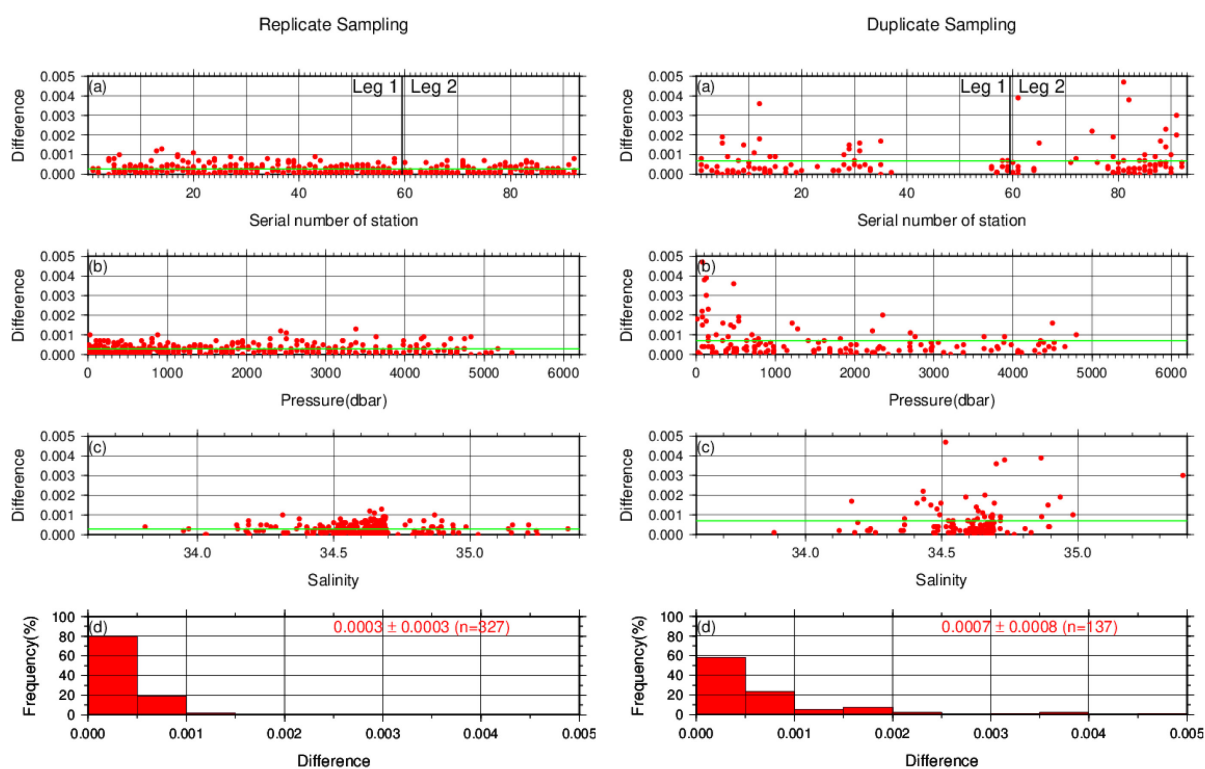


Figure 5.2.2. Results of (left) replicate and (right) duplicate analyses during the cruise against (a) station number, (b) pressure (c) salinity, and (d) histogram of the measurements. Green line indicates the mean of the differences of salinity of replicate/duplicate analyses.

e. Summary of assigned quality control flags

Table 5.2.2. Summary of assigned quality control flags

Flag	Definition	Number of samples
2	Good	2578
3	Questionable	0
4	Bad (Faulty)	238
5	Not reported	0
6	Replicate measurements	334
Total number of samples		3150

5-2-2. Bottle Oxygen

a. Instrument

Detector: DOT-01X (Kimoto Electronic, Japan)

Burette: APB-510 (Kyoto Electronic, Japan)

b. Sampling and measurement

Methods of seawater sampling, measurement, and calculation of dissolved oxygen concentration were based on an IOCCP Report (Langdon, 2010). Standard KIO₃ solutions were prepared gravimetrically using the highest purity standard substance KIO₃ (Lot. No. TLG0272, Wako Pure Chemical, Japan). Table 5.2.3 shows the batch list of prepared standard KIO₃ solutions.

Table 5.2.3. Batch list of the standard KIO₃ solutions.

KIO ₃ batch	Concentration and uncertainty (k = 2) at 20°C. Unit is mol L ⁻¹ .	Purpose of use
20160330-3	0.0016670 ± 0.0000007	Standardization (main use)
20160329-2	0.0016667 ± 0.0000007	Mutual comparison

c. Standardization

The concentration of the Na₂S₂O₃ titrant was determined with the standard KIO₃ solution “20160330-3”, based on the methods of an IOCCP Report (Langdon, 2010). Figure 5.2.3 shows the results of standardization during the cruise. The standard deviation of the concentration at 20°C was determined through standardization and was used in the calculation of uncertainty.

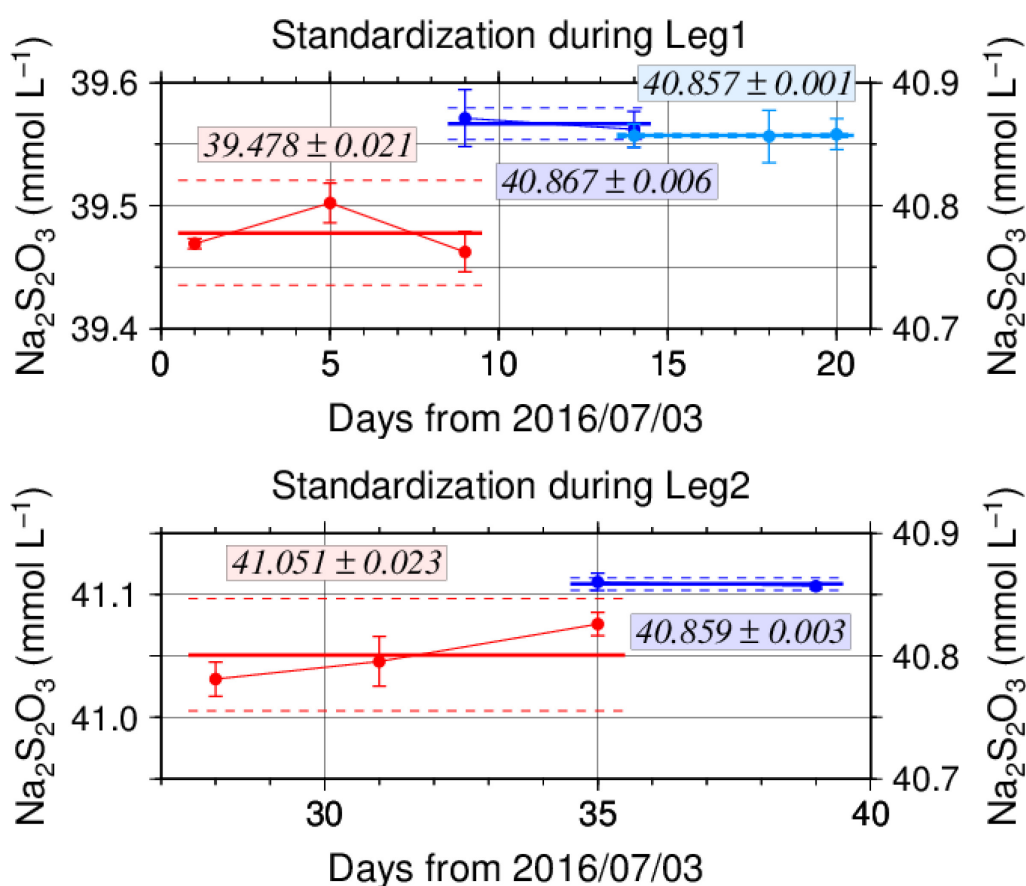


Figure 5.2.3. Calculated concentration of $\text{Na}_2\text{S}_2\text{O}_3$ solution at 20°C in standardization during Leg 1 (top) and Leg 2 (bottom). Different colours of plots indicate different batches of $\text{Na}_2\text{S}_2\text{O}_3$ solution; red (blue and light blue) plots correspond to the left (right) y-axis. Error bars of plots show standard deviations of concentration of $\text{Na}_2\text{S}_2\text{O}_3$ in the measurements. Thick and dashed lines denote the mean and twice the standard deviations for the batch measurements, respectively.

d. Blank

The blank in an oxygen measurement (reagent blank ; V_{blk}) is equal to the sum of two terms as follows:

$$V_{\text{blk}} = V_{\text{blk, ep}} + V_{\text{blk, reg}}$$

where $V_{\text{blk, ep}}$ represents a blank due to differences between the measured end-point and the equivalence point, and $V_{\text{blk, reg}}$ is a blank associated with oxidants or reductants in the reagent. The reagent blank V_{blk} was determined by the methods described in the IOCCP Report (Langdon, 2010). Because we used two sets (set A and B) of pickling reagent I and II, the blanks in each set were determined separately (Figure 5.2.4).

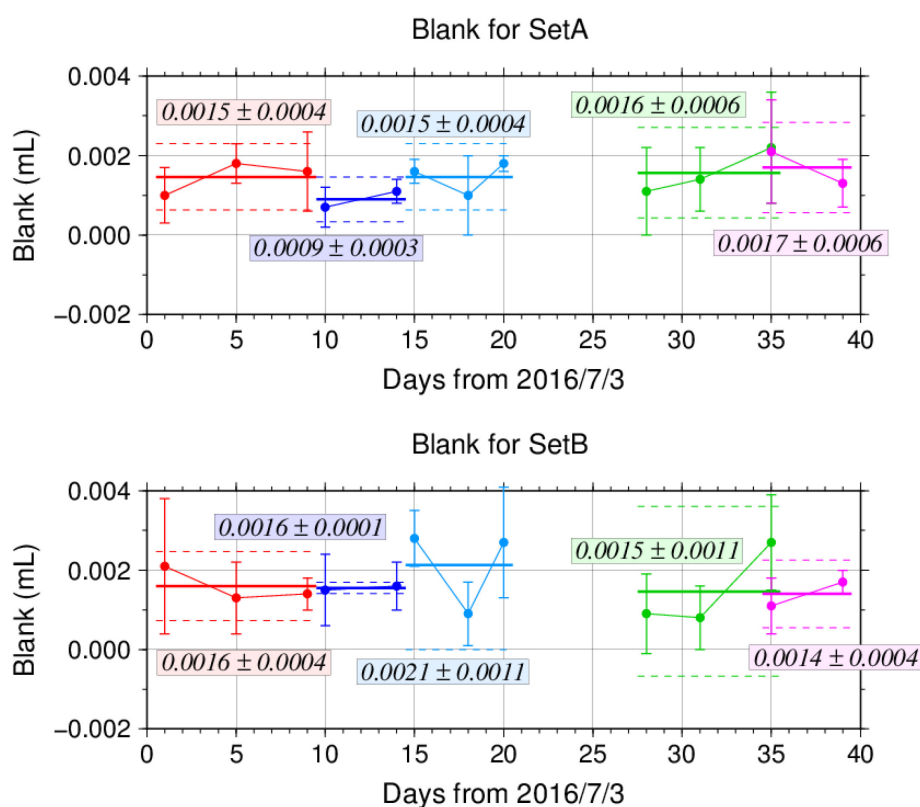


Figure 5.2.4. Reagent blank ($V_{\text{blk, dw}}$) determination for set A (top) and set B (bottom). Error bars of plots show standard deviations of the measurements. Thick and dashed lines denote the mean and the mean \pm twice the standard deviation for the batch measurement, respectively.

e. Replicate and duplicate analyses

We took replicate and duplicate samples of dissolved oxygen throughout the cruise. Table 5.2.4 summarizes the results of the analyses. Figure 5.2.5 shows details of the results. The calculation of the standard deviation from the difference of sets was based on a procedure (SOP 23) in DOE (1994).

Table 5.2.4. Summary of replicate and duplicate measurements.

Measurement	Average magnitude of difference \pm S.D. ($\mu\text{mol kg}^{-1}$)
Replicate	0.14 ± 0.13 (N = 348)
Duplicate	0.26 ± 0.26 (N = 165)

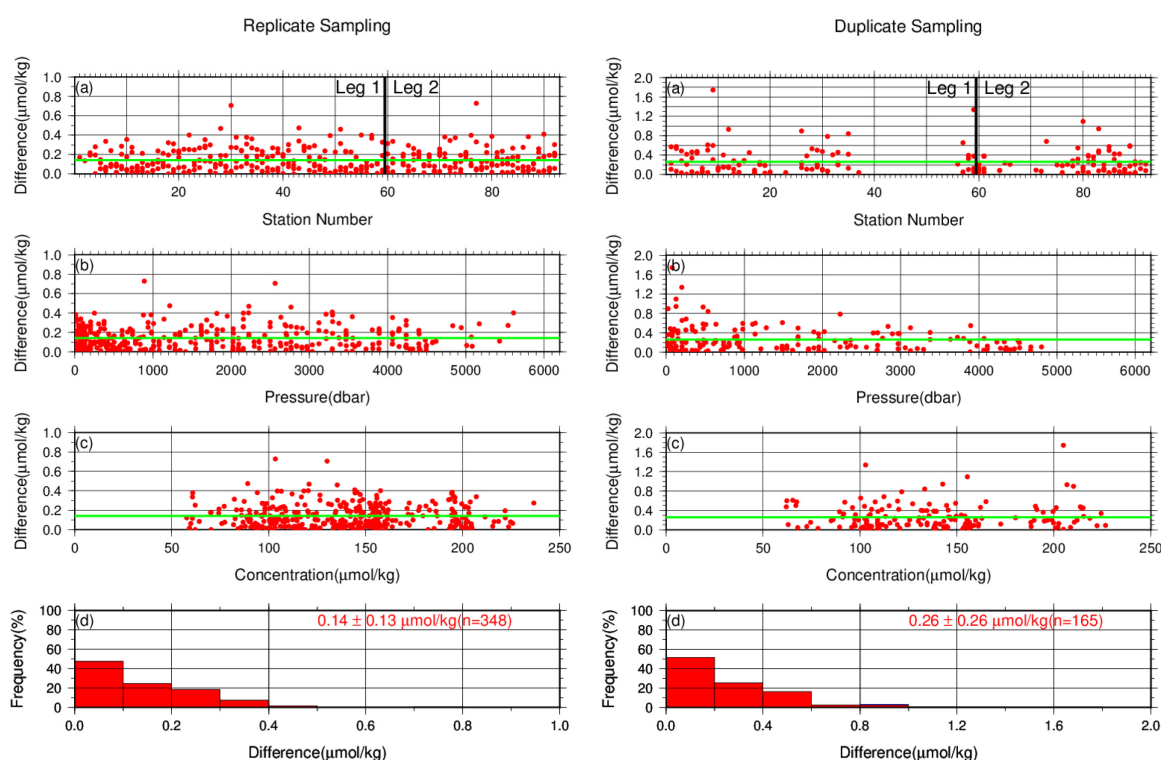


Figure 5.2.5. Results of (left) replicate and (right) duplicate measurements during the cruise against (a) station number, (b) pressure, and (c) concentration of dissolved oxygen. Green lines denote the average of the measurements. Bottom panels (d) show histograms of the measurements.

f. Comparisons between standard KIO_3 solutions

During the cruise, comparisons were made between different lots of standard KIO_3 solutions to confirm the accuracy of our oxygen measurements and the bias of a standard KIO_3 solution. A concentration of the standard KIO_3 solution “20160329-2” was determined using $\text{Na}_2\text{S}_2\text{O}_3$ solution standardized with the KIO_3 solution “20160330-3”, and the difference between the measured value and the theoretical one. Good agreement between two standards confirmed that there was no systematic shift in oxygen measurements during the cruise (Figure 5.2.6).

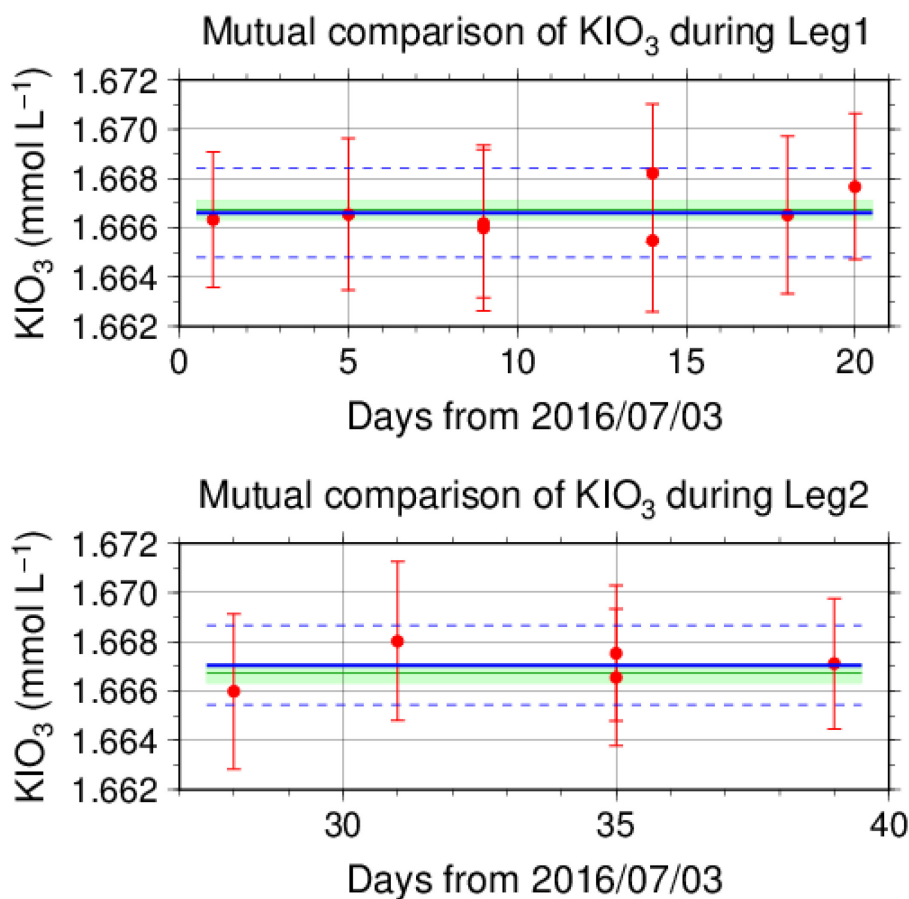


Figure 5.2.6. Result of comparison of standard KIO_3 solutions during Leg 1 (top) and Leg 2 (bottom). Circles and error bars show mean of the measured value and its uncertainty ($k = 2$), respectively. Thick and dashed lines in blue denote the mean and the mean \pm twice the standard deviations, respectively, for the measurements throughout the leg. Green thin line and light green thick line denote the nominal concentration and its uncertainty ($k = 2$) of standard KIO_3 solution “20160329-2”.

g. Quality control flag assignment

A quality flag value was assigned to oxygen measurements, as shown in Table 5.2.5, using the code defined in IOCCP Report No. 14 (Swift, 2010).

Table 5.2.5. Summary of assigned quality control flags.

Flag	Definition	Number of samples
2	Good	2871
3	Questionable	10
4	Bad (Faulty)	19
5	Not reported	0
6	Replicate measurements	348
Total number of samples		3248

h. Uncertainty

Oxygen measurement involves various uncertainties; determination of glass bottles volume, repeatability and systematic error of burette discharge, repeatability of pickling reagent discharges, determination of reagent blank, standardization of $\text{Na}_2\text{S}_2\text{O}_3$ solution, and uncertainty of KIO_3 concentration. After taking into consideration the above uncertainties that could be evaluated, the expanded uncertainty of bottle oxygen concentrations ($T = 20$, $S = 34.5$) was estimated, as shown in Table 5.2.6. However, it is difficult to determine a strict uncertainty for oxygen concentration because there is no reference material for oxygen measurement.

Table 5.2.6. Expanded uncertainty ($k = 2$) of bottle oxygen during the cruise.

O_2 conc. ($\mu\text{mol kg}^{-1}$)	Uncertainty ($\mu\text{mol kg}^{-1}$)
20	0.33
30	0.34
50	0.35
70	0.36
100	0.39
150	0.45
200	0.53
250	0.61
300	0.70
400	0.89

5-2-3. Nutrients

a. Instrument

The nutrient analyses were carried out on a four-channel AutoAnalyzer III (BL TEC K.K., Japan) for four nutrients: nitrate+nitrite, nitrite, phosphate, and silicate.

b. In-house standard solutions

The batches of the reagents used for in-house standards are listed in Table 5.2.7.

Table 5.2.7. List of reagents for the standards used in the cruise.

	Name	CAS No	Lot. no	Industries
Nitrate	Potassium nitrate 99.995 suprapur®	7757-79-1	B0771365	Merck KGaA
Nitrite	Sodium nitrite GR for analysis ACS, Reag. Ph Eur	7632-00-0	A0723349	Merck KGaA
Phosphate	Potassium dihydrogen phosphate anhydrous 99.995 suprapur®	7778-77-0	B1144508	Merck KGaA
Silicate	Silicon standard solution 1000 mg/l Si*	-	HC54715536	Merck KGaA

* Traceable to NIST-SRM3150

c. Certified reference material

Certified reference material for nutrients in seawater (hereafter CRM), which was prepared by the General Environmental Technos company (KANSO Technos, Japan), was used for every analysis at each hydrographic station. Use of CRMs for the analysis of seawater ensures stable comparability and uncertainty of data.

CRMs used in the cruise are shown in Table 5.2.8.

Table 5.2.8. Certified concentration and uncertainty ($k = 2$) of CRMs. Unit is $\mu\text{mol kg}^{-1}$.

	Nitrate	Nitrite	Phosphate	Silicate
CRM-BY	$0.024 \pm 0.019^*$	$0.019 \pm 0.0085^*$	$0.039 \pm 0.010^*$	1.763 ± 0.063
CRM-BW	24.59 ± 0.20	0.067 ± 0.010	1.541 ± 0.014	60.01 ± 0.42
CRM-CB	35.79 ± 0.27	0.116 ± 0.0057	2.520 ± 0.022	109.2 ± 0.62
CRM-BZ	43.35 ± 0.33	0.215 ± 0.011	3.056 ± 0.033	161.0 ± 0.93

* Reference value because concentration is under limit of quantitation

The CRM-BY and -CB were analyzed every analytical run using a newly opened CRM bottle at each hydrographic station. The CRM-BW and -BZ were also analyzed every run but were newly opened every 2 or 3 runs. Although this use of CRMs might be less common, we have confirmed the stability of the opened CRM bottles to be acceptable for oceanographic research. The CRM bottles were stored in a laboratory in the ship, where the temperature was maintained at $\sim 25^\circ\text{C}$.

d. Replicate and duplicate analyses

We took replicate and duplicate samples of nutrients throughout the cruise. Table 5.2.9 summarizes the results of the analyses. Figures 5.2.7–5.2.9 show details of the results. The calculation of the standard deviation from the difference of sets of samples was based on a procedure (SOP 23) in DOE (1994).

Table 5.2.9. Average and standard deviation of difference of replicate and duplicate measurements throughout the cruise. Unit is $\mu\text{mol kg}^{-1}$.

Samples	Nitrate+nitrite	Phosphate	Silicate
Replicates	0.021 ± 0.019 (N = 336)	0.002 ± 0.002 (N = 351)	0.058 ± 0.058 (N = 351)
Duplicates	0.041 ± 0.048 (N = 168)	0.004 ± 0.004 (N = 169)	0.100 ± 0.099 (N = 170)

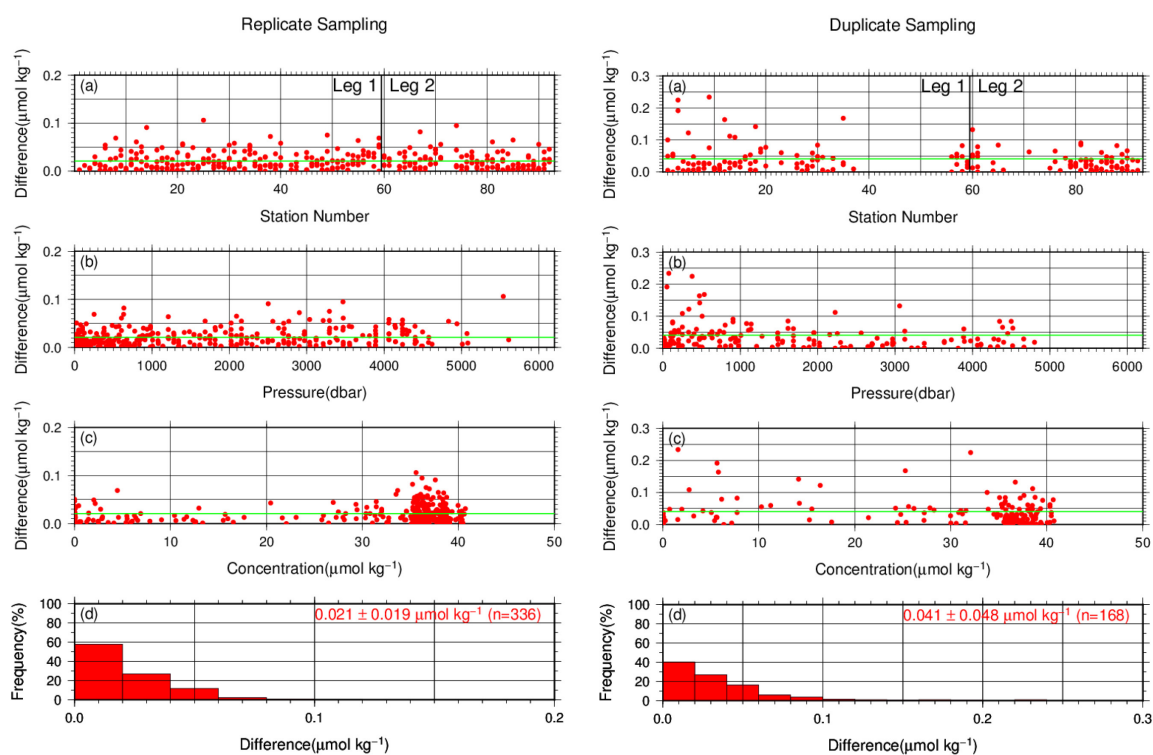


Figure 5.2.7. Results of (left) replicate and (right) duplicate measurements of nitrate+nitrite throughout the cruise versus (a) station number, (b) sampling pressure, (c) concentration, and (d) histogram of the measurements. Green lines indicate the mean of the differences of concentrations based on replicate/duplicate analyses.

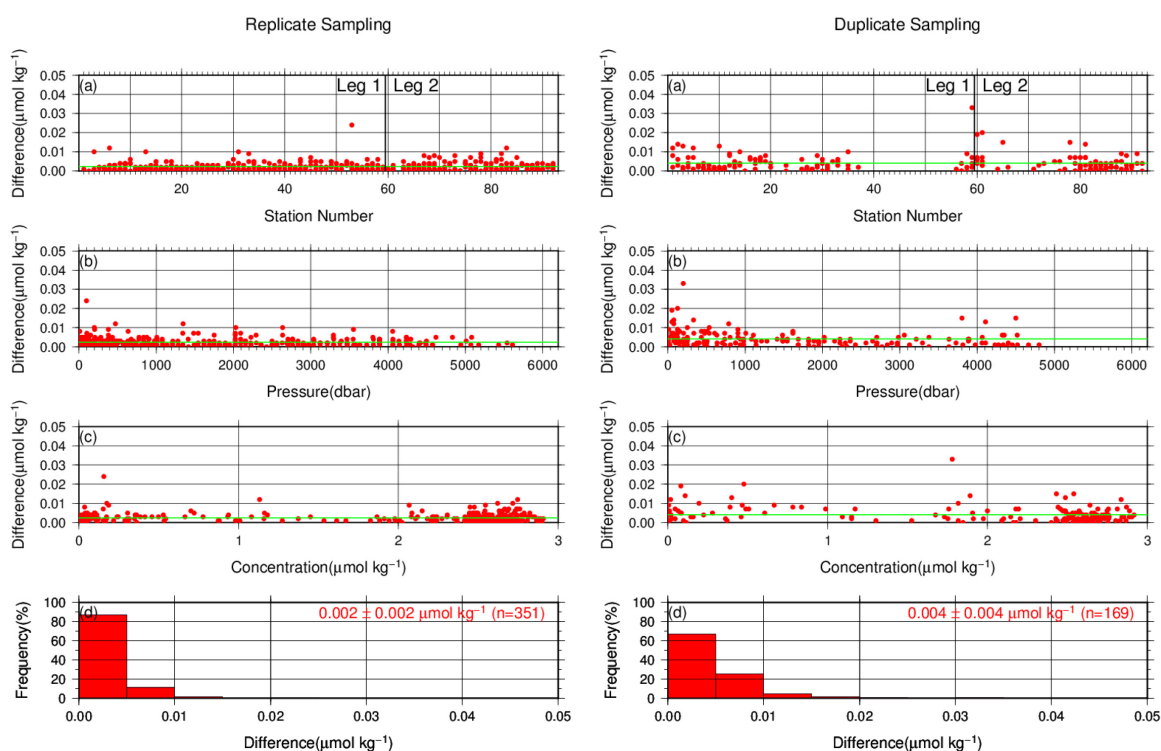


Figure 5.2.8. Same as Figure 5.2.7, but for phosphate.

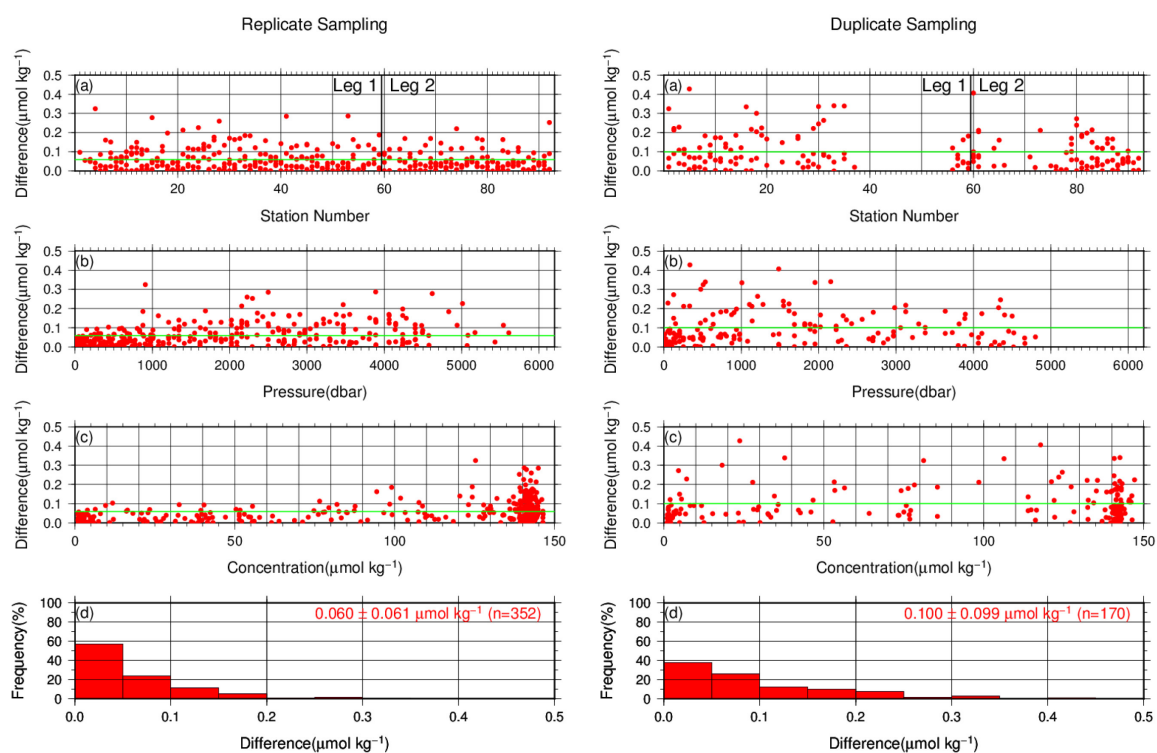


Figure 5.2.9. Same as Figure 5.2.7, but for silicate.

e. Measurement of CRMs

Table 5.2.10 summarizes the CRM measurements during the cruise. The CRM concentrations were assigned with in-house standard solutions. Figures 5.2.10–5.2.13 show the measured concentrations of CRM-BZ throughout the cruise.

Table 5.2.10. Summary of (upper) mean concentration and its standard deviation (unit: $\mu\text{mol kg}^{-1}$), (middle) coefficient of variation (%), and (lower) total number of CRM measurements throughout the cruise.

	Nitrate+nitrite	Nitrite	Phosphate	Silicate
CRM-BY	0.094 ± 0.027	0.023 ± 0.003	0.030 ± 0.011	1.71 ± 0.06
	28.36%	12.05%	37.86%	3.63%
	(N = 172)	(N = 180)	(N = 180)	(N = 180)
CRM-BW	24.71 ± 0.06	0.073 ± 0.002	1.54 ± 0.01	59.93 ± 0.10
	0.27%	2.34%	0.72%	0.16%
	(N = 122)	(N = 128)	(N = 127)	(N = 128)
CRM-CB	35.97 ± 0.08	0.122 ± 0.002	2.52 ± 0.01	109.39 ± 0.13
	0.25%	1.64%	0.45%	0.12%
	(N = 172)	(N = 180)	(N = 180)	(N = 180)
CRM-BZ	43.66 ± 0.09	0.221 ± 0.003	3.06 ± 0.01	161.04 ± 0.19
	0.21%	1.22%	0.39%	0.12%
	(N = 122)	(N = 128)	(N = 128)	(N = 128)

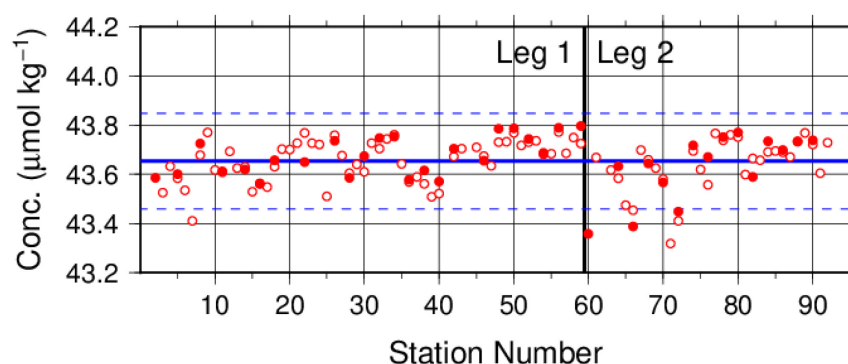


Figure 5.2.10. Time-series of measured concentration of nitrate+nitrite of CRM-BZ throughout the cruise. Closed and open circles indicate the newly and previously opened bottle, respectively. Thick and dashed lines denote the mean and the mean \pm twice the standard deviations of the measurements throughout the cruise, respectively.

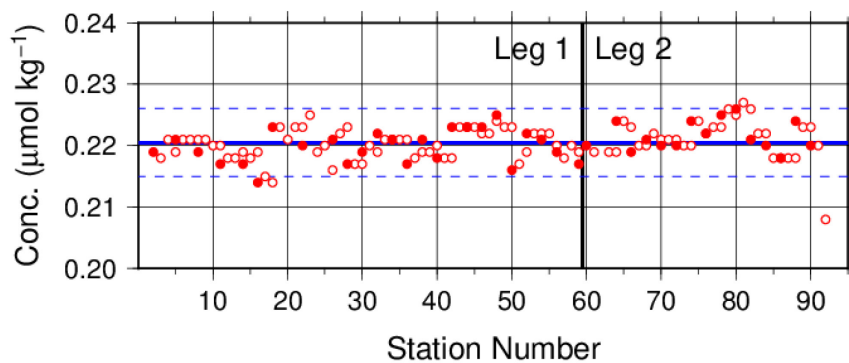


Figure 5.2.11. Same as Figure 5.2.10, but for nitrite.

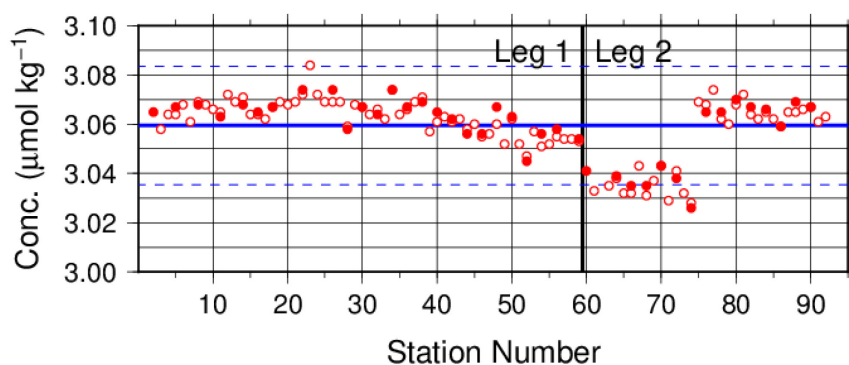


Figure 5.2.12. Same as Figure 5.2.10, but for phosphate.

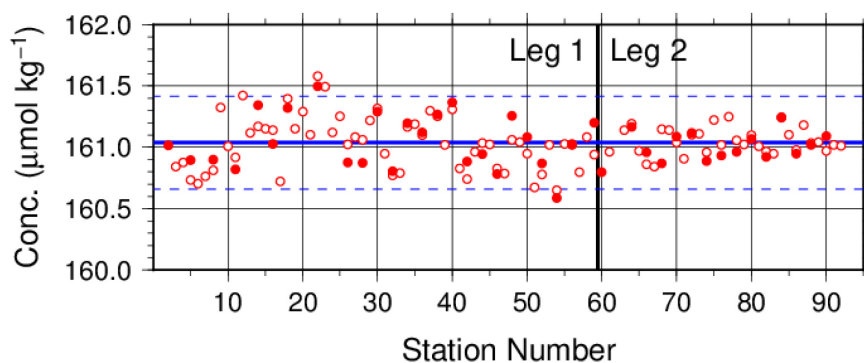


Figure 5.2.13. Same as Figure 5.2.10, but for silicate.

f. Precision of analysis in a run

To monitor the precision of the analyses, the same samples were repeatedly measured in a sample array during a run. For this purpose, a C-5 standard solution was randomly inserted in every 2–10 samples as a “check standard” (the number of standards was about 8–9) in the run. The precision was estimated in terms of the coefficient of variation of the measurements. Table 5.2.11 summarizes the results. The time series are shown in Figures 5.2.14–5.2.17.

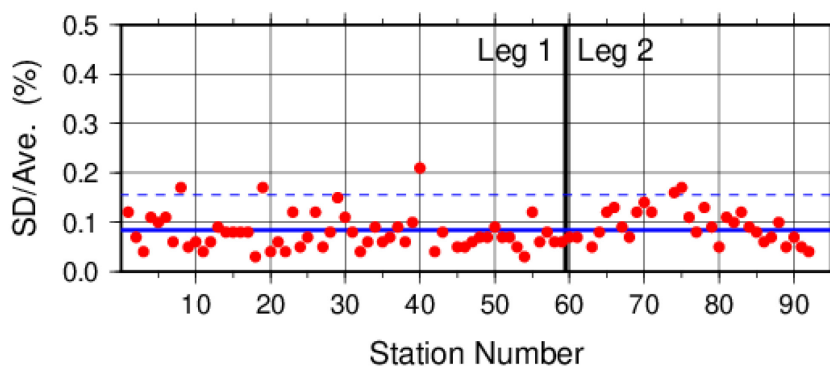


Figure 5.2.14. Time-series of the coefficients of variation of “check standard” measurements of nitrate+nitrite throughout the cruise. Thick and dashed lines denote the mean and the mean \pm twice the standard deviations of the measurements throughout the cruise, respectively.

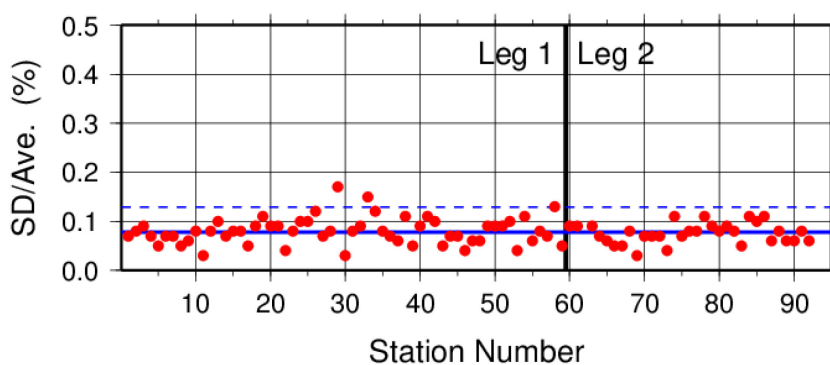


Figure 5.2.15. Same as Figure 5.2.14, but for nitrite.

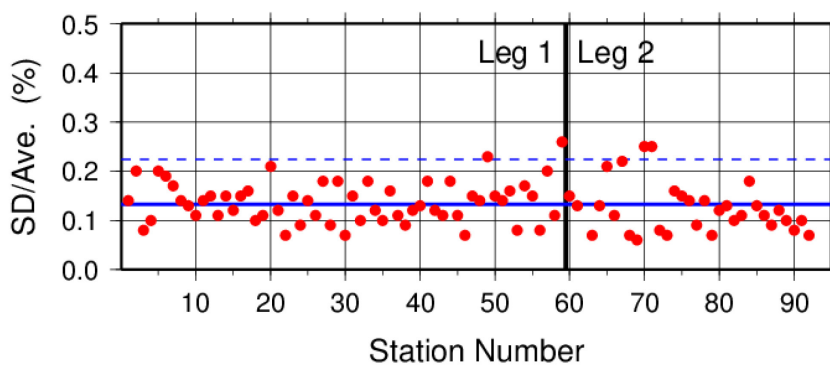


Figure 5.2.16. Same as Figure 5.2.14, but for phosphate.

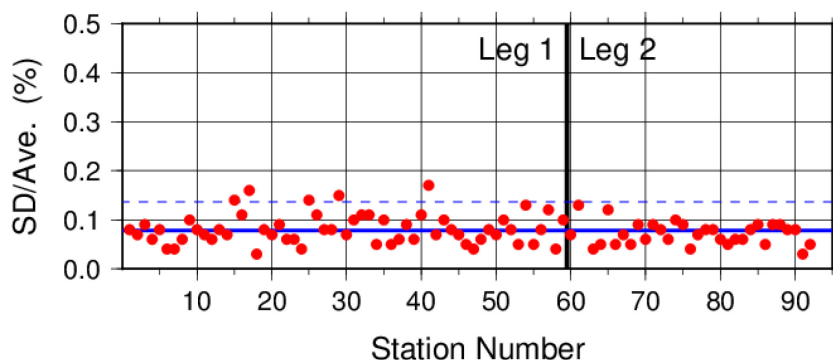


Figure 5.2.17. Same as Figure 5.2.14, but for silicate.

Table 5.2.11. Summary of precisions of nutrient assays during the cruise.

	Nitrate+nitrite	Nitrite	Phosphate	Silicate
Median	0.08%	0.08%	0.13%	0.08%
Mean	0.08%	0.08%	0.13%	0.08%
Minimum	0.03%	0.03%	0.06%	0.03%
Maximum	0.21%	0.17%	0.26%	0.17%
Number	87	91	91	91

g. Carryover

Carryover coefficients were determined during each analytical run. The C-5 standard (high standard) was followed by two C-1 standards (low standards). Figures 5.2.18–5.2.21 show the time series of the carryover coefficients.

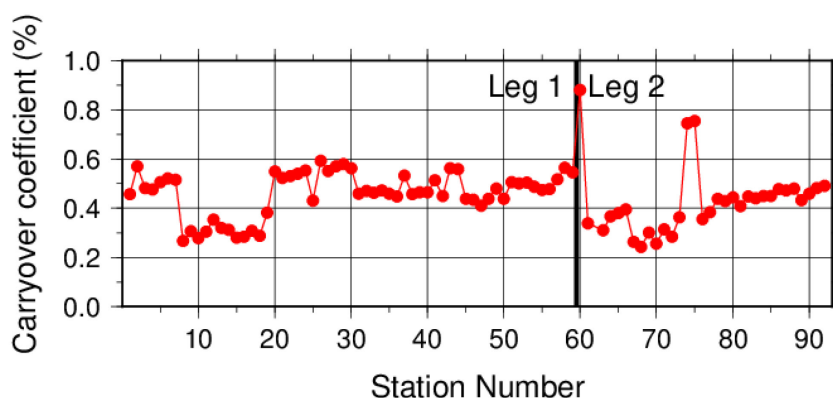


Figure 5.2.18. Time-series of carryover coefficients in measurement of nitrate+nitrite throughout the cruise.

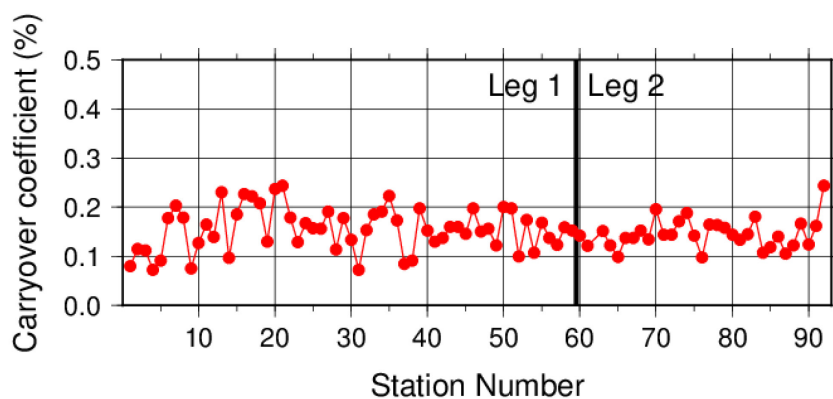


Figure 5.2.19. Same as Figure 5.2.18, but for nitrite.

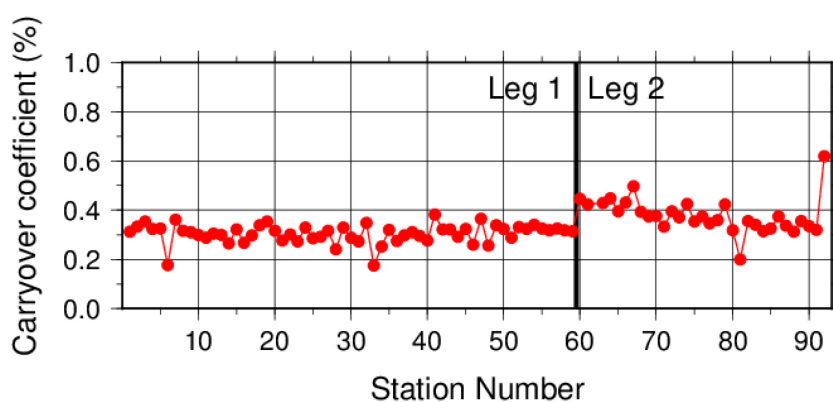


Figure 5.2.20. Same as Figure 5.2.18, but for phosphate.

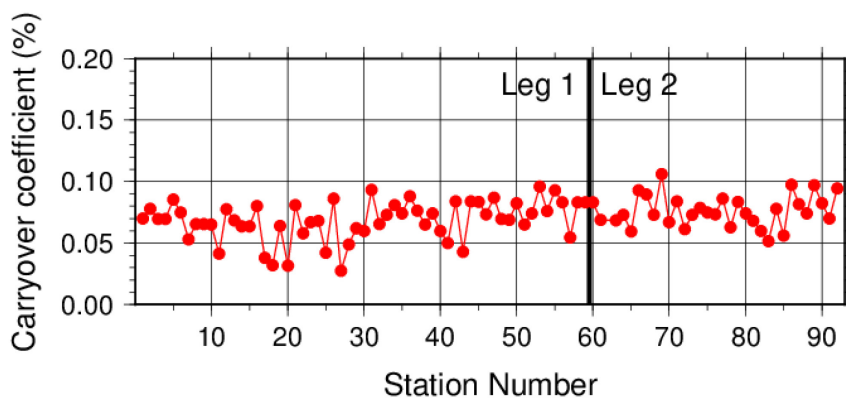


Figure 5.2.21. Same as Figure 5.2.18, but for silicate.

h. Quality control flag assignment

A quality flag value was assigned to nutrient measurements, as shown in Table 5.2.12, using the code defined in IOCCP Report No.14 (Swift, 2010).

Table 5.2.12. Summary of assigned quality control flags.

Flag	Definition	Nitrate+nitrite	Nitrite	Phosphate	Silicate
2	Good	2751	2884	2868	2885
3	Questionable	148	0	9	0
4	Bad (Faulty)	13	12	20	12
5	Not reported	0	0	0	0
6	Replicate measurements	336	352	351	351
Total number of samples		3248	3248	3248	3248

i. Uncertainty

Uncertainty associated with concentration level: U_c

Generally, an uncertainty of nutrient measurement is expressed as a function of its concentration level which reflects that some components of uncertainty are relatively large in low concentration. Empirically, the uncertainty associated with concentrations level (U_c) can be expressed as follows;

$$U_c (\%) = a + b \cdot (1/C_x) + c \cdot (1/C_x)^2,$$

where C_x is the concentration of sample for parameter X.

Using the coefficients of variation of the CRM measurements throughout the cruise, uncertainty associated with concentrations of nitrate+nitrite, phosphate, and silicate were determined as follows:

$$U_{c-no3} (\%) = 0.018 + 2.071 \cdot (1/C_{no3}) - 0.022 \cdot (1/C_{no3})^2$$

$$U_{c-po4} (\%) = -0.054 + 0.361 \cdot (1/C_{po4})$$

$$U_{c-sil} (\%) = 0.02 + 3.66 \cdot (1/C_{sil}) + 1.10 \cdot (1/C_{sil})^2,$$

where C_{no3} , C_{po4} , and C_{sil} represent concentrations of nitrate+nitrite, phosphate, and silicate, respectively, in $\mu\text{mol kg}^{-1}$. Figures 5.2.22–5.2.24 show the calculated uncertainty graphically.

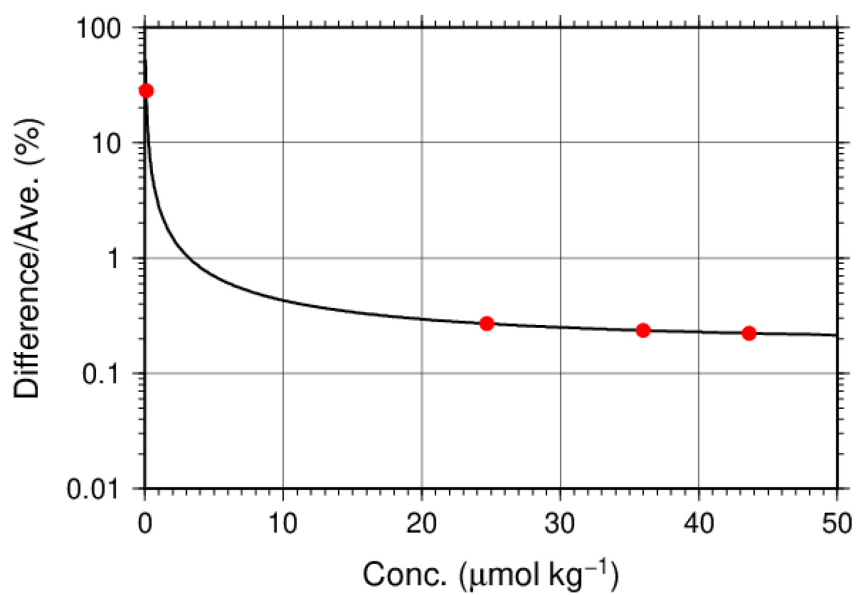


Figure 5.2.22. Uncertainty of nitrate+nitrite associated with concentrations.

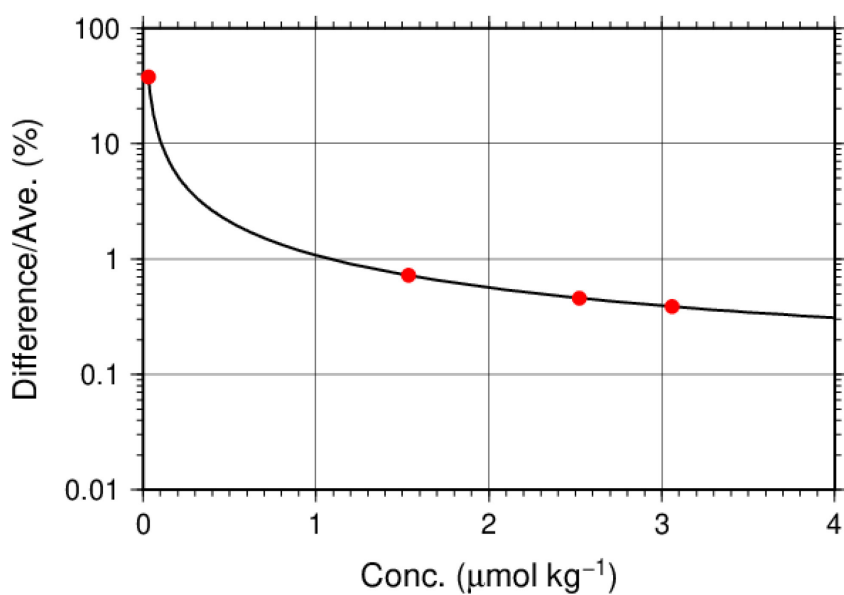


Figure 5.2.23. Same as Figure 5.2.22, but for phosphate.

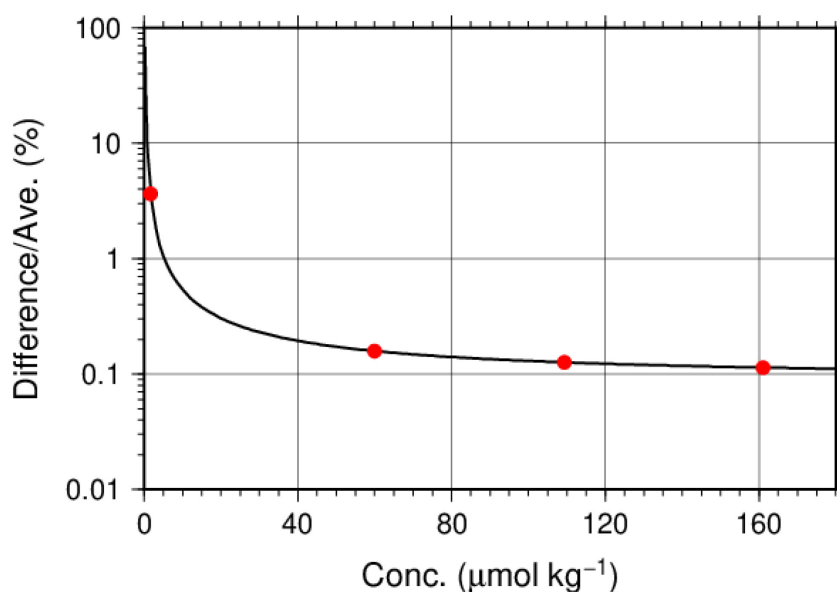


Figure 5.2.24. Same as Figure 5.2.22, but for silicate.

Uncertainty of analysis between runs: U_s

Uncertainty of analysis among runs (U_s) was evaluated based on the coefficient of variation of measured concentrations of CRM-BZ with the highest concentration among the CRM lots throughout the cruise, as shown in subsection (5-2-3e). The reason for using the CRM lot BZ to state U_s is to exclude the effect of uncertainty associated with lower concentration described previously. As is clear from the definition of U_c , U_s is equal to U_c at nutrients concentrations of lot BZ. It is important to note that U_s includes all of uncertainties during the measurements throughout stations, namely uncertainties of concentrations of in-house standard solutions prepared for each run, uncertainties of slopes and intercepts of the linear calibration curve or coefficients of quadric calibration curve, precision of measurement in a run (U_a) and between-bottle homogeneity of the CRM.

Uncertainty of analysis in a run: U_a

Uncertainty of analysis in a run (U_a) was evaluated based on the coefficient of variation of repeated measurements of the “check standard” solution, as shown in subsection (5-2-3f). The U_a reflects the conditions associated with chemistry of colorimetric measurement of nutrients, and stability of electronic and optical parts of the instrument throughout a run. Under a well-controlled condition of the measurements, U_a might show Poisson distribution with a mean as shown in Figures 5.2.14-5.2.17 and Table 5.2.11 and treated as a precision of measurement. U_a is a part of U_c at the concentration as stated in a previous section for U_c .

However, U_a may show larger value which was not expected from Poisson distribution of U_a due to the malfunction of the instruments, larger ambient temperature change, human errors in handling samples and chemistries and contaminations of samples in a run. In the cruise, we observed that U_a of

our measurement was usually small and well-controlled in most runs as shown in Figures 5.2.14–5.2.17 and Table 5.2.11. However, in a few runs, U_a showed high values which were over the mean \pm twice the standard deviations of U_a , suggesting that the measurement system might have some problems.

Uncertainty of CRM concentration: U_r

In the certification of CRM, the uncertainty of CRM concentrations (U_r) was stated by the manufacturer (Table 5.2.8) as expanded uncertainty at $k=2$. This expanded uncertainty reflects the uncertainty of the Japan Calibration Service System (JCSS) solutions, characterization in assignment, between-bottle homogeneity, and long term stability. We have ensured comparability between cruises by ensuring that at least two lots of CRMs overlap between cruises. In comparison of nutrient concentrations between cruises using KANSO CRMs in an organization, it was not necessary to include U_r in the conclusive uncertainty of concentration of measured samples because comparability of measurements was ensured in an organization as stated previously.

Conclusive uncertainty of nutrient measurements of samples: U

To determine the conclusive uncertainty of nutrient measurements of samples (U), we use two functions depending on U_a value acquired at each run as follows:

When U_a was small and measurement was well-controlled condition, the conclusive uncertainty of nutrient measurements of samples, U , might be as below.

$$U = U_c$$

When U_a was relative large and the measurement might have some problems, the conclusive uncertainty of nutrient measurements of samples, U , can be expanded as below.

$$U = \sqrt{U_c^2 + U_a^2}.$$

When U_a was relative large and the measurement might have some problems, the equation of U is defined as to include U_a to evaluate U , although U_a partly overlaps with U_c . It means that the equation overestimates the conclusive uncertainty of samples. On the other hand, for low concentration there is a possibility that the equation not only overestimates but also underestimates the conclusive uncertainty because the functional shape of U_c in lower concentration might not be the same and cannot be verified. However, we believe that the applying the above function might be better way to evaluate the conclusive uncertainty of nutrient measurements of samples because we can do realistic evaluation of uncertainties of nutrient concentrations of samples which were obtained under relatively unstable conditions, larger U_a as well as the evaluation of them under normal and good conditions of measurements of nutrients.

5-2-4. Total Dissolved Inorganic Carbon (DIC)

a. Instrument

The measurements of DIC were carried out with a DIC/TA analyzer (Nihon ANS Co. Ltd, Japan). We used two analyzers concurrently. These analyzers are designated as apparatus A and B.

b. Sampling and measurement

Methods of seawater sampling, poisoning, measurement, and calculation of DIC concentrations were based on the Standard Operating Procedure (SOP) described in PICES Special Publication 3, SOP-2 (Dickson et al., 2007). DIC was determined by coulometric analysis (Johnson et al., 1985, 1987) using an automated CO₂ extraction unit and a coulometer.

c. Calibration

The concentration of DIC (C_T) in moles per kilogram (mol kg⁻¹) of seawater was calculated from the following equation:

$$C_T = N_S / (cV \cdot \rho_S)$$

where N_S is the counts of the coulometer (C), cV is the calibration factor (gC (mol L⁻¹)⁻¹), and ρ_S is the density of seawater (kg L⁻¹), which is calculated from the salinity of the sample and the water temperature. The values of cV were determined by measurements of CRMs that were provided by Dr. Andrew G. Dickson of the Scripps Institution of Oceanography. Table 5.2.14 provides information about the CRM batches used in this cruise.

Table 5.2.14. Certified concentration and uncertainty ($k = 2$) of CRMs. Unit of DIC is $\mu\text{mol kg}^{-1}$. More information is available at the NOAA web site (https://www.nodc.noaa.gov/ocads/oceans/Dickson_CRM/batches.html).

Batch number	150
DIC	2017.88 ± 0.36
Salinity	33.343

The CRM measurement was carried out at every station. After the cruise, a value of cV was assigned to each apparatus (A, B). Table 5.2.15 summarizes the cV values. Figure 5.2.25 shows details.

Table 5.2.15. Assigned cV and its standard deviation for each apparatus during the cruise. Unit is gC (mol L⁻¹)⁻¹.

Apparatus	cV
A	0.189806 ± 0.000232 (N = 85)
B	0.190251 ± 0.000205 (N = 110)

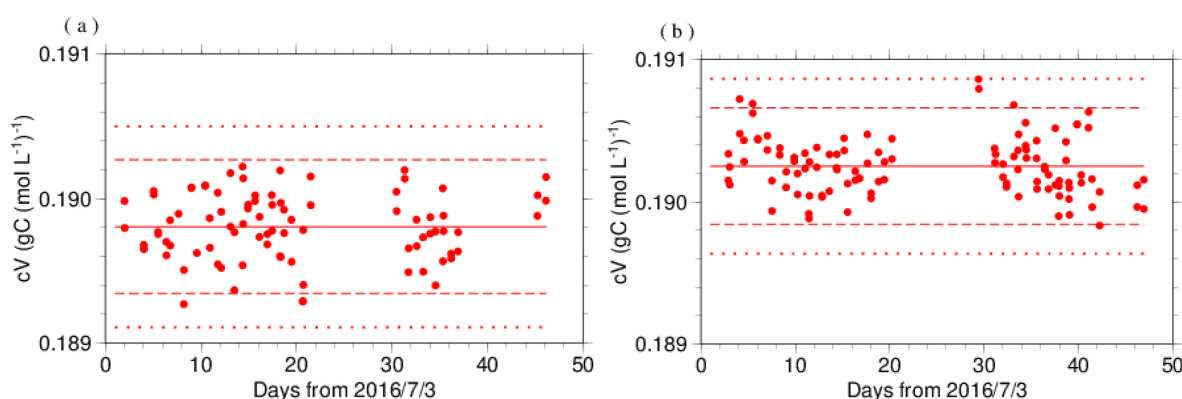


Figure 5.2.25. Results of the cV at each station assigned for apparatus (a) A and (b) B. The solid, dashed, and dotted lines denote the mean, the mean \pm twice the standard deviations, and the mean \pm thrice the standard deviations for all measurements, respectively.

The precision of the cV was equated to its coefficient of variation and was 0.122% for apparatus A and 0.108% for apparatus B. These precisions correspond to uncertainties of C_T of $2.5 \mu\text{mol kg}^{-1}$ and $2.2 \mu\text{mol kg}^{-1}$, respectively, in the standardization.

Finally, the value of C_T was multiplied by 1.00067 ($= 300.2/300.0$) to correct for the effect of dilution of the DIC concentration due to addition of 0.2 mL of mercury (II) chloride (HgCl_2) solution in a sampling bottle with a volume of ~ 300 mL.

d. Replicate and duplicate analyses

We took replicate and duplicate samples of DIC throughout the cruise. Table 5.2.16 summarizes results of the measurements with each apparatus. Figures 5.2.26–5.2.27 show details of the results. The calculation of the standard deviation from the difference of sets was based on a procedure (SOP 23) in DOE (1994).

Table 5.2.16. Summary of replicate and duplicate measurements. Unit is $\mu\text{mol kg}^{-1}$.

Measurement	Apparatus A	Apparatus B
	Average magnitude of difference \pm S.D.	
Replicate	2.2 ± 2.0 (N = 51)	1.4 ± 1.3 (N = 67)
Duplicate	2.1 ± 1.9 (N = 30)	1.7 ± 1.5 (N = 42)

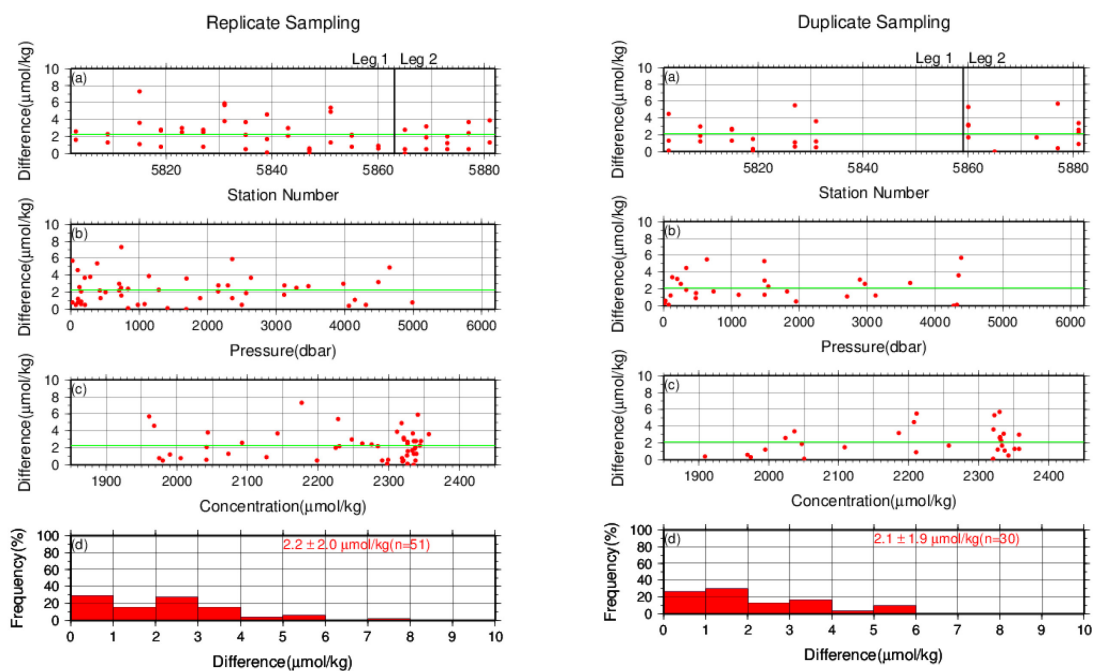


Figure 5.2.26. Results of (left) replicate and (right) duplicate measurements during the cruise versus (a) station number, (b) pressure, and (c) C_T determined by apparatus A. Green lines denote the average of the measurements. Bottom panels (d) show histograms of the measurements.

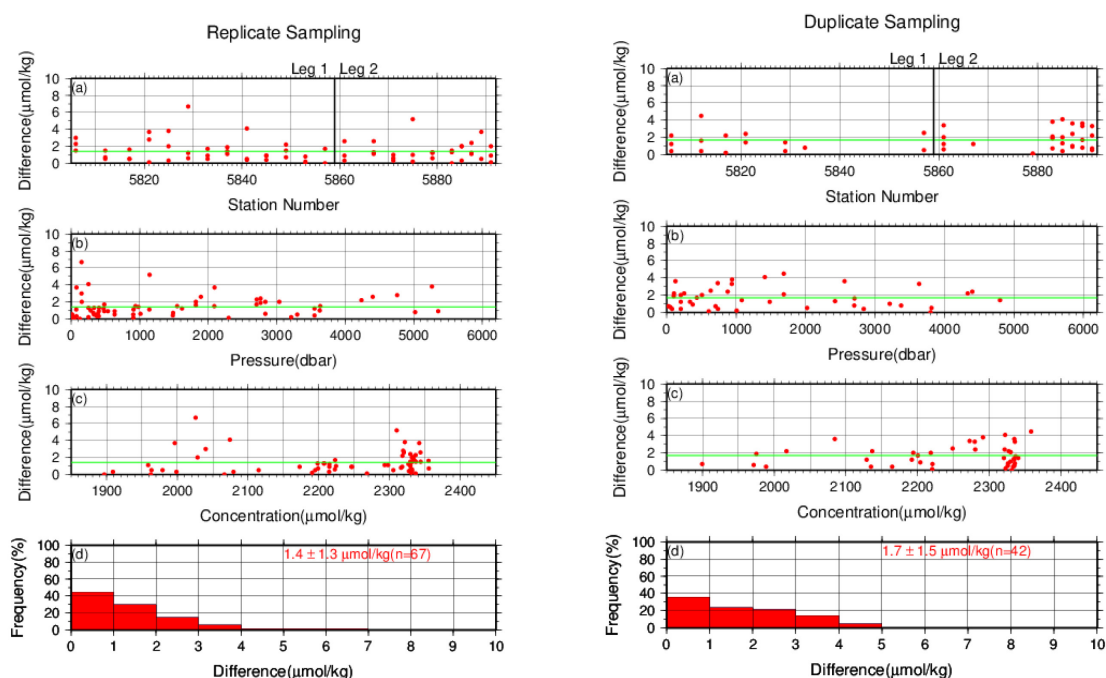


Figure 5.2.27. Same as Figure 5.2.26, but for apparatus B.

e. Measurements of CRMs and working reference materials

The precision of the measurements was monitored by using the CRMs and non-certified working reference materials bottled at our laboratory. The CRM (batch 150) and working reference material measurements were carried out at every station. In the measurements at a station, we measured the working reference material first and the CRM second. If the results of these measurements were confirmed as good, measurements on seawater samples were begun. At the end of a sequence of measurements at a station, another CRM bottle was measured. A CRM measurement was repeated twice from the same bottle. Table 5.2.17 summarizes the differences in the repeated measurements of the CRMs, the mean C_T of the CRM measurements, and the mean C_T of the working reference material measurements. Figures 5.2.28–5.2.30 show the detailed results.

Table 5.2.17. Summary of difference and mean of C_T in the repeated measurements of CRM and the mean C_T of the working reference material. These data are based on good measurements.

Unit is $\mu\text{mol kg}^{-1}$.

Apparatus	CRM	Working reference material	
	Average magnitude of difference \pm S.D.	Mean Ave. \pm S.D.	Mean Ave. \pm S.D.
A	2.6 ± 2.4 (N = 44)	2017.9 ± 2.0 (N = 88)	2081.6 ± 3.3 (N = 22)
B	1.7 ± 1.5 (N = 59)	2018.1 ± 2.2 (N = 118)	2082.0 ± 1.9 (N = 27)

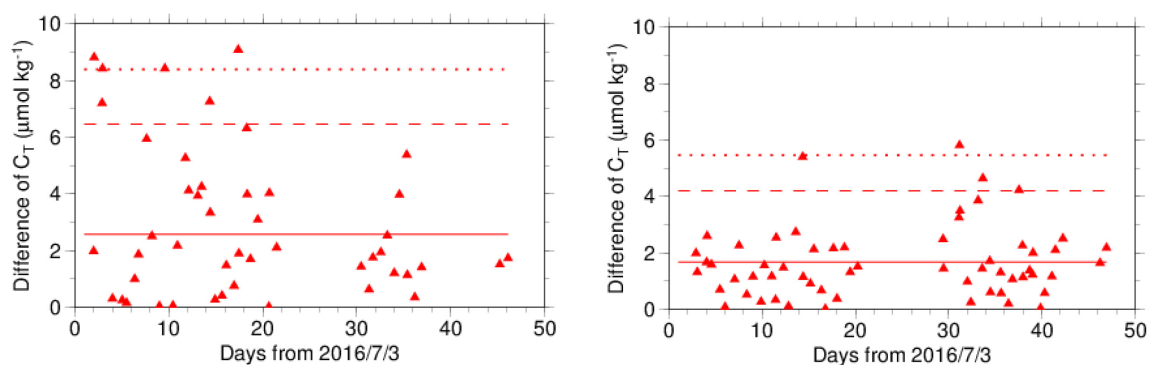


Figure 5.2.28. The absolute difference (R) of C_T in repeated measurements of CRM determined by apparatus A (left) and B (right). The solid line indicates the average of R (\bar{R}). The dashed and dotted lines denote the upper warning limit ($2.512\bar{R}$) and upper control limit ($3.267\bar{R}$), respectively (see Dickson et al., 2007).

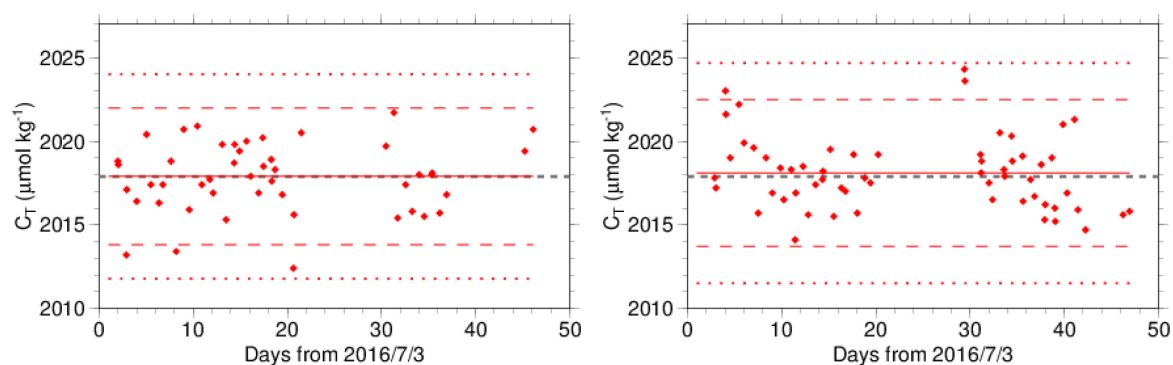


Figure 5.2.29. The mean C_T of measurements of CRM. The left (right) panel shows the results for apparatus A (B). The solid line indicates the mean of the measurements throughout the cruise. The dashed and dotted lines denote upper/lower warning limits (mean \pm 2S.D.) and upper/lower control limit (mean \pm 3S.D.), respectively. The gray dashed line denotes certified concentration of the DIC of CRM.

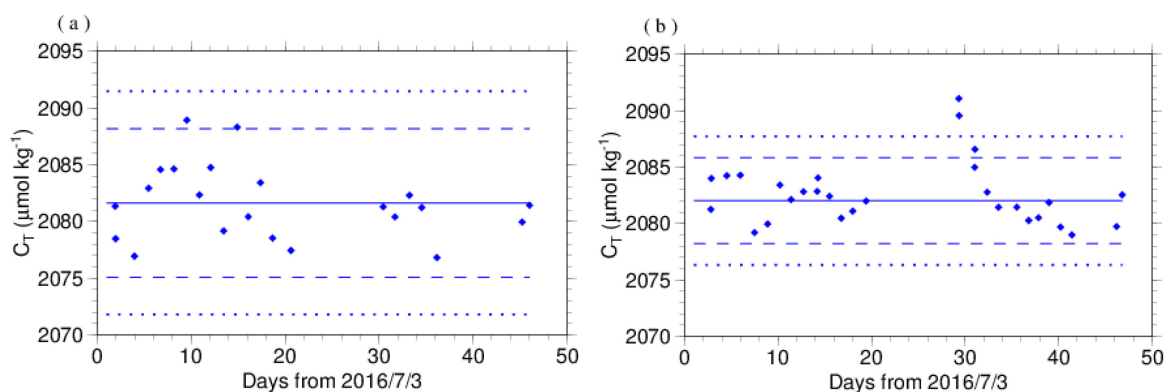


Figure 5.2.30. Calculated C_T of working reference material measured by apparatus (a) A and (b) B. The solid, dashed, and dotted lines are the same as in Figure 5.2.29.

f. Comparison with other CRMs

At every few stations, other CRM batches (140, 145, 147, and 155) were measured to provide comparisons with batch 150 to confirm the determination of C_T in our measurements. For these CRM measurements, C_T was calculated from the cV determined from batch 150 measurement. Figure 5.2.31 shows the difference between the certified and calculated C_T values.

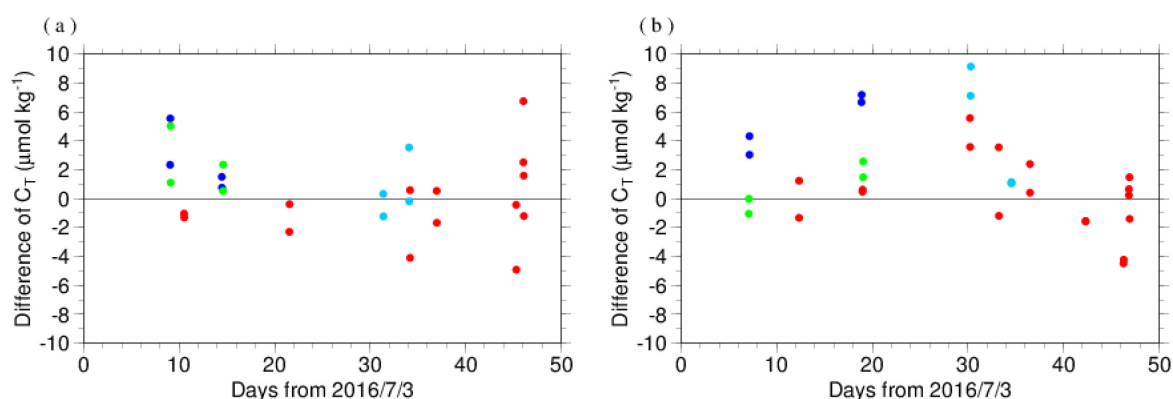


Figure 5.2.31. The differences between certified C_T and calculated C_T from batch 150 measurements. Left and right panels show the results for apparatus A and B, respectively. Colors indicate CRM batches: light blue: 140, blue: 145, green: 147, and red: 155.

g. Quality control flag assignment

A quality flag value was assigned to DIC measurements (Table 5.2.18) using the code defined in the IOCCP Report No.14 (Swift, 2010).

Table 5.2.18. Summary of assigned quality control flags.

Flag	Definition	Number of samples
2	Good	1383
3	Questionable	3
4	Bad (Faulty)	8
5	Not reported	0
6	Replicate measurements	118
Total number of samples		1512

5-2-5. Total Alkalinity (TA)

a. Instrument

The measurement of TA was carried out with DIC/TA analysers (Nihon ANS Co. Ltd., Japan). The methodology that these analysers use is based on an open titration cell. We concurrently used two analysers, designated as apparatus A and B.

b. Sampling and measurement

The procedure of seawater sampling of TA bottles and poisoning with mercury (II) chloride (HgCl_2) were based on the Standard Operating Procedure (SOP) described in PICES Special Publication 3 (Dickson et al., 2007).

TA measurement is based on a one-step volumetric addition of hydrochloric acid (HCl) to a known amount of sample seawater with prompt spectrophotometric measurement of excess acid using the sulfonephthalein indicator bromocresol green sodium salt (BCG) (Breland and Byrne, 1993). We used a mixed solution of HCl, BCG, and sodium chloride (NaCl) as reagent.

c. Standardization of HCl reagent

HCl reagents were prepared in our laboratory and divided into bottles (HCl batches). The concentrations of HCl in the bottles were determined using measured CRMs provided by Dr. Andrew G. Dickson of the Scripps Institution of Oceanography.

Table 5.2.19 provides information about the CRM batch used during this cruise.

Table 5.2.19. Certified concentration and uncertainty ($k = 2$) of CRM. Unit of TA is $\mu\text{mol kg}^{-1}$. More information is available at the NOAA web site (https://www.nodc.noaa.gov/ocads/oceans/Dickson_CRM/batches.html).

Batch number	150
TA	2214.71 ± 0.87
Salinity	33.343

The CRM measurement was carried out at every station. The apparent molarity of HCl_A of the titrant was determined from the certified concentration of CRM.

The value of HCl_A was assigned for each HCl batch for each apparatus, as summarized in Table 5.2.20 and detailed in Figure 5.2.32.

Table 5.2.20. Summary of assigned HCl_A for each HCl batch. The values reported are means and standard deviations. Unit is mmol L^{-1} .

Apparatus	Days	HCl Batch	HCl_A
A	2–9	A_1	49.9489 ± 0.0395 (N = 33)
	9–15	A_2	49.9847 ± 0.0303 (N = 34)
	15–21	A_3	49.9924 ± 0.0342 (N = 33)
	21–36	A_4	50.0075 ± 0.0213 (N = 32)
B	2–9	B_1	50.0684 ± 0.0401 (N = 35)
	9–16	B_2	50.0617 ± 0.0400 (N = 35)
	16–20	B_3	50.0652 ± 0.0235 (N = 17)
	20–36	B_4	50.0491 ± 0.0313 (N = 33)
	36–42	B_5	50.0937 ± 0.0390 (N = 33)

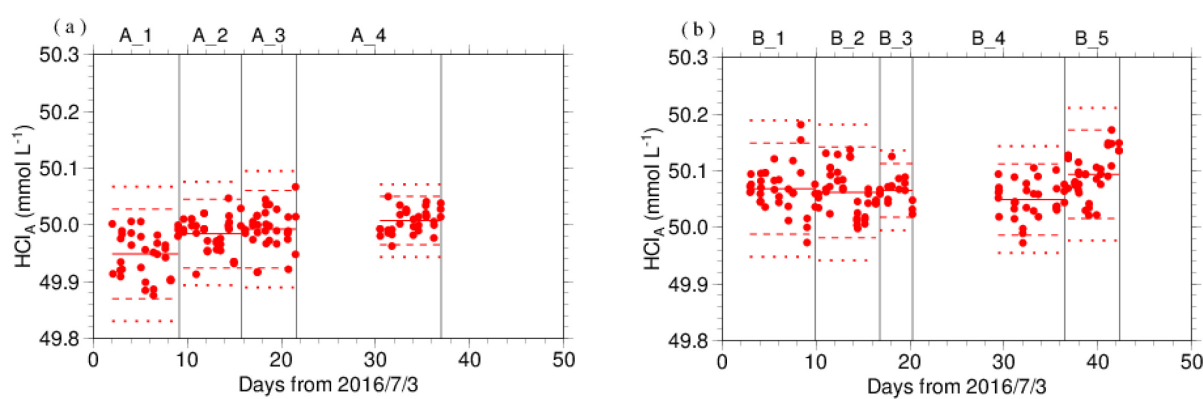


Figure 5.2.32. Results of HCl_A measured by (a) apparatus A and (b) B. The HCl batch name is indicated at the top of each graph, and vertical lines denote the day when the HCl batch was switched. The red solid, dashed, and dotted lines denote the mean and the mean \pm twice the standard deviations and thrice the standard deviations for each HCl batch, respectively.

The precisions of HCl_A , defined as the coefficient of variation, were 0.0427–0.0791% for apparatus A and 0.0470–0.0802% for apparatus B. They correspond to uncertainties of A_T of 0.99 – $1.84 \mu\text{mol kg}^{-1}$ and 1.09 – $1.87 \mu\text{mol kg}^{-1}$, respectively, in the standardization.

d. Replicate and duplicate analyses

We took replicate and duplicate samples of TA throughout the cruise. Table 5.2.21 summarizes results of the measurements by each apparatus. Figures 5.2.33–5.2.34 show detailed results. The calculation of the standard deviation from the difference of sets was based on a procedure (SOP 23) in DOE (1994).

Table 5.2.21. Summary of replicate and duplicate measurements. Unit is $\mu\text{mol kg}^{-1}$.

Measurement	Apparatus A	Apparatus B
	Average magnitude of difference \pm S.D.	
Replicate	0.7 ± 0.6 (N = 54)	1.0 ± 0.9 (N = 68)
Duplicate	0.9 ± 0.9 (N = 29)	1.1 ± 1.1 (N = 42)

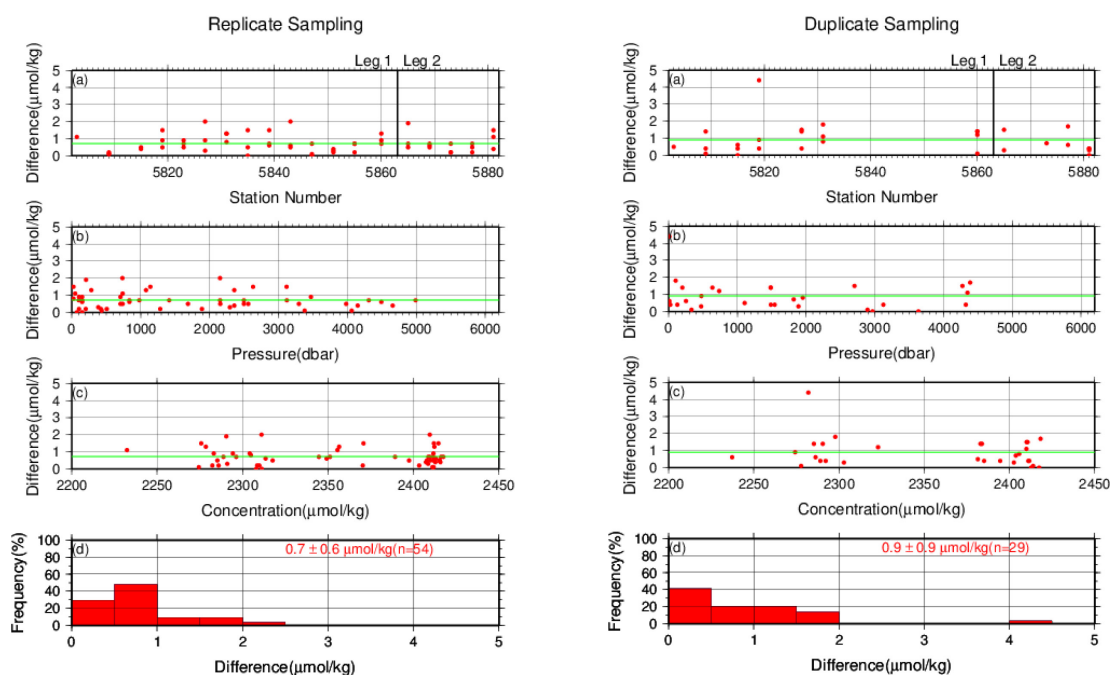


Figure 5.2.33. Results of (left) replicate and (right) duplicate measurements during the cruise against (a) station number, (b) pressure, and (c) equivalents of TA determined by apparatus A. Green lines denote the averages of the measurements. Bottom panels (d) show histograms of the measurements.

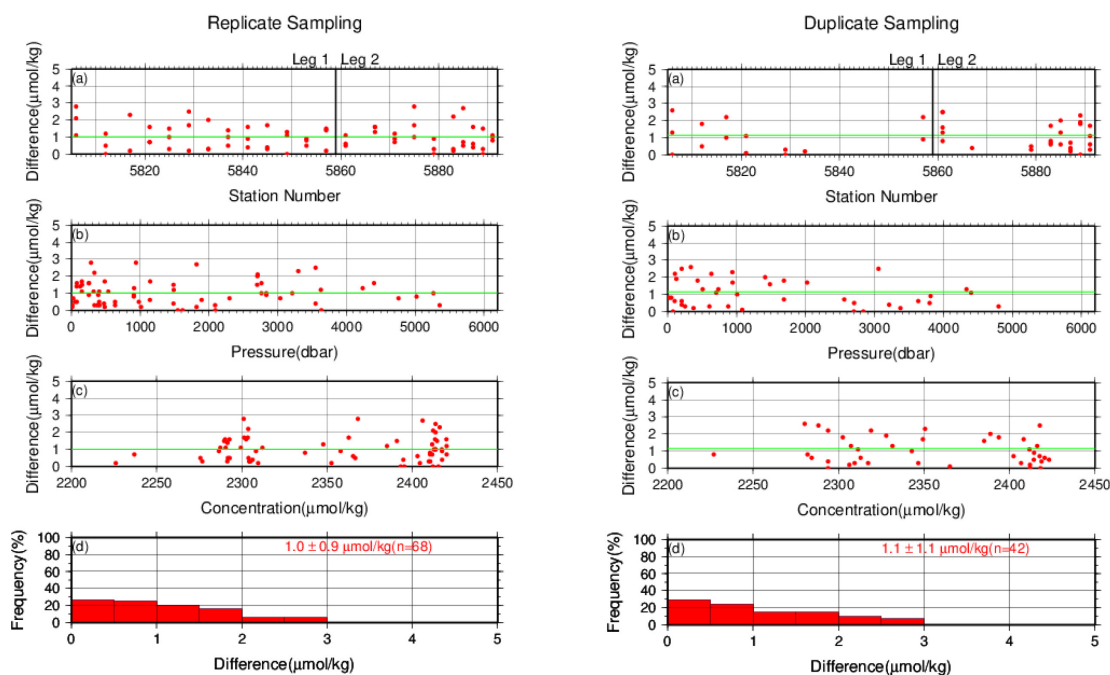


Figure 5.2.34. Same as Figure 5.2.33, but by apparatus B.

e. Measurement of CRMs and working reference materials

The precision of measurements was monitored by using the CRMs and non-certified working reference materials bottled in our laboratory. The measurements of the CRMs and working reference materials were the same as those used to measure DIC, except that the CRM measurement was repeated 3 times from the same bottle. Table 5.2.22 summarizes the differences in the repeated measurements of CRM, the mean A_T of the CRM measurements, and the mean A_T of working reference material measurements. Figures 5.2.35–5.2.37 show details.

Table 5.2.22. Summary of difference and mean of A_T in the repeated measurements of CRM, and mean of A_T of the working reference material. These data are based on good measurements. Unit is $\mu\text{eq kg}^{-1}$.

Days	HCl Batches	CRM		Working reference material
		Average magnitude of difference \pm S.D.	Mean Ave. \pm S.D.	Mean Ave. \pm S.D.
2–9	A_1	1.5 ± 1.2 (N = 10)	2214.7 ± 1.6 (N = 39)	2282.8 ± 1.6 (N = 5)
9–15	A_2	0.9 ± 0.8 (N = 10)	2214.7 ± 1.2 (N = 36)	2285.3 ± 1.3 (N = 6)
15–21	A_3	2.0 ± 1.6 (N = 11)	2214.7 ± 0.7 (N = 33)	2284.6 ± 0.5 (N = 3)
21–36	A_4	0.9 ± 0.7 (N = 10)	2214.7 ± 0.8 (N = 33)	2285.1 ± 1.0 (N = 5)
2–9	B_1	1.4 ± 1.1 (N = 11)	2214.7 ± 1.6 (N = 36)	2282.4 ± 3.0 (N = 5)
9–16	B_2	0.8 ± 0.7 (N = 11)	2214.7 ± 1.8 (N = 36)	2285.9 ± 2.8 (N = 6)
16–20	B_3	0.8 ± 0.7 (N = 6)	2214.7 ± 0.9 (N = 18)	2285.5 ± 0.4 (N = 3)
20–36	B_4	1.3 ± 1.0 (N = 11)	2214.3 ± 1.8 (N = 36)	2284.4 ± 1.4 (N = 7)
36–42	B_5	1.4 ± 1.1 (N = 11)	2214.7 ± 1.6 (N = 33)	2285.0 ± 1.7 (N = 5)

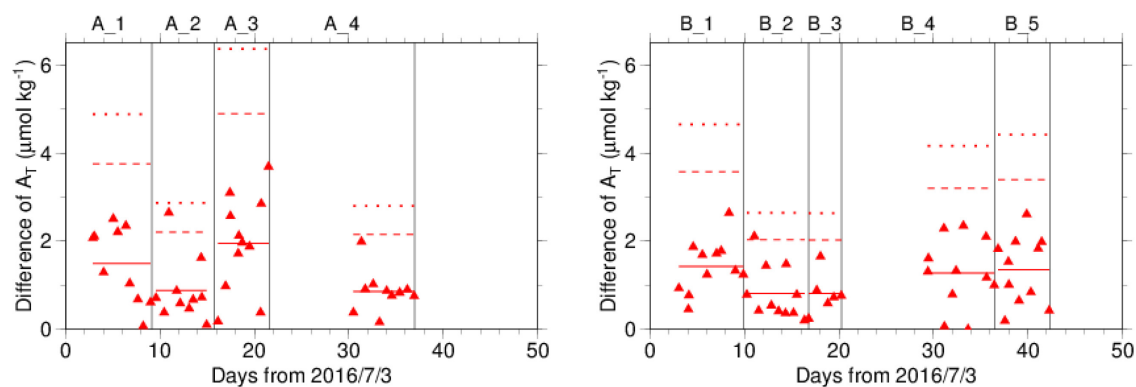


Figure 5.2.35. The absolute difference (R) of A_T in repeated measurements of CRM determined by apparatus A (left) and B (right). The solid line indicates the average of R (\bar{R}). The dashed and dotted lines denote the upper warning limit ($2.512\bar{R}$) and upper control limit ($3.267\bar{R}$), respectively (see Dickson et al., 2007).

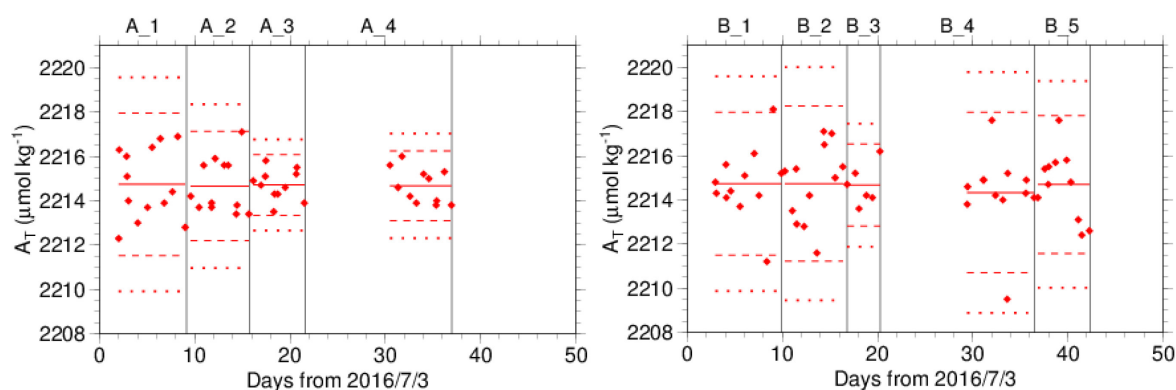


Figure 5.2.36. The mean A_T of measurements of CRM. Left (right) panel shows the results for apparatus A (B). The solid line indicates the mean of the measurements. The dashed and dotted lines denote the upper/lower warning limit (mean \pm 2S.D.) and upper/lower control limit (mean \pm 3S.D.), respectively. The labels at the top of the graph and vertical lines have the same meaning as in Figure 5.2.32.

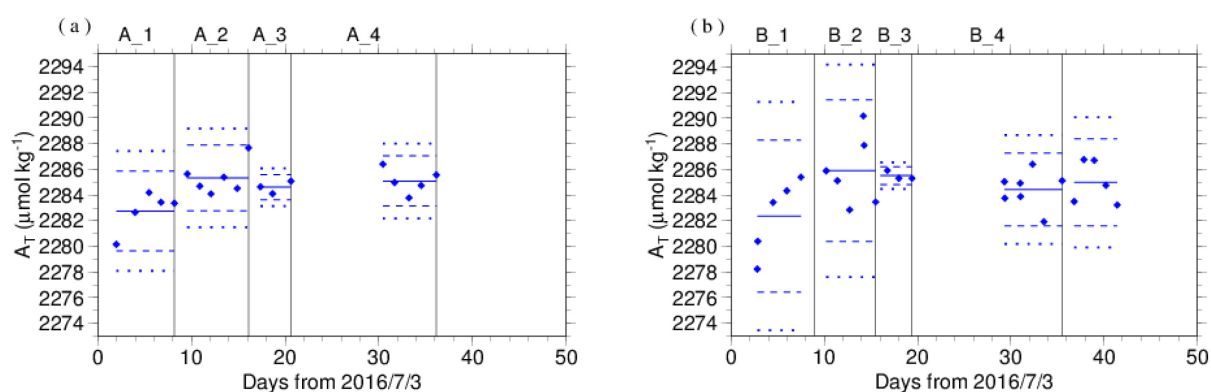


Figure 5.2.37. Calculated A_T of working reference material measured by (a) apparatus A and (b) B. The solid, dashed, and dotted lines have the same meaning as in Figure 5.2.36. The labels at the top of the graph and vertical lines have the same meaning as in Figure 5.2.32.

f. Comparisons with other CRMs

Every few stations, other CRM batches (140, 145, 147, and 155) were measured to provide comparisons with batch 150 and to confirm the determination of A_T in our measurements. For these CRM measurements, A_T was calculated from HCl_A determined by batch 150 measurement. Figure 5.2.38 shows the differences between the certified and calculated A_T .

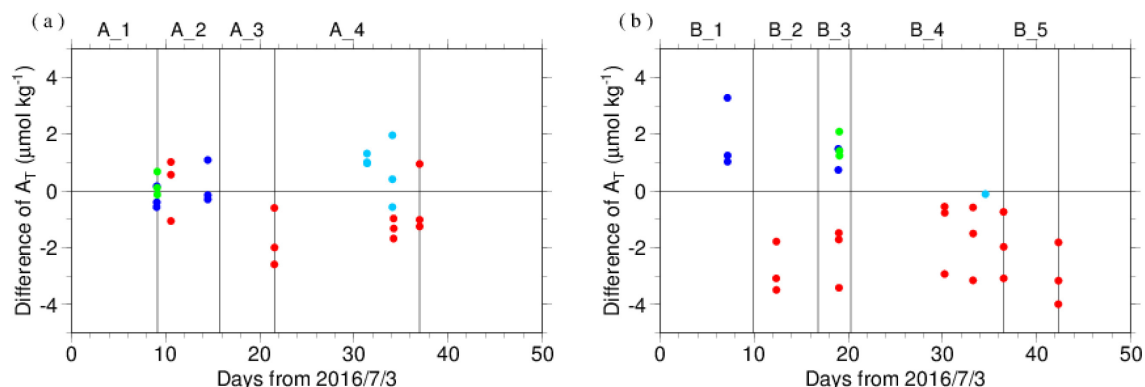


Figure 5.2.38. The differences between the certified A_T and calculated A_T from batch 150 measurements. The panels show the results for (a) apparatus A and (b) B. The labels at the top of the graph and vertical lines have the same meaning as in Figure 5.2.32. Colors indicate CRM batches; light blue: 140, blue: 145, green: 147, and red: 155.

g. Quality control flag assignment

A quality flag value was assigned to the TA measurements (Table 5.2.23) using the code defined in IOCCP Report No.14 (Swift, 2010).

Table 5.2.23. Summary of assigned quality control flags.

Flag	Definition	Number of samples
2	Good	1362
3	Questionable	19
4	Bad (Faulty)	9
5	Not reported	0
6	Replicate measurements	122
Total number of samples		1512

5-2-6. pH

a. Instrument

The measurement of pH was carried out with a pH analyzer (Nihon ANS Co. Ltd, Japan).

b. Sampling and measurement

Methods of seawater sampling, spectrophotometric measurements using the indicator dye *m*-cresol purple (hereafter *m*CP), and calculation of pH_T (on the total hydrogen ion scale) were based on Saito *et al.* (2008). Finally, pH_T was reported as the value at a temperature of 25°C.

c. Replicate and duplicate analyses

We took replicate and duplicate samples for pH determination throughout the cruise. Table 5.2.24 summarizes the results of the measurements. Figure 5.2.39 shows details of the results. The calculation of the standard deviation from the difference of sets of measurements was based on a procedure (SOP 23) in DOE (1994).

Table 5.2.24. Summary of replicate and duplicate measurements of pH.

Measurement	Average magnitude of difference \pm S.D.
Replicate	0.0016 \pm 0.0015 (N = 125)
Duplicate	0.0017 \pm 0.0015 (N = 73)

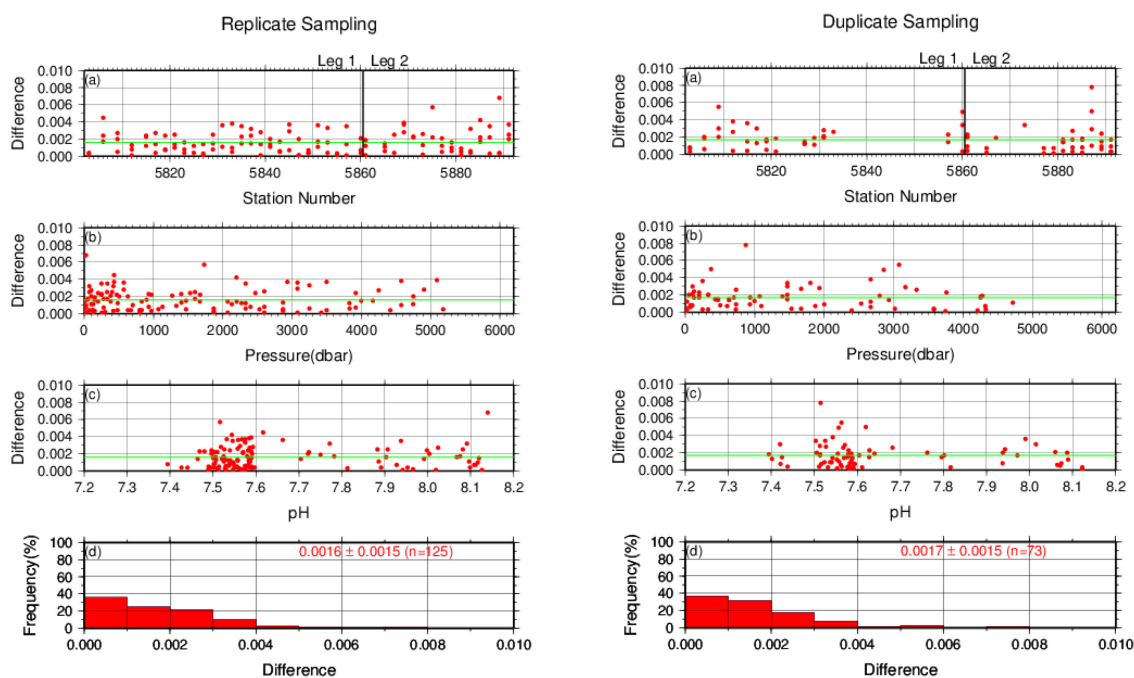


Figure 5.2.39. Results of (left) replicate and (right) duplicate measurements during the cruise versus (a) station number, (b) pressure, and (c) pH. Green lines denote the averages of the measurements. Bottom panels (d) show histograms of the measurements.

d. pH measurements of CRM and working reference materials

The precision of the measurements was monitored by using the CRMs and a non-certified working reference material bottled in our laboratory. Although the pH value of the CRM was not defined, it could be calculated from certified parameters (https://www.nodc.noaa.gov/ocads/oceans/Dickson_CRM/batches.html) based on the chemical equilibrium of the DIC system. The pH of the CRM (batch 150) so calculated was estimated to be 7.8807. Working reference material measurements were carried out first at every station. If the results of the measurements were estimated to be good, sampling was begun. CRM (batch 150) measurements were done at every few stations. One measurement was made from a bottle for sample analysis and two measurements were made from a bottle for CRM.

The pH_T of a CRM and a working reference material was immediately calculated with provisional coefficients estimated from the first station to the given station. Table 5.2.25 summarizes the difference and mean of the pH_T values between two measurements from a CRM bottle and the pH_T value from a working reference material. Figures 5.2.40–5.2.42 show detailed results.

Table 5.2.25. Summary of difference and means of the pH_T values for two measurements from a CRM bottle, and mean of pH_T from a working reference material, which was calculated with data with the exception of questionable or bad data.

Days	mCP Batches	CRM	Working reference material	
		Magnitude of difference Ave. \pm S.D.	Mean Ave. \pm S.D.	Mean Ave. \pm S.D.
2–9	1	0.0016 \pm 0.0013 (N = 8)	7.8768 \pm 0.0020 (N = 8)	7.8607 \pm 0.0026 (N = 17)
9–21	2	0.0010 \pm 0.0009 (N = 7)	7.8769 \pm 0.0024 (N = 7)	7.8614 \pm 0.0020 (N = 20)
21–40	3	0.0013 \pm 0.0011 (N = 6)	7.8751 \pm 0.0024 (N = 6)	7.8606 \pm 0.0018 (N = 21)

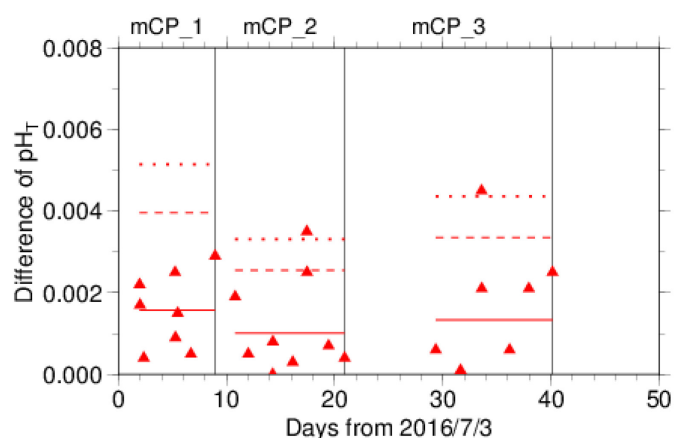


Figure 5.2.40. Difference of pH_T between two measurements of a CRM bottle. The *mCP* batch name is shown above the graph, and vertical lines denote the day *mCP* batches were changed. The solid, dashed, and dotted lines denote the average range (\bar{R}), upper warning limit ($2.512\bar{R}$), and upper control limit ($3.267\bar{R}$) for each *mCP* batch bottle, respectively (see Dickson et al., 2007).

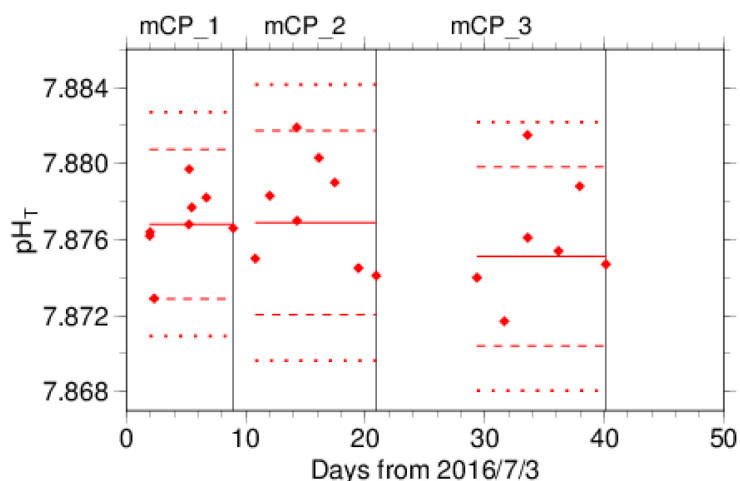


Figure 5.2.41. Mean of pH_T values between two measurements of a CRM bottle. The *mCP* batch name is shown above the graph, and vertical lines denote the day when the *mCP* batch was changed. The solid, dashed, and dotted lines denote the mean, upper/lower warning limit (mean \pm 2S.D.), and upper/lower control limit (mean \pm 3S.D.) for each *mCP* batch bottle, respectively (see Dickson et al., 2007).

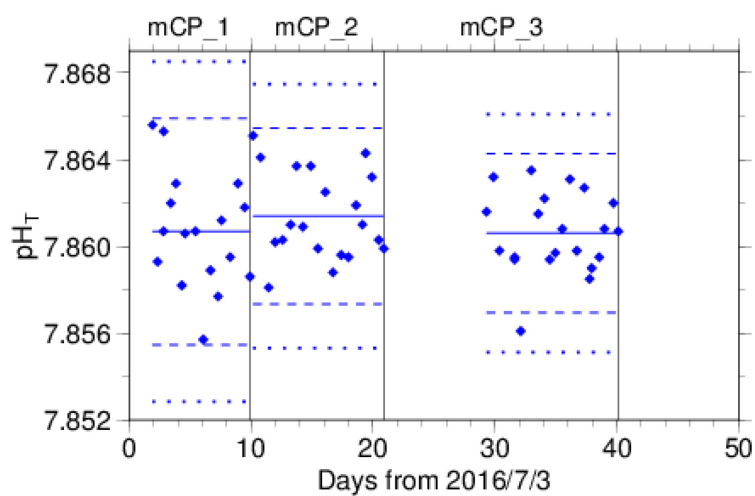


Figure 5.2.42. Same as Figure 5.2.41, but for the mean pH_T of the working reference material.

e. Quality control flag assignment

A quality flag value was assigned to pH measurements (Table 5.2.26) using the code defined in IOCCP Report No.14 (Swift, 2010).

Table 5.2.26. Summary of assigned quality control flags.

Flag	Definition	Number of samples
2	Good	1381
3	Questionable	3
4	Bad (Faulty)	8
5	Not reported	0
6	Replicate measurements	120
Total number of samples		1512

5-3. Quality control for trace metals in seawater during the R.V. Hakuho Maru KH-09-5 cruise (AORI, University of Tokyo)

GEOTRACES is an international research project with the goal of improving understanding of biogeochemical cycles in the ocean. The Japan GEOTRACES group carried out a GEOTRACES section cruise in the Indian Ocean during cruise KH-09-5 of the R.V. Hakuho Maru (Principle Investigator: Dr. Toshitaka Gamo). The group also performed quality control of the trace metal data in accord with the GEOTRACES guide, whose latest version is indicated in Figure 5.3.1.

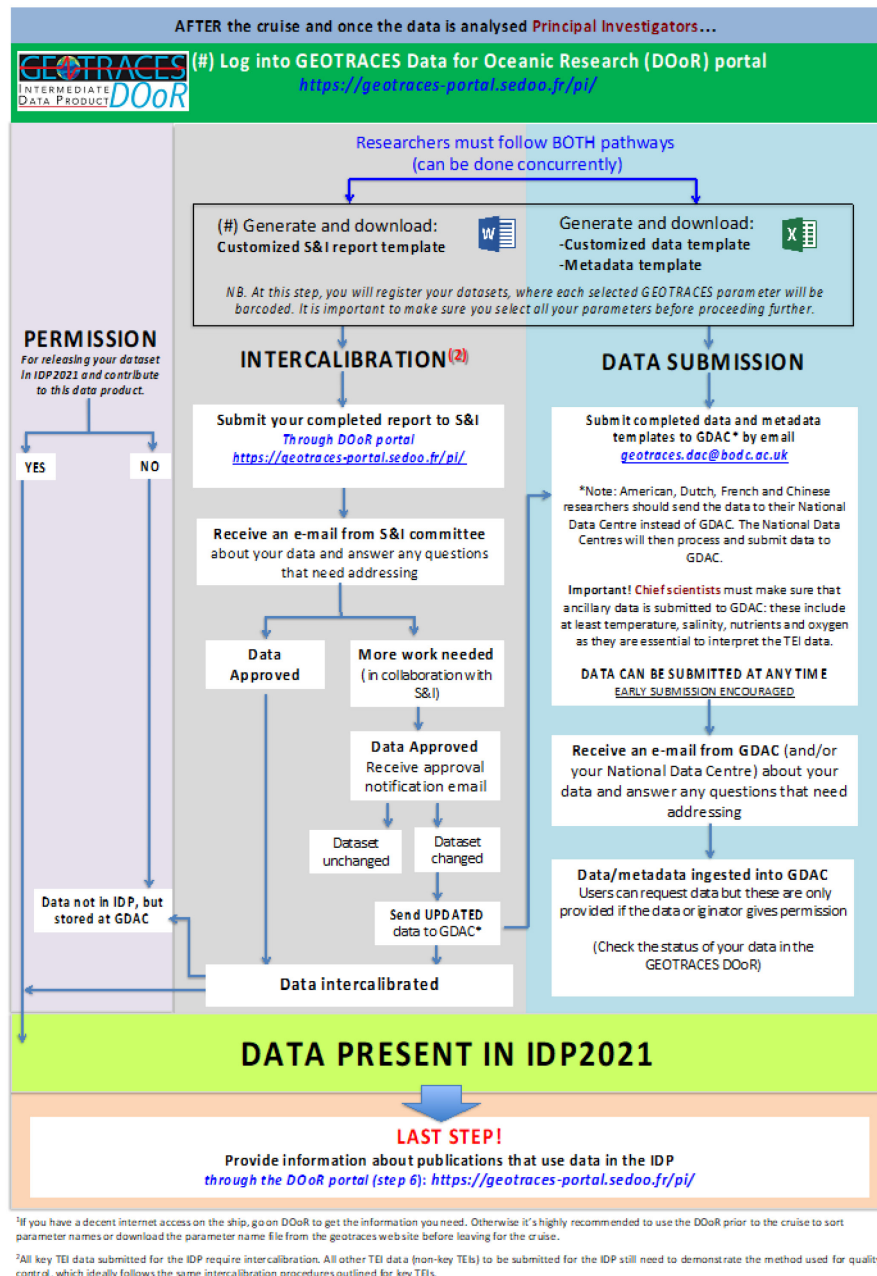


Figure 5.3.1. Flow chart of data submission for GEOTRACES, cited from the webpage (<https://www.geotraces.org/how-to-ensure-that-your-data-are-in-idp-flow-chart/>).

Before the cruise, the scientists were required to submit a pre-cruise metadata sheet (<https://www.bodc.ac.uk/geotraces/cruises/documentation/>).

After the cruise, the scientists were submitted a cruise report (Gomo, 2010).

5-3-1. Metadata

- Sampling

The sampling procedure has been briefly described in Guideline of Ocean Observations Volume 2, Chapter 1. Detailed sampling methods are also described in the GEOTRACES “cookbook”, published on the web site (<http://www.geotraces.org/images/Cookbook.pdf>).

- Analysis

The analytical methods have been described in the post-cruise metadata (Appendix II-3) for the KH-09-5 cruise. The detection limit and the blank measurement values should be included in the analytical methods. Analytical results of reference seawater samples (Guideline of Ocean Observations Volume 3, Chapter 3) should also be reported in the post-cruise metadata.

5-3-2. Intercalibration

The trace metal data are expected to be published in “Intermediate Data Product of GEOTRACES (IDP)”. The data must be intercalibrated. The details of the intercalibration are described in Figure 5.3.2.

How does the GEOTRACES S&I committee assess data quality for IDP2017?

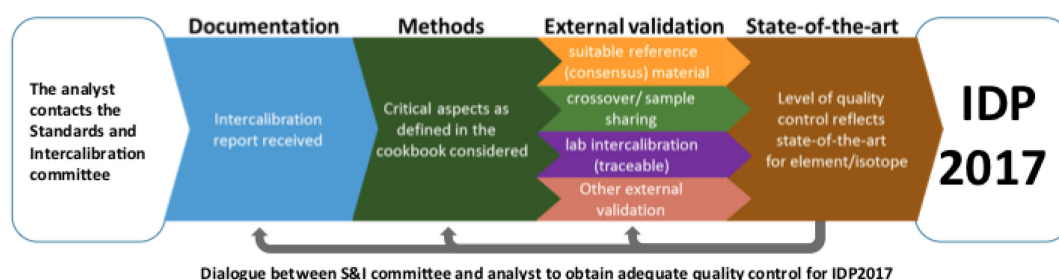


Figure 5. 3. 2. Schematic concept of intercalibration process for GEOTRACES data. This figure was prepared for data submission to IDP2017(cited from the website, http://www.geotraces.org/images/stories/documents/intercalibration/2017_SI_Flowchart.jpg).

First, we have to submit the post-cruise metadata, including sampling and analytical methods. During the GEOTRACES section cruise, it was recommended that at least one crossover station be occupied. If the data from other laboratories at the crossover station are available, we can compare and evaluate our data at the crossover station. Because there was no crossover station during the KH-09-5 cruise, we collected seawater samples at six depths in replicate at one station and distributed the samples from these intercalibration depths to another laboratory in Taiwan for trace metal determinations.

Because we submitted the post-cruise metadata and intercomparison data, our data during the KH-09-5 cruise were included in the GEOTRACES 2014 Intermediate Data Product (The GEOTRACES Group, 2015).

5-4. General procedure of quality control flag assignment

To distinguish between flags of 2, 3, and 4 for water sample measurements, we need followed the flagging procedure in general as below:

- a. Concentration of bottle sample water at the sampling layer was plotted against sampling pressure. Any points not lying on a generally smooth trend were noted.
- b. Vertical sections against pressure and potential density were drawn. If a datum was anomalous on the section plots, the datum flag was degraded from 2 to 3, or from 3 to 4.
- c. If there was a problem in the measurement, the datum was flagged 4.
- d. If the bottle flag was 4 (did not trip correctly), the datum was flagged 4 (bad). In case the bottle flag was 3 (leaking) or 5 (unknown problem), the datum was flagged based on steps a, b and c.

It is also very important, when assessing data, to look through the whole suite of data collected concurrently with "suspect" data. An error in drawing an sample, or an error in a single chemical analysis, will have a much different signature in the overall data set than would an error due to a leaky or mistripped bottle, or a genuine seawater anomaly. One of the most important considerations in assessing a water sample is determining the actual level (from what actual pressure) the water in the Niskin bottle represents. Consider that did the bottle close early or late and the bottle showed leak. Yet leaking, improperly closed, and late/early closed bottles are one of the leading causes of errors in water sample data, and not always easy to find.

There is no single QC method for trace metals, such as for hydrographic data. We initially checked whether the results of replicate samples were reasonable compared with the analytical precision. It has also been recommended that subsamples be measured every 10 samples to check for possible drift of the instrumental sensitivity and sudden contamination. If any data were questionable, we re-analyzed the samples.

Great care must be taken to avoid contamination, especially during sampling, filtration, and measurement. During sampling and filtration, it is important to check the concentrations of contamination-prone trace metals like Fe and Zn in the same water sample. During the KH-09-5 cruise, we did not detect any obvious contamination during sampling and filtration.

6. Quality control by 2D/3D property-property plots by Ocean Data View

6-1. Recommended softwares

Quality control with a control chart and duplicate measurements can provide an immediate alert of a problem just after a measurement. To visualize property-property characteristics, we need appropriate applications that enable visualization of 2D and/or 3D property-property plots.

At this moment the authors recommend use of Ocean Data View (ODV), which is a free software package for the interactive exploration, analysis, and visualization of oceanographic and other geo-referenced profile, time-series, trajectory, or sequence data. ODV runs on Windows, Mac OS X, Linux, and UNIX (Solaris, Irix, AIX) systems. ODV data and configuration files are platform-independent and can be exchanged between different systems (<https://odv.awi.de/>, accessed 19 October 2019). ODV provides property/property plots of selected stations, scatter plots for sets of stations, color sections along arbitrary cruise tracks, colour distributions on general iso-surfaces, temporal evolution plots of tracer fields, differences of tracer fields between repeats, geostrophic velocity sections, animations, and interrupted maps.

Some oceanographers use Java OceanAtlas (<http://joa.ucsd.edu>, accessed on 19 March 2020), which predates ODV and has many similar capabilities. Java Ocean Atlas (JOA) is a multi-OS application for viewing and exploring ocean vertical profile data. Along with a broad collection of data, JOA is the culmination of a long dream: a collection of some of the most useful oceanographic section data from the World Ocean with a multi-platform computer application for exploring those data.

Also, other applications such as Matlab are in wide use (<https://sea-mat.github.io/sea-mat/> accessed on 19 March 2020). Time Series Tools, Mapping Tools, Hydrographic Tools, Data Interface Tools, Atmosphere and Other Tools are available.

6-2. 2D/3D property/property plot by ODV

In this section, we show comparison among historical data achieved in World Ocean Database, WOD and P6 cruises in 2003 and 2009. Property/property scatter plots generated with ODV for sets of stations in the South Pacific Ocean over a region from 32–35°S and 170–178°W in the South Pacific Ocean during the period from 1928 to 2017 are presented in this section. The data were downloaded from the WOD select web page at <https://www.nodc.noaa.gov/OC5/SELECT/dbsearch/dbsearch.html>.

The format of the downloaded data is compatible with ODV software, so it is very easy to handle the dataset.

We also show two examples from a part of the P06 line that was observed in 2003 and 2017.

We have prepared view files to present a map of stations, two vertical profiles of temperature and salinity, 3D property/property plots for salinity vs. temperature with phosphate as colour shading and phosphate vs. nitrate with oxygen as colour shading for long-term history. A plot of total carbon vs. nitrate with nitrate as colour shading has also been added for the 2003 cruise and 2017 cruise.

We can easily look at relationships among parameters using ODV software, as shown in Figures 6.1, 6.2, and 6.3. In general, if we look at a small region, we can assume that properties in the region are homogenous. For example, a phosphate vs. nitrate plot would be a sharp line, as shown in Figures 6.2

and 6.3. However, we do not see a sharp line for phosphate vs. nitrate in Figure 6.1. The implication is that the quality of phosphate and nitrate data in previous years was not good. We discuss this issue later in section 7. We can also see outliers in the oxygen vs. phosphate plot in Figure 6.1, but no similar outliers appear in Figures 6.2 and 6.3. The data suggest that on some cruises in the extensive WOD database, which contains data from many cruises, there unrecognized problems with phosphate measurements

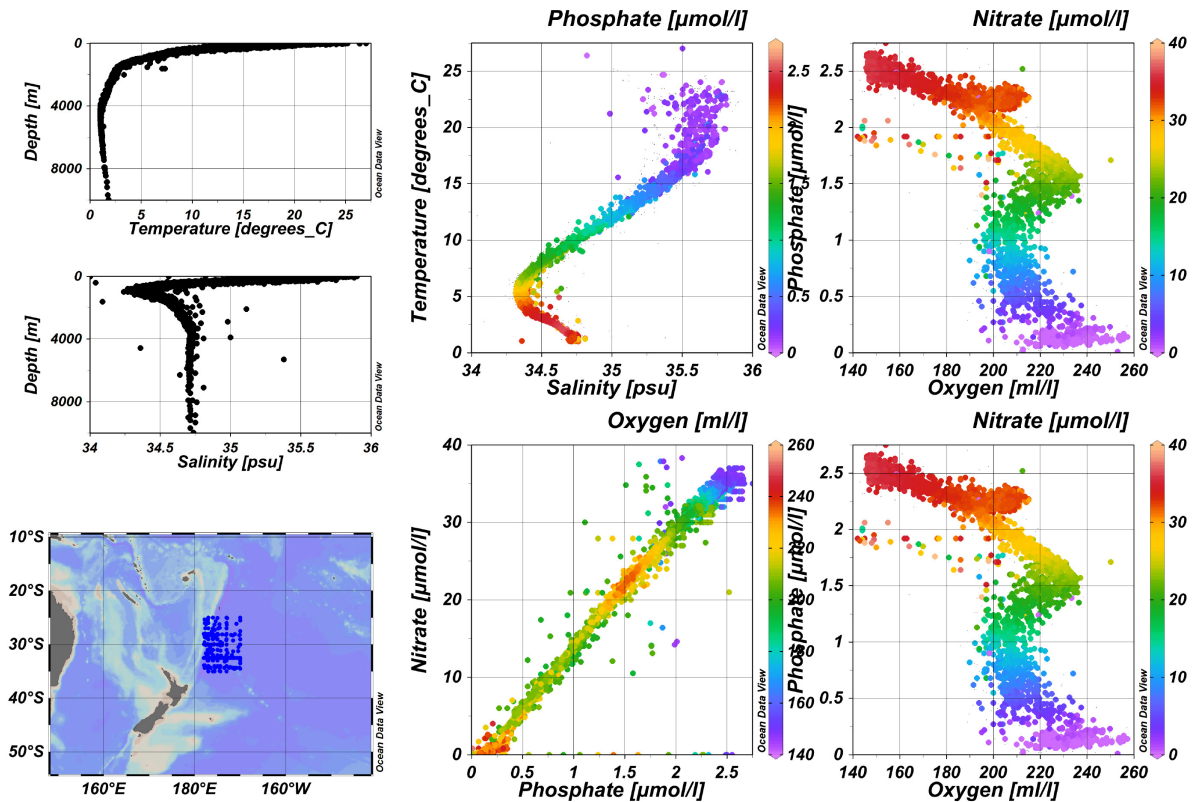


Figure 6.1. 2D/3D property/property plots from 1928 to 2017

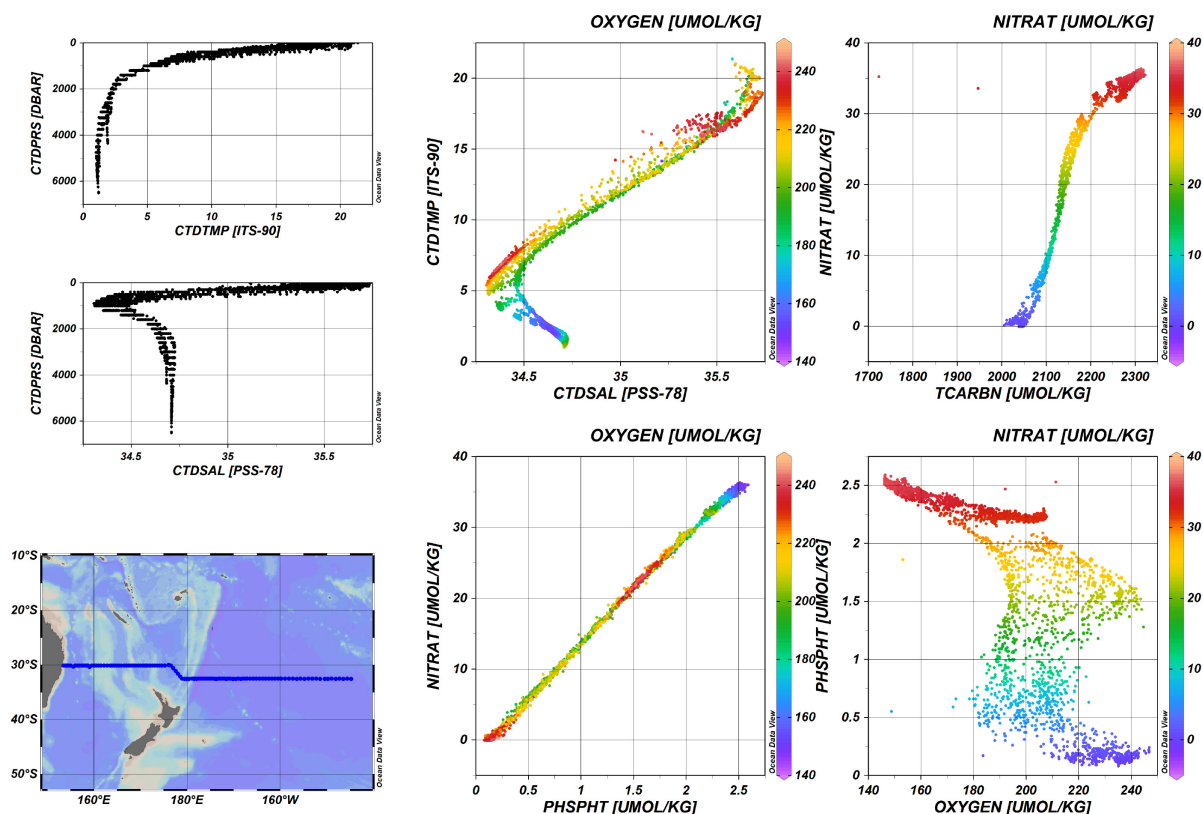


Figure 6.2. 2D/3D property/property plots for a part of P06 line obtained during 2003 by Japanese scientists.

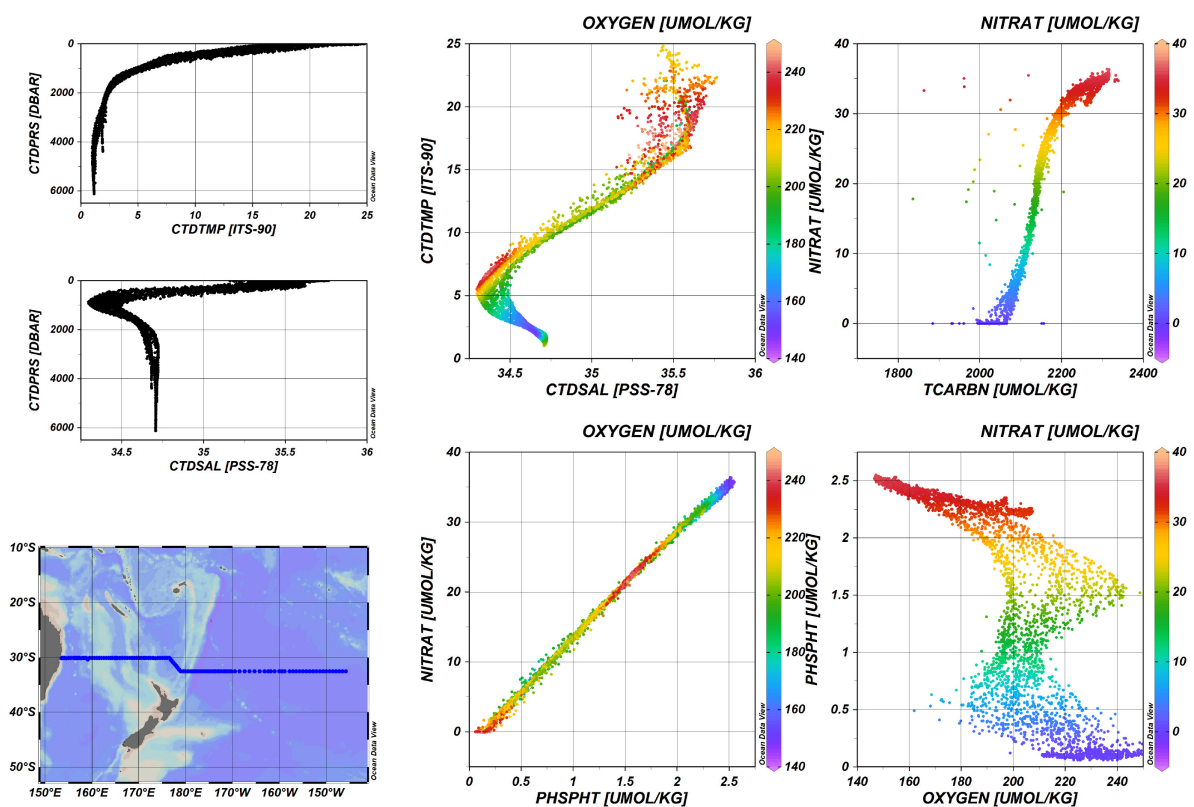


Figure 6.3. 2D/3D property/property plots of a part of P06 line in 2009 by U.S. scientists

Guideline of Ocean Observation Vol.1 Chap.4 Quality control by comparison with standards, control charts, duplicated measurements, and property-property characteristics, and the report of metadata ©Michio Aoyama, Hiroshi Uchida, Daisuke Sasano, Hajime Obata 2019 G104EN:001-134

7. History of a region, 32°–35°S and 178°–170°W, in the South Pacific Ocean: evidence of improvement of data quality by different organizations

Figure 7.1 shows a long-term history of reported phosphate concentration in the region bounded by 32–35°S and 170–178°W (the region of interest), in the South Pacific Ocean. We have data from 1928 to 2017. After 2003, phosphate concentrations were measured using RM or CRM. Vertical profiles in this region obtained in 2003 and 2017 therefore showed good consistency and showed the same patterns as vertical profiles in the region of interest (Figure 7.1), whereas vertical profiles obtained before 1980 were much more scattered, and concentrations were not consistent with those obtained after 2003. This is a good example of how good quality control, and especially the use of RM/CRM, can reveal more realistic characteristics of phosphate profiles.

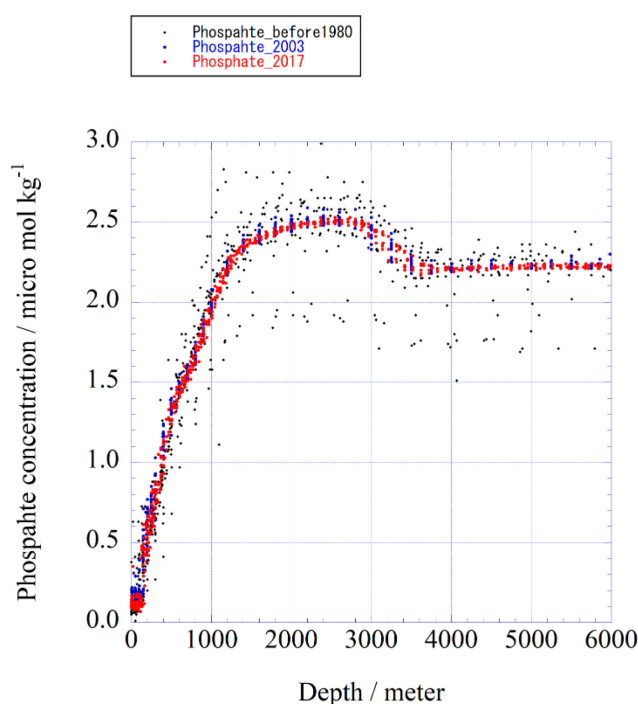


Figure 7.1. Reported phosphate concentration for samples collected deeper than 1900 m in the region of interest from 1928 to 2017

In addition to the history of phosphate concentrations, we observed that nitrate vs. phosphate for the same region but at depths greater than 1900 meters were also scattered before 1980, whereas the molar ratio of nitrate to phosphate of samples obtained after 2003 was almost constant at 14.32 ± 0.15 ($n = 901$), as shown in Figure 7.2.

The good quality control procedures articulated in Chapter 4 of Volume 1 of the Guideline of Ocean Observations surely resulted in a good quality dataset, as shown in this section as well as in the next section 8. These high quality datasets are the basis for scientific research into how the marine environment is changing or not. We believe that continuing to produce high quality datasets over the long term will be the basis of our research on marine environmental and climate change.

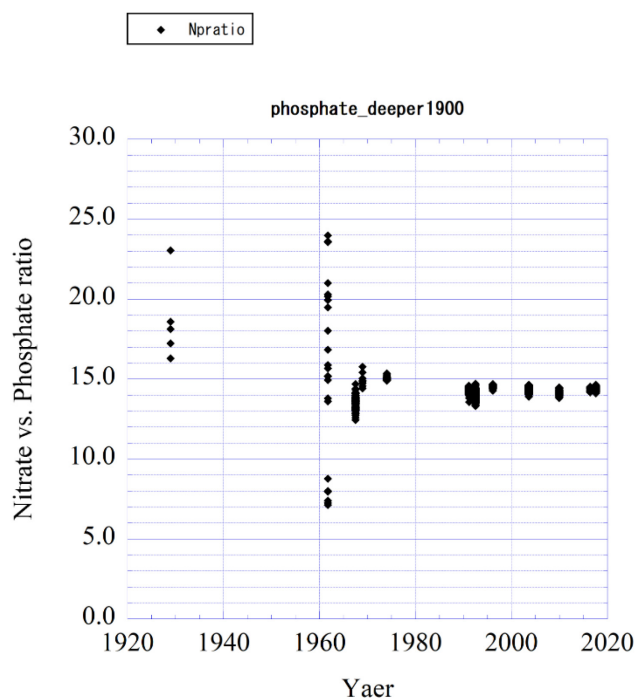


Figure 7.2 N:P atomic ratios based on reported nitrate and phosphate concentration for samples collected at depths greater than 1900 m in the region of interest from 1928 to 2017.

8. History along the P09 section: evidence of improvement of quality of data collected by the same organization

The JMA has measured nutrient concentrations in each layer and has reported the concentrations measured using in-house standard solutions. Since April 2010, nutrient CRMs (more than two concentrations) have been analysed at all stations to ensure comparability between cruises and stations. As a confirmation of the validity of the analysis, it has been confirmed that the result of the nutrient CRM analysis, which is obtained with a home-made standard solution prepared for each measurement station, is included in the uncertainty of the CRM certified value range. In addition, the same batch of CRM with more than one concentration level is continuously measured between cruises to maintain comparability between cruises. However, because the comparability is not ensured for the values given with the in-house standard solution, even if there is a difference in the analytical value between the measurement points and between the cruises, it is difficult to judge whether the difference depends on the analysis error or environmental fluctuation. This section gives examples of spatial and temporal variations of nitrate+nitrite (hereinafter referred to as nitrate), phosphate, and silicate from 1967 to 2017 along the 137°E longitude line (137°E line) monitored by the Japan Meteorological Agency. We then discuss the effect of ensuring traceability and comparability by correcting the values obtained with in-house standard solutions using nutrient CRMs. Nutrient data from April 2010 onwards are based on the relationship between the CRM analysis values of 2–4 concentrations analyzed at each measurement point and the certified values. The nutrient concentration was used after being corrected. Thereby, comparability and traceability could be ensured for the data within this period. Nutrient and dissolved oxygen uncertainties ($k = 2$) were calculated by Nakano (2010).

8.1 Comparability among stations

Figure 8.1 shows the N:P ratio cross-section of the 2016 P09 (137°E) re-visited cruise. Although the N:P ratio based on the inhouse standard solution prepared at each station did not fluctuate with depth, there was a slight gradient in the meridional direction. However, application of the CRM that ensured comparability among stations caused the gradient to disappear. This example means that the nutrient concentration based on in-house standard solutions might include systematic/random errors among stations, and the ability to perform analyses with relatively small uncertainties is not enough to ensure accuracy. In addition, the observational results that the N:P ratio was uniformly distributed in the latitudinal direction in the deep layer along the 137°E line was detected for the first time by using the nutrient CRM. Thus, scientific knowledge was obtained because of maintaining comparability and traceability.

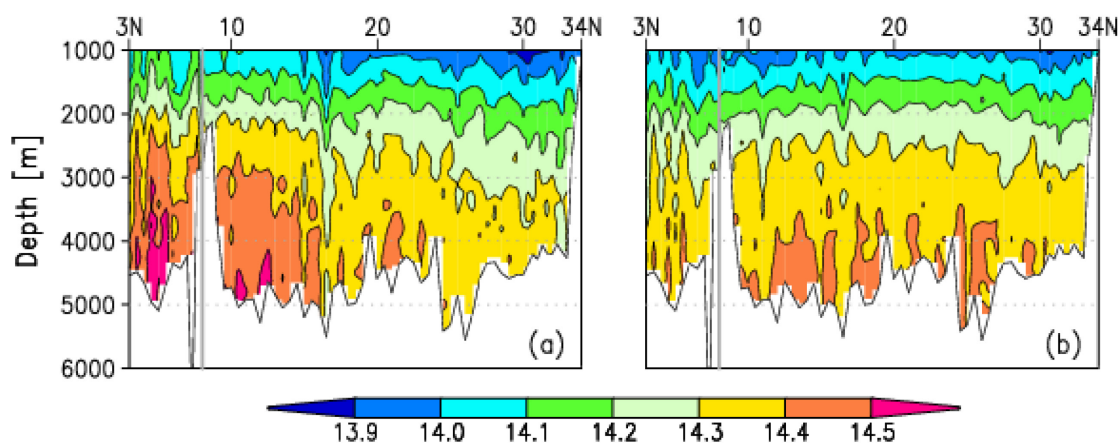


Figure 8.1. Vertical sections of atomic N:P ratio based on (a) in-house standard and (b) CRM below 1000 m along the 137°E section in July–August 2016. Gray line indicates boundary of legs. (This figure is reproduced from a figure in Current Situation and Future Perspective for Environmental Standards of Seawater: Commencing with Certified Reference Materials (CRMs) for Nutrients, Umi no kenkyuu, by permission of Oceanographic Society of Japan)

8.2 Comparability among cruises

Examination of the time series data at a depth of 2000 m, 20°–25°N of the 137°E line revealed almost no temporal variation in dissolved oxygen concentration (Figure 8.2). This result indicates that the natural variability/change of dissolved oxygen at a depth of 2000 m might be small, the analyses of dissolved oxygen concentrations have compared relatively well, and systematic errors between cruises have been relatively small. On the other hand, there have been relatively large variations in nutrient concentrations, especially in the data leading up to the 1980s. Considering that the Redfield ratio (N:P:O₂ = 16:1:170; Anderson and Sarmiento, 1994) is considered to reflect the average chemical composition of organisms in the ocean, the temporal variation of nutrient concentrations is obviously large. If the metric NO or PO reflects the relationship between nutrient concentrations and oxygen (NO = O₂ + NO₃ · 170/16, PO = O₂ + PO₄ · 170; Broecker, 1974) the Redfield ratio corrected by Anderson and Sarmiento (1994)) showed large variations during the same period. Because NO and PO are quasi-preserved components that do not change with photosynthesis or respiration, if nitrate and phosphate fluctuations depended on natural variations through biological activity, they should vary in the direction opposite to variations of oxygen. Another possibility is that there may be a bias from the Redfield ratio in area of interest, or the Redfield ratio and the NO and PO of the source water may change over time. However, because the dissolved oxygen concentration did not change, it is reasonable to judge that the temporal variation found in the old nutrient data was not a natural variation but a systematic error that depended on the magnitude of the analytical error.

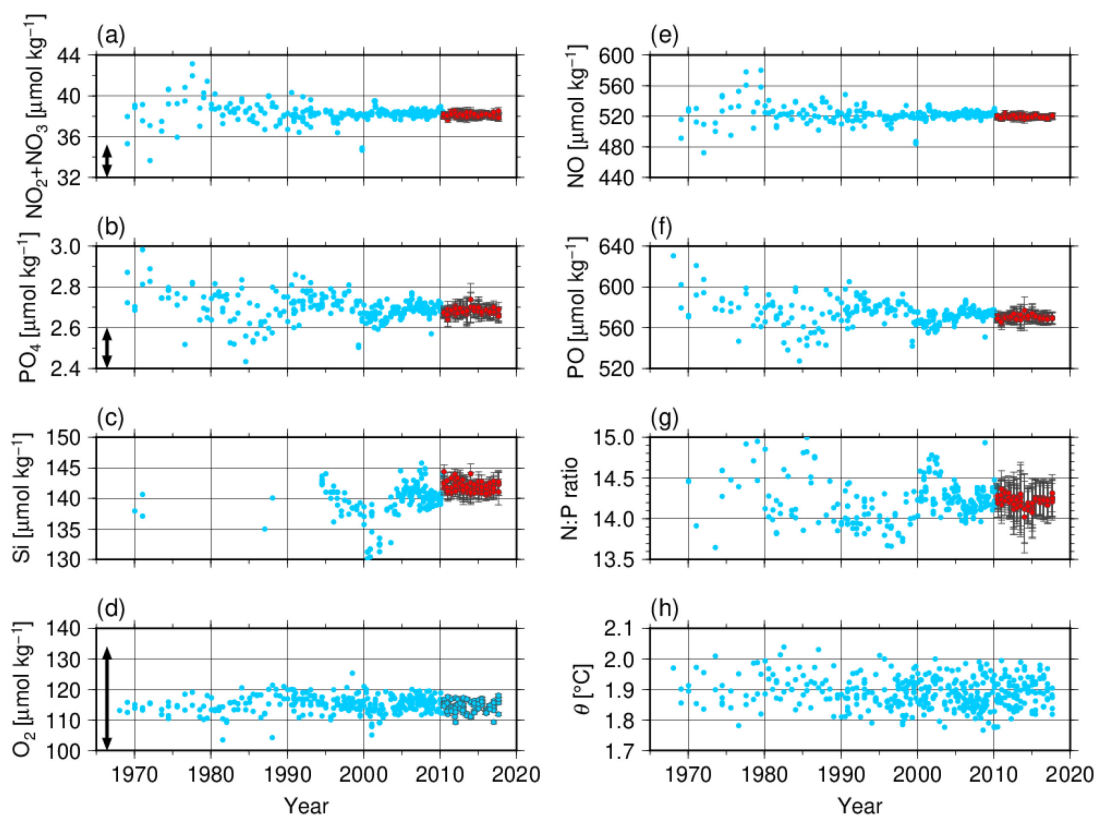


Figure 8.2. Time series of (a) nitrate+nitrite, (b) phosphate, (c) silicate, (d) dissolved O₂, (e) NO, (f) PO, (g) N:P atomic ratio, and (h) potential temperature at 2000 m at 20°–25°N along the 137°E section. Light blue and red symbols indicate in-house standard-based and CRM-based data, respectively. Error bars for some symbols denote uncertainty ($k = 2$). Arrows mean relationship of Redfield ratio among N:P:O₂ (Anderson and Sarmiento, 1994). (This figure is reproduced from a figure in Current Situation and Future Perspective for Environmental Standards of Seawater: Commencing with Certified Reference Materials (CRMs) for Nutrients, Umi no kenkyuu, by permission of Oceanographic Society of Japan)

Close examination of the variation of dissolved oxygen reveals that the data after 2010 show small fluctuations of $\sim 5 \mu\text{mol kg}^{-1}$. Because the uncertainty of the oxygen measurement was small ($\sim 0.5 \mu\text{mol kg}^{-1}$ ($k = 2$) for a dissolved oxygen concentration of $120 \mu\text{mol kg}^{-1}$), this variation is a statistically significant difference. However, this uncertainty is based on the KIO₃ standard, which is the standard solution for oxygen analysis, and not an O₂ standard itself. This variation of O₂ is significantly correlated with the water temperature, so there is no doubt that natural variation contributes. However, a systematic error in analysis due to the lack of comparability among stations and cruises should be considered. Development of certified reference materials for dissolved oxygen is therefore needed to evaluate the changes of dissolved oxygen concentration changes in an appropriate scientific manner.

8.3 Use of nutrient CRMs

Examination of the nutrient concentration time-series data reveals that the accuracy of the analyses has improved since the 1990s when WOCE observations were carried out (Figure 8.2). Since 2000, the accuracy of nutrient analysis has further improved. This improvement is clear from the fact that the magnitude of temporal fluctuations in nutrients has approached that of dissolved oxygen concentrations. Furthermore, after 2010, nutrient concentrations have been corrected with CRMs, and all nutrient components have been consistent within uncertainty. It should be noted that the values have been consistent not only in quasi-preserved components such as NO and PO, but also in silicates and N:P ratios. These results indicate that there has been no significant change in nutrient concentrations or their derived components, at least within this period. A comparison of nutrient concentration changes in the 1990s and 2000s with those after 2010 reveals that there have been changes over time, including the derived components in the 1990s and 2000s. However, comparability was not ensured before 2009 because CRMs were not used before 2009. It is therefore difficult to determine whether this change was a natural change or the result of analytical errors. Assuming that there have been no natural variations in the deeper layers adapted in international integrated datasets such as PACIFICA (Suzuki et al., 2013) and GLODAP (Olsen et al., 2016), it is still possible to study changes from the epipelagic to the mesopelagic, where changes may have been relatively large. However, such an analysis cannot be made of natural variation in the bathypelagic or abyssopelagic. In addition, this method makes it difficult to evaluate the Redfield ratio. However, if we use nutrient CRMs, we do not need the offset correction to data obtained from the surface layer to the deep layer, and we can make a rigorous evaluation of the Redfield ratio by ensuring traceability and comparability. Single chemical components as well as derived components (e.g., a quasi-preserving component such as NO) that combine multiple components based on the Redfield ratio can be obtained accurately. It is very likely that new scientific knowledge about the role of nutrients in the carbon cycle and climate change will be obtained.

Acknowledgements

The authors thank for the authors of cruise reports of R/V Mirai and R/V Ryofu Maru which were cited in this article. The authors also thank Dr. T. Gamo for providing GEOTRACE post-cruise metadata. We also thank Dr. T. Nakano and Dr. J. Swift for their suggestions and comments on this article.

References

- Akaike, H. (1974): A new look at the statistical model identification. *IEEE Transactions on Automatic Control*, 19:716–722.
- Anderson, L. A., and J. L. Sarmiento (1994): Redfield ratios of remineralization determined by nutrient data analysis. *Global Biogeochemical Cycles*, 8(1), 65–80. <https://doi.org/10.1029/93GB03318>.
- Aoyama M., and Joyce T.M. (1996) WHP property comparisons from crossing lines in North Pacific. In Abstracts, 1996 WOCE Pacific Workshop, Newport Beach, California.
- Aoyama, M., (2006) 2003 Intercomparison Exercise for Reference Material for Nutrients in Seawater in a Seawater Matrix, Technical Reports of the Meteorological Research Institute No.50, 91pp, Tsukuba, Japan.
- Aoyama, M., Susan B., Minhan, D., Hideshi, D., Louis, I. G., Kasai, H., Roger, K., Nurit, K., Doug, M., Murata, A., Nagai, N., Ogawa, H., Ota, H., Saito, H., Saito, K., Shimizu, T., Takano, H., Tsuda, A., Yokouchi, K., and Agnes, Y. (2007). Recent Comparability of Oceanographic Nutrients Data: Results of a 2003 Intercomparison Exercise Using Reference Materials. *Analytical Sciences*, 23: 1151-1154.
- Aoyama M., J. Barwell-Clarke, S. Becker, M. Blum, Braga E. S., S. C. Coverly, E. Czobik, I. Dahllof, M. H. Dai, G. O. Donnell, C. Engelke, G. C. Gong, Gi-Hoon Hong, D. J. Hydes, M. M. Jin, H. Kasai, R. Kerouel, Y. Kiyomono, M. Knockaert, N. Kress, K. A. Kroglund, M. Kumagai, S. Leterme, Yarong Li, S. Masuda, T. Miyao, T. Moutin, A. Murata, N. Nagai, G. Nausch, M. K. Ngirchchol, A. Nybakk, H. Ogawa, J. van Ooijen, H. Ota, J. M. Pan, C. Payne, O. Pierre-Duplessix, M. Pujo-Pay, T. Raabe, K. Saito, K. Sato, C. Schmidt, M. Schuett, T. M. Shammon, J. Sun, T. Tanhua, L. White, E.M.S. Woodward, P. Worsfold, P. Yeats, T. Yoshimura, A. Youenou, J. Z. Zhang, (2008) 2006 Intercomparison Exercise for Reference Material for Nutrients in Seawater in a Seawater Matrix, Technical Reports of the Meteorological Research Institute No. 58, 104pp.
- Aoyama, M., Ota, H., Kimura, M., Kitao, T., Mitsuda, H., Murata, A., and Sato, K.: (2012). Current Status of Homogeneity and Stability of the Reference Materials for Nutrients in Seawater, *Analytical Sciences*, 28, 911-916. DOI: 10.2116/analsci.28.911.
- Aoyama, M., Carol, A., Janet, B.-C., Baurand, F., Becker, S., Blum, M., Coverly, S. C., Czobik, E., d'Amico, F., Dahllof, I., Dai, M., Dobson, J., Pierre-Duplessix, O., Duval, M., Engelke, C., Gong, G.-C., Grosso, O., Hirayama, A., Inoue, H., Ishida, Y., Hydes, D. J., Kasai, H., Kerouel, R., Knockaert, M., Kress, N., Kroglund, K. A., Kumagai, M., Leterme, S. C., Mahaffey, C., Mitsuda, H., Morin, P., Moutin, T., Munaron, D., Murata, A., Nausch, G., Ogawa, H., Ooijen, J. v., Pan, J., Paradis, G., Payne, C., Prove, G., Raimbaul, P., Rose, M., Saito, K., Saito, H., Sato, K., Schmidt, C., Schutt, M., Shammon, T. M., Olafsdottir, S., Sun, J., Tanhua, T., Weigelt-Krenz, S., White, L., Woodward, E. M. S., Worsfold, P., Yoshimura, T., Youenou, A., and Zhang, J.-Z. (2010) 2008 Inter-laboratory Comparison Study of a Reference Material for Nutrients in Seawater, the Meteorological Research Institute 60,
- Aoyama, M., Abad, M., Anstey, C., P. M. A., Bakir, A., Becker, S., Bell, S., Berdalet, E., Blum, M., Briggs, R., Caradec, F., Cariou, T., Church, M., Coppola, L., Crump, M., Curless, S., Dai, M., Daniel, A., Davis, C., Braga, E. d. S., Solis, M. E., Ekern, L., Faber, D., Fraser, T., Gundersen, K., Jacobsen, S., Knockaert, M., Komada, T., Kralj, M., Kramer, R., Kress, N., Lainela, S., Ledesma, J., Li, X., Lim, J.-H., Lohmann, M., Lønborg, C.,
- Guideline of Ocean Observation Vol.1 Chap.4 Quality control by comparison with standards, control charts, duplicated measurements, and property-property characteristics, and the report of metadata ©Michio Aoyama, Hiroshi Uchida, Daisuke Sasano, Hajime Obata 2019 G104EN:001-134

- Ludwichowski, K.-U., Mahaffey, C., Malien, F., Margiotta, F., McCormack, T., Murillo, I., Naik, H., Nausch, G., Ólafsdóttir, S. R., Ooijen, J. v., Paranhos, R., Payne, C., Pierre-Duplessix, O., Prove, G., Rabiller, E., Raimbault, P., Reed, L., Rees, C., Rho, T., Roman, R., Woodward, E. M. S., Sun, J., Szymczycha, B., Takatani, S., Taylor, A., Thamer, P., Torres-Valdés, S., Trahanovsky, K., Waldron, H., Walsham, P., Wang, L., Wang, T., White, L., Yoshimura, T., and Zhang, J.-Z. (2016) IOCCP-JAMSTEC 2015 Inter-laboratory Calibration Exercise of a Certified Reference Material for Nutrients in Seawater JAMSTEC, Yokosuka, Japan.
- Aoyama, M., Abad, M., Aguilar-Islas, A., P, M. A., Azetsu-Scott, K., Bakir, A., Becker, S., Benoit-Cattin-Breton, A., Berdalet, E., Björkman, K., Blum, M., Braga, E. d. S., Florian Caradec, T. C., Chiozzini, V. G., Collin, K., Coppola, L., Crump, M., Dai, M., Daniel, A., Davis, C., Solis, M. E., Edelvang, K., Faber, D., Fidel, R., Fonnes, L. L., Frank, J., Frew, P., Funkey, C., Gallia, R., Giani, M., Gkritzalis, T., Grage, A., Greenan, B., Gundersen, K., Hashihama, F., Ibar, V. F. C., Jung, J., Kang, S. H., Karl, D., Kasai, H., Kerrigan, L. A., Kiyomoto, Y., Knockaert, M., Kodama, T., Koo, J.-H., Kralj, M., Kramer, R., Kress, N., Lainela, S., Ledesma, J., Lewandowska, J., López, M. d. C. Á., García, P. L., Ludwichowski, K.-U., Mahaffey, C., Malien, F., Margiotta, F., Márquez, A., Mawji, E. W., McCormack, T., McGrath, T., Merrer, Y. L., Møgster, J. S., Nagai, N., Naik, H., Normandeau, C., Ogawa, H., Ólafsdóttir, S. R., Ooijen, J. v., Paranhos, R., Park, M.-O., Parmentier, K., Passarelli, A., Payne, C., Pierre-Duplessix, O., Povazhnyi, V., Quesnel, S.-A., Raimbault, P., Rees, C., Rember, R., Rho, T. K., Ringuette, M., Riquier, E. D., Rodriguez, A., Roman, R. E., Rosero, C., Woodward, E. M. S., Saito, S., Schuller, D., Segal, Y., Silverman, J., Sørensen, D., Stedmon, C. A., Stinchcombe, M., Sun, J., Thamer, P., Urbini, L., Wallace, D., Walsham, P., Wang, L., Waniek, J., Yamamoto, H., Yoshimura, T., and Zhang, J.-Z. (2018) IOCCP-JAMSTEC 2018 Inter-laboratory Calibration Exercise of a Certified Reference Material for Nutrients in Seawater, JAMSTEC, Yokosuka, Japan.
- Aoyama, M. (2016). Ocean variables and the International system of units (SI), G101EN:001-006 in Guideline of Ocean Observations, Vol. 1 Chap. 1, 3rd Edition, Oceanographic Society of Japan, Tokyo.
- Aoyama, M. (2020) Global certified-reference-material- or reference-material-scaled nutrient gridded dataset GND13, Earth Syst. Sci. Data, 12, 487–499, <https://doi.org/10.5194/essd-12-487-2020>.
- Aoyama M, Joyce T, Kawano T, Takatsuki Y. (2002) Standard seawater comparison up to P129. Deep Sea Research Part I. 49:1103-14.
- Aoyama, M., Uchida, H., Hayashi, K. (2019) Device for measurement and measurement standard (Etalons) , G102EN:001-012, in Guideline of Ocean Observations, Vol. 1 Chap. 2, 4th Edition, Oceanographic Society of Japan, Tokyo.
- Bockmon, E. and Dickson, A.G. (2015) An inter-laboratory comparison assessing the quality of seawater carbon dioxide measurements. Marine Chemistry, 171, 36-43
- Breland, J. A., and Byrne, R. H., (1993) Spectrophotometric procedures for determination of sea water alkalinity using bromocresol green, Deep Sea Research Part I: Oceanographic Research Papers, 40, 3, 629-641, doi:10.1016/0967-0637(93)90149-W.
- Broecker, W. S. (1974): “NO”, a conservative water-mass tracer, Earth Planet. Sci. Lett., 23, 100–107.
- Dickson, A.G. et al. (2003) Reference materials for oceanic CO₂ analysis: a method for the certification of total alkalinity. Mar. Chem. 80, 185-197.
- Dickson, A. G., C. L. Sabine, and J. R. Christian (Eds.) (2007), Guide to best practices for ocean CO₂ measurements. *PICES Special Publication 3*, 191 pp.
- Dickson, A. G. (2010). The carbon dioxide system in sea water: equilibrium chemistry and measurements, In Guide for Best Practices in Ocean Acidification Research and Data Reporting, Office for Official Publications of the European Union, Luxembourg.

- DOE (1994), Handbook of methods for the analysis of the various parameters of the carbon dioxide system in sea water; version 2. *A. G. Dickson and C. Goyet (eds), ORNL/CDIAC-74.*
- Edwards, B., D. Murphy, C. Janzen and N. Larson (2010): Calibration, response, and hysteresis in deep-sea dissolved oxygen measurements, *J. Atmos. Oceanic Technol.*, 27, 920–931.
- Gamo (2010): Preliminary Report of The Hakuho Maru Cruise KH-09-5 Leg1,2,3 (The Indian Ocean and the Antarctic Sea) -ERIDANUS Expedition-.
https://www.bodc.ac.uk/resources/inventories/cruise_inventory/reports/hakuhomaru_kh-09-5.pdf (accessed on 20 March 2020).
- García, H. E. and L. I. Gordon (1992): Oxygen solubility in seawater: Better fitting equations. *Limnol. Oceanogr.*, 37 (6), 1307–1312.
- Gouretski, V.V. and Jancke, K. 2001. Systematic errors as the cause for an apparent deep water property variability: global analysis of the WOCE and historical hydrographic data • REVIEW ARTICLE, *Progress In Oceanography*, 48: Issue 4, 337-402.
- Johnson, K. M., A. E. King and J. McN. Sieburth (1985), Coulometric TCO₂ analyses for marine studies; an introduction. *Marine Chemistry*, 16, 61–82.
- Johnson, K. M., J. McN. Sieburth, P. J. IeB Williams and L Brändström (1987), Coulometric total carbon dioxide analyses for marine studies: Automation and calibration. *Marine Chemistry*, 21, 117–133.
- Joyce, T. and Corry, C. 1994. Requirements for WOCE hydrographic programmed data reporting. WHPO Publication, 90-1, Revision 2, WOCE Report No. 67/91.
- Kawano (2010), The GO-SHIP Repeat Hydrography Manual: A Collection of Expert Reports and Guidelines. IOCCP Report No. 14, ICPO Publication Series No. 134, Version 1.
- Kawano, T., Aoyama, M., Joyce, T and Takatsuki., Y. (2006) The latest batch-to-batch difference table of standard seawater and its application to the WOCE onetime sections. *J Oceanogr* 62, 777–792.
<https://doi.org/10.1007/s10872-006-0097-8>
- Langdon, C. (2010), Determination of dissolved oxygen in seawater by Winkler titration using the amperometric technique, IOCCP Report No.14, ICPO Pub. 134, 2010 ver.1
- McTaggart, K. E., G. C. Johnson, M. C. Johnson, F. M. Delahoyde, and J. H. Swift (2010): The GO-SHIP Repeat Hydrography Manual: A Collection of Expert Reports and guidelines. IOCCP Report No 14, ICPO Publication Series No. 134, version 1, 2010.
- Lesley Rickards, L. and Nast, F. (2007): IODE data flow (National Oceanographic Programmes (NOPs) and Cruise Summary Reports (CSRs)), Nineteenth Session of the IOC Committee on International Oceanographic Data and Information Exchange (IODE-XIX), IOC/IODE-XIX/ 12, INTERGOVERNMENTAL OCEANOGRAPHIC COMMISSION (of UNESCO).
- Mantyla AW. (1987) Standard Seawater Comparisons Updated. *Journal of Physical Oceanography* 17: 543-548.
- Murray, C.N., J.P. Riley, T.R.S. Wilson (1968) The solubility of oxygen in Winkler reagents used for the determination of dissolved oxygen, *Deep Sea Research and Oceanographic Abstracts*, 15, 2, 237-238, doi :10.1016/0011-7471(68)90046-6.
- Mordy, C.W., Aoyama, M., Gordon, L.I., Johnson, G.C., Key, R.M., Ross, A.A., Jennings, J.C. and Wilson. J. 2000. Deep water comparison studies of the Pacific WOCE nutrient data set. *Eos Trans- American Geophysical Union*. 80 (supplement), OS43.
- Nakano, T. (2010): R/V Ryofu Maru Cruise Report: P09. [Available online at http://cchdo.ucsd.edu/data_access/show_cruise?ExpoCode=49RY20100706] .Saito, S., M. Ishii, T. Midorikawa and H.Y. Inoue 2008. Precise Spectrophotometric Measurementf Seawater pH_T with an Guideline of Ocean Observation Vol.1 Chap.4 Quality control by comparison with standards, control charts, duplicated measurements, and property-property characteristics, and the report of metadata ©Michio Aoyama, Hiroshi Uchida, Daisuke Sasano, Hajime Obata 2019 G104EN:001-134

- Automated Apparatus using a Flow Cell in a Closed Circuit. *Technical Reports of Meteorological Research Institute*, **57**, 1–28.
- Olsen, A., R. M. Key, S. van Heuven, S. K. Lauvset, A. Velo, X. Lin, C. Schirnick, A. Kozyr, T. Tanhua, M. Hoppema, S. Jutterström, R. Steinfeldt, E. Jeansson, M. Ishii, F. F. Pérez and T. Suzuki (2016): The Global Ocean Data Analysis Project version 2 (GLODAPv2) – an internally consistent data product for the world ocean, *Earth Syst. Sci. Data*, **8**, 297–323, 2016, doi:10.5194/essd-8-297-2016.
- Sato, K., Aoyama, M., Becker, S., 2010. CRM as Calibration Standard Solution to Keep Comparability for Several Cruises in the World Ocean in 2000s. In: Aoyama, M., Dickson, A.G., Hydes, D.J., Murata, A., Oh, J.R., Roose, P., Woodward, E.M.S., (Eds.), *Comparability of nutrients in the world's ocean*. Tsukuba, JAPAN: MOTHER TANK, pp 43-56.
- Sea-Bird Electronics (2009): SBE 43 dissolved oxygen (DO) sensor – hysteresis corrections, Application note no. 64-3, 7 pp.
- Shanno, David F. (1970): Conditioning of quasi-Newton methods for function minimization. *Math. Comput.* **24**, 647–656. MR 42 #8905.
- Suzuki, T., M. Ishii, M. Aoyama, J. R. Christian, K. Enyo, T. Kawano, R. M. Key, N. Kosugi, A. Kozyr, L. A. Miller, A. Murata, T. Nakano, T. Ono, T. Saino, K. Sasaki, D. Sasano, Y. Takatani, M. Wakita and C. Sabine (2013): PACIFICA Data Synthesis Project. ORNL/CDIAC-159, NDP-092. Carbon Dioxide Information Analysis Center, Oak Ridge National Laboratory, U.S. Department of Energy, Oak Ridge, Tennessee. doi:10.3334/CDIAC/OTG.PACIFICA_NDP092.
- Swift, J. H. (2010), Reference-quality water sample data: Notes on acquisition, record keeping, and evaluation. *IOCCP Report No.14, ICPO Pub. 134, 2010 ver.1.*
- The GEOTRACES Group (2015): The GEOTRACES Intermediate Data Product 2014. *Mar. Chem.*, **177**, 1–8.
- Uchida, H., G. C. Johnson, and K. E. McTaggart (2010): CTD oxygen sensor calibration procedures, The GO-SHIP Repeat Hydrography Manual: A collection of expert reports and guidelines, IOCCP Rep., No. 14, ICPO Pub. Ser. No. 134.
- Uchida, H., K. Ohyama, S. Ozawa, and M. Fukasawa (2007): In situ calibration of the Sea-Bird 9plus CTD thermometer, *J. Atmos. Oceanic Technol.*, **24**, 1961–1967.
- Uchida, H., T. Kawano, I. Kaneko, and M. Fukasawa (2008): In-situ calibration of optode-based oxygen sensors. *J. Atmos. Oceanic Technol.*, **25**, 2271–2281.
- Uchida, H., K. Katsumata, and T. Doi (2015a): WHP P14S, S04I Revisit Data Book, JASTEC, Yokosuka, 187 pp.
- Uchida, H., T. Nakano, J. Tamba, J. V. Widiatmo, K. Yamazawa, S. Ozawa and T. Kawano (2015b): Deep ocean temperature measurement with an uncertainty of 0.7 mK, *J. Atmos. Oceanic Technol.*, **32**, 2199–2210.
- Uchida, H., Y. Maeda, and S. Kawamata (2018): Compact underwater slip ring swivel, Minimizing effect of CTD package rotation on data quality, *Sea Technology*, 30-32, November.
- UNESCO (1981), Tenth report of the Joint Panel on Oceanographic Tables and Standards. UNESCO Tech. Papers in Mar. Sci., **36**, 25 pp.

Appendix

I IOC data policy 2003

II Examples of cruise summary report

II-1 *Examples of cruise summary report of KH-09-5*

II-2 *Examples of post cruise metadata of the same cruise KH-09-05 as shown above*

II-3 *An example of cruise summary report, expanded version by R/V Ryofu Maru*

Appendix I: IOC data policy 2003

During its twenty-second session (24 June - 4 July 2003) the IOC Assembly adopted Resolution IOC-XXII-6 entitled 'IOC Oceanographic Data Exchange Policy

RESOLUTION IOC-XXII-6

(Agenda item 4.3.2)

IOC OCEANOGRAPHIC DATA EXCHANGE POLICY

The Intergovernmental Oceanographic Commission,

1 Recalling Resolution XX-11 on Oceanographic Data Exchange Policy (1999),

2 Noting:

- (i) WMO Resolution 40 (Cg-XII) which defined a policy and practice for the international exchange of meteorological and related data and is intended to promote the free and unrestricted exchange of basic data,
- (ii) The “Statement on Data Management Policy for Global Ocean Programmes” as submitted by the IOC Committee on IODE (Recommendation IODE-XIV.6, December 1992) and adopted by the IOC Assembly at its 17th Session (Paris, 25 February–11 March 1993) (para. 220 of the Summary Report of the Session),

3 Considering the reports of deliberations of:

- (i) The Ad hoc Working Group on Oceanographic Data Exchange Policy (Paris, 15–17 May 2000),
- (ii) The First Session of the Intergovernmental Working Group on IOC Oceanographic Data Exchange Policy (Brussels, 29–31 May 2001),
- (iii) The Second Session of the Intergovernmental Working Group on IOC Oceanographic Data Exchange Policy (Paris, 17–18 June 2002),

4 Adopts the IOC Oceanographic Data Exchange Policy as detailed in the Annex to this Resolution.

Financial implications: none

ANNEX TO DRAFT RESOLUTION IOC-XXII/DR.3 IOC OCEANOGRAPHIC DATA EXCHANGE POLICY

Preamble

The timely, free and unrestricted international exchange of oceanographic data is essential for the efficient acquisition, integration and use of ocean observations gathered by the countries of the world for a wide variety of purposes including the prediction of weather and climate, the operational forecasting of the marine environment, the preservation of life, the mitigation of human-induced changes in the marine and coastal environment, as well as for the advancement of scientific understanding that makes this possible.

Recognising the vital importance of these purposes to all humankind and the role of IOC and its programmes in this regard, the Member States of the Intergovernmental Oceanographic Commission **agree** that the following clauses shall frame the IOC policy for the international exchange of oceanographic data and its associated metadata.

Clause 1

Member States shall provide timely, free and unrestricted access to all data, associated metadata and products generated under the auspices of IOC programmes.

Clause 2

Member States are encouraged to provide timely, free and unrestricted access to relevant data and associated metadata from non-IOC programmes that are essential for application to the preservation of life, beneficial public use and protection of the ocean environment, the forecasting of weather, the operational forecasting of the marine environment, the monitoring and modelling of climate and sustainable development in the marine environment.

Clause 3

Member States are encouraged to provide timely, free and unrestricted access to oceanographic data and associated metadata, as referred to in Clauses 1 and 2 above, for non-commercial use by the research and education communities, provided that any products or results of such use shall be published in the open literature without delay or restriction.

Clause 4

With the objective of encouraging the participation of governmental and non-governmental marine data gathering bodies in international oceanographic data exchange and maximizing the contribution of oceanographic data from all sources, this Policy acknowledges the right of Member States and data originators to determine the terms of such exchange, in a manner consistent with international conventions, where applicable.

Clause 5

Member States shall, to the best practicable degree, use data centres linked to IODE's NODC and WDC network as long-term repositories for oceanographic data and associated metadata. IOC programmes will co-operate with data contributors to ensure that data can be accepted into the appropriate systems and can meet quality requirements.

Clause 6

Member States shall enhance the capacity in developing countries to obtain and manage oceanographic data and information and assist them to benefit fully from the exchange of oceanographic data, associated metadata and products. This shall be achieved through the non-discriminatory transfer of technology and knowledge using appropriate means, including IOC's Training Education and Mutual Assistance (TEMA) programme and through other relevant IOC programmes.

Definitions

'Free and unrestricted' means non-discriminatory and without charge. "Without charge", in the context of this resolution means at no more than the cost of reproduction and delivery, without charge for the data and products themselves.

'Data' consists of oceanographic observation data, derived data and gridded fields.

'Metadata' is 'data about data' describing the content, quality, condition, and other characteristics of data.

'Non-commercial' means not conducted for profit, cost-recovery or re-sale.

'Timely' in this context means the distribution of data and/or products, sufficiently rapidly to be of value for a given application

'Product' means a value-added enhancement of data applied to a particular application

II-1: Cruise summary report of KH-09-5

Reference No. : 20100060
 Ship Name : HAKUHO MARU
 Ship Type : Research Ship
 Cruise No./Name : KH-09-5
 Cruise Period : 2009/11/06 to 2010/01/09
 Responsible Laboratory :
 Atmosphere and Ocean Research Institute, The University of Tokyo
 Chief Scientist(s) : Toshitaka Gamo, Marine Inorganic Chemistry Lab., Ocean Research Institute, Univ. Tokyo
 General Ocean Area(s) : Indian Ocean
 Geographic Coverage : 28, 66, 30, 329, 364, 401, 438, 474, 510, 547, 548, 512, 476, 477, 441
 Project Name : GEOTRACES
 Coordinating Body : SCOR, Atmosphere and Ocean Research Institute (Univ. Tokyo)
 Principal Investigators : A: Toshitaka Gamo the University of Tokyo
 : B: Yoshihisa Kato Tokai University
 : C: Yoshifumi Nogi National Institute of Polar Research
 : D: Toshio Suga JAMSTEC
 : E: Yuko Takahashi Senshu University

Objectives and Brief Narrative of Cruise:

This cruise has been internationally authorized as the first GEOTRACES meridional study in the Indian Ocean. GEOTRACES means an international study of the marine biogeochemical cycles of trace elements and their isotopes (TEIs) in a global scale. The determination of trace elements has recently become a central focus of many research programs that seek information on the biogeochemical processes in the ocean. The study of TEIs has graduated from a curiosity to understand how the chemical diversity of trace elements, in their various redox and chemical states, interacts with the physical and biological processes occurring in the ocean. This is particularly important in the case of micronutrients such as Fe, whose oceanic distributions seem to be a crucial link to climatic processes. Together with other biologically required TEIs, perturbations of their cycles induced by the climate change may have fundamental consequences for the global carbon cycle, which is firmly associated with global climate. Although our knowledge on the behavior of TEIs in the ocean is fairly small at the present stage, recent advances on analytical and clean sampling techniques have just enabled us to get precise information on TEIs in the ocean, which is the powerful background to initiate a new international program, GEOTRACES. As the GEOTRACES initiative in the Indian Ocean, the main study theme of this cruise was marine geochemical observations in the northern (chiefly in the Bengal Bay) and western Indian Ocean from the Arabian Sea to the Antarctic Sea along a meridional line. Our ability to predict the future environmental change caused by the global warming depends upon knowledge on the distribution of biologically important chemical species in the ocean and their exchange flux at the air-sea and sediment-water interfaces. The Indian Ocean occupies a vast area of the world ocean, but little is known about the marine biogeochemical cycles on TEIs. Thus, it is important to understand the role of the Indian Ocean in the global carbon cycle including its temporal variations recorded in marine sediments.

Moorings, Bottom Mounted Gear and Drifting Systems:

PI	LAT.	LON.	DATATYPE	DESCRIPTION
D	30-.1:S	64-59.5:		Argo float
D	37-45.4	57-36.8:		Argo float
D	44-20:S	28-55.3:		Argo float

Summary of Measurements and Samples Taken:

PI	NO	UNITS	DATATYPE	DESCRIPTION
A	12	station	H09, H10, H11, H16, H21, H22, H	Seabird Carousel-32 Multi Bott
B	11	core	G04	Surface sediment (20~40 cm de
B	2	core	G04	Sediment core samples (~15 m)
C	9	station	H10, H13	XBTs and XCTDs
C	1	track	G27, G74	Underway geophysical measurement

II-2: Post cruise metadata of the cruise KH-09-05

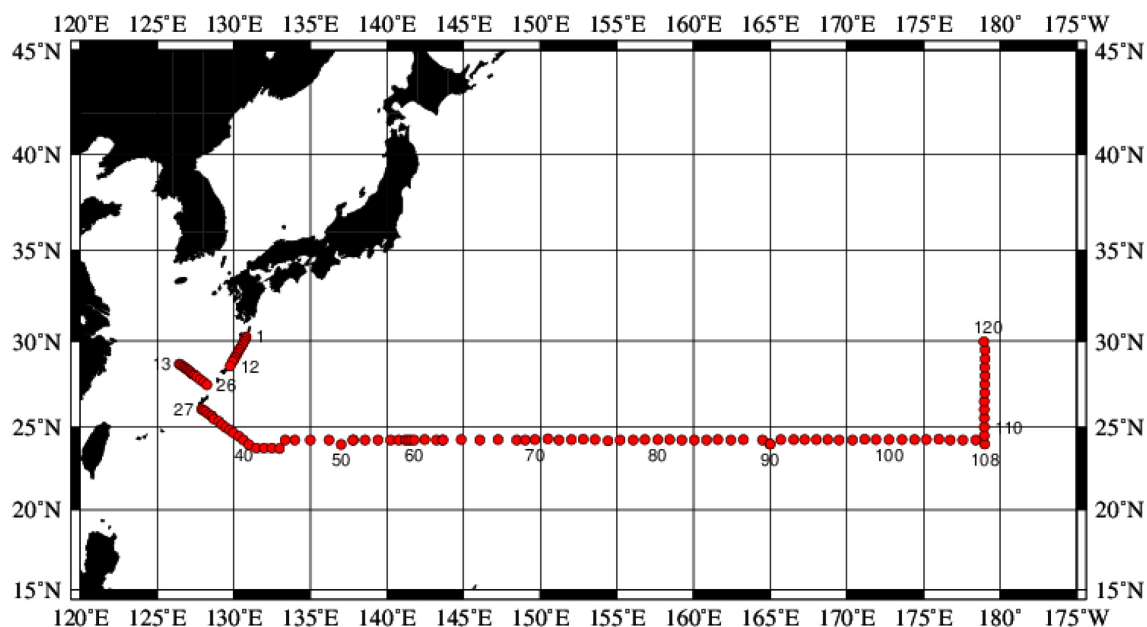
Cruise Name: <i>[any identifier (acronyms), Including technical name]</i>	KH-09-5 cruise leg-1, 2, and 3	
Platform Name and type: Research Vessel Hakuho Maru <i>[vessel, mooring, satellite,, towed vehicle,]</i>		
Project: GEOTRACES Indian Ocean <i>[associated project or program name related to funding]</i>		
Lead Nation: Japan		
Chief scientist (Lead scientist / Principal Investigator) contact details		
Name: Toshitaka Gamo	Email:	Phone:
Mailing Address: Ocean Research Institute, the University of Tokyo 1-15-1 Minamidai, Nakano-ku, Tokyo 161-8639 (JAPAN)		
Co-Chief scientist contact details: <i>[GEOTRACES point of contact if different from Chief scientist]</i>		
Name:	Email:	Phone:
Mailing Address:		
Cruise Details		
Start Port and Country: Tokyo, Japan	Start date: November 6, 2009	
End Port and Country: Cape Town, South Africa	End Date: January 10, 2010	
Location: <i>[general description of study area; map if possible]</i> Indian Ocean, Antarctic Sea (cruise track is shown in the attached map)		
Cruise Overview: <i>[proposal abstract]</i> The KH-09-5 Cruise leg-1, -2, and -3 of R/V <i>Hakuho Maru</i> was planned to pursue Trace Element Oceanography in Japan as part of the international project SCOR-GEOTRACES (study of the marine biogeochemical cycles of trace elements and isotopes). The cruise aimed at precise and detailed measurements of trace elements and isotopes in the Indian Ocean including the atmosphere and bottom sediment, in order to identify processes and fluxes that control the distribution of trace elements in water columns, and to elucidate their important linkage with the global climatic change. We collected seawater, air, plankton and sediment samples for the measurement of trace elements including the GEOTRACES key parameters, dissolved gases, stable- and radio-isotopes at 12 locations chiefly along meridional lines (~65°E and ~30°E) in the western Indian Ocean and the Antarctic Sea.		
Intercalibration activities: <i>Please provide details of how each element was calibrated to meet the requirements of the GEOTRACES programme e.g. use of SaFe standards, collaborative sampling.</i> For small- volume elements (Fe, Al, Zn, Mn, Cd, Cu, Co, Pb), analysts will use the SaFe standards to verify their own methods. For large-volume elements (²³⁰ Th, ²³¹ Pa and Nd isotopes), analysts will reveal vertical profiles of these elements at the baseline station in Arabian Sea (15 N, 65 E), recommended in the GEOTRACES Intercalibration Planning Document. A subset of samples collected at the baseline station will be distributed to GEOTRACES collaborators for analyses and verification of accuracy. We took two sets of clean samples for comparison between the usual CTD hydrocast with Ti armored cable and the special hydrocast using Kevlar wire at two stations ER-3 and ER-10.		
List of parameters to be submitted to GDAC: <i>Key parameters listed, please list any other parameters measured and the PI's contact information. Also include information in regards to the phase i.e. dissolved or</i>		

particulate and how the samples were collected. i.e. *Fe (dissolved)- CTD –Bottle or Fe (dissolved) –Insitu pumps.*

Could PI provide information on when samples are expected to be analysed so GDAC can estimate data delivery date.

Trace elements:	Contact for each element (PI); [name and email]	Internationally calibrated (Yes or No)	Expected date of analysis
<input type="checkbox"/> Fe <input type="checkbox"/> Al <input type="checkbox"/> Zn <input type="checkbox"/> Mn <input type="checkbox"/> Cd <input type="checkbox"/> Cu <input type="checkbox"/> Other <input type="checkbox"/> Other <input type="checkbox"/> Other	J. Nishioka Y. Sohrin Y. Sohrin Y. Sohrin Y. Sohrin Y. Sohrin	Yes Yes Yes Yes Yes Yes	
Radioactive isotopes: <input type="checkbox"/> ²³⁰ Th <input type="checkbox"/> ²³¹ Pa <input type="checkbox"/> Other <input type="checkbox"/> Other <input type="checkbox"/> Other <input type="checkbox"/> Other	A. Okubo A. Okubo	Yes Yes	
Stable isotopes: <input type="checkbox"/> $\delta^{15}\text{N}$ <input type="checkbox"/> $\delta^{13}\text{C}$ <input type="checkbox"/> Other	U. Tsunogai Y. Kumamoto	Yes Yes	
Radiogenic isotopes: <input type="checkbox"/> Nd isotopes <input type="checkbox"/> Pb isotopes <input type="checkbox"/> Other	H. Amakawa and H. Tazoe E. Boyle	Yes Yes	
NON TEI data set (add as required) <input type="checkbox"/> <input type="checkbox"/> <input type="checkbox"/> <input type="checkbox"/> <input type="checkbox"/> <input type="checkbox"/>			
Other parameters: Se: Y. Nakaguchi Cr: K. Isshiki ¹⁴ C: Y. Kumamoto			

List CTD hydrographic parameters [<i>sensors including make; salinity, temperature, oxygen, nutrients etc</i>] Carousel Multi-bottle sampler (SBE-32) Sea-Bird's 911 plus CTD (salinity, temperature, oxygen, fluorescence, light transimission)
Particles/Aerosols: Sampled
List Underway data: [<i>Met data, navigation hull mounted sensors including make and model</i>]
Is there a national data centre: (name and contact) [<i>If not GDAC should be used</i>] <i>JODC (Japan Oceanographic Data Center; http://www.jodc.go.jp/index.html) will serve as the national data center for GEOTRACES in Japan. The contact person is Mr. Akihiro SETA .</i>
Other relevant information:

II-3: Cruise summary report, expanded version by R/V Ryofu Maru**CRUISE REPORT: P03W***(Updated AUG 2018)***Highlights****Cruise Summary Information**

Section Designation	P03W (RF13-06, RF13-07)
Expedition designation (ExpoCodes)	49UP20130619
Chief Scientists	Kazuhiro NEMOTO Hitomi KAMIYA
Dates	2013-06-24 to 2018-09-18
Ship	<i>Ryofu Maru</i>
Ports of call	Naha, Japan - Tokyo, Japan
Geographic Boundaries	30° 14.59' N 126° 26.85' E 179° 3.76' E 23° 42.63' N
Stations	120
Floats and drifters deployed	1 float and 2 drifting ocean data buoys
Moorings deployed or recovered	0

Contact Information:

Kazuhiro NEMOTO
Hitomi KAMIYA

Marine Division • Global Environment and Marine Department • Japan Meteorological Agency

(JMA) 1-3-4, Otemachi, Chiyoda-ku, Tokyo 100-8122, JAPAN

Phone: +81-3-3212-xxxx Ext. xxxx

A. Cruise narrative

1. Highlights

Cruise designation: RF13-06 and RF13-07 (WHP-P03W revisit)

- a. EXPOCODE: 49UP20130619
- b. Chief scientist: RF13-06 Kazuhiro NEMOTO
- c. RF13-07 Hitomi KAMIYA
Marine Division

Global Environment and Marine Department Japan Meteorological Agency
(JMA)

1-3-4, Otemachi, Chiyoda-ku, Tokyo 100-8122, JAPAN

Phone: +81-3-3212- x x x x

Ext. x x x x

- d. Ship name: R/V Ryofu Maru
- e. Ports of call: RF13-06 Leg 1: Tokyo–Naha, Leg 2: Naha–Tokyo RF13-07 Leg
1: Tokyo–Pohnpei, Leg 2: Pohnpei–Tokyo
- f. Cruise dates: RF13-06 Leg 1: 19 June 2013–1 July 2013 RF13-06
Leg 2: 5 July 2013–24 July 2013 RF13-07 Leg 1: 31
July 2013–21 August 2013

RF13-07 Leg 2: 25 August 2013–18 September 2013

- g. Floats and drifters deployed: RF13-06: 1 float and 2 drifters
RF13-07: 5 floats

2. Cruise Summary Information

RF13-06 and RF13-07 cruises were carried out during the period from June 19 to September 18, 2013. The observation line along approximately 24°N was observed by Scripps Institution of Oceanography (SIO), USA in 1985 and Japan Agency for Marine-Earth Science and Technology (JAMSTEC), Japan in 2005–2006. These cruises were carried out as ‘WHP-P03’, which is a part of WOCE (World Ocean Circulation Experiment) Hydrographic Programme, CLIVAR (Climate Variability and Predictability Project) and GO-SHIP (Global Ocean Ship-based Hydrographic Investigations Program).

A total of 120 stations was occupied using a Sea-Bird Electronics (SBE) 36 position carousel equipped with 10-liter Niskin water sample bottles, a CTD system (SBE911plus) equipped with SBE35 deep ocean standards thermometer, JFE Advantech oxygen sensor (RINKO III), Teledyne Benthos altimeter (PSA-916D), and Teledyne RD Instruments L-ADCP (300kHz). Cruise track and station location are shown in [Figure 1](#).

At each station, full-depth CTDO₂ (temperature, conductivity (salinity) and dissolved oxygen) profile and up to 36 water samples were taken and analyzed. Water samples were obtained from 10 dbar to approximately 10 m above the bottom. In addition, surface water was sampled using a stainless steel bucket at each station. Sampling layer is designed as so-called staggered mesh as shown

in [Table 1](#) (Swift, 2010). The bottle depth diagram is shown in [Figure 2](#).

Water samples were analyzed for salinity, dissolved oxygen, nutrients, dissolved inorganic carbon (DIC), total alkalinity (TA), pH, CFC-11, CFC-12 and phytopigment (chlorophyll-a and phaeopigments). Underway measurements of partial pressure of carbon dioxide ($p\text{CO}_2$), temperature, salinity, chlorophyll-a, subsurface current, bathymetry and meteorological parameters were conducted along the cruise track.

RF13-06

RF13-06 cruise was carried out during the period from June 19 to July 24, 2013. Before the observation at the first station, all watch standers were drilled in the method of sample drawing and CTD operations at the point (34°22'N, 138°30'E). At first, the cruise started from Stn.13 (28°42'N, 126°27'E; RF4757) and sailed south-eastward to Stn.26 (27°30'N, 128°15'E; RF4770). After observation of Stn.26 we observed from Stn.1 (30°14'N, 130°50'E; RF4771) to Stn.12 (28°35'N, 129°45'E; RF4782) and from Stn.27 (26°04'N,

127°55'E; RF4783) to Stn.31 (25°39'N, 128°34'E; RF4787). Leg 1 consisted of 31 stations. We finished Stn.31 on June 29. She called for Naha (Japan) on July 1 (Leg 1). She left Naha on July 5, we restarted observation from Stn.32 (25°39'N, 128°34'E; RF4788) that was same the station of Stn.31. Owing to the typhoon (T1307), after observation of Stn.45 (23°43'N,

133°00'E; RF4801), we sailed to Stn.63 (24°15'N, 143°38'E; RF4802). After observation of Stn.63, we sailed to westward, and observed from Stn.59 (24°14'N, 141°34'E; RF4803) to Stn.52 (24°15'N, 137°47'E; RF4810). We gave up at the station of Stn.52 and turned toward Tokyo (Japan). Leg 2 consisted of 23 stations. We arrived at Tokyo on July 24, 2013 (Leg 2).

One float and two drifting ocean data buoy were deployed along the cruise track. The information of deployed the float and the buoy are listed in [Table 2a](#).

RF13-07

RF13-07 cruise was carried out during the period from July 31 to September 18, 2013. Before the observation at the first station, all watch standers were drilled in the method of sample drawing and CTD operations at the point (34°41'N, 139°51'E). We restarted observation from Stn.46 (24°14'N, 133°21'E; RF4812) on August 3 to Stn.51 (24°14'N, 137°49'E; RF4817)

that was same the station of Stn.52, and from Stn.60 (24°15'N, 141°46'E; RF4818) and Stn.62 (24°15'N, 143°14'E; RF4820). We continued observation from Stn.64 (24°15'N, 143°39'E; RF4821) that was the same station of Stn.63. We sailed eastward and finished at Stn.89 (24°00'N, 164°59'E; RF4846) on August 15. Leg 1 consisted of 35 stations. She called for Pohnpei (Federated States of Micronesia) on August 21 (Leg 1). She left Pohnpei on August 25, 2013. The hydrographic cast of CTDO₂ was restarted at the same station (Stn.90 (24°00'N, 165°01'E; RF4847)) of Stn.89 on August 28. We observed eastward to Stn.108 (24°00'N, 179°00'E; RF4865), we turned northward and finished Stn.120 (29°58'N, 178°58'E; RF4877). Leg 2 consisted of 31 stations from Stn.90 to Stn.120. Stn.120 was finished on September 7. She arrived at Tokyo (Japan) on September 18, 2013 (Leg 2).

Five Argo floats were deployed along the cruise track. The information of deployed the float and the buoy are listed in Table 2b.

Location data of stations is shown in Table 3.

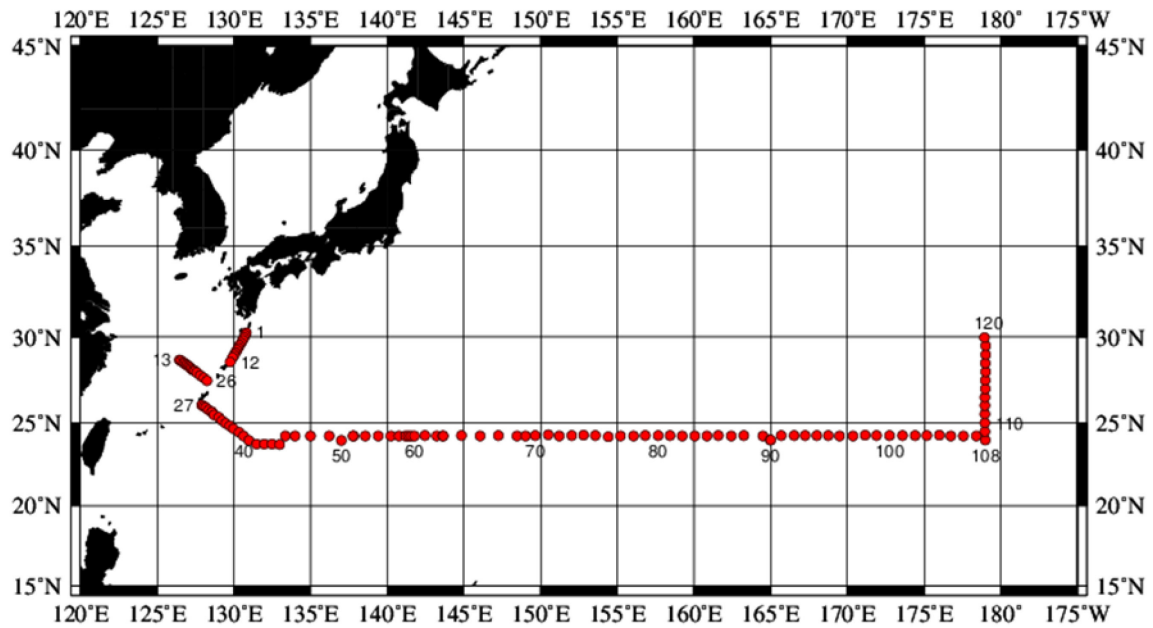


Figure 1: Cruise track of RF13-06 and RF13-07.

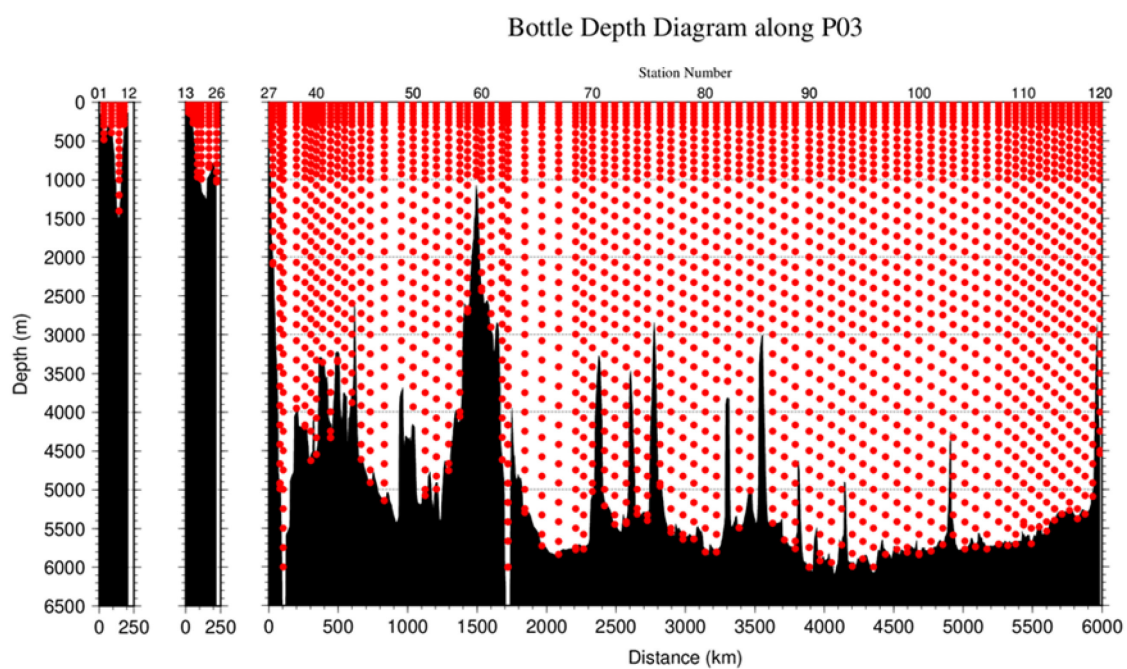


Figure 2: The bottle depth diagram for WHP-P03 revisit.

Table 1. The scheme of sampling layer in meters.

<i>Bottle count</i>	<i>scheme1</i>	<i>scheme2</i>	<i>scheme3</i>
<i>1</i>	10	10	10
<i>2</i>	50	50	50
<i>3</i>	100	100	100
<i>4</i>	150	150	150
<i>5</i>	200	200	200
<i>6</i>	250	250	250
<i>7</i>	300	330	280
<i>8</i>	400	430	370
<i>9</i>	500	530	470
<i>10</i>	600	630	570
<i>11</i>	700	730	670
<i>12</i>	800	830	770
<i>13</i>	900	930	870
<i>14</i>	1000	1070	970
<i>15</i>	1200	1270	1130
<i>16</i>	1400	1470	1330
<i>17</i>	1600	1670	1530
<i>18</i>	1800	1870	1730
<i>19</i>	2000	2070	1930
<i>20</i>	2200	2270	2130
<i>21</i>	2400	2470	2330
<i>22</i>	2600	2670	2530
<i>23</i>	2800	2870	2730
<i>24</i>	3000	3080	2930
<i>25</i>	3250	3330	3170
<i>26</i>	3500	3580	3420
<i>27</i>	3750	3830	3670
<i>28</i>	4000	4080	3920
<i>29</i>	4250	4330	4170
<i>30</i>	4500	4580	4420
<i>31</i>	4750	4830	4670
<i>32</i>	5000	5080	4920
<i>33</i>	5250	5330	5170
<i>34</i>	5500	5580	5420
<i>35</i>	5750	5830	5670
<i>36</i>	6000	6000	6000

Table 2a. Information of deployed float and buoy at RF13-06.

<i>Float WMO number</i>	<i>Date and Time (UTC) of Deployment</i>	<i>Position of deployment</i>		<i>PI</i>	
		<i>Latitude</i>	<i>Longitude</i>		
2902430	2013 July 9 01:32	23-42.54 N	132-56.59 E	JMA	APEX
<i>Buoy WMO number</i>	<i>Date and Time (UTC) of Deployment</i>	<i>Position of deployment</i>		<i>PI</i>	
		<i>Latitude</i>	<i>Longitude</i>		
21679	2013 June 25 01:32	28-42.30 N	126-27.04 E	JMA	YTSS-2100
21704	2013 July 6 00:42	25-32.74 N	128-44.72 E	JMA	YTSS-2100

APEX : Teledyne Webb Research (USA)

YTSS-2100: JVC KENWOOD Co., Japan

Table 2b. Information of deployed float and buoy at RF13-07.

<i>Float WMO number</i>	<i>Date and Time (UTC) of Deployment</i>	<i>Position of deployment</i>		<i>PI</i>	
		<i>Latitude</i>	<i>Longitude</i>		
2902453	2013 August 12 05:30	24-16.70 N	157-39.46 E	JAMSTEC	ARVOR
2902461	2013 August 29 21:59	24-16.84 N	168-02.16 E	JAMSTEC	ARVOR
2902462	2013 August 31 20:45	24-18.38 N	172-47.57 E	JAMSTEC	ARVOR
2902463	2013 September 2 11:45	24-16.08 N	176-47.13 E	JAMSTEC	ARVOR
2902464	2013 September 3 10:20	24-00.89 N	178-59.85 E	JAMSTEC	ARVOR

ARVOR : nke Instrumentation (France)

Table 3a. Station data of RF13-06 cruise. The 'RF' column indicates the JMA station identification number.

<i>EXPOCODE</i>	<i>Leg</i>	<i>Station</i>		<i>Position</i>	
<i>sub number</i>		<i>Stn.</i>	<i>RF</i>	<i>Latitude</i>	<i>Longitude</i>
1	1	1	4771	30-14.47 N	130-50.26 E
1	1	2	4772	30-05.87 N	130-44.66 E
1	1	3	4773	29-58.18 N	130-40.29 E
1	1	4	4774	29-48.88 N	130-34.72 E
1	1	5	4775	29-40.04 N	130-28.82 E
1	1	6	4776	29-32.26 N	130-23.37 E
1	1	7	4777	29-23.21 N	130-17.82 E
1	1	8	4778	29-15.26 N	130-12.34 E
1	1	9	4779	29-06.58 N	130-06.60 E
1	1	10	4780	28-58.18 N	130-01.36 E
1	1	11	4781	28-50.25 N	129-55.28 E
1	1	12	4782	28-35.19 N	129-45.09 E
1	1	13	4757	28-42.01 N	126-26.87 E
1	1	14	4758	28-38.37 N	126-34.13 E
1	1	15	4759	28-33.26 N	126-41.28 E
1	1	16	4760	28-29.59 N	126-48.44 E
1	1	17	4761	28-24.62 N	126-54.41 E
1	1	18	4762	28-21.11 N	127-01.79 E
1	1	19	4763	28-16.09 N	127-08.65 E
1	1	20	4764	28-10.72 N	127-14.80 E
1	1	21	4765	28-06.17 N	127-21.50 E
1	1	22	4766	28-02.56 N	127-28.39 E
1	1	23	4767	27-57.76 N	127-34.77 E
1	1	24	4768	27-48.18 N	127-48.09 E
1	1	25	4769	27-38.76 N	128-02.00 E
1	1	26	4770	27-30.08 N	128-15.29 E
1	1	27	4783	26-04.15 N	127-54.85 E
1	1	28	4784	26-00.11 N	128-02.11 E
1	1	29	4785	25-54.71 N	128-09.77 E
1	1	30	4786	25-47.16 N	128-21.45 E
1	1	31	4787	25-39.13 N	128-33.96 E
2	2	32	4788	25-38.74 N	128-33.71 E
2	2	33	4789	25-29.81 N	128-43.41 E
2	2	34	4790	25-20.88 N	129-00.74 E
2	2	35	4791	25-09.31 N	129-14.70 E

Table 3a. Continue.

<i>EXPOCODE</i>	<i>Leg</i>	<i>Station</i>		<i>Position</i>	
		<i>Stn.</i>	<i>RF</i>	<i>Latitude</i>	<i>Longitude</i>
2	2	36	4792	24-59.45 N	129-29.38 E
2	2	37	4793	24-50.65 N	129-44.33 E
2	2	38	4794	24-40.71 N	129-58.82 E
2	2	39	4795	24-28.09 N	130-19.53 E
2	2	40	4796	24-14.71 N	130-38.28 E
2	2	41	4797	23-59.02 N	130-58.98 E
2	2	42	4798	23-45.49 N	131-28.65 E
2	2	43	4799	23-45.05 N	131-59.11 E
2	2	44	4800	23-45.30 N	132-29.45 E
2	2	45	4801	23-43.71 N	133-00.00 E
2	2	52	4810	24-14.55 N	137-47.36 E
2	2	53	4809	24-15.12 N	138-33.99 E
2	2	54	4808	24-14.40 N	139-26.01 E
2	2	55	4807	24-13.83 N	140-14.17 E
2	2	56	4806	24-14.62 N	140-46.37 E
2	2	57	4805	24-14.60 N	141-11.02 E
2	2	58	4804	24-14.47 N	141-23.34 E
2	2	59	4803	24-14.07 N	141-33.75 E
2	2	63	4802	24-15.23 N	143-37.66 E

Table 3b. Station data of RF13-07 cruise. The 'RF' column indicates the JMA station identification number.

<i>EXPOCODE</i>	<i>Leg</i>	<i>Station</i>		<i>Position</i>	
		<i>Stn.</i>	<i>RF</i>	<i>Latitude</i>	<i>Longitude</i>
3	1	46	4812	24-13.57 N	133-21.00 E
3	1	47	4813	24-14.06 N	133-59.75 E
3	1	48	4814	24-15.17 N	134-59.94 E
3	1	49	4815	24-15.03 N	136-12.54 E
3	1	50	4816	23-59.27 N	137-00.24 E
3	1	51	4817	24-14.25 N	137-48.60 E
3	1	60	4818	24-15.40 N	141-45.91 E
3	1	61	4819	24-15.84 N	142-26.98 E
3	1	62	4820	24-15.32 N	143-13.93 E
3	1	64	4821	24-15.11 N	143-38.58 E
3	1	65	4822	24-15.63 N	144-50.93 E

Table 3b. Continue.

<i>EXPOCODE</i>	<i>Leg</i>	<i>Station</i>		<i>Position</i>	
		<i>Stn.</i>	<i>RF</i>	<i>Latitude</i>	<i>Longitude</i>
3	1	66	4823	24-14.65 N	146-03.68 E
3	1	67	4824	24-15.78 N	147-15.35 E
3	1	68	4825	24-15.50 N	148-28.09 E
3	1	69	4826	24-14.47 N	149-01.46 E
3	1	70	4827	24-16.36 N	149-39.23 E
3	1	71	4828	24-17.59 N	150-30.54 E
3	1	72	4829	24-14.47 N	151-14.05 E
3	1	73	4830	24-16.08 N	152-02.72 E
3	1	74	4831	24-16.71 N	152-49.03 E
3	1	75	4832	24-16.19 N	153-33.69 E
3	1	76	4833	24-10.97 N	154-26.25 E
3	1	77	4834	24-14.91 N	155-12.52 E
3	1	78	4835	24-14.85 N	156-03.86 E
3	1	79	4836	24-15.89 N	156-50.46 E
3	1	80	4837	24-15.92 N	157-39.77 E
3	1	81	4838	24-15.76 N	158-27.00 E
3	1	82	4839	24-14.67 N	159-14.71 E
3	1	83	4840	24-14.30 N	160-04.14 E
3	1	84	4841	24-14.98 N	160-50.69 E
3	1	85	4842	24-15.82 N	161-35.29 E
3	1	86	4843	24-15.13 N	162-26.54 E
3	1	87	4844	24-15.55 N	163-16.16 E
3	1	88	4845	24-15.36 N	164-03.30 E
3	1	89	4846	24-00.15 N	164-59.37 E
4	2	90	4847	24-00.48 N	165-00.85 E
4	2	91	4848	24-15.67 N	165-42.12 E
4	2	92	4849	24-16.16 N	166-31.51 E
4	2	93	4850	24-15.57 N	167-15.59 E
4	2	94	4851	24-15.88 N	168-00.59 E
4	2	95	4852	24-15.95 N	168-46.09 E
4	2	96	4853	24-14.85 N	169-30.85 E
4	2	97	4854	24-14.74 N	170-21.82 E
4	2	98	4855	24-16.58 N	171-10.76 E
4	2	99	4856	24-15.76 N	171-55.30 E
4	2	100	4857	24-16.08 N	172-44.98 E
4	2	101	4858	24-15.52 N	173-36.53 E

Table 3b. Continue.

<i>EXPCODE</i>	<i>Leg</i>	<i>Station</i>		<i>Position</i>	
		<i>Stn.</i>	<i>RF</i>	<i>Latitude</i>	<i>Longitude</i>
4	2	102	4859	24-16.26 N	174-25.87 E
4	2	103	4860	24-16.23 N	175-10.65 E
4	2	104	4861	24-16.94 N	175-59.98 E
4	2	105	4862	24-15.37 N	176-45.70 E
4	2	106	4863	24-14.52 N	177-35.05 E
4	2	107	4864	24-15.14 N	178-24.54 E
4	2	108	4865	24-00.31 N	179-00.35 E
4	2	109	4866	24-30.64 N	178-58.68 E
4	2	110	4867	25-01.28 N	178-58.69 E
4	2	111	4868	25-31.64 N	178-59.31 E
4	2	112	4869	26-01.69 N	178-59.23 E
4	2	113	4870	26-30.91 N	178-58.88 E
4	2	114	4871	27-01.13 N	178-59.51 E
4	2	115	4872	27-30.64 N	179-00.24 E
4	2	116	4873	27-59.88 N	179-00.67 E
4	2	117	4874	28-30.42 N	178-59.89 E
4	2	118	4875	29-00.36 N	179-01.84 E
4	2	119	4876	29-29.78 N	179-01.18 E
4	2	120	4877	29-58.17 N	178-57.70 E

List of Principal Investigators for all Measurements

The principal investigator (PI) and the person in charge responsible for major parameters measured on the cruise are listed in Table 4a (RF13-06) and Table 4b (RF13-07).

Table 4a. List of principal investigator and the person in charge on the ship for RF13-06.

Item	Principal Investigator (PI)	Person in charge on the ship
<u>Hydrography</u>		
CTDO ₂ / LADCP	Toshiya NAKANO	Tomoyuki KITAMURA
Salinity	Toshiya NAKANO	Sho HIBINO
Dissolve oxygen	Toshiya NAKANO	Takashi MIYAO
Nutrients	Toshiya NAKANO	Sonoki IWANO
Phytopigment	Toshiya NAKANO	Naoshi KUBO
DIC	Toshiya NAKANO	Kyoichi KAWAHARA
Total Alkalinity	Toshiya NAKANO	Kyoichi KAWAHARA
pH	Toshiya NAKANO	Kyoichi KAWAHARA
CFCs	Toshiya NAKANO	Akira WADA

Underway

Meteorology	Toshiya NAKANO	Kazuhiro NEMOTO
Thermo-Salinograph	Toshiya NAKANO	Kyoichi KAWAHARA

Guideline of Ocean Observation Vol.1 Chap.4 Quality control by comparison with standards, control charts, duplicated measurements, and property-property characteristics, and the report of metadata ©Michio Aoyama, Hiroshi Uchida, Daisuke Sasano, Hajime Obata 2019 G104EN:001-134

$p\text{CO}_2$	Toshiya NAKANO	Kyoichi KAWAHARA
Chlorophyll-a	Toshiya NAKANO	Naoshi KUBO
ADCP	Toshiya NAKANO	Tomoyuki KITAMURA
Bathymetry	Toshiya NAKANO	Tomoyuki KITAMURA

Float and Buoy

Argo float (JMA)	Kazuhiro NEMOTO	Kazuhiro NEMOTO
Buoy (JMA)	Kazuhiro NEMOTO	Kazuhiro NEMOTO

Table 4b. List of principal investigator and the person in charge on the ship for RF13-07.

Item	Principal Investigator (PI)	Person in charge on the ship
<u>Hydrography</u>		
CTDO ₂ / LADCP	Toshiya NAKANO	Kiyoshi MURAKAMI
Salinity	Toshiya NAKANO	Keizo SHUTTA
Dissolve oxygen	Toshiya NAKANO	Hiroyuki FUJIWARA
Nutrients	Toshiya NAKANO	Chihiro KAWAMURA
Phytopigment	Toshiya NAKANO	Tomohiro UEHARA
DIC	Toshiya NAKANO	Shu SAITO
Total Alkalinity	Toshiya NAKANO	Shu SAITO
pH	Toshiya NAKANO	Shu SAITO
CFCs	Toshiya NAKANO	Etsuro ONO
<u>Underway</u>		
Meteorology	Toshiya NAKANO	Hitomi KAMIYA
Thermo-Salinograph	Toshiya NAKANO	Shu SAITO
$p\text{CO}_2$	Toshiya NAKANO	Shu SAITO
Chlorophyll-a	Toshiya NAKANO	Tomohiro UEHARA
ADCP	Toshiya NAKANO	Keizo SHUTTA
Bathymetry	Toshiya NAKANO	Keizo SHUTTA
<u>Float</u>		
Argo float (JAMSTEC)	Shigeki HOSODA	Hitomi KAMIYA

Toshiya NAKANO (x x x @ x x x .kishou.go.jp)

Marine Division, Global Environment and Marine Department, JMA 1-3-4,
Otemachi, Chiyoda-ku, Tokyo 100-8122, JAPAN
Phone: +81-3-3212- x x x x Ext. x x x x

Kazuhiro NEMOTO (x x x @ x x x .kishou.go.jp)

Marine Division, Global Environment and Marine Department, JMA 1-3-4,
Otemachi, Chiyoda-ku, Tokyo 100-8122, JAPAN
Phone: +81-3-3212- x x x x Ext. x x x x

Shigeki HOSODA (x x x x @jamstec.go.jp)

Ocean Circulation Research Group,

Guideline of Ocean Observation Vol.1 Chap.4 Quality control by comparison with standards, control charts, duplicated measurements, and property-property characteristics, and the report of metadata ©Michio Aoyama, Hiroshi Uchida, Daisuke Sasano, Hajime Obata 2019 G104EN:001-134

Research and Development Center for Global Change (RCGC), Strategic Research
and Development area,
Japan Agency for Marine-Earth Science and Technology (JAMSTEC) 2-15
Natsushima, Yokosuka-shi, Kanagawa 237-0061, JAPAN

Reference

Swift, J. H. (2010): Reference-quality water sample data: Notes on acquisition, record keeping, and evaluation. *IOCCP Report No.14, ICPO Pub. 134, 2010 ver.1*

Data Publication and International Exchange

○Toru SUZUKI (Marine Information Research Center, Japan Hydrographic Association),

Yutaka MICHIDA (Atmosphere and Ocean Research Institute, the University of Tokyo)

1. Introduction

Oceanographic data show observational values, which are attached to dates, times, and positions. Recent developments and improvements to observational techniques and instruments have been associated with data accuracy and quality control, so that the importance of the related information increases the exchange, sharing and integration of oceanographic data. This chapter therefore describes a mechanism of international exchange and sharing in the ocean sciences and other science fields for oceanographic data observed by research vessels and other ships. In this chapter, ‘data’ includes observed data and related information; the latter indicates ‘metadata’ – data of data – if needed. Specimens such as marine organisms or sea bottom materials are also included in data but only numerical data are treated in this chapter.

2. Importance of Data Publication

There is no doubt about the importance of data for all scientific research. Working Group on Scientific Data Network Facilitation (2004) expressed that geophysics is a subject which studies the accumulation of unexpected and not replicable phenomena on the earth and vicinities since 4.6 billion years ago, so as many continuous observations as possible are required, all records should be archived and collected in principle and left as the common heritage of mankind. What is true for geophysics is true for the marine sciences as well. UNESCO’s IOC established the IODE in 1961 because common understanding in the world through oceanographic data exchange and sharing among the member states is important.

3. Outline of Data Publication and International Exchange

The result of various observations by research vessels, including training, survey, chartered and voluntary ships, is published by a chief scientist or someone who belongs to an organization (hereafter, data originator) as cruise reports through preliminary and cruise summary reports. Real time data is reported before publication of their reports. In the past, observed data were recorded on paper as an expression in numerical form of visual observations, while more recently, massive amounts of digital data are being stored directly on mass storage devices, such as optical-magnetic disks or flash memory, for developing instruments and improving accuracy. Moreover, observed data is directly distributed by data originators with the spread of the network system, i.e., full-time connection and unlimited access to the Internet, and cruise reports are also outputted in digital document formats such as PDF.

The NODC, established under a program of the IODE of the IOC/UNESCO, has the role of

providing national oceanographic data and information in a usable format to a wider user community and for international exchange. The JODC was established in the Hydrographic Department of the Japan Maritime Safety Agency (presently, the Hydrographic and Oceanographic Department of the Japan Coast Guard) in 1965 in accordance with a resolution adopted by the IOC/UNESCO in 1961 as well as reports from the Council for Marine Scientific Technology in 1963 and 1964. The JODC provides various oceanographic data through its JODC Data On-line Service System (J-DOSS) and also submits its data to the NCEI (formerly, National Oceanographic Data Center of the United States) which houses the World Data Center for Oceanography under the ICSU WDS according to an IODE recommendation of the WOD project. Japanese data occupy 11% of total observations in the WOD, placing Japan second of 96 countries for contributions. Long time archiving is also one of the roles of the NODC in order to prevent data loss by principle investigator transfer or retirement, or the discontinuance of data distribution or archiving in his/her organization due to various reasons. Particularly in Japan, it is necessary to pay attention to the potential of lost data and information due to a natural disaster such as an earthquake or tsunami. It is therefore strongly recommended to submit the published data and metadata to the JODC.

On the other hand, several data management offices of international projects have continued to collect specific data and information after the end of the projects. The CDIAC Ocean Carbon Data Management Project was organized in 1993 and collects discrete and underway measurements of ocean carbon dioxide from various platforms, e.g., research vessels, commercial and volunteer ships, and buoys. The CCHDO delivers the highest quality global CTD and hydrographic data, including ocean carbon dioxide and its related parameters, which have been acquired during WOCE, CLIVAR and other international oceanographic research programs. The OBIS was created as the information component of the Census of Marine Life and serves to document the ocean's diversity, distribution and abundance of life, and is one of the projects of the IODE at the present. These data management offices target specific parameters and therefore should be called special data centers, against the NODC which collects all oceanographic data. The IODE cooperates with the special data centers for data collection and distribution, and recommends registering as an ADU, a new component of the IODE similar to the NODC. The Japan Ocean Biogeographic Information System Center of JAMSTEC is a Japan regional OBIS node that was registered as an ADU of the IODE in January 2015. It is also recommended that data originators submit their own data to the special data centers at the same time. As for the ICSU World Data System, the IODE is a network member, and some organizations in IOC member states are regular members: the World Data Service for Oceanography in the United States, the World Data Center for Oceanography in NODCs in China and the Russian Federation, the Flanders Marine Institute, the Data Centre in Belgium, and Ocean Networks Canada.

4. National Oceanographic Programs and Cruise Summary Reports

As complementary information until the Cruise Report is published, it is recommended that NOPs and CSRs be submitted.

A NOP provides information on when, where and what kind of oceanographic cruises are planned

at domestic research organizations, in order to enhance the effective use of oceanographic research opportunities and oceanographic data. NOPs are registered and searched on the Marine Information Clearing House Network operated by the Hydrographic Department of the Japan Coast Guard. Please see <http://www.mich.go.jp/> for more information.

A CSR is intended to fill the gap between the first announcement of an oceanographic program and the eventual catalogue of data available to users. As timely inventories of data to ensure prompt exchange, the CSR contains such information as the ocean area where the investigation was carried out, a track chart of the cruise, the name of the person who holds the data, and the name and volume of the data written in the IOC's CSR form. Please see <http://www.jodc.go.jp/info/csr.html> for more information.

5. Standardization for Oceanographic Data Exchange

The JODC collects oceanographic data from domestic research institutes and submits them to the NCEI every year. Those data are stored in the WOD. In addition, non-Japanese data are extracted from the WOD and registered to J-DOSS all together. Recently, oceanographic data and information exchange is being carried out for not only oceanography but also marine meteorology. The IOC established JCOMM in cooperation with the WMO in 1999, and JCOMM coordinates, and develops and recommends standards and procedures for, a fully integrated marine observing, data management and services system. In order to standardize data processing, formats and codes are required for promoting data and information exchange between researchers in oceanography and other sciences. The Task Team for Ocean Data Standards established under the Joint JCOMM/IODE Expert Team on Data Management Practices reviews the proposals for standardization of oceanographic data exchange practices, and accepted proposals are recommended and published in the IOC Manuals and Guides No. 54 series. At present, three recommendations have been published for country codes, representation of date and time, and a quality flag scheme. It would be useful if data originators would consider the above recommendations when publishing data.

5-1. Country Codes

Adoption of ISO 3166-1 and 3166-3 is recommended for identifying countries (IOC, 2010). Japan is defined as JP and JPN in ISO 3166-1 alpha-2 and alpha-3, respectively. The former is known as a top level domain at the highest level in the hierarchical Domain Name System of the Internet, and the latter is often seen in broadcasts of games or events such as the Olympics and international soccer matches.

5-2. Representation of Date and Time

Adoption of ISO 8601:2004 is recommended for representation of date and time (IOC, 2011). The basic date notation is YYYYMMDD, where YYYY is the year, MM is the month of the year between 01 (January) and 12 (December), and DD is the day of the month between 01 and 31 (e.g., 20150624 or 2015-06-24), and the time notation is hhmmss, where hh is the number of complete hours between

00 and 24 (note that 24 is only allowed to indicate the end of the calendar day), mm is the number of complete minutes between 00 to 59, and ss is the number of complete seconds between 00 and 60 (note that 60 is used to indicate a positive leap second; e.g., 141531 or 14:15:31). The recommended representation is therefore familiar to Japanese. For more examples, see IOC (2011). The time zone must be clearly specified. In particular, biological observation during a long voyage or transoceanic cruise often uses the ship's time, not JST or GMT, in order to distinguish between day and night, so it is difficult to standardize the date and time for data exchange.

5-3. Quality Flag Scheme

Although development and improvement of observational techniques and instruments earn wider observation coverage and accurate data and information, it is difficult to avoid the inclusion of error data derived from the malfunction of instruments, and missing or failed measurements. Quality control by data originators is highly reliable and their results are extremely helpful for data exchange. After the error data are eliminated or flagged as 'bad data' by data originators in advance, doubtful data are detected through quality control by data centers or users and are flagged as 'questionable data'. Some of the questionable data will be changed to 'unknown data' if it is difficult to make a decision because there is little historical data and a lack of metadata. It is not to be denied that for observational records of unexpected and not replicable phenomenon, all data should be archived and published with quality flags. It is noted that missing value which has no missing flag, and vice versa, may be misunderstood for data processing.

There are many observed data exchange formats with quality flags, e.g., the WHP-exchange format (Swift and Diggs, 2008) is the de facto standard format for CTDs and bottle sampling data with nine level quality flags added by data originators. On the other hand, data center formats, such as the WOD and FETI of the J-DOSS, determine their own quality flags to header information and observed data in each depth, respectively, because historical data usually have no information for data quality. The problem here is that there is a different definition of the flags in each format, e.g., flag '0' means good in one format but flag '2' means good in another format. For that reason, the recommended quality flag scheme (IOC, 2013) defines five flags: 1 as good, 2 as unknown, 3 as questionable, 4 as bad, and 9 as missing at the primary level, and other results for quality control procedures or data processing in detail are described at the second or lower level. The other purpose for the above simplified quality flag scheme is to promote data exchange between researchers in oceanography and other sciences. There is no format which adopts this quality flag scheme at present, but the Ocean Data View (ODV; Schlitzer, 2015) defines quality flags similar to the primary level flags of the above scheme, and the ODV can import 14 different existing formats with its own quality flags.

5-4. Ship Codes and Cruise Numbers

There is no proposal for standardization of ship codes and cruise numbers at present, but a de facto standard that has been adopted by several data centers exists. It facilitates the management of observed data and metadata from each cruise, so ship codes and cruise numbers are required to identify the cruises. A cruise number assigned by a data originator is a primary, compatible identification of a

cruise by a ship with a timeline. For example, a cruise from September 23 to October 3 by the Ryofu Maru of the JMA is assigned as RF14-08, where RF is the ship code from the JMA, 14 means the year 2014, and 08 means the 8th cruise in 2014.

Former JODC ship codes were assigned as two alphanumeric characters, and the JODC now adopts the international radio call sign for ship identification because it is possible that the old ship codes will expire in the near future. On the other hand, the NCEI assigns three kinds of ship codes: the NODC code, which consists of two figures for the country code and two alphanumeric characters for ship identification, the WOD code with three or more figures, and a call sign (see <http://www.nodc.noaa.gov/General/NODC-Archive/platformlist.txt>). The NODC codes also synchronize with ICES ship codes, which are assigned by the ICES data center. For example, the Ryofu Maru of the JMA has been assigned 49UP, 49RY and 49UX from newest to oldest. Note that the country code in the NODC code is an original one, different from ISO 8601:2004 described in the previous section.

As for cruise identification, the CCHDO and CDIAC use an EXPOCODE that consists of a NODC ship code and cruise departure date (Swift and Diggs, 2008). For example, the EXPOCODE is automatically determined as 49UP20140923 for the above-mentioned cruise of the Ryofu Maru of the JMA. Nevertheless the data originator's cruise number should be recorded on database as metadata because of compatibility and continuity.

6. Data Policy

The intellectual property rights to the observed data basically belong to the organization that provides the facilities and equipment, and the data originator usually has a priority of data use rights in order to research, study and write documents. Unfortunately, its term is frequently unclear in regulation and several further parameters need a long time to fix values by calibration or quality control, so data publishing is often behind schedule. Working Group on Scientific Data Network Facilitation (2004) pointed out that some data originators are not so conscientious to publish and share observed data using the public facilities and equipment, so they often monopolize the data.

The NODC basically follows the IOC data exchange policy (IOC, 2003), while the JODC requests that users express that they have used its materials and submit one copy of the document and product to the JODC, and no reproduction of data can be provided to a third party without permission. As described in a previous section, the JODC submits their data to the NCEI in order to have it merged with that of the WOD, according to IODE recommendations of the WOD and GODAR, and the JODC shares WOD data with the J-DOSS.

7. Data Citation

Cruise reports are published with oceanographic data, and the scientific findings are also published in scientific journals through the peer review process. Both are used as references in other reports and articles; however, it is difficult to refer to oceanographic data because there is no citation information

in the data or databases such as the WOD and the J-DOSS, so the referenced data is mentioned in thanks at the end of an article or in the acknowledgements, which means the referenced data is not countable in the number of citations. The IODE therefore discussed this problem in cooperation with the SCOR, the BODC, and the MBLWHOI (Leadbetter et al., 2013).

On the other hand, the ocean carbon synthesis community has established projects, such as SOCAT for ocean surface and GLODAPv2 for ocean interior, and results of data synthesis from both projects were submitted to the ESSD, a data publication journal. Furthermore, the CDIAC archives other products from the projects, including technical documents and all cruise data, attached citations and DOIs. An increase in the number of references for oceanographic data will be rated highly by data originators and managers. The ESSD and DOIs are also important for digitizing historical data, and identification and citation of massive databases. The data citation issue is also being discussed in one of the working groups of the RDA in cooperation with researchers of other scientific fields.

8. Concluding Remarks

In this paper, we have explained that observed data and metadata are submitted to the NODC of the IODE so that the data is available for international exchange and sharing among researchers in the ocean sciences and other science fields. In addition, it is also important to recover or digitize historical data that were recorded to analog media such as paper using recent technologies, but it is not so easy to guarantee resources for such a project. The IODE created the GODAR project in order to search for and rescue historical data in the IOC member states, and the JODC conducted GODAR-WESTPAC, one of the regional GODAR projects. The global and regional GODAR projects have been terminated but GODAR has been recommended by the IODE again and their results have been summarized in the WOD.

Acknowledgements

We would like to thank staff of the JODC for useful comments and suggestions.

References

- IOC (2003): IOC Oceanographic Data Exchange Policy, Resolution XXII-6, IOC-XXII/3 Annex II, 7–9.
- IOC (2010): Recommendation to adopt IOS 3166-1 and 3166-3 Country Codes as the Standard for Identifying Countries in Oceanographic Data Exchange, Ocean Data Standards, Vol. 1, IOC Manuals and Guides No. 54, Vol. 1, Paris, IOC of UNESCO, 15 pp.
- IOC (2011): Recommendation to adopt ISO 8601:2004 as the Standard for the Representation of Dates and Times in Oceanographic Data Exchange, Ocean Data Standards, Vol. 2, IOC Manual and Guides No. 54, Vol. 2, Paris, IOC of UNESCO, 17 pp.
- IOC (2013): Recommendation for a Quality Flag Scheme for the Exchange of Oceanographic and Marine Meteorological Data, Ocean Data Standards, Vol. 3, IOC Manual and Guides No. 54, Vol. 3, Paris, IOC of UNESCO, 12 pp.

- Leadbetter, A., L. Raymond, C. Chandler, L. Pikula, P. Pissierssens, and E. Urban (2013): Ocean Data Publication Cookbook. IOC Manual and Guides No. 64, Paris, IOC of UNESCO, 41 pp.
- Schlitzer, R. (2015): Ocean Data View, <http://odv.awi.de/>
- Swift, J. H. and S. C. Diggs (2008): Description of WHP-Exchange Format for CTD/Hydrographic Data, CLIVAR and Carbon Hydrographic Data Office, UCSD Scripps Institution of Oceanography, 19 pp.
- Rigaku dēta nettowāku suishin wākingu gurūpu* [Working Group on Scientific Data Network Facilitation] (2004): *Rigaku dētabēsu kouchiku sokushin to dēta nettowāku taisei no seibi ni mukete* [Heading towards Facilitation of Scientific Database Construction and Development of a Data Network System], Subcommittee of Science Data Network Promotion, Section No. 4, 17th phase of the Science Council of Japan, 182 pp. (in Japanese) [Available on line at <http://center.stelab.nagoya-u.ac.jp/rigakunet/rigakunet.html>]

Abbreviations and Acronyms

ADU	Associate Data Unit
BODC	British Oceanographic Data Centre
CCHDO	CLIVAR and Carbon Hydrographic Data Office
CDIAC	Carbon Dioxide Information Analysis Center
CLIVAR	Climate and Ocean: Variability, Predictability, and Change
CSR	Cruise Summary Report
CSV	Comma-Separated Values
CTD	Conductivity, Temperature and Depth profiler
DOI	Digital Object Identifier
ESSD	Earth System Science Data
FETI	Format of Exchange and Translation for Integration
GLODAPv2	Global Ocean Data Analysis Project Version 2
GMT	Greenwich Mean Time
GODAR	Global Oceanographic Data Archeology and Rescue
ICES	International Council for Exploration of the Sea
ICSU	International Council for Science
IOC	Intergovernmental Oceanographic Commission of UNESCO
IODE	International Oceanographic Data and Information Exchange of IOC of UNESCO
JAMSTEC	Japan Agency for Marine-Earth Science and Technology
JCOMM	Joint WMO-IOC Technical Commission for Oceanography and Marine Meteorology
JMA	Japan Meteorological Agency
JODC	Japan Oceanographic Data Center
JST	Japan Standard Time
MBLWHOI	Marine Biological Laboratory, Woods Hole Oceanographic Institution

NCEI	National Center for Environmental Information (USA)
NODC	National Oceanographic Data Center
NOP	National Oceanographic Program
OBIS	Ocean Biogeographic Information System
PDF	Portable Document Format
RDA	Research Data Alliance
SCOR	Scientific Committee on Oceanic Research
SOCAT	Surface Ocean CO ₂ Atlas
UNESCO	United Nations Educational, Scientific and Cultural Organization
WDS	World Data System
WHP	WOCE Hydrographic Programme
WMO	World Meteorological Organization
WOCE	World Ocean Circulation Experiment
WOD	World Ocean Database

Calculation of the Thermophysical Properties of Seawater (2010)

A manual of “Calculation of the Thermophysical Properties of Seawater (2010)”, Manuals and Guides 56, IOC, can be obtained from a GO-SHIP web site as below.

http://www.go-ship.org/Manual/TEOS-10_Manual_06Jul10.pdf

This page left intentionally blank.

Water sampling

○Toshiya NAKANO (Japan Meteorological Agency), Hajime OBATA (The University of Tokyo), Kenichi KATAYAMA, Satoshi OZAWA and Hiroshi MATSUNAGA (Marine Works Japan Ltd.)

To obtain the data of physical and biogeochemical parameters in the ocean, we often need to collect water samples. By selecting the suitable water sampling method for the parameters to be measured, we will be able to get high-quality data. It is also necessary to maintain the sampling tools at better conditions by washing them and/or replacing some parts periodically.

1. Outline for water sampling

In order to obtain high quality data, it is important to use suitable water sampling bottles for the parameters to be measured. For the hydrographic observation in the open ocean, the Nansen water sampling bottle had been used until the CTD (Conductivity Temperature Depth profiler) system was developed in the 1970s. At present, the multi-bottle sampling system (e.g. Carousel Water Sampler by Sea-Bird Electronics, Inc., USA and Intelligent Rosette Water Sampling System by General Oceanics, Inc., USA) with CTD system is available. The multi-bottle sampling system is optimized for use of 12/24/36 water sampling bottles, from 1.2 to 30 L. On the other hand, the Niskin water sampler, Van Dorn water sampler and Kitahara's water bottle (RIGO-B) are used in the coastal regions.

2. Seasurface water sampling (Sea-bucket method)

For surface water (well-mixed sea water from the depth of 1 to 2 m), the sea-bucket method and the intake method are commonly used. For sea-bucket method, the bucket (about 5 L) is used to collect the sea water from the side of the ship (Japan Meteorological Agency, 2015). For the intake method, seasurface water is pumped up by inlet pipe in the bottom of the ship

The sea-bucket method is as follows:

- 1) To not lose a bucket, the end of the rope should be tied to the deck rail as a matter of precaution.
- 2) After filling the bucket with seawater and discarding them two or three times for rinsing, the water should be collected from the sea surface, and the water temperature should be measured on deck. During sampling, it is necessary to keep the bucket in water for a few minutes to get filled, and then haul the bucket up quickly to the deck.
- 3) To not contaminate the water sample, water should not be collected near the drain from the engine and kitchen of the ship.
- 4) The temperature of the seawater should be measured in a shady area. During the measurement, the water in the bucket should be continuously stirred. The temperature should be measured quickly using thermometer, when it attains a steady value after about 1 minute.

- 5) Water sample for measurements of salinity, dissolved oxygen etc., should be obtained after water temperature measurement.
- 5) After temperature measurement and water sampling, the sea water in the bucket should be dumped quickly, and the bucket should be washed with fresh water and turned upside down

3. CTD multi-bottle sampling system

The Niskin water sampling bottle (Niskin bottle, Figure 1) by General Oceanics or Ocean Test Equipment is frequently used for the CTD multi-bottle sampling system. The Niskin bottle consists of a body and end stoppers by hard vinyl chloride, spring for closing end stoppers, and rod. The volume of Niskin bottle is available 1.2 L, 1.7 L, 2.5 L, 5L, 8 L, 10 L, 12 L, 20 L and 30 L. The structure of Niskin sampling bottle is simple. The water inside of the bottle is easily exchanged. After collecting the water, leakage is rarely observed. We can customize Niskin bottles for the targeted parameters by coating the inside of the bottle, or selecting stainless spring or rubber to close the end stoppers, or changing the materials of O-ring. Detailed maintenance procedures of Niskin bottle and multi-bottle sampling system are described in Appendix A.1.

Moreover, we can also equip the Niskin bottle with a reversing thermometer/pressure gauge to confirm the depth where the sampling bottle is closed.

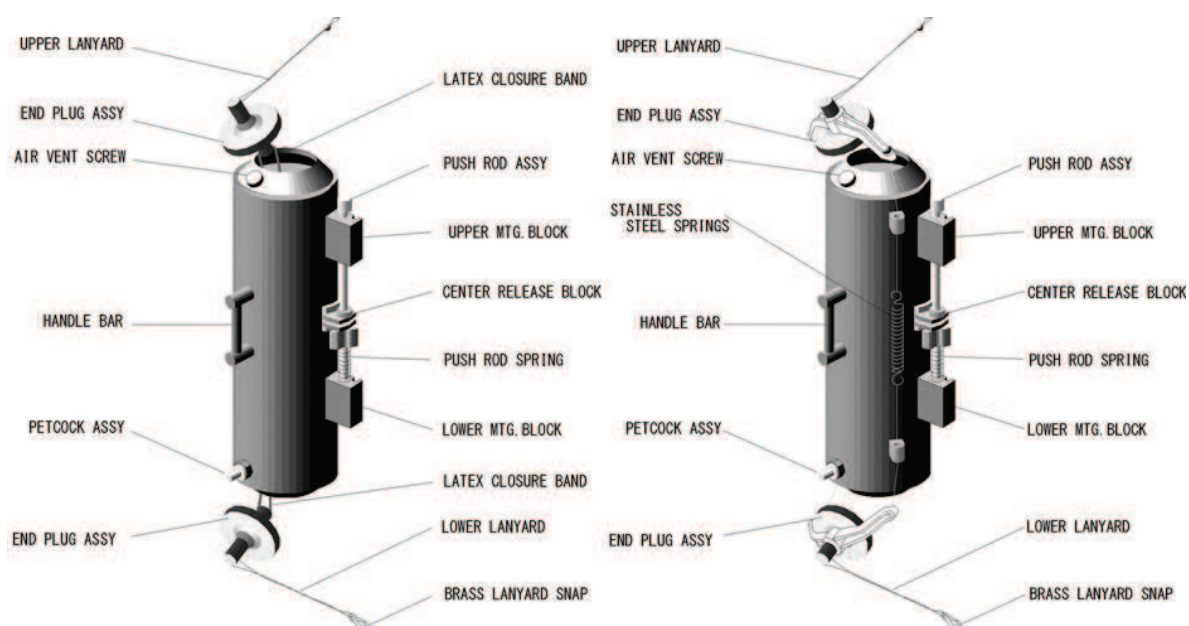


Figure 1. Overview of water sampling bottle (Left: Niskin sampling bottle, Right: Niskin-X sampling bottle ; General Oceanics, Inc., USA)

4. Clean seawater sampling

Trace metals in seawater are now important topics in oceanographic researches because some of them are limiting factors for phytoplankton growth in High Nutrient, Low Chlorophyll (HNLC) areas.

Guideline of ocean observations Vol.2 Chap.1 Water sampling

©Toshiya NAKANO, Hajime OBATA, Kenichi KATAYAMA, Satoshi OZAWA, Hiroshi MATSUNAGA 2018

G201EN:001-019

Despite their importance, we don't have enough data to discuss trace metal distributions and their biogeochemical cycles. Some essential trace metals for phytoplankton growth, like Fe and Zn, are categorized as contamination-prone elements in the ocean science because Fe is ubiquitous in the research ship and Zn is also frequently used in ocean observation equipments as sacrificial anode. Once the trace metals in seawater are contaminated during seawater sampling, it is impossible to study their distributions and biogeochemical cycles. Therefore, we need to apply the clean sampling method for the study of trace metals in seawater.

For the last three decades, the clean seawater sampling system has been developed rapidly. Especially through the international project, GEOTRACES, we have established the clean sampling method for trace metals in seawater. Here, the clean sampling method for trace metals in seawater is described briefly.

4-1. Seawater sampler

Seawater sampler is the most important equipment for clean sampling because it directly gets in contact with seawater. To prevent metal contamination to seawater samples, many original samplers have been developed, but now commercial samplers are available for clean sampling. For example, GO-Flo samplers (General Oceanics, Fig. 2) have often been used by US group for a long time (Brulad et al., 1979). Recently, Niskin-X samplers (General Oceanics, Fig. 3) have been used for clean sampling by Japanese group, too (Kim et al., 2015). For clean sampling, we have to exchange the original petcocks to Teflon ones, and original O-ring to Viton ones. Also, we can prevent metal contamination from the sampler's wall to seawater by Teflon coating.

To collect contamination-free seawater, we have to clean the samplers before the research cruise. After removing the organic compounds on the wall of the samplers with surfactants, we fill the inside of the samplers with 0.1M hydrochloric acid to remove the adsorbed metals. Since remaining acid in the samplers often causes a serious contamination problem, we fill the inside of the samplers with ultra-high purity water (UHPW) for one day. Otherwise, the samplers are soaked with open ocean seawater to remove the remaining acid. After cleaning the samplers, we have to keep the samplers clean so as not to be contaminated by air dusts.

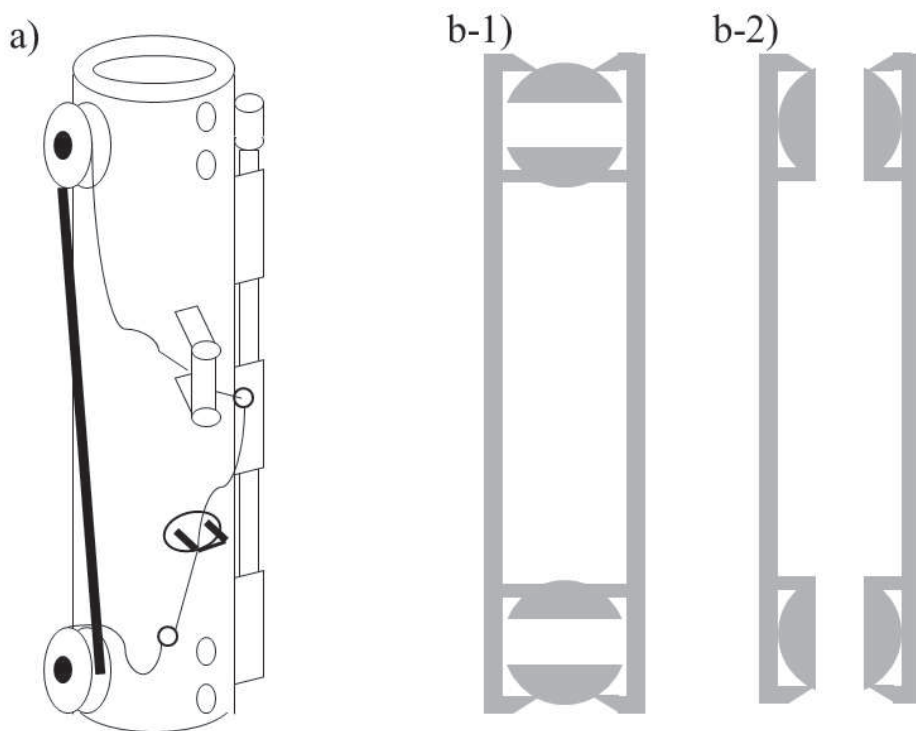


Figure 2. Schematic diagram of GO-Flo sampler (a. whole picture, b-1. closed, b-2. open)

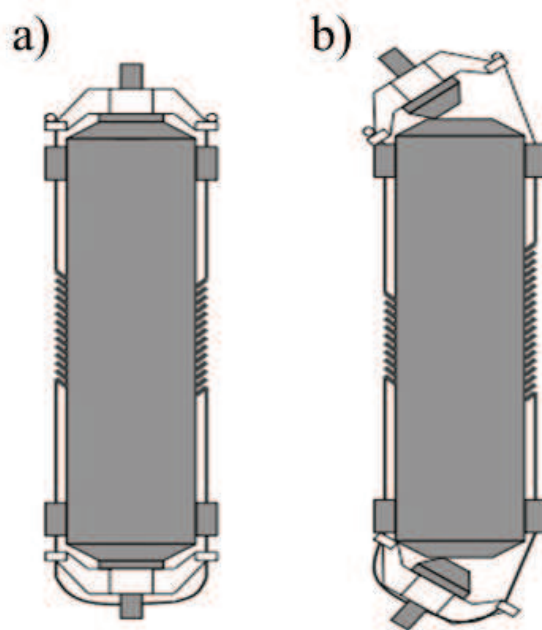


Figure 3. Niskin-X sampler (a. closed, b. open)

4-2 Sampling Procedure

When we use the clean samplers, we also have to be careful about contamination from the wire by which the samplers were hung. We can hang the samplers directly onto the hydrowire, but the seawater samples are often contaminated from the hydrowire itself, especially for trace metals like Fe. Moreover, the hydrowire is usually coated with grease, which possibly causes contamination on organic compounds in seawater. These contamination problems can be solved by using polyamide rope, like Kevlar rope, or titanium wire. For a long time, the most reliable sampling method was to hang the GoFlo sampler onto Kevlar rope (Burland et al., 1979). We also have to keep the sheaves clean where the direction of the rope is changed because grease is often used on the sheaves. By using plastic sheaves, this problem will be avoided. To keep the sampler at the desired depth, we hang some weights at the end of the wire. The distance between the weight and sampler should be long enough not to cause contamination on seawater sample. Messengers, to close the sampler, should be made with Teflon or be Teflon-coated. The Teflon-coated messenger can be commercially obtained.

Recently, it has become common to get the clean seawater samples with CTD sensors and multiple sampling system (Measures et al., 2008; Cutter and Bruland, 2012). During international GEOTRACES projects (<http://www.geotraces.org/>), it is required to perform spatially dense observations for mapping distributions of the trace elements and their isotopes. When CTD sensors and a multiple sampling system are used for investigations on trace elements and their isotopes in seawater, seawater samples might be contaminated from normal armoured cable. Contaminations are also caused by grease released from the normal armoured cable. Now, polyarylate (e.g., Vectran) armoured cable is available and widely-used for CTD observation in the world. In Japan, titanium armoured cable has been used for clean sampling in R.V. Hakuho-maru, which enabled us to determine trace elements in seawater. Recently it has been difficult to get the Ti-cable. Alternatively, Vectran armoured cable are now available in Japan. Care must be taken on the sheave not to contaminate the cable with greese and rust. We also have to keep the frame, onto which clean samplers are deployed, contamination-free. In the GEOTRACES project, epoxy-coated aluminium frames have often been used (Sohrin and Bruland, 2011). However, it is known that Zn sacrificial anodes, used on the frame, easily contaminate Zn in seawater, hence the anodes must be removed from the frame prior to the sampling. On the other hand, original titanium frame, for which Zn anodes are not necessary, was built in the Netherlands (De Baar et al., 2008). For sub-sampling from the Niskin-X sampler, the sampler was taken into a clean-air area (filled with air which was passed through HEPA filter) and samples were collected in sample bottles with positive air pressure.

Detailed sampling methods of the international GEOTRACES project are described in “cookbook,” published on the web site (2013 GEOTRACES Standards and Intercalibration Committee, 2014, <http://www.geotraces.org/science/intercalibration>).

5. Water sampling in the coastal region

The Van Dawn water sampler and Kitahara style (Rigaud B number) water sampler are widely used in the coastal region, river and lake (Figure 4). Since the Van Dawn water sampler is consist of a plastic body with rubber cap, it is often used for sampling for radionuclides, phytoplankton and bacteria. On the other hand, Kitahara's style (RIGO-B) water sampler is used for quality survey of water and sewerage.

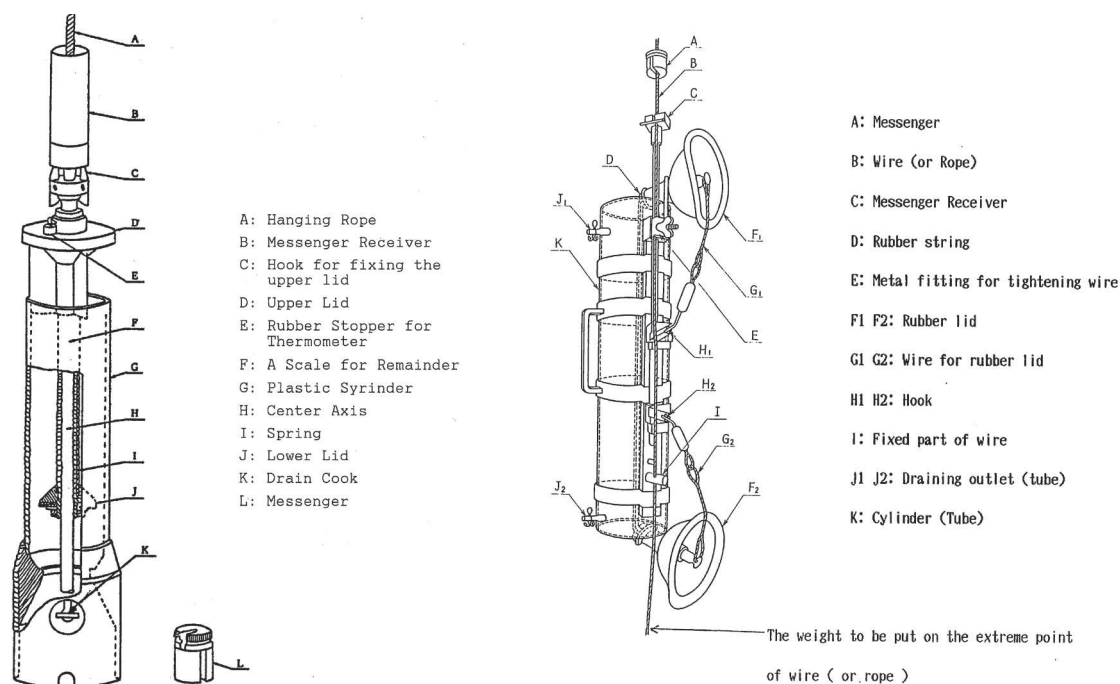


Figure 4. Van Dorn Water Sampler (Left) and Kitahara's type (RIGO-B) Water Sampler (Right)

6. Water sampling layer and order

The standard sampling depths in m samples are: 0 (bucket), 10, 20, 30, 50, 75, 100, 125, 150, 200, 250, 300, 400, 500, 600, 700, 800, 900, 1000, 1250, and below (intervals of 250 m). However, we can change the sampling interval for the purposes and/or region of hydrographic observation. For basin-scale hydrographic observation, such as the GO-SHIP (Global Ship-Based Hydrographic Investigation Program; <http://www.go-ship.org>) program, we can adopt a staggered scheme sampling pattern (Swift, 2010) for getting a high resolution data set.

During the water sampling, seawaters in the sampler are easily warmed to the room temperature and affected by surrounding air. Therefore, we should preserve the seawaters for dissolved gas (e.g. chlorofluorocarbon, dissolved oxygen and dissolved inorganic carbon) into bottles immediately. Samples of log sheets for information of station (date, time, position and water depth, etc.) and water sampling (sampling layer, bottle number, sampling parameter and bottle flag etc.) are denotes in Table 1 and 2.

Table 1 CTD operation log sheet

CTO2 obs. sheet

Stn. No.		Ship name		Cruise No		Leg	
	Cast No.	Sub-stn. No.:		-			

Current							
Date/Time	/	:					
Position	°	.	'N,	°	.	'E	
m	°	.	kt ()	Heading	°		
m	°	.	kt ()	Course	°		
m	°	.	kt ()	ship speed	kt		
m	°	.	kt ()	W.	:		
m	°	.	kt ()	Depth	m		

Operator							
BEGIN	.	/	:				
Position	°	.	'N,	°	.	'E	
W. Depth	m	Flag					
BOTTOM	.	/	:				
Position	°	.	'N,	°	.	'E	
W. Depth	m	Flag					
END	.	/	:				
Position	°	.	'N,	°	.	'E	
W. Depth	m	Flag					
Wire out	m	Altimeter					

Remarks							
----------------	--	--	--	--	--	--	--

Table 2 Sampling log sheet

Water Sampling Sheet

Cruise No.		Leg No.			Lat.		Stn. No.			
Scheme		W. Depth			Long.					
No.	Sampling Layer								No.#	BottleF.
	<i>Pump</i>									
*	<i>Bucket</i>								<i>Bucket</i>	
36									36	
35									35	
34									34	
33									33	
32									32	
31									31	
30									30	
29									29	
28									28	
27									27	
26									26	
25									25	
24									24	
23									23	
22									22	
21									21	
20									20	
19									19	
18									18	
17									17	
16									16	
15									15	
14									14	
13									13	
12									12	
11									11	
10									10	
9									9	
8									8	
7									7	
6									6	
5									5	
4									4	
3									3	
2									2	
1									1	
Remarks							Bottle Flag 0: Bucket 1: Bottle information unavailable 2: No problems noted 3: Leaking 4: Did not trip correctly 5: Not reported 9: Samples not drawn from this bottle			

Acknowledgements

Figures of Niskin sampling bottle was provided by Mr. Tanaka (K-Engineering Co. Ltd.). Figures of Van Dorn water sampler by Mr. Matumoto (RIGO Co., Ltd.).

References

- 2013 GEOTRACES Standards and Intercalibration Committee (2014) : Sampling and Sample-handling Protocols for GEOTRACES Cruises.
<http://www.geotraces.org/images/stories/documents/intercalibration/Cookbook.pdf>
- Bruland, K. W., R. P. Franks, G. A. Knauer, and J. H. Martin (1979): Sampling and analytical methods for the determination of copper, cadmium, zinc, and nickel at the nanogram per liter level in sea water. *Analytica et Chimica Acta*, 105, 233-245.
- Cutter, G. A., and K. W. Bruland (2012): Rapid and noncontaminating sampling system for trace elements in global ocean surveys. *Limnology and Oceanography: Methods*, 10, 425–436.
- De Baar, H. J. W., K. R. Timmermans, P. Laan, H. H. De Porto, S. Ober, J. J. Blom, M. C. Bakker, J. Schilling, G. Sarthou, M. G. Smit, and M. Klunder (2008) : Titan: A new facility for ultraclean sampling of trace elements and isotopes in the deep oceans in the international GEOTRACES program. *Marine Chemistry*, **111**, 4-21.
- Japan Meteorological Agency (2015) : Guide to Weather Observations for Ships. 72pp.
- Kim, T., H. Obata, T. Gamo, and J. Nishioka (2015): Sampling and onboard analytical methods for determining subnanomolar concentrations of zinc in seawater. *Limnology and Oceanography: Methods*, 13, 30–39.
- Measures, C. I., W. M. Landing, M. T. Brown, and C. S. Buck (2008): A commercially available rosette system for trace metal–clean sampling. *Limnology and Oceanography: Methods*, 6, 384–394.
- Sohrin, Y. and K. W. Bruland (2011): Global status of trace elements in the ocean. *Trends in Analytical Chemistry*, **30**, 1291 -1307.
- Swift, J. H. (2010) : Reference-quality water sample data: Notes on acquisition, record keeping, and evaluation. IOCCP Report No.14, ICPO Pub. 134, 2010 ver.1

Appendix

This section describes the maintenance and management of CTD – multi-layer water sampling system, comprised of water sampling bottles (Niskin bottles) and multi-bottle sampling arrays (Sea-Bird Electronics carousel), used widely in many institutes today.

A.1 Managing Water Sampling Bottle (Washing and Maintenance)

Niskin bottles must be washed before sampling. After sampling, all Niskin bottles must be washed and stored or prepared for next sampling.

A.1-1 How to Wash Niskin Bottles

① Preparation

- Neutral detergent (products not subject to PRTR (Pollutant Release and Transfer Register) Law, enacted on July 13, 1999, must be used, e.g. S-CLEAN WO-23 produced by Sasaki Chemical Co., Ltd)
- Plastic beaker
- Sponge
- Bucket

② If you have extra time

- 1) Fill Niskin bottle with 1% solution of S-CLEAN WO-23, and leave it for more than 12 hours.
- 2) Drain the solution. While draining, drain from petcock, to wash petcock as well.
- 3) Using the sponge and the drained solution used to clean inside the Niskin bottles, clean the outside of Niskin bottle. Rinse both the inside and outside of the Niskin bottle with fresh water, making sure bubbles are washed off. While draining, drain from petcock, to rinse petcock as well. (Note: Do not apply sponge inside Niskin bottle.)

③ If your time is limited

- 1) Make 1% solution of S-CLEAN WO-23.
- 2) Using the sponge, clean the outside of Niskin bottle. (Note: Do not apply sponge inside Niskin bottle.)
- 3) Fill Niskin bottle with 1 liter of 1% solution of S-CLEAN WO-23. Shake the bottle thoroughly more than 10 times, to wash every part inside the bottle. Drain from petcock, to wash petcock as well.
- 4) Fill Niskin bottle with fresh water, shake the bottle and rinse until bubbles are completely washed off inside the Niskin bottle. Drain from petcock, to rinse petcock as well.

④ Storing Niskin Bottle

If Niskin bottle is not used in next cruise, or if storing Niskin bottle for an extended period, allow the inside of the Niskin bottle to dry, and cover with tarpaulin to avoid dust.

A.1-2 Preparing Niskin Bottle for Sampling

A.1-2-1 Adjusting and checking tension to ensure sealing

To close the upper and lower lids, Niskin bottles have latex tube or spring (closure spring) inside the bottle. Use spring scale to adjust the tension of 12-liter closure spring Niskin bottles to be around 12 kg (± 0.5 kg). On the other hand, X-type Niskin bottles have external lanyard and closure spring. For adjusting tension of X-type Niskin bottle tension, adjust the length of the lanyard. Use spring scale to check the tension of 12-liter X-type Niskin bottle tension to be around 12 kg (± 0.5 kg).

A.1.2-2 Checking O-Ring

Check the O-rings at top and bottom of the Niskin bottle, and the O-rings at top and bottom valves (hereafter top valve is referred to as “air vent”, and bottom valve is referred to as “petcock”), for any apparent damage such as scratch and crack. If any abnormality is found, replace the part.

A.1-2-3 Checking for Leaks

① Perform leak check while preparing for sampling, can improve the quality of samples. Even during the sampling, always perform leak check, and record the results (Swift, 2010).

Make sure petcock and air vent are closed, and fill the bottle fully. First, check if there is not any leakage.

② Push in the petcock, and:

- 1) If there is leakage from the petcock, check the tension of the closure spring. If the tension is normal, replace the O-ring at air vent, and replace the O-ring at the top lid. If it continues to leak after replacing the O-rings, check the body of the bottle for sound of air leakage, especially around the mounting blocks. If you hear the sound of air leakage, replace the Niskin bottle.
- 2) If there is a leak from outside the petcock, replace the O-ring in the center of the petcock.
- 3) If taking actions in above steps 1) and 2) does not improve the situation, replace the petcock. And, check and see where the petcock is attached to the body of the bottle (hereafter referred to as petcock bushing), for any scratch or crack. If anything is not normal, replace or repair the bottle.

③ Pull the petcock and open the air vent.

- 1) If there is a leak from the petcock, replace two O-rings inside the petcock.
- 2) If there is a leak from outside the petcock, check and see inside the petcock bushing for any scratch. If there is no scratch, replace both of the two O-rings.

- 3) If there is a leak from lower lid, first check the tension of the closure spring. If there is no problem with the tension, replace the O-ring of the lower lid.

If above leak checks have been done, but leaking persists, and the cause and location of the leak (entry of air) cannot be identified, stop using the Niskin bottle, and use another Niskin bottle.

A.1-2-4 Attach upper and lower lanyard

Specifications of lanyard to use, will vary depending on the type of Niskin bottle and type of Carousel. Please be sure to use the appropriate lanyard. Lanyard used with Niskin bottles is often made of nylon, and #150 (2mm) is recommended for use with Carousel.

A.1-2-5 Adjust upper and lower lanyard

If lanyard attached to Niskin bottle is too short, Niskin bottle may not close even after sending the fire command. Therefore, length of lanyard must be adjusted before sampling.

- ① Prepare Niskin bottle for sampling (hook outside, as shown in Photo A.1-2-1).
- ② In the state described in previous step ①, press and hold the lower lid to make sure the lid does not close (as shown in Photo A.1-2-1).
- ③ While keeping both the upper and lower lid closed, hook the lower lid lanyard, and check the tension of lanyard (as shown in Photo A.1-2-2).

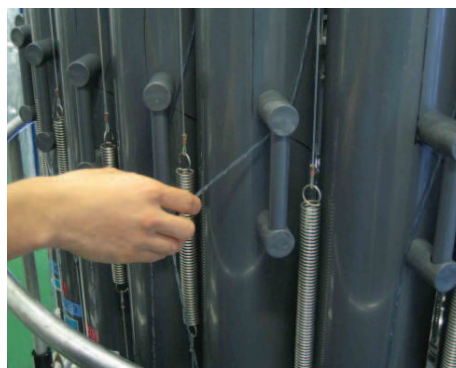


Photo A.1-2-1 Checking tension of lower lid lanyard. Photo A.1-2-2. Checking tension of upper lid lanyard.

References

Swift, J.H. (2010) : Reference-quality water sample data: Notes on acquisition, record keeping, and evaluation. IOCCP Report No.14, ICPO Pub. 134, 2010 ver.1

A.2 Checking and Maintaining Carousel

Carousel is composed of trigger part and housing part. This section describes how to maintain each part.

①Preparation

- Hex Wrench (Inches)
- Monkey Wrench (Small)
- Flat head screwdriver
- Phillips screwdriver
- Precision screwdriver
- 3 Jack-up Screws
- Mallet
- Ethanol (if necessary)
- Carousel pedestal (Nice to have dedicated pedestal having height of 40 cm or more, to prevent carousel from falling out)
- Silicon grease
- Silicon sealant (if necessary)
- Wiper (JK Wiper, Kimwipes, etc)
- Molybdenum grease
- Threadlocker (Loctite 222, etc)

A.2-1 *Disassemble and Reassemble Carousel*

Be aware that disassembling and reassembling 36-bottle carousel will be different from that of 12-bottle carousel or 24-bottle carousel. Depending on the material used in the housing, its parts may be using different materials and screws. Therefore do not mix the parts used with 6,800 m carousel with the parts used with 10,500 m carousels. Furthermore, triggers used uniquely with 36-bottle carousels will have imprints of “36” on its sides, and are different from those used with 12-bottle carousels and 24-bottle carousels.

A.2-2 Detach Latch Assembly

Hereafter, the location where the triggers are attached, is collectively referred to as latch assembly.

① 12-bottle, 24-bottle

- 1) Remove titanium screws located in the center of the top.
(Use 1/8 inch hex wrench for 6,800 m type, and use monkey wrench for 10,500 m type).

<References>

- 6,800 m type: Stainless steel hex socket head cap screw
- 10,500 m type: Titanium hex bolt

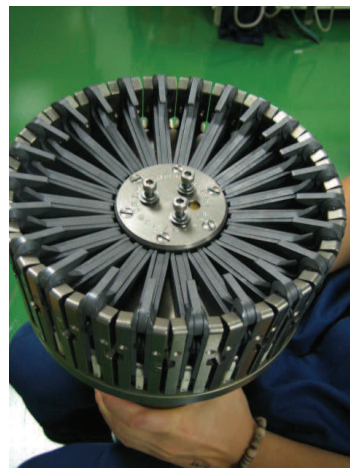


Photo A.2-2-1 Latch Assembly

- 2) Detach latch assembly from housing.

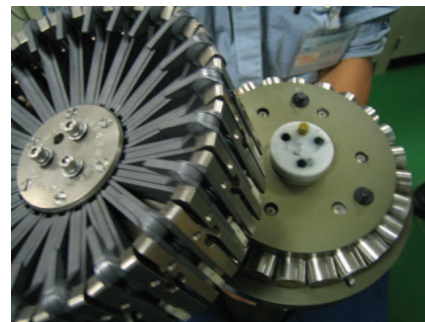


Photo A.2-2-2 Removing from housing

- 3) Use driver to remove 6 titanium screws on retainer disc.
Depending on housing type, screw head may be Phillips or Flat.

- Phillips: Stainless
- Flat head: Titanium

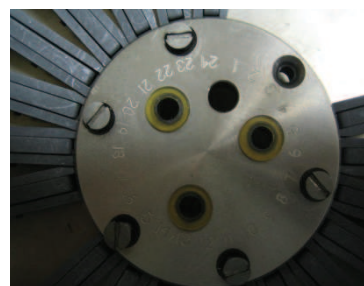


Photo A.2-2-3 Retainer Disc part

- 4) When removing retainer disc, mark the trigger #1.
- 5) Remove retainer disc at top center of carousel. When it is stuck, hit lightly from bottom (back) to remove it with ease.

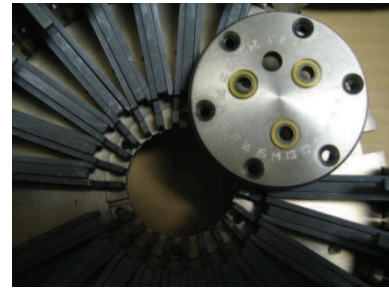


Photo A.2-2-4. Removing Retainer Disc

- 6) Remove the trigger attached to #1, mark the corresponding part with #1. Remove the corresponding trigger.



Photo A-2-2-5 Removing trigger from mount disc.

② 36-Bottle

1) Use 5/32 inch hex wrench to remove 3 white color plastic screws (some carousels may not have those screws).

2) Use Phillips driver to remove 6 titanium screws on retainer disc.

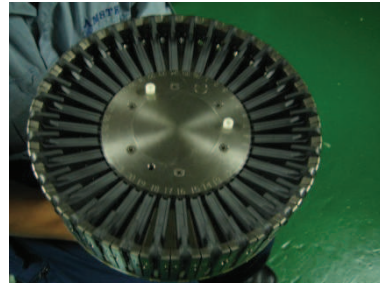


Photo A.2-2-6 Top of 36-bottle carousel (top center part is retainer disc)

3) In the holes where screws were removed in the step 1) , insert 3 jack-up screws, use 1/8 inch hex wrench to tighten the 3 screws equally, and lift up the retainer disc. If jack-up screws are not tighten equally, disc may distort.

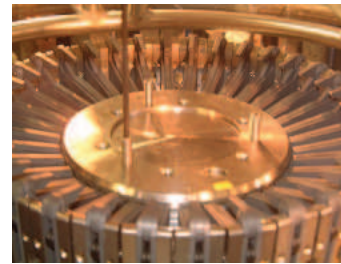


Photo A.2-2-7 Lifting up disc by inserting jack-up screws

4) When disc lifts up, remove it straight upward.

5) Remove triggers from trigger mount disc.

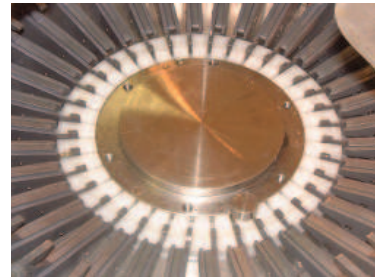


Photo A.2-2-8 After removing retainer disc (trigger mount disc)

A.2-3 Reassemble Latch Assembly

① 12-Bottle 24-Bottle

- 1) Put the triggers back onto trigger mount disc.
- 2) When putting the triggers back to trigger mount disc, look for the marking that says “Trigger #1” and use this location as base location. Make sure trigger mount disc holds triggers firmly.
- 3) Place the retainer disc at position of trigger #1.
- 4) Apply small amount of molybdenum grease on the 6 titanium screws, use driver to tighten the screws equally, and complete reassembling the latch assembly part.
- 5) Place the latch assembly on the housing.
- 6) Use the 3 screws to secure the latch assembly on the housing. Apply small amount of molybdenum grease on the screws. Tighten all the screws equally, to avoid one part being tighter than the other part. Use 1/8 inch hex wrench for 6,800 m type, and use small monkey wrench for 10,500 m type.
- 7) Make sure triggers operate smoothly.

② 36-Bottle

- 1) Attach the triggers to trigger mount disc on the housing part.
- 2) Attach retainer disc at top center part of carousel. Adjust the locations of the triggers for the retainer disc to fit smoothly. If the disc does not fit, use a mallet to hit lightly on it to allow it to fit.
- 3) Use Phillips driver and hex wrench to secure retainer disc with 6 titanium screws. Apply molybdenum grease on the screws. Tighten all the screws equally, to avoid one part being tighter than the other part.
- 4) Make sure triggers operate smoothly again.

A.2-4 Maintain trigger part

This part describes maintenance of triggers. Keep oil and grease away from trigger function part. The gray paint on the triggers reduce resistance under water, and this paint is easily removed by scratches from shock or friction. For more details on trigger, refer to the drawings and references offered by the manufacturer, which describes how to assemble triggers. Top of screws used in triggers are easily damaged. Please use right size of tools.

① Wash trigger part

Remove carousel from CTD frame, and leave it in fresh water for a day and a night, to remove salt deposit. If time allows, remove the triggers, and put the carousel housing and triggers separately in fresh water for a day and a night. After removing salt deposit, make sure housing part and trigger part are normal, and reassemble the triggers, reversing the steps to separate them.

If trigger parts have visible salt deposit, wash them well in lukewarm water of temperature 40°C mixed with neutral detergent. Move the movable parts while washing. Rinse well to wash off bubbles, and soak them in fresh water.

② Visual check trigger part

If conditions like below are visually apparent in the triggers, consider to replace triggers or parts of triggers (Photo A.2-4-1).

- Paint on the trigger has been removed
- Trigger hook is worn out
- Trigger side plate is visually and apparently distorted
- Severe corrosion on back of the actuator disc
- Wear and bend in shaft such as trigger pivot shaft
- Severe wear in trigger lever

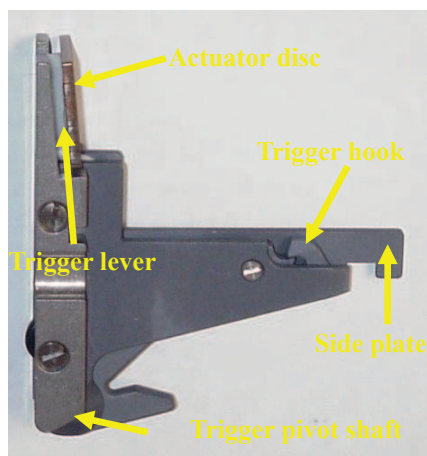


Photo. A.2-4-1 Trigger parts

Hold the trigger as shown in picture below, trigger hook pointing straight down (Photo A.2-4-2), and push the white lever (encircled in red) with a finger, in the direction indicated by the arrow in the picture (handle the lever with care, pushing too strong may damage the lever). While doing this motion, if trigger hook freely drops down, this is normal. If the hook does not drop down, or there is some interference preventing the hook to drop down, loosen 2 screws holding the actuator disc, and adjust them so that the hook is released smoothly. If screws seem already loosen, apply threadlocker on the screws and tighten the screws. However, tightening the screws too much, may damage the trigger lever.

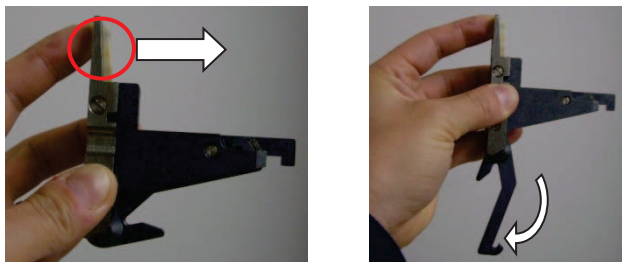


Photo A.2-4-2 Check trigger function

A.2-5 Check and maintain carousel housing part

This section describes how to check and maintain the housing part.

① External visual check on housing part

Remove latch assembly from the housing.

Look closely on electromagnet part, and check if there is no tear or wear on the rubber that coats the electromagnets. If the part is rusty, this check must be done extra carefully.

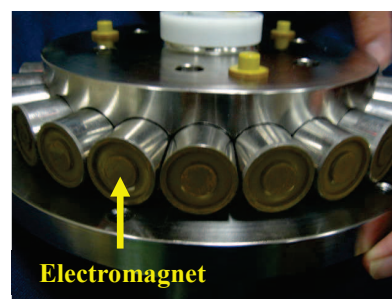


Photo A.2-5 Electromagnet part

If there is major damage on the rubber, spread silicon grease thinly on the damaged part, and leave until it is dry and hardened. And after reassembly, make sure triggers are released normally. If damage is too severe to use, consider to repair by repair service provider. If rust and salt crystals are seen, remove them to the possible extent.

This page left intentionally blank.

Water temperature

○Toshiya NAKANO (Japan Meteorological Agency)

Water temperature (temperature) is the most fundamental physical properties of sea water with pressure and salinity in the International Thermodynamic Equation Of Seawater–2010 (TEOS-10). The vertical and horizontal distributions of temperature are associated with the thermal and dynamic structure in the ocean. Temperature is a key variable that supports oceanic condition, ocean and weather prediction, and air-sea interaction leading to understanding and forecasting short- and long-term climate variability.

1. Definition and Unit

In 1990 the International Practical Temperature Scale 1968 (IPTS-68) was replaced by the International Temperature Scale of 1990 (ITS-90) defined by 17 fixed temperature points. The triple point of water (273.16K or 0.01°C) remains unchanged on ITS-90, however, the definition of boiling point of water at the atmospheric pressure falls to 99.974°C (Rusby, 1991). Since many algorithms for calculating physical properties of seawater had been based largely on IPTS-68, it was necessary to discriminate between IPTS-68 and ITS-90. In the field of oceanography it is common to distinguish using subscripts as t_{90} with the Celsius scale (°C). The relation between ITS-90 (t_{90}) and IPTS-68 (t_{68}) can be adequately represented by the expression

$$t_{90} = 0.99976 \cdot t_{68} \quad (1)$$

This linear transformation is accurate within 0.5×10^{-3} K throughout the oceanographic temperature range -2°C to 40°C (Saunders, 1990). Temperature reported in the literature is used ITS-90 and be labelled t_{90} . In order to use the International Equation of State of Seawater 1980 (EOS-80) with t_{90} data, t_{68} may be calculated using

$$t_{68} = 1.00024 \cdot t_{90} \quad (2)$$

2. Calibration of thermometers

To ensure traceability to the national standards, all thermometers need to be calibrated by a standard device such as a Standard Platinum Resistance Thermometer (SPRT). The standard device also needs to be calibrated by a higher standard device or by ITS-90 fixed point cells. These higher standard device or fixed point cells need to be traceable to the national measurement standards maintained by the National Metrology Institute (e.g. National Metrology Institute of Japan [NMIJ] and National Institute of Standards and Technology [NIST]). The oceanographic temperature range is realized by use of a SPRT calibrated at the ITS-90 defining points of the water triple point, 0.01°C and the gallium melting point, 29.7646°C . Calibrations of thermometers are made regularly with the

standard thermometer fully submerged in a water bath. The temperature correction that must be applied to the thermometer is estimated for agreement with the reading of the standard thermometer.

References

- Rusby, R. L. (1991): The conversion of thermal reference values to the ITS-90. *J. Chem. Thermodynamics*, **23**, 1153-1161.
- Saunders, P. (1990): The International Temperature Scale of 1990, ITS-90. *WOCE Newsletter* **10**, IOS, Wormley, UK.
- UNESCO (1981): The Practical Salinity scale 1978 and the International Equation of State of Seawater 1980. UNESCO technical papers in marine science **36**, 25pp.

Salinity

○Takeshi Kawano (Japan Agency for Marine-earth Science and Technology)

A manual of “Method for Salinity (Conductivity Ratio) Measurement” can be obtained from a GO-SHIP web site as below.

http://www.go-ship.org/Manual/Kawano_Salinity.pdf

This page left intentionally blank.

Density of Seawater

○Hiroshi UCHIDA (Research and Development Center for Global Change / Japan Agency for Marine-Earth Science and Technology)

The density of seawater is defined as its weight per unit volume; in accord with the International System of Units (SI), it is expressed in units of kilograms per cubic meter (kg/m^3). The density of seawater may be estimated as a function of pressure, temperature, and Absolute Salinity by using the International Thermodynamic Equation of Seawater – 2010 (TEOS-10) or by direct measurement using a densitometer. Seawater density data used in the TEOS-10 standards were obtained from density measurements (Millero, 2010).

The density of seawater can be measured with a hydrostatic weighing apparatus or a vibrating-tube densitometer. The former measures the buoyancy of a sinker suspended in a seawater sample. The volume and mass of the sinker must be calibrated in advance. The latter measures the natural period of a vibrating glass tube filled with a seawater sample. The natural period is proportional to the density of the sample. A hydrostatic weighing apparatus can directly measure seawater density traceable to the SI without a reference solution. However, the measuring time for a sample is quite long (longer than several hours), and a hydrostatic weighing apparatus cannot be used on a moving ship. Use of a single-crystal silicon sinker has made it possible to reduce the measurement uncertainty to about 0.001 kg/m^3 with traceability to national density standards based on silicon spheres. However, the tendency of a silicon sphere to dissolve in seawater is a problem that needs to be solved. In contrast, for a vibrating tube densitometer, which can be used on a moving ship, the measuring time for a sample is short (several minutes). Although a reference solution is required for calibration, the resolution of the densitometer is high (0.001 kg/m^3). Because the uncertainties of the commercially available, SI-traceable density reference solutions are large (0.01 kg/m^3 for pure water), a substitution method is normally used for seawater density measurements. In the substitution method, the density difference between a seawater sample and pure water is measured, and the density of pure water, calculated from the TEOS-10 standards, is added to the difference.

An international guideline for seawater density measurements based on vibrating tube densitometers is now in preparation [Wolf, H., S. Weinreben, H. Uchida and R. Pawlowicz: Best practice guide for the measurement of seawater density. The Joint Committee on the Properties of Seawater (IAPSO/SCOR/IAPWS)]. However, seawater densities measured by the substitution method relative to pure water tend to be lower (by as much as 0.01 kg/m^3) than densities calculated from TEOS-10 standards (e.g., Uchida et al., 2011). Although the systematic differences are hypothesized to be the result of systematic errors in the TEOS-10 standards or nonlinearities of vibrating-tube densitometers, a consensus has not yet been reached on the cause of the systematic differences. To solve this problem, a precise determination of the density determined by hydrostatic weighing is planned for IAPSO Standard Seawater, the composition of which is considered to be close to the Reference Composition defined in the TEOS-10 standards.

References

- IOC, SCOR, and IAPSO (2010): The international thermodynamic equation of seawater – 2010: Calculation and use of thermodynamic properties. Intergovernmental Oceanographic Commission, Manuals and Guides No. 56, UNESCO, 196 pp.
- Millero, F. J. (2010): History of the equation of state of seawater. *Oceanography*, 23, 18–33, doi:10.5670/oceanog.2010.21.
- Uchida, H., T. Kawano, M. Aoyama and A. Murata (2011): Absolute salinity measurements of standard seawaters for conductivity and nutrients. *La mer*, 49, 119–126.

Transparency

○Toshiya NAKANO (Japan Meteorological Agency)

Transparency is one of the observed elements for an index of clarity or turbidity of the sea water. Transparency is measured with a Secchi disk, which is the simplest and the most effective tools for estimating marine pollution and temporal changes in water quality.

1. Secchi disk

A Secchi disk is a circular white plate, 30 cm diameter with a graduated line for lowering into the sea water, attached an about 5 kg weight to hold the line vertical (photo 1).

2. Measuring transparency using the secchi disk

The depth where the Secchi disk can no longer be seen through the sea water is the Secchi disk depth. To obtain the Secchi disk depth, the disk is lowered into the water on the shady side of the ship in the daytime, while observing the depth at which it disappears. The disk is then slowly raised, while observing the depth which it reappears. The measurement of the Secchi disk depth is obtained as the average of the two observations.

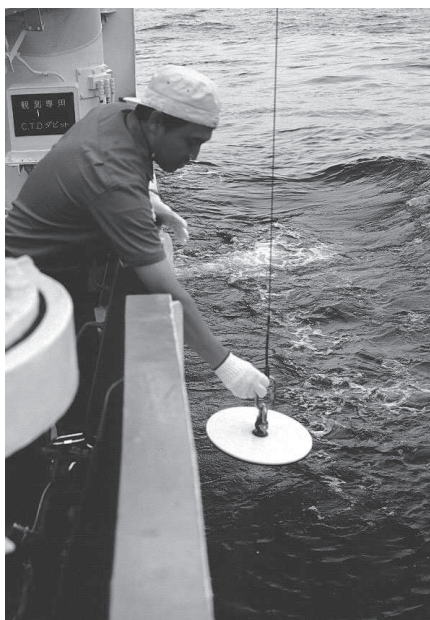


Photo1 Transparency observation (left) 、 Secchi disk (upper right and lower right)

This page left intentionally blank.

Dissolved Oxygen

○Yuichiro KUMAMOTO (Japan Agency for Marine-Earth Science and Technology),
Daisuke SASANO (Japan Meteorological Agency), Hironori SATO (Marine Works Japan Ltd.),
Keitaro MATSUMOTO (Marine Works Japan Ltd.)

1. Introduction

In this chapter, we describe the method for the measurement of oxygen (oxygen molecule, O₂) dissolved in seawater. Surface seawater is saturated with oxygen in the air due to gas exchange between the atmosphere and ocean. The photosynthesis by phytoplankton can supersaturate oxygen concentration in the euphotic zone in surface layers. On the other hand, when seawater leaves the surface layer and sinks into the aphotic zone, the dissolved oxygen concentration decreases due to the decomposition of organic matter. Therefore, the dissolved oxygen concentration in seawater is one of the most essential variables in oceanographic studies on the atmospheric-ocean gas exchange, seawater mixing, and biogeochemistry.

The analysis of dissolved oxygen in seawater has a long history; volumetric analysis, gas analysis, colorimetric method, etc. have been reported (Kitano, 1964). One of the most traditional methods among them is iodometric titration, which is one of the volumetric analyses. This titration method is called the Winkler method named after the first reporter (Winkler, 1888). After modifications by Carpenter (1965a), this simple and sensitive analysis without expensive instruments became a standard analytical method for dissolved oxygen concentration in seawater (Strickland and Parsons, 1972; Grasshoff, 1976; Culberson et al., 1991; Joint Global Ocean Flux Study, 1994; Dickson, 1996; Hansen, 1999; Langdon, 2010). In addition, colorimetric methods utilizing the measurement principle of the Winkler method have been also reported (Broenkow and Cline, 1969; Pai et al., 1993; Labasque et al., 2004). In Japan, Japan Meteorological Agency (JMA) particularly described the modified Winkler method (hereinafter simply referred to as the Winkler method) in the Manual on Oceanographic Observation (JMA, 1999), which has been widely used by the Japanese oceanographic researchers/engineers. The Winkler method uses the starch-iodine reaction (bluish purple) in the determination of the titration endpoint to heighten the analytical sensitivity. In recent years, a photometric automatic titration without starch, which measures the absorbance at the yellow color range (around 350 nm) due to liberated iodine, becomes common because affordable automatic titrators have been easily available (Miyao et al., 2013).

Since the 2000s, we have measured dissolved oxygen concentration in seawater collected in the open ocean using the Winkler method with a photometric automatic titrator and acquired about 0.1 $\mu\text{mol kg}^{-1}$ of the analytical precision of repeat measurements (repeatability). As a result, uncertainty arisen from interfering substances ($< 1 \mu\text{mol kg}^{-1}$) of the Winkler method is

recognized, which has been ignored in the past. The Winkler method does not determine dissolved oxygen directly. Instead, it measures dissolved oxygen indirectly by reducing titration of free iodine (I_2), which is equivalent to dissolved oxygen, to iodide ion with sodium thiosulfate. Therefore, substances contributing to this reduction reaction in the titration condition, namely the interfering substances are measured as "dissolved oxygen" in seawater. The dissolved oxygen and interfering substances contained in added reagents are corrected using predetermined values. On the other hand, the interfering substances contained in seawater itself should be corrected strictly on each sample measurement of the Winkler method. Otherwise, dissolved oxygen concentration measured by the Winkler method would be a total concentration of dissolved oxygen and interfering substances. In the following sections, however, the uncorrected concentration is simply referred to as "dissolved oxygen concentration" in order to avoid complication. The interfering substances of the Winkler method are discussed in section 10.

In this chapter, we describe the Winkler method with the photometric automatic titrator. In addition, the interfering substances and the uncertainty of this method are discussed. We hope that this chapter will be helpful for marine researchers and engineers who need the high analytical precision of dissolved oxygen concentration in seawater samples. For the method of the conventional manual titration with starch, please refer to the Manual on Oceanographic Observation (JMA, 1999). This chapter consists of ten sections. This introduction (1) is followed by nine sections; units (2), principle of measurement (3), reagent preparation (4), apparatus (5), sampling (6), analysis (7), calculation of concentration (8), uncertainty (9), and traceability and interfering substances (10). One can overview all the procedures of the measurement in order of the actual works in the sections from 4 to 9. Section 10 would help readers understand more about the measurement of dissolved oxygen concentration using the Winkler method. Although methods for calculation of pure water and seawater density, and calibration of volumetric apparatus (sample flasks, burettes, and pipettes) were described in the Japanese version in this chapter (Kumamoto et al., 2015), those are omitted in this English version. Please refer to other manuals (e.g. Dickson et al., 2007) for these methods.

2. Units

Dissolved oxygen concentration has been expressed as its volume at the standard condition ($0\text{ }^{\circ}\text{C}$, $1\text{ atm} = 101325\text{ Pa}$) [$\text{mL}\cdot\text{L}^{-1}$] or mass [$\text{mg}\cdot\text{L}^{-1}$] in 1 liter of seawater. However, it is recommended to use the molar concentration (molarity), the amount of substance per liter [$\mu\text{mol}\cdot\text{L}^{-1}$], partly because of change of the atmospheric pressure in the standard condition in 1997 (International Union of Pure and Applied Chemistry, 1997). Recent manuals use the molal concentration (molality) [$\mu\text{mol}\cdot\text{kg}^{-1}$] that is not affected by the change in sample temperature. In this chapter, we use the molal concentration [$\mu\text{mol}\cdot\text{kg}^{-1}$] that is converted from the molar

concentration [$\mu\text{mol}\cdot\text{L}^{-1}$] using seawater density. Conversion equations for [$\mu\text{mol}\cdot\text{L}^{-1}$] from [$\text{mL}\cdot\text{L}^{-1}$] or [$\text{mg}\cdot\text{L}^{-1}$] are as follows.

$$[\mu\text{mol}\cdot\text{L}^{-1}] = [\text{mL}\cdot\text{L}^{-1}] \cdot \frac{1000}{22.392} = [\text{mg}\cdot\text{L}^{-1}] \cdot \frac{1000}{(15.9994 \times 2)} \quad (1)$$

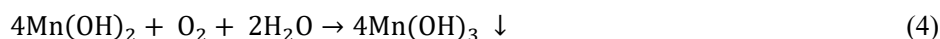
where 22.392 is the volume of 1 mol O_2 in the standard condition (0°C , 101325 Pa) [$\text{L}\cdot\text{mol}^{-1}$]. 15.9994 is the atomic weight of 1 mol O [$\text{g}\cdot\text{mol}^{-1}$].

3. Principle of measurement

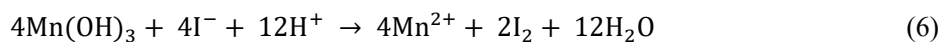
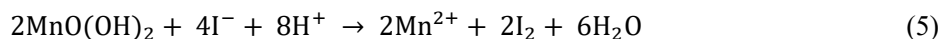
Manganese chloride solution is added to a seawater sample, which is immediately followed by the addition of potassium iodide/sodium hydroxide solution. The white precipitate of manganese hydroxide in colloidal state is formed in the strong alkaline condition.



Some of the precipitate is oxidized with dissolved oxygen and turns brown, which is called "oxygen fixation".



In the acidic condition, the precipitate dissolves, manganese is reduced, and iodine is liberated.



In the two reactions, two moles of I_2 are formed for each mole of O_2 . The liberated iodine reacts with excess iodide ion and changes into triiodide ion. The amount of I_3^- in the solution is determined by titration with standardized sodium thiosulfate solution.



Two moles of thiosulfate ion are required to titrate each mole of triiodide ion. Therefore, the final stoichiometry of one mole of O_2 is four moles of thiosulfate ion. The amount of dissolved oxygen

can be obtained from this stoichiometry.

4. Reagent preparation

All the reagents should be higher than the special grade. Record their lot number, arrival date, and use start date. With preparing the reagent solutions, record the working date, names of workers, apparatus used, and the lot number and usage amount of the reagents. These records will help you find reasons when questions arise in the measurement results. The preparation should be carried out in a fume hood in a laboratory by more than one person. The workers are recommended to wear gloves and safety glasses to insure themselves against risk from deleterious and dangerous reagents, including strong acids and alkalis.

4-1. Manganese chloride solution (3 M): Pickling reagent I

Approximately 600 g of manganese chloride tetrahydrate (molecular weight 197.90) was slowly added into about 600 mL of deionized water (DIW) in a beaker and stir with a magnetic stirring bar until all the crystals have dissolved. Allow the solution to reach room temperature because it becomes cool due to the endothermic reaction. Then DIW is added to make the final volume of 1 L. The concentration is approximately 3 M ($\text{mol}\cdot\text{L}^{-1}$). If you find any particles in the solution, filter the solution through with a glass fiber filter. Store the solution in a light-shieldable bottle.

4-2. Sodium iodide (4 M) · Sodium hydroxide (8 M) mixed solution: Pickling reagent II

Approximate 320 g of sodium hydroxide (molecular weight 39.997) is dissolved in about 600 mL of DIW in a beaker. The solution becomes hot due to the exothermal reaction. Allow it to cool in a water tub. About 600 g of sodium iodide (molecular weight 149.89) is dissolved and allowed it to reach room temperature again. Then, DIW is added to make the total volume of 1 L. If you find any particles in the solution, which could contribute to the reagent blank (7-3), filter the solution through with a glass fiber filter. Store the solution in a light-shieldable plastic bottle. Sodium iodide is easy to be oxidized by exposure to the air or daylight and liberates iodine. The original color of sodium iodide is white, and a yellowish reagent should not be used.

4-3. Sulfuric acid solution (5 M)

Approximate 600 mL of DIW is placed in a beaker in a cooling water tub and slowly poured about 280 mL of concentrated sulfuric acid (molecular weight 98.079, density $1.84\text{ g}\cdot\text{mL}^{-1}$) little by little with gentle stirring. Be careful about a great deal of heat given off as the acid and water

mix. Never add DIW into concentrated sulfuric acid conversely, or the DIW may boil explosively (bump). Allow the solution to cool to ambient temperature and then make up the final volume to 1 L by adding DIW.

4-4. Sodium thiosulfate solution (0.025 M)

6.25 g of sodium thiosulfate pentahydrate (molecular weight 248.19) is dissolved in 1 L of DIW to obtain a solution of approximate 0.025 M. The concentration may decrease with time because sodium thiosulfate is decomposed by the reaction with oxygen/carbon dioxide and activity of bacteria in the solution. To prevent the decomposition, a preservative may be added to the solution, for example, sodium carbonate (Strickland and Parsons, 1972), sodium borate (Joint Global Ocean Flux Study, 1994), and 3-methyl-1-butanol (Fujifilm Wako Pure Chemical Corporation, 2018). Tanaka et al. (2007) reported that the concentration does not change when boiling DIW is used. Even without a preservative, it has been found empirically that the solution is more stable and consistent if it is left a few days after the preparation (Langdon, 2010). This could be explained by the slowdown of the decomposition rate by the aging. This titrant solution has been often called "hypo" wrongly, which is derived from a confusion between sodium thiosulfate and sodium hyposulfite.

The concentration of the sodium thiosulfate solution should be determined by the volume of the burette for the titration (5-2-1). To titrate 100 mL of seawater whose oxygen concentration is as high as $400 \mu\text{mol}\cdot\text{L}^{-1}$ ($40 \mu\text{mol}$), 6.4 mL of 0.025 M sodium thiosulfate solution is required. If the volume size of the titration burette is 5 mL, the concentration of the titrant solution must be increased.

4-5. Potassium iodate standard solution (1/600 M)

The standard solution in the Winkler method is a solution of potassium iodate (molecular weight 214.001, density $3.89 \text{ g}\cdot\text{mL}^{-1}$). Iodate ion oxidizes iodide ion to iodine in the acidic condition.



The liberated iodine reacts with excess iodide ion and changes into triiodide ion that is reduced with sodium thiosulfate (equations 7 and 8). In these reactions, 1 mole of iodate ion corresponds to 6 moles of thiosulfate ion. The concentration of sodium thiosulfate solution is determined from the volume of the titrant solution required for the titration of triiodide ion (the endpoint of the titration) and the concentration of the potassium iodate solution, which is called the

standardization of the sodium thiosulfate solution (7-2). Although the special grade of potassium iodate powder is affordable, it is recommended to use the certified standard substance. In Japan, National Metrology Institute of Japan (NMIJ) supplies "NMIJ CRM 3006-a" (NMIJ, 2015). Procedures for preparing the standard solution of potassium iodate by the gravimetric method are as follows. It should be noted that the uncertainty of the oxygen measurement by the Winkler method is dependent on the care you take with the preparation of this standard solution. The standard solution of potassium iodate is commercially available. For example, Fujifilm Wako Pure Chemical Corporation provides Cooperative Study of Kuroshio Standard Solution (0.0100 N = 1/600 M, sales code 034-10251). However, this standard solution cannot be used for the oxygen measurement with less than 1% of the analytical uncertainty.

4-5-1. Preparation of electronic balances

Prepare a precision electronic balance with 200 g of weighing capacity and 0.01 mg of readability for weighing potassium iodate. To eliminate disturbance due to static electricity, a precision balance with an electrostatic eliminator and a shield made of conductive acrylic fiber is recommended. Also, prepare another balance with about 10 kg of weighing capacity and 10 mg of readability for weighing of the standard solution. The electronic balances must be calibrated by standard weights before use.

4-5-2. Drying potassium iodate

About 0.5 g of high-purity potassium iodate is pulverized in a mortar, taken in a beaker, dried at 130 °C for about 2 hours, and allowed to cool in a desiccator with silica gels.

4-5-3. Weighing potassium iodate

Weigh out about 0.36 g of potassium iodate in a weighing bottle with a lid and measure the weight with the precision balance.

4-5-4. Transfer of potassium iodate

Place a 1-L volumetric flask on the balance for the solution and measure the tare weight. Open the lid of the weighing bottle and transfer potassium iodate to the flask using a powder funnel. Potassium iodate powders on the funnel are washed out into the flask using DIW. At this time, do not moisten the weighing bottle with DIW. Measure the weight of the empty weighing bottle with the lid using the precision balance. Calculate the weight of potassium iodate (w_{KIO_3} [g]) transferred from the weighing bottle to the flask from a difference between the weights of the weighing bottle

before and after the transfer.

4-5-5. DIW addition and weight measurement

Add DIW to the volumetric flask and dissolve potassium iodate. Then dilute the solution to a final volume of 1 L in the volumetric flask and record the sum of weights of the potassium iodate and DIW ($w_{\text{dw}} + w_{\text{KIO}_3}$ [kg]). At this time, you do not have to make up to exactly 1 L because the concentration is calculated not by the volume but the weight.

4-5-6. Stirring

Cap the volumetric flask with a stopper and mix the solution in the flask by overturning. Then stir the solution using a magnetic stirring bar for 1 hour or more to completely dissolve the potassium iodate.

4-5-7. Storage

Aliquot the solution into brown glass bottles (250 or 500 mL volume). An aliquot of the solution should be used up once for each of the standardizations. Do not reuse the opened solution after the first use. The potassium iodate solution is chemically stable. However, evaporation from the narrow gap between the glass bottle and the screw cap results in the rise of the concentration during a long-time storage. This can be prevented by sealing the glass bottle with an airtight vinyl bag using a vacuum sealer machine for kitchen packaging, which allows the standard solution to be used for a few years.

5. Apparatus

5-1. Sampling apparatus

5-1-1. Sample flasks (Oxygen bottles)

Use an "iodine titration" glass flask of 100 mL nominal volume with a flared neck and ground glass stopper, which is called "oxygen bottle". The oxygen bottle is a container for collecting seawater and serves as a flask for titration. The flared neck is used to prevent contamination from atmospheric oxygen during the water sampling and storage. The ground glass stopper should be long enough to make a headspace in the oxygen bottle for the titrant solution added. The volume of the bottle with the stopper must be calibrated by a weighing with the buoyancy correction (Dickson et al., 2007). An oxygen bottle whose volume has already been measured is commercially available. However, the volume calibration is recommended for the confirmation.

The oxygen bottle and stopper should be handled with care because scratches or chips on the inner wall of the bottle or stopper may change the volume calibrated, which results in the error in the measurement. Each bottle/stopper pair must be numbered so as not to confuse it with other pairs. It is sometimes difficult to remove the stopper from the dry bottle because of the ground glass joint. To avoid this, the bottle and stopper should be stored separately or with a slip of paper between the bottle and stopper. In the former case, be careful not to pollute the inside of the bottle. After use, the bottle and stopper should be washed with DIW and dried at room temperature (never use a heating oven). When the ground glass joints become brown, soak the bottles and stoppers in hydroxylammonium chloride solution (about $200 \text{ g}\cdot\text{L}^{-1}$) for about ten minutes and wash out.

5-1-2. Water sampling tubes

A transparent plastic tube, such as a silicone tube, is recommended so that air bubbles in it can be easily found. A new tube should be soaked in DIW before use, which may prevent air entrapment in the tube (Dickson, 1996). A flexible thin-walled tube is convenient for restricting and stopping the flow of seawater during the sampling. A length of the tube should be long enough to reach from the petcock of the Niskin water sampler (or the bottom of the water sampling bucket) to the bottom of the oxygen bottle.

5-1-3. Dispensers for pickling reagents

Prepare two plunger-type dispensers to add the pickling reagents I (4-1) and II (4-2) 1 mL each into seawater in the oxygen bottle. The bottles for the dispensers (1 L) should also be light-shieldable to avoid degradation due to sunlight. The pickling reagent II will stick/bind to the plunger. In that case, soak it in hydroxylammonium chloride solution (about $200 \text{ g}\cdot\text{L}^{-1}$) and wash out in the same way as the oxygen bottle. Disassembly of the dispenser before the soaking is recommended when the fouling is severe. A total volume (2 mL) of the pickling reagent I and II is included in the calculation of dissolved oxygen concentration. Therefore, high repeatability in dispensing is required. The Poulten & Graf FORTUNA OPTIFIX[®] works well. In addition, the volumes of the dispensers (V_{reg} [mL]) must be calibrated by the weighing at room temperature (Dickson et al., 2007).

5-1-4. Thermometer for water temperature

Prepare a battery-type digital thermometer with a thermistor on a thin flexible cable long enough to reach the bottom of the oxygen bottle. The thermistor is inserted into the oxygen bottle for recording the temperature of the seawater during the sampling (6-8). The thermometer should measure the temperature to $0.1 \text{ }^{\circ}\text{C}$ and be calibrated by a comparison with a calibrated mercury

thermometer. Specifically, compare the temperatures from the thermistor and the mercury thermometer at several points in a temperature range of the seawater sample (usually 0–30 °C) and calculate a regression equation between them.

5-1-5. DIW bottles

Plastic "squeeze" bottles (250 or 500 mL volume) filled with DIW are prepared to add DIW to the neck of the oxygen bottle.

5-2. Titration apparatus

5-2-1. Photometric automatic titrator

A photometric automatic titrator (Fig. 1) optically detects the endpoint of the titration. The titrator is equipped with a motorized microsyringe pump (piston burette) capable of discharging 5–10 mL of the sodium thiosulfate solution (4-4) by 1 μ L of the minimum dose. The volume of the burette must be calibrated by the weighing (Dickson et al., 2007). From the calibrations at several volumes between zero and the maximum capacity volume, a regression equation for the volume calibration is calculated. The titration is automatically performed by monitoring the

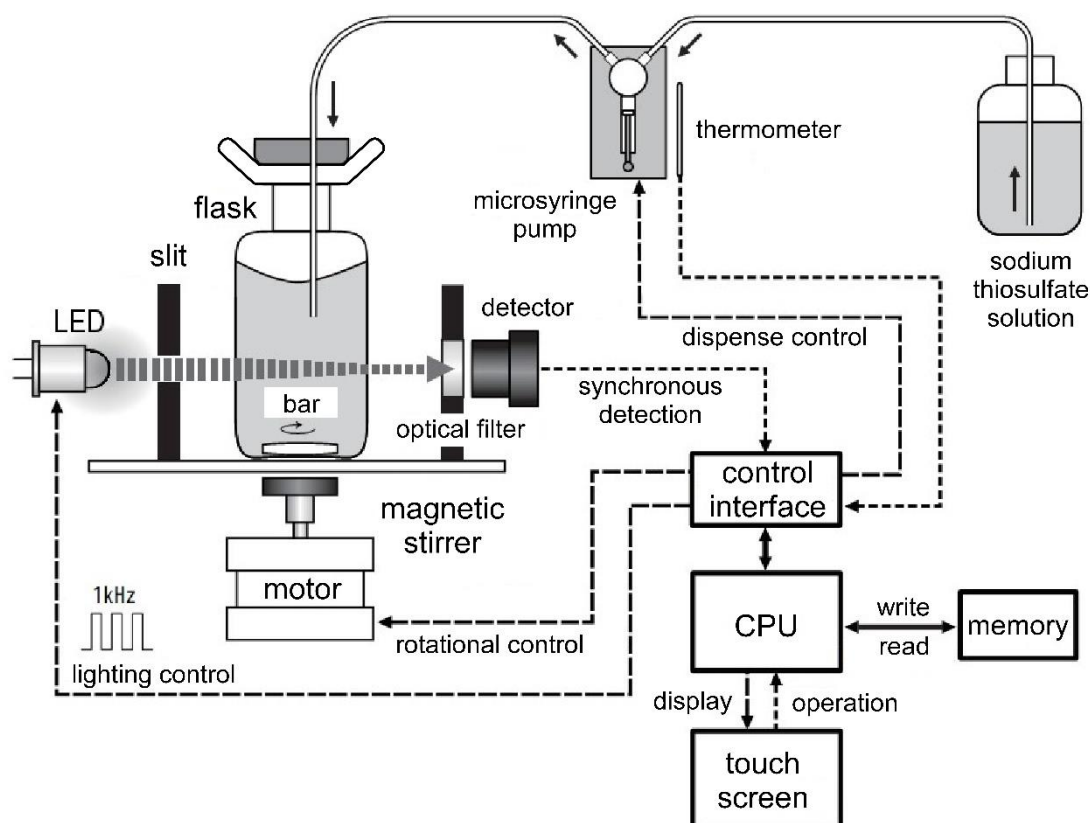


Fig.1 Schematic view of photometric automatic titrator (modified from Kimoto Electric Co., LTD. (2009))

absorbance at around 350–400 nm wavelength and finding the titration endpoint from the titration curve optimized by the titration rate and stirring speed. The method of the endpoint calculation in the titration program should be confirmed before the sample measurement. The automatic titration can avoid human errors in the detection of the endpoint. An amperometric detector, instead of a photometric one, can also determine the titration endpoint. There is no significant difference in analytical results obtained using the amperometric and photometric automatic titrators (Langdon, 2010).

5-2-2. Stirring bars

Use a rod-shaped magnet bar (25–30 mm) coated with fluoro-resin. One stirring bar is required for each titration. Prepare enough number of the stirring bar cleaned and dried before use. If the stirring bar does not rotate smoothly in oxygen bottles, refrain from the use of these bottles that may have a problem in the flatness of its bottom.

5-2-3. Dispenser for sulfuric acid solution

Prepare a dispenser for adding 1 mL of the sulfuric acid solution (4-3). Unlike the dispensers for the pickling reagents (5-1-3), the volume calibration is not necessary because the dispensing volume of the sulfuric acid solution added is not included in the calculation of dissolved oxygen concentration. However, the concentration and volume of dispensing of the pickling reagents and the sulfuric acid should not deviate from the targeted values by 5% and more because those are determined so that the sample pH in the titration become 2 (Carpenter, 1965a).

5-2-4. Burette for potassium iodate standard solution

To dispense 10 mL of the potassium iodate standard solution accurately (4-5), a motorized automatic burette is recommended. The volume (10 mL, $V_{\text{KIO}_3}(t_C)$) must be calibrated by the weighing (Dickson et al., 2007) before use. It should be noted that the accurate dispensing of the standard solution in the standardization (7-2) can reduce the uncertainty of the oxygen measurement by the Winkler method.

5-2-5. Thermometers for water temperature

Prepare a calibrated thermometer for measuring the temperature of the potassium iodate standard solution in the standardization (7-2). The thermometer for the measuring temperature of the seawater sample (5-1-4) can also be used for this purpose. In addition, another thermometer is necessary for monitoring temperature of the sodium thiosulfate solution. You can use the

thermometer for the seawater sample again or one attached to the automatic titrator (Fig.1). The thermometer for the titrant solution is not necessary to be calibrated, because it only monitors the temporal variation in the titrant temperature, which ensures the accurate measurement of dissolved oxygen concentration.

5-2-6. DIW bottles

Prepare a plastic "squeeze" bottle (250 or 500 mL volume) filled with DIW or use the squeeze bottle for the seawater sampling (5-1-5). Another empty squeeze bottle is used as a suction bottle for DIW in the flared neck of the oxygen bottle.

5-2-7. Magnetic stirrer

A magnetic stirrer is equipped with the automatic titrator (5-2-1). If you have another one, the efficiency of the oxygen analysis is improved because you can prepare the next sample during the measurement of the present sample.

6. Sampling

The seawater collected by the Niskin or other sampling devices (a bucket etc.) must be transferred into the oxygen bottle as soon as possible without exposure to air or change in the water temperature. The seawater sample for dissolved oxygen must be collected before those for non-gas samples when you also collect seawater samples for other elements. When the seawater samples are collected from different depths using a multiple sampler, the sampling must start from the deepest sampler because the seawater sample in this sampler has undergone the greatest change in temperature. The procedures of the collecting seawater from the water sampler into the oxygen bottle are as follows. When you use a bucket as a water sampler, prepare a longer water sampling tube and siphon the seawater from the bottom of the bucket into the oxygen bottle according to the following procedures. Never scoop up the seawater in the bucket by the oxygen bottle.

6-1. Setup

Prepare a set of oxygen bottle/stopper (5-1-1), the dispensers of the pickling reagent solutions I and II (5-1-3), the thermometer (5-1-4), the DIW bottle (5-1-5), and a field note at the sampling location. A tube stand for the stoppers is useful. Keep the temperature of the pickling reagent solutions at room temperature by wrapping a heat-insulation sheet around the dispenser bottles and avoiding exposure to direct sunlight. This is because the concentration of dissolved oxygen

in the pickling reagent solutions, which is corrected in the calculating the dissolved oxygen concentration, is assumed to be the saturated concentration at 25.5 °C (Murray et al., 1968).

6-2. Preparation of oxygen bottle

The oxygen bottles/stoppers should be dried. If you wet a bottle before the drawing accidentally, use another dried one (Dickson, 1996). When dried bottles are not ready for use, it is recommended to increase an overflow time (6-5) from two to three times of the bottle volume (Horibe et al., 1972).

6-3. Connection of water sampling tube

Connect the water sampling tube (5-1-2) to the nipple of the petcock on the Niskin sampler. Open the vent screw and push the nipple down over the metal peg to start the flow of seawater. Dislodge any air bubbles within the tube by tapping and squeezing.

6-4. Drawing

Squeeze the water sampling tube to stop the water flow, insert the tube all the way to the bottom of the oxygen bottle, and then gradually loosen the tube to start the water flow. Always keep the tip of the tube at the bottom of the bottle and restrict the flow at the beginning to minimize the bubbles in the seawater and the surge on the surface of the seawater in the bottle.

6-5. Overflow

When the oxygen bottle is filled with the seawater, loosen the sampling tube and overflow the seawater by about the two bottle volumes. Do not allow water droplets to fall into the bottle from overhead stand flames for the Niskin water samplers during the overflowing. It is helpful for estimating the overflow volume to measure how long it takes to fill the oxygen bottle. Ensure that there are no bubbles inside the oxygen bottle, and then gently draw out the sampling tube. Just before the tip of the sampling tube leaves the surface of the seawater, squeeze the tube to stop the water flow completely. At that time, pay attention not to allow water droplets to drip from the tip of the sampling tube.

6-6. Stop of drawing

Pull the nipple of the petcock up to stop the seawater flow. Hold the neck of the oxygen bottle and immediately carry it to where the dispensers of the pickling reagent solutions are located (or pass the bottle to a person who carries it there) before the temperature change of the seawater

sample.

6-7. Addition of pickling reagents

Gently add 1 mL of the pickling reagent I and then 1 mL of the pickling reagent II. The nozzle tip of the dispenser should be submerged at least 1 cm below the neck of the oxygen bottle before the dispensing. Because the pickling reagent solutions are denser than seawater, they sink to the bottom of the oxygen bottle and a total of 2 mL of the seawater sample, which corresponds to the volume of the pickling reagent solutions added, flows over from the oxygen bottle. Small air bubbles in the nozzle of the dispenser should be flushed out by several times dispensing before use. Droplets and stains on the nozzle should be wiped out using a wiping paper.

6-8. Temperature measurement and plugging

Immediately insert the thermometer into the seawater sample and note the sampling temperature (t_s [°C]) and the bottle number. The stopper is then inserted carefully in the oxygen bottle. Do not wash a dried stopper with the sample seawater before insert. Turn over the bottle and make sure that there are no air bubbles inside. If bubbles are contained, collect the seawater sample again using another oxygen bottle. The seawater temperature just before the plugging is essential to accurate computing the density of the seawater sample in the oxygen bottle. Meanwhile, it is necessary to shorten an interval between the overflow and plugging as much as possible to minimize contamination from the atmospheric oxygen. For example, results from an experiment with seawater whose dissolved oxygen concentration was low (about $100 \mu\text{mol}\cdot\text{L}^{-1}$) suggested that the oxygen concentration in the seawater sample plugged two minutes after the overflow was about 0.3 % higher significantly than that plugged just after the overflow. Therefore, when you collect seawater with a low dissolved oxygen concentration, it is recommended that the sampling temperature (and the bottle number) is recorded during the overflow (6-5) using the thermometer and then the stopper is inserted immediately after the addition of the pickling reagents.

6-9. Shaking

Shake the bottle vigorously about 20 times with "snapping of the wrist" to thoroughly mix the precipitate using your thumb to secure the stopper. If the mixing is insufficient, the chemical reaction between manganese hydroxide and dissolved oxygen does not complete, which results in an error in the measurement.

6-10. Storage

Add DIW to the neck of the oxygen bottle using the squeeze bottle. This creates a water seal and prevents oxygen contamination from the air during storage. Without DIW in the neck, the air will penetrate the bottle inside through a narrow gap between the bottle and stopper, which may increase oxygen concentration in the seawater sample. A mixing between the seawater sample in the bottle and DIW in the neck through the gap, which may also result in the contamination of dissolved oxygen, is restricted because of the difference in density between them. Store the oxygen bottles in a covered crate in an air-conditioned laboratory.

6-11. Second shaking and storage

A second shaking of the oxygen bottle is recommended approximately 30 minutes after the first shaking in the same method as the first one to ensure that all the oxygen in the bottle has fully reacted with the pickling reagents. Then, add DIW to the neck of the bottle again and store the bottles in the air-conditioned room before measurement. We found no significant difference in the measurement results of a pair of seawater samples, whose dissolved oxygen concentration was less than $200 \mu\text{mol}\cdot\text{L}^{-1}$, with the shaking once and twice. However, the second shaking is effective in preventing errors due to the wrong mixing in the first shaking. Meanwhile, it was reported that dissolved oxygen concentration in the oxygen bottle turned over by accident just before the measurement increased by about 1 %. This was probably because the manganese hydroxide precipitate isolated by the anoxic supernatant seawater reacted with dissolved oxygen in the DIW in the flared neck that had gradually penetrated into the bottle through the narrow gap between the bottle and stopper. Therefore, the second shaking is not allowed a few hours after the first shaking.

7. Analysis (titration)

Manganese hydroxide precipitate oxidized with dissolved oxygen is dissolved by the acidification, and iodine corresponding to dissolved oxygen is liberated. The liberated iodine reacts with excess iodide ion and changes into triiodide ion, which is determined by titration with the sodium thiosulfate solution. Therefore, to calculate the dissolved oxygen concentration in the sample, the concentration of the sodium thiosulfate solution must be determined in advance. This is called the standardization of the titrant solution. In addition, trace amounts of impurities, including redox species, in the pickling reagents and sulfuric acid solution affects the titration with the sodium thiosulfate solution. This interference by the impurities, which is called the reagent blank, should be determined prior to the sample measurement as well as the standardization. In this section, we describe a method of the sample measurement (7-1) continued

from the previous section, prior to those of the standardization (7-2), and the determination of the reagent blank (7-3).

7-1. Sample measurement

If the water seal by the DIW in the neck of the oxygen bottle is maintained, the bottle can be stored for many days without any noticeable change in the oxygen concentration (Langdon, 2010). We confirmed no significant change in the oxygen concentration within 72 hours. Usually the titration can start from approximately a few hours after the sampling when the precipitate has settled down at the bottom of the bottle. Before the measurement, check that the oxygen bottle and the sodium thiosulfate solution are warmed up to room temperature.

7-1-1. Setup of automatic titrator

Place the sodium thiosulfate solution near the photometric automatic titrator (5-2-1) and draw the solution into the flow tubes and piston burette of the titrator. No bubbles are allowed in them. Immerse the thermometer (5-2-5) in the sodium thiosulfate solution and record its temperature. If possible, a continuous monitoring of the solution temperature is recommended. Record the oxygen bottle number. Prepare the sulfuric acid solution.

7-1-2. Removal of DIW

Pour out the sealing DIW in the neck of the bottle using the empty squeeze bottle (5-2-7) without disturbing the precipitate in the bottle and use a tissue or cotton ball to remove any remaining water.

7-1-3. Addition of sulfuric acid

Remove the stopper from the oxygen bottle and pour 1 mL of the sulfuric acid into the bottle along the stopper. Pour the remaining sulfuric acid solution on the stopper into the bottle using DIW. If you pour the acid solution directly into the bottle, the precipitate may be disturbed.

7-1-4. Addition of stirring bar

Add a stirring bar (5-2-2) in the bottle without scatters of the seawater sample from the bottle. Wipe the outside of the bottle with a tissue and set it in the bottle holder of the automatic titrator.

7-1-5. Titration

Start the rotation of the stirring bar. After the rotation is stabilized (about 7 rps) and all the precipitate are dissolved, start the automatic titration. Air bubbles generated by the faster rotation of the stirring bar could result in an error of the oxygen concentration determination because atmospheric oxygen in the air bubbles oxidizes iodine ion to iodine. This interference, however, hardly disturbs the endpoint determination if the titration time is less than 10 minutes because of the slow reaction rate of this oxidization.

7-1-6. Record of results

The titration is automatically terminated. Record the titration endpoint (V_{tit} [mL]) and the temperature of the sodium thiosulfate solution. If you find something unusual in the titration curve, check whether the titration endpoint has been properly determined.

7-2. Standardization of sodium thiosulfate solution

The standardization of the sodium thiosulfate solution should be carried out at least twice, just before and after a series of sample measurements to verify that the concentration of the titrant solution has not changed during the sample measurements. The standardization should be performed after the titrant solution is warmed up to room temperature.

7-2-1. Setup of automatic titrator

Setup the automatic titrator as same as that in 7-1-1. Prepare the pickling reagents and sulfuric acid solution.

7-2-2. Preparation of oxygen bottle

Fill an oxygen bottle approximately two thirds full with DIW and add a stirring bar into the bottle.

7-2-3. Addition of potassium iodate standard solution

Add 10 mL of the potassium iodate standard solution (4-5) to the oxygen bottle using the volume-calibrated automatic burette (5-2-4). Immediately thereafter, measure the temperature of the standard solution (t_L [°C]) remaining in the brown glass bottle using the calibrated thermometer (5-2-5) and record it.

7-2-4. Addition of sulfuric acid

Add 1 mL of the sulfuric acid and stir thoroughly using the magnetic stirrer (5-2-6).

7-2-5. Addition of pickling reagent II

Add 1 mL of the pickling reagent II solution and stir thoroughly. The solution turns yellowish due to liberated iodine.

7-2-6. Addition of pickling reagent I

Add 1 mL of the pickling reagent I solution and stir thoroughly. Fill the oxygen bottle up to the neck of it with DIW. If you add the pickling reagent I prior to the reagent II, manganese hydroxide precipitate locally produced in the bottle may cause the measurement errors.

7-2-7. Titration

Wipe the outside of the bottle and set it in the bottle holder of the automatic titrator. When the titration is completed, check whether the titration curve and endpoint have been recorded. Record the temperature of the sodium thiosulfate solution.

7-2-8. Calculation of endpoint

Repeat the above procedures 3 to 5 times and the endpoints are averaged (V_{std} [mL]). When the concentrations of the potassium iodate standard and sodium thiosulfate solutions are $1/600 \text{ mol}\cdot\text{L}^{-1}$ and 0.025 M, respectively, the titration volume (endpoint) of the sodium thiosulfate solution is 4 mL, which corresponds to $250 \mu\text{mol}\cdot\text{kg}^{-1}$ of dissolved oxygen concentration. The calculation method of the concentration of the titrant solution from the titration volume is described in section 8-2.

7-3. Reagent blank determination

The reagent blank should be determined at least twice, just before and after a series of sample measurements to verify that it has not changed during the sample measurements, as well as the standardization. The reagent blank determination should be also performed after the titrant solution is warmed up to room temperature. Because the contribution of dissolved oxygen in the pickling reagents is not included in this reagent blank, it is corrected by another way (8-3-1).

7-3-1. Determination method

The reagent blank is the volume of the sodium thiosulfate solution required for the titration of the interfering substances in the reagent solutions added. The reagent blank (V_{blk} [mL]) is obtained as follows.

$$V_1 = V_p + V_{\text{blk}} \quad (10)$$

$$V_2 = 2 \cdot V_p + V_{\text{blk}} \quad (11)$$

$$V_{\text{blk}} = 2 \cdot V_1 - V_2 \quad (12)$$

where V_1 [mL] is the titration endpoint of the sodium thiosulfate solution for a volume (usually 1 mL) of the potassium iodate standard solution, V_2 [mL] is that for the precise double volume of the same standard solution, and V_p [mL] is the equivalent point of the titrant solution for the volume of the standard solution. There are two specific methods. The standard solutions added twice in an oxygen bottle are titrated sequentially, or the single and double volumes of the standard solutions in two different oxygen bottles are titrated separately. In the former method, the total volume of the sodium thiosulfate solution added in the first titration must be also recorded in addition to the first endpoint. Here, we describe the latter method that requires the same procedures in the first and second titrations.

Strictly, the reagent blank determined by equation 12 (V_{blk}) is resulted not only from the interfering substances in the reagents but also from the difference between the apparent and true equivalent points due to unknown causes in the titrator (Carpenter, 1965b). This was suggested by significant differences among the "reagent blanks" from an inter-laboratory experiment using the same pickling reagents (Culberson, 1991). However, the temporal variation in this instrumental error inherent to each titrator seems to be small. Therefore, there is no problem in the calculation of the dissolved oxygen concentration using the apparent reagent blank. It is possible to estimate the true reagent blank and instrumental error separately. A series of the reagent blank determinations with the pickling reagents of single, double, triple, and four times volumes provides a regression line between the volume of the reagents added and the apparent reagent blank. The true reagent blank and instrumental error are identical to the slope and y-intercept of the regression line, respectively.

7-3-2. Setup of automatic titrator

Setup the automatic titrator as same as that in 7-1-1.

7-3-3. Preparation of oxygen bottles

Fill two oxygen bottles approximately two thirds full with DIW and add a stirring bar into each bottle.

7-3-4. Addition of potassium iodate standard solution

Add 1 and 2 mL of the potassium iodate standard solution into the first and second bottles, respectively, using the volume-calibrated automatic burette. Because the volume of "2 mL" is required to be exactly the double of "1 mL", add "1 mL" twice into the second oxygen bottle. Alternatively, you may add 2 and 4 mL of the standard solution into the first and second bottles, respectively.

7-3-5. Addition of sulfuric acid

Add 1 mL of the sulfuric acid to the first oxygen bottle and stir thoroughly using the magnetic stirrer.

7-3-6. Addition of pickling reagent II

Add 1 mL of the pickling reagent II solution and stir thoroughly. The solution turns yellowish due to liberated iodine.

7-3-7. Addition of pickling reagent I

Add 1 mL of the pickling reagent I solution and stir thoroughly. Fill the oxygen bottle up to the neck of it with DIW.

7-3-8. Titration of first bottle

Wipe the outside of the bottle and set it in the bottle holder of the automatic titrator. When the titration is completed, check whether the titration curve and endpoint (V_1 [mL]) have been recorded. Record the temperature of the sodium thiosulfate solution.

7-3-9. Titration of second bottle

The second bottle with 2 mL of the standard solution is titrated along the same procedures from sections 7-3-5 to 7-3-8 to obtain the endpoint (V_2 [mL]).

7-3-10. Calculation of reagent blank

The reagent blank is calculated by substituting V_1 and V_2 into equation 12. Repeat the above procedures 3 to 5 times and the reagent blanks are averaged (V_{blk} [mL]).

8. Calculation of concentration

Dissolved oxygen concentration is calculated from the titration volume of the sodium thiosulfate solution standardized with the potassium iodate standard solution. The calculation methods for concentrations of the potassium iodate standard solution (8-1), sodium thiosulfate solution (8-2), and dissolved oxygen in the seawater sample (8-3) are described below. It is assumed that the concentration of the interfering substance in the DIW used in the reagent preparation can be neglected.

8-1. Concentration of potassium iodate (KIO_3) standard solution

8-1-1. Molal concentration (molality)

The molal concentration of the KIO_3 standard solution C_{KIO_3} [$\text{mol}\cdot\text{kg}^{-1}$] is expressed by the following equation.

$$C_{KIO_3} = \frac{p_{KIO_3} \cdot w_{KIO_3} \cdot f_{\text{buoy},KIO_3}}{m_{KIO_3} \cdot (w_{\text{dw}} + w_{KIO_3}) \cdot f_{\text{buoy},\text{dw}}} \quad (13)$$

where p_{KIO_3} : purity of KIO_3 ,
 w_{KIO_3} : weight of KIO_3 [g] (4-5-4),
 f_{buoy,KIO_3} : factor of buoyancy correction (Dickson et al., 2007) for KIO_3 weighing,
 m_{KIO_3} : molecular weight of KIO_3 (= 214.001 [$\text{g}\cdot\text{mol}^{-1}$]),
 $w_{\text{dw}} + w_{KIO_3}$: weight of DIW + KIO_3 [kg] (4-5-5),
 $f_{\text{buoy},\text{dw}}$: factor of buoyancy correction (Dickson et al., 2007) for DIW + KIO_3 weighing.

8-1-2. Molar concentration (molarity)

The molar concentration of the KIO_3 standard solution at the temperature t_L [$^{\circ}\text{C}$] (7-2-3), $C_{KIO_3}(t_L)$ [$\text{mol}\cdot\text{L}^{-1}$] is expressed by the following equation.

$$C_{KIO_3}(t_L) = \frac{C_{KIO_3} \cdot \rho_w(t_L)}{1000} \quad (14)$$

where C_{KIO_3} : molal concentration [$\text{mol}\cdot\text{kg}^{-1}$] of KIO_3 standard solution (8-1-1),
 $\rho_w(t_L)$: density of DIW at temperature t_L [$\text{kg}\cdot\text{m}^{-3}$] (Dickson et al., 2007). Strictly,
 $\rho_w(t_L)$ should be the density of the KIO_3 standard solution. However, no significant
 difference occurs when you use the density of DIW because it is a dilute solution (about
 0.04%).

8-2. Concentration of sodium thiosulfate ($\text{Na}_2\text{S}_2\text{O}_3$) solution

8-2-1. Dispensed volume of potassium iodate standard solution

The burette volume for the dispensing of the KIO_3 standard solution depends on the
 temperature of the standard solution, t_L [$^{\circ}\text{C}$] (7-2-3), which should be corrected. The dispensed
 volume of the KIO_3 standard solution at the temperature t_L [$^{\circ}\text{C}$], $V_{\text{KIO}_3}(t_L)$ [mL] is calculated by
 the following equation.

$$V_{\text{KIO}_3}(t_L) = V_{\text{KIO}_3}(t_C) \cdot \{1 + \alpha_v(t_L - t_C)\} \quad (15)$$

where t_C : temperature [$^{\circ}\text{C}$] of DIW when burette volume was calibrated (5-2-4),
 $V_{\text{KIO}_3}(t_C)$: dispensed volume of KIO_3 standard solution [mL] at temperature t_C [$^{\circ}\text{C}$],
 α_v : coefficient of volumetric expansion of burette [K^{-1}]. The coefficient of borosilicate
 glass is approximately $1 \times 10^{-5} \text{ K}^{-1}$ (Japanese Industrial Standards, 1994).

8-2-2. Molar concentration (molarity)

Since 1 mole of potassium iodate corresponds to 6 moles of sodium thiosulfate (4-5), the molar
 concentration of the sodium thiosulfate solution, $C_{\text{Na}_2\text{S}_2\text{O}_3}$ [$\text{mol}\cdot\text{L}^{-1}$] obtained by the following
 equation.

$$C_{\text{Na}_2\text{S}_2\text{O}_3} = 6 \cdot C_{\text{KIO}_3}(t_L) \cdot V_{\text{KIO}_3}(t_L) / (V_{\text{std}} - V_{\text{blk}}) \quad (16)$$

where $C_{\text{KIO}_3}(t_L)$: molar concentration of KIO_3 standard solution [$\text{mol}\cdot\text{L}^{-1}$] at temperature t_L
 [$^{\circ}\text{C}$] (8-1-2),
 $V_{\text{KIO}_3}(t_L)$: dispensed volume of KIO_3 standard solution [mL] at temperature t_L [$^{\circ}\text{C}$] (8-
 2-1),
 V_{std} : average volume (endpoint) of $\text{Na}_2\text{S}_2\text{O}_3$ solution used to titrate KIO_3 standard
 solution [mL] (7-2-8),
 V_{blk} : average of reagent blank [mL] (7-3-10).

8-3. Concentration of dissolved oxygen in sample

8-3-1. Amount of oxygen in sample

The total number of O₂ moles in the seawater sample collected in the oxygen bottle, n_{sam} [mol] is given by the following equation.

$$n_{\text{sam}} = \frac{1}{4} \cdot C_{\text{Na}_2\text{S}_2\text{O}_3} \cdot \frac{V_{\text{tit}} - V_{\text{blk}}}{1000} - \text{DO}_{\text{reg}} \quad (17)$$

where $C_{\text{Na}_2\text{S}_2\text{O}_3}$: molar concentration of Na₂S₂O₃ solution [mol·L⁻¹] (8-2-2),
 V_{tit} : volume (endpoint) of Na₂S₂O₃ solution used to titrate seawater [mL] (7-1-6),
 V_{blk} : average of reagent blank [mL] (7-3-10),
 DO_{reg} : saturated amount of O₂ at 25.5 °C in 2 mL of pickling reagent solutions I and II, 7.6×10^{-8} [mol] (Murray et al., 1968). Strictly, this should be calculated using the calibrated volume of the pickling reagents added, V_{reg} [mL] (5-1-3). However, no significant difference occurs when you use "2 mL" because its contribution to the calculation of the dissolved oxygen concentration is small.

Equation 17 is correct only when the molar concentrations of the Na₂S₂O₃ solution, $C_{\text{Na}_2\text{S}_2\text{O}_3}$ [mol·L⁻¹] used in the sample measurement (7-1), standardization (7-2), and reagent blank determination (7-3) are equal. Therefore, the standardization and blank determination should be carried out just before and after the series of the sample measurements, which allows reducing temporal changes in the temperature and molar concentration of the Na₂S₂O₃ solution. According to equations 16 and 17, 1 mol of KIO₃ corresponds to 1.5 mol of dissolved oxygen. Namely, the amount of KIO₃ (about 16.7 μmol) used in the standardization of the Na₂S₂O₃ solution (7-2) corresponds to 25 μmol of O₂, or the amount of O₂ in 100 mL of seawater whose dissolved oxygen concentration is 250 μmol·L⁻¹.

8-3-2. Volume of oxygen bottle

The volume of the oxygen bottle at the sampling temperature t_s [°C] (6-8), $V_{\text{flask}}(t_s)$ [mL] is obtained by the following equation.

$$V_{\text{flask}}(t_s) = V_{\text{flask}}(t_c) \cdot \{1 + \alpha_v(t_s - t_c)\} \quad (18)$$

where t_c : temperature [°C] of DIW when oxygen bottle volume was calibrated (5-1-1),
 $V_{\text{flask}}(t_c)$: volume of oxygen bottle [mL] at temperature t_c [°C],

α_V : coefficient of volumetric expansion of the burette [K^{-1}]. The coefficient of borosilicate glass is approximately $1 \times 10^{-5} K^{-1}$ (Japanese Industrial Standards, 1994).

8-3-3. Molar concentration (molarity)

The molar concentration of dissolved oxygen in the seawater sample at the sampling temperature t_s [$^{\circ}C$], $C_{sam}(t_s)$ [$mol \cdot L^{-1}$] is obtained by the following equation.

$$C_{sam}(t_s) = 1000 \cdot n_{sam} / (V_{flask}(t_s) - V_{reg}) \quad (19)$$

where n_{sam} : amount of dissolved oxygen in seawater sample [mol] (8-3-1),
 $V_{flask}(t_s)$: volume of oxygen bottle [mL] at sampling temperature t_s [$^{\circ}C$] (8-3-2),
 V_{reg} : calibrated volume of pickling reagents I and II added at room temperature [mL] (5-1-3). The change due to temperature change is ignored.

8-3-4. Molal concentration (molality)

The conversion from the molar concentration ($C_{sam}(t_s)$ [$mol \cdot L^{-1}$]) to the molal concentration (C_{sam} [$mol \cdot kg^{-1}$]) is obtained by the following equation.

$$C_{sam} = 1000 \cdot C_{sam}(t_s) / \rho_{sam}(t_s, S) \quad (20)$$

where t_s : sampling temperature [$^{\circ}C$] (6-8),
 S : salinity of seawater sample,
 $\rho_{sam}(t_s, S)$: density [$kg \cdot m^{-3}$] of seawater sample with temperature t_s [$^{\circ}C$] and salinity S (Dickson et al., 2007).

9. Uncertainty

To evaluate the reliability of the measurement result (accuracy), the ideas of "precision" and "trueness" have been used. Because these ideas assume "measurement error" and "true value", which are unknowable in principle, there has been confusion in the use of the terminology. In 1993, "Evaluation of measurement data - Guide to the expression of uncertainty in Measurement" was published by seven international organizations including the International Organization for Standardization (ISO) (ISO, 2008). In this guide, the concept of "uncertainty" was introduced as a new indicator of the reliability of the measurement result. The "uncertainty" is defined as "parameter, associated with the result of a measurement, that characterizes the dispersion of the values that could reasonably be attributed to the measurement" and all the factors related to the

reliability of the measurement are expressed as dispersion. The standard uncertainties ($u_1, u_2, u_3, \dots, u_n$), which are caused by all the factors, are combined in by the following equation.

$$u_c = \sqrt{\sum_{i=1}^n (u_i)^2} \quad (21)$$

where u_c is the combined standard uncertainty. Here we show an example of estimating the uncertainty of the measurement of dissolved oxygen concentration using the Winkler method.

9-1. Sources of uncertainty

From equations 17 and 19, the molar concentration $C_{\text{sam}}(t_s)$ [$\text{mol} \cdot \text{L}^{-1}$] can be obtained by the following equation.

$$C_{\text{sam}}(t_s) = 1000 \cdot \left(\frac{1}{4} \cdot C_{\text{Na}_2\text{S}_2\text{O}_3} \cdot \frac{V_{\text{tit}} - V_{\text{blk}}}{1000} - \text{DO}_{\text{reg}} \right) / (V_{\text{flask}}(t_s) - V_{\text{reg}}) \quad (22)$$

where $C_{\text{Na}_2\text{S}_2\text{O}_3}$: molar concentration of $\text{Na}_2\text{S}_2\text{O}_3$ solution [$\text{mol} \cdot \text{L}^{-1}$],
 V_{tit} : volume of $\text{Na}_2\text{S}_2\text{O}_3$ solution used to titrate seawater [mL],
 V_{blk} : average of reagent blank [mL],
 DO_{reg} : saturated amount of O_2 at 25.5 °C in 2 mL of pickling reagent solutions,
 7.6×10^{-8} [mol],
 $V_{\text{flask}}(t_s)$: volume of oxygen bottle [mL] at sampling temperature t_s [°C],
 V_{reg} : calibrated volume of pickling reagents I and II added at room temperature [mL].

Because DO_{reg} corresponds to about $1 \mu\text{mol} \cdot \text{kg}^{-1}$ of dissolved oxygen concentration, its contribution to the total uncertainty of dissolved oxygen concentration is negligible. The uncertainty of V_{reg} is probably less than 1/50 of the $V_{\text{flask}}(t_s)$ uncertainty. Thereby, we assume that the uncertainty of the molar concentration of dissolved oxygen depends mainly on those derived from $C_{\text{Na}_2\text{S}_2\text{O}_3}$, V_{tit} , V_{blk} , and $V_{\text{flask}}(t_s)$. If the uncertainty due to the seawater density can be ignored, the uncertainties of the molar [$\text{mol} \cdot \text{L}^{-1}$] and molal [$\text{mol} \cdot \text{kg}^{-1}$] concentrations are equal.

9-2. Uncertainties of concentration of sodium thiosulfate solution and reagent blank

The molar concentration of the sodium thiosulfate solution, $C_{\text{Na}_2\text{S}_2\text{O}_3}$ is calculated by the molar concentration of the KIO_3 standard solution ($C_{\text{KIO}_3}(t_L)$), its dispensing volume ($V_{\text{KIO}_3}(t_L)$), the volume of the $\text{Na}_2\text{S}_2\text{O}_3$ solution used to titrate the KIO_3 standard solution (V_{std}), and the reagent blank (V_{blk}) (8-2-2). The uncertainty of $V_{\text{KIO}_3}(t_L)$, which is corrected appropriately using a

calibrated electronic balance, seems to be smaller than that those from other sources. Therefore, we assume that the uncertainty of $C_{\text{Na}_2\text{S}_2\text{O}_3}$ depends on those from $C_{\text{KIO}_3}(t_L)$, V_{std} , and V_{blk} . Equations 13 and 14 suggest that the uncertainty of $C_{\text{KIO}_3}(t_L)$ is mainly derived from those of the purity of KIO_3 (p_{KIO_3}), the molecular weight of KIO_3 (m_{KIO_3}), and the weight of KIO_3 (w_{KIO_3}). When the certified standard substance "NMIJ CRM 3006-a" is used as the KIO_3 standard, the standard uncertainty due to its purity is 0.0090 %. The standard uncertainty of the molecular weight is about 0.0080%. The uncertainty of the reagent weighing using the calibrated electronic balance is estimated to be about 0.027 %. Therefore, the combined standard uncertainty of $C_{\text{KIO}_3}(t_L)$ is calculated to be 0.03 % by substituting the above three standard uncertainties into equation 21. Meanwhile, the standard uncertainties of V_{std} and V_{blk} can be estimated from the standard deviation of the repeat measurements of the standardization (7-2) and reagent blank determination (7-3) to be about 0.001 mL and 0.002 mL, respectively. Then the standard uncertainty of $(V_{\text{std}} - V_{\text{blk}})$ can be calculated to be 0.002 mL, which corresponds to 0.05 % of the relative standard uncertainty. Finally, the combined standard uncertainty of $C_{\text{Na}_2\text{S}_2\text{O}_3}$ is calculated to be approximately 0.06% from the relative standard uncertainties of $C_{\text{KIO}_3}(t_L)$ and $(V_{\text{std}} - V_{\text{blk}})$. Note that this uncertainty does not include the uncertainty derived from the temporal change in temperature of the $\text{Na}_2\text{S}_2\text{O}_3$ solution (8-3-1), because the temperature dependency of the $\text{Na}_2\text{S}_2\text{O}_3$ solution density is unknown. According to the temperature dependency of pure water, the deviation of ± 5 °C from 20 °C corresponds to about 0.1 % deviation of water density.

9-3. Uncertainty of sample titration

The standard uncertainty of V_{tit} can be derived from the standard deviation of the measurements of the same sample pairs (replicate measurement). The standard deviation of the replicate measurements (S) can be calculated from the difference between the two measurement results of n pairs ($d_1, d_2, d_3, \dots, d_n$).

$$S = \sqrt{\sum_{i=1}^n (d_i)^2 / 2n} \quad (23)$$

The standard deviation is estimated to be about $0.1 \mu\text{mol}\cdot\text{kg}^{-1}$, which corresponds to the standard deviation of 0.002 mL (0.04 %) to 4 mL of titration ($250 \mu\text{mol}\cdot\text{kg}^{-1}$ of dissolved oxygen concentration). The uncertainty of V_{tit} (0.002 mL) is larger than that of V_{std} (0.001 mL, 9-2) probably because of those derived from the seawater sampling (6). Then the standard uncertainty of $(V_{\text{tit}} - V_{\text{blk}})$ can be calculated to be 0.003 mL, which corresponds to 0.07 % of the relative standard uncertainty.

9-4. Uncertainty of oxygen bottle volume

The standard uncertainty of the oxygen bottle volume, $V_{\text{flask}}(t_s)$ can be estimated from the standard deviation of the repeat measurement in the bottle volume calibration (5-1-1), which is calculated to be about 0.015 %.

9-5. Combined standard uncertainty

Finally, the combined standard uncertainty of the dissolved oxygen concentration is calculated from the standard uncertainties of $C_{\text{Na}_2\text{S}_2\text{O}_3}$ (0.06 %, 9-2), $(V_{\text{tit}} - V_{\text{blk}})$ (0.07 %, 9-3), and $V_{\text{flask}}(t_s)$ (0.015 %, 9-4) to be 0.09 %, which corresponds to the standard deviation of 0.23 $\mu\text{mol}\cdot\text{kg}^{-1}$ relative to 250 $\mu\text{mol}\cdot\text{kg}^{-1}$. Therefore, the expanded uncertainty ($k = 2$) is 0.18 % or 0.46 $\mu\text{mol}\cdot\text{kg}^{-1}$. The standard uncertainty of V_{tit} becomes larger when the dissolved oxygen concentration is low. Therefore, you should pay much attention to the determination of V_{tit} to reduce the uncertainty of the dissolved oxygen measurement by the Winkler method. Note that the combined standard uncertainty (0.09 %) does not include those derived from the interfering substances (10-2).

10. Traceability and interfering substances

10-1. Traceability

Traceability is defined by "property of a measurement result whereby result can be related to a reference through a documented unbroken chain of calibrations, each contributing to the measurement uncertainty (ISO, 2015)". If you use "NMIJ CRM 3006-a" as a reference material, the dissolved oxygen concentration measured using the Winkler method can be comparable. To establish the comparability, an "unbroken chain of calibrations" should be planned. Fortunately, the concentration of the KIO_3 standard solution appropriately stored does not change for a few years. When a batch of the KIO_3 standard solution is changed, the standardization of the titrant solution should be conducted with both new and old batches of the standard solution at the same time so that you can cross-check the concentration of the new batch solution against that of the old one. It is also recommended a comparison between your standard solution and those prepared in other institutions.

Seawater includes several interfering substances for the measurement of dissolved oxygen concentration by the Winkler method. The total concentration of the interfering substances, which is converted into the dissolved oxygen concentration, is called the seawater blank concentration. The determination of the seawater blank concentration is necessary for ensuring the traceability of the dissolved oxygen concentration. The seawater blank concentration in the open-ocean water

is less than $1 \mu\text{mol}\cdot\text{kg}^{-1}$ except those in suboxic and anoxic waters (10-2). If it is assumed that the concentration is $0.50 (\pm 0.50) \mu\text{mol}\cdot\text{kg}^{-1}$ and the distribution of the possible values is uniform or rectangular, its standard uncertainty is calculated to be $0.29 \mu\text{mol}\cdot\text{kg}^{-1}$ ($= 0.50/\sqrt{3}$). This value corresponds to the standard uncertainty of 0.12 % relative to $250 \mu\text{mol}\cdot\text{kg}^{-1}$ of dissolved oxygen concentration, which is larger than the standard uncertainty of 0.09 % derived from the other sources (9-5). The combined standard uncertainty, which includes the uncertainty of the seawater blank concentration, is calculated to be 0.15 % or $0.37 \mu\text{mol}\cdot\text{kg}^{-1}$ (the extended uncertainty is 0.30 % or $0.74 \mu\text{mol}\cdot\text{kg}^{-1}$). Finally, it is necessary to subtract the seawater blank concentration ($0.5 \mu\text{mol}\cdot\text{kg}^{-1}$) from "the dissolved oxygen concentration", C_{sam} (8-3-4).

10-2. Interfering substances

The major interfering substances in the open-ocean water are iodate ions, nitrite ions, and hydrogen peroxide. The total concentration of them, which is converted into the dissolved oxygen concentration, is called the seawater blank concentration. In this section, a method for the determination of the seawater blank concentration (10-2-1), interferences by iodate ions (10-2-2), nitrite ions (10-2-3), hydrogen peroxide (10-2-4), and others (10-2-5) are described.

10-2-1. Determination of seawater blank concentration

The seawater blank ($V_{\text{sw-blk}}$ [mL]) is the volume of the titrant solution used to titrate the interfering substances in the seawater sample and can be estimated by the following equations.

$$V_1 = V_P + V_{\text{blk}} \quad (24)$$

$$V_3 = V_P + V_{\text{sw-blk}} + V_{\text{blk}} \quad (25)$$

$$V_{\text{sw-blk}} = V_3 - V_1 \quad (26)$$

where V_1 : titration endpoint of $\text{Na}_2\text{S}_2\text{O}_3$ solution for amount of KIO_3 standard solution [mL],
 V_3 : titration endpoint of $\text{Na}_2\text{S}_2\text{O}_3$ solution for amount of KIO_3 standard solution and seawater sample [mL],
 V_P : equivalent point of the titrant for amount of KIO_3 standard solution [mL],
 V_{blk} : reagent blank [mL].

V_1 has been measured in the reagent blank determination (7-3). V_3 can be obtained by similar procedures of the reagent blank determination from sections 7-3-3 to 7-3-8, in which "DIW" is replaced by "seawater sample". And sections 7-3-3 and 7-3-4 are revised as follows.

7-3-3r: "Fill an oxygen bottle with the seawater sample and measured water temperature (t_s

[°C]). The stopper is then inserted carefully in the oxygen bottle. Pour out and wipe off the seawater in the neck of the bottle. Remove the stopper and pour the remaining seawater on the stopper into the bottle using DIW. Add a stirring bar".

7-3-4r: "Add 1 mL of the KIO₃ standard solution into the oxygen bottle using the volume-calibrated automatic burette".

The seawater blank concentration $C_{\text{sw-blk}}(t_s)$ [mol·L⁻¹] is calculated from the following equation.

$$C_{\text{sw-blk}}(t_s) = \frac{1}{4} \cdot C_{\text{Na}_2\text{S}_2\text{O}_3} \cdot V_{\text{sw-blk}} / V_{\text{flask}}(t_s) \quad (27)$$

where $C_{\text{Na}_2\text{S}_2\text{O}_3}$: molar concentration of Na₂S₂O₃ solution [mol·L⁻¹] (8-2-2),

$V_{\text{sw-blk}}$: seawater blank [mL],

$V_{\text{flask}}(t_s)$: volume of oxygen bottle [mL] at sampling temperature t_s [°C] (8-3-2).

It would be impractical to determine the seawater blank concentration on each sample using this method. It is recommended that investigators report the dissolved oxygen concentration corrected by the assumed concentration of the seawater blank ($0.5 \pm 0.5 \mu\text{mol} \cdot \text{kg}^{-1}$) as shown in section 10-1 when they measure the oxygen concentration in the open-ocean water whose seawater blank concentration is less than $1 \mu\text{mol} \cdot \text{kg}^{-1}$. However, if you measured the dissolved oxygen concentration using the Winkler method in coastal waters, in which the concentrations of the interfering substances could be higher than those in the open-ocean water as shown below, the seawater blank concentration should be measured for the correcting of the oxygen concentration at least once in a series of measurements. Anyway, when you report the concentration of dissolved oxygen, you have to specify whether the seawater blank is corrected or not.

10-2-2. Iodate

The seawater blank in open-ocean water is mainly caused by iodate ions. Fig. 2 shows vertical profiles of the seawater blank concentration in the subtropical area of the North Pacific Ocean, which were obtained by the method described in section 10-2-1. The concentrations in the surface (0–150 m) and deep (150 m–bottom) layers are $0.4\text{--}0.5$ and $0.6\text{--}0.7 \mu\text{mol} \cdot \text{kg}^{-1}$, respectively. On the other hand, the concentration of iodate ion in the surface and deep layers are approximately 0.35 and $0.5 \mu\text{mol} \cdot \text{kg}^{-1}$, respectively and their horizontal variations are small (Wong and Li, 2009). In the Winkler method, 1.5 times of iodate concentration corresponds to the dissolved oxygen concentration (8-3-1). Therefore, 0.35 and $0.5 \mu\text{mol} \cdot \text{kg}^{-1}$ of iodate concentrations correspond to 0.52 and $0.75 \mu\text{mol} \cdot \text{kg}^{-1}$ of dissolved oxygen concentrations, respectively, which are in good agreement with the seawater blank concentrations shown in Fig. 2.

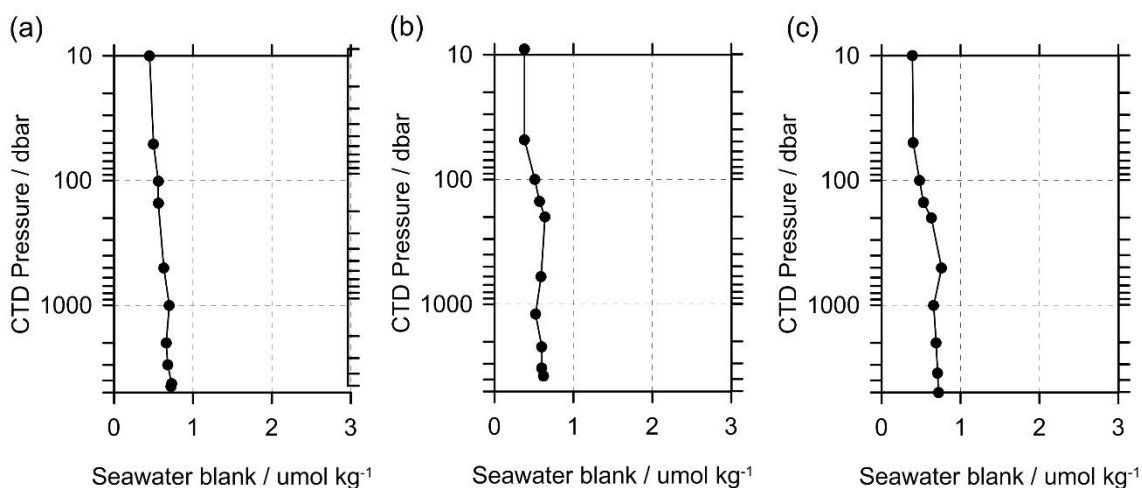


Fig.2 Vertical profiles of the seawater blank concentration ($\mu\text{mol}\cdot\text{kg}^{-1}$) at stations in the subtropical area of the North Pacific Ocean between November 2005 and January 2006. (a) $29.1^{\circ}\text{N}/123.9^{\circ}\text{W}$, (b) $25.5^{\circ}\text{N}/164.3^{\circ}\text{W}$, (c) $24.2^{\circ}\text{N}/172.8^{\circ}\text{E}$.

10-2-3. Nitrite

Nitrite ion oxidizes iodide ion to iodine in the acidic condition.



Because 1 mol of iodine corresponds to 0.5 mol of dissolved oxygen in the Winkler method, 1 mol of nitrite corresponds to 0.25 mol of dissolved oxygen. When dissolved oxygen is present in the sample, the nitric oxide produced in equation 28 reacts with dissolved oxygen, and nitrite ion is regenerated.



The regenerated nitrite ion oxidizes iodide ion again according to equation 28. Therefore, if the reactions of equations 28 and 29 proceed completely under the condition that there is enough iodine ion and dissolved oxygen, the total reaction is summarized as follow.



In this case, 1 mol of nitrite corresponds to 0.5 mol of dissolved oxygen. According to results of an experiment, the molar ratio of the concentrations of nitrite ion to dissolved oxygen is about 0.35 between 0.25 and 0.5 (Wong, 2012). In the open ocean, a maximum concentration of nitrite up to about $1 \mu\text{mol}\cdot\text{kg}^{-1}$ is observed in a subsurface layer. Therefore, the positive bias to dissolved

oxygen concentration due to nitrite ion ranges between 0 and $0.35 \mu\text{mol}\cdot\text{kg}^{-1}$ in the open ocean. On the other hand, higher concentrations of nitrite ion ($\sim 10 \mu\text{mol}\cdot\text{kg}^{-1}$) have been observed in suboxic areas such as the offshore area of Peru, where the interference in oxygen measurement by nitrite ion could be a few $\mu\text{mol}\cdot\text{kg}^{-1}$.

The interference by nitrite ion can be prevented by adding sodium azide (NaN_3) to the pickling reagent (Barnett and Hurwitz, 1939).



This method is called "the modified Winkler method with sodium azide" and commonly used in the determination of dissolved oxygen concentration in industrial wastewater with high concentration of nitrite (Japanese Industrial Standards, 2013). The procedures of the modified method are the same as the original method except that 10 g of sodium azide is added to 1 L of the pickling reagent II solution (4-2). According to Wong (2012), there is no significant difference in results of oxygen concentration measurements between the modified and original Winkler methods. If you measured dissolved oxygen concentration in seawater with a high concentration of nitrite, the modified Winkler method is recommended. However, the solutions and wastes with sodium azide must be handled with care because it is toxic.

10-2-4. Hydrogen peroxide

Hydrogen peroxide is a positive interfering substance in the measurement of dissolved oxygen concentration using the Winkler method as same as iodate and nitrite ions. Hydrogen peroxide oxidizes iodide ion to iodine in the acidic condition.



Because 1 mole of iodine corresponds to 0.5 mole of dissolved oxygen in the Winkler method, 1 mole of hydrogen peroxide corresponds to 0.5 mole of dissolved oxygen. Although the rate of this chemical reaction is slow in DIW, hydrogen peroxide can interfere with the Winkler method because manganese ions (Mg^{2+}) in the pickling reagent facilitate the reaction as a catalyst (Wong et al., 2010). Hydrogen peroxide is mainly generated by the photochemical reaction of organic matter in the surface layer. As a result, the concentrations in the surface and deep layers in the open ocean are $0.06\text{--}0.3 \mu\text{mol}\cdot\text{kg}^{-1}$ and less than $0.01 \mu\text{mol}\cdot\text{kg}^{-1}$, respectively (Wong et al., 2010), which correspond to up to $0.15 \mu\text{mol}\cdot\text{kg}^{-1}$ of dissolved oxygen concentration. The interference by hydrogen peroxide is smaller than those by iodate and nitrite ions in the open ocean. However, you should pay much attention to the seawater blank in seawaters collected in coastal areas and

estuaries, where more than $1 \mu\text{mol}\cdot\text{kg}^{-1}$ of hydrogen peroxide concentrations have been observed (Wong et al., 2010).

10-2-5. Others

In anoxic water depleted of dissolved oxygen, sulfuric acid is reduced to sulfite acid and sulfide. In addition, metallic ions may be eluted from sea-floor sediments into the anoxic bottom water on the seafloor. Sulfite ions, sulfides, and metallic ions are also the interfering substances of the Winkler method. In addition, there are other problems such as contamination from atmospheric oxygen during the water sampling and difficulty in the determination of the titration endpoint for the trace amount of oxygen. Therefore, it would be impractical to measure dissolved oxygen concentration less than $1 \mu\text{mol}\cdot\text{kg}^{-1}$ using the Winkler method.

References

- Barnett, G. R. and E. Hurwitz (1939): The use of sodium azide in the Winkler Method for the determination of dissolved oxygen, *Sewage Works Journal*, 11, 781–787.
- Broenkow, W. W. and J. D. Cline (1969): Colorimetric determination of dissolved oxygen at low concentrations, *Limnology and Oceanography*, 14, 450–454.
- Carpenter, J. H. (1965a): The Chesapeake Bay Institute technique for the Winkler dissolved oxygen method. *Limnology and Oceanography*, 10, 141–143.
- Carpenter, J. H. (1965b): The accuracy of the Winkler method for dissolved oxygen analysis. *Limnology and Oceanography*, 10, 135–140.
- Culberson, C. H. (1991): Dissolved Oxygen. In *WOCE Operations Manual, Part 3.1.3 : WHP Operations and Methods*, WHP Office Report WHPO 91-1, WOCE Report No. 68/91. Available online at: http://www.nodc.noaa.gov/woce/woce_v3/wocedata_1/whp/manuals.htm.
- Culberson, C. H., G. Knapp, R. T. Williams, and F. Zemlyak (1991): A comparison of methods for the determination of dissolved oxygen in seawater, WHP Office Report WHPO 91-2, WOCE Report No. 73/91. Available online at: <http://darchive.mblwhoilibrary.org/bitstream/handle/1912/243/WHPO-91-2.pdf?sequence=1&isAllowed=y>
- Dickson, A. G. (1996): Determination of dissolved oxygen in sea water by Winkler titration. In *WOCE Operations Manual, Part 3.1.3 : WHP Operations and Methods*, WHP Office Report WHPO 91-1, WOCE Report No. 68/91. Available online at: http://www.nodc.noaa.gov/woce/woce_v3/wocedata_1/whp/manuals.htm.
- Dickson, A. G., C. L. Sabine, and J. R. Christian (2007): Guide to best practices for ocean CO₂ measurements. *PICES Special Publication 3*, North Pacific Marine Science Organization, Sidney, pp. 191.

- Fujifilm Wako Pure Chemical Corporation (2018): 0.01mol/l Sodium Thiosulfate Solution. Available online at: http://www.siyaku.com/uh/Shs.do?dspWkfcodes=191-05565&_ga=2.197871663.122721241.1534985899-1808556025.1534985899 (in Japanese).
- Grasshoff, K. (1976): 4. Determination of oxygen, p. 59–70. In *Methods of Seawater Analysis*, first edition, edited by K. Grasshoff, Verlag Chemie, Weinheim.
- Hansen, H. P. (1999): 4. Determination of oxygen, p. 76–89. In *Methods of Seawater Analysis*, third, completely revised and extended edition, edited by K. Grasshoff, K. Kremling, and M. Ehrhardt, WILEY-VCH, Weinheim.
- Horibe, Y., Y. Kodama, and K. Shigehara (1972): Errors in sampling procedure for the determination of dissolved oxygen by Winkler Method. *Journal of Oceanographical Society of Japan*, 28, 203–206.
- ISO (2008): ISO/IEC Guide 98-3:2008, Uncertainty of measurement Part 3: Guide to the expression of uncertainty in measurement (GUM:1995). Available at: http://www.iso.org/iso/home/store/catalogue_ics/catalogue_detail_ics.htm?csnumber=50461
- ISO (2015): Guide 30:2015 Reference materials -- Selected terms and definitions. Available at: http://www.iso.org/iso/home/store/catalogue_ics/catalogue_detail_ics.htm?csnumber=46209
- International Union of Pure and Applied Chemistry (1997): *Compendium of Chemical Terminology*, 2nd ed. (the "Gold Book"). Compiled by A. D. McNaught and A. Wilkinson. Blackwell Scientific Publications, Oxford. Available online at: <http://goldbook.iupac.org/>
- Japanese Industrial Standards (1994): Glass apparatus for chemical analysis, JIS-R3503. Available online at: <http://kikakurui.com/r3/R3503-2007-01.html> (in Japanese).
- Japanese Industrial Standards (2013): Current of testing method for industrial wastewater, JIS-K0102. Available online at: <http://kikakurui.com/k0/K0102-2013-01.html> (in Japanese).
- Japan Meteorological Agency (1999): *the Manual on Oceanographic Observation Part 1*, Japan Meteorological Agency, Tokyo, 200 pp (in Japanese).
- Joint Global Ocean Flux Study (1994): Chapter 6. Determination of dissolved oxygen by Winkler procedure, p. 25–33. In *JGOFS Protocols*. Available online at: http://usjgofs.whoi.edu/JGOFS_19.pdf.
- Kimoto Electric Co., LTD. (2009): *Manual of Titrator for Dissolved Oxygen DOT-05*, 60pp. Available online at: http://www.kimoto-electric.co.jp/support/pdf/DOT05_manual.pdf (in Japanese).
- Kitano, Y. (1964): Determination of dissolved oxygen concentration in freshwater and seawater. "*Bunsekikagaku*", 13, 573–577 (in Japanese).
- Kumamoto, Y., Y. Takatani, T. Miyao, H. Sato, K. Matsumoto (2015): Dissolved Oxygen, p. G301JP:001–030. In *Guideline of Ocean Observations Volume 3 Seawater Analysis (Dissolved Substances)*, The Oceanographic Society of Japan, Tokyo (in Japanese).
- National Metrology Institute of Japan (2015): NMIJ CRM 3006-a. <https://www.nmij.jp/service/C/> (in Japanese).

- Labasque, T., C. Chaumery, A. Aminot, and G. Kergoat (2004): Winkler determination of dissolved oxygen: re-examination of critical factors and reliability, *Marine Chemistry*, 88, 53–60.
- Langdon, C. (2010): Determination of dissolved oxygen in seawater by Winkler titration using the amperometric technique. In the GO-SHIP Repeat Hydrography Manual: A Collection of Expert Reports and Guidelines, edited by E. M. Hood, C. L. Sabine, and B. M. Sloyan, ICPO Publication Series Number 134. Available online at: <http://www.go-ship.org/HydroMan.html>.
- Miyao, T., S. Umeda, Y. Takatani, N. Nagai (2013): High-precision determination of dissolved oxygen. *Weather Serv. Bull.*, 80, S149–S157 (in Japanese).
- Murray, C. N., J. P. Riley, and T. R. S. Wilson (1968): The solubility of oxygen in Winkler reagents used for the determination of dissolved oxygen. *Deep-Sea Research*, 15, 237–238.
- Pai, S.-C., G.-C. Gong, and K.-K. Liu (1993): Determination of dissolved oxygen in seawater by direct spectrophotometry of total iodine, *Marine Chemistry*, 41, 343–351.
- Strickland, J. D. H. and T. R. Parsons (1972): *A Practical Handbook of Seawater Analysis*. Fisheries Research Board of Canada, Ottawa, 310 pp.
- Tanaka, T., H. Hayashi, Y. Komiya, H. Nabekawa, H. Hayashi (2007): Stability of sodium thiosulfate solution and constant-current coulometric iodometric titration of potassium iodate, "*Bunsekikagaku*", 56, 327–332 (in Japanese with English abstract).
- Winkler, L. W. (1888): Die Bestimmung des in Wasser gelösten Sauerstoffes. *Berichte der Deutschen Gesellschaft*, 21, 2843–2854.
- Wong, G. T. F. (2012): Removal of nitrite interference in the Winkler determination of dissolved oxygen in seawater, *Marine Chemistry*, 130–131, 28–32.
- Wong, G. T. F. and K.-Y. Li (2009): Winkler's method overestimates dissolved oxygen in seawater: Iodate interference and its oceanographic implications, *Marine Chemistry*, 115, 86–91.
- Wong, G. T. F., Y.-C. Wu, and K.-Y. Li (2010): Winkler's method overestimates dissolved oxygen in natural waters: Hydrogen peroxide interference and its implications, *Marine Chemistry*, 122, 83–90.

This page left intentionally blank.

The precise and accurate determination of dissolved inorganic nutrients in seawater, using Continuous Flow Analysis methods

○Michio AOYAMA

(Japan Agency for Marine-Earth Science and Technology and University of Tsukuba)

An original version of GO-SHIP nutrients manual by Hydes et al. (2010) is revised and new nutrients manual was published in August 2019 as “The precise and accurate determination of dissolved inorganic nutrients in seawater, using Continuous Flow Analysis methods” by Becker et al. (2019).

This revised manual reviews basic sample collection and storage, aspects of continuous flow analysis (CFA) using an Auto-Analyzer, and specific nutrient methods in use by many laboratories doing repeat hydrography. The document also covers laboratory best practices including quality control and quality assurance (QC/QA) procedures to obtain the best results, and suggests protocols for the use of reference materials (RM) and certified reference materials (CRM). This revised manual was scientific public comments procedure in 2018 and all comments were incorporated where appropriate.

The revised GO-SHIP manual is available at the following website:

<http://www.go-ship.org/HydroMan.html>. DOI: <http://dx.doi.org/10.25607/OBP-555>

References

- D. J. Hydes, M. Aoyama, A. Aminot, K. Bakker, S. Becker, S. Coverly, A. Daniel, A. G. Dickson, O. Grosso, R. Kerouel, J. van Ooijen, K. Sato, T. Tanhua, E. M. S. Woodward, J. Z. Zhang (2010): Determination of Dissolved Nutrients (N, P, SI) in Seawater with High precision and Inter-Comparability Using Gas-Segmented Continuous flow Analysers. In: The Go-ship Repeat Hydrography Manual: A Collection of Expert Reports and Guidelines, UNESCO-IOC, IOCCP Report Number 14, ICPO Publication Series Number 134
- S. Becker, M. Aoyama E. Malcolm S. Woodward, K. Bakker, S. Coverly, C. Mahaffey, T. Tanhua, (2019): The precise and accurate determination of dissolved inorganic nutrients in seawater, using Continuous Flow Analysis methods. In: The GO-SHIP Repeat Hydrography Manual: A Collection of Expert Reports and Guidelines. Available online at: <http://www.go-ship.org/HydroMan.html>. DOI: <http://dx.doi.org/10.25607/OBP-555>

This page left intentionally blank.

Trace metals

○Hajime Obata (AORI, Univ. Tokyo)

For determination of trace metals in seawater, contamination is one of the most critical problems. Concentrations of most metals are very low in seawater of open ocean, but the metals are ubiquitous in the research ship and laboratories. We need to be very careful to avoid contamination at each step, collection, filtration, pretreatment, and analysis of seawater. In this chapter, clean techniques for each step are described to prevent the contamination. Clean sampling techniques are described in Vol. 2, Chap. 1, “Clean sampling”.

1. Filtration of seawater

We usually study “dissolved” trace metals because dissolved fraction of bioactive trace metals in seawater is considered to be available for marine microorganisms. This “dissolved fraction” is also investigated on other non-bioactive trace metals. Filtration of seawater samples is necessary to obtain the dissolved fraction of the samples, but we often suffer from contaminations during this process. To avoid the contamination, initially we have to confirm that the materials of filters and filtering apparatuses are clean enough for the target metals, and establish their cleaning method. For example, 0.2 or 0.4 μm pore-size Nucleopore filters are frequently used to filter seawater samples for trace metal analyses, but these filters must be cleaned with diluted ultra-pure grade of acids before use. During the cleaning process, the acids remaining in the filters may cause the contamination of the seawater samples. The remaining acids should be removed thoroughly with ultra high purity water (UHPW). Filtering apparatuses, like filter holders, are usually made of Teflon, polycarbonate or polysulfon. Suitable cleaning methods for the materials should be established not to damage the apparatuses.

Capsule filters are easy to handle and frequently used for filtration. For example, many research groups in the international GEOTRACES project use 0.2 μm pore-size polysulfon capsule filters (Acropak, PALL). To clean the filters, we fill the capsule filters with 0.1 M ultra pure hydrochloric acid for one day. The acid solution should be completely removed by passing UHPW through the capsule filters. We can effectively remove the acid solution by filling the capsule filters with UHPW for more than one day. Onboard the research vessel, one capsule filter is repeatedly used throughout the observation at several stations. In this case, to prevent the growth of bacteria inside of the capsule, the filters are preserved in the refrigerator between the stations.

2. Onboard analyses

For studying the marine biogeochemistry of contamination-prone trace metals, it is better to determine them onboard the ship. Onboard analyses will allow us to notice the contamination, which prevents the damage to the entire samples during the cruise. In GEOTRACES project, it is recommended to determine some contamination-prone trace metals like Fe and Zn in seawater onboard the ship. Since the clean laboratory space is limited in the research ship, we should apply the compact closed flow system for the analytical method. Several methods have already been developed for onboard analyses of trace metals in seawater (e.g. Al, Brown & Bruland, 2008. Fe: Lohan et al., 2006; Measures et al.,

1995; Obata et al., 1993. Zn: Gosnell et al., 2012; Jakuba et al., 2008; Lohan et al., 2003). Onboard analyses often enable the in situ determination of each species of trace metals in seawater. Therefore, it would be also better to determine trace metals, whose speciations are easily variable, onboard the ship.

3. Preservation and pre-treatments

Some trace metals in seawater will be measured after coming back to the land-based laboratory. Especially, some metals and their isotopes will be determined by using large-sized analytical facilities, so that we have to establish the preservation methods of the samples without loss and contamination. Many trace metals are easily adsorbed onto the wall of the storing bottles at neutral to alkaline pH conditions. An optimal pH of seawater sample for preservation should be examined for each target metal in the laboratory. For most of the metals, it is better to lower the pH of the samples to less than 2 with hydrochloric acid or nitric acid. Since impurities in the acids directly cause contaminations, we need to check the blank values of the acids before use. If the samples are preserved for a long time, leachates of the target metals from the stored bottles should also be evaluated. By choosing the optimal material for the storing bottles and establishing their cleaning methods, we can preserve the seawater samples for a long time. During the production of polymers, some metals might be added to the material as catalysts. We need to examine which storing bottles are suitable for the target metals. For many trace metals, low-density polyethylene or Teflon bottles are known to be useful for storage.

On the other hand, by lowering the sample pH, the speciation of metals will be changed in seawater. In this case, we can temporally preserve the seawater samples by freezing at lower than -18 degree (e.g., Buck et al., 2012). However, we should not use dry ice for freezing because the pH of samples might be changed. It would be better to examine how long we can preserve the samples.

4. Analyses at land-based laboratory

Many analytical methods have been developed to determine trace metals in seawater at land-based laboratory (Sohrin and Bruland, 2011). To determine many trace metals simultaneously, inductively coupled plasma mass spectrometry (ICP-MS) is frequently used. In the ICP-MS system, a high-temperature ICP source converts the atoms of the target metals to their ions. The produced ions are introduced to the mass spectrometer where the ions are separated and detected. The ions are separated by their mass-to-charge ratio with the quadrupole mass filter. This quadrupole mass filter can sufficiently resolve the mass-to-charge ratios of heavy elements, but this resolution is not enough to separate overlapping molecular or isobaric interferences from the isotopes of some trace metals (e.g., Fe, Cu and Zn). To obtain higher resolution, magnetic sector mass spectrometers are common in ICP-MS, which allow us to eliminate or reduce the effect of interferences.

Since seawater contains so much sea-salts, it is difficult to introduce seawater samples to ICP-MS directly. We have to separate target metals from the sea-salts before ICP-MS analyses. For this separation, several methods have been developed, such as magnesium hydroxide coprecipitation method and chelating resin preconcentration method. During these preconcentration processes, the samples are possibly contaminated, hence the processes should be performed under clean air condition or within the flow system. Moreover, the isotope dilution method, adding enriched isotope spike solution, is applied

for the precise measurement. We should select suitable methods for the target metals.

Recently, many methods have been developed by combining ICP-MS with preconcentration using chelating resin column. Among these methods, several methods, often used, are shown in the table below. To successfully determine trace metals in seawater, the analysts should have high levels of analytical skill and experience for clean sample handling. For example, we should check whether procedural blank values are low enough to measure the concentration level in oceanic water.

5. Reference seawater sample

Table. Determination methods of trace metals in seawater by combining chelating resin preconcentration with ICP-MS.

References	Sohrin et al. (2008)	Milne et al. (2010)	Lee et al. (2011)	Billier and Bruland (2012)	Lagerstrom et al. (2013)	Minami et al. (2015)
Elements	Al, Mn, Fe, Co, Ni, Cu, Zn, Cd, Pb	Mn, Fe, Co, Ni, Cu, Zn, Cd, Pb	Fe, Cu, Cd, Pb	Mn, Fe, Co, Ni, Cu, Zn, Cd, Pb	Mn, Fe, Co, Ni, Cu, Zn	Al, Mn, Fe, Co, Ni, Cu, Zn, Cd, Pb
Resin	Nobias-chelate PA1	Toyopearl Chelate-650 IDA resin	NTA Superflow	Nobias-chelate PA1	Nobias-chelate PA1	Nobias-chelate PA1
ICP-MS	Quadrupole	Magnetic Sector	Quadrupole	Magnetic Sector	Magnetic Sector	Magnetic Sector
Detection Limit (nM)				Automatic	Automatic	Automatic
Fe	0.036	0.021	0.07	0.014	0.014	0.09
Cu	0.005	0.007	0.12	0.052	0.003	0.02
Pb	0.001	0.0002	0.0005	0.00056	-	0.0009
Mn	0.01	0.007	-	0.002	0.002	0.003
Zn	0.06	0.005	-	0.03	0.016	0.1

Before determination of trace metals in seawater samples, we usually examine the precision of the analytical methods. Moreover, to get the right number, it is required to analyze reference seawaters and report the results. It is better to choose and analyze reference seawaters in which the concentrations of the target metals are as the same level as those in actual samples. As reference seawaters, consensus values should be reported by several different groups with different methods. We can commercially obtain some reference seawaters, like NASS-series (National Research Council Canada). In these reference seawaters, the concentrations of trace metals are a little higher than those in Atlantic Ocean, Southern Ocean, Indian Ocean and Pacific Ocean. In the international GEOTRACES project, reference seawaters for main key parameters are widely distributed with their consensus values (e. g. SAFe, GEOTRACES seawaters) and available for Geotraces. The details of the reference seawaters are shown at the web site (<http://es.ucsc.edu/~kbruland/GeotracesSaFe/kwbGeotracesSaFe.html>). However, this distribution to the wide community is a voluntary work and the numbers of stocked seawaters are limited. Hence, the reference seawaters cannot be provided everlastingly. It is not easy to keep the reference seawaters for a long time at the same quality level. We will have to find the way to distribute the high-quality reference seawater continuously.

References

- Billier, D. V., and K. W. Bruland (2012): Analysis of Mn, Fe, Co, Ni, Cu, Zn, Cd, and Pb in seawater using the Nobias-chelate PA1 resin and magnetic sector inductively coupled plasma mass spectrometry (ICP-MS). *Mar. Chem.*, 130-131, 12–20.
- Buck, K. N., J. Moffett, K. A. Barbeau, R. M. Bundy, Y. Kondo, and J. Wu (2012): The organic complexation of iron and copper: an intercomparison of competitive ligand exchange–adsorptive cathodic stripping voltammetry (CLE-ACSV) techniques. *Limnol. Oceanogr.: Methods*, 10, 496–515.
- Brown, M.T. and K. W. Bruland (2008): An improved flow-injection analysis method for the determination of dissolved aluminium in seawater. *Limnol. Oceanogr.: Methods*, 6, 87-95.
- Gosnell, K.J., W. M. Landing, A. Milne (2012): Fluorometric detection of total dissolved zinc in the southern Indian Ocean. *Mar. Chem.*, 132-133: 68-76.
- Jakuba, R.W., J. W. Moffett, and M. A. Saito (2008): Use of a modified, high-sensitivity, anodic stripping voltammetry method for determination of zinc speciation in the North Atlantic Ocean. *Anal. Chim. Acta*, 614, 143-152.
- Lagerström, M. E., M.P. Field, M. Séguret, L. Fischer, S. Hann, R.M. Sherrell (2013): Automated on-line flow-injection ICP-MS determination of trace metals (Mn, Fe, Co, Ni, Cu and Zn) in open ocean seawater: Application to the GEOTRACES program. *Mar. Chem.*, 155, 71–80.
- Lee, J.M., E. A. Boyle, Y. Echevoyen-Sanz, J. N. Fitzsimmons, R. Zhang, R. A. Kayser, (2011): Analysis of trace metals (Cu, Cd, Pb, and Fe) in seawater using single batch nitrilotriacetate resin extraction and isotope dilution inductively coupled plasma mass spectrometry. *Anal. Chim. Acta*, 686, 93–101.
- Lohan, M. C, D. W. Crawford, D. A. Purdie, P. J. Statham (2003): Iron and zinc enrichments in the northeastern subarctic Pacific: Ligand production and zinc availability in response to phytoplankton growth. *Limnol. Oceanogr.*, 50, 1427-1437.
- Lohan, M.C., A. M. Aguilar-Islas, K. W. Bruland (2006): Direct determination of iron in acidified (pH 1.7) seawater samples by flow injection analysis with catalytic spectrophotometric detection: Application and intercomparison. *Limnol. Oceanogr.: Methods*, 4, 164-171.
- Measures, C. I., J. Yuan, J. A. Resing (2005): Determination of iron in seawater by flow injection analysis using in-line preconcentration and spectrophotometric detection. *Mar. Chem.*, 50, 3-12.
- Milne, A., W. Landing, M. Bizimis, P. Morton (2010): Determination of Mn, Fe, Co, Ni, Cu, Zn, Cd and Pb in seawater using high resolution magnetic sector inductively coupled mass spectrometry (HR-ICP-MS). *Anal. Chim. Acta* 665, 200–207.
- Minami, T., W. Konagaya, L. Zheng, S. Takano, M. Sasaki, R. Murata, Y. Nakaguchi, Y. Sohrin (2015): An off-line automated preconcentration system with ethylenediaminetriacetate chelating resin for the determination of trace metals in seawater by high-resolution inductively coupled plasma mass spectrometry. *Anal. Chim. Acta*, 854,183–190.
- Obata, H., H. Karatani, E. Nakayama (1993): Automated determination of iron in seawater by chelating resin concentration and chemiluminescence detection. *Anal. Chem.*, 65, 1524-1528.

Sohrin, Y., S. Urushihara, S. Nakatsuka, T. Kono, E. Higo, T. Minami, K. Norisuye, S. Umetani (2008):
Multielemental determination of GEOTRACES key trace metals in seawater by ICPMS after

preconcentration using an ethylenediaminetriacetic acid chelating resin. *Anal. Chem.*, 80, 6267–6273.

Sohrin, Y. and K. W. Bruland (2011): Global status of trace elements in the ocean. *Trends in Anal. Chem.*, 30,
1291-1307.

This page left intentionally blank.

DIC

A Standard Operation Protocol of “Determination of total dissolved inorganic carbon in sea water” is available from the following CDIAC web site:

http://cdiac.ornl.gov/ftp/oceans/Handbook_2007/sop02.pdf

http://cdiac.ornl.gov/oceans/Handbook_2007.html

This page left intentionally blank.

Determination of total alkalinity in sea water by spectrophotometry

○Masao ISHII and Naohiro KOSUGI (Meteorological Research Institute, JMA)

1. Scope

This procedure describes a method for the determination of total alkalinity in sea water by spectrophotometry. A method for the determination of total alkalinity by potentiometric titration has been described in SOP 3a and SOP 3b in Chapter 4 of Dickson, A.G., Sabine, C.L. and Christian, J.R. (Eds.) 2007, “Guide to best practices for ocean CO₂ measurements. PICES Special Publication 3, 191 pp. (http://cdiac.ornl.gov/oceans/Handbook_2007.html). The method is suitable for assaying oceanic levels of total alkalinity (2000–2500 μmol kg⁻¹).

2. Terms and definition

The total alkalinity of a sea water sample is defined as the number of moles of hydrogen ion equivalent to the excess of proton acceptors (bases formed from weak acids with a dissociation constant $K \leq 10^{-4.5}$ at 25°C and zero ionic strength) over proton donors (acids with $K > 10^{-4.5}$) in 1 kilogram of sample:

$$\begin{aligned}
 A_T = & [\text{HCO}_3^-] + 2[\text{CO}_3^{2-}] + [\text{B}(\text{OH})_4^-] + [\text{OH}^-] + [\text{HPO}_4^{2-}] \\
 & + 2[\text{PO}_4^{3-}] + [\text{SiO}(\text{OH})_3^-] + [\text{NH}_3] + [\text{HS}^-] + \dots \\
 & - [\text{H}^+]_F - [\text{HSO}_4^-] - [\text{HF}] - [\text{H}_3\text{PO}_4] - \dots
 \end{aligned} \tag{1}$$

Brackets represent total concentrations of these constituents in solution, $[\text{H}^+]_F$ is the free concentration of hydrogen ion, and the ellipses represent additional minor acid or base species that are either unidentified or present in such small amounts that they can be ignored.

3. Principle

A known amount of sea water is placed in a container such as beaker or directly in an optical cell where it is first acidified to a pH between 3.8 and 4.2 with a known amount of hydrochloric acid. The acid titrant is made up in a sodium chloride background to approximate the ionic strength of sea water so as to maintain approximately constant activity coefficients during the measurement procedure. The solution of an indicator dye bromocresol green is also added to the sea water sample. The solution is then stirred for a period of time to allow for the escape of CO₂ that has evolved, and subsequently pH of the sample is measured precisely with spectrophotometric technique. Total alkalinity is computed from the volume of sample ($V_{\text{SW}}/\text{dm}^3$), concentration ($c_{\text{HCl}} / \text{mol dm}^{-3}$) and volume ($V_{\text{HCl}}/\text{dm}^3$) of hydrochloric acid titrant added to the sample, $[\text{H}^+]_T (=10^{-\text{pH}})$, and the density of sea water sample when placed in the container ($\rho_{\text{SW}} / \text{kg dm}^{-3}$):

$$A_T = \frac{c_{\text{HCl}} \cdot V_{\text{HCl}} \cdot 10^6 - [\text{H}^+]_T \cdot (V_{\text{SW}} + V_{\text{HCl}}) \cdot \rho_{\text{SW}}}{V_{\text{SW}} \cdot \rho_{\text{SW}}} \quad (2)$$

It is necessary to measure the temperature of sample when it is placed into the container and when spectrophotometric measurement is made in order to compute the density of sea water sample and to correct for the effect of temperature change on spectrophotometric measurements.

4. Apparatus

4-1 An example of apparatus set-up

An example of apparatus set-up is shown in Figure 1. Usually, hydrochloric acid and indicator dye are added in a beaker, and spectrophotometric measurement is made in an optical cell separately. However, in an example shown here, measurements are made precisely and efficiently by adding a mixed solution of acid titrant and indicator dye to a seawater sample and making spectrophotometric measurement in the same cell in a spectrophotometric system that uses optical fibers.

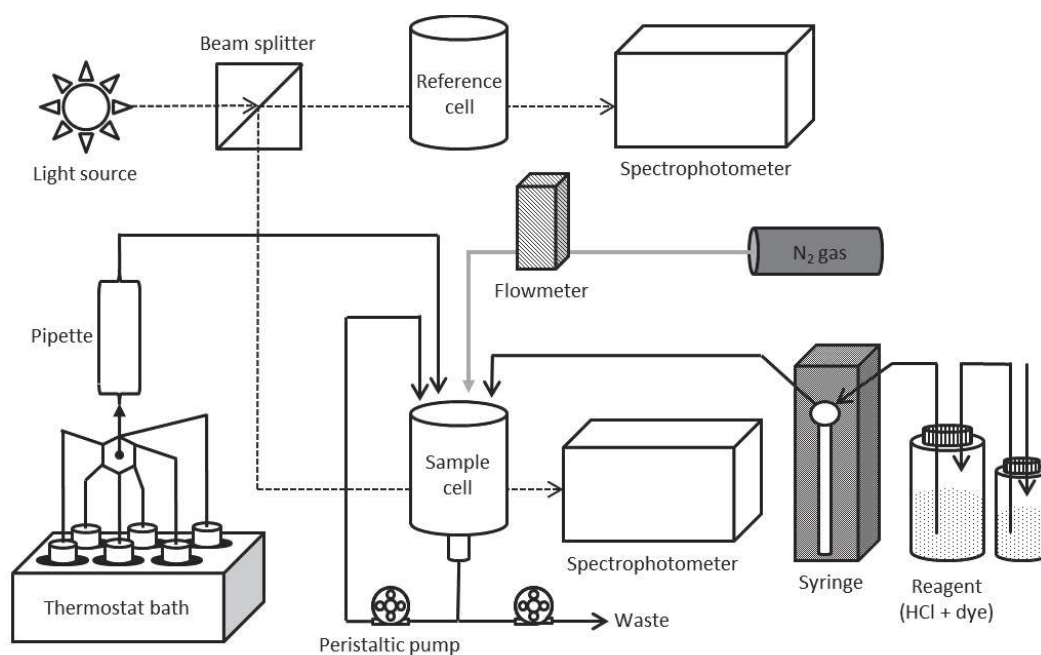


Figure 1 Schematic diagram of an apparatus to determine total alkalinity in sea water.

4-2 Transferring sea water sample

Volumetric pipette ($\sim 50 \text{ cm}^3$) is used to transfer sea water sample from a sample bottle into an optical cell (or beaker). In Figure 1, water-jacketed volumetric pipette with stopcocks at both ends are used to keep the sample temperature unchanged during the transfer. The pipette needs to be calibrated prior to use. In order to obtain the highest quality results with repeatability of total alkalinity analysis at around

$\pm 1 \mu\text{mol kg}^{-1}$, it is necessary to measure the temperature of the sea water sample within the uncertainty of $\pm 0.1^\circ\text{C}$.

4-3 Beaker or optical cell

Hydrochloric acid and indicator dye (it is convenient to use their mixed solution) are added to a sea water sample in a beaker or in an optical cell. It is then stirred and stripped of CO_2 with a stream of N_2 gas.

4-4 Addition of hydrochloric acid and indicator dye solution

Hydrochloric acid (and indicator dye) is added to a sample seawater using a dispensing burette with its dispensing volume of 5 cm^3 at its maximum. In order to obtain the highest quality results, it is necessary to use a highly reproducible burette ($\pm 0.001 \text{ cm}^3$). Although such a burette is commercially available, its accuracy is typically not as good, and the burette system must be also calibrated prior to use. It is also recommended to keep the temperature of the acid unchanged.

The concentration of hydrochloric acid shifts as it is used and thereby the head space in the bottle increases. To minimize the change, the room air is introduced into the head space of the bottle after it flows through the same hydrochloric acid stored in another bottle.

4-5 Aeration of acidified sea water sample

Cylinder of N_2 gas mounted with pressure regulator and a flowmeter to indicate gas flow rate (ca. $200 \text{ cm}^3 \text{ min}^{-1}$) is used to remove CO_2 from the acidified sea water sample.

4-6 Spectrophotometer and optical cell

Absorbances of the acidified seawater in an optical cell and deionized water in a reference cell are measured at wavelengths of 444nm, 616nm and 750nm with a spectrophotometer. For a better repeatability of the spectrophotometric measurements, it is necessary to use an optical cell of long path-length (8 cm or 10 cm). It is also required to control the temperature of the sample sea water in an optical cell by circulating the temperature-controlled water in the cell-holder, and measure the temperature of the sample at the time of spectrophotometric measurement by putting the temperature probe in the optical cell in the position where the probe does not disturb the light path.

4-7 Thermostat bath

Thermostat bath is mounted with a circulation pump and capable of maintaining temperature at $25.0 \pm 0.1^\circ\text{C}$. This is used to control the temperature of a sea water sample transferred for measurement and that in an optical cell.

4-8 Thermometer

Calibrated thermometer is readable to 0.01°C . This is used to measure the solution temperature when transferring from sampling bottle and to provide the value of solution temperature in optical cell for use

in subsequent calculations.

5. Reagents/Supplies

5-1 Nitrogen gas

Stream of N₂ is supplied from a gas cylinder as described in 4-5 in order to remove CO₂ from the sea water sample that has been acidified with hydrochloric acid.

5-2 Deionized water

Beaker or optical cell is washed thoroughly with deionized water each time after the measurement is finished.

5-3 Mixed titrant-indicator dye solution

A mixed solution of titrant and indicator dye of concentration approximately 0.05 mol dm⁻³ in hydrochloric acid (0.05 mol dm⁻³), 0.65 mol dm⁻³ in sodium chloride, and 80 μmol dm⁻³ in bromocresol green is prepared in the following procedure.

5-3-1 Instruments

- Calibrated balance to weigh 200g to within 0.01 mg.
- Oven capable of drying reagents at 600°C.
- Thermostat bath capable of controlling 25.0± 0.1°C and deep enough to immerse a 3 dm³ volumetric flask to around its marked line.

5-3-2 Tools

- 1×3 dm³ borosilicate glass volumetric flask.
- 3×1 dm³ plastic screw-cap borosilicate glass bottle with Teflon-liner cap such as those of Schott Duran^R.
- 1×100 cm³ capacity porcelain crucible.
- Desiccator with silica gel to store the porcelain crucible.
- 1× a few cm³ capacity weighing bottle.
- 1×500 cm³ measuring cylinder.
- 1×300 cm³ capacity beaker.

5-3-3 Reagents

- High purity primary standard grade sodium chloride (>99.98%).
- Hydrochloric acid (0.5 mol dm⁻³).
- Bromocresol green sodium salt.

5-3-4 Procedures

In a day before:

- Put approximately 120g of sodium chloride in a porcelain crucible and dry it in an oven at 600°C for > 1 hour. Allow to cool it in a desiccator over silica gel and put it near the balance.
- Clean up and dry weighing bottle and beaker, and put them near the balance.

On the day of preparation:

- Weigh out 113.9180 g (1.95 mol) dried sodium chloride in a beaker.
- Weigh out 0.1818 g (240 μ mol) bromocresol green sodium salt in a weighing bottle.
- Pour 0.30 dm³ of 0.5 mol dm⁻³ hydrochloric acid (0.15 mol HCl) into measuring cylinder, and transfer it thoroughly into a volumetric flask by rinsing with deionized water.
- Using a funnel, transfer the weighed sodium chloride and bromocresol green to the volumetric flask. Rinse the beaker and weighing bottle into the flask to ensure quantitative transfer of the sodium chloride and bromocresol green salt into the flask.
- Pour approximately 1 dm³ of deionized water into volumetric flask, shake it gently and let the solutes dissolved.
- Once sodium chloride was dissolved, pour deionized water up to below the calibration mark and shake the flask again to ensure a consistent composition.
- Immerse the flask in the thermostat bath being controlled at 25.0 \pm 0.1°C, and allow the temperature of the mixed solution to reach an equilibrium value (> 20 minutes).
- Adjust the volume of solution contained in the flask to the calibration mark.
- Once it is closed, shake the flask gently to mix the solution.
- In case that the solution looks turbid because of the undissolved bromocresol green salts, filter out the undissolved salts.
- Fill 2 \times 1 dm³ screw-cap bottles with the solution. Store the surplus solution in another screw-cap bottle.

6. Procedures of the measurement

6-1 Outline

An analysis session, starting with clean up the burette, consists of the sequence of activities outlined in Table 1. At each stage of this procedure, compare the results obtained with the system's previous history to ensure that the method is performing according to prescribed specifications. Once the initial tests are complete, water samples can be analyzed.

Table 1. Recommended sequence of activities in an analysis session.

Activity
<ul style="list-style-type: none"> • Clean up the pipette and burette, and calibrate them. Clean up the optical cell. • Set the bottle of acid titrant and indicator dye mixed solution in place. Turn on the power of thermostat bath, spectrophotometer, and so on. Wait until their performances get stabilized. • Rinse the burette and tubings with the acid titrant and indicator dye mixed solution. • Analyze two “junk” sea water samples to condition the system. Check the performance of spectrophotometer and confirm no bubbles in acid titrant and indicator dye mixed solution in the burette and tubings. If any problems are found, resolve it and analyze “junk” sea water sample again. • Analyze sea water reference material. • Analyze sea water samples. • Analyze seawater reference material again. • Calibrate the burette. Clean up the optical cell.

6-2 Clean up the optical cell

It is critical to keep the optical cell always clean. If it gets stained, small bubbles tend to attach on the cell. They disturb precise spectrophotometric measurements and concurrently raise the baseline of absorbance. Optical cell is washed with brush and detergent but not with cleanser. Use of an ultrasonic cleaning machine is also recommended.

6-3 Clean up and calibrate pipette and burette

Volumetric pipette used to transfer sea water samples and volumetric burette used to deliver acid titrant to sea water sample in beaker or in optical cell are required to be kept clean and calibrated. Before and after a series of analysis, pre- and post-calibrations are required. In case that the apparatus is set on board a ship, their delivery volume should be confirmed by collecting several replicate samples that can be returned to the shore-based laboratory to be weighed. Deliver an aliquot of deionized water into a pre-weighed serum bottle using the volumetric pipette and burette. Seal the bottle and save it to be reweighed later (on return to shore).

The procedure has been described in Dickson, A.G., Sabine C. L., and Christian, J. R. (Eds.) 2007, “Guide to best practices for ocean CO₂ measurements. PICES Special Publication 3, 191 pp.”, chapter 4, SOP12 and SOP13 (http://cdiac.ornl.gov/oceans/Handbook_2007.html).

6-4 Analyze sea water reference material and sea water sample

6-4-1 Transfer sea water sample and measure absorbances of cell + sea water background

Transfer a sea water sample into the optical cell, and measure absorbances at 730 nm (baseline), at

610 nm (maximum absorbance wavelength of base form of indicator dye (I^{2-})), and at 444 nm (maximum absorbance wavelength of acid form of indicator dye (HI^-)). They are the background absorbances of the sea water sample.

6-4-2 Dispense acid titrant and indicator dye mixed solution to the sample sea water

Transfer a known amount of sea water sample to a beaker or optical cell using a volumetric pipette and measure the sample temperature. Dispense acid titrant and indicator dye to the sample. The volume of acid titrant to be delivered is presumed from the site and depth of sampling and the salinity of the sample so that the pH of sea water sample becomes in the range between 3.8 - 4.2 after acid titrant is added and the evolved CO_2 escapes from the solution. After dispensing the acid titrant and indicator dye to the sample, stir the sample and aerate it with a stream of N_2 .

6-4-3 Measure absorbances of cell + sea water + dye

Measure absorbance at the same three wavelengths as those measured in 6-4-1. The same optical cell as used to measure the background absorbances has to be used. Confirm that baseline absorbance at 730 nm agrees with that in cell + sea water background measurement within ± 0.01 . In case that the difference in the baseline exceeds 0.01, it is possible that small air bubbles attached on the cell and disturbed the spectrophotometric measurement, and the measurement should be done again after the cell is cleaned.

6-4-4 Clean up the cell

Clean up the optical cell each time after the absorbance of the acidified sea water sample was measured.

6-4-5 Remarks

Titrant acid in a screw-cap bottle should be replaced by another bottle of titrant acid when the head-space in the bottle exceeded half of the volume (500 cm^3) since the concentration of hydrochloric acid is prone to change as the head-space increases. Once the acid titrant was replaced, substitute the titrant that remains in the burette and tubings with the new one. It is also critical to ensure that there are no bubbles in the burette and tubings.

It is desirable to repeat the measurement three times by changing the amount of acid titrant dispensed to the sample at least for the reference material. In case that the measurements have been properly done within the pH range of 3.8 – 4.2, the values of total alkalinity calculated will agree well irrespective of the volume of acid titrant dispensed to the sea water sample.

6-5 Calculation of total alkalinity

6-5-1 Correction of absorbance

If the spectrophotometer that outputs the light intensity is used, users need to calculate absorbance A_λ from the light intensity at each of the three wavelengths for each measurement before and after delivering acid titrant and indicator dye.

$$A_{\lambda} = -\log_{10}\left(\frac{I}{I_0}\right) \quad (3)$$

In the next, subtract the absorbances measured before adding acid and dye from that after. The absorbance measured at a non-absorbing wavelength, *i.e.*, 730 nm, is used to monitor and correct for any baseline shift. This assumes that the magnitude of any observed baseline shift is identical across the visible spectrum. To do this, subtract the measured shift from the background - corrected absorbances at wavelengths 610 nm and 444 nm to obtain the final corrected absorbance value at each wavelength.

These final absorbance values, corrected for background absorbances and any observed baseline shifts, are used to calculate the absorbance ratio A_{616}/A_{444} that describes the extent of protonation of the dye.

6-5-2 Calculation of the pH of the sea water + acid + dye

The pH of the sea water + acid + dye in the cell is computed from

$$\text{pH} = \text{p}K_2 + \log_{10}\left(\frac{(A_{616}/A_{444})_{25} - \varepsilon_{616}(\text{HI}^-)/\varepsilon_{444}(\text{HI}^-)}{\varepsilon_{616}(\text{I}^{2-})/\varepsilon_{444}(\text{HI}^-) - (A_{616}/A_{444})_{25} \varepsilon_{444}(\text{I}^{2-})/\varepsilon_{444}(\text{HI}^-)}\right) \quad (4)$$

The equilibrium constant K_2 of the indicator dye bromocresol green at 25°C is a function of salinity and has been determined by careful laboratory measurements,

$$\text{p}K_2 = 4.2699 + (2.758 \times 10^{-3}) \cdot (35 - S) \quad (5)$$

where S denotes salinity of the sample. A_{616} and A_{444} represent final corrected absorbance values at 616 nm and 444 nm, respectively, and $(A_{616}/A_{444})_{25}$ represents A_{616}/A_{444} ratio at sample temperature of 25°C. $(A_{616}/A_{444})_{25}$ is calculated from Eq(6) using (A_{616}/A_{444}) and sample temperature t (in °C) in optical cell when the spectrophotometric measurement is made.

$$(A_{616}/A_{444})_{25} = (A_{616}/A_{444}) [1 + 0.00907 (25 - t)] \quad (6)$$

The various extinction coefficient terms ε used in Eq(4) correspond to values measured for the specified species at wavelengths 616 nm and 444 nm, respectively (Table 2).

Table 2. Extinction coefficient ratios for bromocresol green

$\varepsilon_{616}(\text{HI}^-) / \varepsilon_{444}(\text{HI}^-)$	0.00131
$\varepsilon_{616}(\text{I}^{2-}) / \varepsilon_{444}(\text{HI}^-)$	2.3148
$\varepsilon_{444}(\text{I}^{2-}) / \varepsilon_{444}(\text{HI}^-)$	0.1299

6-5-3 Calculation of total alkalinity

Total alkalinity in sea water sample is calculated from Eq(2). The density of sea water is calculated from salinity that has been measured separately and temperature of sea water sample when it is transferred from the sample bottle.

In case that the mercury chloride solution was added to the sample as a bactericide, further minor corrections may need to be made to compute the total alkalinity in the original sea water sample:

$$A_T = 1.0002 A_T' \quad (7)$$

1.0002 is the coefficient when mercury chloride solution is added to the sample at the solution to sample volume ratio of 0.02/100.

6-5-4 Confirmation of the procedure

- In case that the spectrophotometer outputs the light intensity, it is critical that the output at 444 nm and 616 nm before and after acid – dye addition to the sea water sample is within the range that the output changes linearly with the change in the light intensity.
- pH of sea water sample is within the range of 3.8 – 4.2 when the spectrophotometric measurements is made after acid is added and CO₂ is removed.
- Absorbance at 730nm before and after the addition of acid and dye to a sea water sample should agree within ± 0.01 .

If any of these conditions have not been satisfied, problems have to be found and resolved, and the measurement has to be done again for the same sample. In principle, increase in the headspace air in the sampling bottle will not effect on the value of total alkalinity in sea water sample. Therefore, measurement of total alkalinity in a single bottle can be repeated if enough sea water sample to transfer to beaker or optical cell by volumetric pipette remains in the bottle.

7. Analysis of reference material

It is necessary that concentration of hydrochloric acid used to determine total alkalinity as a titrant has been calibrated within the uncertainty of $\pm 0.02\%$. However, in case that such an accurate calibration is not possible on board a ship or in a laboratory on land, circumstances may force one to use the Certified Reference Material (CRM) for dissolved inorganic carbon and total alkalinity analyses provided by Dr. A. G. Dickson in Scripps Institute of Oceanography to determine the concentration of the hydrochloric acid.

7-1 Procedure

Determine total alkalinity of the CRM according to the procedure described in 6.4. In order to evaluate the uncertainty due to the non-linearity in the response of spectrophotometer and due to the error in the volume of acid dispensed from a burette and so on, measurements should be repeated three times while changing the volume of acid titrant dispensed to the sample but keeping its resultant pH fall within the range of 3.8 – 4.2.

7-2 Calculation of the concentration of hydrochloric acid

Calculate the concentration of hydrochloric acid in the titrant:

$$c_{\text{HCl}} = \frac{\{A_{\text{T}}^{\text{CRM}} \cdot V_{\text{CRM}} + [\text{H}^+]_{\text{T}} \cdot (V_{\text{CRM}} + V_{\text{HCl}})\} \cdot \rho_{\text{CRM}}}{V_{\text{HCl}} \cdot 10^6} \quad (8)$$

$A_{\text{T}}^{\text{CRM}}$ represents the certified value of total alkalinity in the CRM. V_{CRM} represents the volume of CRM used for the analysis. The same volumetric pipette as that used for the sea water sample should be used so that V_{CRM} and V_{SW} in Eq(2) become identical. ρ_{SW} is calculated from the salinity of the CRM that has been determined and the temperature of the CRM when it is transferred from the bottle using the volumetric pipette.

8. Example calculations

8-1 Determination of the concentration of hydrochloric acid in titrant using CRM

Certified value of total alkalinity in CRM $A_{\text{T}}^{\text{CRM}}$	2224.65 $\mu\text{mol kg}^{-1}$
Salinity of CRM	33.357
Volume of pipette V_{CRM}	42.7495 cm^3
Volume of acid titrant added to the sample	2.05 cm^3

Measured data:

Temperature and density of CRM	25.14 °C, 1.0221 g cm^{-3}
Temperature of the sample at the time of spectrophotometric measurement	25.32° C

Measured light intensity and absorbance:

Wavelength	Sea water		Dye + acid + sea water		Absorbance
	Sample	Reference	Sample	Reference	
444 nm	25827	21890	18305	21863	0.1490
616 nm	36417	38894	27596	38868	0.1202
730 nm	13883	12699	13816	12679	0.0014

Result

$$A_{616}/A_{414} = \frac{0.1202 - 0.0014}{0.1490 - 0.0014} = 0.8050$$

$$(A_{616}/A_{414})_{25} = 0.8026$$

$$\text{pH}_{\text{T}} = 3.8483$$

$$[\text{H}^+]_{\text{T}} = 141.8 \mu\text{mol kg}^{-1}$$

$$c_{\text{HCl}} = 0.050577 \text{ mol dm}^{-3}$$

8-2 Total alkalinity in sea water sample

Salinity of sea water sample	34.424
Volume of pipette V_{SW}	42.7495 cm ³
Concentration of hydrochloric acid c_{HCl}	0.050577 mol dm ⁻³
Volume of acid titrant added to the sample	2.15 cm ³

Measured data

Temperature and density of sea water sample	25.22 °C, 1.0228 g cm ⁻³
Temperature of the sample at the time of spectrophotometric measurement	25.73° C

Measured light intensity and absorbance:

Wavelength	Sea water		Dye + acid + sea water		Absorbance
	Sample	Reference	Sample	Reference	
444 nm	25876	21904	18460	21891	0.1464
616 nm	36542	38921	25615	38912	0.1542
730 nm	13936	12734	13873	12736	0.0020

Results

$$A_{616}/A_{414} = \frac{0.1542-0.0020}{0.1464-0.0020} = 1.0540$$

$$(A_{616}/A_{414})_{25} = 1.0470$$

$$\text{pH}_{\text{T}} = 3.9678$$

$$[\text{H}^+]_{\text{T}} = 107.7 \mu\text{mol kg}^{-1}$$

$$A_{\text{T}} = 2373.8 \mu\text{mol kg}^{-1}$$

9. Quality assurance**9-1 Quality of each titration data**

In order to assure the data quality of each sample, absorbance (light intensity), pH after adding acid to sample, and change in the baseline of spectrum (730nm) before and after the addition of acid and dye need to be controlled. Repeatability of analysis should be also evaluated by making replicate analyses by adding a constant volume and different volumes of acid titrant to the same sea water sample.

9-2 Analysis of reference material

A stable reference material should be analyzed regularly. Plot the results on a property control chart.

9-3 Duplicate analyses

A duplicate analysis should be made regularly on sea water sample and sea water reference material by adding a constant volume and different volumes of acid titrant. Plot the difference between each pair of analyses on a range control chart. The standard deviation expected is within 2 $\mu\text{mol kg}^{-1}$.

Reference

- Breland II, J. A. and R. H. Byrne, 1993. Spectrophotometric procedures for determination of sea water alkalinity using bromocresol green. *Deep-Sea Res. I*, 40, 629–641.
- Dickson, A.G. 1981. An exact definition of total alkalinity and a procedure for the estimation of alkalinity and total inorganic carbon from titration data. *Deep-Sea Res.* 28A: 609–623.
- Dickson, A.G., Afghan, J.D. and Anderson, G.C. 2003. Reference materials for oceanic CO₂ analysis: a method for the certification of total alkalinity. *Mar. Chem.* 80: 185–197.
- Yao, W., and Byrne, R. H. 1998. Simplified seawater alkalinity analysis - application to the potentiometric titration of the total alkalinity and carbonate content in sea water, *Deep-Sea Res. I*, 45: 1383-1392.

Acknowledgment

We have prepared this guideline by referring to and in a similar format to Dickson, A.G., Sabine, C.L. and Christian, J.R. (Eds.) 2007, “Guide to best practices for ocean CO₂ measurements”. PICES Special Publication 3, 191 pp.

pH

A Standard Operation Protocol of “Determination of the pH of sea water” is available from the following CDIAC web site:

http://cdiac.ornl.gov/ftp/oceans/Handbook_2007/sop06a.pdf

http://cdiac.ornl.gov/ftp/oceans/Handbook_2007/sop06b.pdf

http://cdiac.ornl.gov/oceans/Handbook_2007.html

This page left intentionally blank.

***p*CO₂**

A Standard Operation Protocol of “Determination of $p(\text{CO}_2)$ in air that is in equilibrium with a discrete sample of sea water” is available from the following CDIAC web site:

http://cdiac.ornl.gov/ftp/oceans/Handbook_2007/sop04.pdf

http://cdiac.ornl.gov/oceans/Handbook_2007.html

This page left intentionally blank.

Chlorofluorocarbons and sulfur hexafluoride

A standard method of “sampling and measurement of chlorofluorocarbon and sulfur hexafluoride in seawater” is available from the following GO-SHIP repeat hydrography manual web site:

https://www.go-ship.org/Manual/Bullister_Tanhua_CFCSF6.pdf

This page left intentionally blank.

Carbon isotopic ratios ($\Delta^{14}\text{C}$, $\delta^{13}\text{C}$) of dissolved inorganic carbon

Yuichiro KUMAMOTO (Japan Agency for Marine-Earth Science and Technology),

Takafumi ARAMAKI (National Institute for Environmental Studies)

1. Introduction

There are three isotopes of carbon, ^{12}C , ^{13}C , and ^{14}C in the environment and the abundance ratios of ^{13}C and ^{14}C to ^{12}C are about 10^{-2} and 10^{-12} , respectively. Both ^{12}C and ^{13}C are stable isotopes while ^{14}C is a radionuclide (radiocarbon) with a half-life of about 5730 years that is naturally derived from the reaction of atmospheric nitrogen and cosmic rays in the atmosphere. The $^{13}\text{C}/^{12}\text{C}$ and $^{14}\text{C}/^{12}\text{C}$ ratios vary due to the isotopic fractionation in the environment. Unlike the $^{13}\text{C}/^{12}\text{C}$ ratio, the $^{14}\text{C}/^{12}\text{C}$ ratio decreases with time due to the radioactive decay. In addition, the $^{13}\text{C}/^{12}\text{C}$ and $^{14}\text{C}/^{12}\text{C}$ ratios have been disturbed by the fossil fuel combustion and utilization of nuclear energy and weapons by humans, respectively. Thereby, the two isotopic ratios of dissolved inorganic carbon (DIC), which is the sum of carbonate ion, bicarbonate ion, and molecular carbon dioxide (CO_2), in seawater are useful indicators for studies on the gas exchange at sea surface, marine carbon cycle, and the ocean circulation.

The high-precision measurement of the stable carbon isotopic ratio, $^{13}\text{C}/^{12}\text{C}$ was achieved by a stable isotope ratio mass spectrometer (SIRMS) equipped with a dual-inlet device (McKinney et al., 1950). To measure the $^{13}\text{C}/^{12}\text{C}$ of DIC in seawater by a SIRMS, DIC in seawater is stripped as CO_2 gas. In recent years, continuous measurements of the $^{13}\text{C}/^{12}\text{C}$ of DIC in surface seawater using a SIRMS or cavity-ringdown spectrometer, which is equipped with a pretreatment device for CO_2 extraction and purification, have been reported (e.g. Oguma et al., 2012; Becker et al., 2012). Since the $^{14}\text{C}/^{12}\text{C}$ ratio varies with the two factors: the isotopic fractionation and radioactive decay, the correction for the isotopic fractionation using the $^{13}\text{C}/^{12}\text{C}$ ratio is necessary to estimate the effect of the radioactive decay on the $^{14}\text{C}/^{12}\text{C}$ ratio. Therefore, the two isotopic ratios of DIC are usually measured together. In this chapter, we describe analytical methods for the simultaneous measurements of the $^{13}\text{C}/^{12}\text{C}$ and $^{14}\text{C}/^{12}\text{C}$ ratios in CO_2 gas extracted from a seawater sample.

In the late 1940s, the natural ^{14}C derived from the cosmic rays was discovered and the radiocarbon dating for a time range of 10^3 to 10^4 years was proposed (Anderson et al., 1947; Libby et al., 1949). The ^{14}C has been measured by the analysis of its radioactivity, in which beta rays emitted by the radioactive decay of ^{14}C are measured using a gas proportional or liquid scintillation counting device. The measurement of ^{14}C of DIC in seawater samples started in the 1950's (e.g., Linick et al., 1978). In the early stage, observational data from deep layers were limited, because the radioactivity analysis of ^{14}C needs a few hundred liters of seawater. In the Geochemical Ocean Section Study (GEOSECS) conducted by oceanographers of the United

States in the 1970s, 250 L of seawater was collected at 18 layers from the surface to bottom at 125 stations using a large-volume water sampler. The DIC in the sample was stripped as CO₂ gas and absorbed in sodium hydroxide solution on board. After the conversion from the recovered CO₂ gas to acetylene gas in an onshore laboratory, radiocarbon in the gas sample was measured using gas proportional counters (Stuiver and Östlund 1980; Östlund and Stuiver, 1980; Stuiver and Östlund, 1983). In Japan, in addition to the acetylene method (Gamo and Horibe, 1983), radiocarbon has been measured by the liquid scintillation since the 1980s, in which benzene synthesized from acetylene is dissolved in organic solvent (Tsunogai et al., 1995).

The accelerator mass spectrometer (AMS) developed in the late 1970s (Muller, 1977; Purser, 1977) can measure ¹⁴C with a sample amount of 1/1000 or less as compared to that for the radioactivity measurement because ¹⁴C atoms are determined directly in the AMS method. As the smaller AMS with low acceleration voltage (2–3 MV) was newly developed in the early 1990s, the AMS has been widely used in the oceanography. In the World Ocean Circulation Experiment (WOCE) conducted in the world ocean in the 1990's, more than 15,000 of seawater samples (500 mL or less) were collected at 785 stations and ¹⁴C of DIC was measured by the AMS method (Key et al., 2004). Because the analytical sensitivity of the AMS method is high, it is possible to obtain a measurement result with an uncertainty of about 0.5% by the AMS measurement with a carbon content of 1 mg for 30 minutes. As a result, most of the ¹⁴C measurements are conducted using the AMS method these days.

A manual on the radiocarbon measurement by the AMS method, which was prepared for the WOCE, has been widely used (McNichol and Jones, 1992). The manual was revised in 2010 (McNichol et al., 2010), but there is no major change in it. In Japan, Aramaki (1999) reported methods for the seawater sample pretreatment and ¹⁴C measurement at the AMS facility of the Japan Atomic Energy Research Institute (the Japan Atomic Energy Agency since 2005). In these manuals, methods of water sampling on shipboard and sample pretreatment were mainly described, and there is not much description about the sample analysis using the AMS. In this chapter, we describe the water sampling, sample pretreatment, and analytical method along the order of the actual procedures, so that the readers can overview all the analytical procedures of the carbon isotopic ratios of DIC in the seawater sample. The definition and unit (2), sampling (3), sample pretreatment (4, 5), and analyses (6) are described in the following sections.

2. Definition and unit

2-1. $\delta^{13}C$

The difference in the ¹³C/¹²C ratio between the sample (R_{SA}) and standard material (R_{ST}) is expressed as a permillage ($\delta^{13}C$ [‰]).

$$\delta^{13}\text{C} = (R_{\text{SA}} / R_{\text{ST}} - 1) \times 1000 \quad (1)$$

Belemnites fossils from the Pee Dee Formation in North Carolina, the USA (PDB), is the primary standard material of the $^{13}\text{C}/^{12}\text{C}$ ratio. $\delta^{13}\text{C}$ should be written as $\delta^{13}\text{C}_{\text{PDB}}$ precisely. However, the demand for the PDB exhausted the supply and secondary standards calibrated to the PDB are distributed by the International Atomic Energy Agency (IAEA) in Vienna, Austria. The value of $\delta^{13}\text{C}$ relative to the secondary standard (Vienna PDB) is expressed as $\delta^{13}\text{C}_{\text{VPDB}}$.

2-2. $\Delta^{14}\text{C}$

As with the $^{13}\text{C}/^{12}\text{C}$ ratio, the difference in the $^{14}\text{C}/^{12}\text{C}$ ratio between the sample (A_{SA}) and standard material (A_{ST}) is expressed as a permillage ($\delta^{14}\text{C}$ [‰]).

$$\delta^{14}\text{C} = (A_{\text{SA}} / A_{\text{ST}} - 1) \times 1000 \quad (2)$$

The primary standard material of the $^{14}\text{C}/^{12}\text{C}$ ratio is wood in the 19th century (AD 1890), whose $^{14}\text{C}/^{12}\text{C}$ ratio was not disturbed by human activities. However, it is practically impossible to obtain such wood. Therefore, oxalic acid supplied by the National Institute of Standards and Technology (NIST), SRM 4990 (Oxalic Acid I) and SRM 4990C (Oxalic Acid II) have been widely used as the standard materials. The measured $^{14}\text{C}/^{12}\text{C}$ ratio of the oxalic acid (A_{OX}) is converted into that of the standard wood ($A_{\text{ON}} = A_{\text{ST}}$) in modern times by the following approximate expression (Karlén et al, 1966).

$$A_{\text{ON}} = 0.95 A_{\text{OX}} [1 - \{2 (19 + \delta^{13}\text{C}_{\text{PDB}}) / 1000\}] \quad (3)$$

where $\delta^{13}\text{C}_{\text{PDB}}$ is the $\delta^{13}\text{C}$ value of Oxalic Acid I. The equation 3 corrects the difference in the isotopic fractionation effect between the oxalic acid and wood, and indicates that the isotopic fractionation effect on the $^{14}\text{C}/^{12}\text{C}$ ratio is approximately twice that of the $^{13}\text{C}/^{12}\text{C}$ ratio. Strictly, the isotopic fractionation effect can be obtained by the following equation.

$$A_{\text{ON}} = 0.95 A_{\text{OX}} (1 - 19/1000)^2 / (1 + \delta^{13}\text{C}_{\text{PDB}}/1000)^2 \quad (4)$$

Because the $\delta^{13}\text{C}$ of Oxalic Acid I is -19.3 ‰, the difference in results from the equations 3 and 4 is negligibly small ($< 0.001\%$).

Oxalic Acid I is no longer commercially available at present. Thus, Oxalic Acid II is the current

standard material, whose $^{14}\text{C}/^{12}\text{C}$ ratio (A_{NOX}) is converted into that of the standard wood ($A_{\text{ON}} = A_{\text{ST}}$) in modern times by the following approximate expression (Stuiver, 1983).

$$A_{\text{ON}} = 0.7459 A_{\text{NOX}} [1 - \{2 (25 + \delta^{13}\text{C}_{\text{VPDB}}) / 1000\}] \quad (5)$$

where $\delta^{13}\text{C}_{\text{VPDB}}$ is the $\delta^{13}\text{C}$ value of Oxalic Acid II. The isotopic fractionation effect can be precisely calculated by the following equation. However, the difference in results from the equations 5 and 6 is negligibly small ($< 0.02\%$) because the $\delta^{13}\text{C}$ of Oxalic Acid II is -17.8% ,

$$A_{\text{ON}} = 0.7459 A_{\text{NOX}} (1 - 25/1000)^2 / (1 + \delta^{13}\text{C}_{\text{VPDB}}/1000)^2 \quad (6)$$

Because radiocarbon in the oxalic acid declines by the radioactive decay, the $^{14}\text{C}/^{12}\text{C}$ ratio of the standard material (A_{ON}) decreases with time. The A_{ON} decay-corrected to AD 1950 is called as the absolute $^{14}\text{C}/^{12}\text{C}$ ratio of the standard material (A_{ABS}) (Stuiver & Polach, 1977).

$$A_{\text{ABS}} = A_{\text{ON}} e^{\lambda(y - 1950)} \quad (7)$$

where y is the measurement year, and λ is the radioactive decay constant of ^{14}C ($1/8267 \text{ yr}^{-1}$). Finally, $\delta^{14}\text{C}$ is calculated by substituting A_{ABS} for A_{ST} in the equation 2.

$$\delta^{14}\text{C} = (A_{\text{SA}} / A_{\text{ABS}} - 1) \times 1000 \quad (8)$$

$\delta^{13}\text{C}$ of wood (the primary standard material) is about -25% . On the other hand, $\delta^{13}\text{C}$ of marine organic matter and DIC in seawater are about -15% and 0% , respectively. Therefore, $\delta^{14}\text{C}$ in samples with different $\delta^{13}\text{C}$ values cannot be compared directly. For geochemical samples including seawater, $\Delta^{14}\text{C}$ [‰] is used instead of $\delta^{14}\text{C}$.

$$\Delta^{14}\text{C} = (A_{\text{SN}} / A_{\text{ABS}} - 1) \times 1000 \quad (9)$$

where A_{SN} is the corrected A_{SA} (the $^{14}\text{C}/^{12}\text{C}$ ratio of the sample) using the $\delta^{13}\text{C}$ value of the sample ($\delta^{13}\text{C}_{\text{VPDB}}$) as follows.

$$A_{\text{SN}} = A_{\text{SA}} [1 - \{2 (25 + \delta^{13}\text{C}_{\text{VPDB}}) / 1000\}] \quad (10)$$

or

$$A_{\text{SN}} = A_{\text{SA}} (1 - 25/1000)^2 / (1 + \delta^{13}\text{C}_{\text{VPDB}}/1000)^2 \quad (11)$$

The equation 10 is the approximate expression of the equation 11, and the range of $\delta^{13}\text{C}_{\text{VPDB}}$ from -30‰ to 5‰ corresponds to the difference between them from 0.02% to -0.13% . The value of $\Delta^{14}\text{C}$ is identical to the $\delta^{14}\text{C}$ in the sample that would have the same $\delta^{13}\text{C}$ as that of wood (-25‰). The difference between $\delta^{14}\text{C}$ and $\Delta^{14}\text{C}$ of DIC is about 50‰ . In addition, if the sampling year (z) and the measurement year (y) are different, A_{SA} in the equation 8 for $\delta^{14}\text{C}$ and A_{SN} in the equation 9 for $\Delta^{14}\text{C}$ should be replaced by $A_{\text{SA}} \cdot e^{\lambda(y-z)}$ and $A_{\text{SN}} \cdot e^{\lambda(y-z)}$, respectively.

In the radiocarbon dating for archaeological samples, the A_{ABS} in the equations 8 and 9 is replaced by A_{ON} because the radioactive decay in the sample and standard cancel each other (Stuiver and Polach, 1977).

$$d^{14}\text{C} = (A_{\text{SA}} / A_{\text{ON}} - 1) \times 1000 \quad (12)$$

$$D^{14}\text{C} = (A_{\text{SN}} / A_{\text{ON}} - 1) \times 1000 \quad (13)$$

Although $d^{14}\text{C} [\text{‰}]$ and $D^{14}\text{C} [\text{‰}]$ are confusable with $\delta^{14}\text{C}$ and $\Delta^{14}\text{C}$, they should be distinguished strictly. The $A_{\text{SN}}/A_{\text{ON}}$ and $A_{\text{SN}}/A_{\text{ABS}}$ ratios in a percentage are called the percent modern carbon (pMC) and absolute pMC, respectively. The notation for the radiocarbon measurement described in this section follows those in Stuiver and Polach (1977), which has not been displaced yet by a new less-confused notation proposed by Mook and van der Plicht (1999).

3. Sampling

As stated in the section 1, the method for the simultaneous measurements of ^{13}C and ^{14}C of DIC in seawater is described. The sampling (3) and CO_2 gas stripping (4) are common to both of the measurements.

3-1. Apparatus and reagents

3-1-1. Sample bottle

To prevent contamination from atmospheric CO_2 gas, use a glass bottle of 250 ml (or 500 ml) nominal volume and a ground glass stopper with grease. The weights of carbon necessary for the ^{14}C and ^{13}C measurements are approximate 1 mg (= about 100 μmol) and 0.1 mg (= about 10 μmol), respectively. The required volume of the seawater sample is 100 ml because the DIC concentration in seawater is about $2000 \mu\text{mol} \cdot \text{L}^{-1}$. After use, wipe the grease on the bottle/stoppers with acetone, soak in alkaline detergent and 10% hydrochloric acid subsequently, and wash with pure water. Then bake them in an electric furnace at 450 °C overnight and let them cool. Finally, each bottle/stopper pair is numbered and weighed (tare measurement).

3-1-2. Grease

Apiezon greases L, M, N are recommended. Transfer grease into a plastic syringe with a 10 mL volume for easier handling.

3-1-3. Mercury chloride (II) saturated solution

Approximately 10 g of special-grade mercuric chloride (II) powder is added to about 100 mL of pure water in a plastic bottle and dissolved. Because the solubility of mercuric chloride (II) at room temperature is about 7 g/100 mL, the powder remains in the bottom of the bottle. The solution and waste with mercury chloride (II) must be handled with care because mercury chloride (II) is very toxic.

3-1-4. Pipettes

Prepare a micro pipette for dispensing 50 μ L of the saturated solution of mercuric chloride (II) into seawater samples. Another pipette with 10-mL volume is also necessary to pour off the seawater sample in the bottle for making a headspace (3-2-2).

3-2. Water sampling

3-2-1. Water drawing

The method of the seawater drawing from a water sampler into the sample bottle is in accordance with the sampling method for DIC analysis (Dickson et al., 2007). The seawater sample for the carbon isotopes measurement is usually drawn just after the seawater sampling for DIC.

3-2-2. Poisoning

The seawater sample in the bottle must be poisoned with mercuric chloride (II) as soon as possible to prevent the change in DIC concentration due to biological activity, which is called the "fixation" of the sample. Remove the stopper from the bottle and wipe off the seawater on the stopper using a piece of paper. Pour off the seawater in the bottle using the 10-ml pipette (3-1-4) and wipe off the seawater on the inside wall of the bottle neck. Then, 50 μ L of the saturated solution of mercuric chloride (II) is added to the seawater sample using the micro pipette (3-1-4). Apply an appropriate amount of the grease to the ground glass joint of the stopper, return it to the bottle, and twist it around while applying pressure to ensure that a good seal is made. If the amount of the grease is insufficient, the grease seal does not work while the excess amount of the grease could result in a drop of the grease into the bottle, which causes stains on an air bubbler (4-5). Fix

the stopper to the bottle tightly using a clip or rubber bands. Store the seawater sample in a cool and dark place until pretreatment.

4. Pretreatment I (CO₂ stripping)

To measure the carbon isotopic ratios of DIC, DIC should be stripped from the seawater sample as CO₂ gas. There are a few methods for the stripping. In the precipitation method (Drimmie et al., 1991), DIC is precipitated as strontium carbonate or barium carbonate and then CO₂ gas is recovered by soaking the precipitates into acid solution. In the headspace method (Ishii et al., 2000; Salata et al., 2000), CO₂ in a headspace in a closed bottle, which degassed from acidified seawater in the bottle, is recovered. In the bubbling method (McNichol and Jones, 1992), acid is added to the seawater sample to reduce the solubility of CO₂ and then the CO₂ is stripped from the seawater by bubbling of an inert gas such as pure N₂. The bubbling method is most popular among them for seawater samples (McNichol et al., 2010). In this section, we describe a bubbling method using a vacuum device for the stripping and purification of CO₂ gas currently conducted in the National Institute for Environmental Studies (NIES), in which all the procedures proceed manually. However, semi-automated devices have also been reported (Aramaki et al., 2000; Honda et al., 1999; McNichol and Jones, 1992).

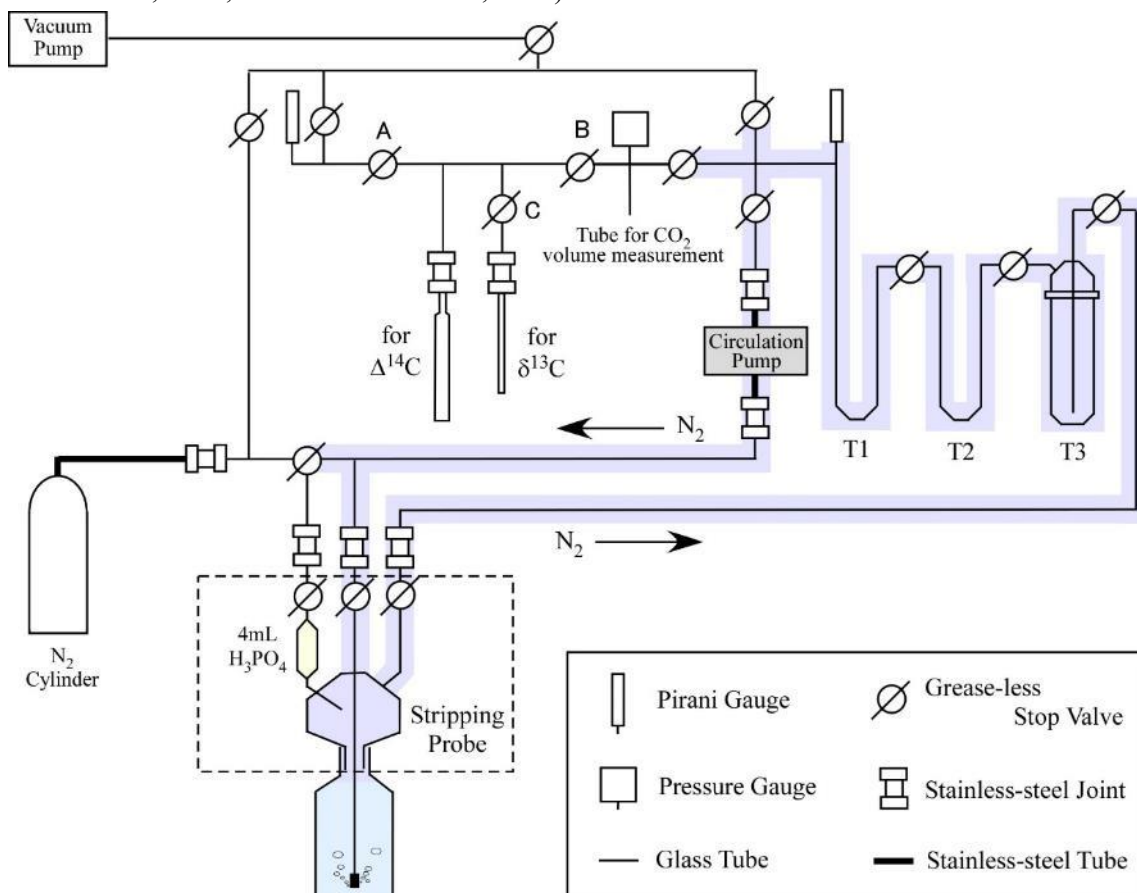


Fig. 1 A schematic view of the vacuum device for the CO₂ stripping.

4-1. Vacuum device for stripping

Fig. 1 is a schematic view of the vacuum device for the CO₂ stripping installed in NIES. Most of the parts of this vacuum device (< 0.1 Pa vacuum degree) is made of borosilicate glass except for some metal or resin parts (e.g. valves and joints). Because the borosilicate is easily-worked, it is possible to reduce uses of joints that may cause leakage. Grease-less stop valves are recommended for keeping low vacuum degree. In recent years, the vacuum device composed by stainless steel pipes and joints are also used widely.

4-2. Stripping probe

Weigh the seawater sample bottle and calculate the weight of the seawater sample by subtracting the tare weight (3-1-1) from the bottle weight. A stripping probe (Fig. 2) is placed on the seawater sample bottle in a N₂-filled glove bag or box. Prior to that, 4 mL of 85% phosphoric acid (H₃PO₄) solution is set in the stripping probe. After confirming that the three vacuum valves of the probe are closed, the sample bottle + stripping probe is connected to the vacuum device using a joint (Fig. 1).

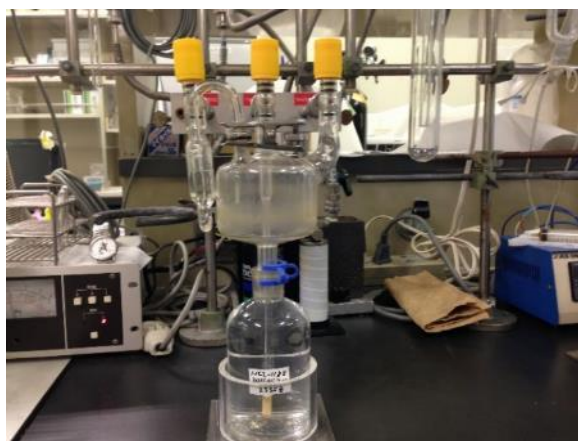


Fig. 2 The sample bottle + the stripping probe.

4-3. Nitrogen gas filling

The air in the vacuum device is exhausted and then filled with pure N₂ gas (>99.9999%) to a pressure of about 1.2 atm using a pressure gauge. The N₂ gas in the circulation flow path (a shaded area in Fig. 1) is isolated by closing the valves. The three vacuum valves of the stripping probe remain closed.

4-4. Injection of phosphoric acid

Open the vacuum valve of the stripping probe above the phosphoric acid solution, and the solution is poured into the sample bottle by the pressure difference between the vacuum device (1.2 atm) and sample bottle (1 atm). pH of the seawater sample drops and the DIC in the sample changes to gaseous CO₂.

4-5. Stripping

After the phosphoric acid solution is dropped into the sample bottle, close the vacuum valve for the acid solution and open the two others of the stripping probe, and turn on the circulation pump. The N₂ gas in the circulation flow path starts to circulate, and air bubbles are released from the bubbler inserted in the sample bottle (Fig. 1). The flow rate of the N₂ circulation is 0.5 to 1.0 liter/min. It takes about 10 minutes for the CO₂ stripping from 250 ml of the seawater sample. Prior to the sample stripping, it is necessary to estimate the proper flow rate and time to obtain more than 95% of CO₂ recovery (4-6). During the recirculation of the N₂ gas, the cold traps for CO₂ (T1 and T2) and water (T3) should be cooled to -196°C by liquid nitrogen and -72°C by ice slush of dry ice/ethanol, respectively. After the stripping is complete, turn off the circulation pump, isolate the water trap (T3) and the stripping probe/sample bottle by closing the valves, and then exhaust the N₂ gas in the vacuum device using the vacuum pump.

4-6. Recovery

The extracted CO₂ in the traps T1 and T2 is purified by changing the cryogen from the liquid nitrogen to the ice slush. Then only the gaseous CO₂ is transferred to the tube for CO₂ volume measurement (cold finger) just under the pressure gauge (Fig. 1) using liquid nitrogen. The volume of the section with the cold finger and pressure gauge isolated by the two valves must be measured in advance, using a tube with a grease-less valve whose inner volume is determined by a gravimetric calibration using mercury or water. Then, remove the liquid nitrogen from the cold finger and measured the pressure of the CO₂ gas filled in the isolated section at room temperature using the pressure gauge. The amount (mol) of the CO₂ recovered is calculated by the pressure, the room temperature, and the volume of the isolated section with the cold finger. Meanwhile, the amount of CO₂ (mol) contained in the seawater sample is calculated from the DIC concentration and the weight of the seawater sample (4-2). Then, calculate the recovery rate from the amounts of CO₂ recovered from and contained in the seawater. To prevent the isotopic fractionation effect during the CO₂ stripping, this recovery rate should be larger than 95% (McNichol and Jones, 1992).

4-7. Storage

The recovered CO₂ gas is split into two subsamples as follows. The CO₂ gas is transferred to the glass tube for ¹⁴C from the isolated section with the cold finger using liquid nitrogen and close the valves A and B (the valve C remains open) (Fig. 1). Then the liquid nitrogen is removed, and the CO₂ gas spreads in the small section isolated by the valves A and B. After a brief interval for the CO₂ gas diffusion, the valve C is closed. Then, the CO₂ gas below the valve C is condensed

cryogenically and sealed in the glass tube for ^{13}C using a gas torch. Meanwhile, the CO_2 gas that remains in the section isolated by the valves A, B, and C is also condensed and sealed in the glass tube for ^{14}C . If the interval for the CO_2 gas diffusion is insufficient, the isotopic fractionation between the CO_2 gas for ^{14}C and ^{13}C may occur. In the NIES vacuum device (Fig. 1), the interval time for the gas diffusion was empirically estimated to be more than 5 minutes. It is necessary to estimate the proper interval time in advance for each vacuum device. The split ratio of the CO_2 gases for ^{14}C and ^{13}C is about 4:1 in the NIES vacuum device, suggesting that the amount of the CO_2 gases for ^{14}C and ^{13}C are about 400 and 100 μmol , respectively. The CO_2 gas sealed in the glass tubes are semi-permanently stable. The CO_2 gases for ^{14}C and ^{13}C are converted to graphite powder for the AMS measurement (5) and analyzed by the SIRMS (6-1), respectively.

5. Pretreatment II (graphitization)

To measure radiocarbon using the AMS, the CO_2 gas extracted from the seawater sample has to be reduced to solid carbon. A few methods for the CO_2 reduction were proposed. CO_2 gas can be reduced to amorphous carbon using magnesium (Yoshikawa et al., 1987). The amorphous carbon, however, has no electric conductivity that is required for the AMS measurement. CO_2 gas can also be reduced to graphite carbon, which has electric conductivity unlike amorphous carbon, using metallic lithium and electrodeposits (Gurfinkel, 1987) or iron powder and hydrogen gas

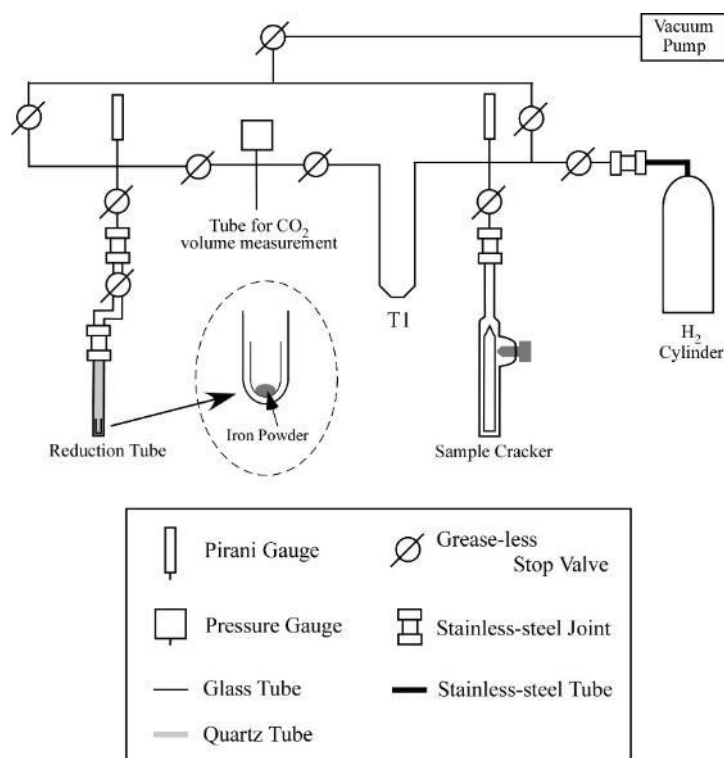


Fig. 3 A schematic view of the vacuum device for the graphitization.

(Vogel et al., 1984). The graphitization with hydrogen is the simplest and yields the highest recovery rate among the three methods. In this section, we describe a graphitization method currently conducted in NIES, which was modified by Kitagawa et al. (1993).

5-1. Vacuum device for graphitization

Fig. 3 is a schematic view of the vacuum device for the graphitization of CO₂ gas in NIES. As with the vacuum device for the CO₂ stripping (4), most of the parts of this device are made of borosilicate glass.

5-2. Iron powder (catalyst)

Prepare pure iron powder used as a catalyst for the CO₂ reduction reaction. The particle size should be as fine as possible, and we use that with a particle size of 10 μm or less. The iron powder commercially available may be contaminated with organic matter or oxidized slightly. Therefore, it is recommended that the iron powder is heated at 650 °C for 1 hour with hydrogen gas before use to decompose the organic matter and reduce the iron oxide. The procedures of this pre-heating of the iron powder are in accordance with those in the sections 5-5 and 5-6 without the sample CO₂ gas.

5-3. Graphite reactor

The weight of the iron powder (mg) should be equal to that of the graphite powder produced from the CO₂ gas (Kitagawa et al., 1993). When the graphite powder is less than 1 mg, the recovery rate of graphite is improved by doubling the amount of the iron powder. Measure the tare weight of a small quartz tube with a length of about 2 cm and an outer diameter of 6 mm (4 mm inner diameter) and weigh the iron powder in the quartz tube. Transfer the small quartz tube with the iron powder gently into a quartz tube with a length of about 20 cm and an outer diameter of 9 mm (“reduction tube” in Fig. 3). Quartz is available in an electric furnace at 650 °C (5-6). The reduction tube is attached to a tube with a grease-less valve, which is called the graphite reactor (Fig. 4). The approximate inner volume of the graphite reactor must be estimated in advance for the determination of H₂ pressure injected into the reactor (5-5). Then the graphite



Fig. 4 The graphite reactor.

reactor is connected to the vacuum device using a joint and the air in it is exhausted using the vacuum pump.

5-4. Transfer of CO₂ gas

The glass tube in which the sample CO₂ gas for ¹⁴C measurement is sealed (4-7) is set in a glass-tube cracker, or a sample cracker (Fig. 5). Then the sample cracker with the sample glass tube is connected to the vacuum device using a joint and the air in it is exhausted. The glass tube is broken by screwing a rod attached to the cracker (Fig. 5) and the sample CO₂ gas is transferred into the vacuum device and condensed in the T1 trap (Fig. 3) cooled to –196 °C using liquid nitrogen. The condensed CO₂ in the T1 trap is purified by changing the cryogen from liquid nitrogen to the dry ice/ethanol slush. Then only the gaseous CO₂ is transferred to the tube for CO₂ volume measurement (cold finger) just under the pressure gauge (Fig. 3) using liquid nitrogen. As with the vacuum device for the CO₂ stripping (4-6), the volume of the small section with the cold finger and pressure gauge isolated by the two valves must be measured in advance. Remove liquid nitrogen from the cold finger and measured the pressure of the CO₂ gas



Fig. 5 The sample cracker..

filled in the isolated section at room temperature using the pressure gauge. The CO₂ amount (mol) is calculated from the pressure, the room temperature, and the volume of the isolated section.

5-5. Injection of hydrogen gas

Graphite powder (C) is generated from CO₂ gas and hydrogen (H₂).



To reduce the CO₂ gas to the graphite powder completely, the amount (mol) of the hydrogen gas should be the double of that of the sample CO₂ gas, which is calculated from the inner volume of the graphite reactor (5-3) and H₂ pressure in it. The recovery rate of the graphite powder is improved by using 2.1–2.2 times the amount of the hydrogen gas (Kitagawa et al., 1993). After condensation of the CO₂ gas in the graphite reactor using liquid nitrogen, pure H₂ gas (>99.9999%) is injected into the vacuum device. Although the graphite reactor is cooled to

–196 °C to retain the sample CO₂ in it, the injected H₂ gas is not trapped in the graphite reactor. Adjust the pressure of the H₂ gas using the pressure gauge. Close the valve of the graphite reactor and remove liquid nitrogen from it. The inner volume of the graphite reactor should be determined by the total pressure of the sample CO₂ and H₂ in it at room temperature. If the total pressure is higher than 1.5 atm, the sealing of the graphite reactor may be broken.

5-6. Graphitization

Remove the graphite reactor from the vacuum device and insert the quartz tube of the graphite reactor into a hole (about 10 mm diameter) of an electric furnace heated at 650 °C for about 6 to 12 hours to reduce the sample CO₂ gas to the graphite powder on the iron powder. Water droplets derived from the reduction reaction (the equation 14) appear on the inner wall of the L-shaped part of the graphite reactor (Fig. 4). A cooling of the L-shaped part using a Peltier cooler or another cryogen facilitates the reaction (Aramaki, 1999). The L-shape part prevents a back slip of the water droplets into the quartz tube after the cease of the heating.

5-7. Weighing of graphite

Weigh the small quartz tube with the recovered graphite and iron powder. Calculate the weight of the graphite by subtracting the weight of the quartz tube and the iron (5-3) from the total weight. The graphitization recovery is estimated from the amounts of the graphite and the CO₂ used for the graphitization (5-4) and ranges normally between 70% and 90%. When the recovery is less than 60%, the isotope fractionation may occur in the process of the graphitization (Kitagawa et al., 1993).

6. Analyses

6-1. $\delta^{13}\text{C}$

6-1-1. Standard gas

Prepare the CO₂ gas with a known $\delta^{13}\text{C}$ value, namely the standard gas to measure $\delta^{13}\text{C}$ using the dual inlet SIRMS. The standard substance of calcium carbonate supplied by IAEA (2-1). The method for the recovering CO₂ gas from the standard calcium carbonate was described by Verkouteren and Klinedinst (2004). Otherwise, the commercial products of the standard CO₂ gas with a known $\delta^{13}\text{C}_{\text{VPDB}}$ value are available (e.g., Oztech Trading Corporation).

6-1-2. Injection of sample gas

Connect a container containing the standard CO₂ gas to the standard inlet of the SIRMS. Meanwhile, the glass-tube cracker (5-4) with the sample glass tube for ¹³C measurement (4-7) is connected to the sample inlet, which allows injecting the sample CO₂ gas into the SIRMS. An automatic sample cracker for the sample glass tube is equipped with the SIRMS as an option. When you use the manual tube cracker for the injection of the sample CO₂, it is necessary to take sufficient time for the gas diffusion so as not to cause the isotopic fractionation.

6-1-3. $\delta^{13}\text{C}$ determination and uncertainty

The sample and standard CO₂ gases are measured sequentially several times automatically by a computer program. The $\delta^{13}\text{C}$ value of the standard CO₂ gas should be input into the program in advance. The program outputs an average $\delta^{13}\text{C}$ value and its standard deviation for the several repeat measurements. This standard deviation, however, indicates only the uncertainty of the repeat measurement of the same sample gas. The standard deviation in the replicate measurement of the same seawater sample is estimated to be about 0.03 ‰ (McNichol et al., 2010), which includes the uncertainty derived from not only the SIRMS analysis but also the sampling and sample pretreatment.

6-2. $\Delta^{14}\text{C}$

The AMS consists of the ion source, accelerator, mass spectrometry systems, electromagnets, and detectors (Fig. 6). There are several models of the AMS. Here, we describe the AMS system

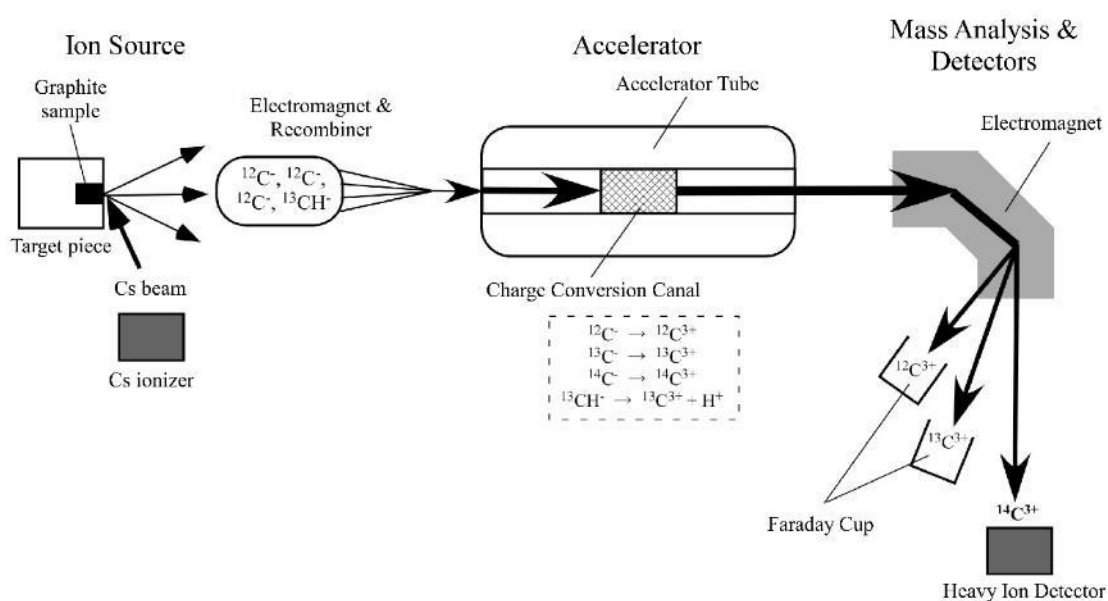


Fig. 6 A schematic view of the tandem tandem accelerator.

manufactured by High Voltage Engineering Europe, Netherlands, called the tandetron tandem accelerator. This model has been installed at Nagoya University and Japan Atomic Energy Agency in Japan.

6-2-1. Standard

As with the ^{13}C measurement by the SIRMS, the AMS measures ^{14}C in the sample and standard sequentially. Procedures of a combustion method for the graphitization of the NIST Oxalic Acid II (2-2) are as follows. Pack about 5 mg of the oxalic acid, which corresponds to about 1 mg of graphite, and about 1 g of copper oxide into a borosilicate glass tube with a length of about 7 cm and an outer diameter of 6 mm (4 mm inner diameter). Then insert it in a borosilicate glass tube with a length of about 30 cm and an outer diameter of 9 mm (7 mm inner diameter) together with about 0.5 g of reduced copper and about 1 mg of a silver piece. Silver prevents generation of interfering gas during the combustion. After the exhausting of the air in the glass tube using a vacuum pump, seal the upper part of the glass tube with a gas torch. The sealing can be conducted using the vacuum device for the stripping or graphitization. Heat the sealed tube in an electric furnace at 550 °C for 8 hours. The metallic luster of the reduced copper in the glass tube is the indicator for the successful combustion of the oxalic acid. After cooling the glass tube to room temperature, purify and graphitize the CO_2 gas in the tube according to the procedures in the section 5. The graphitization of the standard CO_2 gas must be conducted using the same vacuum device as that for the sample CO_2 graphitization. For the quality control of the AMS results, it is recommended to measure the reference materials supplied by IAEA (e.g., IAEA-C7 Oxalic Acid, pMC = 49.53%) together with the sample and standard graphite powders. In addition, results of the standard graphite newly prepared should be compared with those prepared in previous measurements. Please refer other reports (e.g., Tuniz et al., 1998; Nakamura, 2003) for further details on the quality control of the AMS measurement.

6-2-2. Target press

The sample/standard graphite should be measured by the AMS as soon as possible or stored in a desiccator to prevent reaction between the atmospheric oxygen/moisture and the iron catalyst. To measure radiocarbon in the graphite powder using the AMS, it is loaded into an aluminum sample holder or a target piece under high pressure, which is called the target press. Each AMS facility decides the press pressure for the target press empirically. You must avoid cross contamination during the target press.

6-2-3. Ion beam

The cesium-sputter negative-ion source is generally used to extract a carbon beam from the graphite sample. The aluminum target with the graphite sample is installed in the ion source device and negative ions of carbon ($^{12}\text{C}^-$, $^{13}\text{C}^-$, $^{14}\text{C}^-$, $^{13}\text{CH}^-$, etc.) are extracted from the graphite sample in the target by sputtering of cesium ions from the cesium ionizer. The negative-ion source has an advantage that negative ions of nitrogen, which are the major interfering ions in the AMS radiocarbon measurement, are hardly formed while the negative ions of carbon are easily generated because of its positive electron affinity. The negative ions are separated according to their mass by the electromagnet and interfering ions are rejected from the three ion beams of atomic/molecular weight 12, 13, and 14. Then the three ion beams are converged into one by the recombiner and injected into the accelerator.

6-2-4. Tandem acceleration

The combined ion beam injected into the accelerator is accelerated toward the high voltage terminal charged positively in the center of the accelerator tube, where the negative ions are converted into positive monoatomic ions ($^{12}\text{C}^{3+}$, $^{13}\text{C}^{3+}$, and $^{14}\text{C}^{3+}$) because its electrons are stripped. In addition, the molecular ions are destroyed by argon gas in the charge conversion canal. Then the positive monoatomic ions are accelerated again in the latter half of the accelerator. The "tandem" accelerator comes from this two-step acceleration.

6-2-5. Detectors

The positive ions ejected from the accelerator are separated by the other electromagnet again according to their mass. The ion beams of ^{12}C and ^{13}C are measured by the Faraday cups, which capture charged ions in vacuum. The ^{14}C atoms are counted by the heavy ion detector. The detection efficiency of ^{14}C by the AMS method is about 1%. The $^{14}\text{C}/^{12}\text{C}$ and $^{13}\text{C}/^{12}\text{C}$ ratios can be obtained from those outputs

6-2-6. $\Delta^{14}\text{C}$ calculation and uncertainty

The method for the $\Delta^{14}\text{C}$ calculation from the $^{14}\text{C}/^{12}\text{C}$ and $^{13}\text{C}/^{12}\text{C}$ ratios was explained in the section 2-2. If a precise $^{13}\text{C}/^{12}\text{C}$ ratio can be obtained by the AMS method, it should be used in the $\Delta^{14}\text{C}$ calculation instead of that measured by the SIRMS (6-1), because the isotopic fractionation effect in the graphitization and AMS measurement can be corrected (Nakamura, 2003). The method of the $\delta^{13}\text{C}$ measurement should be reported with the $\Delta^{14}\text{C}$ data. The standard deviation derived from the replicate measurement of the same seawater sample is about 5 ‰

(Aramaki et al., 2010; Kumamoto et al, 2013; McNichol et al., 2010). This uncertainty includes those derived from the sampling, stripping, graphitization, and AMS measurement, but probably not those from the preparation and measurement of the oxalic acid standard. The contaminations of radiocarbon in the AMS measurement and graphitization are evaluated by the AMS measurement results of the iron powder (5-2) and ^{14}C -free reference material (IAEA-C1 Carbonate, pMC = 0.00%), respectively. On the other hand, it is difficult to estimate that in the CO_2 stripping because the preparation of ^{14}C -free seawater is not easy.

References

- Anderson, E. C., W. F. Libby, S. Weinhouse, A. R. Reid, A. D. Kirshenbaum, and A. V. Grosse (1947): Radiocarbon from cosmic radiation. *Science*, 105, 576–577.
- Aramaki, T. (1999): Chemical treatment method for AMS-measurement of radiocarbon in seawater samples. Japan Atomic Energy Research Institute Research 99-007, pp.22 (In Japanese with English abstract).
- Aramaki, T., T. Mizushima, Y. Mizutani, T. Yamamoto, O. Togawa, S. Kabuto, T. Kuji, A. Gott dang, M. Klein and D.J.W. Mous (2000): The AMS facility at the Japan Atomic Energy Research Institute (JAERI). *Nuclear Instruments and Methods in Physics Research*, B172, 18-23.
- Aramaki T, Y. Nojiri, H. Mukai, S. Kushibashi, M. Uchida, and Y. Shibata (2010): Preliminary results of radiocarbon monitoring in the surface waters of the North Pacific. *Nuclear Instruments and Methods in Physics Research B*, 268, 1222–1225.
- Becker, M., N. Andersen, B. Fiedler, P. Fietzek, A. Körtzinger, T. Steinhoff, and G. Friedrichs (2012): Using cavity ringdown spectroscopy for continuous monitoring of $\delta^{13}\text{C}(\text{CO}_2)$ and $f\text{CO}_2$ in the surface ocean. *Limnology and Oceanography: Methods*, 10, 752–766.
- Dickson, A. G., C. L. Sabine, and J. R. Christian (2007): Guide to best practices for ocean CO_2 measurements. PICES Special Publication 3, North Pacific Marine Science Organization, Sidney, pp. 191.
- Drimmie, R. J., R. Aravena, L. I. Wassenaar, P. Fritz, M. J. Hendry, G. Hut (1991): Radiocarbon and stable isotopes in water and dissolved constituents, Milk River aquifer, Alberta, Canada. *Applied Geochemistry*, 6, 381–392.
- Gamo, T. and Y. Horibe (1983): Abyssal circulation in the Japan Sea. *Journal of Oceanographical Society of Japan*, 39, 220–230.
- Gurfinkel, D. M. (1987): An assessment of laboratory contamination at the Isotracer Radiocarbon Facility. *Radiocarbon*, 29, 335-346.

- Honda, M., Y. Kumamoto, N. Harada, M. Kusakabe, M. Katagiri, K. Nakao, K. Hayashi, and N. Kisen (1999): Semi-automated samplepreparation system for ^{14}C measurement on seawater sample. JAMSTECR, 39, 1–16 (In Japanese with English abstract).
- Ishii, M., H.Y. Inoue, H. Matsueda (2000): Coulometric precise analysis of total inorganic carbon in seawater and measurements of radiocarbon for the carbon dioxide in the atmosphere and for the total inorganic carbon in seawater. Technical Reports of the Meteorological Research Institute, 40, pp.62 (In Japanese with English abstract).
- Karlén I., I. U. Olsson, P. Källberg, S. Killiççi (1966): Absolute determination of the activity of two ^{14}C dating standards. Arkiv for Geofysik, 6, 465–471.
- Key, R. M., A. Kozyr, C. L. Sabine, K. Lee, R. Wanninkhof, J. L. Bullister, R. A. Feely, F. J. Millero, C. Mordy, and T.-H. Peng (2004): A global ocean carbon climatology: Results from Global Data Analysis Project (GLODAP). Global Biogeochemical Cycles, 18, GB4031, doi:10.1029/2004GB002247.
- Kitagawa, H., T. Masuzawa, T. Nakamura, and E. Matsumoto (1993): A batch preparation method for graphite targets with low background for AMS ^{14}C measurements. Radiocarbon, 35, 295–300.
- Kumamoto, Y., A. Murata, T. Kawano, A. Watanabe, and M. Fukasawa (2013): Decadal changes in bomb-produced radiocarbon in the Pacific Ocean from the 1990s to 2000s. Radiocarbon, 55, 1641–1650.
- Libby, W. F., E. C. Anderson, and J. R. Arnold (1949): Age determination by radiocarbon content: world-wide assay of natural radiocarbon. Science, 109, 227–228.
- Linick, T. W. (1978): La Jolla measurements of radiocarbon in the oceans. Radiocarbon, 20, 333-359.
- Mckinney, C. R., J. M. McCrea, S. Epstein, H. A. Allen, and H. C. Urey (1950): Improvements in mass spectrometers for the measurement of small differences in isotopic abundance ratios. the Review of Scientific Instruments, 21, 724–730.
- McNichol, A. P. and G. A. Jones (1992): Measuring ^{14}C in seawater ΣCO_2 by accelerator mass spectrometry. In WOCE Operations Manual, Part 3.1.3 : WHP Operations and Methods, WHP Office Report WHPO 91-1, WOCE Report No. 68/91. Available online at: http://www.nodc.noaa.gov/woce/woce_v3/wocedata_1/whp/manuals.htm.
- McNichol, A. P., P. D. Quay, A. R. Gagnon, and J. R. Burton1 (2010): Collection and measurement of carbon isotopes in seawater DIC. edited by E. M. Hood, C. L. Sabine, and B. M. Sloyan, ICPO Publication Series Number 134. Available online at: <http://www.go-ship.org/HydroMan.html>.
- Mook., W. G. and J. van der Plicht (1999): Reporting ^{14}C activities and concentrations. Radiocarbon, 41, 227–239.
- Muller, R. A (1977): Radioisotope dating with a cyclotron. Science, 196, 489–494.
- Nakamura, T. (2003): High sensitivity measurements of environmental and tracer radioisotopes with Accelerator Mass Spectrometry. Radioisotopes, 52, 145–171 (in Japanese).

- Oguma, S., T. Ono, and T. Asumaya (2012): Measurements of carbon and oxygen stable isotope ($\delta^{13}\text{C}_{\text{DIC}}$ · $\delta^{18}\text{O}_{\text{H}_2\text{O}}$) of seawater using a GasBench II continuous-flow-through preparation system. *Journal of Fisheries Technology*, 4, 65–71 (in Japanese with English abstract).
- Östlund, G. H. and M. Stuiver (1980): GEOSECS Pacific radiocarbon. *Radiocarbon*, 22, 25-53.
- Purser, K.H. (1977): Ultra-sensitive spectrometer for making mass and elemental analyses. United States patent, 4037100.
- Salata, G. G., L. A. Roelke, L. A. Cifuentes (2000): A rapid and precise method for measuring stable carbon isotope ratios of dissolved inorganic carbon. *Marine Chemistry*, 69, 153–161.
- Stuiver, M. (1983): International agreements and the use of the new oxalic acid standard. *Radiocarbon*, 25, 793–795.
- Stuiver, M. and G. H. Östlund (1980): GEOSECS Atlantic radiocarbon. *Radiocarbon*, 22, 1–24.
- Stuiver, M. and G. H. Östlund (1983): GEOSECS Indian Ocean and Mediterranean. *Radiocarbon*, 25, 1–29.
- Stuiver, M. and H. A. Polach (1977): Discussion: Reporting of ^{14}C data. *Radiocarbon*, 19, 355–363.
- Tsunogai S., S. Watanabe, M. Honda, and T. Aramaki (1995): North Pacific Intermediate Water studied chiefly with radiocarbon. *Journal of Oceanography*, 51, 519–536.
- Tuniz, C., W. Kutschera, D. Fink, G. F. Herzog, J. R. Bird (1998): *Accelerator Mass Spectrometry: Ultrasensitive Analysis for Global Science* 1st Edition. CRC Press, Boca Raton, pp.400.
- Verkouteren, M. and D. B. Klinedinst (2004): Value assignment and uncertainty estimation of selected light stable isotope reference materials: RMs 8543-8545, RMs 8562-8564, and RM 8566. NIST Special Publication 260-149 2004 Edition, pp.56.
- Vogel, J. S., D. E. Nelson, and J. R. Southon (1984): Performance of catalytically condensed carbon for use in accelerator mass spectrometry. *Nuclear Instruments and Methods in Physics Research B*, 233, 289–293.
- Yoshikawa, H., K. Sato, K. Yoshida, K. Kobayashi, T. Miura, M. Imamura, Y. Homma, H. Nakahara, and T. Nozaki (1987): Contamination of modern carbon in sample preparation for measurement of carbon-14 by accelerator MS. *Bunseki Kagaku*, 36, 755–759 (in Japanese with English abstract).

This page left intentionally blank.

Dissolved organic carbon (DOC), nitrogen (DON), and phosphorus (DOP)

Hiroshi OGAWA (Atmosphere and Ocean Research Institute, the University of Tokyo)

The methods for measuring DOC, DON (total dissolved nitrogen: TDN) and DOP (total dissolved phosphorus: TDP) in seawater are published on the websites of several institutions and research projects.

- DOC-TDN sampling guide
Hansell Lab, Rosenstiel School of Marine and Atmospheric Science, University of Miami
http://margolab.com/pubs/Margolin_et_al_2015.pdf

- Determination of DOC-TDN
PICES Scientific Report34
http://www.jodc.go.jp/geotraces/docs/PICESReport34_DOC_DON.pdf

NASA Ocean Color Web Site
<https://oceancolor.gsfc.nasa.gov/fsg/instrumentreports/>

California Current Ecosystem LTER Program
<http://cce.lternet.edu/data/methods-manual/augmented-cruises/dissolved-organic-carbon-and-total-nitrogen>

HOT (Hawaii Ocean Time-series) Field Laboratory Protocols
<http://hahana.soest.hawaii.edu/hot/protocols/protocols.html#>

BATS (Bermuda Atlantic Time-series Study), Methods Chapter 16
<http://bats.bios.edu/wp-content/uploads/2017/07/chapter16.pdf>

- Consensus reference material (CRM) for DOC and TDN measurements
Hansell Lab, Rosenstiel School of Marine and Atmospheric Science, University of Miami
<https://hansell-lab.rsmas.miami.edu/consensus-reference-material/index.html>
- Determination of DOP
Book Chapter (provide for non-commercial research and educational use)
http://cmore.soest.hawaii.edu/summercourse/2015/documents/Karl_05-27/Karl-and-Bjorkman-2015.pdf

HOT (Hawaii Ocean Time-series) Field Laboratory Protocols
<http://hahana.soest.hawaii.edu/hot/protocols/protocols.html#>

This page left intentionally blank.

Particulate organic carbon (POC), particulate nitrogen (PN), and particulate phosphorus (PP)

○ Takeshi YOSHIMURA (Central Research Institute of Electric Power Industry)

1. Scope and field of application

This procedure describes methods for the sampling and the analysis of particulate organic carbon (POC), particulate nitrogen (PN), and particulate phosphorus (PP) in seawater samples. For analytical methods, the high temperature combustion (HTC) method with an elemental analyzer for POC and PN, and the HTC and acid hydrolysis (HTC-AH) method and persulfate oxidation (PO) method for PP are described. Descriptions for POC and PN are based on the JGOFS protocol (Knap et al., 1996). Since many analytical methods for POC, PN, and PP have been published in past studies, analysts should select an appropriate method and establish an in-house protocol for the method based on their own situation. The HTC method for nitrogen has been adopted as the standard method for organic nitrogen analysis in research fields in Japan (Murakami and Shirai, 2015), and thus new technologies and related insights for the HTC method that can be incorporated into seawater POC and PN analysis may be published in the near future.

2. Definition

POC, PN, and PP in seawater are defined as carbon, nitrogen, and phosphorus in mainly non-volatile organic suspended matter derived from filtering seawater onto a filter, and expressed as moles per volume or weight of seawater. POC and PN can be analyzed simultaneously in a filter sample, and PP is analyzed using another filter sample. Samples for POC and PN are acidified prior to analysis, thus particulate inorganic carbon (PIC) is eliminated and we can measure POC. For PN, however, the acidification procedure cannot eliminate particulate inorganic nitrogen (PIN), thus we analyze PN but not particulate organic nitrogen (PON). In principle, total particulate carbon (TPC) is measured if a non-acidified sample is analyzed, therefore PIC can be estimated as the difference between TPC and POC. For PP, samples are decomposed and the liberated phosphate is analyzed, therefore particulate inorganic phosphorus (PIP) and particulate organic phosphorus (POP) cannot be differentiated and thus PP is measured.

3. Principles of the Analysis

For POC and PN, samples are generally combusted at temperature higher than 900 °C with oxygen. If a tin cup is used for the sample container, the combustion temperature of the sample can reach higher than 1800 °C. The combustion gas flows through a combustion column eliminating halogens, and then through a reduction column reducing nitrogen oxides to N₂ gas and eliminating excess oxygen. N₂ and CO₂ gases are separated with gas-chromatography or gas-specific adsorptions, and then quantified with a thermal conductivity detector. Principles of POC and PN analysis by elemental analyzer are detailed in JSAP (2008).

For PP, samples are combusted at 500 °C and then hydrolyzed by acid in the HTC-AH method or

are decomposed in persulfate solution under high temperature and high pressure conditions in the PO method. Liberated phosphate is quantified colorimetrically using the molybdenum blue method. Detailed procedures for colorimetry analysis are practically described in Oku (2002).

4. Apparatus

Simultaneous analysis of POC and PN requires use of an elemental analyzer, which have been developed by various manufacturers. Various methods for combustion of the sample, separation of combustion gases, and detection of the target gas are adopted by each elemental analyzer. Currently available analyzers in Japan are reviewed in JSAP (2008).

For PP analysis, we need a hotplate, electric oven, heating device such as a hot water bath, and colorimeter for the HTC-AH method, and an autoclave and colorimeter for the PO method. For the colorimeter, a spectrophotometer for manual analysis or a nutrient autoanalyzer can be used.

5. Reagents

All reagents should be of an analytical reagent grade quality unless otherwise specified.

For POC and PN analyses, concentrated HCl for the removal of PIC and acetanilide (C_8H_9NO) for standards are required. Acetanilide is suitable as the standard for POC and PN because it has a C:N molar ratio of 8 that is a similar value to marine suspended particulate matter.

For PP analysis, sodium sulfate (Na_2SO_4), magnesium sulfate ($MgSO_4 \cdot 7H_2O$), and HCl in the HTC-AH method, and potassium persulfate ($K_2S_2O_8$) (for nitrogen and phosphorus analysis) in the PO method are required to decompose the samples. For liberated phosphate analysis, ammonium heptamolybdate tetrahydrate ($(NH_4)_6MoO_{24} \cdot 4H_2O$), L-ascorbic acid ($C_6H_8O_6$), potassium antimony tartrate ($K(SbO)C_4H_4O_6$), and potassium dihydrogen phosphate (KH_2PO_4) (superpure grade of Merck) for standards are required.

6. Sampling

If subsampling of seawater is not conducted immediately after the recovery of Niskin bottles, settling of large particles in the Niskin bottle will create a non-uniform distribution of the particles. Therefore, the Niskin bottle should be shaken before subsampling or the entire volume should be used as the sample. If needed, large zooplankton should be removed using a net e.g. by sieving through a 200 μm mesh plankton net.

Particles in seawater are collected on binder-free glass fiber filters such as Whatman 25 mm GF/F filter. For POC and PN sampling, the filters are pre-combusted at 450 $^{\circ}C$ for 5 hours to eliminate carbon and nitrogen contamination. For PP analysis, the pre-combusted filters are washed using an acid. For this, a 10 mL aliquot of 1 N HCl is poured onto the filter attached to a filter funnel and the HCl removed by vacuum, and then the filter is thoroughly washed using Milli-Q water. After filtering the seawater for PP, rinse the filter twice with 2 mL aliquots of 0.17 M Na_2SO_4 (Solórzano and Sharp, 1980). Filter samples for POC and PN, and PP are wrapped in pre-combusted (550 $^{\circ}C$, 5 h) aluminum foil and stored at a temperature lower than $-20^{\circ}C$. If the filter samples are stored in a plastic container, the samples may be contaminated by carbon (Sharp, 1974). If the samples are stored in a freezer with organic

solvents or biological samples, the samples may be contaminated by carbon and nitrogen.

It is important to take a significant quantity of filter blank samples. The filter blank sample is processed by an identical procedure to the sample except filtering Milli-Q water is carried out instead of the seawater sample.

7. Analytical procedures

7-1 POC and PN

Stored filter samples are dried and acidified prior to the analysis. Samples are dried in a drying oven at 60 °C or in a freeze-dryer. Then, the samples are placed in a desiccator saturated with HCl fumes for 24 h. The air in the desiccator is kept saturated by leaving concentrated HCl in an open container in the desiccator, which is placed under a fume hood. Thereafter, the filter samples are placed in a vacuum desiccator with granulated NaOH to dry and remove the HCl that has detrimental effects on the subsequent elemental analysis. To vacuum the desiccator, a water-circulating aspirator should be used since a vacuum pump is not resistant to corrosion by HCl. While the filter sample can be dried in open aluminum foil that was used to store the sample in freezer, the sample has to be acidified in an acid-resistant container. The sample may be contaminated by carbon if the filter sample is placed on a plastic container (Sharp, 1974), therefore a glass container is appropriate for the acidification procedure.

Carbon and nitrogen contents of the filter sample are analyzed with an elemental analyzer following the guidelines given by the manufacturer. Reagents for the combustion column and the reduction column are sieved to remove any fine powder prior to packing into the column. To lower blank values the reagents should be pre-combusted prior to packing if applicable to the reagent. Then the reagents are packed into the column appropriately with consideration for the design of a furnace (vertical or horizontal) and the internal pressure of the columns. The analyzer should run overnight to stabilize the baseline before sample analysis. If you use a brand-new column, it is important that equilibrium conditions for adsorption-desorption between reagents and the analyte gas are achieved by processing with standard samples at the maximum concentration of the working curve several times before the start of the analysis run. Empty tin cups are used as blanks to confirm the baseline stability of the analyzer. Prior to sample analysis, a five-point working curve and three filter blank samples are analyzed. A blank and standard sample with a predetermined concentration is measured every 5–10 samples to ensure that problems have not developed. Details of the preparation, analysis run, and maintenance of an analyzer are described in JSAP (2008).

7-2 PP

First, an example procedure of the HTC-AH method (Solórzano and Sharp, 1980) is described. A filter sample is placed in a glass vial with a screw cap. A two mL aliquot of 0.017 M MgSO₄ is poured into the vial, and the solution in the vial without the cap is dried on a hotplate. After combusting the sample in an electric oven at 500 °C for 2 h, the sample is treated in 0.2 M HCl in the vial with the cap at 80 °C for 30 min using a hot water bath. After cooling, the sample solution is filtered through a 0.22 µm pore size syringe filter. A four mL aliquot of the filtrate is added into a 50 mL volumetric flask and

make to 50 mL with Milli-Q water, and then the phosphate concentration is colorimetrically analyzed. It is important to confirm beforehand that the acid concentration of the sample solution does not inhibit color development of the molybdenum blue method. Although the sample solution may be neutralized with NaOH solution when the acid concentration is high enough to inhibit molybdenum blue color development, caution is required because excess addition of NaOH make the solution alkaline and then generates precipitation that adsorb and remove the phosphate from the sample solution. This may cause a serious underestimate or no detection of phosphate in the sample solution.

Second, an example procedure of the PO method is described. A filter sample is placed in potassium persulfate solution in an airtight container, and treated under high temperature and high pressure using an autoclave. After cooling, the sample solution is filtered through a 0.22 μm pore size syringe filter. Since a high concentration of potassium persulfate inhibits color development of molybdenum blue method, the concentration is reduced to less than 2 %. Finally the phosphate concentration is measured colorimetrically with the molybdenum blue method. Although the PO method of Parsons et al. (1984) or equivalent has been widely used, it has been reported that the PO method may underestimate the PP concentration compared to the HTC-AH method. However, Suzumura (2008) shows that an increase in potassium persulfate concentration of the previous PO method under 120 °C for 30 min conditions can generate the same PP concentration to the HTC-AH method. They conclude that the improved PO method is a simpler procedure and a less time-consuming method than the HTC-AH method.

Regardless of the PP decomposition method, liberated phosphate is colorimetrically quantified with the molybdenum blue method of Parsons et al. (1984) for a single solution method or Hansen and Koroleff (1999) for a double solution method. Since the color development of molybdenum blue can be inhibited due to the combination of the decomposition method and colorimetry method, prior examinations to confirm a normal color development are necessary. Similarly, a manual and an automated analysis can generate a different color development, so it is important that the phosphate concentration in the sample solution has to be calculated with a working curve using standards in the same matrix to the sample solution.

8. Factors for errors

POC, PN, and PP have to be analyzed to a high precision using a small amount of sample, and therefore factors leading to errors should be eliminated as much as possible. A tin cup for the POC and PN sample container should be washed with ethanol and acetone to reduce absolute values and variability of blanks. If any volume of air is contained in a sample container with a sample filter, nitrogen in the air also is detected with the nitrogen derived from the sample and thus a cause of contamination (1 μL of air is equivalent to 1 μg of nitrogen). Although the organic and inorganic carbon and nitrogen dissolved in an approximately 0.1 mL aliquot of the seawater that is retained on a GF/F filter as a residue of filtered seawater does not affect the carbon and nitrogen values derived from the sample itself (Sharp, 1974), it has not been determined whether adsorption of dissolved matter in the sample seawater to the GF/F filter through filtering the sample seawater has a significant impact on the sample analysis value. Karl et al. (1998) and Morán et al. (1999) reported that a significant amount of dissolved organic carbon (DOC) produced during an incubation for the measurement of primary production with ^{14}C method is

adsorbed onto a GF/F filter. Moran et al. (1999) reported that adsorption of DOC onto a GF/F filter is a cause of a 2–4 times higher value for several liters of filtered POC sample derived from a Niskin bottle than for several hundred liters filtered POC sample derived from an in situ pump. Wang et al. (2011) corrected their POC concentrations by subtracting 2 μmol of carbon from the detected value of a filter sample to cancel out the effect of DOC adsorption. Adsorption of dissolved matter onto a GF/F filter can also cause a positive error for nitrogen and phosphorus, but the extent to which nitrogen and phosphorus adsorb onto a filter has not been clarified.

Furthermore, the utilization of a reference material (RM) is recommended to manage the quality of analytical results and to establish comparability to the results reported by different analysts. For example, an in-house secondary standard (plankton sample) for POC and PN analysis and apple leaves (NIST 1515) for PP analysis are used as a check standard in the Hawaii Ocean Time-series Program (<http://hahana.soest.hawaii.edu/hot/methods/results.html>). In Japan, National Institute for Environmental Studies (NIES) distributes RMs for environment measurements (<http://www.nies.go.jp/labo/crm/index.html>). In their list, water hyacinth (*Eichhornia crassipes*) (NIES CRM No. 29) has a certified value for phosphorus and a reference value for carbon and nitrogen, and thus this can be used as a RM for POC, PN, and PP analysis. A dataset for carbon, nitrogen, and phosphorus in particulate organic matter in the global ocean has recently been established by Martiny et al. (2014), and it is expected that the dataset is utilized in a wide range of research including modeling studies. More high quality data derived through better sampling and analytical protocols as reported here are needed to better understand the marine biogeochemical cycle of carbon, nitrogen, and phosphorus.

References

- Hansen, H. P. and F. Koroleff (1999): Determination of nutrients, p. 159–228. In *Methods of Seawater Analysis*, Third Edition, edited by K. Grasshoff, K. Kremling, and M. Ehrhardt, Wiley-VCH Verlag GmbH, Weinheim, Germany.
- Japan Society for Analytical Chemistry (JSAP), The Association of Organic Micro-analysts (2008): *Practical Microorganic Analysis*. Mimizukusha, Tokyo, 195 pp (in Japanese).
- Karl, D. M., D. V. Hebel, K. Björkman, and R. M. Letelier (1998): The role of dissolved organic matter release in the productivity of the oligotrophic North Pacific Ocean. *Limnology and Oceanography*, 43, 1270–1286.
- Knap, A., A. Michaels, A. Close, H. Ducklow, and A. Dickson (1996): *Protocols for the Joint Global Ocean Flux Study (JGOFS) Core Measurements*. JGOFS Report Nr. 19, vi+170 pp. Reprint of the IOC Manuals and Guides No. 29, UNESCO 1994.
- Martiny, A. C., J. A. Vrugt, and M. W. Lomas (2014): Concentrations and ratios of particulate organic carbon, nitrogen, and phosphorus in the global ocean. *Scientific Data*, 1, 140048, doi:10.1038/sdata.2014.48
- Moran, S. B., M. A. Charette, S. M. Pike, and C. A. Wicklund (1999): Differences in seawater particulate organic carbon concentration in samples collected using small- and large-volume methods: the importance of DOC adsorption to the filter blank. *Marine Chemistry*, 67, 33–42.
- Morán, X. A., J. M. Gasol, L. Arin, and M. Estrada (1999): A comparison between glass fiber and membrane filters for the estimation of phytoplankton POC and DOC production. *Marine Ecology Progress Series*, 187, 31–41.

- Murakami, T. and Y. Shirai (2015): Organic elemental analysis by combustion method. *BUNSEKI*, 2015, 108–114 (in Japanese).
- Oku, O. (2002): *Know-How for Spectrophotometry: Qualitative Analysis of Silicic Acid, Phosphate, and Nitrate*. Gihodoshuppan, Tokyo, 137 pp (in Japanese).
- Parsons, T. R., Y. Maita, and C. M. Lalli (1984): *A Manual of Chemical and Biological Methods for Seawater Analysis*. Pergamon Press, Oxford, 173 pp.
- Sharp, J. H. (1974): Improved analysis for “particulate” organic carbon and nitrogen from seawater. *Limnology and Oceanography*, 19, 984–989.
- Solórzano, L., and J. H. Sharp (1980): Determination of total dissolved phosphorus and particulate phosphorus in natural waters. *Limnology and Oceanography*, 25, 754–758.
- Suzumura, M. (2008): Persulfate chemical wet oxidation method for the determination of particulate phosphorus in comparison with a high-temperature dry combustion method. *Limnology and Oceanography: Methods*, 6, 619–629.
- Wang, G., W. Zhou, W. Cao, J. Yin, Y. Yang, Z. Sun, Y. Zhang, and J. Zhao (2011): Variation of particulate organic carbon and its relationship with bio-optical properties during a phytoplankton bloom in the Pearl River estuary. *Marine Pollution Bulletin*, 62, 1939–1947.

Biogenic silica

○Fuminori HASHIHAMA (Tokyo University of Marine Science and Technology)

1. Introduction

Biogenic silica (BSi) is an amorphous silica that is produced primarily by diatoms, silicoflagellates, radiolarians, and sponges. Among these organisms, planktonic diatoms are an important group and are currently responsible for 40% of primary production in the world's oceans (Nelson et al., 1995). Assimilation of dissolved silicic acid (DSi) by diatoms, dissolution of diatom frustules, and downward export and sedimentation of diatom debris are the major processes in the marine silicon cycle. To understand these processes, information regarding BSi is generally essential.

Analytical procedures for the measurement of BSi include wet-alkaline extractions, X-ray diffraction, and infrared absorption. Among them, the wet-alkaline extraction method appears to be the most versatile for the BSi measurement of suspended particulate matter (DeMaster, 1991). This method involves the alkaline extraction of BSi on filter samples and the subsequent determination of DSi using conventional colorimetry. Herein is described a modified literature procedure using NaOH for the extraction (Paasche, 1973). This procedure features a more rapid extraction and higher extraction efficiency than other wet-alkaline extraction methods (Krausse et al., 1983).

2. Sampling

Water samples should be collected using a silicon-free, alkaline- and acid-cleaned sampler such as a Niskin or Van Dorn sampler. Water collected in the sampler is then dispensed into a plastic bottle (and not a glass bottle) directly or using a vinyl tube. The use of silicon tubing instead of the vinyl tubing should be avoided, because silicon tubing can contaminate the BSi. The required sample volume, approximately equal to the filtration volume, is roughly several tens of milliliters to several liters for the coastal, high latitude, and equatorial upwelling regions; and several liters to several tens of liters for subtropical and equatorial warm pool regions. In practice, the required sample volume is determined based on the analytical detection limit of the colorimetry and the previously reported BSi concentration in a target region (see below).

3. Filtration

The sample water is accurately measured using a plastic graduated cylinder or a plastic bottle of known-volume (such as the plastic bottle used for sampling). The measured water is filtered using a plastic filtration device (with no glass components). If silicon packing is used in the filter holder, it should be replaced with a silicon-free packing, such as Teflon. There are many filters used for collecting suspended particulate matter, and a polycarbonate filter, such as a Whatman Nuclepore filter (GE Healthcare), is appropriate for BSi determination. A glass fiber filter cannot be used because it would introduce significant silicon contamination. A polycarbonate filter with a 47 or 25 mm diameter is commonly used, and its 0.4–0.8 μm pore size is effective for collecting most diatoms. The filtration is performed using an aspirator with a gentle suction of <150–200 mmHg. After the filtration, the

particulate matter attached to the inside of the filter funnel, and the DSi adsorbed onto the filter, are washed with several tens of milliliters of low-DSi filtered seawater. The low-DSi filtered seawater is prepared by passing oligotrophic open water through a 0.2 μm pore size polycarbonate filter. The filter sample is folded and placed into a polypropylene centrifuge tube, e.g., 28 mL Oak Ridge Centrifuge Tubes, Nalgene. A tightly sealable and heat-resistant tube is preferred because it will be held at 100 $^{\circ}\text{C}$ during the extraction of BSi (see below).

4. Extraction procedure

If a drying oven is available in the field, the filter sample is immediately dried at 60 $^{\circ}\text{C}$ for approximately 2 h. However, if one is unavailable in the field, the filter sample is temporarily stored at -20°C , and after the field observation is complete the sample is dried at a land-based laboratory. BSi on the filter sample is extracted according to a procedure using a NaOH solution. First, 10 mL of 0.2 M NaOH is added to a filter-containing polypropylene centrifuge tube. At this point, the screw top of the tube should be wrapped using a Teflon seal tape to ensure a tight seal. After the tube is sealed and the filter is soaked in the NaOH solution, the sample is placed in a water bath at 100 $^{\circ}\text{C}$ for 15 min. The sample is then cooled to ambient temperature and neutralized using 10 mL of 0.2 M HCl.

5. Colorimetry

BSi in the sample should be transformed into DSi after the extraction. The DSi concentration is then measured using a molybdenum blue colorimetry (see Vol. 3, Chap. 2).

During the DSi measurement, the blank and the matrix of standard solutions should be prepared using equal volumes of 0.2 M NaOH and 0.2 M HCl. A correction of filter blank is generally not required because Nuclepore filters are not contaminated with BSi. However, if other filter types are used, the absorbance of filter blank might require subtraction from the absorbance of the sample. A filter blank is prepared through the extraction and neutralization of a fresh filter that has not been exposed to sample water.

6. Calculation

From the DSi concentration determined using colorimetry, the BSi concentration is calculated as follows:

$$\text{BSi } (\mu\text{M}) = \text{DSi } (\mu\text{M}) * 0.02 \text{ (L)} / \text{FV (L)}$$

where FV is the filtered volume, and 0.02 that is multiplied by DSi concentration is the total volume of 0.2 M NaOH and 0.2 M HCl used.

The FV is a critical term because it directly influences on the detection of DSi. If given a detection limit of 0.1 μM DSi and an ambient concentration of 0.01 μM BSi, the FV is calculated as follows:

$$0.01 \text{ } (\mu\text{M BSi}) = 0.1 \text{ } (\mu\text{M DSi}) * 0.02 \text{ (L)} / \text{FV (L)}$$

$$\text{FV (L)} = 0.2$$

In this case, >200 mL FV is required for the detection of BSi. Therefore, the DSi detection limit and the ambient BSi concentration should be reviewed before sampling, and an appropriate sample volume should be collected for the accurate determination of BSi.

7. Remarks

The wet-alkaline extraction method appears to be the most versatile, but it requires particular attention when used for samples collected from estuarine and coastal regions. In these regions, lithogenic silica (LSi) contributes significantly to the total particulate silica and its dissolution during the alkaline extraction often results in overestimation of the BSi concentration (Ragueneau and Tréguer, 1994). To determine the BSi concentration in high-LSi water, a method that corrects for the contribution of LSi to BSi should be applied (Ragueneau et al., 2005).

References

- DeMaster, D. J. (1991): Measuring biogenic silica in marine sediments and suspended matter, p. 363–368. In *Marine Particles: Analysis and Characterization*, edited by D. C. Hurd and E. W. Spenser, American Geophysical Union.
- Krause, G. L., C. L. Schelske, and C. O. Davis (1983): Comparison of three wet-alkaline methods of digestion of biogenic silica in water. *Freshwater Biol.*, 13, 73–81.
- Nelson, D. M., P. Tréguer, M. A. Brzezinski, A. Leynaert, and B. Quéguiner (1995): Production and dissolution of biogenic silica in the ocean: Revised global estimates, comparison with regional data and relationship to biogenic sedimentation. *Global Biogeochem. Cycles*, 9, 359–372.
- Paasche, E. (1973): Silicon and the ecology of marine plankton diatoms. I. *Thalassiosira pseudonana* (*Cyclotella nana*) grown in a chemostat with silicate as limiting nutrient. *Mar. Biol.*, 19, 117–126.
- Ragueneau, O., and P. Tréguer (1994): Determination of biogenic silica in coastal waters: applicability and limits of the alkaline digestion method. *Mar. Chem.*, 45, 43–51.
- Ragueneau, O., S. Nicolas, Y. Del Amo, J. Cotton, B. Tardiveau, and A. Leynaert (2005): A new method for the measurement of biogenic silica in suspended matter of coastal waters: using Si:Al ratios to correct for the mineral interference. *Continental Shelf Res.*, 25, 697–710.

This page left intentionally blank.

Carbon and Nitrogen Stable Isotopes in Particulate Organic Matter

Yu UMEZAWA (Tokyo University of Agriculture and Technology)

1. Introduction

Particulate Organic Matter (POM) in the ocean is an important food source for a variety of the marine organisms such as filter feeders and fishes. POM also functions as a reservoir of dissolved organic matter (DOM) and nutrients, which are generated during bacterial decomposition of POM, especially in oligotrophic pelagic waters. Furthermore, evaluation of the export flux of POM into the deep layers of the ocean is important for comprehending the Earth's carbon, nitrogen and phosphorus cycles.

Carbon and nitrogen stable isotopes ($\delta^{13}\text{C}$ · $\delta^{15}\text{N}$) in POM in the euphotic layer primarily reflect the $\delta^{13}\text{C}$ · $\delta^{15}\text{N}$ values of source materials, that is, dissolved inorganic carbon (DIC) and dissolved inorganic nitrogen (DIN), which are taken up by phytoplankton. POM isotopes also reflect the mixed POM carried from the other sources such as rivers. In addition to source values, the isotope values of POM reflect processes including isotope discrimination (kinetic isotope effect), such as due to prior uptake and biosynthesis of lighter isotopes by phytoplankton, and heterogenic modification such as due to bacterial decomposition of specific parts of the POM pool.

Of course we need to pay special attention to the interpretation of $\delta^{13}\text{C}$ · $\delta^{15}\text{N}$ values in POM, because POM itself is an aggregation and/or mixture of different materials (i.e., phytoplankton, zooplankton and organic debris). Despite these potential complications, $\delta^{13}\text{C}$ · $\delta^{15}\text{N}$ values can be an effective tool for investigating food web dynamics and material cycles (i.e., the source and pathways of the materials) in the aquatic systems, as far as we understand the characteristics of stable isotopes and interpret values in the context of other physical, chemical and biological parameters (Tables 3-1, 2).

The concentration of POM is variable in space and time, and therefore, field and laboratory sample processing for POM $\delta^{13}\text{C}$ · $\delta^{15}\text{N}$ can be time-consuming since we need to collect many samples to capture the spatio-temporal variation, as well as needing to adjust filtration volumes (see below). However POM $\delta^{13}\text{C}$ · $\delta^{15}\text{N}$ analyses should be considered an important parameter in field observations of the ocean, now and in the future. It is also advantageous that the outsourcing of isotope analyses is available relatively cheaply, costing 2,000 to 5,000 JPY per sample, and the number of mass spectrometers in university or research institutes is increasing.

In this section, the basic protocols and devices for POM sampling, sample processing, and $\delta^{13}\text{C}$ · $\delta^{15}\text{N}$ analyses are briefly explained. Because these protocols are not completely unified between researchers, previous articles dealing with $\delta^{13}\text{C}$ · $\delta^{15}\text{N}$ analyses should also be consulted, depending on the conditions (e.g., Teece and Fogel, 2004; Miyajima, 2008; Ogawa et al., 2010; Ogawa et al., 2013). POM $\delta^{13}\text{C}$ · $\delta^{15}\text{N}$ analyses are generally conducted using elemental analyzer-isotope ratio mass spectrometry (EA-IRMS), with POM generally defined as the particles trapped on a glass fiber filter with a pore size of 0.7 or 0.8 μm (e.g., GF/F, Whatman). Filters with smaller pore size (e.g., GF-75, ADVANTEC) may be used in surface waters of the tropical and subtropical ocean, where the biomass of pico-plankton is not negligible. The appropriate filter pore size should be selected depending on the conditions of the target ocean, and the purpose of the observation.

This chapter focuses on $\delta^{13}\text{C}$ and $\delta^{15}\text{N}$ analysis of bulk POM according to the above definition. On the other hand, it is possible to analyze $\delta^{13}\text{C}$ and $\delta^{15}\text{N}$ in size-fractionated POM and those in chlorophylls and amino acids extracted and purified from POM. By analyzing these compound-specific isotopic values, there is an advantage to understand the phytoplankton dynamics and the trophic level of POM (i.e., contribution of heterotrophs and related debris). Please refer to previous literatures for sample processing, analytical methods and applications for these parameters (e.g., Sato et al., 2006; McCarthy et al., 2007; Yamaguchi & McCarthy, 2018).

Table 3-1. Factors causing variation in $\delta^{13}\text{C}$ -POM and associated fluctuations of other parameters(※ An opposing pposite shift in $\delta^{13}\text{C}$ values is often caused by the reverse case)

Factors causing a relative increase of $\delta^{13}\text{C}$ -POM	Probable phenomena observed simultaneously
• Increase in photosynthesis (DIC uptake)	1) Increase in irradiance, temperature, and nutrients supply 2) Increase in photosynthetic pigments (e.g., chlorophyll) 3) Increase in $\delta^{15}\text{N}$ values
Factors causing a relative decrease of $\delta^{13}\text{C}$ -POM	Probable phenomena observed simultaneously
• Supply of DIC with lighter $\delta^{13}\text{C}$ (e.g., freshwater DIC)	1) Decrease in salinity
• Contribution of terrestrial plants and freshwater plankton	1) Increase in C/N ratio (higher C/N ratio of terrestrial plants) 2) Decrease in salinity 3) Increase in organic polymers in vascular plants (e.g., lignin)

Table 3-2. Factors causing the variation of $\delta^{15}\text{N}$ -POM and associated fluctuations of other parameters(※ An opposing pposite shift in $\delta^{13}\text{C}$ values is often caused by the reverse case)

Factors causing a relative increase of $\delta^{15}\text{N}$ -POM	Probable phenomena observed simultaneously
• Contribution of wastewater-derived DIN with high $\delta^{15}\text{N}$	1) Decrease in salinity, Short distance from the shore
• Increase in $\delta^{15}\text{N}$ -nitrate due to denitrification	1) Decrease in dissolved oxygen 2) Increase in denitrifying bacteria (e.g., molecular approach) 3) Increase in $\delta^{18}\text{O}$ -nitrate
• Increase of photosynthesis (DIN uptake)	1) Increase in irradiance, temperature, and nutrients supply 2) Increase in photosynthetic pigments (e.g., chlorophyll) 3) Increase in $\delta^{13}\text{C}$ -DIC 4) Decrease in DIN concentration by uptake (Inverse correlation between $\delta^{15}\text{N}$ -POM & log-transformed DIN)
• Contribution of upwelling-derived NO_3 to primary production, compared with N_2 -fixation in pelagic water	1) Decrease in temperature, Increase of salinity 2) Developed vertical mixing
• Higher contribution of heterotrophs-derived organic matter with relatively heavier $\delta^{15}\text{N}$	1) Increase in heterotrophs (microscopic analysis) (Increase of amino acid trophic level in POM) 2) Decrease in Chl/POC 3) Increase in water depth below euphotic zone
Factors causing a relative decrease of $\delta^{15}\text{N}$ -POM	Probable phenomena observed simultaneously
• Contribution of rainwater- NO_3 to primary production	1) Increase in $\delta^{18}\text{O}$ -nitrate 2) Decrease in salinity 3) Increase in DIN/P ratio in nutrient
• Increase in nitrogen fixation	1) Increase in nitrogen fixing bacteria 2) Increase in photosynthetic pigment, phycoerythrin
• Contribution of remineralized NH_4 (lower f -ratio) compared with NO_3 from deep water in pelagic ocean	1) Increase in small-sized phytoplankton 2) Increase in nitrifying bacterial activity 3) Development of stratification

2. Sampling

For the analysis of $\delta^{13}\text{C} \cdot \delta^{15}\text{N}$ in organic matter, it is recommended to prepare samples such that they contain 60-100 μg nitrogen in order to minimize the effect of contamination (i.e., atmospheric nitrogen, and organic matter attached to the glass fiber filter and tin capsules) on the real isotope values of the samples. The amount of carbon is not such a focus because the carbon to nitrogen ratio in natural organic matter is generally larger than 1. On the other hand, it is necessary to minimize the volume of glass fiber filter used and to maintain good analysis conditions, especially for small samples (see 3-4) because the incombustible glass fiber filters accumulate in the combustion column as debris often causing incomplete combustion of organic matter and blockage of gas passing, resulting in erroneous $\delta^{13}\text{C} \cdot \delta^{15}\text{N}$ values. Therefore, it is necessary to change the volume of water filtered depending on the concentration of POM. For example, c.a. 10 L or more may be necessary over coral reefs, in the surface layers of offshore waters, and in very deep layers, compared to 2 or 10 L in the chlorophyll maximum layer or just several hundred mL for samples taken from a phytoplankton bloom in the coastal area. Increasing the amount of POM by increasing the water volume of the filtration results in an increase in filtration time. Furthermore, as POM trapped on the filter increases, it may partly fill the filter pores and then small particles less than the nominal pore size may also get trapped on the filter. We need to take care regarding the volume of water chosen for filtration to prevent an imbalance in the size of POM collected on the filter (Uematsu et al., 1978).

Seawater samples for POM $\delta^{13}\text{C} \cdot \delta^{15}\text{N}$ are generally collected across water depths using a water sampler (e.g., Van Dorn sampler or Niskin water sampler equipped into RMS: Rosette Multibottle Samplers), and the water is transferred to a plastic container through a tube via a nylon net of 200 or 300 mesh size to remove large zooplankton or debris. Surface seawater can be collected by a bucket and transferred to the container with a funnel containing the nylon net. Water samples are then filtered on pre-combusted (3 hours at 450°C to remove the organic matter) glass fiber filters using an aspirator to keep suction pressure about 20–25 kPa (150–200 mmHg) to prevent larger particles from passing the filter. The entire water sample is generally introduced into the filtration system continuously using a siphon system, but it is necessary to regularly shake the container to keep an even POM concentration in suspension. At the final step of the filtration, rinse the inner wall of the funnel with filtered seawater, then wash the salt out of the filter with a few ml of the ultrapure water. Ammonium carbonate solution is also used for washing to minimize the possibility of lysis of phytoplankton cells due to the osmolar difference (e.g., Uematsu et al., 1978), but there is a risk of ammonium contamination in water samples for nutrient analysis during the sample processing. After filtration, the filter is removed from filter folder by forceps while maintaining suction pressure, and placed into pre-combusted aluminum foil or a petri dish and stored at a temperature of -20°C .

As suggested in Tables 3-1, 2, there are many environmental factors causing shifts in $\delta^{13}\text{C} \cdot \delta^{15}\text{N}$ values in POM. To properly interpret POM $\delta^{13}\text{C} \cdot \delta^{15}\text{N}$ values in the context of environmental conditions, collection of not only basic parameters such as water temperature, salinity, chlorophyll, and dissolved oxygen, but also other data sets such as nutrients, predominant phytoplankton species, and bacteria may also be required during the field survey depending on the study purpose.

3. Sample Processing

Filter samples stored in the freezer are dried in a vacuum freezing oven or heating oven at about 60°C, and transferred to clean glass petri dish one by one. The filter samples are then stored in a tight box with a beaker of 20-40 ml concentrated hydrochloric acid (conc. HCl) for 1 day to remove inorganic carbon (e.g., HCO_3^- , CaCO_3) by acid fumigation. After acidification, the petri dishes are placed in a vacuum desiccator equipped with no metal parts (or vacuumed by water aspirator) from several days to 1 week. There is the option to place granular sodium hydrate together with the samples to promote neutralization of the acid gas. At the final step, the filter is completely dried on a hotplate or in the oven for 1 day, and stored in a desiccator with silica gel.

In the next step, the marginal white portion of the filter, which contains no organic matter, is removed using ethanol-washed forceps and scissors to minimize the amount of glass fiber filter relative to the amount of organic matter. Some researcher also slightly peel the back side of the filter for the same purpose. However, this is not recommended, because, although this method may increase the number of samples analyzed with single combustion column, carbon and nitrogen amounts are then underestimated and $\delta^{13}\text{C} \cdot \delta^{15}\text{N}$ values can potentially deviate from the real values. Glass fiber filter samples are wrapped in a tin or silver capsule, and tightly folded into a pellet using 2 set of forceps. Generally organic matter, especially organic carbon, attaches to the surface of tin capsule. The contamination of organic matter can be minimized by soaking and washing with a clean organic solvent such as methanol or acetone. The use of disk-type smooth tin foil without wrinkles or smaller sized tin capsules decreases the amount of contaminated organic matter. Furthermore, in the case of silver capsules having a higher melting point, pre-combustion at 400-450°C effectively decreases the organic matter contamination (Ogawa et al., 2010).

To adjust the amount of organic matter to one appropriate for analysis, the filter is divided after confirmation that the samples were homogeneously trapped into the filter. The relative weights of the whole filter and the filter part are measured, and used for calculation of organic matter concentration in the sample (e.g., mg-C/L, mg-N/L) based on the following equation.

POC conc. (mg-C/L) =

$$\text{POC (mg-C) in the filter part} \times \frac{\text{weight of whole filter (mg)}}{\text{weight of the filter part (mg)}} \times \frac{1}{\text{filtration volume (L)}}$$

When the amount of organic matter is large, some oxidant such as vanadium pentoxide (V_2O_5) or cobalt oxide (Co_2O_3) may be added with POM samples to promote complete combustion of the organic matter (Kanda et al., 1998), after checking the blank size (i.e., the contaminated organic matter in the oxidant). When tin capsules burn with a flash in the combustion column at about 1000°C, the temperature increases up to above 1800°C. Therefore, a small piece of tin-foil placed on the POM sample and wrapped together with the filter may promote complete combustion of the POM in the glass fiber filter. The sample roughly compressed with forceps can be further compacted with a handy tablet punch & dies with a pressure of 3 – 5 MPa to completely remove atmospheric nitrogen gas contained in the glass fiber. Atmospheric nitrogen remaining in the filter can cause overestimation of nitrogen

contents and inaccurate estimation of the $\delta^{15}\text{N}$ of the samples. In order to accurately evaluate the contamination of atmospheric nitrogen, it is necessary to prepare blank filter samples in the same manner as samples (see 3.4). The samples should be kept in a desiccator until analysis, but it is recommended they should be analyzed as soon as possible to minimize contamination by atmospheric nitrogen.

4. Sample analysis

The $\delta^{13}\text{C} \cdot \delta^{15}\text{N}$ values of the filter samples in tin capsules are determined by EA-IRMS (Elemental Analyzer coupled to Isotope Ratio Mass Spectrometry) in the same way as the analysis of solid organic samples.

Generally $\delta^{13}\text{C} \cdot \delta^{15}\text{N}$ values in the samples are first determined relative to the $\delta^{13}\text{C} \cdot \delta^{15}\text{N}$ values in reference CO_2 and N_2 gas, respectively, and then these temporal values are converted to real values referring to the difference between the real values and measured values of standards having known $\delta^{13}\text{C} \cdot \delta^{15}\text{N}$ values (Fig. 3-1). The $\delta^{13}\text{C}$ and $\delta^{15}\text{N}$ values often shift depending on the amount of carbon or nitrogen in the sample. In particular $\delta^{15}\text{N}$ values in small samples tend to be lighter than the real values. Ideally the size of samples should be adjusted so that they contain enough nitrogen for the $\delta^{15}\text{N}$ values to be minimally shifted, however this is often difficult for the POM samples (Fig. 3-1). The mass-dependent shift in $\delta^{15}\text{N}$ values of standards can be modelled by a regression fit, and the real stable isotope values of unknown samples then corrected based on the mass of N injected and the regression equation for the standards (Fig. 3-1).

Amino acids having similar C/N ratio to that of particulate organic matter (e.g., 3.0 for alanine, 5.0 for proline, and 9.0 for phenylalanine) are often used as standards. These standard amino acids are generally secondary standards produced based on the primary international standard samples and are available through many domestic or foreign companies. The basic mechanisms of EA-IRMS, the details of machine-specific operation (e.g. based on the apparatus of Thermo Fisher Scientific Inc.), and details on the analysis of the data obtained are also available in previous reports (e.g., Brand, 2004, Ogawa et al., 2013) in addition to the manuals of the product makers.

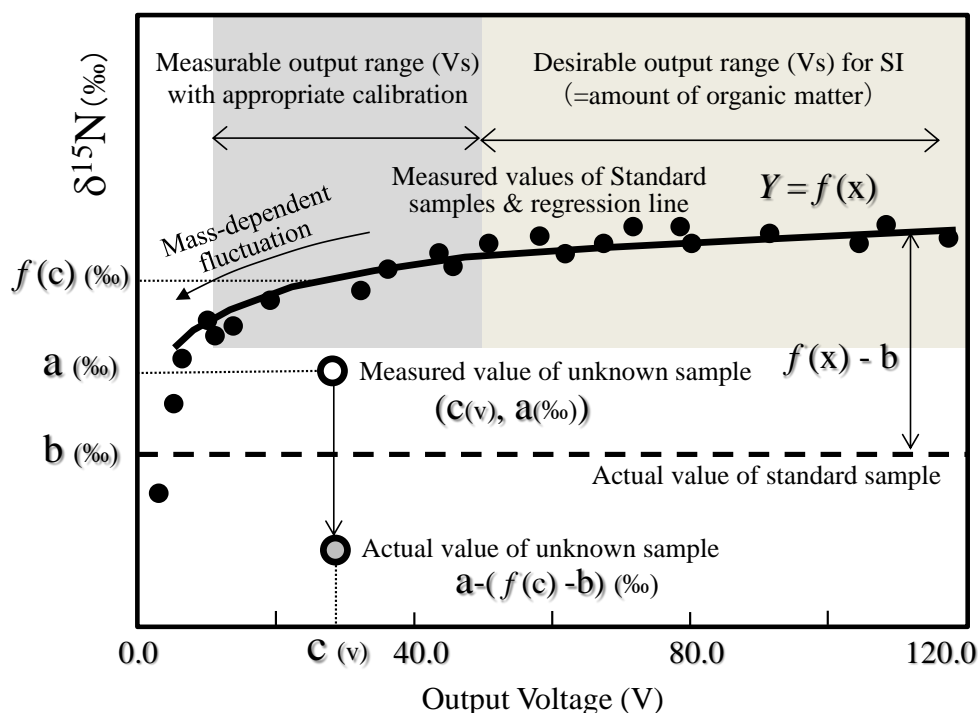


Figure 3-1. Calculation of actual stable isotope values of unknown samples based on the analyses of standards

Several points about which we should be extra careful in the analysis of filter samples having lower organic matter include: 1) to precisely measure the blank sample (i.e., tin capsule and glass fiber filter) and compensate the measured values of targeted samples by subtracting the blank size; 2) to confirm the accuracy and repeatability of $\delta^{13}\text{C}$ and $\delta^{15}\text{N}$ values in standards having similar carbon and nitrogen content to that of targeted samples through repeated analyses; and, 3) to monitor the deterioration of the analytical conditions (e.g., clogging and contamination in the combustion column) and make a proactive decision regarding suspension of the analysis. Deterioration of the analytical conditions can be objectively judged based on a shift of $\delta^{13}\text{C}$, $\delta^{15}\text{N}$ and C/N ratios in the standards, a shift in carrier gas flow speed (ml/s) and retention time of the sample peaks, an increase the background values, and instability in repeatedly injected reference gases.

As mentioned in Section 3., nonflammable glass fiber filters accumulate as debris in the combustion column, and potentially cause incomplete combustion of organic matter and/or block the passage of the carrier gasses. These phenomena cause delays in the retention time of the sample peak and peak tailing, resulting in a shift in $\delta^{13}\text{C}$ and $\delta^{15}\text{N}$ values when the peaks overlap with the reference gas peak and the peak is not correctly evaluated. An inner ceramic or quartz tube placed in the combustion column may improve analytical conditions for glass fiber filter samples. Since the inner tube is easily replaced with a new tube when the symptoms of incomplete combustion are observed, many more filter samples can be analyzed using the same combustion and reduction columns (Kanda et al., 1998; Ogawa et al., 2013).

Furthermore, quartz tubes with smaller internal diameter (ϕ 8-10 mm) than the normal tubes with ϕ 14-16 mm ID decrease the dilution ratio of generated gasses (CO_2 and N_2) with carrier He gas, and are therefore useful for increasing the accuracy of analyses of samples with lower organic matter (Ogawa

et al., 2010). Although the number of the samples that can be analyzed in the narrower tube is smaller than that of normal tubes, an increase in the analytical accuracy for small samples is an indispensable merit, in addition to saving the materials filled in the quartz tubes.

As introduced above, special care is needed for the analysis of filter samples. A longer time is required for these analyses to minimize interference with the reference gas peaks due to incomplete combustion and tailing peaks. Manual modification of the peak width on the chromatogram and calibration of the values based on the standards and blanks are needed for each sample analysis. Unlike the analyses of animal and plant samples, the accurate analysis of POM filter samples will be accomplished based on the accumulated experience and techniques used by each researcher.

References

- Brand, W. A. (2004): Mass Spectrometer Hardware for Analyzing Stable Isotope Ratios. p.835-856. In Handbook of Stable Isotope Analytical Techniques, Vol. 1, Edited by P.A. de Groot, Elsevier, Amsterdam.
- Kanda, J., K. Sada, I. Koike, and K. Yokouchi (1998): Application of an automated carbon-nitrogen analyzer for elemental and isotopic analysis of samples retained on glass-fiber filters. *International Journal of Environmental Analytical Chemistry*, 72, 163-171.
- McCarthy M.D., R. Benner, C. Lee, and M.L. Fogel (2007): Amino acid nitrogen isotopic fractionation patterns as indicators of heterotrophy in plankton, particulate, and dissolved organic matter. *Geochim. Cosmochim. Acta*, 71, 4727–4744.
- Miyajima, T. (2008) Chapter 4: Estimation of the source of particulate organic matter in the estuary. P.163-186, (In) *Stable Isotopes in Environmental Assessment of Watersheds –Progress Towards an Integrated Approach-* (eds. T. Nagata and T. Miyajima), Kyoto University Press, Kyoto. (in Japanese)
- Ogawa, N., and N. Ogura (1997): Dynamics of Particulate Organic Matter in the Tamagawa Estuary and Inner Tokyo Bay. *Estuar. Coast. Shelf S.*, 44, 263-273.
- Ogawa, N. O., T. Nagata, H. Kitazato, and N. Ohkouchi (2010): Ultra sensitive elemental analyzer/isotope ratio mass spectrometer for stable nitrogen and carbon isotopic analyses. P.339-353, In *Earth, Life, and Isotopes*, edited by N. Ohkouchi, I. Tayasu, K. Koba, Kyoto University Press, Kyoto.
- Ogawa, N. O., Wang, S., Shinohara, H., and N. Ohkouchi, (2013): Protocol for precise analyses of stable isotope ratio – Carbon and nitrogen stable isotope analyses –, Japan Chemical Analysis Center (in Japanese)
- Sato, T., T. Miyajima, H. Ogawa, Y. Umezawa, and I. Koike (2006): Temporal variability of stable carbon and nitrogen isotopic composition of size-fractionated particulate organic matter in the hypertrophic Sumida River Estuary of Tokyo Bay. *Estuarine, Coastal and Shelf Science*, 68, 245-258.
- Teece, M. A., and M. L. Fogel (2004): Preparation of Ecological and Biochemical Samples for Isotope Analysis. p.177-202. In *Handbook of Stable Isotope Analytical Techniques*, edited by P.A. de Groot, Elsevier, Amsterdam.
- Uematsu, M., Minagawa, M., Arita, H., and Tsunogai, S. (1978): Determination of dry weight of total suspended matter in seawater, *Bulletin of the Faculty of Fisheries Hokkaido University*, 29(2), 164-172. (In Japanese)
- Yamaguchi Y. T., and M. D. McCarthy (2018): Sources and transformation of dissolved and particulate organic nitrogen in the North Pacific Subtropical Gyre indicated by compound-specific $\delta^{15}\text{N}$ analysis of amino acids.

Geochimica et Cosmochimica Acta, 220, 329-347.

This page left intentionally blank.

Algal pigments

Koji Suzuki (Hokkaido University)

1. Introduction

Concentrations of chlorophyll *a* or total chlorophyll *a* (chlorophyll *a* + divinyl chlorophyll *a*) have often been used as indices of phytoplankton (cyanobacteria and eukaryotic microalgae) biomass. All marine phytoplankton except cyanobacterium *Prochlorococcus* possess chlorophyll *a* as the principal photosynthetic pigment (Jeffrey et al., 2011), whereas *Prochlorococcus*, which occurs in sunlit subtropical and tropical waters, contains divinyl chlorophyll *a* (Chisholm et al., 1998). These chlorophylls can be quantified easily by fluorometry or the other methods. However, it is well known that algal cellular chlorophyll *a* concentration can significantly change with differences among species and/or their habitats (intensity and quality of light, nutrient availability, etc.; Harrison et al., 1977; Falkowski and Owens, 1990). Therefore, in general, it is difficult to convert chlorophyll *a* concentration to carbon biomass. At present, fluorometry and high-performance liquid chromatography (HPLC) have been widely used for the analysis of chlorophyll *a* in seawater. In this chapter, the methodology for the determination of chlorophyll *a* concentration in seawater by fluorometry is mainly introduced.

2. Sampling, filtration and pigment extraction

Seawater sampling is generally carried out by using a plastic bucket and/or water samplers. Because algal pigments are highly photosensitive, it would be preferable to conduct further experimental procedures under subdued light conditions after sampling. Before starting seawater filtration, seawater volume must be measured correctly using a graduated cylinder or other apparatus. In general, glass-fiber filters (e.g. Whatman® GF/F, nominal pore size 0.7 µm) with 25 or 47 mm in diameter are often used for the seawater filtration. Also, to estimate cell sizes in phytoplankton community, membrane filters with precise pore sizes (e.g. 20 µm, 2.0 µm, 0.2 µm) are utilized. Also, the membrane filters should be tolerant for the organic solvents used for pigment extraction. For example, in the case that *N,N*-dimethylformamide (DMF) is applied for pigment extraction, polycarbonate track-etch membrane filters (e.g. Whatman® Nuclepore) are not recommended because of its intolerance to DMF. Therefore, in our laboratory, nylon membrane or polystyrene track-etch membrane filters (e.g. GVS Life Sciences) have been used for DMF pigment extraction. For the filtration volume, the required seawater could be around 50–200 mL and 200–300 mL for coastal and oceanic waters, respectively. Vacuum filtration should be made under ≤ 0.016 MPa (12 cm Hg) to prevent the cells from significant damages. After filtration, the filters should be transferred into glass tubes or organic-solvent-tolerant vials containing the known amount (5–10 mL) of DMF, 90% acetone (acetone : water = 90 : 10 in volume) or methanol. It is known that DMF, which is often used in the field of oceanography in Japan, has higher chlorophyll *a* extraction efficiency and less volatile at room temperature, and little produces break-down pigments during extraction (Suzuki and Ishimaru, 1990). However, DMF is toxic, so operators must put DMF-tolerant gloves and pay attention to ventilation in laboratory. In the case that the volume of organic solvent for pigment extraction is minimized, seawater remained in the glass-fiber used for filtration may

significantly affect the extraction volume. For example, 25 mm Whatman® GF/F filters can contain 200–250 µL of seawater, so the filters should be folded in half to keep the filtration side inside, and then blotted with filter papers to remove the extra seawater. Algal pigments including chlorophyll *a* can be extracted in organic solvent for 24 h in the dark at –20°C.

3. Calibration curve

Once an authentic solid chlorophyll *a* standard from a manufacturer (e.g. Sigma-Aldrich Co. Ltd.) is dissolved in the organic solvent used for pigment extraction, its absorbance can be determined spectrophotometrically. In the case of DMF, chlorophyll *a* absorbance at 750.0 nm and 663.8 nm are measured, and then the difference in absorbance between 663.8 nm and 750.0 nm can be regarded as the true chlorophyll *a* absorbance (hereafter *A*) assuming that the absorbance of chlorophyll *a* at 750 nm is nil. Using the Beer-Lambert law, chlorophyll *a* concentration (*c*) is expressed as the Equation 4.1:

$$c = A / (\varepsilon \cdot l) \quad (4.1)$$

where ε is the absorption coefficient ($\text{L g}^{-1} \text{cm}^{-1}$) for chlorophyll *a*, *l* is the pathlength (cm) of the solution. Table 4.1 indicates the values of absorption coefficient for chlorophyll *a* in each organic solvent (DMF, 90% acetone, and methanol). Once the concentration of chlorophyll *a* is determined, the standard solution should be diluted with the same organic solvent to make standards with different levels, followed by the fluorometric analyses described below for examining the relationship between chlorophyll *a* concentration and its fluorescent value (i.e. calibration curve).

4. Fluorometric analysis

Fluorometers specifically for the determination of chlorophyll *a* concentration are commercially available from some manufactures such as Turner Designs, Inc. If such a fluorometer is used, operators should follow the manufacture's protocol. In the case that a common fluorometer is utilized, the excitation and emission wavelengths can be set at 436 nm and 680 nm, respectively, with a slit width between 5–20 nm (cf. Welshmeyer, 1994). If higher sensitivity is required due to low chlorophyll *a* concentration, the slit width needs to be expanded. However, such a broader slit width condition may cause some errors due to the interference with chemical compounds other than chlorophyll *a*.

Prior to sample measurement, an appropriate volume of the organic solvent used for pigment extraction is dispensed into a quartz cuvette for the determination of a blank value. After that the glass-fiber filter, which was used for filtration, is removed from the organic solvent, fluorescence values of each sample can be measured. From the difference in fluorescence values between sample and blank, the true sample fluorescence intensity can be determined. Then chlorophyll *a* concentration (*C*; g L^{-1}) in seawater is estimated from the Equation 4.2:

$$C = x \cdot v / V \quad (4.2)$$

where x is chlorophyll a concentration in the organic solvent used for pigment extraction, v and V are each volume (L) of the organic solvent and seawater filtration, respectively. In general, the unit of chlorophyll a concentration in seawater is $\mu\text{g L}^{-1}$ (or mg m^{-3}).

Table 4–1 Absorption coefficients of chlorophyll a in each solvent at specific wavelength.

Solvent	Wavelength (nm)	Absorption coefficient ($\text{L g}^{-1} \text{cm}^{-1}$)	References
DMF	663.8	88.74	Porra et al. (1989)
90% acetone	664.3	87.67	Jeffrey and Humphrey (1975)
Methanol	665.2	79.95	Porra et al. (1989)

5. High-performance liquid chromatography (HPLC) and ultra-high-performance liquid chromatography (UHPLC)

Analytical procedures for the fluorometry described above is rather simple, and the technique can estimate chlorophyll a concentration with high sensitivity. However, this method may overestimate chlorophyll a values due to the presence of chlorophyll breakdown compounds which have the same fluorescence properties as the photosynthetic pigment and/or with chlorophyll b (Welshmeyer, 1994). Therefore, to estimate chlorophyll a concentration more precisely, high-performance liquid chromatography (HPLC) or ultra-high-performance liquid chromatography (UHPLC) need to be employed. For the algal pigment analyses using HPLC, the methods of Zapata et al. (2000) or Van Heukelem and Thomas (2001) have often been used. Recently, Jayaraman et al. (2011) and Sanz et al. (2015) succeeded in the improvement of separation between divinyl and monovinyl forms of chlorophylls using a C_{16} -Amide column and a pentafluorophenyl octadecyl silica column, respectively. The HPLC and UHPLC techniques allow us to analyze not only chlorophylls, but also carotenoids simultaneously. The UHPLC systems recently developed are equipped with analytical columns with particle sized less than $2 \mu\text{m}$ and instrumentation that is capable of delivering pressures above 40 MPa (up to ca. 130 MPa), therefore they can analyze algal pigments with high speed and high resolution (Guillarme and Veuthey, 2012). In general, it takes ca. 30 min or more to analyze algal pigments with HPLC, whereas the UHPLC technique developed by Suzuki et al. (2015) can complete the separations of chlorophylls and carotenoids from marine phytoplankton within 7 min with similar resolution as conventional HPLC methods. Abundance and composition of phytoplankton assemblages in seawater can be estimated with taxonomically unique algal pigments. The relative contributions of each phytoplankton group at the class level to chlorophyll a concentration have often been calculated using the factorization program CHEMTAX (Mackey et al., 1996) or multiple regression analysis (e.g. Suzuki et al., 2002).

References

- Chisholm, S. W., R. J. Olson, E. R. Zettler, R. Goericke, J. B. Waterbury, and N. A. Welshmeyer (1988): A novel free-living prochlorophyte abundant in the oceanic euphotic zone. *Nature*, 334, 340–343.
- Guillarme, D. and J. -L. Veuthey (2012): *UHPLC in Life Sciences*. RSC Publishing, 447 pp.
- Falkowski, P. G. and T. G. Owens (1980): Light–shade adaptation. *Plant Physiol.*, 66, 592–595.
- Harrison, P. J., H. L. Conway, R. W. Holmes, and C. O. Davis (1977): Marine diatoms grown in chemostat under silicate or ammonium limitation. III. Cellular chemical composition and morphology of *Chaetoceros debilis*, *Skeletonema costatum*, and *Thalassiosira gravida*. *Mar. Biol.*, 43, 19–31.
- Jayaraman, S., M. L. Knuth, M. Cantwell, and A. Santos (2011): High performance liquid chromatographic analysis of phytoplankton pigments using a C₁₆-Amide column. *J. Chromatogr. A*, 1218, 3432–3438.
- Jeffrey, S. W. and G. F. Humphrey (1975): New spectrophotometric equations for determining chlorophylls *a*, *b*, *c*₁ and *c*₂ in their higher plants, algae and natural phytoplankton. *Biochem. Physiol. Pflanzen*, 167, 191–194.
- Jeffrey, S. W., S. W. Wright, and M. Zapata (2011): Microalgal classes and their signature pigments, p. 3–77, In *Phytoplankton Pigments: Characterization, Chemotaxonomy, and Applications in Oceanography*, edited by S. Roy, C. A. Llewellyn, E. S. Egeland and G. Johnsen, Cambridge University Press, Cambridge.
- Mackey, M. D., D. J. Mackey, H. W. Higgins, and S. W. Wright (1996): CHEMTAX – a program for estimating class abundances from chemical markers: application to HPLC measurements of phytoplankton. *Mar. Ecol. Prog. Ser.*, 144, 265–283.
- Porra, R. J., W. A. Thomas, and P. E. Kriedemann (1989): Determination of accurate extinction coefficients and simultaneous equations for assaying chlorophyll *a* and *b* extracted with four different solvents: verification of the concentration of chlorophyll standards by atomic absorption spectroscopy. *Biochim. Biophys. Acta*, 975, 384–394.
- Sanz, N., A. García-Blanco, A. Gavalás-Olea, P. Loures, and J. L. Garrido (2015): Phytoplankton pigment biomarkers: HPLC separation using a pentafluorophenyl octadecyl silica column. *Meth. Ecol. Evol.*, 6, 1199–1209.
- Suzuki, K., C. Minami, H. Liu, and T. Saino (2002): Temporal and spatial patterns of chemotaxonomic algal pigments in the subarctic Pacific and the Bering Sea during the early summer of 1999. *Deep-Sea Res. II*, 49, 5685–5704.
- Suzuki, K., A. Kamimura, and S. B. Hooker (2015): Rapid and highly sensitive analysis of chlorophylls and carotenoids from marine phytoplankton using ultra-high performance liquid chromatography (UHPLC) with the first derivative spectrum chromatogram (FDSC) technique. *Mar. Chem.*, 176, 96–109.
- Suzuki, R. and T. Ishimaru (1990): An improved method for the determination of phytoplankton chlorophyll using N,N-dimethylformamide. *J. Oceanogr. Soc. Japan*, 46, 190–194.
- Van Heukelem, L. and C. S. Thomas (2001) Computer-assisted high-performance liquid chromatography method development with applications to the isolation and analysis of phytoplankton pigments. *J. Chromatogr. A*, 910, 31–49.
- Welshmeyer, N.A. (1994) Fluorometric analysis of chlorophyll *a* in the presence of chlorophyll *b* and pheopigments. *Limnol. Oceanogr.* 39, 1985–1992.

Zapata, M., F. Rodóriguez, and J. L. Garrido (2000): Separation of chlorophylls and carotenoids from marine phytoplankton: a new HPLC method using a reversed phase C₈ column and pyridine-containing mobile phases. *Mar. Ecol. Prog. Ser.*, 195, 29–45.

This page left intentionally blank.

Direct Counting Methods of Prokaryote and Heterotrophic Nanoflagellates by Epifluorescence Microscopy

○Taichi YOKOKAWA (Japan Agency for Marine-Earth Science and Technology, JAMSTEC)

Prokaryotes and heterotrophic nanoflagellates (HNF) are abundant in the aquatic environment and play important roles in biogeochemical processes in the aquatic ecosystem (Konhauser, 2007; Madsen, 2008; Kirchman, 2008). A typical liter of water from the surface of a lake or ocean contains $\sim 10^9$ prokaryotic cells and 10^5 HNF cells, depending on the environment (Kirchman 2012). Studying the dynamics of the abundance and activities of microbes is important because microbes are the most abundant organisms in aquatic environments and mediate many essential biogeochemical processes.

Methods for enumeration of aquatic microbes have been established and described in several papers and books (e.g., Sherr et al. 1993; Turley 1993, Caron 2001; Sherr et al. 2001). It is recommended to read those references before starting your experiments. The methods described in this chapter and in the references are not appropriate for all purposes. Users must modify the method to suit their own purpose.

This chapter is composed of the following four sections:

- 1) Sampling
- 2) Sample fixation
- 3) Staining, filtration, and producing sample slides
- 4) Sample observation and enumeration

Procedures

1. Sampling

Sampling apparatus

The sampling apparatus (bucket, bottle) should be washed and sterilized before collecting samples to avoid any biological or chemical contamination. Rinsing with the sample water is also recommended to avoid contamination. Other apparatuses for sampling (tubing, funnel) and sample bottles should also be washed and sterilized before use. Use of a pre-washed, sterilized, and disposable plastic apparatus for sampling and sample storage is convenient.

Sampling

Wear plastic laboratory gloves and use the apparatus described above during sampling to avoid contamination. Store samples in a refrigerator (dark, 4°C) immediately following sampling, and preserve the samples using a fixative as soon as possible. Long-term storage of samples without fixation may result in growth or death of microbes and grazing of HNF on prokaryotes. Freezing of samples without fixation is not recommended because the freeze-thaw process may disrupt microbial cells.

2. Sample fixation

Fixation should be performed immediately following sampling. Prokaryote samples (1–20 mL) should be preserved in neutral-buffered formalin solution (final concentration, 1%) that has been passed through a 0.2 μm filter. Samples should be refrigerated (4°C) until being subjected to filtration (~ 12 h).

HNF samples (1–100 mL) should be preserved in glutaraldehyde solution (final concentration, 1%). Samples should be refrigerated (4°C) until being subjected to filtration (~12 h). The type of fixative and its final concentration should be selected according to the objective, particularly for molecular biology techniques.

3. Staining, filtration, and producing sample slides

Cell staining

Both prokaryote and HNF cells must be stained with a fluorochrome for enumeration using an epifluorescence microscope because these cells do not auto-fluoresce. Cells that exhibit auto-fluorescence (those containing chlorophyll *a*, phycoerythrin, phycocyanin, bacteriochlorophyll, etc.) can be detected using an epifluorescence microscope without staining.

For prokaryotic cells, fluorochromes that bind to DNA—such as acridine orange (AO, Hobbie et al., 1977), 4',6-diamidino-2-phenylidole (DAPI, Porter and Feig, 1980), and SYBR Green I (Marie et al., 1997)—are generally used (Sherr et al. 2001). Fluorochromes that bind to protein are also used for enumeration of microbial cells. For precise determination of bacterial cell size, use of a protein-binding fluorochrome is more appropriate (Straza et al. 2009).

For HNF cells, fluorochromes that bind to DNA, such as AO and DAPI, are generally used (Sherr et al. 1993). Double-staining with a DNA- and protein-binding fluorochrome is also used for enumeration of HNF cells (Fukuda et al. 2007).

Each fluorochrome has specific excitation/emission wavelengths (Table 1). Optical filter sets for each fluorochrome must be used. The fluorochrome should be selected depending on the objectives of the experiment. DAPI is generally used for visualization of prokaryotes, whereas FITC is used for HNFs. Staining of prokaryotic cells with DAPI and of HNF cells with FITC are described below.

Prokaryotic cell staining

Add DAPI solution to the sample at a final concentration of 1 $\mu\text{g mL}^{-1}$, followed by storage in the dark for 5–10 min. Large-volume samples (> 5 mL) should be reduced to 2 mL using a filtration funnel (to reduce the amount of DAPI required) and then stained with DAPI (final concentration, 1 $\mu\text{g mL}^{-1}$) in the dark (cover the funnel with aluminum foil) for 5–10 min. After staining, the remaining sample should be filtered.

HNF cell staining

Reduce the sample volume to 2 mL using the filtration funnel, and then release the vacuum. Add FITC solution to the sample at a final concentration of 0.4 mg mL^{-1} , and then incubate the sample in the dark for 5–10 min. After the staining period, rinse the funnel and filter twice using a few milliliters of 0.1 M sodium carbonate buffer (pH 9.5).

Sample filtration

The filtration apparatus should be washed with 0.2 μm -filtered (e.g., ADVANTEC, 25AS020AS) deionized water before use and between each sample.

Place a 0.45 μm cellulose membrane backing filter (Millipore, HAWP02500) onto a 25 mm filtration bottom (note: this backing filter is to spread cells evenly on the filter; the same backing filter can be used for multiple samples; replace daily). Soak with a few drops of 0.2 μm -filtered deionized water. Place a 0.2 μm polycarbonate membrane filter or 0.8 μm polycarbonate membrane filter for prokaryotes and HNF, respectively, onto the wetted backing filter. Place the filtration funnel on top of the filter. For enumeration of prokaryote cells, a filter with an effective diameter (16–25 mm) is appropriate. For enumeration of HNF cells, a filter with an effective diameter of 4 mm is appropriate (a smaller filter area provides higher concentration efficiency). Use forceps to handle filters, and try not to touch the filter area.

For prokaryotes, filter an aliquot of DAPI-stained sample through a 0.2 μm membrane filter. For HNFs, filter an aliquot of fixed sample through a 0.8 μm membrane filter. The sample volume required is dependent upon the cell concentration. A maximum vacuum of 80 mmHg is appropriate for filtration to avoid damage to cells and ensure their random distribution. Rinse with a few milliliters of 0.2 μm -filtered deionized water for prokaryotes or a few milliliters of 0.1 M sodium carbonate buffer for HNF. With the vacuum on, carefully remove the membrane filter from the underlying backing filter. Proceed to the next step, “Slide preparation,” immediately.

Slide preparation

For prokaryotic cells, place the filter onto a slide and place immersion oil (~10 μL) on the center of the filter. Mount a new coverslip on top of the filter and gently press down until the oil moves out to the edge of the filter and forms a seal. For HNF cells, use FA mounting fluid (pH 9.0–9.6) instead of immersion oil.

4. Sample observation and enumeration

Observation

Prepare the optical filters appropriate for the fluorochrome (Table 1). Samples are visualized using a 100 \times oil immersion objective and 10 \times eyepiece. Prokaryotic cells are 0.2–2.0 μm in length and bright blue-white in color. You may distinguish bacilli, cocci, and spirilli among prokaryotic cells. Plate 4 in Pernthaler et al. (2001) shows a representative image of a prokaryotic cell. HNF cells are 2–20 μm in length and fit into a small quadrant of squared graticule. You may observe flagella attached to the cells. Figure 3 in Sherr et al. (1993) and Figure 7.1 in Kirchman (2012) show several representative images of HNF cells.

Table 1. Fluorochrome characteristics.

Fluorochrome	Excitation peak (nm)	Emission peak (nm)
AO	490	530, 640
DAPI	372	456
FITC	490	520
SYBR Green I	494	521
SYPRO Ruby	280	610

Enumeration

Randomly choose 10 large quadrants ($100 \times 100 \mu\text{m}$) and count the cells in each. Thirty to fifty cells per large quadrant are appropriate for counting. If the cell density is outwith this range, the sample volume should be adjusted appropriately. Counting errors and variations of this method are described in Kirchman (1993).

Calculate prokaryotic and HNF cell concentrations as follows:

$$\text{Cells mL}^{-1} = [\text{SC} \times \text{CF}] / \text{V},$$

where SC is the mean sample count/quadrant, CF is the effective filter area/quadrant area, and V is the volume of preserved sample (not including the fixative volume).

Biomass estimates of prokaryotes and HNF are convenient for comparing the carbon budget to other microbial groups or prokaryotes and HNF in other environments. Two methods can be used to convert cell abundance to carbon biomass. One is to convert cell volume to carbon content per cell (Norland 1993), and the other is using a conversion factor (e.g., 20 fg of C per cell, Fukuda et al., 1998). For calculation of HNF biomass, please see Chapter 6 of this guideline.

It should be noted that the fixatives and fluorochromes described here could cause personal injury and health problems. Appropriate protective equipment (e.g., protective eyewear, gloves, laboratory coat, etc.) should be worn and procedures conducted under appropriate laboratory conditions (e.g., clean bench and fume hood).

The methods described here are appropriate for current studies but may not be in the future. More appropriate fluorochromes, more efficient methods of concentrating cells, or more convenient enumeration techniques may be developed. The enumeration methods should be updated as appropriate. Cells have been enumerated by flow cytometry (described in the next section) in recent studies.

Materials required

Equipment and Supplies

Microscope: Epifluorescence microscope with a 100 W mercury lamp, a 100 \times oil immersion objective, and an ocular grid of 10 \times 10 squares.

Filtration apparatus (for prokaryotes): apparatus fit for 25 mm ϕ filters (e.g., ADVANTEC filter manifold KG25 or Hoefer Ten-Place Filtration Manifold FH225V).

Filtration apparatus (for HNF): apparatus fit for 25 mm ϕ filters with a small effective filter area (e.g., ADVANTEC filter manifold KGS-04)

Also, 0.2 μm pore size, 25 mm polycarbonate membrane filters (for prokaryotes), and 0.8 μm pore size, 25 mm polycarbonate membrane filters (for HNF). Black-stained filters of those types are useful for reducing strong background intensity (e.g., ADVANTEC polycarbonate filter K020N025A).

Backing filter: 0.45 μm pore-size, 25 mm cellulose membrane filter

Vacuum pump

Glass slides and cover slips

Immersion oil and FA mounting fluid (Vmrdr, Inc.)

Solutions

DAPI stock solution, 0.5 mg mL⁻¹. Dissolve 10 mg DAPI in 20 mL filtered distilled water. Dispense 0.5 mL aliquots of the DAPI stock solution into plastic vials and store at -20°C.

FITC staining solution

0.25 ml 0.5 M sodium carbonate buffer (pH 9.5)

1.1 mL 0.01 M potassium phosphate buffer (pH 7.2)

1.1 mL 0.85% sodium chloride

1.0 mg FITC

References

- Caron, D. A. (2001): Chapter 15, Protistan herbivory and Bacteriovory, pp. 289–316. In *Methods in Microbiology*, volume 30, edited by J. H. Paul, Academic Press.
- Fukuda, H., R. Sohrin, T. Nagata, and I. Koike (2007): Size distribution and biomass of nanoflagellates in meso- and bathypelagic layers of the subarctic Pacific. *Aquat. Microb. Ecol.* 46, 203–207.
- Hobbie, J. E., R. J. Daley, and S. Jasper (1977): Use of nucleopore filters for counting bacteria by fluorescence microscopy. *Appl. Environ. Microbiol.* 3, 1225–1228.
- Kirchman, D. L. (1993): Chapter 14, Statistical analysis of direct counts of microbial abundance, pp. 117–120. In *Handbook of Methods in Aquatic Microbial Ecology*, edited by P. F. Kemp, R. F. Sherr, E. B. Sherr and J. J. Cole, Lewis Publisher.
- Kirchman, D. L. (2008): *Microbial Ecology of the Oceans*, 2nd edition. Wiley.
- Kirchman, D. L. (2012): *Processes in Microbial Ecology*. Oxford.
- Konhauser, K (2007): *Introduction to Geomicrobiology*. Blackwell Publishing.
- Madsen, E. L. (2008): *Environmental Microbiology*. Blackwell Publishing.
- Marie, D., F. Partensky, S. Jaquet, and D. Vaultot (1997): Enumeration and cell cycle analysis of natural populations of marine picoplankton by flow cytometry using the nucleic acid stain SYBR Green I. *Appl. Environ. Microbiol.* 63, 186–193.
- Pernthaler, J., F-O Glöckner, W Schönhuber, and R. Amann (2001): Chapter 11, Fluorescence in situ hybridization with rRNA-targeted oligonucleotide probes, pp. 207–226. In *Methods in Microbiology*, volume 30, edited by J. H. Paul, Academic Press.
- Porter, K. G. and Y. S. Feig (1980): The use of DAPI for identifying and counting aquatic microflora. *Limnol. Oceanogr.* 25, 943–948.
- Sherr, B., E. Sherr, and P del Giorgio (2001): Chapter 8, Enumeration of total and highly active bacteria, pp. 129–159. In *Methods in Microbiology*, volume 30, edited by J. H. Paul, Academic Press.
- Sherr, E. B., D. A. Caron, and B. F. Sherr (1993): Chapter 26, Staining of heterotrophic protists for visualization via epifluorescence microscopy, pp. 213–228. In *Handbook of Methods in Aquatic Microbial Ecology*, edited by P. F. Kemp, R. F. Sherr, E. B. Sherr and J. J. Cole, Lewis Publisher.
- Straza, T. R. A., M. T. Cottrell, H. W. Ducklow, and D. L. Kirchman (2009): Geographic and phylogenetic variation in bacterial biovolume as revealed by protein and nucleic acid staining. *Appl. Environ. Microbiol.* 75, 4028–4034.

Turley, C. M. (1993): Chapter 18, Direct estimates of bacterial numbers in seawater samples without incurring cell loss due to sample storage, pp. 143–148. In *Handbook of Methods in Aquatic Microbial Ecology*, edited by P. F. Kemp, R. F. Sherr, E. B. Sherr and J. J. Cole, Lewis Publisher.

Enumeration of prokaryotes by flow cytometry

○Mitsuhide SATO (Graduate School of Agricultural and Life Sciences, the University of Tokyo)

1. Instrument and reagents

- A flow cytometer and its ancillaries
- Black plastic bottles of volume > 50 mL
- Micropipettes (1 mL and 10 μ L)
- Standard fluorescent bead suspension (with a diameter of \sim 1 μ m)
- SYBR Green I (or SYBR Gold) solution
- A vortex mixer

For sample fixation

- Glutaraldehyde or paraformaldehyde solution
- Disc filters (with a pore size < 0.2 μ m) and a syringe
- Microdispenser
- Cryovials and canes
- A dry shipper
- A deep freezer

To measure samples onboard, a flow cytometer with an optical system that can be readily adjusted by a user is necessary. For oceanographic requirements, an argon ion laser or a solid laser that can emit blue light is recommended, because it can excite chlorophyll, phycoerythrin and various artificial fluorescent probes including SYBR Green I and SYBR Gold. Light channels should include forward scatter (FSC), side scatter (SSC), green fluorescence (FL1) for fluorescent probes, orange fluorescence (FL2) for phycoerythrin and red fluorescence (FL3) for chlorophyll. The cytometer should be installed on a vibration isolation table in a dry laboratory, and its power should be supplied by a noise-free source. Before and after measurements, instrumental settings should be checked using standard fluorescent beads. Before sampling, plastic bottles should be soaked in detergent and rinsed well with distilled water. The bottles must be rinsed immediately after use, and air-dried. The standard bead suspension should be diluted depending on the intended use and stored in a refrigerator. The concentration should be measured using an epifluorescence microscope. SYBR Green I or SYBR Gold should be stored in a freezer after being diluted 100 times.

2. Sampling and measurement

Seawater can be dispensed directly into black plastic bottles or through silicon tubing from water samplers. The bottles must not be subjected to direct sunlight, to avoid temperature change. A cooler is useful to minimize the temperature change until further analysis.

Fluorescent beads are added to the sample before analysis for the following two reasons. The first is to serve as a standard for the flow rate. The flow rate of a flow cytometer is unstable onboard, except when installed with a syringe pump, which can serve a sample at a controlled rate, as it is affected by the ship's motion and engine vibration. To know an exact flow rate, a bead suspension with a known

particle concentration is added. The second is to serve as a standard of scatter and fluorescence intensities. The light intensities measured by a cytometer can be affected by machine sensitivity, configuration of optical systems, life of the laser, and run length. To compare the values among different samples, they should be normalized to those of the standard beads. The intensity of forward and side scatters is essential to estimate cell size (Ackleson and Spinrad, 1988). The concentration of the beads added must not be too low or too high, relative to the total particle concentration in the sample.

For sheath fluid, either commercially available fluid, filtered seawater (< 0.2 μm), or Milli-Q water can be used, although each of the three has advantages and disadvantages. Commercially available fluid can prevent adhesion of microbes to the tubing inner wall; however, it costs more than the other two alternatives. Milli-Q water is the most economical, and does not induce biofouling. Filtered seawater is advantageous in estimating cell size, because it has the same refractive index as the samples (Cucci and Sieracki 2003), although it frequently induces biofouling. Any of the three above-mentioned materials can be used as sheath fluid, depending on the purpose of the measurement. After using filtered seawater as sheath fluid, it is necessary to clean the tubing vigorously using commercially available sheath fluid or detergent diluted with Milli-Q water. Sonication treatment of sheath fluid may be effective in decreasing noise, by removing the microbubbles present in it.

For enumeration of phytoplankton, which requires no staining procedures, the appropriate volume of seawater is poured into a sample cell. The sample should be measured using FL3 as a trigger parameter, while arranging the gains so that targeted populations are properly captured on FL2-FL3 and FL3-FSC (or SSC) cytograms. The flow rate should be properly set, with a tradeoff of efficiency and sensitivity or precision. When focusing on *Prochlorococcus*, which has an extremely faint autofluorescence, large eukaryotic phytoplankton or nano-sized cyanobacteria are sometimes omitted from the detection range. When this occurs, the same sample should be measured twice using different settings. For detailed processes of categorization of different phytoplankton populations on cytograms, see Marie et al., (1999) or Sato et al., (2010).

For enumeration of heterotrophic prokaryotes, which include bacteria and archaea, fluorescent probes for nucleic acids are generally used, among which SYBR Green I (Marie et al., 1997) is the most widely used, followed by SYTO 13 or PicoGreen. SYBR Gold can be used as an alternative to them (Patel et al., 2007). When added at high concentrations, the fluorescent probe can stain unfixed marine prokaryotes efficiently for detection by flow cytometry (Kamiya et al., 2007). Ten minutes before measurement, 1 mL of seawater sample should be mixed with 10 μL of SYBR Green I working solution and vortexed. FL1 is used for as trigger parameter. The cluster of prokaryotes that appears on an FL1-FSC (or SSC) cytogram includes the cyanobacterium *Prochlorococcus* with faint chlorophyll fluorescence; it is required to correct for it (Sieracki et al., 1995). On the cytogram, more than two clusters with different FL1 intensities are sometimes observed, which possibly reflect their ecological difference (Gasol and del Giorgio, 2000). Differentiation of the clusters becomes easier when membrane permeability is enhanced by chemical fixation (Kamiya et al., 2007).

After measurement, tubing should be rinsed repeatedly, which is followed by an appropriate shutdown procedure. Because the residual stains in the tubing may cause noise, the use of a surfactant detergent is recommended after using a staining reagent. The machine operating time should be recorded

for quality control of the laser.

3. Sample preservation

Owing to the limitation of space or time, samples collected for flow cytometry are sometimes preserved. Among the various preservation methods available, most include chemical fixation by aldehyde, snap freezing in liquid nitrogen, and storage at $-80\text{ }^{\circ}\text{C}$. Glutaraldehyde, paraformaldehyde, or a combination of the two is widely used as fixative. Since preservation efficiency depends on species composition, its physiological status and the method used (Vaulot et al., 1989; Trousselier et al., 1995; Sato et al., 2007), the optimum method applicable to every marine microbial community is yet to be established. Here, I introduce a simple preservation method using glutaraldehyde, which has high fixation efficiency.

Prior to sampling, 20% glutaraldehyde solution (for electron microscopy) should be filtered through a disc filter by using a syringe to remove particles that may cause noise. Using a micropipette, dispense the samples into cryovials ($\sim 5\text{ mL}$), and then add the glutaraldehyde solution at a final concentration of 1% by using a microdispenser. Tightly close the lids, mix the solution within the cryovials by gentle shaking, and leave them still for 10 min in a refrigerator before snap-freezing in liquid nitrogen. If the dry shipper is not large enough to contain all samples, some samples can be stored in a deep freezer after snap freezing. For transportation, dry ice is recommended to maintain the lowest possible temperature. The preserved samples should be thawed in running water just before measurement. Ensure that there is no ice remaining in the samples. Refreezing of the samples is not recommended. Recently, it was reported that glutaraldehyde fixation with the addition of small amounts of surfactant can greatly improve cell preservation (Marie et al., 2014).

References

- Ackleson, S. G. and R. W. Spinrad (1988): Size and refractive index of individual marine particles: a flow cytometric approach. *Appl. Opt.*, 27, 1270-1277.
- Cucci, T. L. and M.E. Sieracki (2001): Effects of mismatched refractive indices in aquatic flow cytometry. *Cytometry*, 44, 173-178.
- Gasol, J. M. and P. A. del Giorgio (2000): Using flow cytometry for counting natural planktonic bacteria and understanding the structure of planktonic bacterial communities. *Sci. Mar.*, 64: 197-224.
- Kamiya, E., S. Izumiyama, M. Nishimura, J. G. Mitchell, and K. Kogure (2007): Effects of fixation and storage on flow cytometric analysis of marine bacteria. *J. Oceanogra.*, 63: 101-112.
- Marie, D., F. Partensky, S. Jacquet, and D. Vaulot (1997): Enumeration and cell cycle analysis of natural populations of marine picoplankton by flow cytometry using the nucleic acid stain SYBR Green I. *Appl. Environ. Microbiol.*, 63: 186-193.
- Marie, D., F. Partensky, D. Vaulot, S. Brussaard (1999): Enumeration of phytoplankton, bacteria, and viruses in marine samples. In *Current Protocols in Cytometry Supplement 10*, ed. by J. P. Robinson, Z. Darzynkiewicz, P. N. Dean, A. Orfao, P. S. Rabinovitch, C. C. Stewart, H. J. Tanke, L. L. Wheelless and L. G. Dressier, Wiley, New York.

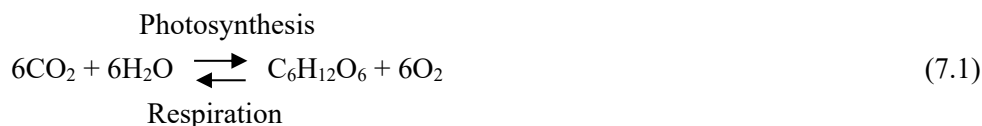
- Marie, D., F. Rigaut-Jalabert, and D. Vaultot (2014): An improved protocol for flow cytometry analysis of phytoplankton cultures and natural samples. *Cytometry A*, 85: 962-968.
- Patel, A., R. T. Noble, J. A. Steele, M. S. Schwalbach, I. Hewson, and J. A. Fuhrman (2007): Virus and prokaryote enumeration from planktonic aquatic environments by epifluorescence microscopy with SYBR Green I. *Nature Protocols*, 2: 269–276.
- Sato, M., S. Takeda, and K. Furuya (2006): Effects of long-term sample preservation on flow cytometric analysis of natural populations of pico- and nanophytoplankton. *J. Oceanogr.*, 62: 903-908.
- Sato, M., F. Hashihama, S. Kitajima, S. Takeda, and K. Furuya (2010): Distribution of nano-sized *Cyanobacteria* in the western and central Pacific Ocean, *Aquat. Microb. Ecol.*, 59, 273-282.
- Sieracki, M. E., E. M. Haugen, and T. L. Cucci (1995): Overestimation of heterotrophic bacteria in the Sargasso Sea: direct evidence by flow and imaging cytometry. *Deep-Sea Res. I*, 42: 1399-1409.
- Troussellier, M., C. Courties and S. Zettelmaier (1995): Flow cytometric analysis of coastal lagoon bacterioplankton and picophytoplankton: fixation and storage effects. *Est. Coast. Shelf Sci.*, 40, 621-633.
- Vaultot, D., C. Courties and F. Partensky (1989): A simple method to preserve oceanic phytoplankton for flow cytometric analyses. *Cytometry* 10: 629-635.

Primary Production

Koji Suzuki (Hokkaido University)

1. Introduction

Production of organic matter through phytoplankton photosynthesis (i.e. primary production) can be simply expressed as Equation 7.1:



Global annual net primary production (gross primary production minus respiration) by phytoplankton on the basis of carbon is estimated to be ca. 50×10^{15} g C, which is roughly equivalent to those produced by terrestrial plants (Raven, 2009). As field techniques for determining the primary production by phytoplankton, carbon fixation, oxygen evolution and chlorophyll fluorescence measurements have been used (Marra, 2002). Here I introduce the ^{13}C technique (Hama et al., 1983), because this method has been widely used in Japan for the determination of primary production by marine phytoplankton. For the ^{13}C technique which is one of the carbon fixation methods, a small amount of sodium bicarbonate labelled with ^{13}C ($\text{NaH}^{13}\text{CO}_3$) is enriched into seawater sample, followed by incubation for a certain time period, and measure the fixed organic carbon labelled with ^{13}C to estimate primary productivity (i.e. primary production rate). For the measurements of primary production by marine phytoplankton, the higher-sensitive, radioisotope labelled ^{14}C technique has been widely used in the world. However, in some countries including Japan where the use of radioisotopes outside has been severely limited, the ^{13}C method would be in use more conveniently. A good agreement between ^{14}C - and ^{13}C -based primary productivity has been observed (Hama et al., 1983). Marra (2009) pointed out that ^{14}C uptake over daytime (dawn to dusk) periods estimates net primary production, whereas 24-h ^{14}C assimilation approximates daily net community production (i.e. net primary production minus heterotrophic respiration) based on the O_2 method, but the former is perhaps slightly higher than the latter.

2. Sample collection and incubation

Seawater samples are generally collected by using water samplers (e.g. Niskin bottles, which are pre-washed with neutral detergent, followed by diluted hydrochloric acid and pure water to avoid any metal contamination). First seawater for the determination of total dissolved inorganic carbon (DIC) concentrations should be transferred into glass bottles without air bubbles. To suspend any biological activity, saturated mercury chloride (II) solution (0.02% (in volume) at the final concentration) is added to each DIC bottle. The sample bottles are closed tightly and then stored at room temperature. The DIC concentrations can be determined by coulometry, pH sensor, and so on (see Vol. 3, Chapter 4) soon after the sample collection. As incubation bottles for primary production measurement, more than four

polycarbonate bottles, which are pre-washed by neutral detergent and 10% (in volume) hydrochloric acid, with ca. 250 and 500–1000 ml for coastal and oceanic waters, respectively, should be prepared, and the two are for light bottles and one is for dark bottle (covered with black tape, etc.). One can be prepared for the determination of particulate inorganic carbon (PIC) concentrations before the addition of ^{13}C . Size of the incubation bottles used for primary production measurement is dependent on the amount of organic matter in seawater, but larger bottles would be better to minimize the physical effect of bottle walls (i.e. bottle effect). A certain amount of seawater is filled into each incubation bottle. Furthermore, a small amount of $\text{NaH}^{13}\text{CO}_3$ solution is added to the light and dark bottles to become ca. 10% in terms of ^{13}C abundance. For reference, DIC concentrations in surface oceanic waters are generally ca. 2 mmol kg^{-1} (corresponding to 24 mg C L^{-1} ; Zeebe and Wolf-Gladrow, 2001). However, the DIC concentrations can vary in other marine environments, therefore approximate DIC levels should be estimated before experiments. Incubation can be conducted from a few hours to 1 day using in situ or simulated in situ methods. For the in situ technique, the seawater samples collected from surface layers of the water column are dispensed into incubation bottles, followed by ^{13}C addition, returned the bottles to the sampling layers using a moored system, and incubated for a certain time period. For the simulated in situ method, on the other hand, the samples are incubated in a water tank on land or on board for a certain period by simulating the sampling site environments (light and temperature) using temperature controllers, neutral light screen and/or filters. Immediately after the start of incubation, seawater samples for the determination of natural ^{13}C abundance of particulate organic carbon (POC) (i.e. before ^{13}C enrichment) should be filtered with pre-combusted (450°C , $\geq 4 \text{ h}$) glass-fiber filter (e.g. 25 mm Whatman GF/F) soon (in the case of vacuum filtration, the pressure should be $< 0.016 \text{ MPa}$). The filter combustion can be made in an electric furnace to remove organic carbon attached to the filter. The sample filters obtained are stored in a freezer at $< -20^\circ\text{C}$. After incubation, seawater from the light and dark bottles also should be filtered soon and the filters obtained can be stored in the same manner as above.

3. Sample pre-treatment

The frozen filters stored are melted at room temperature and exposed to the vapor from hydrochloric acid in order to remove PIC from them. After the procedures, the filters should be completely dried in a desiccator.

4. Sample pre-treatment

The concentration and ^{13}C abundance of POC are determined with an elemental analyzer and a mass spectrometer or an infrared spectrometer, respectively. For the POC concentration, refer to the text in Vol. 4, Chapter 1. Also, for the determination of ^{13}C abundance, follow the manufacture's manual.

To estimate the primary production by phytoplankton using ^{13}C method, the following mass balance equation of ^{13}C abundance before and after incubation can be set:

$$a_{\text{is}} \cdot \text{POC} = a_{\text{ns}} \cdot (\text{POC} - \Delta\text{POC}) + a_{\text{ic}} \cdot \Delta\text{POC} \quad (7.2)$$

where a_{is} and a_{ns} are ^{13}C abundance (^{13}C atom%) in POC after incubation and that before ^{13}C addition, respectively. POC is the concentration of POC after incubation. ΔPOC is the concentration of POC increased during incubation. By solving the Equation 7.2 for ΔPOC , the following Equation 7.3 can be obtained:

$$\Delta POC = POC \cdot (a_{is} - a_{ns}) / (a_{ic} - a_{ns}) \quad (7.3)$$

Primary productivity (i.e. primary production rate; P) can be estimated by dividing ΔPOC in the Equation 7.3 by the time period of incubation T and these are multiplied by the fractionation factor of ^{13}C (=1.025; Hama et al., 1983).

$$P = \Delta POC \cdot f / T = [POC \cdot (a_{is} - a_{ns})] \cdot f / [(a_{is} - a_{ns}) \cdot T] \quad (7.4)$$

For the estimates of P , the mean and its standard deviation can be calculated using the values from light and dark bottles. Also, for the correction of non-photosynthetic carbon fixation and the adsorption of ^{13}C , values from light bottles should be subtracted from those from dark bottles.

Values of P normalized by chlorophyll a concentration (see Vol. 4, Chapter 4) have been used for an index of phytoplankton-abundance specific primary productivity.

References

- Hama, T., T. Miyazaki, Y. Ogawa, T. Iwakuma, M. Takahashi, A. Otsuki, S. Ichimura (1983): Measurement of photosynthetic production of a marine phytoplankton population using a stable ^{13}C isotope. *Mar. Biol.*, 73, 31–36.
- Marra, J. (2002): Chapter 4, Approaches to the measurement of plankton production, p. 78–108, In *Phytoplankton Productivity: Carbon Assimilation in Marine and Freshwater Ecosystems*, edited by P. J. le B. Williams, D. N. Thomas and C. S. Reynolds, Blackwell Science, Oxford.
- Marra, J. (2009): Net and gross productivity: weighing in with ^{14}C . *Aquat. Microb. Ecol.* 56, 123–131.
- Raven, J. A. (2009): Volume 4, Primary production processes, p. 585–589. In *Encyclopaedia of Ocean Sciences*, 2nd Edition, edited by, J. H. Steele, S. A. Thorpe and K. K. Turekian, Academic Press, London.
- Zeebe, R. E., Wolf-Gladrow, D. (2001) *CO₂ in Seawater: Equilibrium, Kinetics, Isotopes*, Elsevier, 346 pp.

This page left intentionally blank.

Seabed sediment sampling

○Hisashi NARITA (Tokai University)/ Shigeyoshi OTOSAKA (Japan Atomic Energy Agency)

Seabed sediments are classified into coastal, hemipelagic, and pelagic sediments. The sedimentation rate, grain size, and chemical and mineralogical characteristics of these sediments vary greatly depending on the cycling of materials in the marine environment and sedimentary environments of the respective region. The collection and analysis of marine sediments clarifies the characteristics of this cycling allowing determination of the source material deposited on the seafloor and understanding the nature of primary production in the surface layer. In addition, the information recorded in the seabed sediments serves as historical markers to unravel past regional and global changes in environment, circulation, and climate.

1. Selection of sampling location

Collection of seabed sediment is typically referred to as “bottom sampling”. A rope or cable with a bottom sampler attached is lowered from the ship to the seabed. Because the sedimentation process of various seafloor materials is greatly influenced by the topography of the site, it is necessary to carefully select sampling points considering the surrounding topography and the bottom environment. Abundant topographical data are available for the coastal area, including much of the continental shelf. Chart symbols/abbreviations (R, S, M, Sh, etc.) can be used as approximate information on the seafloor, where R, S, M, and Sh indicate rock, sand, mud, and shell, respectively. However, detailed topographical and sedimentary information required to determine sampling points is generally limited in much of the open ocean. Therefore, when collecting seabed sediments, especially several meters of core samples, it is recommended to obtain information on bottom sediments and topographical information before selecting sampling points.

To acquire topographic information of the seabed, systematic observation using either a precision depth recorder (PDR) or multi-beam echo sounder is necessary. To understand the nature of the underlying sediments, a sub-bottom profiler is often utilized. This system transmits a ~3.5 kHz sound pulse from the research vessel and receives reflections from the seabed and underlying sediments. Based on this system, it is possible to obtain acoustic images of geological profiles up to several tens of meters below the seafloor with high resolution.

2. Sediment samplers

“Sediment sampling” means to collect sediments, rocks and benthic organisms from seabed sediments. A variety of bottom samplers have been developed according to purpose and sediment types. They are roughly classified into dredges, grab samplers, and core samplers. A steel cable generally used to deploy this heavy equipment. To confirm that the sampler has landed on the seabed or that the sample enters the sampler, a tensiometer is commonly used to monitor the tension of the cable.

2-1 Dredge samplers

A dredge sampler consists of a cylinder or a box-shaped, steel bucket. Sediments, rocks, and benthos are collected by towing this device on the seafloor. To tow a dredge sampler, the cable length needs to be longer than the water depth. However, care should be taken because the cable may be damaged if it is extended too long. Because this device dredges on the seafloor for a given distance, the obtained sediments will show an average composition in certain areas. For this reason, this device is not suitable for the collection of samples at a fixed point on the seafloor. In addition, samples may be disturbed or decomposed during the dredging, and some samples may selectively flow out when the sampler is retrieved on board the ship.

2-2 Grab samplers

The grab sampler collects sediment samples by rotating and closing two opposed semicylindrical buckets. It collects the upper (~10 cm) sediments with minimal disturbance across a relatively wide surface area, even in sand or gravel. The trigger for closing the buckets may be activated by either a shock upon landing on the seafloor (Smith-McIntyre sampler) or by operating a trigger with a “messenger” weight after landing (Ekman-Burge sampler). Both samplers can be used to precisely identify the sampling point and are suitable for understanding the inventory of chemical substances and the standing stock of the benthic organisms in the sediment because of collection along a constant surface area. Because they are compact and lightweight, grab samplers are also widely used for sampling by small boats in shallow water.

An OKEAN-type grab sampler using a balance as a bottom trigger is used for sediment collection in the deep sea. Although the sample is sometimes disturbed by the operation wire used for closing the bucket, it can collect coarse sediments, such as gravel, because of its heavy weight.

The box corer is an improved type of grab sampler, which was designed to collect sediments to a depth of approximately several tens of centimeters without disturbance. It consists of a core box with a 30 cm or 50 cm cube coupled to a core cutter (called a spade) that functions as a bottom cover for the penetrated core box. In addition to being capable of collecting undisturbed surface sediments, it is also suitable for collecting a large volume of sediment. As necessary, core samples can be obtained by penetrating subcores into the core box after retrieval of the box corer on board. Therefore, the box corer is sometimes categorized as a core sampler rather than a grab sampler.

2-3 Core samplers

The core sampler is a device that penetrates a barrel (cylindrical pipe) vertically into the seabed and collects sediments with a length of several tens of cm or more. Devices used to penetrate the barrel include gravity, vibration, push-in corers. The gravity corer is widely used for oceanographic observations. It simply penetrates the barrel into the sediment by its own weight. A piston corer prevents the loss of samples based on the negative pressure in the piston attached to the barrel. Both gravity and piston corers can collect samples from 1 m to several tens of meters but are not suitable to collect sand and gravel. To collect sediments in shallow water, other types of core sampler, such as

the vibration corer and push-in-type thin wall sampler, are used. These corers can also collect sandy sediments and the disturbance of the sample is relatively small.

Recently, multiple (multi-barrel) corers with several polycarbonate pipes with a diameter of 60 to 80 mm and a length of 600 mm are widely used for the collection of surface sediments with a length of about 300 mm. The multiple corer can slowly penetrate cores into sediment by its own weight, with the speed of 5 mm s⁻¹ or less, by regulating the amount of seawater discharged from the cylinder at the center of the main frame of the corer (Barnett *et al.*, 1984). To complete the core penetration based on mechanical characteristics, it is necessary to wait for 1.5~2 min in case of muddy sediments and > 1~2 min for sandy sediments after the corer landed on the seabed. In addition, it is necessary to let out the cable for a few meters to a few tens of meters after the landing of the corer and monitor tension to confirm that the corer is not lifted during the waiting time. In case it is expected that the cable will experience tension during the waiting time due to the movement of the boat, the wire should be extended a few more meters than needed. The advantage of this device is that it can also collect the overlying water above the seafloor without disturbing the sediment-water interface (Shirayama and Fukushima, 1994).

References

- Barnett, P.R.O, J. Watson and D. Connelly (1984): A multiple corer for taking virtually undisturbed samples from shelf, bathyal and abyssal sediments. *Oceanologica Acta*. **7** (4), 399-408.
- Shirayama, Y. and T. Fukushima (1994): Comparisons of deep-sea sediments and overlying water collected using Multiple Corer and Box Corer. *Journal of Oceanography*. **51**, 75-82.

This page left intentionally blank.

Physical properties of sediment (water content, bulk density and porosity)

○Hisashi NARITA (Tokai University) /Shigeyoshi OTOSAKA (Japan Atomic Energy Agency)

Parameters reflecting the physical properties of seabed sediments include water content, porosity, and dry bulk density. In particular, the water content and porosity can be measured relatively easily. These parameters are related to the composition, average density, or the particle size of the sediments (Meade, 1966, Nafe and Drake, 1957). Therefore, the water content and porosity are effective primary information on the sedimentation process and composition of the sediment. In Japan, density and water content are regulated based on the Japan Industrial Standard “Test method for density of soil particles” (JIS A 1202) and “Test method for water content of soils” (JIS A 1203), respectively.

1. Water content

The water content is the ratio of the mass of water lost during drying of homogeneous sediment to the wet sediment. It is defined by the following equation:

$$w = \frac{m_{pw}}{m_{wet}} \times 100$$

where

- w : Water content (%)
- m_{pw} : Mass of water lost during drying (g)
- m_{wet} : Mass of wet sediment (g)

1-1 Measurement method

The measurement method is as follows:

1. Weigh the mass m_c (g) of the container (heat-resistant) after heating and cooling. If the mass of the sample is below 10 g, use an electronic balance capable of reading the mass of 0.0001 g. If the sample mass is between 10~100 g, an electronic balance capable of reading the mass of 0.001 g is used. In addition, it is necessary to confirm that the mass of the container is constant (difference of the minimum digit is within ± 5). Therefore, an average of two consecutive measurements is used as the m_c value.
2. Place the wet sediment sample in a container and measure the gross mass m_a (g).
3. Put the sediment sample in a constant-temperature drying oven together with the container and dry it at 110 ± 5 °C to obtain a constant mass. It generally takes 12 to 24 hr to reach a constant mass depending on the amount of sample to be dried. When measuring pigments and organic matter in the sediment, high-temperature heating should be avoided. In such cases, freeze each container,

Guideline of ocean observations Vol. 5 Chap. 2

Physical properties of sediment (water content, bulk density and porosity)

© Hisashi NARITA, Shigeyoshi OTOSAKA 2018 G502EN:001-013

put the frozen sample together with the container in a vacuum freeze dryer, and dry the sample after completing step 2.

4. Transfer the dried sample to a desiccator together with the container and measure the total mass m_b (g) after cooling it to room temperature. If necessary, the drying and weighing processes are repeated. In case the sediment has high a content of organic matter or biogenic particles, the mass may increase during measurement due to moisture absorption after drying. Therefore, it is desirable that the air temperature and relative humidity of the laboratory is controlled at 20~25 °C and 50~60 %, respectively, during weighing. In addition, weighing should be done quickly after taking out the sample from the desiccator.

1-2 Calculation

The water content is calculated as follows:

$$w = \frac{m_{wc} - m_{sc}}{m_{wc} - m_c} \times 100$$

where

- w : water content (%)
- m_{wc} : Mass of container with wet sediment (g)
- m_{sc} : Mass of container with dried sediment (g)
- m_c : Mass of container (g)

2. Porosity

The porosity is defined as the ratio of the pore volume to the total volume of sediment sample. In general, it is denoted as ϕ :

$$\phi = \frac{V_{pw}}{V_{wet}} \times 100$$

where

- ϕ : Porosity (%)
- V_{wet} : Volume of homogenous wet sediment (ml)
- V_{pw} : Volume of pore water in the wet sediment (ml)

Because it is difficult to directly measure V_{wet} and V_{pw} , volume of wet sediment is calculated by dividing the mass of dried sediment by dry bulk density. Otherwise, the porosity is calculated with the following equation under the assumption that the volume of the wet sediment is the sum of the volume of the solid phase and liquid phase (pore water) and the volume of pore water in the wet sediment is equal to the volume of water reduced by drying. It should be noted that the mass of the

dried sediment includes the mass of the salt precipitated by drying in addition to the mass of sediment particles. Therefore, the dry bulk density and the density of sediment particles used here are the apparent dry bulk density and the density of sediment particles including salts (see 2-8 and 2-4, 2-6).

$$\phi = \frac{m_{pw}/\rho_w^t}{m_s/\rho_{DB}^{ap}} \times 100 = \frac{m_{pw}/\rho_w^t}{m_s/\rho_s^{ap} + m_{pw}/\rho_w^t} \times 100$$

where

ϕ : Porosity

m_{pw} : Mass of water lost during drying (g)

m_s : Mass of dried sediment including salt (g)

ρ_w^t : Density of pure water under room temperature (kg m^{-3})

ρ_{DB}^{ap} : Apparent dry bulk density of the dried sediment with salt (kg m^{-3}) (see section 2.6)

ρ_s^{ap} : Apparent mean density of sediment with salt (kg m^{-3})

Additionally, by dividing the denominator and numerator by the mass of wet sediment m_{wet} (g), the porosity ϕ (%) can also be expressed as a function of water content w (%), water density, and mean density of sediment (Berner, 1971).

$$\phi = \frac{w/100\rho_s^{ap}}{(1-w/100)\rho_w^t + w/100\rho_s^{ap}} \times 100$$

2-1 Measurement method

The measurement method is as follows. Details follow the procedure described in Section 1-1.

1. Measure the mass of the container (beaker or plastic container) m_c (g).
2. Place the wet sediment sample in a container and measure the total mass m_{wc} (g).
3. Put the sediment sample in a constant-temperature drying oven together with the container or in a vacuum freeze dryer after freezing.
4. Transfer the dried sample to a desiccator together with the container and measure the gross mass m_{sc} (g) after cooling it to room temperature.
5. Calculate the water content w according to Section 1-2.

2-2 Calculation

The porosity ϕ is calculated as follows:

$$\phi = \frac{w/100\rho_s^{ap}}{(1-w/100)\rho_w^t + w/100\rho_s^{ap}} \times 100$$

In this calculation, use 998.2 kg m^{-3} (density of pure water at $20.0 \text{ }^\circ\text{C}$) as the density of pure water ρ_w (kg m^{-3}). In general, the mean density of sediment particles ρ_s (kg m^{-3}) is about 2500 kg m^{-3} (Berner, 1980). However, the mean density of sediment particles can be changed due to the composition of sediment (content of organic matter, biogenic carbonate, and biogenic opal). In addition, the apparent density of sediment particles ρ_s^{app} (kg m^{-3}) greatly varies with the amount of salt depending water content. Therefore, it is desirable to directly measure the mean density of and apparent density of sediment particles of each sample or each station. In the following sections, methods for the density measurement of sediment particles are described.

2-3 Measurement method of density of sediment particles using a pycnometer

Measurement of density of sediment particles is as follows. In the measurement, use an electronic balance capable of reading the mass of 0.001 g .

1. Measure mass of a 50-ml pycnometer m_f (g) after dried and cooled.
2. Remove the stopper of the pycnometer, fill with pure water so that bubbles do not stick on the inner surface, replace the stopper, wipe water drops on the outer surface of pycnometer, and measure the total mass m_a^1 (g). The m_a^1 is the sum of the mass of pure water m_w^1 and the mass of a pycnometer m_c .
3. Remove the stopper, insert a thermometer in the pycnometer, and measure the water temperature t_1 ($^\circ\text{C}$)
4. Discard water, dry the pycnometer. Pour about 15 g (about 1 cm height) of dried sediment into the dried pycnometer, and measure the mass m_s (g).
5. Add pure water up to about $2/3$ of the pycnometer and leave it for more than 12 hours to remove air bubbles in the sediment sample.
6. Heat the pycnometer containing the sample with a water bath for 1~2 hours. To remove bubbles, gently shake the pycnometer sometimes during the heating. After air bubbles were sufficiently removed, cool the pycnometer until the water temperature reaches room temperature.
7. Fill the pycnometer with pure water, set the stopper, wipe water drops on the outer surface of pycnometer, and measure the total mass m_a^2 (g). The m_a^2 is the sum of the mass of pure water m_w^2 , the mass of dried sediment m_s , and the mass of a pycnometer m_c .
8. Measure the temperature t_2 ($^\circ\text{C}$) inside the pycnometer.

2-4 Calculation

By the method described in section 2-3, the mass of pure water m_w^s is calculated as follows:

$$m_w^s = m_a^1 + m_s - m_a^2 = m_w^1 - m_w^2$$

The m_w^s corresponds to the volume of sediment particles in the pycnometer. To obtain the volume of the dried sediment, the buoyancy correction is applied to the mass of pure water, and divided by the density of pure

water. Because salt in the dried sediment dissolves to pure water by the step 7 in section 2-3, the obtained volume is regarded as that of sediment particles without salt. However, when the water temperature of pure water is different between steps 2 and 7, it is necessary to consider the volumetric change of the pycnometer due to the density change of the glass.

$$V_{c, \text{calc}}^1 = V_c^1 [1 + \alpha_v (t_2 - t_1)]$$

where

V_c^1 : Volume of pycnometer using at temperature t_1 (ml).

$V_{c, \text{calc}}^1$: Volume of pycnometer using at temperature t_2 (ml).

The mass of a pycnometer $m_{a \text{ calc}}^1$ when it is filled with pure water at temperature t_2 ($^{\circ}\text{C}$) is calculated from the mass of the pycnometer m_a^1 filled with pure water at temperature t_1 ($^{\circ}\text{C}$).

$$m_{a \text{ calc}}^1 = \frac{(\rho_w^2 - \rho_{\text{air}}) [1 + \alpha_v (t_2 - t_1)]}{\rho_w^1 - \rho_{\text{air}}} (m_a^1 - m_c) + m_c$$

where

m_a^1 : Mass of the pycnometer filled with pure water at temperature t_1 ($^{\circ}\text{C}$) (g)

m_a^{2w} : Mass of the pycnometer at when it is filled with pure water at temperature t_2 ($^{\circ}\text{C}$) (g)

t_2 : Temperature inside of the pycnometer at when m_a^1 was measured ($^{\circ}\text{C}$)

t : Temperature inside of the pycnometer at when m_a^2 was measured ($^{\circ}\text{C}$)

m_c : Mass of the pycnometer (g)

ρ_w^1 : Density of pure water at temperature t_1 ($^{\circ}\text{C}$) (kg m^{-3})

ρ_w^2 : Density of pure water at temperature t_2 ($^{\circ}\text{C}$) (kg m^{-3})

ρ_{air} : Density of air (kg m^{-3})

α_v : Coefficient of cubical expansion of the pycnometer (K^{-1})

The density of air is lower than that of pure water, and the coefficient of cubical expansion of glass is negligible if the difference between t_1 and t_2 is within 2 $^{\circ}\text{C}$. Since the relative influence of these terms on $m_{a \text{ calc}}^1$ is less than 0.05%, the above equation can be simplified as the follows:

$$m_{a \text{ calc}}^1 = \frac{\rho_w^2}{\rho_w^1} (m_a^1 - m_c) + m_c$$

Considering the change in temperature during the measurements, the mass of pure water m_w^s is calculated as follows:

$$m_w^s = m_{a\text{ calc}}^1 + m_s - m_a^2 = m_{w\text{ calc}}^1 - m_w^2$$

where

$m_{w\text{ calc}}^1$: Mass of pure water considering the temperature change of the mass of pure water from

$$m_w^1 \text{ (g)}$$

$$m_{a\text{ calc}}^1 = \frac{(\rho_w^2 - \rho_{\text{air}}) [1 + \alpha_v (t_2 - t_1)]}{\rho_w^1 - \rho_{\text{air}}} m_w^1$$

or,

$$m_{w\text{ calc}}^1 = \frac{\rho_w^2}{\rho_w^1} m_w^1$$

Thus, the volume of sediment particles measured by a pycnometer V_{solid} (ml) becomes as follows:

$$V_{\text{solid}} = \frac{(m_{w\text{ calc}}^1 - m_w^2) \frac{1 - \rho_{\text{air}}/\rho_{\text{weight}}}{1 - \rho_{\text{air}}/\rho_w^2}}{\rho_w^2 \times 10^{-3}}$$

where

ρ_{weight} : Density of a balance weight (kg m⁻³)

The mean density of the sediment particles is calculated by dividing the volume of sediment particles V_{solid} by mass of dried sediment m_s . Since the mass of dried sediment m_s includes the mass of salt originated from pore water, the apparent density of sediment particles ρ_s^{ap} is calculated with the following equation:

$$\rho_s^{\text{ap}} = \frac{m_s \frac{1 - \rho_{\text{air}}/\rho_{\text{weight}}}{1 - \rho_{\text{air}}/\rho_s^{\text{ap}}}}{V_{\text{solid}}} \times 10^3$$

$$\rho_s^{\text{ap}} = \left[\frac{m_s}{m_{w\text{ calc}}^1 - m_w^2} (\rho_w^2 - \rho_{\text{air}}) + \rho_{\text{air}} \right] \times 10^3$$

If the above-mentioned processes are performed using the desalted dried sediments, the mean

density of sediment particles ρ_s can be obtained. For the desalting of the dried sediment, a proper amount of dried sediment is put in a 50 ml centrifuge tube, add 50 ml of pure water, centrifuge, and remove the overlying water. These processes are repeated for four times. When the dry mass of the desalted sediment is defined as $m_s^{\text{salt free}}$, the density of sediment particles ρ_s can be calculated by the following equation.

$$\rho_s = \frac{m_s^{\text{salt free}} \frac{1 - \rho_{\text{air}} / \rho_{\text{weight}}}{1 - \rho_{\text{air}} / \rho_s}}{V_{\text{solid}}} \times 10^3$$

$$\rho_s = \left[\frac{m_s^{\text{salt free}}}{m_{\text{w calc}}^1 - m_{\text{w}}^2} (\rho_{\text{w}}^2 - \rho_{\text{air}}) + \rho_{\text{air}} \right] \times 10^3$$

2-5 Measurement method of density of sediment particles using a gas pycnometer

In recent years, density measurement using a helium (He) gas pycnometer has been widely used instead of the wet density measurement described in section 2-3. Fig. 1 shows the principle of the measurement by a gas pycnometer. The volume of the sample used for the analysis is expressed by the following equation

$$V_s' = V_{\text{cell}} - \frac{V_{\text{exp}}}{\frac{p_1 - p_a}{p_2 - p_a} - 1}$$

Using the atmospheric pressure as a reference, the above equation becomes as follows.

$$V_s' = V_{\text{cell}} - \frac{V_{\text{exp}}}{\frac{p_1}{p_2} - 1}$$

where,

- V_s' : Total volume of dried sediment V_s and sample container V_c (ml)
- V_{cell} : Volume of sample cell (ml)
- V_{exp} : Volume of expansion cell (ml)
- p_a : Pressure when all cells are replaced with He gas and at the ambient pressure (kPa)
- p_1 : Pressure when sample cell is replaced and pressurized with He gas (kPa)
- p_2 : Pressure in the entire system when the valve between the both cells is open (kPa)

When measuring the volume of dry sediment with a gas pycnometer, the dry sediment is placed in a glass or plastic container, etc. For this reason, it is necessary to measure the volume of the container first and subtract the volume from the total volume of dry sediment and containers with the following

equation.

$$V_s = V'_s - V_c$$

where,

V'_s : Volume of dry sediment (ml)

V_c : Volume of sample container used for the measurement (ml)

The volume of dry sediment measured by a pycnometer, V'_s , includes volume of salt separated from seawater during the drying process. In order to estimate actual volume of dry sediment, it is necessary to subtract the volume of salt from V'_s .

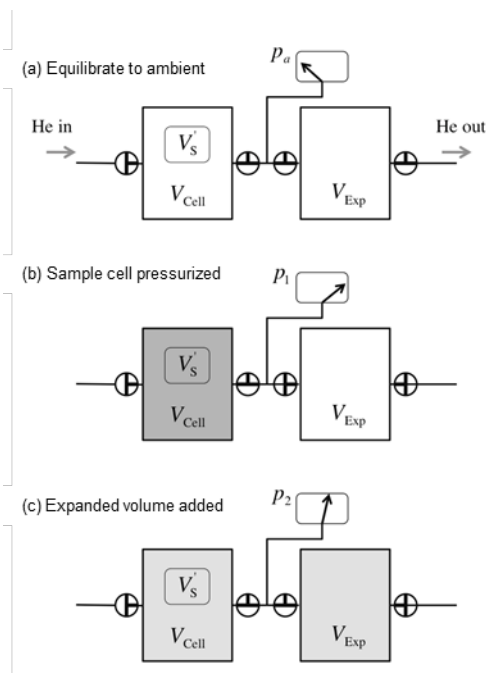


Fig 1: Schematics of operating sequence of a gas pycnometer

2-6 Calculation

The mass of the wet sediment is the sum of the masses of the sediment particles, the water lost by drying and the precipitated salt as shown below.

$$m_{\text{wet}} = m_{\text{solid}} + m_{\text{w}} + m_{\text{salt}}$$

where

m_{wet} : Mass of wet sediment (g)

m_{solid} : Mass of sediment particles (g)

m_{w} : Mass of water lost during drying (g)

m_{salt} : mass of salt evaporated during drying (g)

The mass of dry sediment m_s , described in section 2-4, is the sum of masses of the sediment particles and salt.

$$m_s = m_{\text{solid}} + m_{\text{salt}}$$

Considering that the mass of water lost during the drying m_w is derived from pore water, the mass of the precipitated salt m_{salt} can be estimated using the absolute salinity S . Furthermore, by dividing m_{salt} by the density of the salt (ρ_{salt} : 2200 kg/m³), the volume of the salt V_{salt} can be calculated. The volume of the sediment particles V_{solid} can be determined by subtracting the volume of salt V_{salt} from the total volume of the dry sediment V_s .

In this calculation, it is preferable to use the practical salinity of seawater in the bottom layer at the sampling point as the absolute salinity of pore water.

$$m_{\text{salt}} = \frac{S}{10^3 - S} m_w$$

$$V_{\text{salt}} = \frac{m_{\text{salt}}}{\rho_{\text{salt}} \times 10^{-3}}$$

$$V_{\text{solid}} = V_s - V_{\text{salt}}$$

where

m_{salt} : Mass of salt evaporated during drying (g)

m_w : Mass of water lost during the drying (g)

S : Absolute salinity (g/kg)

V_{salt} : Volume of salt (ml)

ρ_{salt} : Density of salt (2200) (kg m⁻³)

V_s : Volume of dry sediment (ml)

V_{solid} : Volume of sediment particles (ml)

In addition, the density of sediment particles can be calculated by dividing the value obtained by subtracting the mass of salt m_{salt} from the mass of dried sediment with salt m_s by the volume of sediment particles.

$$\rho_s = \frac{m_s - m_{\text{salt}}}{V_{\text{solid}}} \times 10^3$$

2-7 Estimation of porosity from given volume of a container

For the estimation of the porosity as described above, it is necessary to assume or measure the apparent density of the sediment particles in addition to the density of the pure water. The apparent

density values largely affect the porosity. Because the apparent density is necessary to determine the volume of the wet sediment samples, the porosity can be measured without using the apparent density of the sediment particles by filling the wetting sediment into a container with a given volume. The methods are as follows. The detailed procedures are described in Section 2-2.

1. Weigh the mass of a given volume of heat-resistant plastic container, m_c (g), after heating and cooling. If the sample is less than 10 g, use an electronic balance capable of reading a mass of 0.0001 g. The volume of container, V_c (ml), is measured in advance.
2. Fill the wet sediment sample into the container and weigh the gross mass m_{wc} (g). Care should be taken not let bubbles into the container.
3. Put the sediment sample in a constant-temperature drying oven together with the container or in a vacuum freeze dryer after freezing.
4. Transfer the dried sample to a desiccator together with the container and measure the gross mass m_{sc} (g) after cooling it to room temperature.

2-8 Calculation

The porosity ϕ can be calculated using the following equation. This method can be applied to calculate the water content w (%) according to Section 1-2.

$$\phi = \frac{(m_{wc} - m_{sc}) / \rho_w^t}{V_c} \times 100$$

where

ρ_w^t : Density of pure water at temperature t (°C) (kg m^{-3})

m_{wc} : Gross mass of container including wet sediment sample (g)

m_{sc} : Gross mass of container including dried sediment sample (g)

V_c : Volume of the container (ml)

Additionally, by using a container with a given volume, the apparent dry bulk density of sediment ρ_{DB}^{ap} (kg m^{-3}) can be estimated as follows:

$$\begin{aligned} \rho_{DB}^{ap} &= \frac{m_{sc} - m_c}{V_c} \times 1000 \\ &= \frac{m_s}{V_c} \times 1000 \end{aligned}$$

where

- ρ_{DB}^{ap} : Apparent dry bulk density (kg m⁻³)
 m_{sc} : Gross mass of container including dried sediment sample (g)
 m_c : Mass of container (g)
 m_s : Mass of dried sediment containing salt (g)
 V_c : Volume of the container (ml)

The apparent dry bulk density of sediment ρ_{DB} can be calculated by dividing the value obtained by subtracting the mass of salt m_{salt} from the mass of dried sediment containing salt m_s by the volume of sediment particles V_c .

$$\rho_{DB} = \frac{m_s - m_{salt}}{V_c} \times 1000$$

2-9 Effect of salinity on measurement of physical properties of sediment

In the previous sections, except for the measurement using a gas pycnometer, pore water is regarded as pure water in calculations of water content, porosity, mean density of sediment particles and dry bulk density. However, the pore of the sediment collected by the sampling is usually filled with seawater. By evaporating the pore water during drying, the salt in the pore water is precipitated. Consequently, and the mass of dried sample includes the masses of sediment particles and the precipitated salt. Therefore, when considering the pore water as seawater, it is necessary to assume absolute salinity S (g kg⁻¹) of seawater for calculations. The water content, porosity, mean density of the sediment particles, and the dry bulk density are shown in the following equations for cases where the absolute salinity of pore water is S (g kg⁻¹) and the pore water is regarded as pure water.

	In the case of saline water	In the case of pure water
Water content	$w = \frac{10^3 / (10^3 - S) m_w}{m_{wet}} \times 100$	$w = \frac{m_w}{m_{wet}} \times 100$
Porosity	$\phi = \frac{[m_w 10^3 / (10^3 - S)] / \rho_{sw}^t}{(m_s - m_{salt}) / \rho_s + [m_w 10^3 / (10^3 - S)] / \rho_{sw}^t} \times 100$	$\phi = \frac{m_w / \rho_w^t}{m_s / \rho_s^{ap} + m_w / \rho_w^t} \times 100$

When pore water is regarded as pure water, the water content is underestimated by about 3.45% compared with the case saline pore water with salinity of 34.5g kg⁻¹. With regard to the porosity, even when regarding it as pure water, there is practically no problem if the apparent density of particles of sediment containing salt is used as density of sediment. However, it should be noted that the water content will be underestimated by 0.2~0.02% where the water content ranges 50 and 90% and by about 0.7% where the water content is 10%.

Salinity corrected

Salinity uncorrected

Guideline of ocean observations Vol. 5 Chap. 2

Physical properties of sediment (water content, bulk density and porosity)

© Hisashi NARITA, Shigeyoshi OTOSAKA 2018 G502EN:001-013

Density of sediment particles

$$\rho_s = \left[\frac{m_s^{\text{salt free}}}{m_{\text{w calc}}^1 - m_{\text{w}}^2} (\rho_w^2 - \rho_{\text{air}}) + \rho_{\text{air}} \right] \times 10^3 \quad \rho_s^{\text{ap}} = \left[\frac{m_s}{m_{\text{w calc}}^1 - m_{\text{w}}^2} (\rho_w^2 - \rho_{\text{air}}) + \rho_{\text{air}} \right] \times 10^3$$

Dry bulk density

$$\rho_{\text{DB}} = \frac{m_s - m_{\text{salt}}}{(m_s - m_{\text{salt}}) / \rho_s + [m_{\text{w}} 10^3 / (10^3 - S)] / \rho_{\text{sw}}^1} \times 10^3 \quad \rho_{\text{DB}} = \frac{m_s}{m_s / \rho_s^{\text{ap}} + m_{\text{w}} / \rho_{\text{w}}^1} \times 10^3$$

or,

$$\rho_{\text{DB}} = \frac{m_s - m_{\text{salt}}}{V_c} \times 10^3 \quad \rho_{\text{DB}} = \frac{m_s}{V_c} \times 10^3$$

Both the density of sediment particles and the dry bulk density are influenced significantly depending on the presence and its extent of absolute salinity. For example, a sediment sample with a water content of 95%, assuming the absolute salinity of 34.5 g kg⁻¹, the salt contributes 3.39 g on 1.61 g of the weight of sediment particles. In general, salinity of pore water is estimated by measuring the chlorine content and multiplying by 1.86055. However, the absolute salinity of pore water varies vertically due to dissolution of carbonate and biogenic opal, loss of magnesium or potassium due to reverse weathering, does not necessarily have a positive relationship with the chlorine content. Determination of the absolute salinity of pore water is practically difficult. When estimating water content, porosity, mean density of sediment particles and dry bulk density, it is advisable to substitute the practical salinity of seawater in the bottom layer at the sampling point. Changes in water content and porosity due to 1 g kg⁻¹ difference in absolute salinity are less than 0.1%, and the change in mean density of sediment particles is about ~0.3%. When the water content is 90% or more, the dry bulk density varies by up to 7% due to the change in absolute salinity of 1 g/kg, but the variation is less than 1% except this case.

In addition to importance as physical property value the dry bulk density is crucial for estimating inventory I (mol m⁻² or g m⁻²) and flux of a target component F (mol m⁻² yr⁻¹ or g m⁻² yr⁻¹) by the following equations.

$$I = \int_0^z C \rho_{\text{DB}} \times 10^{-3} dz$$

$$F = C \rho_{\text{DB}} \times 10^{-3} S_r$$

where

z : Depth in sediment (m)

C : Concentration of a target component in sediment (mol g⁻¹ or g g⁻¹)

ρ_{DB} : Dry bulk density (kg m⁻³)

S_r : Sedimentation rate (m yr⁻¹)

In general, the concentration of a chemical component of the sediment is measured as the amount or

mass of the component per dry weight of dry sediment containing salt, in order to avoid changes during the desalination process such as desorption of the target component. Therefore, there is no problem to use the pure water-based dry bulk density in calculating the abundance or flux of the target component. Conversely, when calculating the inventory or the flux using the saline water-based dry bulk density, the concentration of the target component in the sediment must be converted as concentration per mass of salt free dry sediment, and multiply the saline water-based dry bulk density.

$$C_{\text{salt free}} = \frac{(10^2 - w)(1 - S/10^3)}{10^2 - S/10 - w} C$$

where

$C_{\text{salt free}}$: Concentration of a component without containing salt (mol g⁻¹ or g g⁻¹)

S : Absolute salinity (g kg⁻¹)

w : Water content (%), equivalent to mass of pure water per 100 g of wet sediment (g)

References

- Meade, R.H. (1966): Factors influencing the early stages of the compaction of clays and sands – review. *J. Sed. Petrology*, **36**, 1085-1101.
- Nafe, J.E. and C.L. Drake (1957): Variation with depth in shallow and deep water marine sediments of porosity, density and the velocities of compressional and shear waves. *Geophysics*, **22**(3), 523-552.
- JIS A 1202, Test method for density of soil particles, Japanese Standard Association, Tokyo, (2009).
- JIS A 1203, Test method for water content of soils, Japanese Standard Association, Tokyo, (2009).
- Berner, R.A. (1971): Principles of Chemical Sedimentology. McGraw-Hill, New York, 92 pp.
- Berner, R.A. (1971): Early Diagenesis A Theoretical Approach. Princeton Series in Geochemistry. Princeton University Press, Princeton, NJ, 241pp.

This page left intentionally blank.

Loss on ignition

○Hisashi NARITA (Tokai University) /Shigeyoshi OTOSAKA (Japan Atomic Energy Agency)

As a method to estimate the organic carbon content in sediments, the loss of weight after combustion at 550 °C (loss on ignition: LOI) is commonly used (e.g., Dean, 1974, Heiri *et al.*, 2001). In the LOI method for suspended and sinking particles in seawater, samples are combusted at 450 °C (e.g., Honjo, 1980; Tsunogai *et al.*, 1982) to estimate the organic carbon content. On the other, the Japan Industrial Standard (2009) recommends combustion at 750 ± 50 °C until the mass of the sample is constant. The conditions used in the LOI method may greatly vary. For example, the incineration temperature ranges from 200~1600 °C, the time varies from 1~16 hours, and the amount of the sample is unreported in most cases (Luczak *et al.*, 1997). Luczak *et al.*, (1997) also pointed out the importance of the combustion temperature, time and sample size and recommended optimum conditions (500 °C and 5 hr for 2 g of sample size).

Results from the LOI method may be affected by the loss of mass due to dehydration and hydrolysis of clay minerals, requiring varying analytical technique, also based on the clay content of sediments (Dean, 1974). The temperature of dehydration and hydrolysis of clay minerals greatly changes depending on the type of clay mineral (Grim and Bradley, 1947). Seabed sediments contain biogenic minerals such as calcium carbonate and opal. It is generally known that calcite is decomposed at 800~850 °C and dolomite, $\text{CaMg}(\text{CO}_3)_2$, is thermally decomposed at 700~750 °C and release CO_2 . Kamatani (2000) pointed out that calcium carbonate is not decomposed at a temperature of ~500 °C, but dolomite is partly decomposed and releases CO_2 . In addition, Hirota and Szyper (1976) reported that the thermal decomposition of calcium carbonate occurs at temperatures above 550 °C and recommend combustion with careful temperature control (500 °C or slightly lower) using an electric muffle furnace. Biogenic opal in sediment contains on average 10% water (Mortlock and Froelich, 1989). This water dehydrates during diagenesis processes and opal undergoes a phase transition first from opal A to opal CT, and then to quartz (Mizutani, 1970). The water in the opal is also lost by heating; the loss is 60-70 % at 200 °C. Approximately 100 % of water in opal dehydrates during heating to 1000 °C (Knauth and Epstein, 1982). These facts indicate that high-temperature incineration at 550 °C or higher should be avoided when performing LOI. The LOI method can also be affected by insufficient temperature control of the electric muffle furnace and unevenness of the temperature in the furnace.

As mentioned above, the LOI method has been widely used as an indicator of the organic matter content; however, the loss of weight is not only due to the combustion of organic matter but also the dehydration and hydrolysis of clay minerals or dehydration of calcium carbonate and opal. Considering the effects of dehydration and hydrolysis, combustion at a temperature below 550 °C is reasonable when measuring the LOI of marine sediments. With regard to detailed temperature conditions for heating, analysts should make decisions based on the sampling locations and composition of major components. Preliminary experiments are strongly recommended to determine optimal heating condition.

1. Measurement method

The measurement method is as follows. The details follow the procedure described in Section 2-2.

1. Measure the mass of a crucible or a glass container (heat-resistant), m_c (g), after heating and cooling. Use a balance with a minimum scale of 0.001 g or less. The mass is measured twice and the average value is used as m_c (g).
2. Place 2 g of dried sediment sample in the container, heat it at 110 °C for 2 hr, and measure the total mass m_a (g). If extra material, such as wood fragments, is present in the sample, it should be removed beforehand. Additionally, it is advisable to pass the sample through a 2 mm sieve.
3. Place the sediment sample in a muffle furnace together with the container and gradually raise the temperature to 550 °C. When it reaches to the target temperature, maintain the temperature, and heat it for 5 hr.
4. After heating, open the door of the muffle furnace for ~10 min, remove the sample containers with a crucible tongs, and expose them to room temperature for a couple of minutes. Transfer the containers to a desiccator and measure the total mass m_b (g) after cooling them to room temperature.

2. Calculation

The LOI (%) is calculated as follows.

$$LOI = \frac{m_a - m_b}{m_a - m_c} \times 100$$

where,

LOI : Loss of ignition (%)

m_a : Mass of container with dried sediment (g)

m_b : Mass of container with combusted sediment (g)

m_c : Mass of container (g)

References

- Dean, W.E. (1974): Determination of carbonate and organic matter in calcareous sediments and sedimentary rocks by loss on ignition: comparison with other methods. *J. Sed. Petrol.* **44**, 242–248.
- Heiri O., A.F. Lotter and G. Lemcke (2001): Loss on ignition as a method for estimating organic and carbonate content in sediments: reproducibility and comparability of results. *J. Paleolim.* **25**, 101–110.
- Honjo, S. (1980): Material fluxes and modes of sedimentation in the mesopelagic and bathypelagic zones. *J. Mar. Res.*, **38**, 53-97.
- Tsunogai, S., M. Uematsu, S. Noriki, N. Tanaka and M. Yamada (1982): Sediment trap experiment in the northern North Pacific: Undulation of settling particles. *Geochem. J.*, **16**, 129-147.
- JIS A1226, Test Method for Ignition Loss of Soils, Japanese Standard Association, Tokyo, (2009).
- Luczak, C., M.-A. Janquin and A. Kupka (1997): Simple standard procedure for the routine determination of organic matter in marine sediment. *Hydrobiologia*, **345**, 87–94.

- Grim, R.E. and W.F. Bradley (1948): Rehydration and dehydration of the clay minerals. *American Mineralogist*, **33**, 50-59: Illinois Geological Survey Report Inv. 134.
- Pansu, M. and J. Gautheyrous (2006): Handbook of soil analysis: Mineralogical, *Organic and Inorganic Methods*. Springer, pp 10.
- Kamatani, A. (2000): Measuring Biogenic Silica of Marine Samples : its Situation and Prospect. *Umi no Kenkyu (Oceanography in Japan)*, **9** (3), 143-159.
- Mortlock, R.A. and P.N. Froelich (1989): A simple method for the rapid determination of biogenic opal in pelagic marine sediments. *Deep-Sea Res.*, 36 (9), 1415-1436.
- Mizutani, S. (1970): Silica mineral in the early stage of diagenesis. *Sedimentology*, **15**, 419-436.
- Knauth, L.P. and S. Epstein (1982): The nature of water in Hydrous silica. *American Mineralogist*, **67**, 510-520.

This page left intentionally blank.

Grain size distribution

○Hisashi NARITA (Tokai University) /Shigeyoshi OTOSAKA (Japan Atomic Energy Agency)

The grain size is fundamental parameters reflecting the basic physical properties of marine sediment. The grain size distribution of the marine sediment is mainly influenced by the composition of terrestrial detritus, biogenic calcium carbonate and opal. Stokes' law indicates that the sinking velocity of a particle in seawater is proportional to the square of its diameter. The grain size of the terrestrial detritus therefore reflects transport and deposition processes, as well as provenance and dispositional environment. It is also known that there is a certain relationship between the size distribution of the terrestrial detritus and its chemical composition (Kitano, 1972; Terashima *et al.*, 2008).

In general, detrital particles in sediment can be classified into stone, gravel, sand, silt, and clay depending on the particle size. However, the boundary value of each size class is not standardized, neither internationally nor academically. In Japan, based on the Japanese Industrial Standard “Test method for particle size distribution of soils” (JIS A 1204), boundaries of particle size classes of ground material are defined in “Method of classification of geomaterials for engineering purposes” (JGS 0051) of the Geotechnical Society standards (Fig.1). The typical sizes of biogenic opal and carbonate in marine sediments are indicated in Fig. 1. The Wentworth size classification (Fig. 1), where particle size is divided into $1/2^n$ mm sections and the phi-scale (ϕ) represents grain size, is often used by geologists (Wentworth, 1922).

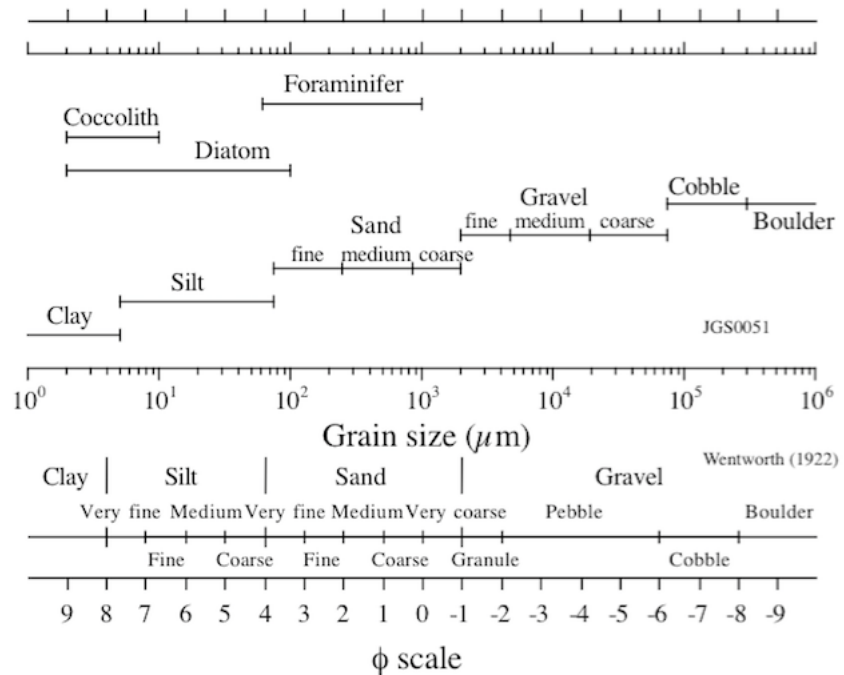


Fig. 1 Typical diameter of various particles in marine sediments

$$\phi = -\log_2(d/d_0)$$

where

d : Particle diameter (mm)

d_0 : 1 mm (unit value for creating a dimensionless parameter)

However, particles in marine sediment are typically not spherical but exhibit various,

irregular shape. Additionally, the particle density is not uniform. When discussing the particle size in sediments under such circumstances, it is necessary to define the particle size. The particle size is defined according to the measurement method. For the measurement of the grain size of the marine sediment, the 1) sieving method, 2) settling method, 3) Coulter counter method, and 4) laser diffraction-scattering method are mainly used.

1. Methods for grain size analysis

1) Sieving method

Sieving is a simple and direct method and is used for grain size measurement of sandy and gravel sediments. Sieves with mesh apertures of 75 μm , 106 μm , 250 μm , 425 μm , 850 μm , 2 mm, 4.75 mm, 9.5 mm, 19 mm, 26.5 mm, 37.5 mm, and 53 mm are used for the sieving analysis (JIS A 1204). Sieve the well-dried sediment sample, shake it with a shaker, and measure the mass of the sample above each sieve. The particles size remaining on the sieve is conceptually proportional to the intermediate axis of the particle.

2) Settling method

In the settling method, sediment particles are suspended and settled in a sedimentation cylinder containing a dispersant such as sodium hexametaphosphate solution. This method is divided into four categories: a) hydrometer method, b) pipette method, c) settling mass method, and d) light transmittance method. The detection method of the temporal change in sedimentation of particles of these methods differs depending on the particle size, density, and density difference between the dispersant and particles.

In method a, the density of the suspension solution is measured with a hydrometer at systematic time intervals. In method b, a given amount of a suspended solution in a cylinder of known-height is withdrawn from a particular depth at appropriate time intervals. In method c, a weighing dish is placed at a certain depth in a sedimentation cylinder and the temporal change in the mass of particles deposited on the weighing dish is measured. In method d, the temporal change in the transmittance caused by the sedimentation of particles is measured by applying light from the side of the sedimentation cylinder. Based on these methods, the particle diameter (Stokes' diameter) can be obtained assuming spherical particles. This particle size is called effective diameter. Using methods a and b, particles with diameters of 1~50 μm can be measured; particles with diameters of 0.2~200 μm and 0.2~100 μm can be measured with methods c and d, respectively (Okubo, 1989).

3) Coulter counter method

The Coulter Counter is an electrical sensing zone method, which determines the number and size of particles suspended in an electrolyte by measuring the electric resistance. A glass tube with pores filled with an electrolyte solution is inserted into a glass vessel filled with the same electrolyte solution and the electric resistance between two electrodes arranged on both sides of the glass tube is measured. Because the inside of the inner glass tube is adjusted to a negative pressure, the particles and solution move through the pores inside the glass tube when the particles are uniformly suspended in the

solution in the outer glass vessel. At this time, the electric resistance of the electrolyte solution changes according to the volume of the particle. The change in resistance is detected as an electrical pulse and the number of particles and volume of each particle can be measured. Because the diameters of the individual particles are calculated from the volume, the particle diameter obtained is an equivalent diameter. It is possible to measure the number and volume of the particles with a particle size ranging from 0.4~1200 μm .

4) Laser diffraction scattering method

The laser diffraction-scattering method is a measurement method using light properties. When a laser enters the suspension solution, light is diffracted or scattered in various directions by the particles. The distributional pattern of the intensity of diffracted and scattered light depends on the particle size. When the particle diameter is larger than the wavelength of the laser light, the Fraunhofer diffraction is dominant and the light converges toward its traveling direction. On the other hand, Mie scattering becomes dominant when the particle diameter is equal to or less than the wavelength of the laser light. Assuming spherical particles, the scattering intensity increases in the traveling direction if the particles are $\sim 1 \mu\text{m}$ in diameter; the scattering intensity increases laterally and backward if the particles are $\sim 0.1 \mu\text{m}$ in diameter.

Because the object to be measured is not a single particle but a group of particles with various shapes, a distributional pattern of intensity of the actual diffracted and scattered light is a superimposition of diffracted and scattered light from individual particles. Therefore, the particle size distribution can be obtained by detecting and analyzing the distributional pattern of the light intensity. However, in the laser diffraction-scattering method, the particle size dependency of the scattered pattern is lost when the particle diameter is less than half of the wavelength of the laser light. In addition, when the particle diameter reaches approximately 1/10 of the wavelength, Rayleigh scattering becomes dominant and the scattering intensity decreases in inverse proportion to the fourth power of the wavelength. Therefore, when measuring a sample including particles with various sizes and shapes, the sensitivity is significantly lowered by the influence of the scattered light of particles with a large particle diameter. Nevertheless, recent improvement of the optical system enabled the measurement of a wide range of particle sizes. It now is possible to measure particles with a particle diameter ranging from 0.02 to 2000 μm . Because the particle diameter is considered to be spherical, an effective diameter is obtained by this method.

The upper limits of the measurable particle size are 50 to 200 μm for of the settling method, 1200 μm for the Coulter counter method, and 2000 μm for the laser diffraction-scattering method. When measuring the particle size distribution of the seabed sediments, it is necessary to use these methods in combination with the sieving method. The sieving and settling method (except for the light transmission method) measure the mass-based distribution of particle size, whereas the light transmission method, Coulter counter method, and laser diffraction-scattering method generally measure the number- or volume-based distribution. Therefore, the volume-based particle size distribution needs to be converted to mass-based distribution using the particle density. Because the seabed sediment consists of particles with various densities, the average density is used for the

conversion. However, except for the sieving and pipette methods, determine the average density of each particle size fraction is fundamentally complicated and subject to uncertainty, and an estimated density value is generally used.

2. Measurement of particle size distribution by sieving and settling methods

Marine sediments consist of various particles, such as detrital particles, biogenic carbonate and opal, and organic matter. If the seabed sediments contain biogenic carbonate, biogenic opal, and organic matter (organisms), these particles may cause bias in the measurement of the particle size distribution. The autogenous mineral coated on the surface of the detritus or salts in the pore water can also bias the results. A combined sieving and settling methods of detrital particles is described in the following section in addition to procedures to exclude the factors that bias the particle size distribution. The dissolution procedure of biogenic carbonate and opal can be omitted, to measure the particle size distribution of bulk sediment. However, application of this method to calcareous and siliceous mud with a high content of carbonate and opal in hemipelagic and pelagic region is extremely difficult because of its difficulties to collect enough volume of sample. It should be considered that this method is applied to sediments that mainly consist of lithogenic material with relatively low content of carbonate and opal such as coastal sediment. To measure the grain size distribution of sediments with high content of carbonate and opal, it is recommended to apply the laser diffraction/scattering method described in Section 3 that permit measurement with a small volume of samples.

2-1 Sample dividing and preparation

Approximately 20 g (wet weight) of the collected sample is taken and used for measurements of water content, ignition loss and various chemical analyses and the remainder is used for particle size analysis. Although the quadrisection method (also known as a “cone and quarter”) is recommended for the division of the sample, there is generally no issue, even if an appropriate amount is sorted for sediment samples consisting of fine particles. From the viewpoint of accuracy, the mass of the sediment sample for particle size analysis is provided in JIS A 1204 as a function of the maximum particle size. The minimum sample mass is ~200 g for the sample with the maximum particle size of 2 mm and ~400 g for the sample with the maximum particle size of 4.75 mm (Table 1). In the settling method, ~115 g (dry mass) of sandy sediment (< 2 mm fraction) is required and ~ 65 g is required for silty or clay sediments.

In JIS A 1204, it is recommended to first divide the sediment sample into two fractions of gravel and sand to clay using a 2 mm sieve. However, in the case of marine sediments, dry samples are used because it is difficult to directly divide the wet sample into two fractions with

Table 1: Average minimum mass of samples based on grain size measurement

Maximum grain size (mm)	2	4.75	19	37.5	75
Mass of sample (g)	200	400	1500	6000	30000

a 2 mm sieve. In such a case, fine particles are agglomerated by heating and drying and it is necessary to physically disperse them before sieving. Also, it is desirable to perform freeze-drying because there is a possibility of breakage of coarse particles during physical dispersion. The sediment sample is relatively easy to disperse after freeze-drying. The mass of the sediment sample is measured before and after drying with an electronic balance capable of reading a mass of 1 mg and the water content w (%) is calculated. The mass of samples after drying is m_s^0 (g).

The dried sample is sieved and divided into two fractions; the fractions are passed through a 2 mm sieve and the residue remains on the 2 mm sieve. When sieving, fine particles adsorbed on the surface of coarse particles on the sieve are removed as much as possible. For this process, it is helpful to use an electromagnetic sieve shaker. However, excessive shaking may cause breakage of particles. When there are many contaminants, such as wood and shell fragments and organisms, the sieving efficiency may be reduced. In such a case, it is desirable to remove them by hand after confirming that the mass of fine particles on their surfaces can be ignored. The mass of the sediment passed through a 2 mm sieve is denoted as m_{1s}^0 (g) and the mass of the residue on the 2 mm sieve is m_{0s}^0 (g).

Based on the above-mentioned procedures, evaporated salt is precipitated on the surface of fine particles. Additionally, the sample may contain a considerable amount of biogenic opal, calcium carbonate, and organic matter. Because such biogenic particles interfere with the particle size measurement during sieving and settling, it is necessary to remove them chemically or physically. The detailed procedures are listed below.

1. For passing sediment samples through a 2 mm sieve, accurately weigh in ~100 g (in dry weight) for sandy sediments and ~60 g for silt and muddy sediments, place the samples in a 1000 ml tall beaker, and record the mass m_{1s}^1 (g). The residue on the 2 mm sieve is washed with pure water to remove fine particles from the surface of coarse particles. Transfer the residue to a beaker, dry it in a constant-temperature oven at 110 °C, and measure the mass m_{0s}^1 (g) after drying. Add 200 ml of pure water to the sample in a beaker such that all samples are immersed in pure water.
2. Add 50 ml of hydrogen peroxide solution, stir thoroughly, leave the solution for 12 hr or more, and heat at 80 °C for about 3 hr on a hotplate to decompose the organic matter. If the sample has a high content of organic matter, bubbles are generated vigorously. Samples containing a large amount of manganese oxide explosively react with hydrogen peroxide and may be blown out together with the solution. In such a case, it is necessary to moderate the reaction by adding pure water as necessary.
3. Add 250 ml of 1 M hydrochloric acid or acetic acid-sodium acetate buffer solution adjusted to pH 5, stir thoroughly, and leave for at least 12 hr to dissolve biogenic calcium carbonate.
4. Add 500 ml of pure water, stir thoroughly, and let it stand for 24 hr or more. For the sample of 2

mm sieve residue, it is enough to let it stand for several minutes. After the sediment particles settle, remove the solution by decantation or centrifugation.

5. Transfer the sample to a 500 ml polyethylene beaker. Add 300 ml of 0.1 mol L⁻¹ sodium carbonate, cover the beaker with a Teflon watch glass, and incubate it in a constant-temperature oven at 85 °C for 1 hr.
6. After allowing the sample to cool, add 120 ml of 0.5 mol L⁻¹ hydrochloric acid solution and stir well to neutralize, let stand for 24 hr or more, and then remove the solution by decantation or centrifugation.
7. Transfer the sediment sample to a centrifuge tube with 80% ethanol and remove the solution by centrifugation. This process also facilitates to remove eluted cations (Jackson, 1956). To remove ethanol, add pure water. The solution is removed by decantation or centrifugation.

The above-mentioned steps 3-6 can be omitted if unnecessary. Especially for samples fractions >2 mm, steps 5 and 6 are not required. Step 5 aims to removal biological opal, but it is known that a considerable proportion of clay minerals also dissolves by this procedure (DeMaster, 1981). Additionally, it is necessary to recognize that the particle size distribution of the sample may be changed to a certain extent.

2-2 Sieving analysis of sediment particles remaining on 2 mm sieve

2-2-1 Sample

The samples for sieving analysis are processed by the following procedure:

1. Wash the residual reagent thoroughly with water.
2. Put the sample in a constant-temperature oven at 110 °C and measure its mass m_{0s}^2 (g).

2-2-2 Sieving

The sieving of the sample is performed according to the following procedure:

1. Sieve the dried sediment samples using 75 mm, 53 mm, 37.5 mm, 26.5 mm, 19 mm, 9.5 mm and 4.75 mm sieves.
2. Sieve using an electromagnetic sieve shaker for 10 min.
3. Measure the accurate mass $m(d_i)$ (g) of the sample remaining on each sieve with the electronic balance. During this process, carefully confirm that the particles remaining in the sieve do not contain any plant and shell fragments. If such contaminants are found on the sieves, remove them by hand using tweezers.

2-3 Settling analysis of sediment particles passed through a 2 mm sieve and sieving analysis of sediment particles after the settling analysis

2-3-1 Sample

Samples to be subjected to settling analysis are prepared by the following procedure:

1. After samples are passed through a 2 mm sieve, they are dried in a vacuum freeze dryer and the total

mass m_{1s}^2 (g) is determined with an electronic balance. Approximately 15 g of the dried sample is separated for density measurement and the mass of the remaining sample m_{1s}^3 (g) is measured with an electronic balance.

2. Add 200 ml of pure water, stir thoroughly such that the whole sample is immersed in pure water, and leave it in a thermostatic chamber for 15 hr or more.
3. After standing, add pure water to reach the total volume of ~700 ml. Add 10 ml of 20 % sodium hexametaphosphate solution by stirring and disperse the sediment particles using a dispersing device or ultrasonic bath.

2-3-2 *Settling analysis*

The sedimentation analysis of samples is performed according to the following procedure:

1. Transfer the dispersed sample to a sedimentation cylinder and adjust the total volume to 1000 ml using pure water.
2. Place the sedimentation cylinder in a thermostatic chamber and leave it until the temperature of the suspension solution is equal to the room temperature. Keep stirring the solution with a magnetic stirrer during this process.
3. Securely cover the open end of the cylinder with a silicon stopper and secure it with the palm of your hand. Subsequently, turn the cylinder upside down and back upright for a few minutes. At this point, it is necessary to avoid the suspension leaking out from the cylinder and to ensure that the sediment is completely mixed in the suspension. Set the cylinder in a thermostatic chamber and record the time.
4. After 1, 2, 5, 15, 30, 60, 240 and 1440 minutes, carefully lower the hydrometer into the cylinder and let it float in the sediment suspension. Record the density and temperature of the suspension. The density read until 0.0005 (half of a minimum scale) at the upper level of the meniscus after stopping the hydrometer bobbing motion. The hydrometer is left in the cylinder for 1 to 2 min. In the other case, the hydrometer is carefully removed from the cylinder after reading. Rinse the hydrometer and thermometer with pure water and completely dry them.

2-3-3 *Sieving analysis after the settling analysis*

The above-mentioned procedures cannot be used to measure the particle size distributions from 250 μm to 2 mm. Therefore, to measure size distributions of this size interval, it is necessary to sieve sediment using settling analysis.

1. After settling analysis, the sedimentation cylinder is vigorously rotated hand-over-hand for a few minutes to generate the suspension solution. All of the suspension solution is passed through a 75 μm sieve. The sediment samples on the sieve are carefully washed with running water to remove fine particles less than 75 μm . Put the sample in a constant-temperature oven at 110 $^{\circ}\text{C}$ and measure its mass m_{1s}^4 (g).
2. Sieve the dried sediment samples using 850 μm , 425 μm , 250 μm , 106 μm , and 75 μm sieves.

3. Sieve using an electromagnetic sieve shaker for 10 min.

Measure the accurate mass $m^1(d_i)$ (g) of the sample remaining on each sieve with the electronic balance.

2-3-4 Hydrometer and its calibration

Use a hydrometer for soil with a scale range of 0.995 to 1.050 g cm⁻³ and a minimum scale of 0.001 g cm⁻³. Because the reference temperature is generally 15 °C when using the hydrometer, it is necessary to obtain the density at that temperature and correct the density with the following equation.

$$\Delta \rho = \rho \alpha_v (15 - t)$$

where

$\Delta \rho$: Difference of density to be corrected (g cm⁻³)

ρ : Reading of density on hydrometer (g cm⁻³)

α_v : Volume expansion coefficient (K⁻¹) of hydrometer glass. A hydrometer should be made of transparent glass that has a volume expansion coefficient of $25 \pm 5 \times 10^{-6}$ (K⁻¹; JIS B 7525). The expansion coefficient is calculated as the third power of linear expansion coefficient.

t : Temperature at the time of measurement (°C)

The scale of a hydrometer must be read with the specified eye level of reading (read the scale at the top or bottom of meniscus, depending on the hydrometer; Fig. 2). When using a level different from the specified level, the difference between the reading values of both levels is corrected as ΔC_m :

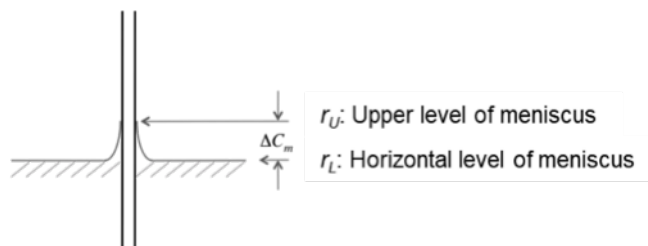


Fig 2: Reading a meniscus

$$\Delta C_m = r_U - r_L$$

where

ΔC_m : Difference of density between the upper and lower levels of meniscus (g cm⁻³)

r_U : Reading after the decimal point at the upper level of the meniscus (g cm⁻³)

r_L : Reading after the decimal point at the horizontal level of the meniscus (g cm⁻³)

Because oil adhering to the neck of the hydrometer influences the measurement, it is necessary to clean the surface of the neck and body surface with detergent and then degrease them with ethanol

or acetone. During the measurement, do not touch the neck with bare hands. The temperature of the hydrometer should be kept at ± 5 °C for the solution to be measured.

When using multiple hydrometers, it is necessary to float them in pure water or a mixed solution of pure water and sulfuric acid and compare their readings. In such a case, the density of pure water ρ is determined from the water temperature and that of the mixed solution is determined using a pycnometer.

Measure the length of the body the hydrometer (L_B : mm), the length from the upper end of the body (level at the joint between the body and neck) to the scale of 1.000 (l_1 : mm), and length to the scale line 1.050 (l_2 : mm) with a micrometer caliper up to 0.1 mm. In addition, measure the volume of the body part of the floating body (V_B : cm³) to 1 cm³ using a 250 ml graduated cylinder and the cross-sectional area of the 1000 ml sedimentation cylinder (A : cm²) up to 0.01 cm².

Based on the measurement results, the effective depth of the center of the body is calculated from the reading of the decimal part of the hydrometer (Fig.3):

$$L = L_1 + \frac{1}{2} \left(L_B - \frac{V_B}{A} \times 10 \right)$$

$$L_1 = l_1 - 20(r + \Delta C_m)(l_1 - l_2)$$

where

L : Effective depth at the center of the float body (mm)

L_1 : Length from the upper end of the float body to the reading r (mm)

l_1 : Length from the upper end of the float body to reading of 1.000 (mm)

l_2 : Length from the upper end of the float body to reading of 1.050 (mm)

r : Reading of the hydrometer after the decimal point (g cm⁻³)

ΔC_m : Difference in density between the upper and lower levels of meniscus (g cm⁻³)

L_B : Length of the body of the hydrometer (mm)

V_B : Volume of the body of the hydrometer (cm³)

A : Cross-sectional area of the measuring cylinder (cm²)

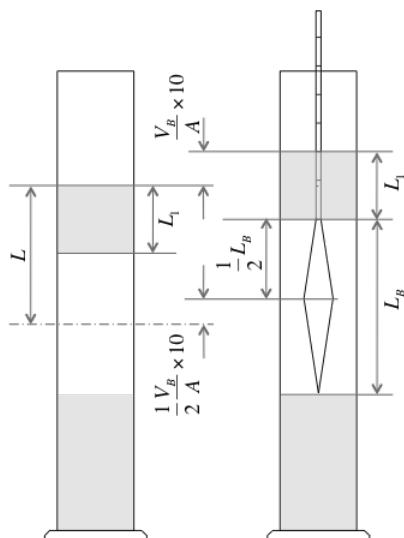


Fig. 3: Calculation of the effective depth at the center of the float body

2-4 Calculation

2-4-1 Calculation of particle size of sediment remaining on the 2 mm sieve by the sieving analysis

The passing mass percentage of the sample remaining on the sieve (nominal mesh size; d_i) of 2 mm or larger is calculated by the following equation:

$$P(d_i) = \frac{m_{0s}^2}{(m_s^0 - m_{0s}^1)m_{1s}^3/m_{1s}^0 + m_{0s}^2} \left(1 - \frac{\sum m(d_i)}{m_{0s}^2} \right) \times 100$$

where

d_i : Nominal mesh size of sieve (mm)

$P(d_i)$: Passing mass percentage of the sample remaining on a sieve with d_i of the nominal mesh size (%)

m_s^0 : Dry mass of the total sediment sample (g)

m_{1s}^0 : Mass of sample passed through the 2 mm sieve (g)

m_{0s}^1 : Dry mass of the remaining sample on the 2 mm sieve after treatment with water (g)

m_{0s}^2 : Dry mass of the remaining sample on the 2 mm sieve after preprocessing (g)

m_{1s}^3 : Mass of the sample on the 2 mm sieve used for the settling analysis (g)

$m(d_i)$: Dry mass of the sample remaining on each sieve of nominal mesh size d_i

$\Sigma m(d_i)$: The sum of dry mass $m(d_i)$ of the sample remaining on sieves of nominal mesh size (d_i) or larger (g)

2-4-2 Calculation of particle size of sediment passed through 2 mm sieve by the settling analysis

During the settling analysis of the sediment sample passing through a 2 mm sieve, the particle size corresponding to each hydrometer reading is calculated by the following equation:

$$d_R = \sqrt{\frac{18\eta L}{g(\rho_s - \rho_w)T}}$$

where

d_R : Particle diameter corresponding the reading number R after the decimal point of the hydrometer

η : Viscosity coefficient corresponding temperature t_w (°C) of the suspension solution at the time of the measurement. The η is calculated with the following equation:

$$\eta = 0.0017772 - 5.8283 \times 10^{-5} t_w + 1.3057 \times 10^{-6} t_w^2 - 1.847 \times 10^{-8} t_w^3 + 1.184 \times 10^{-10} t_w^4$$

This equation can be applied to a temperature range from 10 to 40 °C.

g : Gravitational acceleration (cm s⁻²)

ρ_s : Average density of particles with a diameter < 2 mm (g cm⁻³)

ρ_w : Density of water corresponding to a temperature of the suspension solution (°C) at the time of the measurement (g cm⁻³). The ρ_w is calculated with the following equation.

$$\rho_w = 999.84847 \times 10^{-3} + 6.337563 \times 10^{-5} t_w - 8.523829 \times 10^{-6} t_w^2 + 6.943248 \times 10^{-8} t_w^3 - 3.821216 \times 10^{-10} t_w^4$$

This equation can be applied to a temperature range from 5 to 40 °C.

L : Effective depth at the center of the float body (mm)

T : Elapsed time from the start of standing of the graduated cylinder to the hydrometer reading (s)

The mass percentage of the sample passed through a 2 mm sieve is calculated with the following equation.

$$P(d_R) = \frac{(m_s^0 - m_{0s}^1)m_{1s}^3/m_{1s}^0}{(m_s^0 - m_{0s}^1)m_{1s}^3/m_{1s}^0 + m_{0s}^2} \frac{V \{(R + \Delta C_m + \Delta\rho) - \rho_w\}}{m_{1s}^3} \times 100$$

where

$P(d_R)$: Mass percentage of the sample suspended at the time of hydrometer reading (%) . It corresponds to the passing mass percentage.

V : Volume of the suspension solution (1000 mL)

$\Delta\rho$: Difference in density due to the change in temperature (g cm^{-3})

2-4-3 Calculation of particle size of sediment remaining on the 75 μm sieve after the settling analysis by the sieving analysis

The passing mass percentage of the sample remaining on the sieve (nominal mesh size; d_i) of 75 μm or larger after the settling analysis is calculated with the following equation. The size distribution from 75 μm to 2 mm was generally used for the sieving analysis:

$$P(d_i) = \frac{m_{1s}^4}{(m_s^0 - m_{0s}^1)m_{1s}^4/m_{1s}^0 + m_{0s}^2} \left(1 - \frac{\sum m(d_i)}{m_{1s}^4} \right) \times 100$$

where

d_i : Nominal mesh size of sieve (mm)

$P(d_i)$: Passing mass percentage of the sample remaining on the sieve with d_i of the nominal mesh size (%)

m_s^0 : Dry mass of the total sediment sample (g)

m_{1s}^0 : Mass of the sample passed through the 2 mm sieve (g)

m_{0s}^1 : Dry mass of the remaining sample on the 2 mm sieve after treatment with water (g)

m_{0s}^2 : Dry mass of the remaining sample on the 2 mm sieve after preprocessing (g)

m_{1s}^4 : Mass of the sample on the 75 μm sieve after settling analysis (g)

$m(d_i)$: Dry mass of the sample remaining on each sieve with the nominal mesh size d_i

Guideline of ocean observations Vol. 5 Chap. 4 Grain size distribution

© Hisashi NARITA, Shigeyoshi OTOSAKA 2018 G504EN:001-020

$\Sigma m(d_i)$: The sum of dry mass $m(d_i)$ of the sample remaining on sieves with nominal mesh size (d_i) or larger (g)

2-5 Evaluation of data

The result of the particle size analysis using the combination of the sieving and the sedimentation methods (JIS method) is displayed on a semilogarithmic graph with the particle size on the horizontal axis with the logarithmic scale and the passing mass percentage on the vertical axis. The relationship is shown as a particle accumulation curve. The particle diameter d (mm) when the passing mass percentage is 10%, 30%, 50%, and 60% is read from the accumulation curve, and the particle diameter is defined as d_{10} (mm), d_{30} (mm), d_{50} (mm) and d_{60} (mm), respectively. The d_{10} and d_{50} is called the effective diameter and median diameter, respectively. Based on these diameters, the uniformity coefficient U_c and the curvature coefficient U'_c are calculated by the following equation.

$$U_c = \frac{d_{60}}{d_{10}}$$

$$U'_c = \frac{(d_{30})^2}{d_{10} d_{60}}$$

The uniformity coefficient indicates that as the index of the slope of the particle addition curve. The higher the value, the larger the particle diameter, and the lower value indicates the relatively uniform particle size. The curvature coefficient is an indicator of the smoothness of the curve.

When the particle size analyzed by the JIS method, the passing mass percentage with respect to the particle size of less than 75 μm exceeds 100%, and the particle accumulation curve becomes discontinuous at the junction of sieving analysis and sedimentation analysis (Geotechnical Society of Japan, 2009). The reason that the passing mass percentage exceeds 100% is considered to be in high organic matter content. Such cases can be prevented by facilitating decomposition of organic matter by increasing the concentration of hydrogen peroxide or heating. The discontinuity at the junction is presumed to be caused by (1) different definition of the particle size between the sieve and the sedimentation analysis, (2) unstable suspension of particles at the initial stage of sedimentation analysis, and (3) the interaction between particles and the presence of cylinder walls (Geotechnical Society of Japan, 2009; Katayama, 1997). However, since such discontinuity can occur due to analytical problems such as insufficient dispersion of samples, it is necessary to replicate the analysis if such analytical problems are predicted (Geotechnical Society, 2009).

Although it is necessary to understand the analytical procedure and be proficient, the above-mentioned causes of the data discontinuity (1) - (3) can be regarded as an essential problem of the sedimentation analysis. The particle accumulation curve is theoretically continuous and does not exceed 100%. Therefore, if the discontinuity or the degree of passing mass percentage exceeding

100% is small, the particle accumulation curve is drawn smoothly in accordance with the sieve analysis. Accordingly, the particle accumulation curve may include the subjectivity of the evaluator in some cases.

As a method of correcting the discontinuity of sieve and sedimentation analysis, Kumon *et al.* (1992) and Kishi and Kumon (1993) proposed a weight correction method that calculates iteratively by varying the mass by 0.01 g until the passing percentage at 4.5 ϕ coincided in the both analysis. Furthermore, in Kumon *et al.* (1992) and Kishi and Kumon (1993), the degree of the weight correction is represented by a value obtained by dividing the absolute value of the mass difference before and after the correction by the sample amount (mass before the correction). Sawa and Nakayama (2014) have proposed an evaluation method that considers synthetic uncertainty and expanded uncertainty to the results of particle size analysis using sieve analysis and sedimentation analysis.

3. Measurement of particle size distribution by laser diffraction scattering method

The particle size analysis method (JIS method) which uses the sieve method and sedimentation method described in the previous section has been used as a standard method in a wide range of fields such as civil engineering and geotechnical engineering as well as earth science. However, problems such as length of measurement time, turbulence of suspensions occurring when putting a float for precipitation analysis, inconsistency of results between the analysts, has been pointed out (Geotechnical Society Japan, 1990). In addition, the problem of discontinuity near the junction of sieving method and sedimentation method, which is around 75 μm , may occur, and the correction method depends on the judgment of the analyst and the evaluator.

In the field of powder process industry and engineering, laser diffraction/scattering method (JIS Z 8825, 2013) and image analysis method (JIS Z 8827-1, 2008; JIS Z 8827-2, 2010) have been applied to automate grain size measurement. The laser diffraction/scattering method can measure the particle size of particles with a wide size range of 0.02 to 2000 μm , and it is expected that the method can measure particles to which the JIS method is applied rapidly without sieving. Furthermore, in recent years, it has become possible to measure a wider range of particle sizes by a composite light source consists of a red laser diode and a blue (405 nm) light emitting diode. In addition, the laser diffraction/scattering method has been applied to grain size analysis of geoscientific samples because it requires less volume of samples and can analyze rapidly than JIS method (Ishii *et al.*, 1991; Nakajima and Kanai, 1996; Saito, 1996; Katayama, 1997; Ando *et al.*, 2014; Nishida and Ikehara, 2016).

In the laser diffraction/scattering method, the grain size distribution is estimated from concentric intensity distributions of diffracted and scattered light generated when particles are irradiated with laser light. The Fraunhofer diffraction theory and the Mie scattering theory are used to correlate the pattern of the intensity distribution of the diffracted/scattered light and the particle diameter. When the grain size is at least 10 times of the wavelength of the laser light, the Fraunhofer diffraction theory can be applied for the analysis, and when the grain size is less than about 7 μm (10 times the

wavelength), the Mie scattering theory is applied because lateral and backward scattering is dominant. The analysis theory of grain size distribution depends on manufacturer and equipment. Some cases use Fraunhofer diffraction theory and Mie scattering theory in combination and other case adopt Mie scattering theory only. The Fraunhofer diffraction theory is one of the approximation of the Mie scattering theory, and the algorithm used in the calculation also differs depending on manufacturer and equipment (Tsumura, 1993).

In order to calculate the pattern of the light intensity distribution using Mie scattering theory, it is necessary to set the refractive index of the solution (dispersion medium) and the suspended particles. The refractive index (complex refractive index) N_p is expressed by the following equation.

$$N_p = n_p - k_p i$$

In this equation, the real part n_p is the curvature of light, the imaginary k_p is the extinction coefficient, which represents the absorption of light by the particle. However, in general, the extinction coefficient of the imaginary can be regarded as zero (Kinoshita, 2008). Additionally, if the refractive index of the solution in which the particles are suspended is n_m , the relative refractive index RRI is expressed by the following equation .

$$RRI = N_p / n_m$$

Generally, if particles consist of single component, a literature value of the refractive index is applied. If the particles are not a single component, a literature value of the main component of the particle group or a similar substance should be assumed. However, even if the refractive index is known, the obtained results of size distributions may differ between equipments (Hayakawa *et al.*, 1993), and it is considered that the difference is caused by the optical system or refractive index between the equipments. These issues are black boxed and it is impossible to consider quantitatively (Hayakawa *et al.*, 1993). Hayakawa *et al.* (1993; 1995) reported that the refractive index, at which the median diameter (effective diameter in some cases) based on the particle size distribution of fine ceramics shows the maximum, becomes the optimum value of the device. However, this method is not effective for bimodal size distributions (Hayakawa *et al.*, 1995).

The Mie scattering theory is based on the assumption of complete spherical particles, whereas most of the particles to be actually measured are aspherical. For this reason, the scattered light intensity obtained by the laser diffraction/scattering method is affected not only by the particle size but also by the particle shape. Even if the particles have the same refractive index, the measurement result will be different if the particle shape is different. The refractive index used in the laser diffraction / scattering method is not a refractive index as a physical property value but a parameter specified to the equipment that includes other parameters such as the shape of particles. Therefore, it should be referred as “refractive index parameter” (Kinoshita, 2000; 2008).

Kinoshita (2008), by improving the method of Kinoshita (2000), proposed the optimum refractive index parameter and its evaluation function that minimizes the residual between the detected light

intensity distribution and the estimated distribution calculated from the particle size distribution. However, similar to the method of Hayakawa *et al.* (1993; 1995), the method of Kinoshita (2000; 2008) is also based on the assumption that the particles have uniform size. Furukawa *et al.* (2000) introduced an evaluation function that developed the idea of crushing rate for soil particles by Marsal (1965) and Ishii (1985), and proposed to optimize the relative refractive index by changing the value so that the difference between the particle size distribution obtained by laser diffraction/scattering method and JIS method to be minimum. This method is expected to be applied to seabed sediment composed of various nonspherical particles of minerals. In any case, the setting of the refractive index in the laser diffraction/scattering method is a big problem for analysts. In recent years, the relative refractive index values of 1.17 to 1.24 are used in particle size analysis of seabed sediments using the laser diffraction/scattering method (Ando *et al.*, 2014; Nishida and Ikihara, 2016). However, as mentioned above, it is necessary to pay attention that the refractive index is a parameter that varies depending on the equipment.

In the laser diffraction/scattering method, the particle concentration contained in the dispersion medium also influences the particle size distribution. In general, the accuracy of the data decreases when the particle concentration is low (% transmittance is high), and the shift of particle size distribution to the fine grain side because of the multiple scattering occurs when the concentration is high (% transmittance is low). Therefore, an appropriate particle concentration is indicated for each equipment with the unit of % transmittance. Furukawa *et al.* (2001) recommends that the appropriate % transmittance is $80\pm 5\%$ for laser light, and soil particle concentration is 60 ± 20 mg/100 ml in the dispersion medium.

The maximum diameter that can be measured by the laser diffraction/scattering method varies depending on the equipment used, and it ranges from 2000 to 5000 μm . Therefore, when the maximum particle size of the sample exceeds the measurement range of the equipment, the sample must be sieved in advance. On the other hand, when the range of measurable particle size is between 0.02 and 2000 μm , the ratio of the maximum to the minimum particle size is 10^5 , and it corresponds to 10^{15} in the volume ratio. Therefore, when a particle group having a maximum diameter of 2000 μm is to be measured, it is necessary to increase the particle concentration in the dispersion medium in order to evaluate the volume of fine particle size appropriately. However, as described above, since a proper transmittance is required for the accurate measurement, it is necessary to set the proper maximum grain size for measurement of the laser diffraction/scattering method apart from the measurable maximum grain size of the device. Furukawa *et al.* (2001) compared the result of grain size analysis by the laser diffraction/scattering method and JIS method for a uniform particle group with different particle sizes and a particle group with different particle size (>38 μm), and determined that a proper maximum size for the laser diffraction/scattering analysis is 250 μm . On the other hand, considering the consistency with the JIS method, grain size analysis by the laser diffraction/scattering method should be performed for a fraction that passed through a 75 μm or 44 μm sieve, instead of applying the the maximum particle size of 250 μm (Furukawa *et al.*, 2001).

The validity of the result of analyzing the particle size of the seabed sediment by the laser diffraction/scattering method can only be evaluated by the relative size with reference to the particle

size distribution obtained by JIS method. Katayama (1997) indicated that the result of the laser diffraction/scattering analysis for the fraction passing through the 44 μm (4.5 ϕ) sieve was biased to the coarser grain size compared with that by the JIS sedimentation method, and pointed out that the difference was mainly due to the principal of measurements. Furthermore, as a problem of the sedimentation method, the influence of the algorithm concerning the particle size calculation of the equipment used, the influence by the algorithm of the particle size calculation of the used equipment, the influence of the sedimentation And the possibility of the influence of the relative refractive index used are pointed out. In addition, it is pointed out that turbulence, interaction between particles and decline of sedimentation rate due to Brownian motion affect the grain size analysis by sedimentation method affects. On the other hand, in the laser diffraction/scattering method, the result is influenced by algorithms for particle size calculation of the equipment used, the relative refractive index and the shape of sediment particles. Furukawa *et al.*. (2001) compare the particle size of soil measured by laser diffraction/scattering method and JIS method, and pointed out that the result of laser diffraction/scattering method is biased toward the finer grain compared with JIS method, conversely to the result of Katayama (1997). Since the analysis results are influenced by the algorithm of the equipment used, it is difficult to specify the factor that causes the difference between the results. In the particle size analysis by the laser diffraction/scattering method, it is necessary to understand the characteristics of the equipment through comparison with the JIS method and measurement of a reference material.

As mentioned above, both the laser diffraction/scattering method and the JIS method have merits and demerits regarding the particle size analysis of clay, silt and fine grain sand. Nevertheless, in comparison with the JIS method, the laser diffraction/scattering method requires a smaller volume of sample, enables rapid analysis, and shows high accuracy and reproducibility. These points would be the greatest advantages in applying the laser diffraction/scattering method to the particle size analysis of the seabed sediment.

3-1 Points of attention in splitting and pretreatment of sediment samples

Even when particle size analysis is performed by the laser diffraction/scattering method, basic concepts for splitting and pretreatment of sediment sample, described in section 2-5, can be applied. In this section, some points that should be pay attention in preperation of samples for particle size analysis by laser diffraction/scattering method.

When the maximum particle size of the sample exceeds the upper limit of the measureable range of the equipment, it is necessary to remove the coarse particles by sieving. In the laser diffraction/scattering method, the optimum particle concentration in the dispersion medium introduced into the apparatus is around 60 mg per 100 ml, and the amount is much smaller than that of the JIS method. Therefore, in order to ensure representation, it is necessary to reduce the sample after lyophilization by an appropriate method such as a conical quartering. With respect to clay and silt sediments, considering the consistency with JIS method, the sediment is divided by a 2 mm mesh sieve, the fraction passed through the sieve is preprocessed, and used for particle size analysis. As described in Furukawa *et al.*. (2001), in the case of sandy or sand-containing clay and silt sediments,

it may be necessary to divide the sample further with a sieve such as a 250 μm mesh and use the passed fraction for the particle size analysis in order to avoid bias of particle size distribution due to the presence of sand. However, the characteristics of the bias may be different depending on the equipment, it is necessary to consider the influence of the sand, necessity of sieving, matching of sieves to be used in advance of the analysis. In any case, the mass and percentage of particles remaining in each sieve should be recorded.

Before the particle size analysis of detrital particles in sediment, biogenic carbonates and opals sample are needed to be removed by dissolution. During the pretreatment for dissolving this carbonate or opal, the lithogenic detritus may also slightly dissolve. Therefore, it is recommended to use an acetic acid-sodium acetate buffer solution (adjusted to pH 5) and 0.1 mol/L sodium carbonate (Na_2CO_3) solution to dissolve the carbonate and opal, respectively. The reaction is performed for 1 hour at 85 $^\circ\text{C}$. However, opal may become difficult to decompose with the elapsed time after sedimentation (Müller and Schneider, 1993). If the dissolution of the opal is insufficient, increase Na_2CO_3 concentration or extend the reaction time. For dissolution of the biogenic opal, the solid-liquid ratio is also important in addition to the type and concentration of the alkaline solution and the reaction time and temperature. When the solid-liquid ratio is 1 g L^{-1} or less, silicon dissolves from clay particles, and dissolution of biogenic opal is insufficient at a higher solid-liquid ratio (Loassachan and Tada, 2008). Therefore, it is necessary to set the solid-liquid ratio to 2 ± 0.5 g L^{-1} to dissolve the biogenic opal. Considering that the proper % transmittance of laser light for grain size analysis is $80\pm 5\%$, it is advisable to process 200 ± 50 mg of sediment sample for dissolution of biogenic opal. When replacing the solution during the pretreatment, centrifuge the sample for 10 minutes at 3000 rpm. Also, after removal of the carbonate, it is necessary to wash the particles with pure water.

Samples after dissolution of the biogenic opal are weighed after lyophilization and the mass of the residual particles is measured. Depending on the mass of the residual particles, 0.1% sodium hexametaphosphate solution is added to the dried sample so that the % transmittance of the laser light is $80\pm 5\%$. In the laser diffraction/scattering analysis of the dispersed particles, a circulating flow cell is commonly used. The specifications such as the capacity of the dispersion vessel, flow rate and the ultrasonication option differs between the apparatus. Therefore, it is necessary to investigate the influence of the measurement time on the results in advance of the sample analysis, and the appropriate time parameters should be determined according to the required accuracy. Blank measurement with 0.1% sodium hexametaphosphate solution containing no particles should be performed under the same conditions as the sample measurement.

For analyzing the size distribution of particles with large particle size excluded when used for laser diffraction/scattering analysis, methods described in sections 2-2 and 2-3-3 are applied. However, it is sometimes impossible to precisely measure the particle size distribution because of the lack of sample mass of the particles remaining in the sieve. Therefore, the measurement of grain size of such particles remained on the sieve should be performed independently from the laser diffraction/scattering analysis. In the field of earth science, particle size distribution measurement using a digital image analysis device is being introduced in recent years, and the measurable size range

is 30 μm to 30 mm (Nanayama *et al.*, 2012). The digital image analysis also has an advantage that it can be measure the major axis diameter, the minor axis diameter. It will be an effective tool for evaluating the continuity of results by sieving analysis, sedimentation analysis or laser diffraction/scattering analysis.

References

- Kitano, Y. (1972): Senkai Taisekibutu: Taisekibutu no Kagaku (Shallow water sediments: Chemistry of sediments), ed. Y. Miyake, Tokai Univ. Press., 243-335.
- Terashima, S., N. Imai, K. Ikehara, H. Katayama, T. Okai, M. (Ujiie) Mikoshiba, A. Ohta and R. Kubota (2008): Variation of elemental concentrations of river and marine sediments according to the grain size classification. Bull. Geol. Surv. Japan, 59 (9/10), 439-459.
- JIS A 1204, Test method for particle size distribution of soils, Japanese Standard Association, Tokyo, (2009).
- JGS 0051, Method of classification of geomaterials for engineering purposes, Japanese Deotecgnical Society Standards, Tokyo, (2009).
- Wentworth, C.K. (1922): Method of computing mechanical composition of sediments. Geological Society of America Bulletin, 40, 771-790.
- Ohkubo, T. (1989): Comparison of size distribution measured by serveral methods. Bill. Yamagata Univ. (Eng.), 20 (2), 159-168.
- Jackson, M.L. (1956): Soil chemical analysis: advanced course: Published by the author., Madison, Wis., 895 p.
- DeMaster, D.J. (1981): The supply and accumulation of Silica in the marine environment. Geochimi. Cosmochimi. Acta, 45, 1715-1732.
- JIS B 7525-1, Density fydrometers, Japanese Standard Association, Tokyo, (2013).
- The Geotechnical Sciety of Japan (2009): Test meshods of ground materials, The Geotechnical Sciety of Japan, Tokyo, 533 p.
- Katayama, H. (1997): Comparison between a lazer diffraction-scattering method and a hydrometer method in the grain size analysis for fine-grained sediments. J Sedimentological Soc. Japan, 46, 23-30.
- Kumon, F., T. Kamittani, K. Sutoh, Y. Inouchi (1992): Grain Size Distribution of the Surface Sediments in Lake Biwa, Japan. Mem Geol Sco Japan, 39, 53-60 (in Japanese)
- Kishi, S., F. Kumon (1993): Grain-size analysis combined settling tube method with hydrometer method for muddy sand sediments. Journal of the Sedimentological Soc. Japan, 38, 101-106.
- K. Swa, Y. Nakayama (2014): A study on the evaluation of the uncertainty of particle size distribution test results. Japan Geotechnol. J., 9, 255-274.
- JIS Z 8825, Particle size analysis-Laser diffraction methods, Japanese Standard Association, Tokyo (2013).
- JIS 8827-1, Particle size analysis Image analysis methodsPart 1 : Static image analysis methods, Japanese Standard Association, Tokyo (2008).
- JIS 8827-2, Particle size analysis-Image analysis methods-Part 2: Dynamic image analysis methods, Japanese Standard Association, Tokyo (2010).
- The Geotechnical Sciety of Japan (2009): Test meshods of soils, The Geotech. Soc. Japan, Tokyo, 902 p.

- Ishii, J., T. Yabuta, T. Maeda (1991): Grain size of a core sample from the northern Japan Basin, analyzed by a laser-beam diffraction method. *Proc. Hokkaido Tokai Univ. Sci. Eng.*, 4, 9-25. (in Japanese)
- K. Nakajima, Y. Watanabe (1995): Recurrence Intervals of earthquakes inferred from turbidites near the Epicentral area of the 1983 Japan Sea Earthquake. *J. Seismolog. Soc. Japan. 2nd ser.*, 48, 223-228.
- Saito, Y. (1996): Grain-size and sediment-color variations of Pleistocene slope sediments off New Jersey. In Mountain, G.S., Miller, K.G., Blum, P., Poag, C.W. and Twichel, D.C. eds., *Proceedings of the Ocean Drilling Program, Scientific Results*, 150, 229-239.
- Ando, H, M. Oyama, F. Nanayama (2014): Data report: grain size distribution of Miocene successions, IODP Expedition 313 Sites M0027, M0028, and M0029, New Jersey shallow shelf. In Mountain, G., Proust, J.-N., McInroy, D., Cotterill, C., and the Expedition 313 Scientists, *Proceedings of the Integrated Ocean Drilling Program*, 313.
- N. Nishida, K. Ikehara (2016): Spatial variation of coastal marine sediments of the northern Suruga Bay, central Japan and their depositional processes. *Seamless Geoinformation of Coastal Zone S-5*, 1-23.
- Tomura, S. (1993): Particle-Size Analysis of Clays. *J. Clay Sci. Soc. Japan*, 32, 239-246. (in Japanese)
- Hayakawa, O., K. Nakahara, J. Tsubaki (1993): Estimation of the optimum refractive index by laser diffraction and scattering method. *J. Soc. Powder Technol. Japan*, 30, 652-659. (in Japanese with English abstract)
- Hayakawa, O., Y. Yasuda, M. Naito, J. Tsubaki (1995): The effect of the refractive Index Input value on particle size distribution measured by the laser diffraction & scattering Method. *J. Soc. Powder Technol. Japan*, 32, 796-803. (in Japanese with English abstract)
- Kinoshita, T. (2000): The method to determine the optimum refractive index parameter in laser diffraction and scattering methods. *J. Soc. Powder Technol. Japan*, 37, 354-361. (in Japanese with English abstract)
- Kinoshita, T. (2008): An investigation of evaluation function for the method to determine the optimum refractive index parameter in laser diffraction and scattering method *J. Soc. Powder Technol.*, Japan, 45, 104-109. (in Japanese with English abstract)
- Marsal, R.J. (1965): Soil properties-shear strength and consolidation. *Proc.*, 6th, ICSMF, 310-316.
- Ishii, T. (1989): Physical Significance of Indices for Particle Breakage. *Soils and Foundations*, 29, 155-164
- Furukawa, Y., T. Fujita, T. Kunihiro, M. Fukazawa (2000): Investigation of particle size distribution of soil using a particle size analysis equipment automated by laser and its applicability to soil samples. *Trans. Japan Soc. Civil Eng.*, 687, 219-231. (in Japanese)
- Müller, P.J. and R. Schneider (1993): An automated leaching method for the determination of opal in sediments and particulate matter. *Dep-Sea Res.*, 40, 42-54.
- Loassachan, N. and K. Tada (2008): Effect of solid to solution ratio on biogenic silica determination in coastal sediments. *J. Oceanogr.*, 64, 657-662.
- Nanayama, F., R. Furukawa, M. Ogasawara (2013): How to measure the particle size in sediment? : a planning the sophistication of the equipment and the data integration system of grain size analysis. *GSI Chishitsu News*, 2, 82-85. (in Japanese)

Major component

○Hisashi NARITA (Tokai University), Shigeyoshi OTOSAKA (The University of Tokyo)

As seabed sediment reflects geochemical cycles and the sedimentary environment, the sedimentation rate, particle size and biochemical/mineralogical composition of sediments vary greatly. Therefore, the major composition of sediment provides important information for understanding geochemical cycles and the sedimentary environment in the study area.

Seabed sediment is generally composed of lithogenic, biogenic, or authigenic materials. Lithogenic matter originates from terrestrial rocks, and consists of minerals transported through rivers and the atmosphere. Biogenic material is generally divided into three groups: organic matter, silicates, and carbonates. Organic matter can be further divided into terrestrial (mainly plants) and aquatic organisms. Biogenic silicate is mainly produced by phytoplankton in seawater, and is an amorphous silicate (biogenic opal) formed from silicic acid in seawater. Skeletons of diatoms are a typical biogenic opal, and this substance is also produced by siliceous dinoflagellates, radiolarians, and sponges. Biogenic carbonates in the marine environment are produced by coccolithophores, foraminifera, shellfish, and coral. Seabed sediment also contains small amounts of terrestrial carbonate. For example, large amount of carbonate is contained in soil at the source area of eolian dust (kosa) (Quan *et al.*, 1994). Minerals of aqueous origin from non-biologically (inorganically) from dissolved materials in water, and the minerals that form in the seawater or sediments are generally called authigenic minerals. Authigenic minerals include oxides such as those of Fe and Mn, sulfates, sulfides, phosphates, and carbonates.

Among these substances, lithogenic matter, biogenic opal, biogenic carbonate and organic matter are particularly important as major components of sediment. In some cases, authigenic minerals such as Fe and Mn oxides are present in significant proportions in sediments. This chapter describes an outline and points of attention in analyzing the amounts of lithogenic matter, biogenic opal, biogenic carbonate, and organic matter, which mainly contribute to the composition of sediment.

1. Sediment sampling

For the purpose of analyzing the major components of sediments, sediment samplers such as grab samplers, multiple corers, gravity corers, and piston corers are commonly used. In particular, when analyzing surface sediments, it is recommended to use a multiple corer that minimises disturbance of the sediment surface and can collect water overlying the sediment. Please see Chapter 1 of this volume for details on sediment sampling.

2. Pretreatment of sediment samples

After drying a sediment sample, the size of the sample is reduced by the increment method (JIS Z 8816, 2001) in principle. However, for sediments consisting of fine particles, there is practically no problem if the sample is sorted an appropriate amount arbitrarily. Gravel, shell pieces, and plant and animal material are removed with a sieve before analysis.

Drying of the sediment sample should be carried out by freeze-drying. It is recommended to avoid heat drying as fine grains aggregate during heating and coarse lithogenic particles may be unnecessarily crushed by grinding. Freeze-dried sediment particles are easily dispersed and the loss of coarse particles due to breakage is relatively small. It is possible to calculate water content by measuring the mass of the sediment before and after drying (see Chapter 2 for details). An electronic balance that can read to 1 mg should be used for weighing.

After drying, the sediment sample is sieved with a 2 mm (9 mesh) sieve. During sieving, fine particles on the surfaces of coarse particles should be separated as much as possible. Impurities such as gravel and shell fragments should be removed by hand picking. After being passed through the 2 mm sieve, the sediment sample is passed through a 0.180 mm (80 mesh) sieve. Particles on the 0.180 mm sieve (with particle size between 0.180 and 2 mm) are gently crushed in an agate mortar so that the particles pass through the sieve. With regard to particles passed through the 0.180 mm sieve, no further grinding is required because there is no significant influence from grinding (Imai, 2010) and Si in lithogenic matter may be desorbed from finely ground sediment during analysis of biogenic opal (Mortlock and Froelich, 1989).

For the measurement of major components in seabed sediment, samples passed through a 0.180 mm sieve are used. Except for samples obtained in certain sea areas such as estuaries and coasts, coarse sediments of 2 mm or more, such as gravels and shell fragments, should not be used for analysis because they are less representative.

3. Lithogenic and authigenic matter

There are two ways to estimate the amount of lithogenic matter (% LM). In the first method, concentrations of biogenic opal (% BO), CaCO₃ (% CC), and organic matter (% OM) are measured by the following method, and the sum of the three biogenic components (% TB) is subtracted from 100 % (e.g., Nederbragt *et al.*, 2008).

$$\begin{aligned} \%LM &= 100 - (\%BO + \%CC + \%OM) \\ &= 100 - \%TB \end{aligned}$$

The concentration of organic matter (% OM) is estimated from the organic carbon content (% TOC) by the following equation (Nederbragt *et al.*, 2008).

$$\%OM = 2.2 \times \%TOC$$

The accuracy of the lithogenic matter content estimated by this method is determined based on the propagation of the measurement accuracy of biogenic opal, CaCO₃ and organic matter concentrations as follows:

$$\sigma_{LM} = \sqrt{(\sigma_{BO}^2 + \sigma_{CC}^2 + \sigma_{OM}^2)} \frac{100 - \% TB}{\% TB}$$

The second method is to calculate lithogenic matter content (% LM) from Al concentration in the sediment sample (% Al_{sample}), assuming the average crustal composition ratio (% Al_{crust}; e.g., Taylor, 1964). This method is widely used for estimating the amount of lithogenic matter content in sinking particles collected by sediment traps (e.g, Noriki and Tsunogai, 1985).

$$\%LM = \frac{\%Al_{sample}}{\%Al_{crust}} \times 100$$

It is difficult to estimate the proportion of authigenic minerals in sediments from elemental composition alone, but the concentration coefficient (EF_M; “M” indicates any element of interest) of an element in the sediment against the crustal abundance and excessive concentration of the element relative to the crust [M_{excess}] are commonly used as indicators. These indicators are calculated using the following equation (Ravichandran *et al.*, 1995):

$$EF_M = \frac{(M/Al)_{sample}}{(M/Al)_{crust}}$$

$$[M_{excess}]_{sample} = [M]_{sample} - (M/Al)_{crust} \times [Al]_{sample}$$

where [M]_{sample} is the total concentration of the element of interest in the sediment, (M/Al)_{sample} and (M/Al)_{crust} are the ratio of the element of interest and Al in the sediment sample and the average in the crust, and [Al]_{sample} is the Al concentration in the sediment sample. This method is based on the assumption that the majority of Al in the sediment is of crustal origin.

In estimating such concentration factors and excess concentrations, it is important to carefully select the (M/Al)_{crust} values used for calculation (Turekian and Wedepohl, 1961; Taylor, 1964; Taylor and McLennan, 1985). For example, in estimating excess Ba concentration ([Ba_{excess}]_{sample}), 0.005 to 0.01 is used as the value of the Ba/Al ratio in terrestrial crust, and this range in the Ba/Al ratio causes deviation of up to 50 % (Reitz *et al.*, 2004). In some cases, (Ba/Al)_{crust} is assumed to be similar to Ba/Al ratio in the residue after removing authigenic Ba from the sediment sample by the selective sequential dissolution method (Schenau *et al.* 2001) (Reitz *et al.*, 2004). In addition, because [Al_{excess}]_{sample} is sometimes observed from sinking particles, Ti, which has a short residence time in surface seawater, is used as an indicator of representative lithogenic element (Dymond *et al.*, 1997).

3-1 Determination of elemental composition of sediment

For determination of major elemental composition of sediment samples, X-ray fluorescence analysis is commonly used. In this analysis, a powdered sediment sample and lithium tetraborate are mixed at a ratio of 1:5 to 1:10 and melted at 1100 °C in an Au-Pt alloy crucible to prepare a glass bead for analysis. In general, about 1 g of sediment samples is required for this analysis. With this method, in addition to major elements such as Si, Ti, Al, Fe, Mn, Mg, Ca, Na, K, and P, the trace elements such as V, Cr, Co, Ni, Cu, Zn, Rb, Sr, Y, Zr, Nb, Ba, Pb, Th, and As can be measured. For the quantitative determination of elements, several standard materials are measured, and a calibration curve based on the relationship between the intensity of X-ray fluorescent and the elemental composition of the standard is prepared in advance (e.g., Hokanishi *et al.*, 2015).

There is also a method in which the sediment sample is dissolved with HNO₃-HClO₄-HF and major elements are measured with MP-AES and ICP-AES/ICP-OES or ICP-MS. Because of the sensitivity of these instruments, only about 0.1 to 0.2 g of each sediment sample is required for the analysis. In addition, by combining ICP-MS with MP-AES or ICP-AES/ICP-OES, it is possible to quantify trace elements such as rare earth elements, Sc, and Th. Although decomposition using HF is unsuitable for measurement of Si, it is possible to measure Si by the acid decomposition method using a sealed Teflon vessel combined with calorimetric spectrophotometry (Noriki *et al.*, 1980). In determination of elements, an absolute calibration curve with an added internal standard is used. For an internal standard, In (indium) is used for the MP-AES and ICP-AES/ICP-OES methods. For the ICP-MS method, in addition to In-115, isotopes such as Be-9 and Tl-205 are used for measurements of low and high mass elements, respectively. The internal standards are added such that the concentration is the same for a series of samples and standard solutions. The concentration of an element used as the internal standard should be 100 times or more than the concentration of the element in the sample solution. In addition, it is recommended to analyze a certified reference sample such as JMS-1, JMS-2, or Jlk-1 of the National Institute of Advanced Industrial Science and Technology (AIST), or SRM 2702 or SRM 2703 of the National Institute of Standards and Technology (NIST), simultaneously with the sediment sample. In preparation of the standard and internal standard solution and preprocessing of the sample, reagents of a high purity grade should be used, depending on the concentration of the target component in the sample.

3-2 Decomposition of sediment sample by mixed acid

To completely dissolve the sediment sample, it is necessary to decompose the carbonate, biogenic opal, aluminosilicates, and organic matter contained in the sample. In the past, the alkaline melting method (heating a sample together with Na₂CO₃ and then dissolving it in an acid) was commonly used. As analytical methods using MP-AES, ICP-AES/ICP-OES, or ICP-MS has now become popular, and decomposition of sediment samples in sealed Teflon vessels with mixed acid containing HF followed by simultaneous measurements of multiple elements is becoming mainstream. Because only a small amount of acid is used for decomposition, the use of sealed Teflon vessels can reduce reagent blanks and avoid contamination. As mixed acid, HNO₃-HClO₄-HF or HClO₄-HF is generally used.

However, in the decomposition of samples containing aluminosilicates (i.e., seabed sediment) using HF, fluorides such as insoluble CaAlF_5 and $\text{CaMg}_2\text{Al}_2\text{F}_{12}$ are produced during decomposition. These fluorides may limit precise analysis of trace elements such as Rb, Sr, Y, Cs, Ba, REE, Pb, Th, and U due to coprecipitation with the fluorides (Yokoyama *et al.*, 1999). Therefore, it is necessary to dissolve the generated fluoride and moderately adjust the solution for the measurement.

To dissolve fluorides, a boric acid solution is added directly to the decomposed solution and diluted to a certain volume. Alternatively, the solution after decomposition is once evaporated in a Teflon beaker, the dried residue is dissolved with 5 %~10 % HNO_3 followed by the addition of a certain amount of boric acid solution and then dilution to a certain volume. The addition of boric acid promotes dissolution of fluoride and is also effective in masking excess HF. However, in adding boric acid, care must be taken because measurement sensitivity and sensitivity drift may occur when analyzing by ICP-AES/ICP-OES or ICP-MS because of the increase of matrix.

According to the method of Yokoyama *et al.* (1999), sediment samples are dissolved with a HClO_4 -HF solution, the solution is gradually heated to completely evaporate to dryness, and 1 ml of 7 M HClO_4 is added to the residue, which is then heated to completely evaporate to dryness. By this method, excess HF is completely removed and all fluorides transform to oxide. By dissolving the residue with HCl, evaporating again to dryness, and dissolving in 4 M HNO_3 solution, it is possible to recover nearly 100 % of the trace elements without coprecipitation with fluoride.

4. Biogenic opal

Opal is an amorphous silicate, and that formed by plankton is called biogenic opal. Biogenic opals are distinguished from volcanic amorphous aluminosilicates (volcanic glass). Diatoms, siliceous dinoflagellates, Parmales, radiolarians, and sponges are known producers of biogenic opal. In particular, diatoms and Parmales occupy a significant proportion of the community composition of phytoplankton in the subarctic North Pacific (Komuro *et al.*, 2005). Diatoms and radiolarians can be found in deep-sea sediments and have been used as indicators in stratigraphic and paleoceanographic studies based on their assemblages. In addition, from the vertical change in biogenic opal content in sediment, it is possible to reconstruct past changes in primary production in the ocean (e.g., Narita *et al.*, 2002).

The alkaline extraction method is commonly used for quantitative analysis of biogenic opal in sediments. However, in this method, dissolution of coexisting clay minerals occurs in addition to elution of Si from biogenic opal (e.g., DeMaster, 1981). Generally, desorption of Si from clay minerals increases in the order of illite < montmorillonite < kaolinite (Kamatani and Oku, 2000). Such desorption of Si is more remarkable with NaOH solution than Na_2CO_3 solution. Desorption of Si from sediment tends to increase with increasing concentration of alkaline solution. In addition, amorphous clay minerals such as allophane tend to release Si more quickly than kaolinite (Kamatani and Oku, 2000). At this time, the type and concentration of alkaline solution, dissolution temperature, and time for the measurement of biogenic opal in sediments have not yet been unified (Conley, 1998).

The methods of DeMaster (1981) and Mortlock and Froelich (1989) are widely used for analysis of

biogenic opal in seabed sediment. The difference between the two methods is whether the amount of dissolved Si from clay minerals, including volcanic glasses, is corrected. DeMaster (1981) dissolved Si in the sediment using a 1 % (0.1 M) Na_2CO_3 solution, and assumed that the temporal change of the Si concentration in the extract consisted of two different dissolution curves, for biogenic opal-derived Si (fast dissolution) and mineral-derived Si (slow dissolution). In this method, an intercept obtained from the approximate line of the Si dissolution curve after a sufficient time has been defined as concentration of biogenic opal-derived Si (time step method).

In contrast, Mortlock and Froelich (1989) recommend using a 2 M Na_2CO_3 solution and to heat uniformly for 5 hours at 85 °C to dissolve Si from biogenic opal. They reported that the contribution of Si dissolved from clay minerals was about 2 % to 3 %. Accordingly, this is a very advantageous method for measuring biogenic opal in many samples. However, dissolution of opal in radiolarians and sponge spicules is insufficient under these conditions (Mortlock and Froelich, 1998; Lyle and Lyle, 2002). There is also a method of correcting the contribution of dissolved Si from aluminosilicates using Al concentration eluted in alkaline solution (Kamatani and Oku, 2000). This method is unsuitable for measurement of a large number of samples. In addition, Shimesh *et al.* (1988) reported that dissolution of Si from clay minerals is not related to clay content or the clay/opal ratio in sediment.

Most of the biogenic opal in seabed sediment is derived from diatom, the primary producers (Nelson *et al.*, 1995). With this in mind, this section compares the method of DeMaster (1981) with the method of Mortlock and Froelich (1989) which is advantageous for analysis of biogenic opal of a large number of samples, and describe points to notice when analyzing biogenic opal.

4-1 Weighing sample mass

The content of biogenic opal in sediment greatly varies spatiotemporally. Therefore, when measuring the biogenic opal content, it is necessary to predict the biogenic opal content in advance and to adjust Si concentration in the measurement solution at the final step of the measurement.

According to DeMaster (1981), 10 to 30 mg of dried sediment is precisely weighed into a 50 ml polypropylene centrifuge tube, and 50 ml of 1 % (0.1 M) Na_2CO_3 solution previously heated to 85 °C is then added to dissolve biogenic opal. According to Mortlock and Froelich (1989), 25 to 200 mg of dried sediment is used, and 40 ml of 2 M Na_2CO_3 solution is added after the pretreatment described below. In these two methods, the ratio of sediment to the amount of alkaline solution (solid-liquid ratio) differs by one order of magnitude. In the former case, the solid-liquid ratio, is in the range of 0.2 to 0.6 g L⁻¹, and in the latter case, it is in the range of 0.63 to 5.0 g L⁻¹.

Although the solid-liquid ratio is an important factor when quantifying biogenic opal content by alkaline extraction using solid-liquid equilibrium, few studies have considered this quantitative relationship. Loassachan and Tada (2008) extracted Si by a time step method after the method of DeMaster (1981) with different solid-liquid ratios, and investigated the influence of the solid-liquid ratio on the recovery of biogenic opal. In addition, Lyle and Lyle (2002) examined the effect of extraction of biogenic opal by comparing two types of alkaline solutions, 2 M Na_2CO_3 and 2 M KOH. They found that in the range of the solid-liquid ratio of 1.1 to 2.4 g L⁻¹, when the solid-liquid ratio is small,

opal of biological origin is overestimated due to promotion of the elution of Si from clay minerals, and when the solid-liquid ratio is high, dissolution of Si is suppressed and leads to underestimation of biogenic opal. However, it should be noted that the solid-liquid ratio described here is “the ratio of the amount of sediment particles excluding organic matter and CaCO₃ to the amount of the alkaline solution”. Generally, the influence of organic matter content on the solid-liquid ratio in the extraction of biogenic opal is relatively small. However, when analyzing samples with high or variable CaCO₃ content, it is recommended to analyze biogenic opal content after determined CaCO₃ content.

Strictly speaking, the solid-liquid ratio applied to opal analysis needs to account for the type and concentration of the alkaline solution to be used, the reaction time, and the mineral composition of lithogenic matter in the sediment. Prior to analyzing biogenic opal in a sediment sample, it is preferable to conduct a preliminary experiment using a working standard or the sample to confirm the linear relationship between the sample amount and the extracted Si concentration.

For the biogenic opal analysis, dried sediment is precisely weighed with a balance that can measure to 0.1 mg. It should be noted that samples with high organic content may absorb moisture under a high humidity conditions. It is recommend to use a weighing dish made of non-electrified polystyrene. A boat-shaped weighing dish with sharp edges is helpful for transferring the sample to a centrifuge tube with a small amount of pure water. In addition, it is necessary to add the alkaline solution to the sample with 0.1 ml precision. As an alkaline solution such as 2 M Na₂CO₃ has high viscosity, it may results in low reproducibility when measuring the volume using a volumetric devise such as an automatic pipette. For this reason, measurement of the amount of alkaline solution and dilution for determination of sample and standard solutions are carried out on the basis of the mass.

4-2 Sample pretreatment

Mortlock and Froelich (1989) processes sample for biogenic opal determination to remove inorganic substances (oxides and sulfides) and organic matter covering the surfaces of biogenic opal with 10 % H₂O₂ and 1 M HCl. DeMaster (1981) did not carry out such pretreatment.

Pretreatment with H₂O₂ and HCl is a method widely used in the field of microscopic analysis of diatoms. Such pretreatment is effective for removing sulfide (Akiba *et al.*, 2014) and oxides formed on the surface or inside diatoms' frustules as well as in fecal pellets in coastal sediment. Nevertheless, few studies have examined the influence of this pretreatment on the quantitative analysis of biogenic opal (e.g., Michalopoulos and Aller, 2004). This process should be avoided as pretreatment has been found to be unnecessary, based on the fact that there is no significant difference in the results between those of Mortlock and Froelich (1989) and DeMaster (1981) (Conley, 1998).

During pretreatment, sediment particles must not be lost. For samples with large amounts of organic matter and CaCO₃, the reaction proceeds rapidly when H₂O₂ or HCl is added, or a substance such as manganese oxide in the sample acts as a catalyst to decompose H₂O₂, whereby the solution is ejected from the reaction vessel (centrifuge tube), and the sample may be lost in some cases. To avoid such problems, after the sample is swollen with a small amount of pure water, a further 4 ml of pure water should be added, and 2 mL of 30 % H₂O₂ should be dropped into the smple while confirming the

state of the reaction. The centrifuge tube is allowed to stand for 12 hours or more to decompose the organic matter and then heated in an oil bath for 60 minutes to promote decomposition of H_2O_2 . In this process, when the centrifuge tube is sealed, internal pressure rises because of the generated gas, and the centrifuge tube may rupture. Therefore, a pinhole is opened in the cap of the centrifuge tube (Mortlock and Froelich, 1989), and when the sample is left and heated, the cap should be closed loosely. After the tube is allowed to cool, 5 mL of 1 M HCl should be dropped in while the state of the reaction is checked. After confirming the dissolution of CaCO_3 , pure water is added to make the total volume 40 ml; the sample is then centrifuged at 3000 rpm (about 1500 g) for 10 minutes, and the supernatant solution is removed. Then, 40 ml of pure water is added, the deposit is resuspended, the sample is centrifuged at 3000 rpm (about 1500 g) for 10 minutes, and the supernatant solution is removed. At this stage, the solution becomes almost neutral. The deposit is dried in a vacuum freeze dryer. Heat drying should be avoided as it promotes agglomeration of the particles and prevents the particles from dispersing in the alkaline solution. For this reason, vacuum freeze drying is recommended.

4-3 Extraction conditions

The recommended conditions for extraction of biogenic opal from sediments differ greatly between scientists (Conley, 1998). The extraction of Si from sinking particles and cultivated diatoms can be completed in 20 to 30 minutes even with 1 % (0.1 M) Na_2CO_3 solution and it does not depend on the type or concentration of alkaline solution or processing time (Müller and Schneider, 1993; Kamatani and Oku, 2000). However, for extraction of Si from diatom fossils such as those of Pliocene age and diatomaceous earth, a longer processing time is required, and Na_2CO_3 solution may be insufficient (Müller and Schneider, 1993; Kamatani and Oku, 2000). Also, for radiolarians and sponge spicules, the processing time tends to increase compared that needed for diatom frustules or diatom shells, and dissolution may be insufficient even with 0.1 M NaOH solution (Müller and Schneider, 1993). Indeed, Mortlock and Froelich (1989) pointed out that dissolution of Si from radiolarians may be insufficient after 5 hours of treatment at 85 °C with 2 M Na_2CO_3 solution. Furthermore, Lyle and Lyle (2002) showed that dissolution of biogenic opal from sediments rich in radiolarians from the Miocene and Eocene was insufficient after processing with 2 M Na_2CO_3 solution, and recommended using 2 M KOH solution. However, except for some regions where radiolarian mud accumulates, such as the equatorial Pacific, the contribution of radiolarian-derived opal to total biogenic opal is ~ 2 % (Mortlock and Froelich, 1989).

4-4 Measurement conditions

Spectrophotometric analysis is commonly used for determination of dissolved Si in an alkaline solution, and sometimes it is measured with ICP-AES. In this section, points for determination of Si by the spectrophotometry are described.

The molybdenum blue and molybdenum yellow methods are available for spectrophotometric analysis of Si. Table 1 shows calculated Si concentration in 2 M Na₂CO₃ solution extracted from 100 mg of sediments containing several kinds of biogenic opal. In addition, Fig. 1 shows typical calibration curves from the molybdenum blue and molybdenum yellow methods using a 1 cm cell.

The molybdenum blue method has a high molecular absorptivity at a wavelength of 810 nm of $1.9 \times 10^4 \text{ L mol}^{-1} \text{ cm}^{-1}$ and a dynamic range of about 0 to 60 $\mu\text{mol L}^{-1}$ in the case of using a 1 cm cell. Therefore, for the determination of biogenic opal using the molybdenum blue method, it is necessary to dilute the alkaline solution by about 40 for analysis of a sample with opal content of 5%. When the opal content in the sample is 50%, it is necessary to dilute the alkaline solution by about 400 times. In the molybdenum yellow method, the molecular absorptivity is $2.8 \times 10^3 \text{ L mol}^{-1} \text{ cm}^{-1}$ at a wavelength of 385 nm, and $2.1 \times 10^3 \text{ L mol}^{-1} \text{ cm}^{-1}$ at a wavelength of 400 nm. This method has a wider dynamic range than that of the molybdenum blue method and is suitable for determination of high concentration of Si. The quantitative range when a 1 cm cell is used is from

0 to 400 $\mu\text{mol L}^{-1}$ at 385 nm, and from 0 to 600 $\mu\text{mol L}^{-1}$ at 400 nm. Therefore, when we apply a wavelength of 400 nm for measurement, Si can be measured for all sediment samples with biogenic opal content up to 75% by diluting the extracted alkaline solution by 50 times. Thus, the molybdenum yellow method is advantageous for quantitative determination of wide range of biogenic opals in sediments. However, fading is faster with the molybdenum yellow method than with the molybdenum blue method, and it is necessary to measure within 10 to 30 minutes after colouring is performed.

Table 1: Calculated Si concentration in 40mL of 2 M Na₂CO₃ solution extracted from 100 mg of sediments containing several kinds of biogenic opal content.

Biogenic opal (%)	Si conc. in 2 M Na ₂ CO ₃ ($\mu\text{mol/L}$)
5	1857
10	3715
25	9287
50	18574
75	27860

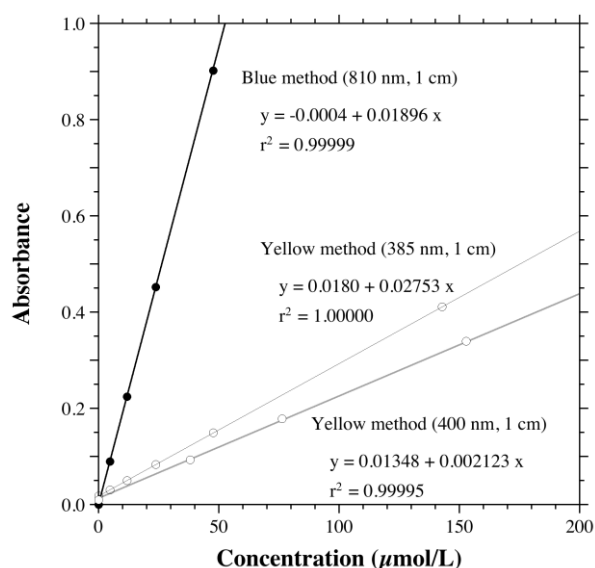


Fig1: Examples of calibration curves using molybdenum blue method and molybdenum yellow method.

4-5 Calculation of biogenic opal content

Because biogenic opal contains ~15 % water molecules in its crystal, the existence of water cannot be ignored when considering the composition of the sediment. Mortlock and Froelich (1989) proposed that the chemical formula of biogenic opal in sediment is $\text{SiO}_2 \cdot 0.4\text{H}_2\text{O}$ and that the molar mass is 67.3. The formula for determining the amount of biogenic opal (%BO) in the sediment from the Si concentration in a diluted alkaline solution is shown below:

$$\% \text{BO} = \frac{C_{\text{dilu}} \times 10^{-3} \cdot w_{\text{dilu}} / w_{\text{div}} \cdot w_{\text{alk}} \cdot 67.3 \times 10^{-6}}{w_{\text{sed}}} \times 100$$

where,

C_{dilu}	: Si concentration in diluted alkaline solution ($\mu\text{mmol kg}^{-1}$)
w_{dilu}	: Mass of diluted alkaline solution (g)
w_{div}	: Mass of dispensed Na_2CO_3 solution before dilution (g)
w_{alk}	: Mass of Na_2CO_3 solution used for extraction of biogenic opal (g)
67.3	: Molar mass of biogenic opal (g mol^{-1})
w_{sed}	: Mass of sediment sample used for analysis (g)

5. Calcium carbonate (CaCO_3)

CaCO_3 in the sediment is classified into material of terrestrial origin and of biological origin. The former is derived from rivers and atmospheric dust represented by kosa, whereas the latter is produced by coccolithophore and foraminifera. In the North Pacific, CaCO_3 is dissolved in the deep sea where water depth exceeds 3000 m, and it can be measured from sediment in the shelf area, continental slope, or seamounts at depths of ~2500 m. Coccolithophores and foraminifera, like diatoms and radiolarians, have been used as stratigraphic and palaeoceanographic proxies based on fossil assemblages. In addition, from vertical changes in the CaCO_3 content of seabed sediments, fluctuation of past primary production in the ocean can be reconstructed.

There are two main methods of analyzing CaCO_3 in sediment. In the first method, CaCO_3 content is obtained from the difference between the total carbon amount and the organic carbon amount measured by a CHN analyzer, and the second method is to quantify the generated CO_2 based on the coulometric titration after acid is added to the sample. As the pretreatment line differs according to its design philosophy, in this chapter, we only describe the points to be noted for CaCO_3 determination based on coulometric titration. Guidelines for handling the coulometric titrator and calibration method of the equipment are provided by Dickson *et al.* (2007).

5-1 Samples and weighing sample mass

The content of CaCO_3 in the sediment varies spatiotemporally. In the coulometric titration method, if a large amount of CO_2 is introduced into the apparatus in a short time, the temperature of the

electrolytic cell increases considerably. In such a case, the dissociation constant of the pH indicator used in the catholyte solution is changed, and the detection sensitivity at the end point of the titration varies for each calibration and sample. Therefore, it is important to minimise the change in temperature of the electrolysis cell between measurements as much as possible, and for that purpose, it is necessary to change the amount of sample to be measured according to the CaCO_3 content.

Dickson *et al.* (2007) recommends replacing the cell solution when the cumulative amount of CO_2 introduced into the electrolysis cell reaches 2 mmol, or if 12 hours have elapsed after the first measurement. If measuring CaCO_3 using 25 mg of a sample containing 25 % of CaCO_3 , 30 samples can be measured with one cell adjustment. The number of samples is 10 when measuring with 25 mg of sample containing 75 % of CaCO_3 . Therefore, when measuring a sample with 75 % CaCO_3 content, the sample amount should be reduced to about 10 mg. In this case, about 25 samples can be measured within the constraint of 2 mmol.

Dry sediment samples to be analyzed are precisely weighed with a semi-microbalance capable of measuring to 0.01 mg or with a microbalance capable of measuring to 0.001 mg. Samples with high contents of organic matter absorb moisture during weighing and may increase in mass. Therefore, when weighing, attention should be paid to control the humidity and temperature of the atmosphere. The balance should be installed under conditions of 45 %~60 % relative humidity and 20 °C ~25 °C temperature. However, when the relative humidity becomes 45 % or less, caution is required because the substance becomes easy to charge, measurement error is caused by the generated static electricity, and the balance display becomes unstable. Recently, a balance with a function of static electricity removal has also become available. To weigh the sample, it is advisable to use a glass container with a diameter of 4 mm~5 mm. When measuring, the container should be inserted together with the sample directly into the reaction tube of the coulometer using tweezers.

5-2 Calibration

Calibration of equipment designed specifically for solid sample is carried out using Na_2CO_3 . For the calibration, Na_2CO_3 (purity 99.95 %) or high-purity inorganic material (CRM3005-a, purity 99.970 ± 0.016 %) distributed by National Metrology Institute of Japan, AIST, Japan is used as the standard material for volumetric analysis. In addition, high-purity CaCO_3 is sometimes used (Mörth and Backman, 2011). For calibration of the instrument, 4 to 5 points of the standard in the range of 10 to 30 mg, and a further 5 to 10 points, including the acid blank, are measured. For calibration, the slope is calculated by linear regression of the amount of introduced CO_2 calculated from the mass of the standard substance and the

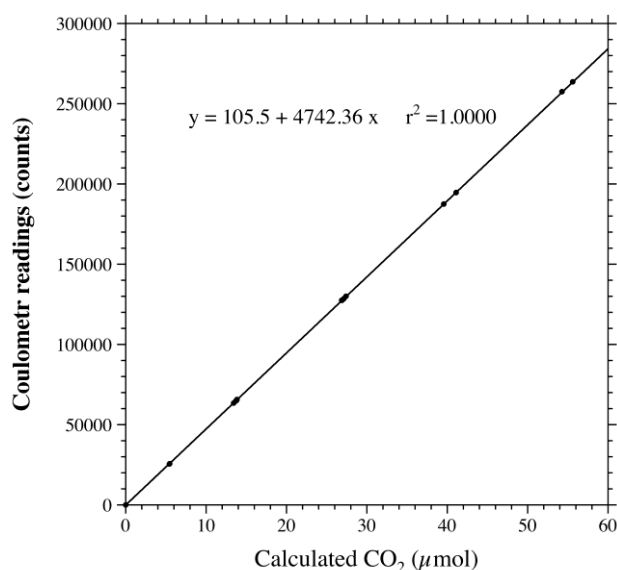


Fig. 2: Relationship between amount of CO_2 and coulometric titration value.

coulometric titration (counts). This slope is used as a calibration factor (counts mol⁻¹) for calculation of CaCO₃ concentration.

If the instrument can process both solid and liquid samples, a Na₂CO₃ solution is used for calibration. The solution is prepared according to Dickson *et al.* (2007). The instrument is calibrated with measurements of 4 to 5 points in the standard solution and 5 to 6 points with the acid blank as described above. As described above, the linear regression slope is obtained from the amount of CO₂ and the coulometric titration value (counts) (Fig. 2) and used as the calibration factor for the following calculation of CaCO₃ content:

$$\%CC = \frac{N_s - b \cdot t - a}{c} \cdot \frac{100.08}{w_{\text{sed}}} \times 100$$

where,

%CC	: CaCO ₃ content in sediment (%)
N_s	: Coulometric titration value (counts)
a	: Acid blank (counts)
b	: Background count rate of the system (counts min ⁻¹)
c	: Calibration factor (counts mol ⁻¹)
t	: Measuring time (min)
100.08	: 100.08: Molar mass of CaCO ₃ (g mol ⁻¹)
w_{sed}	: Mass of sediment sample used for analysis (g)

5-3 Effect of terrestrial carbonate

Seabed sediment contains CaCO₃ (calcite) of terrestrial origin in addition to biogenic carbonates such as coccolithophores and foraminifera. Oba and Pedersen (1999) reported that CaCO₃ derived from atmospheric dust comprises up to 40 % of total CaCO₃ in sediments of the coldest period of the Last Glacial Maximum in the Sea of Japan. In addition, eolian dust from the Eurasian continent such as kosa may contain dolomite (CaMg(CO₃)₂), depending on its source (Li *et al.*, 2007).

Because dolomite has lower solubility in acid than calcite (e.g., Li *et al.*, 2007), dissolution of dolomite using acids such as 8.5 % phosphoric acid (Dickson *et al.*, 2007) and 2 M HCl (Mörth and Backman, 2011), which are generally used in coulometric titration, takes a long time for the reaction to compete. Nevertheless, CaCO₃ content in sediment measured by coulometric titration includes the influence of dolomite in addition to terrestrial calcite. At present, unfortunately, there is no technique to clearly separate biogenic calcite from terrestrial calcite or dolomite.

6. Organic matter

As a technique to estimate the organic carbon content in sediments, the loss on ignition method combusting the sample at 550 °C has been used for a long time (e.g., Dean, 1974, Heiri *et al.*, 2001). However, the loss on ignition also contains the mass associated with dehydration and hydrolysis of clay

minerals, and is therefore also affected by the clay content in sediments in addition to the conditions of the analysis (Dean, 1974). Therefore, in general, the amount of organic matter in the sediment is determined based on the organic carbon content in the sediment analyzed using an elemental analyzer. In recent years, an elemental analyzer/isotope ratio mass spectrometer (EA/IRMS) has commonly been used, and it is possible to measure nitrogen content and stable isotopic ratios of carbon and nitrogen in addition to carbon content from the same sample.

The details of the measurement of organic carbon content using an elemental analyzer are described in Volume 4 Chapter 1 of these guidelines (Yoshimura, 2016), and analysis using an EA/IRMS system is described in Volume 4 Chapter 3 (Umezawa, 2016). In this section, general points to be noted for analysis of organic carbon/nitrogen contents and their stable isotope ratios in sediments using EA/IRMS are described.

6-1 Samples and sample pretreatment

A required amount of dried sediment is transferred into a tin or silver sample capsule and precisely weighed with a microbalance capable of measuring to 0.001 mg. Because a sample with a large amount of organic matter absorbs moisture during weighing, attention must be paid to controlling the humidity and the temperature of the atmosphere in the laboratory. The balance should be installed in an atmosphere with a relative humidity of 45 %~60 % and an air temperature of 20 °C~25 °C. However, when the relative humidity becomes 45 % or less, caution is required; because the substance on the balance will be charged, measurement error will be caused by the generated static electricity, and the display of the balance will become unstable. Recently, a balance with function of static electricity removal has also become available.

Because impurities such as carbon are attached to the surfaces of tin or silver capsules in the manufacturing process, there is a possibility that this carbon may affect the measurement of organic carbon in sample. The sample capsules must be cleaned in advance of organic carbon analysis. In this cleaning process, a 1:1 (v:v) mixture of methanol and dichloromethane is used (Ogawa *et al.*, 2013). In addition to cleaning with this methanol-dichloromethane solution, heating at 150 °C is effective for tin capsules (Maruoka, 2008) and heating for 3 hours at 550 °C is effective for silver capsules (Brodie *et al.*, 2011). Five cleaned sample capsules are measured simultaneously with the samples, and the result is regarded as a capsule blank for background correction.

To measure the organic carbon content and stable isotopic ratio, it is important to completely remove the carbonate in the sample. The dissolution and removal of this carbonate can be carried out by a method of processing the sample using a silver sample capsule, or by processing the sample in a container such as a beaker or a centrifuge tube (Ogawa *et al.*, 2013; Brodie *et al.*, 2011; Schubert and Nielsen, 2010).

When processing in a capsule, a silver sample capsule should be used. The necessary amount of sediment sample is weighed in the capsule, the sample is swollen with pure water, and the capsule is put in a desiccator together with a beaker containing about 40 ml of concentrated HCl and left for about 24 hours to remove carbonate minerals. During this process, care should be taken not to blow up the

sample. Also, as the pressure inside the desiccator rises with HCl vapor or generated CO₂, it is necessary to move the lid and release the pressure every few minutes initially and every few hours after the reaction becomes stable. Because carbonate sometimes does not dissolve completely (Schubert and Nielsen, 2010), the sample capsule is taken out of the desiccator, 4 M HCl is added dropwise, and the presence of reaction is checked. When the reaction is insufficient, 4 M HCl can be dropped into the sample until the reaction is not observed, and the sample can be heated on a hot plate at 50 °C as necessary to reduce the solution and promote dissolution of the carbonate. The above mentioned procedure is carried out in a fume hood. In addition, it is easy to work by placing the sample capsules on a well plate. When dissolution of the carbonate is confirmed, the sample capsules are heated on a hot plate until the moisture and hydrochloric acid odor disappears. Thereafter, the capsule is heated at an oven at 50 °C. Dried samples are kept in a desiccator until analysis. The calcium dissolved in sample capsules precipitates as hygroscopic CaCl₂. If the sample is stored in a desiccator over several days, the sample should be dried in an oven at 50 °C immediately before it is wrapped in a tin capsule.

When processing the sample in a container such as a beaker or a centrifuge tube, attention should be paid to avoid losing the sample particles. It is recommended to use a centrifuge tube to reduce this loss (Brodie *et al.*, 2011). Two to three times the required amount of sample should be weighed for one analysis in a 50 ml centrifuge tube, 5 ml of pure water is added dropwise to swell the sample, and 5 ml of 4 M HCl is gently added dropwise. Another 20 ml of 4 M HCl is added and the sample is left for about 24 hours. Then, 10 ml of pure water is added, and the sample is centrifuged for 10 min at 3000 rpm (about 1500 g). After the supernatant solution is removed with a pipette, 40 ml of pure water is added to wash the sample after removal of carbonate, followed by centrifugation at 3000 rpm (about 1500 g) for 10 minutes. This washing operation is carried out twice. Finally, after the supernatant solution is reduced to 5 ml with a pipette, the sample in the centrifuge tube is frozen in a freezer and dried in a vacuum freeze dryer. The dried samples are kept in the desiccator until analysis. In the analysis of the organic carbon and total nitrogen contents and the stable isotopic ratios of both elements, the required amount of the carbonate-free sample is precisely weighed and transferred into a tin capsule. As the organic carbon and total nitrogen contents measured by this operation are concentrations based on the mass of the sample without sea salt and carbonate, they are converted into the concentrations per bulk sediment based on the water content and CaCO₃ content.

6-2 Important point for analysis using an elemental analyzer/isotope ratio mass spectrometer (EA/IRMS)

In the elemental analyzer/isotope ratio mass spectrometer (EA/IRMS) system, gas is generated in the elemental analyzer by combustion of a sample introduced through the reduction furnace, dehydration column and gas chromatograph. For this reason, isotopic fractionation occurs in each of these processes. Because the value of the stable isotopic ratio measured by the EA/IRMS is relative to the standard material, conditions such as the combustion temperature, the dilution ratio by He gas, and the type of column of the gas chromatograph, as well as the correction method using the measured value of reference materials affect the stability and precision of the measured value. Therefore, it is necessary

to carefully manage the obtained value at all times (e.g., Suzuki *et al.*, 2012; Ogawa *et al.*, 2013).

6-2-1 Preparation and introduction of samples

In the general EA/IRMS analysis, the necessary amount of the element for measurement is 30 μg for C and 80 μg for N. When the introduction amount to the mass spectrometer is decreased, sufficient signal cannot be obtained and the influence of the blank increases. Also, when the introduction amount increases, fractionation caused by the introduction device becomes large (Ogawa *et al.*, 2013). Therefore, with reference to the measurable area of the equipment to be used, it is necessary to draw a scattergram showing the relationship between the isotopic ratio (δ value, which may be a value for the reference gas) and the output (peak area) of m/z 44 in C and m/z 28 in N. In general, the N content in organic matter is significantly lower than the C content, and the C/N ratio in sediments varies spatiotemporally. In EA/IRMS, when measuring C, the introduced CO_2 is diluted by He before the appearance of the CO_2 peak, and the relationship between the output and the measured value changes. When preparing the scattergram, it is recommended to create one for each case of dilution and no dilution (Ogawa *et al.*, 2013). From this scatter plot, the lower and upper limits of the output from which a stable isotopic ratio (± 0.1 to 0.2%) can be obtained are set, and the amount of sample to be used for measurement is determined. With regard to the measurement of N, the measured value may vary due to the influence of N in the air, so it is necessary to ensure extrusion of the air when wrapping the sample with the tin sample capsule. A small amount of carbon contained in the tin/silver sample capsule also influences the measurement as a blank.

6-2-2 Calibration and correction

If pretreatment and introduction of samples are properly performed, a positive correlation is found between the output (peak area) and the introduced amount. From this relationship, it is possible to quantify the amount of C and N. If combustion becomes incomplete or if separation of the peak becomes insufficient because of accumulation of cinders in the combustion furnace and obstruction of the combustion gas, the measured value vary and the correlation coefficient decreases (Umezawa, 2016: Volume 4, Chapter 3). By monitoring the oxygen isotopic ratio measured in the CO_2 measurement mode, it is possible to confirm the oxidation state and the presence of incomplete combustion (Sato and Suzuki, 2010).

When measuring with EA/IRMS, three or more types of work standards with different δ values should be measured for every ten samples. The working standards should be calibrated beforehand with three to four internationally certified reference materials (Ogawa *et al.*, 2013). There is a liner relationship between the δ value of the working standard calibrated with the reference materials (δ_{ISM}) and the provisional δ value of the working standard (δ_{RF} : δ value relative to the reference gas). The δ value of the sample is obtained from linear regression between the δ values ($\delta_{\text{RF}} = a \delta_{\text{ISM}} + b$).

6-2-3 Validation of the memory effect

In analysis by EA/IRMS, because samples are continuously introduced into a combustion furnace with an auto sampler, depending on the properties and the isotopic ratios of the samples, the measured result of a sample introduced later is influenced by the signals derived from the former samples. This is called the memory effect. The memory effect may change depending on the adjustment of the apparatus or the furnace. To validate this effect, it is necessary to measure the working standards with different isotopic ratios five times alternately (Sato and Suzuki, 2010). For this measurement, it is desirable for the sample amount for each analysis to be equalized as much as possible. When an obvious memory effect is observed, the measurement result of a sample with a low δ value immediately after measuring a sample with a high δ value is shifted toward the higher side than the value to be indicated, and becomes gradually lighter from the second measurement. Generally, in the analysis of stable isotopic ratios of C and N, this effect is small, but S isotopic ratio analysis often shows a significant effect (Maruoka, 2008). When a significant memory effect appears, it is necessary to make improvements by adjusting the furnace and to take measures such as revision of measurement methods or measuring samples multiple times (Sato and Suzuki, 2010).

References

- Quan, H., H. Yeru, M. Nishikawa, and M. Morita (1994): Carbonate carbon in the original soil particles of kosa aerosols. *J. Environ. Chem.*, **4**, 677-682.
- JIS 8816, Particulate materials—General requirements for methods of sampling, Standard Association, Tokyo (2001).
- Imai, N. (2010): Investigation of the distribution of elements of the whole of Japan and their applications – Geochemical map of land and sea of Japan—. *Synthesiology*, **3**, 281-291.
- Mortlock, R.A. and P.N. Froelich (1989): A simple method for the rapid determination of biogenic opal in pelagic marine sediments. *Deep-Sea Res.*, **36**, 1415–1426.
- Nederbragt, A.J., J.W. Thurow, and P.R. Bown (2008) : Paleoproductivity, ventilation, and organic carbon burial in the Santa Barbara Basin (ODP site 893, off California) since the last glacial. *Paleoceanography*, **23**, PA1211, doi:10.1029/2007PA0011501.
- Taylor, S.R. (1964) : Abundance of chemical elements in the continental crust: A new table. *Geochim. Cosmochim. Acta*, **28**, 1273-1285.
- Noriki, S. and S. Tsunogai (1985): Particulate fluxes and major components of settling particles from sediment trap experiments in the Pacific Ocean. *Deep Sea Res. Part A*, **33**, 903-912.
- Ravichandran, M., M. Baskaran, P.H. Santschi, and T.S. Bianchi (1995): History of trace metal pollution in Sabine –Neches Estuary, Beaumont, Texas. *Environ. Sci. Technol.*, **29**, 1495-1503.
- Turekian, K.K. and K.H. Wedepohl (1961): Distribution of the elements in some major units of the Earth's crust. *Geol. Soc. Am. Bull.*, **72**, 175-192.

- Taylor, S.R. and S.M. McLennan (1985): *The Continental Crust: Its Composition and Evolution*. Blackwell Sci. Cambridge, Mass.
- Reitz, A., K. Pfeifer, G.J. de Lange, and J. Klump (2004) : Biogenic barium and the detrital Ba/Al ratio: a comparison of their direct and indirect determination. *Mar. Geol.*, **204**, 289-300.
- Schenau, S.J., M.A. Prins, G.J. de Lange, and C. Monnin (2001) : Barium accumulation in the Arabian Sea: Controls on barite preservation in marine sediments. *Geochim. Cosmochim. Acta*, **65**, 1545-1556.
- Dymond, J., R. Collier, J. McManus, S. Honjo, and S. Manganini (1997) : Can the aluminum and titanium contents of ocean sediments be used to determine the paleoproductivity of the oceans? *Paleoceanography*, **12**, 586-593.
- Hokanishi, N., A. Yasuda, and S. Nakada (2015): Major and trace element analysis of silicate rocks using fused glass beads with an X-ray fluorescence Spectrometer. *Bull. Earthq. Res. Inst. Univ. Tokyo*, **90**, 1-14.
- Noriki, S., K. Nakanishi, T. Fukawa, M. Uematsu, T. Uchida, and S. Tsunogai (1980): Use of a sealed Teflon vessel for the decomposition followed by the determination of chemical constituents of various marine samples. *Bull. Faculty Fish. Hokkaido Univ.*, **31**, 354-361.
- Yokoyama, T., A. Makishima, and E. Nakamura (1999) : Evolution of the coprecipitation of incompatible trace elements with fluoride during silicate rock dissolution by acid digestion. *Chem. Geol.*, **157**, 175-187.
- Komuro, C., H. Narita, K. Imai, Y. Nojiri and R.W. Jordan (2005) : Microplankton assemblages at Station KNOT in the subarctic western Pacific, 1999-2000. *Deep Sea Res. II*, **52**, 2206-2217.
- Narita, H., M. Sato, S. Tsunogai, M. Murayama, M. Ikehara, T. Nakatsuka, M. Wakatsuchi, N. Harada and Y. Ujiie (2002): Biogenic opal indicating less productive northwestern North Pacific during the glacial ages. *Geophys. Res. Lett.*, **29**, 10.1029/2001GL014320.
- DeMaster, D.J. (1981): The supply and accumulation of silica in the marine environment. *Geochim. Cosmochim. Acta*, **45**, 1715 – 1732.
- Kamatani, A. and O. Oku (2000): Measuring biogenic silica in marine sediments. *Mar. Chem.*, **68**, 219-229.
- Conley, D.J. (1998): An interlaboratory comparison for the measurement of biogenic silica in sediments. *Mar. Chem.*, **63**, 39-48.
- Lyle, A.O. and M.W. Lyle (2002): 6. Determination of biogenic opal in pelagic marine sediments: a simple method revisited. In *Proceedings of the Ocean Drilling Program, Initial Reports. Volume 199* (Lyle, M., Wilson, P. A., Janecek, T. R., et al., eds), pp. 1-21. College Station, TX (Ocean Drilling Program).
- Shimesh, A., R.A. Mortlock, R.J. Smith, and P.N. Froelich (1988): Determination of Ge/Si ratios in marine siliceous microfossils: separation, cleaning and dissolution of diatoms and radiolaria. *Mar. Chem.*, **25**, 305-323.
- Nelson, D.M., P. Tréguer, M.A. Brzezinski, A. Leynaert, and B. Quéguiner (1995): Production and dissolution of biogenic silica in the ocean: revised global estimate, comparison with regional data and relationship to biogenic sedimentation. *Global Biogeochem.*, **9**, 359-372.
- Loassachan, N. and K. Tada (2008): Effect of solid to solution ratio on biogenic silica determination in coastal sediments. *J. Oceanogr.*, **64**, 657-662.
- Akiba F., Y. Tanimura, T. Oi, S. Ishihama, and R. Matsumoto (2014): Diatom biostratigraphy and diatom-derived black grains of the uppermost Quaternary cores from the Japan Sea, and their paleoceanographic implications. *J. Jap. Assoc. Petroleum Technol.*, **79**, 130-139.

- Michalopoulos, P. and R.C. Aller (2004): Early diagenesis of biogenic silica in the Amazon delta: Alteration, authigenic clay formation, and storage. *Geochim. Cosmochim. Acta*, **68**, 1061-1085.
- Müller, P. J. and R. Schneider (1993): An automated leaching method for the determination of opal in sediments and particulate matter. *Deep-Sea Res.*, **40**, 425–444.
- Dickson, A.G., C.L. Sabine, and J.R. Christian (2007): Guide to best practices for ocean CO₂ measurements. PICES Special Publication 3, https://www.nodc.noaa.gov/ocads/oceans/Handbook_2007.html
- Mörth, C.-M. and J. Backman (2011): Practical steps for improved estimates of calcium carbonate concentrations in deep sea sediments using coulometry. *Limnol. Oceanogr. Methods*, **9**, 565-570.
- Oba, T. and T.F. Pedersen (1999): Paleoclimatic significance of eolian carbonates supplied to the Japan Sea during the last glacial maximum. *Paleoceanography*, **14**, 34-41.
- Li, G., J. Chen, J. Yang, J. Ji, and L. Liu (2007): Dolomite as a tracer for the source regions of Asian dust. *J. Geophys. Res.*, **112**, D17201, doi:10.1029/3007/JD008676.
- Dean, W.E. (1974): Determination of carbonate and organic matter in calcareous sediments and sedimentary rocks by loss on ignition: comparison with other methods. *J. Sed. Petrol.*, **44**, 242–248.
- Heiri O., A.F. Lotter and G. Lemcke (2001): Loss on ignition as a method for estimating organic and carbonate content in sediments: reproducibility and comparability of results. *J. Paleolim.*, **25**, 101–110.
- Yoshimura, T. (2016): Particulate organic carbon (POC), particulate nitrogen (PN), and particulate phosphorus (PP). *Guideline of Ocean Observations*, Vo. 4, Chap. 1, G401EN:001-006.
- Umezawa, Y. (2016): Carbon and Nitrogen Stable Isotopes in Particulate Organic Matter. *Guideline of Ocean Observations*, Vo. 4, Chap. 3, G403EN:001-008.
- Ogawa, N., G. Wang, H. Shinohara, and N. Ohkouchi (2013): Accurate measurements of carbon and nitrogen stable isotope ratio by EA/IRMS : technical guide for isotope ratio mass spectrometry. Japan Chemical Analysis Center.
- Brodie, C. R., M.J. Leng, J.S.L. Casford, C.P. Kendrick, J.M. Lloyd, Z. Yongqiang, and M.I. Bird (2011): Evidence for bias in C and N concentrations and $\delta^{13}\text{C}$ composition of terrestrial and aquatic organic materials due to pre-analysis acid preparation methods. *Chem. Geol.*, **282**, 67-83.
- Maruoka, T. (2008): Isotope analysis of carbon and sulfur in solid materials using continuous-flow isotope ratio mass spectrometer: Improvements for high-precision analysis. *Chikyukagaku (Geochemistry)*, **42**, 201-216.
- Schubert, C.J. and B. Nielsen (2010): Effects of decarbonation treatments on $\delta^{13}\text{C}$ values in marine sediments. *Mari. Chem.*, **72**, 55-59.
- Suzuki, Y., Y. Chikaraishi, K. Yamada, and N. Yoshida (2012): Interlaboratory comparison of carbon, nitrogen, and oxygen isotope ratios in organic chemicals using elemental analyzer-isotope ratio mass spectrometer. *Bunseki Kagaku (Analytical Chemistry)*, **61**, 805-810.
- Sato, R., and Y. Suzuki (2010): Carbon and Nitrogen stable isotope analysis by EA/IRMS. *Res. Org. Geochem.*, **26**, 21-29.

Pore water

○Hisashi NARITA (Tokai University), Shigeyoshi OTOSAKA (Japan Atomic Energy Agency)

Physical, chemical and biological changes that occur during sedimentation and consolidation in the seafloor are collectively termed “diagenesis”. In particular, oxidative decomposition of organic matter occurring several meters beneath the seafloor, and various changes in chemical composition and those due to mineral formation are termed early diagenesis. Changes in the concentration of chemical components due to changes in the sedimentary environments are more pronounced than those due to diagenesis. For this reason, it is extremely difficult to measure diagenesis directly from changes in the chemical composition of sediments, except that of the uppermost surface layer of the sediment. To clarify our understanding of diagenesis, including early diagenesis, measurement of the chemical components of pore water is extremely effective (e.g., Masuzawa and Kitano, 1983; Gamo and Gieskes, 1992). In particular, it is crucial to measure chemical constituents of pore water to determine the migration velocity of substances in the sediment-seawater boundary layer accompanying changes in the redox environment of the sediments (e.g., Berner, 1980; Watanabe and Tsunogai, 1984; Anderson *et al.*, 1989). Moreover, by measuring the stable isotopic ratio of oxygen and hydrogen in pore water and the chloride ion concentration, including a correction of the effect of advection/diffusion, it is possible to reconstruct past salinity fluctuations above the seafloor (Kato *et al.*, 1996a; Adkins *et al.*, 2002; Schrag *et al.*, 2002). Also, using chloride ions and oxygen and hydrogen isotopes, it is possible to infer the existence of the advection of pore water (Kato *et al.*, 1996a), and to estimate the diffusion velocity (e.g., Spivack *et al.*, 2002; Toki *et al.*, 2014).

1. Sediment sampling

Core samplers such as multiple, gravity and piston corers are used for sediment coring for collecting pore water. Details of sediment sampling are described in Chap. 5 of this volume. In particular, for research aimed at estimating the migration rate of substances in the sediment-seawater boundary layer, the use of a multiple corer that can collect the overlying water is recommended. For studies in coastal areas and lakes that require a sediment cores several meters in length or longer, mechanical rotary boring using a hydraulic thin-wall sampler may also be used in sampling.

2. Sampling of pore water

As a method for separating pore water from sediments, the centrifuge method and pressurization method are commonly used. The sediment core is sliced into thin layer immediately following collection, and the subsample is placed in a centrifuge tube or a polyethylene syringe for pore water separation. Manheim (1968) and Kato *et al.* (1996b) are good examples of studies using a polyethylene syringe. When a large amount of pore water is required or pore water must be separated from sediment with low water content, a stainless pressurized container combined with a hydraulic pump can also be used to squeeze pore water (Manheim and Sayles, 1974; Gamo and Gisekousu, 1992). Otherwise, in-situ sampling of pore water using a special suction unit has also been proposed (Sayles *et al.*, 1976; Masuzawa *et al.*, 1991; Beck *et al.*, 2007).

Pore water separated from sediment is filtered through a 0.45 μm (or 0.2 μm) disposable membrane filter and analyzed as quickly as possible. The material of the filter must be tested and selected carefully to reduce the effect of contamination of the target component. For example, a cellulose-mixed ester filter potentially causes contamination of NO_2 . If the sample can not be analyzed immediately and must be stored until analysis, the pore water should be placed in a polyethylene or glass container, depending on the target component; sealed without creating headspace; and stored in a refrigerator. In the case of heavy metal measurement, nitric acid should be added and the sample should be stored in an acidic condition of approximately pH 2. In the case of the measurement of components that may change due to microbial activity, mercuric chloride is added prior to storage. In these cases, it is necessary to accurately obtain the dilution rate of the pore water by adding chemicals. In the case of the analysis of alkali and alkaline earth metals, sulfides, sulfate ions, halogen etc., it is not necessary to acidify the sample. When storing a pore water sample, it is necessary to minimize the evaporation of water.

3. Effects to consider during pore water sampling

Gases in contact with pore water during collection of sediment and separation of pore water may have a significant effect on the concentration of chemical constituents in the separated pore water (e.g., Masuzawa *et al.*, 1980; Toole *et al.*, 1984; Barnes and Cochran, 1988). In particular, to remove the effects of pressure, temperature, and oxygen at the time of separation, the only means is to separate the pore water in the sediments at the site. To solve this problem, an in-situ pore water sampler that can be used in the deep sea has been developed (Sayles *et al.*, 1976; Masuzawa *et al.*, 1991) and an in-situ sampling method for shallow water (Seeberg-Elverfeldt *et al.*, 2005; Beck *et al.*, 2007) has also been developed. If pressure change is excluded, during pore water separation temperature and contamination by oxygen in the atmosphere are important.

3-1 Pressure effect

The difference in pressure between the site where the sediment was collected and that where the pore water is separated influences the concentration of the chemical components in the pore water to a considerable extent. To eliminate this effect, there is no means to separate the pore water at the site. As an example of the influence of pressure change, an increase in uranium concentration in pore water due to dissolution of carbonate has been reported (Toole *et al.*, 1984). It is also known that dissolved gases with low solubility, such as methane, are degassed as pressure decreases from sampling to separation (Jørgensen and Kasten, 2006).

3-2 Temperature effect

In many cases, the temperature of the sediment increases during the sampling process from sediment collection to pore water separation. Therefore, sediment samples should remain refrigerated except when the samples are being sliced or packed. If possible, these processes should be performed in a low-temperature laboratory, and when separating the pore water, it is necessary to use a temperature-

controlled centrifuge or a low-temperature thermostatic tank so that the samples can be remain in a similar environment as that of the sampling site. Temperature control during pore water separation is particularly crucial in measurements of chemical components such as potassium, silicon, boron, magnesium and total alkalinity in pore water, of which the reversible dissolution equilibrium between the solid-liquid phase dominates the concentration in the pore water. To eliminate the influence of temperature from the measurement of these components in pore water, the sediment is sealed in a container such as a syringe, adjusting the temperature to that of the sampling site. After reaching the set temperature, it is maintained for 3 to 4 hours, and then pore water separation is initiated (Masuzawa *et al.*, 1980).

3-3 Effect of contaminants in the atmosphere

Except for pelagic sediments such as red clay, because dissolved oxygen in pore water in sediments is consumed by decomposition of sedimentary organic matter, the concentration is lower than that in the bottom water on the seabed or is zero. Therefore, when separating pore water, it is necessary to avoid sediments contact with the atmosphere, which contains a high concentration of oxygen, following collection. For this purpose, the processes of removing the overlying water of the sediment core, slicing the sediment, and packing the sliced samples in containers must be performed rapidly or under a nitrogen atmosphere. It should be noted that the influence of the concentrations of the target components cannot be sufficiently eliminated for uranium in the pore water of reductive coastal sediments even if such operations are performed (Barnes and Cochran, 1988; Nagao *et al.*, 1992).

As a method of separating the pore water without allowing sediment to come into contact with the atmosphere, a piston is mounted above and below the core tube and the pore water is separated while being pressurized (Bender *et al.*, 1988; Jahnke, 1988). Fig. 1 shows a schematic diagram of a method of compressing and separating pore water by Jahnke (1988). Nagao *et al.* (1992) succeeded in measuring uranium in pore water using this method without the influence of contamination. However, under method it is difficult to control the temperature, unless separation work of pore water is performed in a low-temperature laboratory.

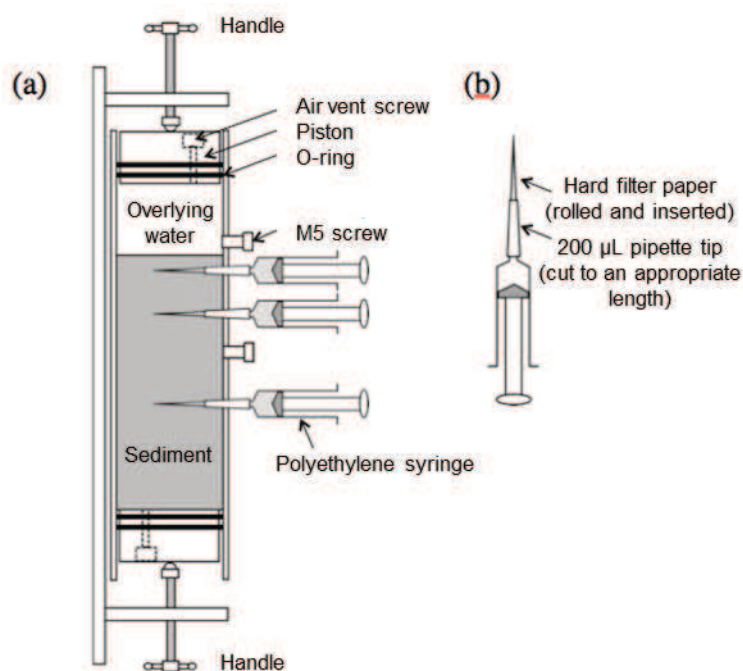


Fig. 1: (a) Overview of the squeeze separation method of pore water and that of the (b) syringe barrel (Jahnke, 1988). Before sediment coring, drill 4.2 mm holes at the side wall of the core barrel with an interval of 2~5 cm, and cut a screw thread (M5) in the holes. Keep the M5 screws in the unused holes. Turn the handle and push up the lower piston to squeeze the pore water. Modified from Narita and Kato (2007).

In recent years, a method of collecting pore water using a Rhizon sampler has been applied as well to seabed sediments (Seeberg-Elverfeldt et al., 2005; Dickens et al., 2007). The Rhizon sampler was developed as an artificial plant root during the 1990s for the purpose of collecting soil water in the field of soil science. This sampler is a capillary composed of a hydrophilic porous polyether sulfone (PES), which has (1) a capillary of a hydrophilic porous polymer (diameter of 2.5 mm, average pore diameter of 0.15 μm), (2) a wire supporting the capillary, (3) a tube of polyvinyl chloride (PVC)/polyethylene (PE) that allows water to pass through the capillary, and (4) a luer connector. When collecting pore water using a Rhizon sampler, insert the Rhizon sampler into the sediment from a small hole at the side of a core barrel, connect the polyethylene syringe or peristaltic tube to the luer connector, and aspirate to collect the pore water. Otherwise, connect the injection needle to the luer connector and collect the pore water via a collection tube which is evacuated. This method can separate the pore water without sediment contact with the atmosphere and without destroying the sediment. It is also possible to collect pore water at sampling intervals of 1 cm (Seeberg-Elverfeldt et al., 2005). However, because the pore water is collected by suction, it is unsuitable for measurement of dissolved gas components such as dissolved inorganic carbon, total alkalinity and pH (Schrum et al., 2012). It has also been noted that, in measuring oxygen and hydrogen isotopic ratios and chloride ion concentration, a systematic difference exists between the measurement results using this method and those of the conventional squeezing method (Miller *et al.*, 2014). In the sampling of pore water using a Rhizon sampler, it may take several tens of minutes to 1 hour for completion suction of the pore water. In the meantime, it is necessary to control the temperature during aspiration by storing the sediment column in a large-sized refrigerator or a low-temperature laboratory. Because it is almost impossible to aspirate the pore water from the deep layers of sediment with a low water content, it is necessary to use the squeezing method together with the Rhizon sampler.

4. Summary

In this chapter, cautions regarding the sampling of pore water are described. Each method has advantages and disadvantages, and it is no exaggeration to say that there is no common method to separate pore water that is applicable for all chemical components. When collecting pore water, it is necessary to select an appropriate sampling method according to the target component, or to change the method of processing the subsample for each component (Schrum *et al.*, 2012). Among the effects of pressure, temperature, and gaseous contaminant, temperature may irreversibly change the concentration of components related to the dissolution equilibrium between sediment and pore water, as well as microbial activity in the sediment, concentrations of organic components, and trace gasses (Ijiki *et al.*, 2013). Therefore, it is necessary to process the samples quickly from sediment sampling to pore water separation, to minimize the temperature change as much as possible, and to separate the pore water at a temperature near that of the sampling site. Furthermore, it is recommended that separation of pore water be performed after the temperature of the sample reaches that of the sampling site (Masuzawa *et al.*, 1980). Depending on the target components, elution of contaminants from the filter or adsorption of the target components to the filter may occur; thus, it is necessary to conduct blank tests and cleaning of the filter in advance.

References

- Masuzawa, T and Y. Kitano (1983) : Interstitial water chemistry in deep-sea sediments from the Japan Sea. *J. Oceanogr. Soc. Japan*, **39**, 171-184.
- Gamo, T., J.M. Gieskes (1992): Shipboard chemical analyses of sedimentary pore waters during the Ocean Drilling Program (ODP) Leg 131. *Chikyukagaku*, **26**, 1-15. (in Japanese)
- Berner, R.A (1980) : Early diagenesis: A theoretical approach. Princeton Univ. Press., Princeton, NY. 256 pp.
- Watanabe, Y. and S. Tsunogai (1984) : Adsorption-desorption control of phosphate in anoxic sediment of a coastal sea, Funaka bay, Japan. *Mar. Chem.*, **15**, 71-83.
- Anderson, R.F., A.P. LeHuray, M.Q. Fleisher, and J.W. Murray (1989) : Uranium deposition in saanich inlet sediments, vancouver island. *Geochim. Cosmochim. Acta*, **53**, 2205-2213.
- Kato, Y., T. Miyata, H. Wada, H. Minami (1996a): Diffusion of chloride in sediments of a brackish lake: distributions of chlorinity in pore waters of drillcores from Lake Hamana. *Umi no kenkyu (Oceanogr. Japan.)*, **5**, 97-106. (in Japanese)
- Adkins, J.F., K. McIntyre, and D.P. Schrag (2002): The salinity, temperature, and $\delta^{18}\text{O}$ of the glacial deep ocean. *Science*, **298**, 1769-1772.
- Schrag, D.P., J.F. Adkins, K. McInerine, J.L. Alexander, D.A. Hodell, C.D. Charles, and J.F. McManus (2002) : The oxygen isotopic composition of seawater during the last glacial maximum. *Quat. Sci. Res.*, **21**, 331-342.
- Toki, T., U. Tsunogai, T. Gamo, S. Kuramoto, and J. Ashi (2004): Detection of low-chloride fluids beneath a cold seep field on the Nankai accretionary wedge off Kumano, south of Japan. *Earth Planet. Sci. Lett.*, **228**, 37-47.
- Manheim, F.T. (1968): Disposable syringe techniques for obtaining small quantities of pore water from unconsolidated sediments. *Journal of sedimentary Research*, **38** (2), 666-668.

- Kato, Y., H. Minami, S. Okabe, H. Wada, H. Kitazato (1996b): Remineralization of biophile elements in anoxic sediments from Lake Hamana. *Umi no kenkyu (Oceanogr. Japan.)*, **5**, 221-234. (in Japanese)
- Manheim, F.T. and F.L. Sayles (1974): Composition and origin of interstitial waters of marine sediments, based on deep sea drill cores. In: *The Sea*, Vol 5 (E.D. Goldberg ed.), 527-568.
- Sayles, F.L., P.C. Mangelsdorf, T.R.S. Wilson, and D.N. Hume (1976) : A sampler for the in situ collection of marine sedimentary pore waters. *Deep Sea Res.*, **23**, 259-264.
- Masuzawa, T., Y. Kato, S. Nakashima and S. Nagao (1991) : An in-situ pore water squeezer for obtaining pore waters at multi-depths in marine sediments. In: *Proc. 3rd Intl. Symp. on Advanced Nuclear Energy Research: Global Environment and Nuclear Energy*, JAERI, Tokai, 258- 261.
- Beck, M., O. Dellwig, K. Kolditz, H. Freund, G. Liebezeit, B. Schnetger, and H.-J. Brumsack (2007) : In situ pore water sampling in deep intertidal flat sediments. *Limnol. Oceanogr. Methods*, **5**, 136–144.
- Toole, J., J. Thomson, T.R.S. Wilson and Baxter, M.S. (1984): A sampling artifact affecting the uranium content of deep-sea porewaters obtained from cores. *Nature*, **308**, 263-266.
- Masuzawa, T., S. Kanamori and K. Kitano (1980) : The reversible effect of temperature on the chemical composition of interstitial water of marine sediment. *J. Oceanogr. Soc. Japan*, **36**, 68-72.
- Seeberg-Elverfeldt, J., M. Schlüter, T. Feseker, and M. Kölling (2005), Rhizon sampling of porewaters near the sediment-water interface of aquatic systems. *Limnol. Oceanogr. Methods*, **3**, 361–371.
- Jørgensen, B.B. and S. Kasten (2006): Sulfur cycling and methane oxidation. In: Schulz, H.H., Zabel, M. (Eds.), *Marine Geochemistry*, second ed. Springer, Berlin, pp. 271–309.
- Barnes, C.E. and J.K. Cochran (1988): The geochemistry of uranium in marine sediments. In: Guary, J.C., Guegueniat, P., Pentreath, R.J. (Eds.), *Radionuclides: A Tool for Oceanography*. Elsevier, London, 162–170.
- Nagao, S., H. Narita, S. Tsunogai, K. Harada and T. Ishii (1992): The geochemistry of pore water uranium in coastal marine sediments from Funka Bay, Japan. *Geochem. J.*, **26**, 63–72.
- Narita, H. and Y. Kato (2007): “2.2.5 Sediment and pore water”, ed. The Chemical Society of Japan, *The Fifth Series of Experimental Chemistry*, Vol. 20-2 Environmental Chemistry, Maruzen Press., Tokyo, p. 105-110.
- Bender, M., W. Martin, J. Hess, F. Sayles, L. Ball and C. Lambert (1987): A whole-core squeezer for interfacial pore-water sampling. *Limnol. Oceanogr.*, **32**, 1214-1225 .
- Jahnke, R.A. (1988): A Simple, reliable, and inexpensive pore-water sampler. *Limnol. Oceanogr.*, **33**, 483-487.
- Dickens, G. R., M. Kölling, D. C. Smith, and L. Schnieders (2007): Rhizon sampling of pore waters on scientific drilling expeditions: An example from the IODP Expedition 302, Arctic Coring Expedition (ACEX), *Sci. Drill.*, **4**, 22–25.
- Schrump, H.N., R.W. Murray, and B. Gribsholt (2012) : Comparison of Rhizon sampling and whole round squeezing for marine sediment porewater. *Sci. Drill.*, **13**, 47–50.

Plankton Net

○Hiroaki SAITO (Atmosphere and Ocean Research Institute, The University of Tokyo)

1. Plankton net

Plankton are drifting organisms in water bodies because they are nonmotile or poor ability to swim against a current. Most of them are tiny <20 mm, but some gelatinous plankton such as jellyfish and tunicates are larger than 100 mm with weak swimming ability. In marine ecosystems, the density is higher for smaller organisms. For small plankton (~0.2 mm), such as bacteria, archaea, phytoplankton, protozoan zooplankton, collecting water samples (milliliters to liters) and concentrating them with various methods (Vol. 4). In order to collect larger metazoan zooplankton which density is much lower, we need to concentrate organisms from much larger volume of water than water bottle sampling. Plankton nets are sampling devices of plankton that are towed thorough water and filter plankton larger than the mesh size. Fig 1 shows a NORPAC (North Pacific Standard) net and a WP-2 (UNESCO Working Party 2) net, which are widely used conical net and cylinder-conical net, respectively.

The minimum size of plankton collected with a plankton net is defined by the mesh size. The maximum size is influenced by variable factors such as tow speed and mouth opening size of the plankton net, swimming speed and visual or mechanosensory recognition ability of plankton. For the sampling of micronekton, which swim faster than zooplankton, larger nets or trawls allowing high speed tow are used (e.g., IKMT、 MOHT、 RMT, Sameoto et al., 2000; Oozeki et al., 2004). Plankton nets are also used for micro phytoplankton and microzooplankton sampling such as diatoms, radiolarians, forminiferans. In this manuscript, we use a term “zooplankton” as metazoan zooplankton which are the main target of plankton net sampling.

2. Filtering efficiency of plankton net and filtering rate

The choice of the type of plankton net, mesh size and towing method are depending on target zooplankton species and groups. A plankton net with larger mouth area filters more water in a certain amount of time and reduces the possibility of net avoidance of zooplankton. On the other hand, requiring larger filtering area (i.e., net length) to minimize the influence of net clogging by phytoplankton and detritus and to sustain the filtering efficiency during tow. The initial filtering efficiency (IFE) of a conical net is 75-85%, and one of conical-cylinder net, such as WP-2 (Fig. 1), reaches around 100% (Keen, 2013). IFE is decreasing with net tow due to net clogging. The decline in the filtering efficiency is more serious in the water with high abundance of chain-forming diatoms and/or sticky organisms such as *Noctiluca*. These organisms are usually abundant in the surface layer of the water column. Thus, the declining of the filtering efficiency means not only decreasing the filtering volume but also inducing the underestimation of the zooplankton abundance distributing in the surface layer and crucial impact on the quantitative sampling.

The Open Area Ratio (R) is the ratio of the filtering mesh area to the mouth area of net.

$$R = a\beta / A$$

Where, a, β , A mean mesh area, mesh porosity, and mouth area, respectively.

$$\beta = m^2 / (d + m)^2$$

m means mesh width, and d the diameter of mesh filament. Since the filtering efficiency declines with filtering volume by net clogging, a plankton net with large R is appropriate using in plankton rich waters. The minimum R for quantitative sampling is represented as follows (Sameoto et al, 2000),

$$\text{Green water} \quad \text{Log}_{10}(R) = 0.38 \times \text{Log}_{10}(V / A) - 0.17$$

$$\text{Blue water} \quad \text{Log}_{10}(R) = 0.37 \times \text{Log}_{10}(V / A) - 0.49$$

where V means the filtering volume of sea water (m^3). In the case of 150-m vertical tow of a NORPAC net (Fig. 1) fitted with 335 μm Nylal mesh ($R=3.7$), the net clogging is estimated to be not serious in blue water (minimum $R=2.1$). But in green water, the filtering efficiency may decline (minimum $R = 4.5$). Tranter and Smith (1968) recommended $R>5$ for a plankton net fitted with mesh >0.33 mm, and $R>9$ for mesh <0.33 mm (Keen, 2013). In Japan, short conical nets have been used because of easy-handling on small ship and also low product price. The users should be careful these low R nets are easy clogging and inappropriate for quantitative sampling in green water.

In order to determine the filtering volume of sea water during net tow, a flow meter is mounted at net mouth as confronted with towing direction. For a plankton net with bridles in front of the net, the flow meter should be set deviated from the mouth center to minimize the interfere of bridles on the flow field (e.g., in quarter of the diameter). The flow meters should be calibrated at calm sea surface condition. Using the plankton net frame without net or a calibration frame, towing more than 7 times to obtain the revolution of the flow meter in a certain distance towed at 100 % filtering efficiency. The revolution per distance can be changed by strong impact such as hitting to the hull or falling on the deck. The flow meter should be rinsed with fresh water to remove salt after use.

3. Plankton net sampling and sample handling

It has been developed various plankton nets to collect zooplankton (Wiebe and Benfield, 2003). The towing methods of plankton nets which widely used in Japan are summarized in Hasumoto (2006).

Towing methods are categorized as: 1) vertical tow, 2) oblique tow, 3) multi-layer sampling with opening-closing nets, 4) neuston sampling. In this manuscript, describing the sampling procedure with vertical tow and sample handling at first, then other towing methods and devices.

3-1 Vertical tow

Vertical tow of a plankton net is widely used sampling method which enable to estimate zooplankton abundance and biomass per area in relatively short sampling time. This method has been widely used for various monitoring projects. Because of relatively low filtering volume, it is inadequate for examining the abundance for minor species.

In the case of using a NORPAC net, a 10-30 kg lead weight is used as a sinker. To avoid twisting bridles and/or rope, use swivel to connect with wire and the weight (Fig. 1). When the net is at the sea surface, make zero-correction of the wire length meter. To prevent the generation of kink of wire, the

pay out speed of the wire is to be adjusted to keep the wire tension, especially when the net is at the sea surface. In the calm sea condition, the pay out speed may reach 1 m s^{-1} .

When the wire length is approaching to the target depth, measure the wire angle and pay extra length (Table 1) out to reach the net to the target depth. Hauling speed is generally $0.5\text{-}1.0 \text{ m s}^{-1}$. It has been observed that zooplankton specimens are taken in poorer condition at higher towing speed. Also, inducing escapement through the mesh due to the high filtration pressure. The decline of the filtering efficiency at high speed towing is more serious for conical net than cylinder-conical net. At the sea surface, it should be careful that the plankton net can be damaged by wind and swell under the rough sea surface condition.

Since some plankton are caught in mesh or stick on due to the mucus, wash the plankton net carefully using an appropriate flow of sea water from the outside of the net to remove plankton. Clogging near the cod end is usually more serious. The cod end is taken off and the obtained samples are transferred into a sampling bottle or jar (see 4). Record the revolution and ID of the flow meter.

In order to collect live zooplankton for experimental studies or obtain less damaged specimen, it is recommended to tow slowly ($<50 \text{ cm s}^{-1}$) and use a large cod end. It has been used several to tens liter of bottle or plastic bag (Fig. 2) for the cod end. It is effective to enlarge the bottom diameter of the plankton net to allow smooth transfer of zooplankton to the cod end. The sample is transferred without net washing to minimize the mixing of damaged plankton stuck on the mesh.

Obtained samples are appropriately processed depending on the purpose. For species enumeration and identification, fix with sodium borate ($\text{Na}_2\text{B}_4\text{O}_7 \cdot 10\text{H}_2\text{O}$) buffered formalin-seawater (final concentration of formaldehyde is 4 %) as soon as possible. It is recommended fixing the sample with 8 % formaldehyde in the case that plankton volume is more than 30% of the sample bottle. Ethylalcohol is used for DNA sequence. Since RNA is labiler than DNA, a zooplankton sample for RNA is kept frozen or with specific chemicals for the preservation. It is recommended to refer latest literatures for RNA preservation. For the measurement of dry weight or carbon and nitrogen weight, filter on precombusted (450°C , 4 hour) glass fiber filter such as Whatman GF/A after dividing the sample using sub-sampling devices such as Folsom's splitter as necessary. Sub-sampling devices is to be set on a bench appropriately to avoid errors through the splitting process. Since some commercial products are not enough stable, determine the variability between splits at land-based laboratory before use. For dry weight measurement, rinse the filter with a small amount of distilled water to remove the salt (Ohmori, 1978). The filter is transferred to petri dish and kept in freezer until measurement. Or, the filter is folded in half, covered with combusted aluminum foil and kept in freezer. The sequential processes of freezing and thawing is required, such as for gut pigment analysis, using mesh for plankton net as a filter inducing less damage than glass fiber filter. For gut pigment analysis, the sample on the mesh is kept in freezer $< -70^\circ\text{C}$ to prevent the degradation of pigments. For any purposes, fix or freeze the sample as soon as possible. Even for the fixation with formalin, leaving a sample more than 30 minutes in room temperature induces significant damage.

The following are potential troubles and mistakes at a plankton net towing and sample handling: 1) wire breakage due to the generation of kink, 2) net breakage by wind and swell, 3) sample loss due to the cod end breakage or fall out of clip, 4) sample loss during transferring sample from cod end, 5)

undescribed or insufficient description of sampling information. We have to be very careful to avoid the case 1) which can induce serious accident. The second case is more probable on clogged net with containing sea water at the recovery. During handling the sample, it should be careful for unexpected rolling and running sea water on deck. To avoid case 5), take care that sampling bottle is properly marked at both lid and bottle. In the case of formalin fixation, input a waterproof paper with describing the information.

3-2 Oblique tow

For an oblique tow, various nets such as WP-2 net, Bongo-net (Fig. 3), ORI net (Fig. 4) have been used. The larger filtering volume than obtained with a vertical tow allows more accurate estimation of the composition of zooplankton population and abundance. Also, reducing the influence of plankton patchiness.

To enhancing the downforce, attaching a depressor or weight (30-100 kg) with a swivel. Setting a small depth sensor or acoustic net monitor at the flume to record the towing depth. Steaming the ship at low speed and put down the net to the sea surface, and then pay the wire off and control the ship speed (1.0-2.5 knot) to make the wire angle 45°. When the net is estimated to reach the target depth from the net sensor or wire length and angle, record the wire length and time, and haul the wire at stable speed (0.2-1.0 m s⁻¹). The net towing speed, i.e., wire speed + ship speed, should be controlled to keep the filtering efficiency high enough. Obtained samples are processed as one of vertical tow.

3-3 Multi layer sampling

In order to collect zooplankton samples from multi-layers in a single tow, plankton nets with an opening-closing system controlled by logging the depth through armored cable with conductor, such as MOCNESS, VMPS, are used. A plankton net with closing system controlled by falling messengers, such as MTD net, had used in the past. However, such a net is hard to detect the exact sampling layer, difficult to exclude the possibility of contamination at paying out the wire, and unstable performance of the closing system. The contamination from outside the target depth induces serious error to examine the vertical distribution of species and developmental stages.

There are various types in MOCNESS, VMPS and another multi-layer sampling gears, and most of them equip various sensors for environmental parameters such as temperature, salinity, phytoplankton fluorescence, etc. In general, the 1st net which is set open during downcasting is not useful for quantitative sampling.

3-4 Neuston sampling

Neuston nets are designed to collect zooplankton, fish eggs and larvae occurring very surface of the water column. A Chigyo-net (Maruchi-net) has been widely used in Japan. A Chigyo-net is towed beside the ship being the upper 1/3 of the ring above the sea surface by controlling wire length. Since it is unable to estimate exactly the filtering volume, only the biomass and abundance per towing time or distance are obtained. To eliminate the influence of ship light, shut the light down at nighttime tow.

ORI-neuston is towed by a bridle attached to one side of the net frame (Fig. 5). This makes free-open area without wire and bridle during the net tow, keeping the net far away from the ship relative to Chigyo-net and minimize the influence of bow wave. Neuston nets stacking multiple nets vertically can examine the fine vertical distribution of zooplankton within the neuston layer (Wiebe and Benfield, 2003).

4. Codend

Zooplankton collected by towing a plankton net are concentrated into a cod end attached at the bottom of the net. The materials of cod end and handling procedure are variable: 1) Cod end with rubber tube at the bottom. Folding the tube and pinched with a clip at sampling. Drain sea water and plankton off by removing the clip, 2) Cod end with screw cap. The cod end is screwed in the bottom of the net. After sampling, screw off the cod end to transfer samples, 3) Canvas or mesh bag. Attach and detach from the net with a hose clamp or strings. The cod end with screw cap is made by plastic or vinyl chloride, opening windows at the side covered by mesh to drain sea water. The mesh opening at the side windows is to be the same or smaller than one of the plankton net. Since strong filtering pressure exert on the windows, check the damage and rinse fully to remove clogging after sampling.

5. Maintenance

Net clogging should be carefully washed off to maintain the filtering efficiency of the net and contamination. Nets should always be checked to be sure without damaged gauze, loozend screws and ropes. Wash metal materials with fresh water to remove salt. It should be noted that metal is more susceptible to corrosion at high temperature-high humid condition. After the cruise, remove all the parts and kept in fresh water for a day to remove salt. Then dry and keep in bags.

References

- Hasumoto, H. (ed) (2006) Kaiyo-Kansoku Manual. ORI, the University of Tokyo, 258 pp. (in Japanese)
- Keen, E. (2013) A practical designer's guide to mesozooplankton nets. 1-52. <http://acsehttp://acsweb.ucsd.edu/~ekeen/resources/Choosing-a-Net.pdf>
- Ohmori, M. (1978) Some factors affecting on dry weight, organic weight and concentrations of carbon and nitrogen in freshly prepared and in preserved zooplankton. *International Review of Hydrobiology*, 63, 261-269.
- Oozeki, Y., Hu, F, Kubota, H., Sugisaki, H., Kimura, R. 2004. Newly designed quantitative frame trawl for sampling larval and juvenile pelagic fish. *Fisheries Science* 70, 223-232.
- Sameoto, D., Wiebe, P, Runge, J., Poste, L., Dunn, J., Miller, C, Coombs, S. 2000. Collecting Zooplankton. In: Harris et al. Ed., *ICES Zooplankton Methodology Manual*, Elsevier Academic Press, London, pp55-81.
- Tranter, D. J., Smith, P. E. (1968) Filtering performance. In: Tranter, D. J. (ed) *Monographs on oceanographic methodology 2, Zooplankton sampling*, UNESCO Press, Paris, 27-56 pp.
- Wiebe, P.C, Benfield, M. H. (2003) From the Hensen net toward four-dimensional biological oceanography. *Progress in Oceanography* 56, 7-136.

NORPAC-net

(conical net)

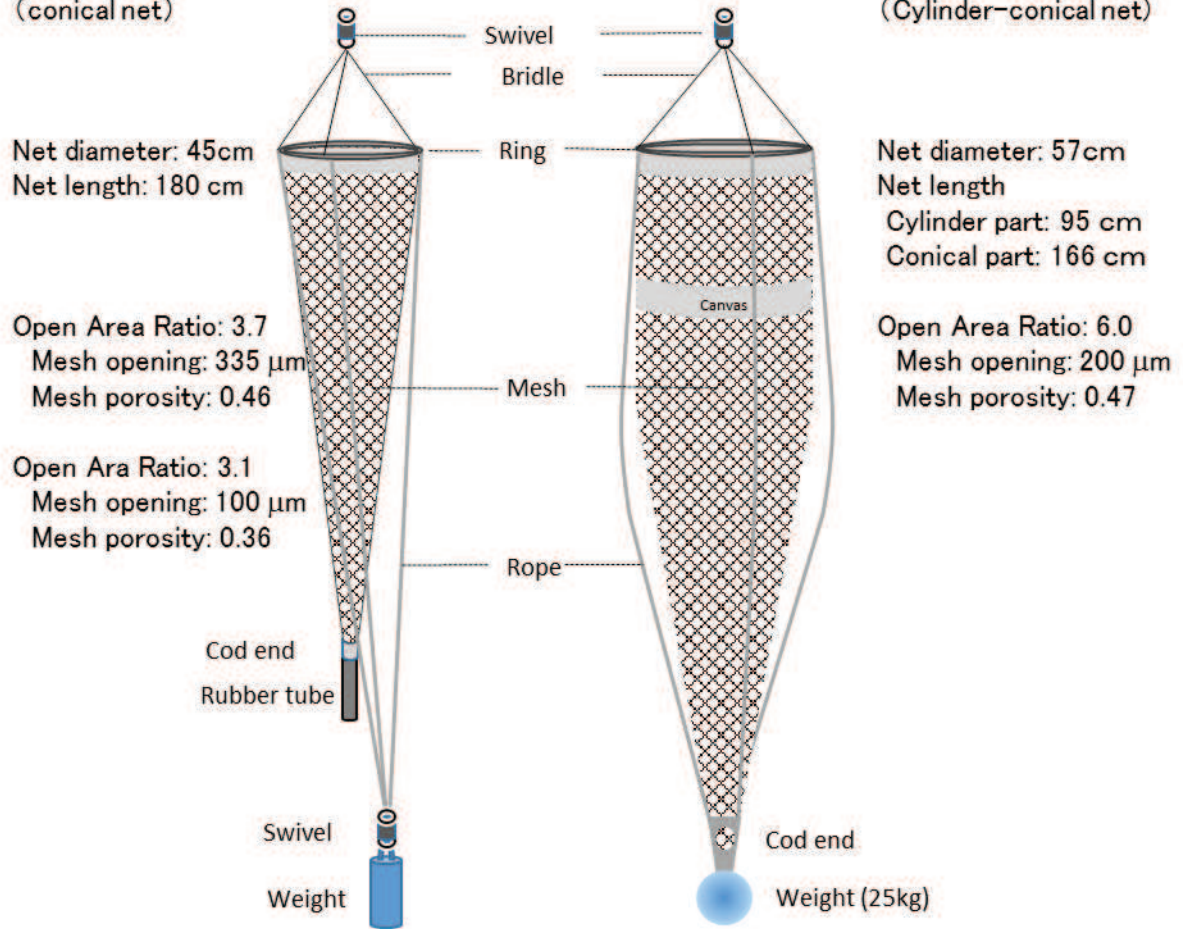


Fig. 6-1 NORPAC(North Pacific Standard) net and WP-2 (UNESCO Working Party No.2) net.



Fig. 2. A plankton net attached large plastic bag as a cod end to collect living zooplankton for incubation experiment.



Fig. 3 BONGO net (70 cm ring diameter). Photo by Dr. Y. Okazaki.

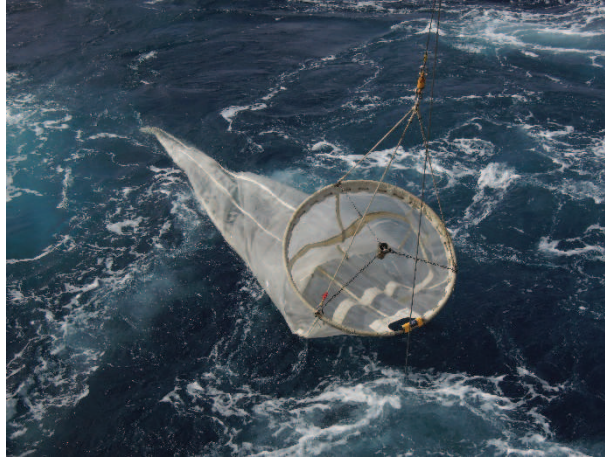


Fig. 4 ORI net (1.6 m ring diameter).

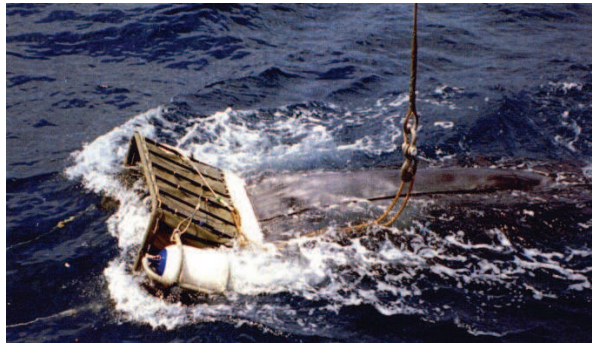


Fig. 5 Neuston net

This page left intentionally blank.

Benthos

○Shigeaki KOJIMA (Graduate School of Frontier Sciences / Atmosphere and Ocean Research Institute, The University of Tokyo)

1. Size categories of benthos

Benthic organisms (benthos) are organisms living on/in bottom sediments. Demersal fishes which spend most time setting on the sea bottom such as soles and eelpouts, or swimming above the bottom to feed as rattails are mostly classified into them. Benthos is conveniently divided into some size categories based on differences in sampling and observing methods. Megabenthos is a category which includes organisms large enough to be visible with the naked eye and sampled by using dragnets such as beam trawls and dredges. Organisms of smaller categories are generally sampled with bottom sediment by using bottom samplers. Among them, organisms remained on a mesh of 0.5 mm or 1 mm openings are called as macrobenthos. Organisms which pass through a mesh of 0.5 mm or 1 mm openings and remained on a mesh of 38 μm openings and those which pass through a mesh of 38 μm openings are meiobenthos and microbenthos, respectively.

2. Sampling and observing methods of megabenthos

Megabenthos has been collected by dragnets such as beam trawls and dredges for a long time. Biological dredges we use have same structures as those used during the research cruise in the Aegean Sea by Edward Forbes in 1840s, which is famous as the first systematic survey of deep-sea organisms. Biological dredges are used at sand and mud bottom at relatively shallow sites. Unlike dredges for geological studies, they collect organisms into light-weight nylon nets. Dredges of various sizes are used according to water depth and/or performance of a winch. During research cruises of R/V *Tansei-Maru* and *Shinsei-Maru*, biological dredges with a 1 m span (Fig. 1) have been used. It consists of a steel frame (1 m x 40 cm x 20 m), an inner net of 5 mm openings and an outer net of 2 cm openings. Usage of plumbic chain bridles, which swirl up mud with organisms, improves the efficiency of collecting organisms. At deep sites, a weight is attached at the codend (the end of a net) to prevent a winch cable from shrinking. Of too high tension cuts a fuse wire (6 mm thickness) between bridles and a winch cable, the dredge leaves bottom by being pulled by a life wire connecting between the winch cable and the side of the frame to protect the winch cable and the dredge. A life wire is tied and attached the frame using plastic tape not to become an obstacle. As dredges are drawn on sea bottom, they are often distorted and broken due to collision with rocks. It is better to think that dredges are consumable goods. When using a biological dredge, it is put into the sea with keeping the mouth of net upward, and lowered at a rate of 0.5 m/s from the vessel sailing at the speed through the water of 1.5 knot. Too fast lowering will loose and damage a winch cable. Grounding of the dredge is confirmed by the decrease of the tension, which is often rather difficult in the case of dredges, or the calculation based on the water depth, the angle of a winch cable, and the length of cable pay out. After grounding, vessel speed is changed to the ground speed of 1.0 knot and the winch cable of 30% of the length already pay out is additionally pay out. After then, the dredge is pulled at the ground speed of 1.0 knot for 5 min and wounded up at a rate of 0.2 m/s,

which gradually increase to 0.5 m/s. After leaving the bottom, the dredge is wound up at a rate of 1 m/s and recovered. During seining, the tension should be monitored. If the tension suddenly rises, seining is terminated and the vessel is immediately stopped. On deck, samples are taken out by opening a zipper at the side of the net. When difficult due to too much samples, it can be easily taken out by hauling up the codend using a winch. After picking out large organisms, bottom sediment is sieved with a mesh of 1 or 4 mm to select organisms. As the mouths of dredges are rather small, collected organisms are mainly infaunal mollusks, annelids, and echinoderms which are relatively small and less-swimming. A dredge is not a quantifiable sampler. As deep-sea animals are patchy distributed, a small difference in sampling points often results in a large difference in amount and composition of collected animals. So, it is difficult to estimate their density or spatial and seasonal changes based on few dredge samples. For biological sampling on rocky bottom where biological dredge and trawl cannot be used, dredges for sampling rocks such as a cylindrical dredge are available. They are, however, seldom used to collect animals as rocks badly damaged specimens in the dredges.



Figure 1 A biological dredge

For sampling larger benthic organisms and demersal fish with high swimming performance, trawls are used. During cruises of R/V *Tansei-Maru* and *Shinsei-Maru*, beam trawls with a 2 m span or a 3 m span (Fig. 2) have been used and those with a 4 m span have been used for R/V *Hakuho-Maru* cruises. A beam trawl consists of two steel poles called as beams, two lateral frames called as heads, and a duplex net. The width of the mouth of the net is fixed by beams. During seining, the frame of a trawl slides on the sea bottom as a sledge and collect sediments near the bottom surface and animals swimming above the bottom. As a biological dredge, a fuse wire and a life wire are used, although the latter is connected to the codend so that the trawl is wound up backwards abandoning sediments if the fuse wire is cut. At the great depth such as 3,000 m, plumbic chains inserted between a winch cable and a trawl or weight(s) attached to a frame and/or codend stabilizes the system in the sea for reliable landing. The variation of beam trawls contain a Sigsbee-Agassiz type beam trawl, which is not distinguished between upper and lower sides, Ocean Research Institute type beam trawl, which is distinguished between upper and lower sides, and so on. Beam trawls are operated in similar manner to biological dredges with the exception that the vessel speed at time when a trawl is put into the sea is 2 knot through the water, a trawl is lowered at a rate of 1 m/s, and the sampling is continued for 30 min. At the great depth, the winch cable is pay out 70% more after grounding. If the tension rapidly decreases or does not increase

during seining, the trawl is suspected to be away from the bottom. In that case, the winch cable is pay out additionally to see how it goes for a while. To collect demersal fish mainly, fast seining around the ground speed of 1.5 knot, and slow seining around the ground speed of 0.5 knot to collect invertebrates are recommended. In the latter case, attachment of a plumbic chain along the underside of the mouth of a net increases sampling efficiency of infauna as it sinks into the bottom sediments. As sampling area of trawls can be calculated based on the width of the net, the seining speed, and the range between grounding and leaving times, the density of organisms can be estimated. The value, however, tends to be underestimated as trawls do not necessary continue to touch the bottom during seining. In order to solve this problem, devises for real-time monitoring of status of trawls were developed (Hasumoto, 2006). An otter trawl is a net sampler used mainly by research vessels of fishery institutes and training ships of fishery high schools and colleges. They are suitable for collecting a large amount of fish and large crustaceans. Two steal boards named otter boards, which are set at both sides of a net, spread the mouth of the net when they receive water flow from the front. Although otter trawls can collect more samples, their quantitativty is inferior to beam trawls. As trawls have no mechanisms to close nets during rising, the by-catch of pelagic organisms cannot be prevented and they need be selected after sampling.

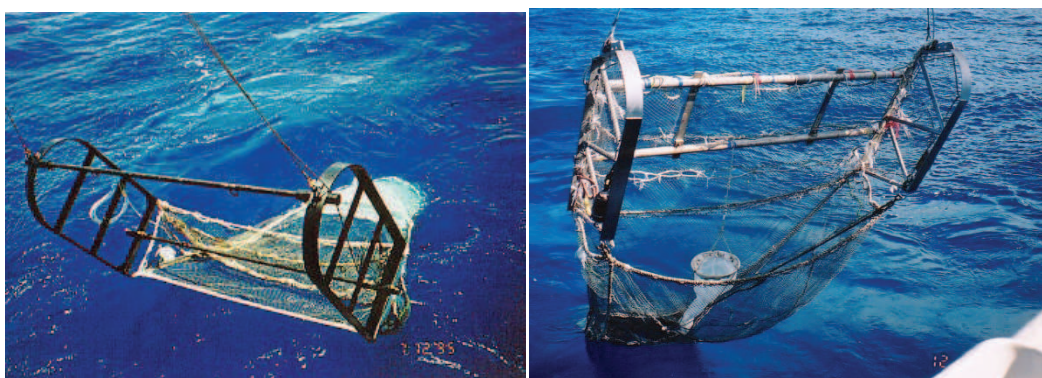


Figure 2 Beam trawls with a 2 m span (left) and a 3 m span (right)

A deep-sea camera system takes photographs of deep-sea bottom. It can obtain data of organisms inhabiting rocky bottom which cannot be sampled by trawls but can record only relatively large epifauna (organisms living on the bottom surface). Using camera(s) and a strobe contained in pressure resistant vessel(s), the system takes pictures at preprogrammed time intervals. Stereographs taken by two cameras enable to determine sizes of organisms. A pinger is turned on just before the start of the operation and the system is lowered at a rate of 1 m/s from drifting vessel. With approaching sea bottom, the lowering rate is decreased and the system is kept about 2m above the bottom. Signals from the pinger are received to monitor the distance between the system and the bottom. After photographing, the system is wound up at a rate of 1 m/s. Using deep-sea cameras attached to mooring systems with a disconnection devise, temporal changes of deep-sea bottom and gathering of large organisms around baits have been observed.

3. Sampling methods of macrobenthos

Macrobenthos, which is smaller than megabenthos, is generally sampled quantitatively with bottom sediment by using bottom samplers. During cruises of R/V *Tanasei-Maru* and *Hakuho-Maru*, 1/10 m² (Fig. 3) and 1/4 m² Box corer (USNEL-type spade corer) have been mainly used, respectively. The former can collect bottom sediment of surface area of 1/10 m² and the latter can collect bottom sediment of surface area of 1/4 m², respectively. Both types of box corers can be used by R/V *Shinsei-Maru*. Box corers are samplers which cut off bottom sediment and sea water above it as they are in a rectangular steel box. A box is set in opened state in deck. The box corer is lowered at a rate of 1 m/s from the vessel which holds fixed point. When landing, the box is inserted into the bottom and a spade is unclashed to turn to close the box when it is pulled out. In addition, water ports are also closed to prevent bottom water from flowing out from the box. After confirming the box corer lands by a rapid decrease of the tension, payout of the winch cable is immediately stopped and the cable is wound up at a rate of 0.5 m/s. In the most cases, the tension rapidly increases just before the box corer leaves the bottom, which decreases to the ordinary level soon. Then, it is wound up at a rate of 1 m/s and recovered. On deck, the box is removed using a dedicated jacking dolly and bottom sediment is taken out from the upper side of the box. As a box full of mud is quite heavy, special attention is required especially on a rolling vessel. If necessary, subcores are inserted into sediment in the box to batch off subsamples. For an analysis of macrobenthos, the sediment is sieved with a mesh of 0.5 mm or 1 mm openings. As it is very difficult to select all macrobenthos by the naked eyes, samples remained on the mesh are fixed by adding neutralized formalin (final 10% in volume). In a laboratory, they are washed and sorted using a stereoscopic microscope. Macrobenthic organisms are preserved in 70% ethanol. Organisms of megabenthos-size are rarely collected by the box corer and organisms heavier than 1 g in wet weight are usually removed from data in order to prevent their presence from having a big influence on density estimation. As mentioned below, recently multiple corers, which show superior quantitativity to box corers, became popular. However, box corers, which can cover a larger sampling area, are still a excellent bottom sampler for studies in macrobenthos.

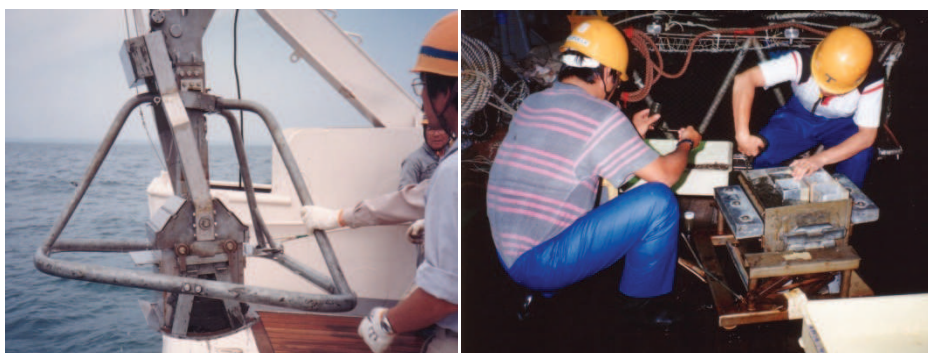


Figure 3 A 1/10 m² Box corer

Before the development of a box corer, grab samplers such as a Smith-McIntyre (SM) bottom sampler and an OKEAN grab were used to collect macrobenthos from research vessels. The latter is even

now used for sampling by small ships. Bottom sediments collected by grab samplers are not uniform in depth as those by box corers and they blow surface sediments when landing, both of which result in the underestimation of density of organisms. Comparison among data obtained using samplers of different types should be conducted carefully. Grab samplers contain a Ekman-Birge grab, which is so small that it can be managed only by human power and used for sampling a small amount of bottom sediment from piers and small ships.

In order to collect benthic-pelagic organisms, that is, animals swimming right over the sea bottom, epibenthic sleds are used. Plankton nets within a stilette frame filter sea water of the near-bottom layer without touching the bottom, which results in damage of nets by inflow of bottom sediments. Some models can mechanically open nets only when the sled is landing for preventing the by-catch of pelagic organisms and can equip video cameras (Brenke, 2005). So-called a “Manbiki (shoplifting)” net, that is, plankton nets set within a trawl net (Fig. 2, right) are also effective to collect benthic-pelagic species.

4. Sampling methods of meio- and microbenthos

Not so much as grab samplers, even box corers blow surface sediment with minute organisms at landing. On the surface of the deep-sea bottom, amorphous materials containing fresh organic matter accumulate to form an extremely unstable layer called as a fluffy layer in some season. Within that layer, bacteria and unicellular eukaryotes propagate themselves. Thus, sampling loss of box corers cannot be ignored in studies of smaller organisms than macrobenthos. To resolve this problem, a multiple corer was developed by increasing quantitativity instead of reduction in sampling area (Fig. 4). It is now used as a standard sampler of meio- and microbenthos. Disturbance of the bottom surface is minimized by landing with “legs” grinding at remote positions from cylindrical acrylic cores for the sediment collection and inserting these tubes into the bottom very slowly. To prevent the multiple corer from leaving the bottom before the insertion completes, a winch cable is pay out a bit after landing. Then, a quarter rope put between the winch cable and the multiple corer looses for the protection of the winch cable. A vinyl tape is wound around the quarter rope and shackles at the both ends to avoid entwining the corer. If bottom sediment is too soft and it overflows from the top of tubes, weights are removed from the corer to lighten it. On deck, cores are set in opened state. The corer is lowered at a rate of 1 m/s from the vessel which holds fixed point. After the corer stands still 50 m above the bottom for 3 min to stabilize the cable, the cable is pulled out again at a rate of 0.3 m/s (0.5 m/s if there is a strong swell). At the great depth where the change of tension at landing is easily overlooked, a pinger is attached to cable 50m above the corer to monitor the altitude of the corer. After landing, the winch cable is additionally (2-3m) pulled out. The winch cable is wound up at a rate of 0.3 m/s 0.5-1 min later. As the case of the box corers, the tension rapidly increases just before the corer leaves the bottom. When the tension decreases to the ordinary level, the winding rate is increased to 1 m/s. When landing, arms attached to lids of cores are released and cores are sealed when they are pulled out from the bottom. On deck, cores are removed, both ends of each core are capped, and they are kept standing up. As soft sediment easily flows out from cores, it had better be quickly held with a large spatula. After sampling, the inner part of the corer and its mechanical parts such as a trigger and arms should be closely washed using fresh water. If gravels are caught within the trigger, it results in a failure in operation. After sampling bottom

sediment containing gravels, trigger had better be released on deck to wash them away. In studies of meibenthos, core samples are often pushed from the lower side and sliced in parallel with the sea bottom. In the near bottom layer with high biomass, sediment sample is sliced at small intervals (0.5-1 mm) while intervals are wide in the deeper layer. Tools for pushing sediment out from cores have been devised by researchers. Sliced sediment samples are fixed with neutralized formalin containing Rose Bengal, which stains living organisms, and preserved. In laboratory, macrobenthos are removed from samples using a mesh of 0.5 mm or 1 mm openings and a fraction remained on a mesh of 38 μm openings are washed. Organisms are picked up under a stereoscopic microscope and preserved in 70% ethanol. When too much organisms are collected, they can be divided equally using a plankton divider. Samples for studies of microbenthos are treated according to purposes suitably. Although multiple corers can obtain 3 to 8 core samples simultaneously, they are not independent. To estimate deviation of data, it is desired to conduct repeated sampling.



Figure 4 A multiple corer

Reference

- Brenke, N (2005): An epibenthic sledge for operations on marine soft bottom and bedrock. *Mar. Technol. Soc. Jour.*, 39, 10-19.
- Hasumoto, H. (supervision) (2006): *The Way to Observe the Ocean*. Ocean Research Institute, The University of Tokyo, Tokyo, 258 pp.(in Japanese)

**Determination of $p(\text{CO}_2)$ in air that is in equilibrium
with a continuous stream of sea water**

Daisuke SASANO (Japan Meteorological Agency),

Shin-ichiro NAKAOKA (National Institute for Environmental Studies)

A standard operating procedure (SOP) of “Determination of $p(\text{CO}_2)$ in air that is in equilibrium with a continuous stream of sea water” in Dickson, A.G., Sabine, C.L. and Christian, J.R. (Eds.) 2007, *Guide to best practices for ocean CO_2 measurements*, PICES Special Publication 3, is available at the following website:

https://www.nodc.noaa.gov/ocads/oceans/Handbook_2007/sop05.pdf

Appendix: Tandem type equilibrator

In the text, we introduce the shower type equilibrator, thus we here describe the tandem one. It consists of a combination of a bubbling component with a mixer and generates the equilibrated air. The structure of the equilibrator is shown in figure 1. The flow rate of the seawater to the equilibrator is approximately $10\text{--}15\text{ dm}^3\text{ min}^{-1}$. The water samples introduced from the upper part hit plates called a mixer and are splashed. This causes the splashed water to increase the surface area in contact with the air in the equilibrator and makes the air easier to reach equilibrium for CO_2 in seawater. In addition, the air in the laboratory or the air adjusted CO_2 concentration is introduced from a bubbler attached to the lower part of the equilibrator, then the bubbles are exchanged with CO_2 in seawater to reach near equilibrium during they are rising from the bubbler to the water surface. The reason why the combination of the bubbling and the mixer components are adopted as a tandem type equilibrator is that it is confirmed that the offset of CO_2 concentration from the shower type equilibrator system can be eliminated experimentally. Although the components of the tandem type equilibrator system such as analyzer, standard gas, dehumidification unit, etc. are quite similar to those of the shower type one, a point that the equilibrated air is discharged out of the system after introducing the analyzer is different from the shower type one, which makes the air circulate in the system. Advantages of the tandem type equilibrator are that there is no clogged part like a shower head of the shower type equilibrator and that the water level in the equilibrator can be kept constant. Consequently, they make it easy to maintain the system. On the other hand, because the size of the equilibrator is larger than the shower type equilibrator system, there is a disadvantage that the installation place is limited.

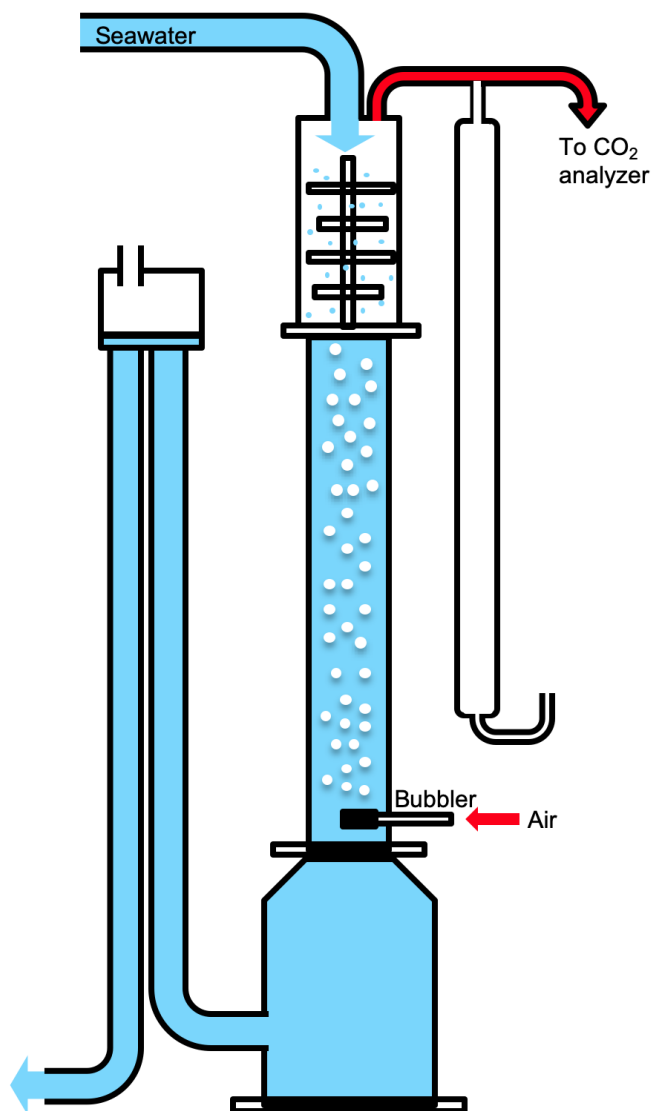


Figure 1 Schematic of the tandem type equilibrator

This page left intentionally blank.

Acoustic Doppler Current Profilers

○Shinya KOUKETSU (Japan Agency for Marine-earth Science and Technology)

Shipboard acoustic Doppler current profilers (SADCPs) mounted on the hulls of sea-going vessels have been widely used to monitor ocean currents. Downward-looking SADCPs transmit sound pulses, measure the Doppler shifts of the reflected pulses, and then calculate the velocity of the ocean water relative to the vessel. SADCPs with working frequencies of 38 kHz, 75 kHz, and 150 kHz have been available from Teledyne RD Instruments (TRDI) since 2000. The lower frequency instruments can measure currents in deeper layers, but vertical resolution declines. According to the TRDI manual, the maximum depths of measurement and typical cell lengths for TRDI SADCPs are respectively 1000 m and 24 m for the 38 kHz SADCP, 700 m and 16 m for the 75 kHz SADCP, and 400 m and 8 m for the 150 kHz SADCP [1]. The choice of instrument should depend on the range of water depths in the research region. However, the maximum depth of current measurements in the field depends on local seawater properties and may be shallower than the published maximum depth.

This guideline provides summary descriptions of data processing and field operations that are presented in greater detail in the Global Ocean Ship-Based Hydrographic Investigations Program (GO-SHIP) manual [2]. Instrument specifications, which are also provided in the GO-SHIP manual, are omitted here, but the operating principles of the SADCP are briefly described. More detailed information about instrument configurations and applicable software should be obtained from the GO-SHIP manual or manufacturer's manuals.

1. Measurement principles

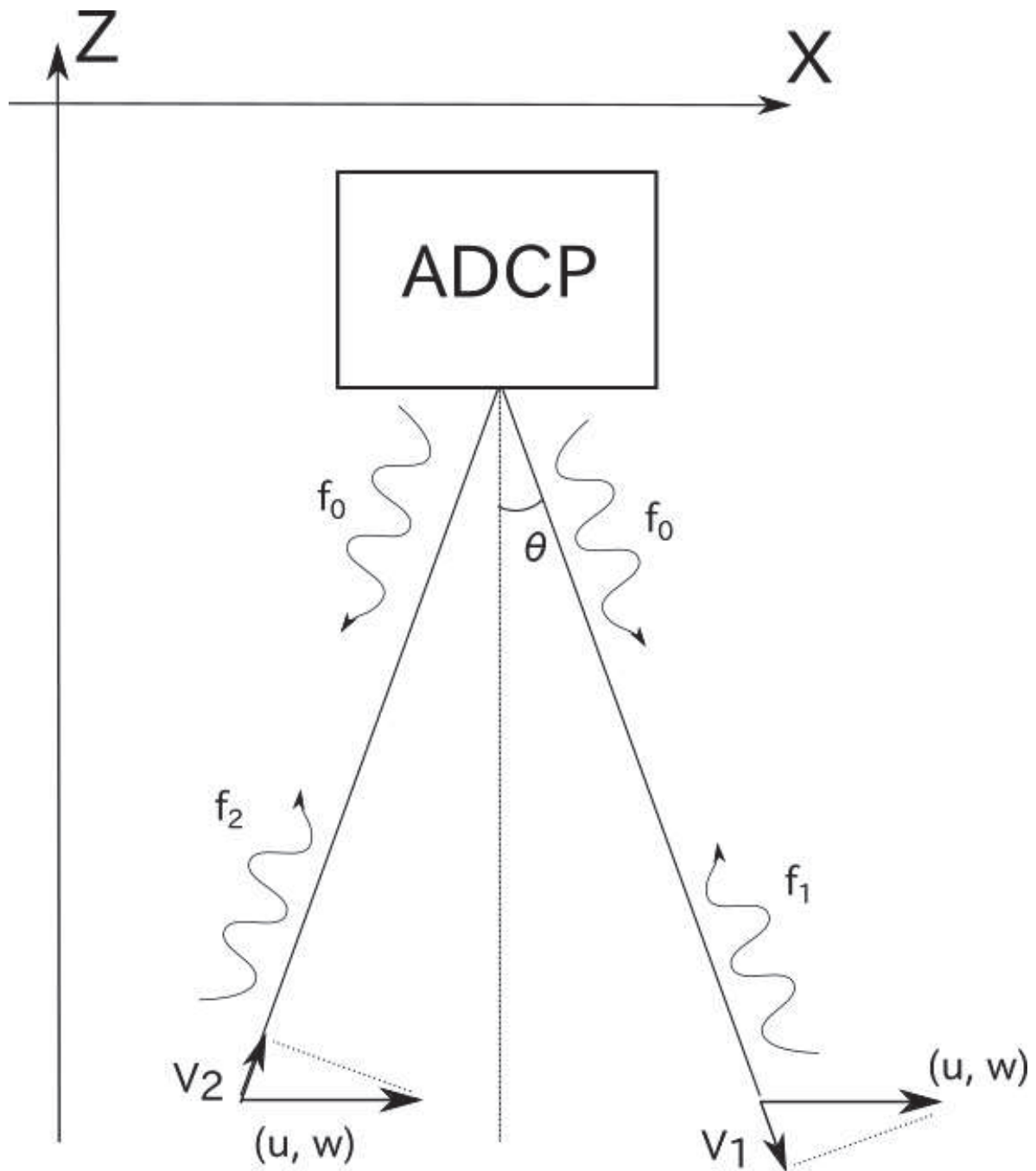


Figure 1 Schematic of acoustic Doppler current profiler (ADCP) observation in the x-z plane. f_0 is the transmitted pulse frequency and f_1 and f_2 are reflected pulse frequencies. V_1 and V_2 are measured velocities in the direction of the pulses. (u, w) is the current in the x-z plane.

The pulses transmitted by the SADCPC are refracted at density stratification boundaries and partially reflected by particles (e.g., plankton, particulate organic matter). Currents and current depths can be calculated from the Doppler shifts and periods between transmitted and reflected pulses.

If a transducer transmits a pulse of frequency f_0 and the pulse is reflected by a particle moving at velocity V_1 , the reflected pulse frequency (f_1) is

$$f_1 = f_0 \frac{c+V_1}{c-V_1}$$

Here, assuming $V_1 \ll C$,

$$V_1 = \frac{f_1 - f_0}{2f_0} C.$$

Thus, the velocity of the current relative to the moving SADCP can be calculated from the Doppler shift ($f_1 - f_0$). As one transducer can obtain a velocity in only one direction (transmitted pulse direction), more than three differently oriented transducers are needed to obtain a three-dimensional velocity. For a SADCP equipped with two transducers oriented at $\pm\theta^\circ$ from the vertical in the x-z plane (Fig. 1) and two transducers oriented at $\pm\varphi^\circ$ from the vertical in the y-z plane, the velocities (V_1, V_2, V_3, V_4) observed by each transducer are

$$V_1 = w \cos\theta + u \sin\theta$$

$$V_2 = w \cos\theta - u \sin\theta$$

$$V_3 = w \cos\varphi + v \sin\varphi$$

$$V_4 = w \cos\varphi - v \sin\varphi$$

From the above equations, we obtain the three-dimensional velocity (u, v, w) relative to the moving vessel. Although it is assumed that all four transducers measure components of the velocity of the same current, measurements can be disturbed by small-scale current fluctuations, fish, and instrument noise. Thus, the differences between the vertical velocities (w) estimated from different transducer pairs (e.g., V_1 and V_2 versus V_3 and V_4 pairs) are generally used as the “velocity error”.

2. Conversion of relative velocity to true velocity

The relative velocity measured by the SADCP should be converted to earth coordinate velocity by using ship heading data (gyro compass or GPS compass data). This conversion can generally be done using software (e.g., [3] and [4]) provided by the instrument manufacturers.

To obtain the true ocean current velocity, ship velocity must be accounted for. If the water depth is shallow enough to obtain bottom track data (recorded by the SADCP), the bottom velocity can be used as the ship velocity. Otherwise, ship velocity can be determined from GPS data.

3. Correction and evaluation of accuracy

Data obtained from individual pings are strongly disturbed by noise, and ship velocities based on GPS data at intervals of a few minutes are not very accurate. Thus, estimates of ocean current velocities are normally averaged over 5–10 minutes, which suppresses the influence of noise. Errors can be evaluated on the basis of the standard deviation of the time-averaged results. However, it is important to note that there will be large uncertainties in current velocity estimates based on data acquired during periods of ship acceleration.

Corrections are needed for the difference of the orientations of the SADCP and gyro sensor (“arrangement angle”), which can cause considerable biases between true ship velocity (usually much faster than currents) and SADCP measurements including ship velocity. For any one cruise, comparison of directions and magnitudes of the ship velocities obtained by SADCP bottom track with those obtained

from GPS data allows estimation of a correction angle and amplitude coefficient for that cruise [5]. The relationships between bottom-track velocity (u_b, v_b) and ship velocity (u_s, v_s) are as follows:

$$\begin{aligned} u_s &= -\beta (u_b \cos \alpha - v_b \sin \alpha) \\ v_s &= -\beta (u_b \sin \alpha + v_b \cos \alpha), \end{aligned}$$

where α is the arrangement angle and β is the amplitude coefficient. Note that the negative signs on the right-hand side of these equations indicate the direction opposite to the direction of the bottom velocity of the ship. Using these relationships and bottom-track data obtained while cruising, the arrangement angle (α) and amplitude coefficient (β) are obtained as follows.

$$\begin{aligned} \tan \alpha &= \frac{\langle u_b v_s - v_b u_s \rangle}{\langle u_b u_s + v_b v_s \rangle} \\ \beta &= -\frac{\langle u_b v_s + v_b u_s \rangle}{\langle u_b^2 + v_b^2 \rangle \cos \alpha}, \end{aligned}$$

where $\langle \dots \rangle$ indicates the ensemble average during the cruise.

Current velocity is corrected to account for the local velocity of sound in water (C_{real} , dependent on water temperature and salinity) by using, for example, TEOS-10 software [6] as follows:

$$V_{corrected} = V_{adcp} \frac{C_{real}}{C_{adcp}},$$

where V_{adcp} and C_{adcp} are raw estimated current velocity and sound velocity recorded at the SADCP, respectively. Note that vertical stratification of the water column does not affect horizontal velocities, and that this correction is not needed if a phased array system is used (e.g., [7]).

The corresponding water depth correction is done according to the following equation:

$$L_{corrected} = L_{adcp} \frac{C_{real}}{C_{adcp}},$$

where $L_{corrected}$ and L_{adcp} are corrected and measured water depth, respectively. If the vertical profile of C_{real} is available, water depths can be obtained by integration of C_{real} .

4. Data required for post-cruise processing

In areas where the water depth is shallow enough to use bottom tracking, the bottom-tracking data are generally used for correction of velocity data and for evaluation of instrument noise. However, the use of bottom-track recording can reduce the accuracy of the velocity data, so bottom tracking should be turned off when working far from the coast.

The following data are needed for post-cruise data processing.

- ADCP raw data
- GPS ship location data
- Heading data based on the ship gyro (or ADCP)

All data are collected and archived by using software provided by the equipment manufacturer (e.g., [4] and [8]). If the GPS and gyro data collected by the vessel's navigation systems are more accurate than the data collected by the ADCP, they should also be archived. Although the software provided by the manufacturer generally generates 5 or 10 minutes averaged data, the raw data (for every ping) should also be archived for future use. Time average data can be simply generated after the cruise by using standard PC software (e.g., [3] and [4]).

Available salinity and temperature measurements (ex. by a Conductivity Temperature Depth profiler) should also be archived for use in sound velocity corrections.

References

- [1] Ocean Surveyor ADCP, Teledyne RD Instruments, <http://www.rdinstruments.com/surveyor.aspx>
- [2] Firing, E., and J.M. Hummon (2010): Shipboard ADCP measurements. The GO-SHIP Repeat Hydrography Manual: A Collection of expert reports and guidelines, IOCP Report (14), ICPO Publication Series (134).
- [3] WinADCP, Teledyne RD Instruments
- [4] UHDAS, University of Hawaii, http://currents.soest.hawaii.edu/uhdas_fromships.html
- [5] Joyce, T. M. (1989): On in situ "Calibration" of Shipboard ADCPs, *J. Atmos. Oceanic Technol.*, 6, 169-172.
- [6] Ocean Observer ADCP, Teledyne RD Instruments, <http://www.rdinstruments.com/observer.aspx>
- [7] TEOS-10, <http://www.teos-10.org>
- [8] VMDAS, Teledyne RD Instruments

This page left intentionally blank.

Bathymetry

Hiroshi UCHIDA (Research and Development Center for Global Change,
Japan Agency for Marine-Earth Science and Technology)
Souichiro SUEYOSHI (Nippon Marine Enterprises, Ltd.)

1. Definition and Units

Water depth is a distance measured vertically between the sea surface and the sea floor, expressed in meters (m), the base unit for distance in the International System of Units (SI). The act of measuring water depths (bathymetry of the sea floor) is referred to as “depth sounding” or often simply as “sounding”.

Because tides cause sea level to rise and fall in time and space, the water depth shown on a chart (charted depth) is defined as the vertical distance between an appropriate reference level (chart datum) and the sea floor. In Japan, the Lowest Low Water, which is approximated by Mean Sea Level minus the sum of the amplitudes of the four major harmonic tidal constituents (M2, S2, K1 and O1), is selected as the chart datum to prevent stranding of vessels in coastal areas with depths shallower than 200 m (Fig. 1) (Horiuchi and Nishishita, 2010).

There are several depth sounding methods: echo sounding by measuring the two-way travel time of an acoustic wave, wire sounding by lowering a line with a lead weight, calculation from measured pressure and density using the hydrostatic relation, and laser induced detection and ranging (LIDAR) by measuring the time interval between the emission of a laser pulse from an aircraft and the reception of its reflection from the sea surface and the sea floor. Echo sounding is the standard method for current research vessels (Japan Meteorological Agency, 1999).

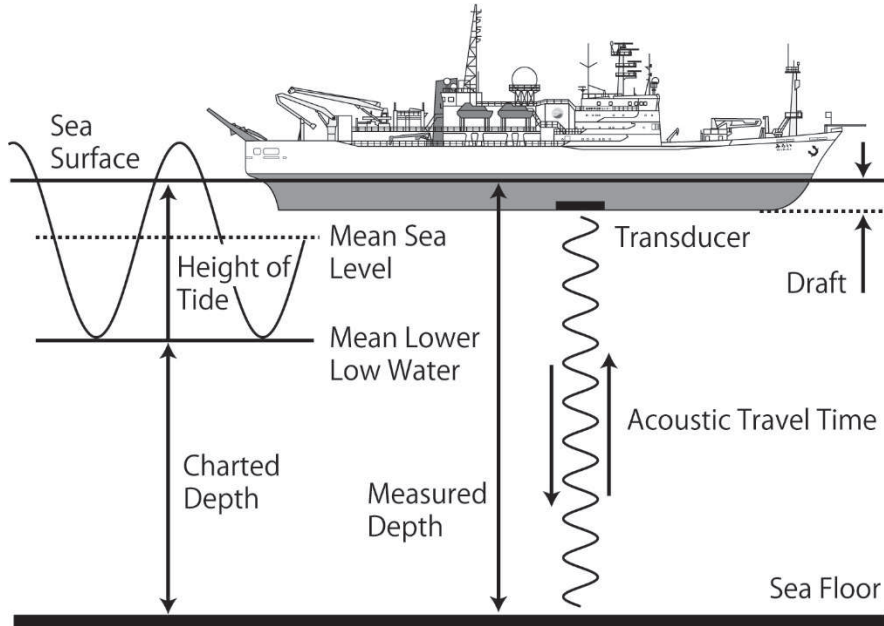


Figure 1. A schematic of echo sounding.

2. Echo Sounding

Echo sounding is a method for estimating water depths by calculation using the two-way travel time of an acoustic pulse between a transducer on the vessel and the sea floor, and the speed of sound in seawater (Fig. 1). The equipment that uses this principle to measure water depth is called an echo sounder.

Echo sounders are classified into two types: single-beam echo sounders and multi-beam echo sounders (Kita et al., 2003). Single-beam echo sounders consist of one transducer that transmits a single acoustic beam and can measure depths directly beneath the vessel. In contrast, multi-beam echo sounders consist of a transducer array that transmits multiple acoustic beams and can measure depths to each side of the vessel's track at several ranges (Fig. 2). Sounding by multi-beam echo sounder is therefore called "swath sounding".

The distance D between a transducer and the sea floor is expressed as

$$D = \frac{1}{2} \int_{t_0}^{t_1} v dt , \quad (1)$$

where t_0 is the time that the sound pulse is transmitted, t_1 is the time that the pulse is received after being reflected at the sea floor, and v is the speed of sound in seawater. Although v is a function of water temperature, salinity, and pressure, D can be estimated by using the average speed of sound \bar{v} over the sound path length:

$$D = \frac{1}{2} \bar{v}(t_1 - t_0) . \quad (2)$$

A value of 1500 m/s is commonly used as a nominal value for \bar{v} (Müller and Schenk, 1991). For multi-beam echo sounders, however, the angle of the sound beam is determined on the basis of the sound speed at the transducer. It is therefore important to use the real-time sound-speed value at the transducer to determine the beam angle because the speed can change along the vessel's track because of changes in water mass or diurnal variation in sea surface temperature. The sound speed measured by a sound-speed sensor or calculated from temperature and salinity measurements is generally used to determine the beam angle.

Before 2010, the speed of sound in seawater was calculated using the equation proposed by Chen and Millero (1977) (Fofonoff and Millard, 1983). However, in "The international thermodynamic equation of seawater—2010: Calculation and use of thermodynamic properties" (TEOS-10) (IOC et al., 2010), the equation for the speed of sound is based on the data provided by Del Grosso (1974) (Feistel, 2003). The difference between the speed of sound in seawater calculated from these two equations is relatively small in surface water, but it becomes larger as pressure increases. The speed calculated from the algorithm of Chen and Millero (1977) at a depth of 3000 m is about 0.5 m/s higher than that from the equation of Del Grosso (1974). Water depths directly measured by bottom pressure

sensors were compared with water depths calculated from Eq. (2) by using two-way acoustic travel-time data from inverted echo sounders (IES) moored about one meter above the sea floor and the average speed of sound in seawater calculated from temperature and salinity profiles for both the Chen and Millero (1977) and Del Grosso (1974) algorithms. The results showed that the algorithm of Del Grosso (1974) is more accurate than the algorithm of Chen and Millero (1977) (Meinen and Watts, 1997).

Although higher frequency sound pulses can be used to measure water depths with higher resolution, the sound energy in higher frequency sound pulses in seawater attenuates more rapidly than those of lower frequency. Therefore, a range of frequencies from 200 kHz and higher is used in shallow water and low frequency sound pulses of about 12 kHz are used for deep-water surveys, including those in submarine trenches.

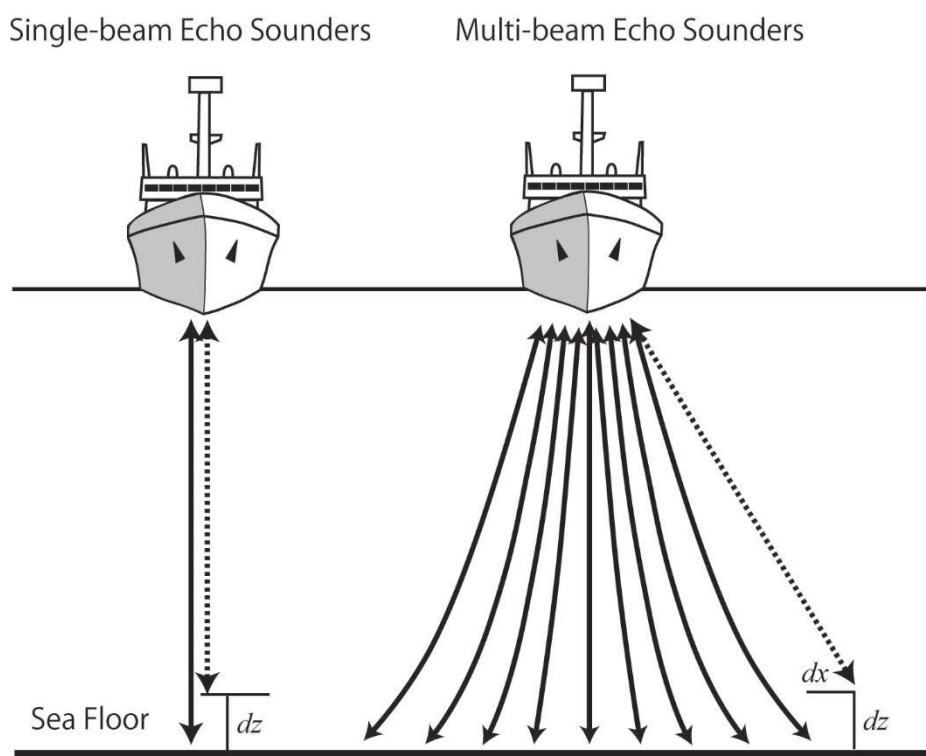


Figure 2. Schematic of echo soundings by single-beam and multi-beam echo sounders. Dotted lines represent changes in the acoustic ray due to errors in the sound-speed profile.

3. Correction of Measured Depth

To obtain the actual water depths from the depths measured between the echo-sounder transducer and the sea floor, the following corrections are needed.

a. Draft correction

The transducer is usually on the bottom of the ship's hull, below the sea surface. A correction is

necessary for this depth (draft) (Fig. 1).

b. Sound-speed correction

The speed of sound in seawater changes according to changes in temperature, salinity and pressure. Therefore, it is necessary to correct for the difference between the depth calculated from the nominal speed of sound (Eq. 2) and the actual speed. For multi-beam echo sounders, the error in water depth measurements may be large for the outer sound beams, because the sound path over a vertical profile with variable sound speed bends locally toward regions of lower speed (Fig. 2). Therefore, detailed vertical profiles of sound speed are needed for the sound-speed correction. Vertical profiles of sound speed can be obtained from a conductivity-temperature-depth (CTD) profiler or from expendable CTD (XCTD) measurements. If CTD/XCTD data are not available during a depth survey, CTD data from ARGO floats (robotic profiling floats) near the vessel's track may be useful for the sound-speed correction (Ota et al., 2011).

c. Vessel motion correction

Water depths measured by single-beam echo sounders vary as a result of the heaving, rolling, and pitching motions of the vessel. The accuracy of water depth measurements by multi-beam echo sounders is also affected by the yawing (side-to-side) angular motion of the bow. Recently, multi-beam echo sounders have included a three-axis fiber optic gyroscope with an accelerometer to precisely correct for vessel motion in real-time.

d. Tide correction

Water depth measurements should be corrected for tidal height by using tidal data. Generally, however, the tide correction has not been applied for water depth measurements in the open ocean because tides and tide reference levels there have been poorly understood. Because ocean tide models have improved markedly, mainly due to the recent accumulation of high-quality sea-level data by satellite altimeters (Stammer et al., 2014), it is now possible to apply a tidal correction for water depth measurements in the open ocean (Horiuchi and Nishishita, 2010).

4. Uncertainty

The International Hydrographic Organization (IHO) developed standards for hydrographic surveys for depth soundings used to compile charts (IHO, 2008). These standards require a detailed estimation of the uncertainty in water depth data acquired by depth soundings. Both the total horizontal uncertainty (THU) and total vertical uncertainty (TVU) must be considered as the total propagation uncertainty (TPU) as follows.

a. Total horizontal uncertainty (THU):

- Positioning system errors
- Range and beam errors
- The error associated with the ray path model (including the sound-speed profile) and the beam

angle

- The error in vessel heading
- System pointing errors resulting from transducer misalignment
- Sensor location
- Vessel motion sensor errors; i.e., roll and pitch
- Sensor position offset errors
- Time synchronisation/data processing latency

b. Total vertical uncertainty (TVU):

- Vertical datum errors
- Vertical positioning system errors
- Tidal measurement errors, including co-tidal errors where appropriate
- Instrument errors
- Sound-speed errors
- Ellipsoidal/vertical datum separation model errors
- Vessel motion errors; i.e., roll, pitch and heave
- Vessel draft
- Vessel settlement and squat
- Sea-floor slope
- Time synchronisation/data processing latency

It can be useful if the uncertainty in measured water depth data also be estimated for general ocean observations not aimed at obtaining sounding data for compiling charts. An example from the Japan Coast Guard is helpful for showing the estimated uncertainty of measurements in the deep ocean. The relative expanded uncertainty was about 1.0% for measurements beneath the vessels and within 2.6% for a beam angle of 60° from the vessels for 16 cases of estimates from combinations of five research vessels and nine multi-beam echo sounders (Oikawa et al., 2010).

The data presented in Figure 3 are an example of the uncertainty in multi-beam echo sounder data obtained over a relatively flat sea floor under calm seas, calculated in the same way as by Oikawa et al. (2010). As with the results of Oikawa et al. (2010), the uncertainty is higher for the wider beam angle from the vessel. The relative expanded uncertainty was below 0.5% (25 m) when the beam angle was within 55°, and was about 0.1% (5 m) directly beneath the vessel, although it was only slightly higher about 3° to each side of the vessel. Note that the uncertainties from causes such as bias and tides are not included in this estimate because these data are from the same section of the same cruise.

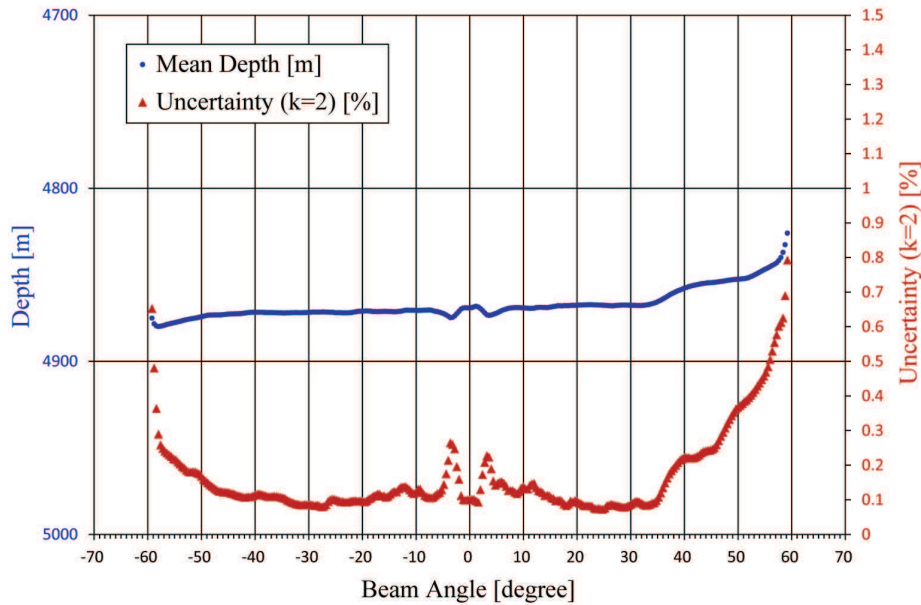


Figure 3. An example of expanded uncertainty (the coverage factor $k = 2$) in multi-beam echo sounder data obtained from R/V *Mirai*.

The water depths measured by echo soundings can be compared with water depths calculated from pressure and density data obtained from CTD observations using the hydrostatic relation. The distance D_p between the sea surface and the sea floor can be calculated from the hydrostatic approximation

$$D_p = \int_0^{p_{\max}} \frac{1}{\rho g} dp + \text{Alt}, \quad (3)$$

where p is the pressure, ρ is the density of seawater, g is the acceleration of gravity, p_{\max} is the maximum pressure from the CTD measurements, and Alt is the height of the CTD above the sea floor at the maximum pressure. Alt is usually measured by an acoustic altimeter attached to the CTD using the same principle as the echo sounder or by an acoustic pinger attached to the CTD frame. In the latter case, the vessel's transducer receives two acoustic signals from the pinger, one arriving directly from the pinger and the other reflected by the sea floor; Alt can be calculated from the difference in arrival times of the two signals. Water depths from echo soundings were compared with water depths calculated using Eq. (3) at CTD stations where the length of wire out during CTD measurements and the depth calculated from CTD data (the first term on the right side of Eq. [3]) are approximately the same (Table 1). The difference between water depths estimated by the two methods was less than 0.13%, and is approximately the same as the estimated uncertainty (0.1%) in the echo-sounder data from directly beneath the vessel (Fig. 3). Such precise validation of echo-sounder data is useful for discovering unexpected problems with the data processing software or the hardware.

Table 1. Comparison of water depths directly beneath the vessel as measured by multi-beam echo sounder and calculated from CTD and acoustic altimeter data (Eq. 3). The water depths from echo soundings were estimated from Eq. (2) by using the mean speed of sound in seawater calculated from the CTD data and corrected for the vessel's draft (6.6 m). The data were obtained during leg 3 of R/V *Mirai* cruise MR12-05 (Southern Ocean, 2012–2013).

Station number	Wire out (m)	CTD depth (m)	CTD height above bottom (m)	CTD depth + height above bottom (m)	Echo sounding (m)	Error in echo sounding (m)
S04I 93	4396	4395	8	4403	4406	3
S04I 94	4414	4416	9	4425	4424	–1
S04I 115	2937	2935	9	2944	2944	0
S04I 116	3934	3934	7	3941	3942	1
S04I 144	4748	4747	9	4756	4762	6
S04I 151	4834	4833	9	4842	4847	5

5. Data Management

In hydrographic surveys by research vessels, especially those including soundings by multi-beam echo sounders, it is possible to accumulate a large amount of data. The data obtained and processed must therefore be appropriately stored at each of the following data processing stage.

- a. Raw data—Echo sounding data before applying various corrections and the data used for the corrections (e.g. sound-speed profiles), including documents (e.g. field notebooks), for future reprocessing of the data
- b. Edited and corrected data—Data processed by applying any necessary noise reduction and corrections
- c. Grid point data—Data thinned by interpolation of the processed data onto grid points of the appropriate horizontal resolution
- d. Metadata—A collection of data comprising, at minimum, the following information (International Hydrographic Organization, 2008):
 - general information about the survey, e.g., purpose, date, area, equipment used, and name of survey platform
 - the geodetic reference system used, i.e., the horizontal and vertical datums, including tides, within a geodetic reference frame based on the International Terrestrial Reference System (ITRS) (<https://www.iers.org/IERS/EN/Science/ITRS/ITRS.html>)

- calibration procedures and results (e.g. draft and vessel motion corrections)
- sound-speed correction method
- sounding datums (tidal correction)
- estimated uncertainties and the respective confidence levels
- special comments
- rules and mechanisms employed for data thinning

6. Noise Reduction and Gridding for Multi-Beam Echo Sounder Data

Raw data obtained by multi-beam echo sounders include outliers resulting from various factors. Data processing software to eliminate such outliers is provided by the manufacturers of echo sounders and those developing software for hydrographic surveys (e.g. HIPS software, Teledyne CARIS Inc.; <http://www.caris.com>). Generally, outliers such as noise spikes can be eliminated visually by plotting the lateral depth profile against the heading of the vessel over earlier profiles. Although this data editing method is reliable, it requires considerable time and manpower for data obtained over a wide area and in shallow waters, and the identification of noise may depend on the subjectivity of the data editor. It is therefore important to set uniform evaluation criteria for all data editors (e.g. setting a minimum percent deviation from the water depth), based on the specifications of the echo sounder used.

Because the horizontal resolution of water depth data from multi-beam echo sounders varies depending on spatial variations in water depth and the cruising speed of the vessel, these data are generally interpolated onto grid points with equal horizontal intervals. To generate the grid-point data, it is necessary to choose the horizontal interval between grid points and a method of interpolation. The time and space intervals for the water depth data change depending on the intervals between transmitted sound pulses (ping rate). For example, sounding data are available at 1-second intervals for shallow water with depths of several tens of meters, but they are only available at intervals of several tens of seconds for deeper water with depths of several thousands of meters. Generally, the ping rate is automatically determined by the echo sounder according to the water depth and the beam angle. Therefore, appropriate horizontal intervals for grid points should be selected in consideration of the horizontal resolution of the water depth data estimated from the ping rate in the survey area and the cruising speed. A typical method for gridding water depth data is to apply spatial averaging with inverse distance weighting by using water depth data from within a certain distance from the grid point (e.g., three or five times the horizontal grid-point interval). Also, for multi-beam echo sounders, the weighting may change in proportion to the beam angle because the uncertainty is larger for the wider angles (Fig. 3).

For processing of multi-beam echo sounder data from hydrographic surveys in coastal waters, the Combined Uncertainty and Bathymetry Estimator (CUBE) algorithm (Calder, 2003), available in the HIPS software, has become popular. CUBE estimates grid-point values for depth from the surrounding data and includes estimates of uncertainty for each grid node.

References

- Calder, B. (2003): Automatic statistical processing of multibeam echosounder data. *International Hydrographic Review*, 4, 53–68.
- Chen, C.-T. and Millero, F. J. (1977): Sound speed of seawater at high pressures. *The Journal of the Acoustical Society of America*, 62, 1129–1135.
- Del Grosso, V. A. (1974): New equation for the speed of sound in natural waters (with comparison to other equations). *The Journal of the Acoustical Society of America*, 56, 1084–1091.
- Feistel, R. (2003): A new extended Gibbs thermodynamic potential of seawater. *Progress in Oceanography*, 58, 43–114.
- Fofonoff, N. P. and R. C. Millard Jr. (1983): Algorithms for computation of fundamental properties of seawater. UNESCO Technical Papers in Marine Science, 44, 53 pp.
- Horiuchi, D. and A. Nishishita (2010): Examination of tidal correlation method based on ocean tide model. *Report of Hydrographic and Oceanographic Researches*, 46, 78–86.
- International Hydrographic Organization (2008): IHO Standard for Hydrographic Surveys (5th edition). Special publication no. 44.
- IOC, SCOR and IAPSO (2010): *The international thermodynamic equation of seawater – 2010: Calculation and use of thermodynamic properties*. Intergovernmental Oceanographic Commission, Manuals and Guides No. 56, UNESCO (English), 196 pp.
- Japan Meteorological Agency (1999): Observations of bathymetry, *Manuals for Oceanographic Observations*, Part 1, Chapter 2, 5–8.
- Kita, T., N. Kurihara, K. Hashimoto, K. Teranishi and K. Okamura (2003): A technical note regarding bathymetric technology with particular reference to swath bathymetry. *Oyo Technical Report*, 23, 113–122.
- Meinen, C. S. and D. R. Watts (1997): Further evidence that the sound-speed algorithm of Del Grosso is more accurate than that of Chen and Millero. *Journal of Acoustical Society of America*, 102, 4, 2058–2062.
- Müller, T. J. and H.-W. Schenk (1991): Near-surface temperature, salinity, and bathymetry measurements. *WHP Operations and Methods*, WHP Office Report WHPO-91-1, WOCE report no. 68/69.
- Oikawa, M., N. Watanabe, T. Hashimoto, T. Yoshida and S. Chiba (2010): The uncertainties and the data management of deep water bathymetric data obtained with multibeam echo sounders. *Report of Hydrographic and Oceanographic Researches*, 46, 39–46.
- Ota, H., W. Tokunaga, N. Nagahama and K. Maeno (2011): Automatic construction of sound speed profiles for multi-beam echo sounders by using ARGO floats. *Proceedings of 2011 spring meeting of Advanced Marine Science and Technology Society*.
- Stammer, D., R. D. Ray, O. B. Andersen, B. K. Arbic, W. Bosch, L. Carrère, Y. Cheng, D. S. Chinn, B. D. Dushaw, G. D. Egbert, S. Y. Erofeeva, H. S. Fok, J. A. M. Green, S. Griffiths, M. A. King, V. Lapin, F. G. Lemoine, S. B. Luthcke, F. Lyard, J. Morison, M. Müller, L. Padman, J. G. Richman, J. F. Shriver, C. K. Shum, E. Taguchi, Y. Yi (2014): Accuracy assessment of global barotropic ocean tide models. *Reviews of Geophysics*, 52, 243–282.

This page left intentionally blank.

Weather Observations

○Toshiya NAKANO (Japan Meteorological Agency)

Meteorology operational services depend on a wide-range of international co-operation. Weather observations by a ship not only benefit its own safety but that of other ships through resultant weather forecasts and storm warnings issued using such weather reports gathered by meteorological services. The Japan Meteorological Agency (JMA), the national meteorological service of Japan, requests individual ships equipped with radio communication facilities to make meteorological observations (weather observations on board ships) and report the data by radio and mail. This chapter, “Guide to Weather Observations for Ships (Third Edition)“, was published in 2015 by JMA.

Guide to Weather Observations for Ships

Third Edition



March, 2015

Global Environment and Marine Department
Japan Meteorological Agency

CONTENTS

CHAPTER 1	General Description	1
CHAPTER 2	Observation of Atmospheric Pressure	6
CHAPTER 3	Observation of Air Temperature and Dew-point Temperature	9
CHAPTER 4	Observation of Wind	16
CHAPTER 5	Observation of Cloud	29
CHAPTER 6	Observation of Visibility	49
CHAPTER 7	Observation of Atmospheric Phenomena and Weather	50
CHAPTER 8	Observation of Sea Surface Temperature	56
CHAPTER 9	Observation of Ocean Waves	57
CHAPTER 10	Observation of Sea Ice	61
CHAPTER 11	Observation of Ice Accretion	69
CHAPTER 12	Port Meteorological Officer (PMO)	71
Appendix 1	List of supplies for ship weather observations and reports	A-1
Appendix 2	Table for saturated vapor pressure	A-3

CHAPTER 1 General Description

1.1 Introduction

The navigation of ships is affected by weather; consequently, methods of weather observation have developed along with those of navigation. In fact, weather forecasting might have originated to facilitate the safe navigation of ships. The commencement of storm warnings in France (1856) followed an incident where allied fleets of the UK and France, gathering off Sevastopol during the Crimean War, were suddenly enveloped by a hurricane-force storm which wrecked several vessels (14 November 1854).

Weather observations by a ship not only benefit its own safety but that of other ships through resultant weather forecasts and storm warnings issued using such weather reports gathered by meteorological services. These forecasts and warnings also help prevent and reduce risks of meteorological disasters affecting industries, transport systems, livelihoods and various other activities on land.

Furthermore, weather reports of ships on the oceans where fewer reports are available play a valuable role in monitoring global-scale climate change, which is an increasingly important issue for mankind affecting global warming.

The Japan Meteorological Agency (JMA), the national meteorological service of Japan, emphasizes the importance of ship weather observations. Meteorology operational services depend on a wide-range of international co-operation. The World Meteorological Organization (WMO), one of the specialized agencies of the United Nations, promotes meteorological observation on board ships under the umbrella “International Convention for the Safety of Life at Sea (SOLAS)” (1974). WMO has established internationally common methods of observation including codes and procedures to report and exchange data among members of WMO.

The WMO Voluntary Observing Ship (VOS) scheme is an international program in which ships are recruited to make and report meteorological observations.

Under this scheme, JMA requests individual ships equipped with radio communication facilities to make meteorological observations (weather observations on board ships) and report the data by radio and mail.

This Guide explains how to make marine meteorological observations and other related matters. In addition to this guide, JMA provides VOSs with the following materials free of charge:

- Guide to Ships’ Weather Reports
- Ships’ Weather Code Card
- Table for Finding the Dew-point
- JMA Cloud Plate
- Beaufort Scale of Wind Force
- OBSJMA (software to make weather reports)
- OBSJMA Operation Manual
- Ship’s Weather Observation Field Note for OBSJMA (see Fig. 1.1)
- Marine Meteorological Logbook

- Envelope to send logbooks, floppy disks or CD-Rs (postage free within Japan)

(see Appendix 1)

1.2 Careful practice

1.2.1 Accurate observations

In order to obtain reliable data, it is important for mariners to perform meteorological observations carefully and rigorously. An inaccurate reported observation may result in an erroneous forecast, whereas one that is valid and reliable could shed light on obscure and complex meteorological phenomena. It is also necessary to ensure that observations are not affected by motion or vibration of the ship, exhaust of gases or liquids, or sea spray. Needless to say, neglecting a scheduled observation should be avoided.

It is worthwhile matching observed values to the context of surrounding meteorological and ocean conditions. For example, change in atmospheric pressure. If a tropical cyclone (e.g. typhoon) or an extra-tropical cyclone is approaching, "wind speed" will increase. If a front is approaching, "direction of wind" will change and "wind waves" will be higher. Being mindful of these factors will reduce errors in reading measures and help determine malfunctioning instruments.

Observed results should be recorded directly in the Marine Meteorological Logbook. As for items requiring calculations (see the corresponding chapters for details), it is recommended to record observed and calculated values on paper at time of determination before making an entry in the logbook:

- Atmospheric pressure; correct to sea level (Chap.2)
- Dew-point temperature (Chap. 3)
 - * dew-point hygrometer, no calculation needed
- Wind speed/direction; observed (apparent) values, correct to true wind (Chap.4)
- Weather (present and past); change during previous 3 or 6 hours required, change should be recorded at any time (Chap.7)

Do not enter any value from memory. Always ensure observation procedures, calculations, and radio weather messages are correct.

Software to make electric logbooks including OBSJMA can assist in accurate weather observations and reports.

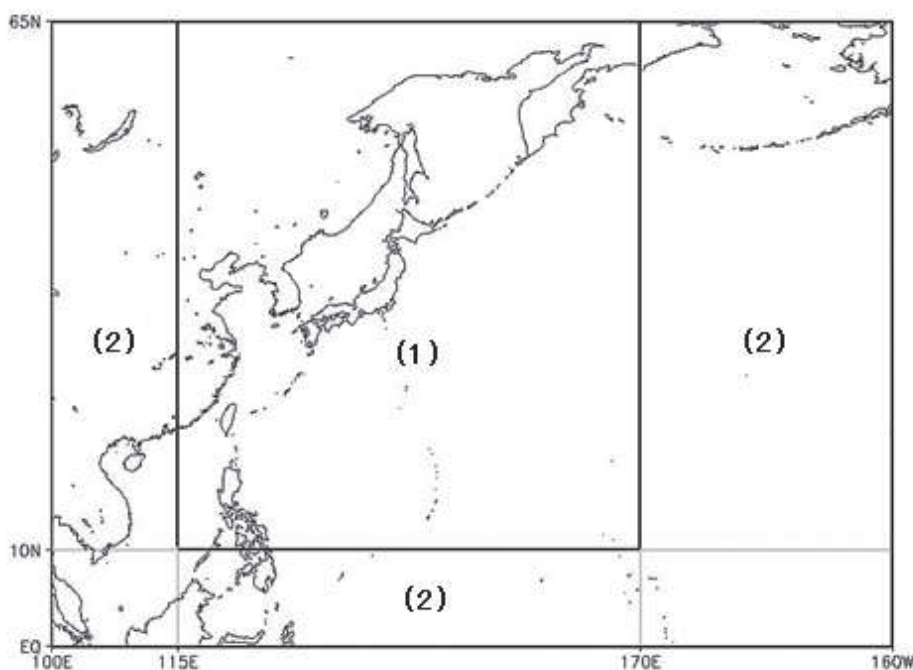


Fig. 1.2 The areas where ships are requested to report weather observations by JMA

1.2.4 Sequence of observations

Although different observations cannot be conducted simultaneously, they should be conducted as close to the reporting time as possible. Non-instrumental observations should be made consecutively rather than instrumental and non-instrumental alternately, since eyes need time to accommodate to the sight over the sea (especially at night). Instrumental observations requiring the use of a light should be made after non-instrumental ones, so that dark adaptation of eyes is not impaired.

With the above remarks in mind, the following sequence of observations is recommended:

- 1) Observation of sea surface temperature (in case of bucket measurement)
- 2) Non-instrumental observations
 - Horizontal visibility
 - Cloud (amount, type, height, etc.)
 - Ocean waves (wind waves, swell)
 - Wind direction and speed (in case of observation by Beaufort scale)
- 3) Instrumental observations
 - Wind direction and speed (in case of observation by anemometer)
 - Air and wet-bulb temperatures (in case of wet-bulb thermometer) or air temperature and dew-point (in case of dew-point hygrometer)
 - Sea surface temperature (in case of intake measurement or hull-attached thermometer)
 - Atmospheric pressure to be measured exactly on time
- 4) Calculation and conversion to codes

- 5) Entry in Marine Meteorological Logbook
- 6) Preparation of Radio Weather Message
- 7) Completion and transmission of weather report

Present and past weather should be observed as necessary (see 1.2.1). Software to make weather reports including OBSJMA can assist in the above procedures 4) - 6).

1.3 Utilization of observed results

JMA receives weather reports from ships directly through Radio Weather Messages and/or later through Marine Meteorological Logbooks mailed from Japanese ports.

Observations reported through Radio Weather Messages are immediately utilized mainly to produce weather and ocean wave forecasts/warnings, and numerical weather and ocean wave prediction models. Observations on board ships are valuable to augment the sparse data available over the oceans. Though meteorological satellites provide observations, these data are insufficient and require corrections based upon observations provided by ships.

Marine meteorological observation data received by JMA as Marine Meteorological Logbooks are archived electronically after being checked for quality, and exchanged internationally to assemble the global database of marine meteorology. These data are being utilized for such activities as monitoring global climate change, development or improvement of numerical climate models and more.

CHAPTER 2 Observation of Atmospheric Pressure

It is widely known from weather maps that atmospheric pressure is the most basic measure used to describe the state of the atmosphere. The distribution or time change of atmospheric pressure is an important indicator of change of weather and/or wind.

2.1 Definition and units

Hecto-pascal (hPa) is the standard unit of atmospheric pressure. Other units include mb, mmHg and inchHg as below:

$$1 \text{ hPa} = 100 \text{ Pa} = 1 \text{ mb}$$

$$1 \text{ mmHg} = 1.33322 \text{ hPa}$$

$$1 \text{ inchHg} = 33.8639 \text{ hPa}$$

A detailed list converting mmHg to hPa is provided in “Guide to Ships’ Weather Reports” issued by JMA.

2.2 Measuring instruments and installation conditions

The marine aneroid barometer measures atmospheric pressure. The marine aneroid barograph records barometric tendencies (e.g. rate of change). The resonator digital barometer, as described later, also records atmospheric pressure and barometric tendencies.

When installing these instruments the following conditions should be considered:

- 1) Avoid exposure to direct sunlight.
- 2) Choose sites with minimum temperature change.
- 3) Minimize effects of vibration and shock caused by engine and/or ocean waves, with insulation material such as sponge rubber.
- 4) The marine aneroid barometer is normally installed horizontally. If fixed on a vertical wall, ensure its indicated value differs no more than 0.5 hPa from that of normal installation.

2.3 Aneroid barometer

The aneroid barometer works on the principle that its capsule made of metal expands or contracts in response to change in atmospheric pressure. A high quality precision marine aneroid barometer (see Fig. 2.1) is recommended for weather observations by ships.

Before reading the atmospheric pressure, tap the glass face with your finger so that the needle vibrates slightly. Then focus your best eye above the needle and read the scale. Only use one eye to avoid parallax error. If you see a reflection of your eye in the glass exactly at the same horizontal position as the needle, your eye is correctly located for observation. If your barometer has a mirror on the scale plate, you can accurately adjust your eye position.

Among high ocean waves, ships undergo large rolling and pitching resulting in displacement and vertical acceleration causing the barometer needle to show horizontal oscillations. In this case, make several readings noting the maximum and minimum values on

the scale and take the average value as the observed value.

Observation of the atmospheric pressure should be made exactly on the observation hour and the pressure should be recorded to within 0.1 hPa.

2.4 Electronic barometers

Two types of electronic barometers are commonly used for weather observations. One is a resonator digital barometer and the other an electric capacitance barometer. The former works on the principle that the frequency of its sensor varies with atmospheric pressure. The latter works on the principle that its electric capacitance varies with atmospheric pressure. Electronic barometers do not indicate current atmospheric pressure but an averaged value over a short period. Thus, accurate observations may be made during rolling and pitching. In addition, since these barometers display digitized values inter- and intra-observer bias is avoided.

2.5 Correction for instrumental error

The indicated value of a barometer differs from the true value to some extent. This intrinsic difference is known as “instrumental error” and should be corrected to obtain the station value (see 2.6) of atmospheric pressure. If the correction value for instrumental error is known from a barometer inspection, the station pressure is obtained by adding the value to the indicated value. Barometers should be inspected every 6 months by Port Meteorological Officers (PMOs) to maintain their accuracy (Chap.12).

2.6 Correction to sea level

The atmospheric pressure at mean sea level may be derived from the observed value of the instrument installed at a height above mean sea level (referred to as station pressure). This derivation is called “correction to mean sea level”. Correction depends not only on the height at which the instrument is installed but on station pressure* and temperature. See “Guide to Ships’ Weather Reports” for a detailed correction table.

The height of the barometer above mean sea level should be determined when a ship is fully loaded and unloaded. If the ship draught level varies by + or - 1 m around the average level, the height of the barometer above the average draught level may be taken as its height for the correction.

Given a station pressure of 997.4 hPa, height of barometer above mean sea level of 6 m, and temperature 13°C, the correction value will be 0.7 hPa according to the table mentioned above. And the corrected value is obtained as follows:

$$\begin{array}{rccccccc}
 997.4 & & + & & 0.7 & = & 998.1 \text{ hPa} \\
 \text{(station pressure)} & & & & \text{(correction)} & & \text{(pressure at mean sea level)}
 \end{array}$$

2.7 Barograph

A barograph is used to check observed values of pressure and record barometric tendencies.

* Station pressure is defined as the pressure at barometer level.

Figure 2.2 shows an aneroid barograph, one of several available types of barographs. The barograph paper, on which a continuous record of the pressure is made, is the barogram. Barograms must be renewed at intervals (from 1 day to 7 days, depending on the instrument). It is recommended that a barograph be installed to reveal whether a high, a low, a trough or a ridge is approaching or moving away indicating improving or worsening weather conditions.

As for where and how to install the barograph, refer to section 2.2.

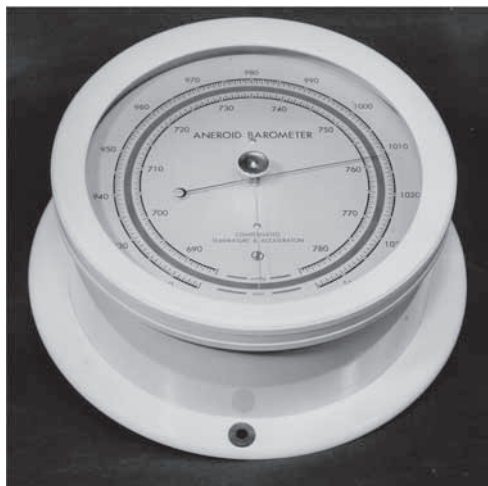


Fig. 2.1 Aneroid barometer

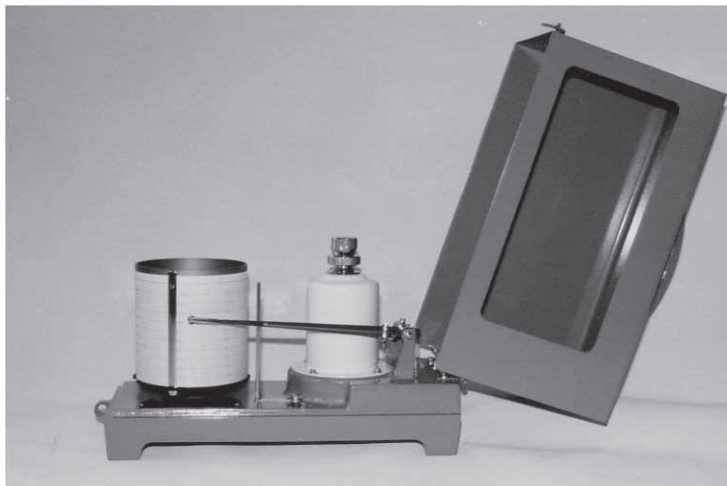


Fig. 2.2 Barograph

CHAPTER 3 Observation of Air Temperature and Dew-point Temperature

The horizontal distribution of temperature in the atmosphere caused by latitudinal differences in incoming sunlight creates regional differences in atmospheric density giving rise to air flow (wind), clouds and precipitation. Therefore, atmospheric temperature is one of the basic elements to be observed in analyzing atmospheric conditions.

Water vapor in the atmosphere is the source of clouds and precipitation. It also transports energy in the form of latent heat through evaporation and condensation. Since water vapor absorbs and emits infrared radiation, it also affects the variation of atmospheric radiation. Therefore water vapor plays an important role in atmospheric phenomena.

3.1 Definition and unit

The temperature of the atmosphere is called air temperature. The partial pressure of water vapor in the atmosphere is called water vapor pressure, or vapor pressure. The maximum value of vapor pressure in the atmosphere, which is called saturated vapor pressure, depends on air temperature and whether the atmosphere faces water or ice. The ratio of vapor pressure to saturated vapor pressure at a given temperature is called relative humidity. Dew-point temperature is defined as the air temperature at which vapor pressure is equal to saturated vapor pressure at constant air pressure. Air and dew-point temperatures should be recorded as degree Celsius to the nearest 0.1.

3.2 Measuring instruments and installation conditions

For observations of air and dew-point temperatures, an aspiration (ventilated) psychrometer, an Assmann psychrometer, a sling psychrometer, and an electric psychrometer (combined resistance thermometer and dew-point hygrometer or electric humidity hygrometer) are commonly used (see Fig. 3.1-Fig. 3.4).

A dew-point hygrometer measures the dew-point temperature directly.

A non-ventilated psychrometer is not recommended because if there is little air movement only air near the instrument is measured, which may not represent the observation site.

An aspiration psychrometer should be screened in an instrument shelter (see Fig. 3.5).

To make accurate temperature observations, instruments should be well exposed to a fresh air stream from the sea, which has not been in contact with or passed over the ship. They should also be adequately shielded from spray, precipitation, and heat radiated by the sun, the sea and the ship itself.



Fig. 3.1 Ventilated psychrometer

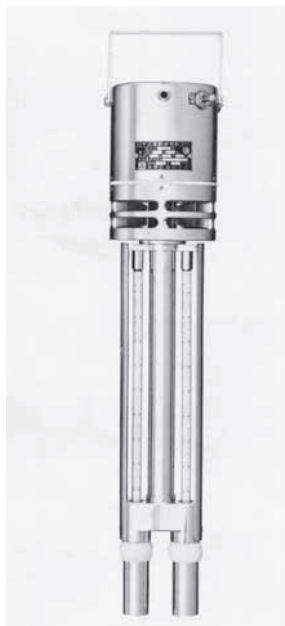


Fig. 3.2 Assmann psychrometer

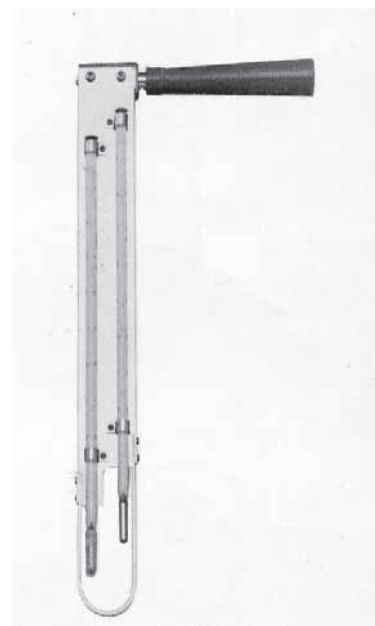


Fig. 3.3 Sling psychrometer



Fig. 3.4 Electric thermometer and hygrometer housed in separate metal envelopes



Fig. 3.5 Instrument shelter called "Screen" in which a psychrometer is housed

3.3 Psychrometers (Dry and wet-bulb thermometers)

3.3.1 Maintenance of wet-bulb thermometer

Psychrometers are instruments with both a wet-bulb and a dry-bulb thermometer. Wet-bulb temperature is measured with the wet-bulb thermometer which is a thermometer with its bulb wrapped in a wet cloth called a sleeve (or muslin wicking). The thermometer without a sleeve is called the dry-bulb thermometer. The wet-bulb thermometer is the one on the left of an aspiration psychrometer or on the outer side of a sling psychrometer. Its sleeve must be wet with the purest water available (preferably distilled). Any minerals or other impurities would change the evaporation characteristics of the water. If the sleeve becomes dirty or contaminated by sea spray, it should be replaced immediately. The sleeve should be renewed at least once a

month with normal use. The thermometer bulbs should also be kept clean. When changing a sleeve, ensure the thermometer bulbs are clean. Fig. 3.6 shows various types of wet-bulbs wrapped in sleeves.

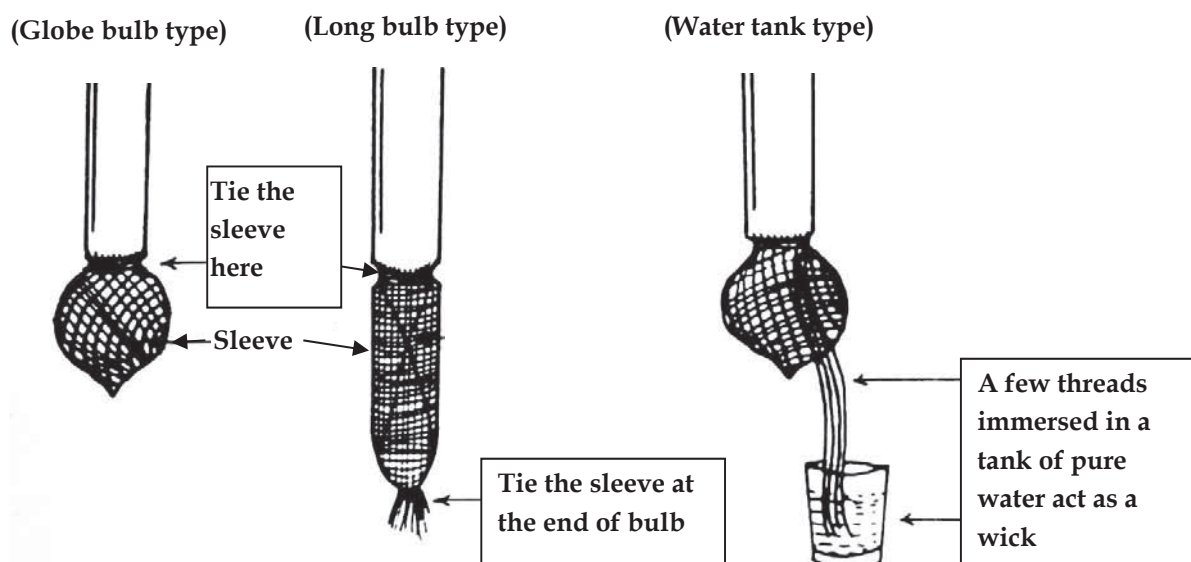


Fig. 3.6 Wet-bulbs wrapped in sleeves

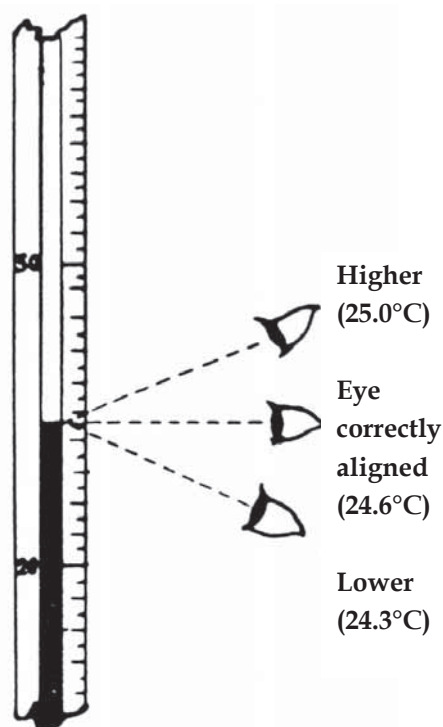


Fig. 3.7 Align eye to avoid parallax error

3.3.2 Observation by psychrometer

Ten minutes before observation, moisten the sleeve with pure (preferably distilled) water using a water dropper careful not to wet other parts of the psychrometer.

Hold the psychrometer out of direct sunlight, facing windward. Ensure the dry-bulb is not downwind of the wet-bulb. It takes about 5 minutes to obtain a stabilized value from a wet-bulb thermometer if the air temperature is above 0°C. But it may take 10 to 20 minutes if the wet-bulb is ice covered. Read the dry-bulb thermometer first then the wet-one taking care to avoid any influence by body heat or breath. Read the 1st decimal place of the scale first, then the higher places.

When reading a thermometer, care should be taken to align the eye with

the measurement point, otherwise there may be a risk of parallax error (see Fig. 3.7).

The minimum interval on a thermometer scale is generally 0.5°C or 0.2°C . For meteorological observations, that of 0.2°C is recommended with the measure estimated to the nearest tenth of a degree.

3.3.3 How to measure dew-point temperature

Unless using a dew-point hygrometer, to obtain the dew-point temperature use “Table for Finding the Dew-point” published by JMA or the table for saturated vapor pressure (see Appendix 2).

(1) Method using “Table for Finding the Dew-point”

The table shows dew-point temperatures under wet-bulb depression values. Wet-bulb depression is the difference between the dry-bulb temperature (t) and the wet-bulb temperature (t'), (wet-bulb depression: $t-t'$). As both $t-t'$ and t' are given at intervals of 0.5°C in the table, the dew-point temperature is obtained as shown in the following examples:

Example A)

Given

dry-bulb temperature (t) = 20.8°C

wet-bulb temperature (t') = 19.4°C

$t-t' = 1.4$ and the nearest values at intervals of 0.5 for t' and $t-t'$ are 19.5 and 1.5, respectively. In the table we find:

dew-point temperature = 18.8°C for $t-t' = 1.5$ and $t' = 19.5$.

t'	$t-t'$			
	0.5	1.0	1.5	2.0
19.0	18.8	18.5	18.3	18.0
19.5	19.3	19.0	18.8	18.5
20.0	19.8	19.5	19.3	19.1

The diagram shows the interpolation process. A box labeled '1.4' is placed above the '1.5' column header. An arrow points down from this box to the intersection of the '1.5' column and the '19.5' row. Another box labeled '19.4' is placed to the left of the '19.5' row header. An arrow points right from this box to the same intersection point.

Example B)

Given

$$t = 1.2^{\circ}\text{C}$$

$$t' = -2.7^{\circ}\text{C} \text{ (wet-bulb not ice covered)}$$

$t-t' = 3.9$ and the values of t' and $t-t'$ are rounded to -2.5 and 4.0 , respectively. In the table (for a wet-bulb not ice covered) we find:

dew-point temperature = -12.1°C for $t-t' = 4.0$ and $t' = -2.5$.

t'	$t-t'$			
	3.0	3.5	4.0	4.5
-3.0	-9.8	-11.3	-13.0	
-2.5	-9.0	-10.5	-12.1	
-2.0	-8.2	-9.6	-11.1	-12.8

Diagram illustrating the interpolation process for Example B. A dot is placed at the intersection of $t-t' = 4.0$ and $t' = -2.5$ (value -12.1). A vertical arrow points up from this dot to the value 3.9 in the $t-t' = 4.0$ column. A horizontal arrow points left from this dot to the value -2.7 in the $t' = -2.5$ row.

Example C)

Given

$$t = 1.2^{\circ}\text{C}$$

$$t' = -2.7^{\circ}\text{C} \text{ (wet-bulb ice covered)}$$

$t-t' = 3.9$ and the values of t' and $t-t'$ are rounded to -2.5 and 4.0 , respectively. In the table (for a wet-bulb ice covered) we find:

dew-point temperature = -11.1°C for $t-t' = 4.0$ and $t' = -2.5$.

t'	$t-t'$			
	3.0	3.5	4.0	4.5
-3.0	-9.4	-10.7	-12.1	
-2.5	-8.6	-9.8	-11.1	
-2.0	-7.7	-8.9	-10.1	-11.5

Diagram illustrating the interpolation process for Example C. A dot is placed at the intersection of $t-t' = 4.0$ and $t' = -2.5$ (value -11.1). A vertical arrow points up from this dot to the value 3.9 in the $t-t' = 4.0$ column. A horizontal arrow points left from this dot to the value -2.7 in the $t' = -2.5$ row.

(2) Method using “Table for saturated vapor pressure (Appendix 2)”

Appendix 2 is a series of tables to determine saturated vapor pressure from air temperature. Different tables are used according to condition:

- 1) Air temperature above 0°C, wet-bulb not ice covered
- 2) Air temperature below 0°C, wet-bulb not ice covered
- 3) Air temperature below 0°C, wet-bulb ice covered.

To calculate dew-point temperature given dry-bulb temperature (t), wet-bulb temperature (t'), and sea level pressure (P) as

$$t = 19.8^{\circ}\text{C}$$

$$t' = 17.3^{\circ}\text{C}$$

$$P = 985.2 \text{ hPa}$$

saturated vapor pressure (E') for t' is 19.74 hPa from Table 1. Vapor pressure (e) is calculated as

$$e = E' - A / 755 \times (t - t') \times P$$

where A is 0.5 (wet-bulb not ice covered) or 0.44 (wet-bulb ice covered). In this case,

$$\begin{aligned} e &= 19.74 - 0.5/755 \times (19.8 - 17.3) \times 985.2 \\ &= 19.74 - 1.63 \\ &= 18.11 \text{ hPa} \end{aligned}$$

The nearest value of (e) in the table 1) is 18.06 hPa, so its corresponding dew-point temperature 15.9°C should be recorded.

3.4 Electric psychrometer

3.4.1 Platinum resistance thermometer

The thermometer has a platinum sensor whose resistance changes with temperature change. It is housed in a ventilated cylinder to shield it from direct sunlight and precipitation, and to provide adequate ventilation. Adequate wind speed ventilation for the sensor is 6 to 8 m/s.

3.4.2 Dew-point hygrometer

The sensor of the dew-point hygrometer is a heater coated with lithium chloride which absorbs water vapor from the air. Dry lithium chloride is non-conductive but with water it becomes conductive. As it absorbs water, conductivity increases and a current flows to the heater which evaporates water from the sensor until a dynamic equilibrium is reached when the water vapor pressure of the lithium chloride matches that of the atmosphere. Then, the temperature of the sensor is closely related to the dew-point temperature of the air. A hygrometer, which generates heat, and a thermometer must be housed separately. Comparison checks with a psychrometer should be conducted frequently. If the difference in dew-point temperature among them exceeds 1°C, apply new lithium chloride.

3.4.3 Electric humidity hygrometer

The hygrometer has a capacitance sensor including a polymer film which absorbs water. As the polymer absorbs water there is a change in capacitance which can be directly converted to the relative humidity of the surrounding atmosphere. The hygrometer is housed in a ventilated cylinder to shield it from direct sunlight and precipitation. Adequate wind speed ventilation for the sensor is about 4 m/s. Comparison checks with a psychrometer should be conducted frequently.

CHAPTER 4 Observation of Wind

Wind is an important meteorological element, closely related to the pattern of atmospheric pressure. Wind speed is proportional to the pressure gradient while wind direction deviates about 15 degrees from the direction of isobars over the oceans in mid-latitudes. Reported observations of wind over the oceans are utilized in real time for weather analysis, forecasting and warnings, and also as statistical data for navigation of ships and aircraft.

4.1 Definition and units

Wind vectors indicate direction (wind direction) and magnitude (wind speed). Values averaged over 10 minutes immediately preceding the observation time should be reported. If the wind characteristics were markedly changeable showing discontinuity during the period, adopt the values averaged over the period since the discontinuity, hence less than 10 minutes..

Wind direction is the direction from which it is blowing. In marine meteorological observation, wind direction is measured as one of 36 direction codes, with the east as 09, the south as 18, the west as 27 and the north as 36. The scale of the direction code increases clockwise with an increment of 1 for each angle increment of 10 degrees. If the wind speed is 0.2 m/s (0.4 knot) or less, the wind direction should be recorded as “calm” and coded as 00 in the logbook. If wind is indeterminate, enter 99 as the direction code.

The unit for wind speed is “knot”.

1 knot = 1 nautical mile/hour

= 1852 m/hour

= 0.5144 m/s

1 m/s = 1.9438 knot



Fig. 4.1 Anemometer (wind vane type)

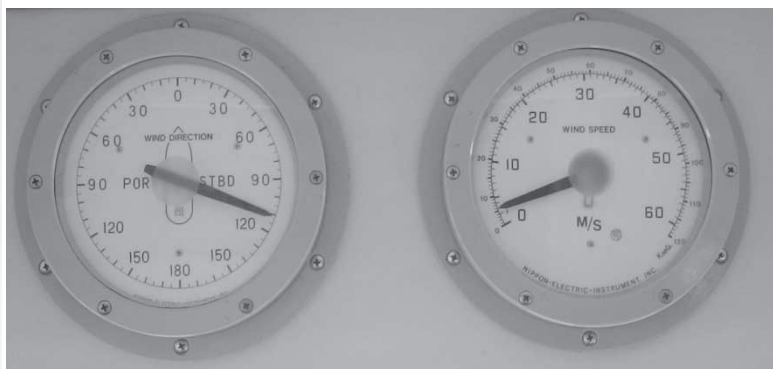


Fig. 4.2 Indicator of wind direction

Fig. 4.3 Indicator of wind speed

4.2 Measuring instruments and installation conditions

A wind vane/anemometer, generally used to measure wind (Fig. 4.1), should be installed where the wind is least affected by the ship structure and it is accessible to repair in case of malfunction.

4.3 Measurement of wind direction and speed

With an anemograph, examine the data recorded over 10 minutes preceding the observation time. Determine the wind direction as the averaged direction at the center of the most densely dotted part in the record. Similarly determine the mean wind speed at the center of the fluctuating values of wind speed. Without an anemograph, determine the average of wind direction values shown by the indicator for about 1 minute. Regarding wind speed, discard the maximum and the minimum values and adopt the value around which fluctuations are most constant.

4.4 Calculation of true wind direction and speed

Unless your instrument is capable of measuring wind compensating for ship motion (true wind), the observed wind obtained on board ship during navigation is taken as apparent wind.

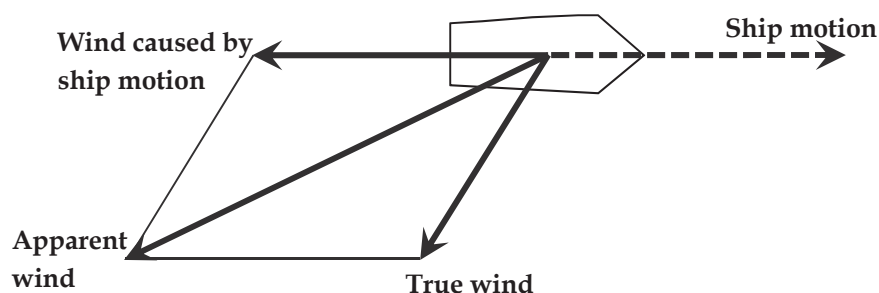


Fig. 4.4 Ship motion vector and wind vectors

True wind is the vector sum of apparent wind and ship motion. A circle graph is useful in its calculation. Plot an angle scale on the circumference in increments of 10 degrees. Then plot a speed scale on the diameter in increments of 10 knots. Example (Fig. 4.5) to find the true wind:

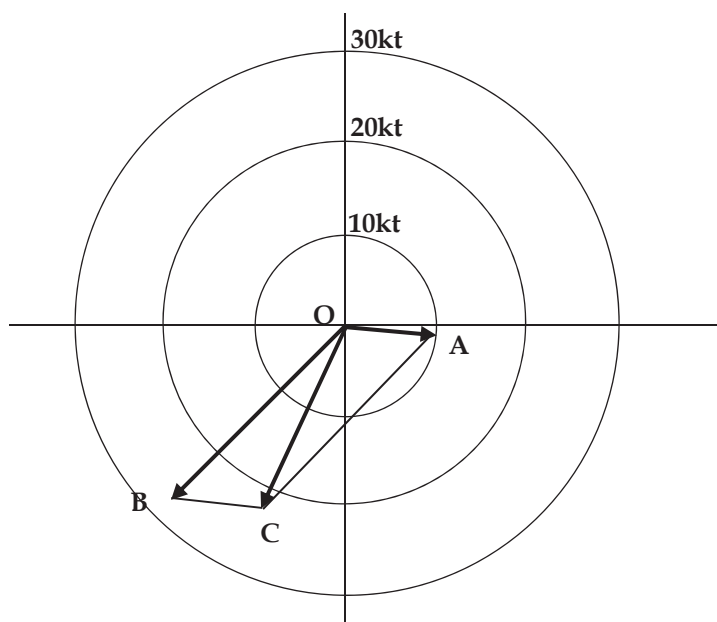


Fig. 4.5 Vectors of ship motion(\overrightarrow{OA}), apparent wind(\overrightarrow{OB}), and true wind(\overrightarrow{OC})

Given

Ship motion (\overrightarrow{OA}):

ship course, 95 degrees

ship speed, 10 knots

Apparent wind (\overrightarrow{OB}):

wind direction, 50 degrees on the port side

wind speed, 27 knots

Calculations:

Mark point A at the angle of 95 degrees and distance of 10 knots from the center. The arrow from the center (O) to A indicates the ship motion vector.

Mark point B at the angle of 225 degrees = 95 (ship course) - 50 (apparent wind direction relative to the bow; negative in case of wind on the port side and positive on the starboard side) + 180 (to obtain the direction to which wind blows) and distance of 27 knots from the center.

The vector direction of apparent wind is the direction to which it is blowing, opposite from which it is blowing. The arrow from the center (O) to B indicates the apparent wind vector.

The true wind vector is the summation of vectors, \overrightarrow{OB} and \overrightarrow{OA} . Form a parallelogram using OA and OB to find point C. This yields \overrightarrow{OC} as the true wind vector and the length of \overrightarrow{OC} as the true wind speed (22 knots). The opposite direction of \overrightarrow{OC} , is the true wind direction (25 degrees) from which the wind blows. True wind can be also calculated using a

wind velocity scale (see Fig. 4.6), which comprises two rotatable disks and a rectangular scale fastened at the center. The lower disk is called the compass disk, and the upper the wind direction disk. The rectangular scale is called a wind speed ruler. To calculate true wind:

- 1) Turn the wind direction disk to set "0" at the direction of the ship bow (95 degrees in the above example) on the compass disk.
- 2) Turn the wind speed ruler to the direction of apparent wind (50 degrees to the left) on the wind direction disk.
- 3) Mark point "A" on the wind direction disk using the wind speed ruler to measure wind speed (27 knots) from the center, and next, mark point "C" going down from "A" at a distance of ship speed (10 knots) in parallel with vertical lines of the wind direction disk.
- 4) Turn the wind speed ruler to "C" to find the true wind speed by reading the scale of the ruler at "C" (it must be 22 knots).
- 5) The cross point of the wind speed ruler and the wind direction disk shows the true wind direction from the bow, and the cross point of the wind speed ruler and the compass disk shows the true wind direction from true north (it must be 25 degrees).

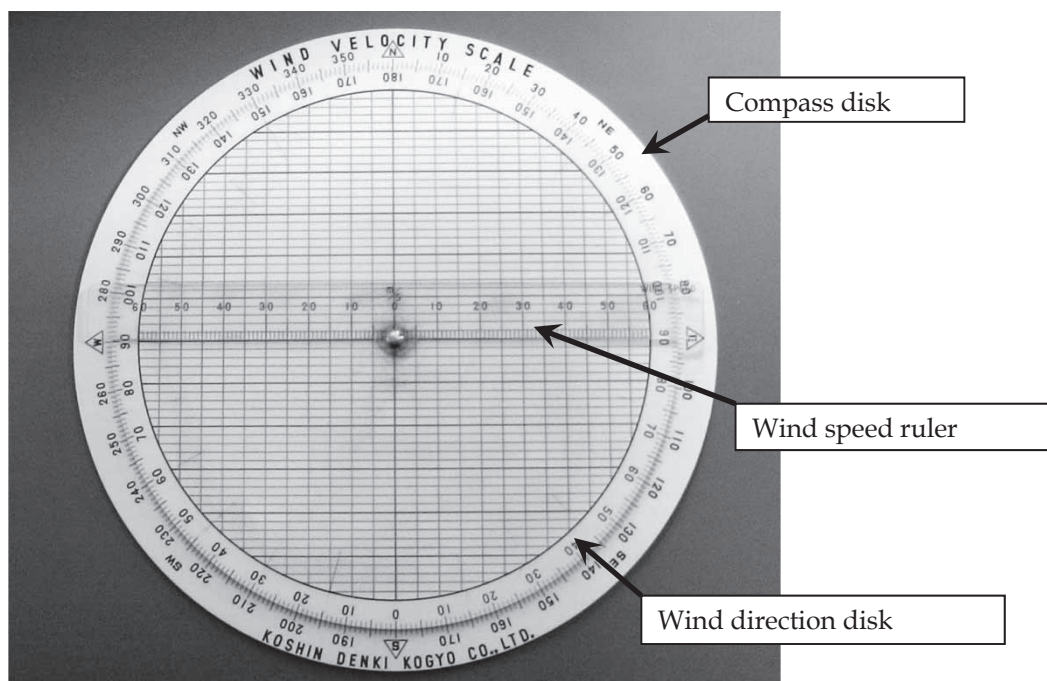


Fig. 4.6 Wind velocity scale

You can confirm the calculated true wind direction by observing wind waves, which travel in almost the same direction as the wind.

4.5 Non-instrument observations

If a wind vane/anemometer is unavailable wind direction and force may be found as below.

4.5.1 Wind direction

True wind direction may be estimated from streaks of foam on the sea surface and/or sea (wind) wave direction with a gyro compass. Consider the following:

- 1) Observe wind waves far enough from the ship that they are not influenced by the ship.
- 2) When wind direction changes abruptly, note the direction of streaks of foam and the orientation of the crests of sea waves other than their overall shape since wave characteristics remain affected by the preceding wind for some time.
- 3) When wind is too weak to cause perceptible waves, estimate wind direction from the deck considering the ship travel direction.
- 4) Do not rely on wind waves near shore or sea ice for proper wind direction.
- 5) At night or in poor visibility (such as heavy rainfall, snow, fog etc.), estimate wind direction from smoke, tape and so on.
- 6) Although windward is preferable, observe wind leeward to avoid dazzle by the sun or its reflection from the sea surface.

4.5.2 Wind force

To estimate wind force from the sea surface, use the Beaufort Scale of Wind Force (see Table 4.1) and refer to photographs. The velocity equivalent in Table 4.1 is for a standard height of 10 meters above the sea surface. When using the table, heed the following:

- 1) Even while wind is strengthening, there are time lags before changes in sea surface characteristics (wave length, wave height, etc.) occur.
- 2) The scale of a wave depends on the fetch (the distance along which a wind is blowing straight) of the wind in question. This is why a wave with land on its upstream side has a different scale from an offshore wave.
- 3) If a tidal or ocean current is predominant, the sea surface does not always correspond to the wind force. Especially, unusual waves are remarkable near an ocean front.
- 4) The sea depth affects the way a wave is formed.
- 5) When a swell is prevailing, it is more difficult to discern wind waves.
- 6) At night, estimation of wind force is not easy. Since it is more difficult to recognize white caps of wind waves, slightly inflate the wind force value.
- 7) Rainfall tends to make the sea surface smoother. Severe rainfall is particularly effective. In such conditions inflate the wind force value accordingly.
- 8) The height of a wind wave depends on the difference between air and sea surface temperatures. Accordingly, adopt a smaller wind force value than estimated from wind waves when the air temperature is lower than the sea surface temperature.

Table 4.1 Beaufort scale of wind force

Beaufort number	Descriptive term	Wind speed equivalents		Specifications for observations
		m/s	knots	
0	Calm	0 - 0.2	< 1	Sea like a mirror
1	Light air	0.3 - 1.5	1 - 3	Ripples with the appearance of scales are formed, but without foam crests
2	Light breeze	1.6 - 3.3	4 - 6	Small wavelets, still short but more pronounced; crests have a glassy appearance and do not break
3	Gentle breeze	3.4 - 5.4	7 - 10	Large wavelets; crests begin to break; foam of glassy appearance; perhaps scattered white horses
4	Moderate breeze	5.5 - 7.9	11 - 16	Small waves, becoming longer; fairly frequent white horses
5	Fresh breeze	8.0 - 10.7	17 - 21	Moderate waves, taking a more pronounced long form; many white horses are formed (chance of some spray)
6	Strong breeze	10.8 - 13.8	22 - 27	Large waves begin to form; the white foam crests are more extensive everywhere (probably some spray)
7	Near gale	13.9 - 17.1	28 - 33	Sea heaps up and white foam from breaking waves begins to be blown in streaks along the direction of the wind
8	Gale	17.2 - 20.7	34 - 40	Moderately high waves of greater length; edges of crests begin to break into the spindrift; the foam is blown in well-marked streaks along the direction of the wind
9	Strong gale	20.8 - 24.4	41 - 47	High waves; dense streaks of foam along the direction of the wind; crests of waves begin to topple, tumble and roll over; spray may affect visibility
10	Storm	24.5 - 28.4	48 - 55	Very high waves with long overhanging crests; the resulting foam, in great patches, is blown in dense white streaks along the direction of the wind; on the whole, the surface of the sea takes on a white appearance; the tumbling of the sea becomes heavy and shock-like; visibility affected
11	Violent storm	28.5 - 32.6	56 - 63	Exceptionally high waves (small and medium-sized ships might be for a time lost to view behind the waves); the sea is completely covered with long white patches of foam lying along the direction of the wind; everywhere the edges of the wave crests are blown into froth; visibility affected
12	Hurricane	32.7 =<	64 =<	The air is filled with foam and spray; sea completely white with driving spray; visibility very seriously affected

**Force 0 Calm**

Wind speed < 1 knot

Sea like a mirror

**Force 1 Light air**

Wind speed 1 – 3 knots

Ripples with the appearance of scales are formed, but without foam crests

**Force 2 Light breeze**

Wind speed 4 – 6 knots

Small wavelets, still short but more pronounced; crests have a glassy appearance and do not break

**Force 3 Gentle breeze**

Wind speed 7 – 10 knots

Large wavelets; crests begin to break; foam of glassy appearance; perhaps scattered white horses

**Force 4 Moderate breeze**

Wind speed 11 – 16 knots

Small waves, becoming longer; fairly frequent white horses

**Force 5 Fresh breeze**

Wind speed 17 – 21 knots

Moderate waves, taking a more pronounced long form; many white horses are formed (chance of some spray)

**Force 6 Strong breeze**

Wind speed 22 – 27 knots

Large waves begin to form; the white foam crests are more extensive everywhere (probably some spray)

**Force 7 Near gale**

Wind speed 28 – 33 knots

Sea heaps up and white foam from breaking waves begins to be blown in streaks along the direction of the wind

**Force 8 Gale**

Wind speed 34 – 40 knots

Moderately high waves of greater length; edges of crests begin to break into the spindrift; the foam is blown in well-marked streaks along the direction of the wind

**Force 9 Strong gale**

Wind speed 41 – 47 knots

High waves; dense streaks of foam along the direction of the wind; crests of waves begin to topple, tumble and roll over; spray may affect visibility

**Force 10 Storm**

Wind speed 48 – 55 knots

Very high waves with long overhanging crests; the resulting foam, in great patches, is blown in dense white streaks along the direction of the wind; on the whole, the surface of the sea takes on a white appearance; the tumbling of the sea becomes heavy and shock-like; visibility affected

**Force 11 Violent storm**

Wind speed 56 – 63 knots

Exceptionally high waves (small and medium-sized ships might be for a time lost to view behind the waves); the sea is completely covered with long white patches of foam lying along the direction of the wind; everywhere the edges of the wave crests are blown into froth; visibility affected

**Force 12 Hurricane**

Wind speed ≥ 64 knots

The air is filled with foam and spray; sea completely white with driving spray; visibility very seriously affected

CHAPTER 5 Observation of Cloud

A cloud is a hydrometeor consisting of water droplets or ice crystals, or a mixture of both, suspended in the air above land or sea. It differs from fog only in that fog is in contact with the earth's surface. Cloud observations help determine the state of the atmosphere with their distribution related to meteorological disturbances including Typhoons or extra-tropical lows. Although wide range observations by meteorological satellites have been introduced, the importance of cloud observation by ships over the oceans remains significant.

5.1 Observation of cloud

Observation of cloud on board ship covers:

- Amount of cloud and type of cloud
- Identification of cloud types
- Height of the base of each cloud

Observe the total amount of cloud first, then from lower cloud to higher cloud. Among the same height of clouds, groups with larger amount should be considered first.

5.1.1 Cloud amount (Cloud cover)

“Total cloud amount” is the proportion of the sky occupied by clouds of all types.

In contrast, the proportion of a specified type of cloud is called “cloud amount” for that type. Observers should estimate each cloud type exclusively, as if no other type were present at different levels, taking into consideration the evolution of the sky. Total summation of the cloud amounts could then exceed the total cloud amount.

Cloud amount for any particular type is recorded as 0 if there is none present, 10 if it covers the whole sky and 1 to 9 according to its coverage. If the amount seems too small to be 1, put 0+. If it is almost 10 but a break is present, put 10-.

Care should be taken as follows:

- 1) If there is fog, haze, or other phenomena preventing observation of any cloud above, record cloud amount as unknown (sky obscured), code 9 in the logbook. If cloud can be seen through the fog, etc., cloud amount should be estimated as well as possible.
- 2) If the sun, moon or stars are visible through the fog, etc., and there is no evidence of cloud above the fog, cloud amount should be estimated as 0.
- 3) If cloud amount cannot be estimated at night, rather than make an ambiguous guess record it as unknown with the code ×.
- 4) If part of the sky is obscured by rain or snow, decide the amount assuming the cloud bringing the rain or snow covers that part of the sky.

5.1.2 Cloud type (genus)

Clouds are classified into 10 principal types (genera), see 5.2. They are incessantly changing,

not necessarily appearing in typical form so care is needed to determine which types are prevailing. If uncertain, record as unknown.

5.1.3 Cloud height

Cloud height is the height of the cloud base above the sea measured in units of 100 m, reaching up to about 10 km. A cloud can be classified according to height as: high level cloud (C_H), middle level cloud (C_M) and low level cloud (C_L). The maximum cloud height observed varies according to latitude, being higher in the tropics than in the higher latitudes. If it is difficult to discern the cloud type, consideration of its height may help.

5.2 Details of cloud types (genera)

Table 5.1 shows 10 types of clouds (genera) by 3 levels of height, and Table 5.2 summarizes the relationship between cloud type and precipitation.

Table 5.1 Approximate heights for high, middle and low clouds

Level	Cloud type (genus)	Polar Regions	Temperate Regions	Tropical Regions
High (C_H)	Cirrus (Ci)	3 - 8 km	5 - 13 km	6 - 18 km
	Cirrocumulus (Cc)			
	Cirrostratus (Cs)			
Middle (C_M)	Alto cumulus (Ac)	2 - 4 km	2 - 7 km	2 - 8 km
	Altostratus (As)			
	Nimbostratus (Ns)	As: usually found in the middle level, but often extends higher. Ns: usually found in the middle level, but often extends into the other levels.		
Low (C_L)	Stratocumulus (Sc)	below 2 km	below 2 km	below 2 km
	Stratus (St)			
	Cumulus (Cu)	Cu, Cb: usually have bases in the low level, but their tops often reach into the middle and high levels.		
	Cumulonimbus (Cb)			

Table 5.2 Hydrometeors consisting of falling particles and the cloud genera

Hydro- meteors \ Genera	As	Ns	Sc	St	Cu	Cb	No cloud
Rain	○	○	○		○	○	
Drizzle				○			
Snow	○	○	○	○	○	○	
Snow grains				○			
Snow pellets			○		○	○	
Diamond dust							○
Hail						○	
Small hail						○	
Ice pellets	○	○					

*Reference: International Cloud Atlas Vol.1 (1975)

The following descriptions of general features of each type of cloud are excerpted from “International Cloud Atlas Vol.1 (WMO-No.407, 1975)”.

5.2.1 High level clouds (C_H)

(1) Cirrus (Ci)

- Cirrus is defined as detached clouds in the form of white, delicate filaments or white or mostly white patches or narrow bands. These clouds have a fibrous (hair-like) appearance, or a silky sheen, or both. Cirrus is composed almost exclusively of ice crystals. Cirrus tufts with rounded tops often form in clear air.

- At all times of day, cirrus not too close to the horizon is white, in fact whiter than any other cloud in the same part of the sky. When the sun sinks below the horizon, cirrus high in the sky is yellow, then pink, red and finally grey. The color sequence is reversed at dawn.

- Cirrus clouds often evolve from virga of cirrocumulus (Cc) or altocumulus (Ac), or from the upper part of a cumulonimbus (Cb).

- Cirrus clouds are distinguished from cirrostratus (Cs) by their discontinuous structure or, if they are in patches or bands, by their small horizontal extent or the narrowness of their continuous parts.

(2) Cirrocumulus (Cc)

- Cirrocumulus is defined as thin, white patch, sheet or layer of cloud without shading, composed of very small elements in the form of grains, ripples, etc., merged or separate, and more or less regularly arranged; most of the elements have an apparent width of less than one degree.

- Cirrocumulus is composed almost exclusively of ice crystals; strongly supercooled water droplets may occur but are usually rapidly replaced by ice crystals.

- Cirrocumulus often forms as a result of the transformation of cirrus (Ci) or cirrostratus (Cs). Cirrocumulus may also form as the result of a decrease in size of the elements of a patch,

sheet or layer of altocumulus (Ac).

- Cirrocumulus differs from cirrus (Ci) and cirrostratus (Cs) in that it is rippled or subdivided into very small cloudlets; it may include fibrous, silky or smooth portions which, however, do not collectively constitute its greater part.

- Cirrocumulus differs from altocumulus (Ac) in that most of its elements are very small (by definition, of an apparent width less than one degree when observed at an angle of more than 30 degrees above the horizon) and without shading.

(3) Cirrostratus (Cs)

- Cirrostratus is defined as transparent, whitish cloud veil of fibrous (hair-like) or smooth appearance, totally or partly covering the sky, and generally producing halo phenomena. Cirrostratus is composed mainly of ice crystals.

- Cirrostratus is never thick enough to prevent objects on the ground from casting shadows, at least when the sun is high above the horizon.

- Cirrostratus differs from altostratus (As) by its thinness and by the fact that it may show halo phenomena. Cirrostratus near the horizon may be mistaken for As. The slowness of the apparent movement and the slowness of the variations in optical thickness and in appearance, both characteristic of cirrostratus, give useful guidance in distinguishing this cloud from As and also from stratus (St).

- Cirrostratus differs from stratus (St) by being whitish throughout, and by the fact that it may have a fibrous appearance. Moreover cirrostratus often displays halo phenomena, whereas St does not, except occasionally at very low temperatures.

- Cirrostratus differs from a veil of haze by the fact that latter is opalescent or has a dirty yellowish to brownish color.

5.2.2 Middle level clouds (C_M)

(1) Altocumulus (Ac)

- Altocumulus is defined as white or grey, or both white and grey, patch, sheet or layer of cloud, generally with shading, composed of laminae, rounded masses, rolls, etc., which are sometimes partly fibrous or diffuse and which may or may not be merged; most of the regularly arranged small elements usually have an apparent width between one and five degrees.

- Altocumulus is, at least in the main, almost invariably composed of water droplets. A corona or irisation is often observed in thin parts of altocumulus.

- An altocumulus layer may sometimes be confused with altostratus (As); in case of doubt, clouds are called altocumulus if there is any evidence of the presence of laminae, rounded masses, rolls, etc.

- Altocumulus, with dark portions, may sometimes be confused with stratocumulus (Sc). If most of the regularly arranged elements have, when observed at an angle of more than 30 degrees above the horizon, an apparent width between one and five degrees, the cloud is altocumulus.

- Altocumulus in scattered tufts may be confused with small cumulus (Cu) clouds; the altocumulus tufts, however, often show fibrous trails (virga) and moreover are, in their majority, smaller than the Cu clouds.

(2) Altostratus (As)

- Altostratus is defined as greyish or bluish cloud sheet or layer of striated, fibrous or uniform appearance, totally or partly covering the sky, and having parts thin enough to reveal the sun at least vaguely, as through ground glass. Altostratus does not show halo phenomena.

- Altostratus is composed of water droplets and ice crystals. Raindrops or snowflakes are often present in altostratus and below its base.

- Pannus clouds may be present; they occur under the altostratus in the lower turbulent layers when these are moistened by evaporation from precipitation.

- Altostratus may evolve from a thickening veil of cirrostratus (Cs); it is sometimes formed by the thinning of a layer of nimbostratus (Ns). Altostratus may also develop from an altocumulus (Ac) layer; this happens when widespread ice crystal trails (virga) fall from the latter. Sometimes, particularly in the tropics, altostratus is produced by the spreading out of the middle or upper part of cumulonimbus (Cb).

- A low, thick layer of altostratus may be distinguished from a similar layer of nimbostratus (Ns) by the presence in altostratus of thinner parts through which the sun is, or could be, vaguely revealed. Altostratus is also of a lighter grey and its under surface is usually less uniform than that of Ns. When, on moonless nights, doubt exists regarding the choice of the designation altostratus or Ns, the layer is by convention called altostratus, if no rain or snow is falling.

- Altostratus is distinguishable from stratus (St), with which it may be confused, by its ground glass effect. Furthermore, altostratus is never white, as thin St may be when observed more or less towards the sun.

(3) Nimbostratus (Ns)

- Nimbostratus is defined as grey cloud layer, often dark, the appearance of which is rendered diffuse by more or less continuously falling rain or snow, which in most cases reaches the ground. It is thick enough throughout to blot out the sun. Low, ragged clouds frequently occur below the layer, with which they may or may not merge.

- Nimbostratus is composed of water droplets (sometimes supercooled) and raindrops, of snow crystals and snowflakes, or of a mixture of these liquid and solid particles.

- The under surface of nimbostratus is often partially or totally hidden by pannus clouds resulting from turbulence in the layers under its base, which are moistened by partial evaporation of precipitation.

- In the tropics, particularly during short lulls in the rainfall, nimbostratus can be seen breaking up into several different cloud layers, which rapidly merge again.

- Nimbostratus usually develops from thickening altostratus (As). It also sometimes forms by the spreading out of cumulonimbus (Cb).

- Nimbostratus is distinguished from thick stratus (St) by the fact that it is a dense cloud

producing rain, snow or ice pellets; the precipitation which may fall from St is in the form of drizzle, ice prisms or snow grains.

- When the observer is beneath a cloud having the appearance of a nimbostratus, but accompanied by lightning, thunder or hail, the cloud should by convention be called cumulonimbus (Cb).

5.2.3 Low level clouds (C_l)

(1) Stratocumulus (Sc)

- Stratocumulus is defined as grey or whitish, or both grey and whitish, patch, sheet or layer of cloud which almost always has dark parts, composed of tessellations, rounded masses, rolls, etc., which are non-fibrous (except for virga) and which may or may not be merged; most of the regularly arranged small elements have an apparent width of more than five degrees.

- Stratocumulus is composed of water droplets. During extremely cold weather stratocumulus may produce abundant ice crystal virga which may be accompanied by a halo. When stratocumulus is not very thick, a corona or irisation is sometimes observed.

- Stratocumulus differs from cumulus (Cu) in that its elements usually occur in groups or patches and generally have flat tops; if however, stratocumulus tops are in the form of domes, they rise, unlike those of Cu, from merged bases.

- Stratocumulus is often formed by the spreading out of cumulus (Cu) or cumulonimbus (Cb).

(2) Stratus (St)

- Stratus is defined as generally grey cloud layer with a fairly uniform base, which may give drizzle, snow or snow grains. When the sun is visible through the cloud, its outline is clearly discernible. Sometimes stratus appears in the form of ragged patches.

- Stratus is usually composed of small water droplets; this cloud may, when very thin, produce a corona round the sun or moon. At low temperatures, stratus may consist of small ice particles. The ice cloud is usually thin and may, on rare occasions, produce halo phenomena.

- A common mode of stratus formation is the slow lifting of a fog layer, due to warming of the earth's surface or an increase in wind speed.

- Stratus fractus clouds may also form as accessory clouds (pannus) under altostratus (As), nimbostratus (Ns), cumulonimbus (Cb) and precipitating cumulus (Cu); they develop as a result of turbulence in the moistened layers under these clouds.

- Stratus fractus is distinguished from cumulus (Cu) fractus in that it is less white and less dense. Furthermore, it shows a smaller vertical development, since it owes its formation mainly to turbulence without thermal convection.

(3) Cumulus (Cu)

- Cumulus is defined as detached clouds, generally dense and with sharp outlines, developing vertically in the form of rising mounds, domes or towers, of which the bulging upper part often resembles a cauliflower. The sunlit parts of these clouds are mostly brilliant

white; their base is relatively dark and nearly horizontal. Sometimes cumulus is ragged.

- Cumulus is composed mainly of water droplets. Ice crystals may form in those parts of a cumulus in which the temperature is well below 0°C; they grow at the expense of evaporating supercooled water droplets, thereby transforming the cloud into cumulonimbus (Cb).

- Cumulus develops in convection currents which occur when the lapse rate in the lower layers is sufficiently steep. Such steep lapse rates result from heating of the air near the earth's surface.

- Since cumulonimbus (Cb) generally results from the development and transformation of cumulus, it is sometimes difficult to distinguish cumulus with a great vertical extent from Cb. The cloud should be named cumulus as long as the sprouting upper parts are everywhere sharply defined and no fibrous or striated texture is apparent. If it is not possible to decide on the basis of other criteria whether a cloud is to be named cumulus or Cb, it should by convention be called cumulus if it is not accompanied by lightning, thunder or hail.

(4) Cumulonimbus (Cb)

- Cumulonimbus is defined as heavy and dense cloud, with a considerable vertical extent, in the form of a mountain or huge towers. At least part of its upper portion is usually smooth, or fibrous or striated, and nearly always flattened; this part often spreads out in the shape of an anvil or vast plume.

- Under the base of this cloud which is often very dark, there are frequently low ragged clouds either merged with it or not, and precipitation sometimes in the form of virga.

- Cumulonimbus is composed of water droplets and, especially in its upper portion, of ice crystals. It also contains large raindrops and, often, snowflakes, snow pellets, ice pellets or hailstones. The water droplets and raindrops may be substantially supercooled.

- Cumulonimbus clouds may appear either isolated clouds or in the form of a continuous line of clouds resembling a very extensive wall. In certain cases, the upper portion of cumulonimbus clouds may be merged with altostratus (As) or nimbostratus (Ns). Cumulonimbus may also develop within the general mass of As or Ns.

- Cumulonimbus most commonly evolves from cumulus (Cu) which was formed in the normal manner. Cumulonimbus sometimes develops from altocumulus (Ac) or stratocumulus (Sc).

5.3 Observation of cloud states and their coding

For forecasters who eventually receive and use observers' reports, reports on what clouds are present in the sky are not so important but reports on distributions or arrangements of clouds, namely the states of clouds are much more valuable.

The state of clouds is coded not only based on 10 cloud types but by the characteristics C_L (low level cloud), C_M (middle level cloud) and C_H (high level cloud), amount, thickness, variation and combination of clouds. Procedures to define the code are shown in Figs. 5.1-5.3.

Typical photos for each code are shown in succeeding pages with explanations taken from "International Cloud Atlas Vol.1 (WMO-No.407, 1975)"

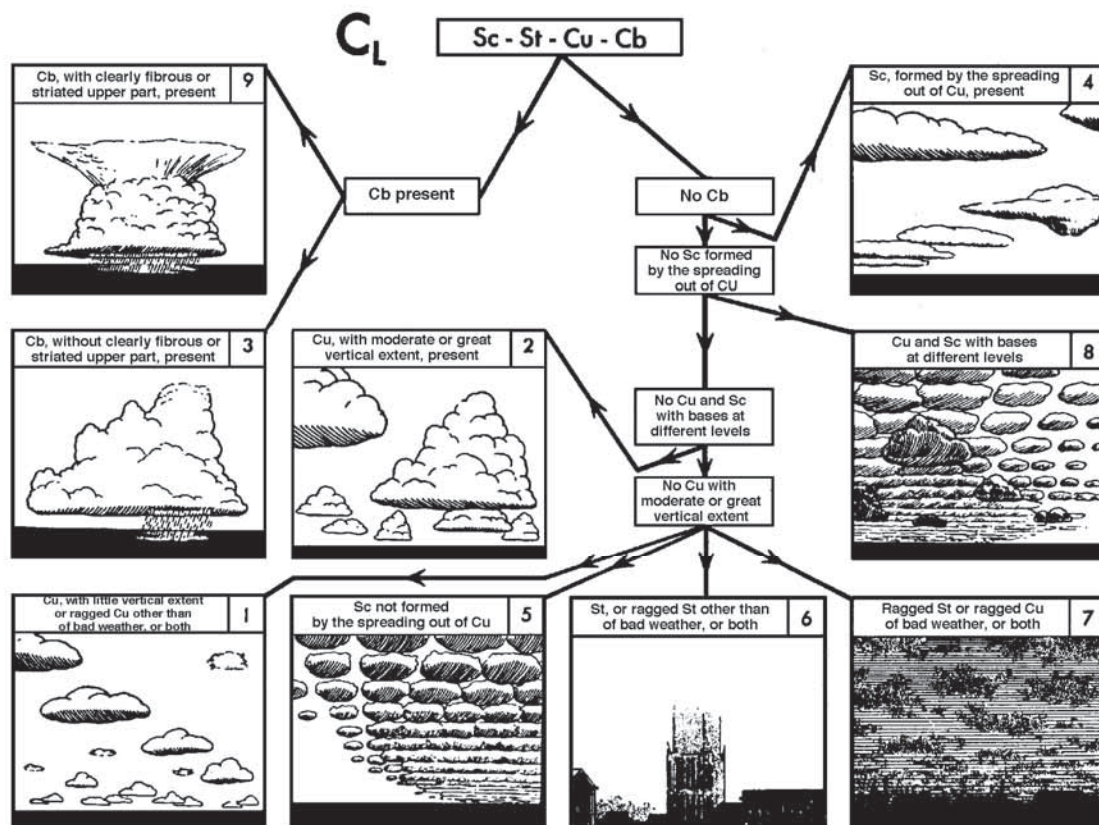


Fig. 5.1 Selection chart to define the code for C_L

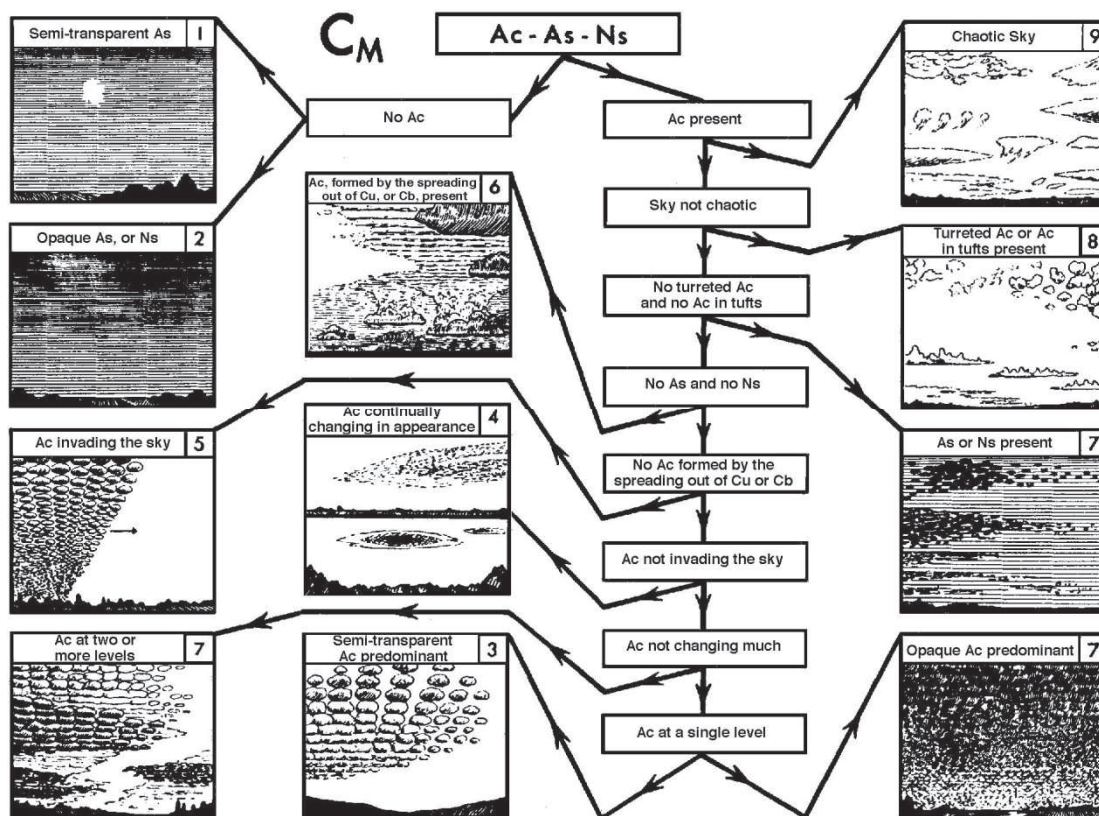


Fig. 5.2 Selection chart to define the code for C_M

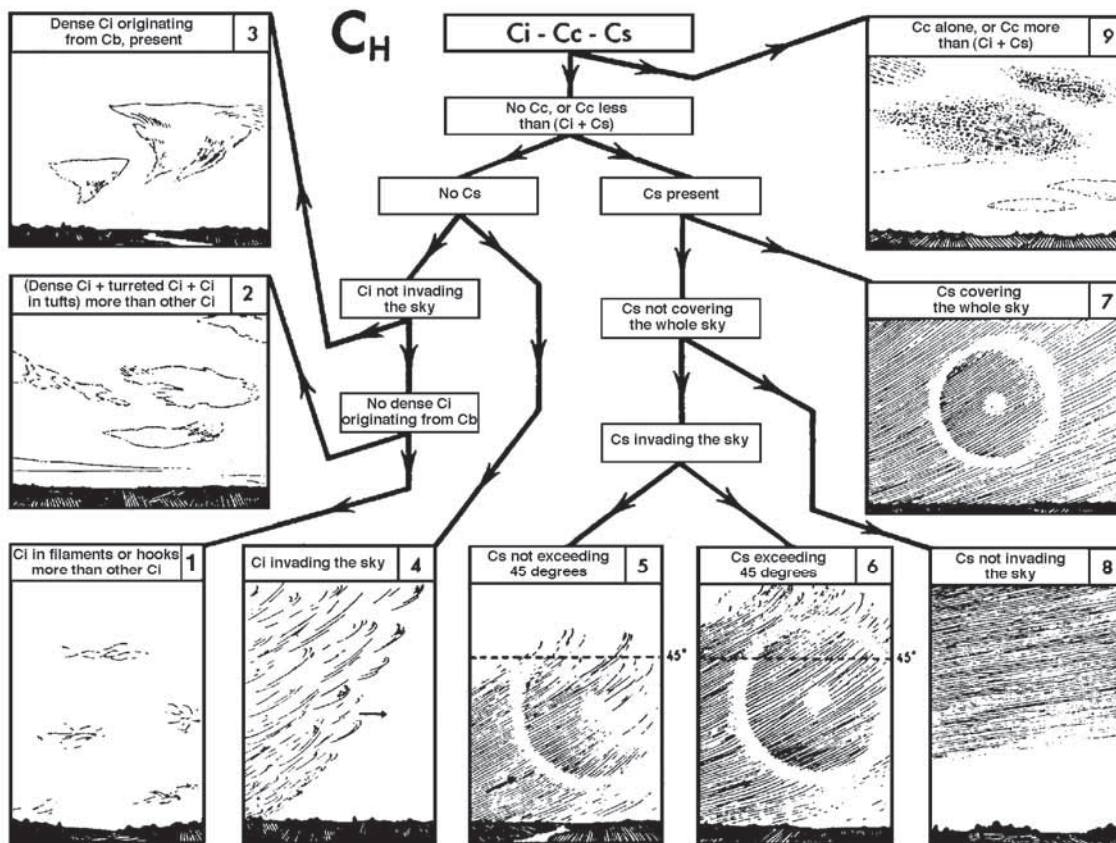


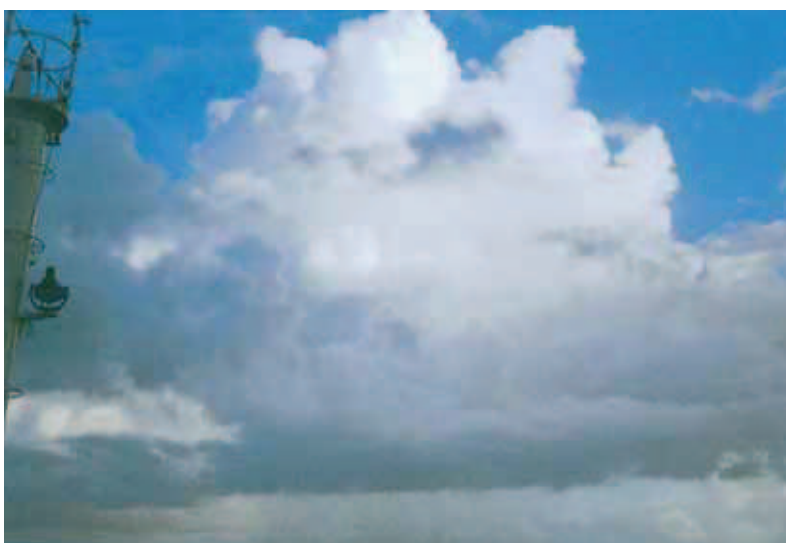
Fig. 5.3 Selection chart to define the code for C_H

**CL:1**

Cu with little vertical extent and seemingly flattened, or ragged Cu other than of bad weather, or both.

**CL:2**

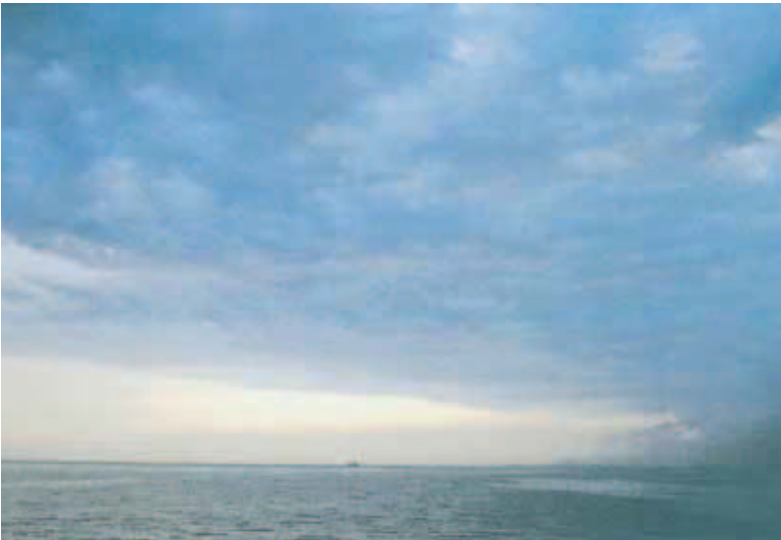
Cu of moderate or strong vertical extent, generally with protuberances in the form of domes or towers, either accompanied or not by other Cu or by Sc, all having their bases at the same level.

**CL:3**

Cb the summits of which, at least partially, lack sharp outlines, but is neither clearly fibrous (cirriform) nor in the form of an anvil; Cu, Sc or St may also be present.

**CL : 4**

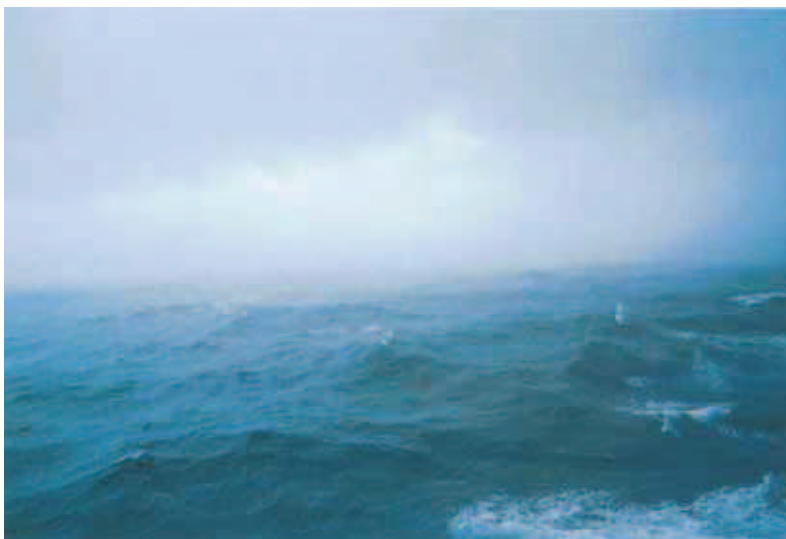
Sc formed by the spreading out of Cu; Cu may also be present.

**CL : 5**

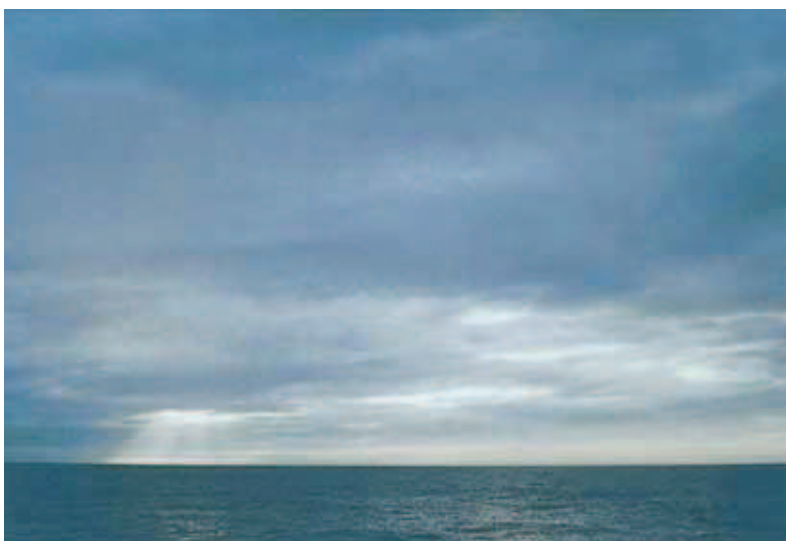
Sc not resulting from the spreading out of Cu.

**CL : 6**

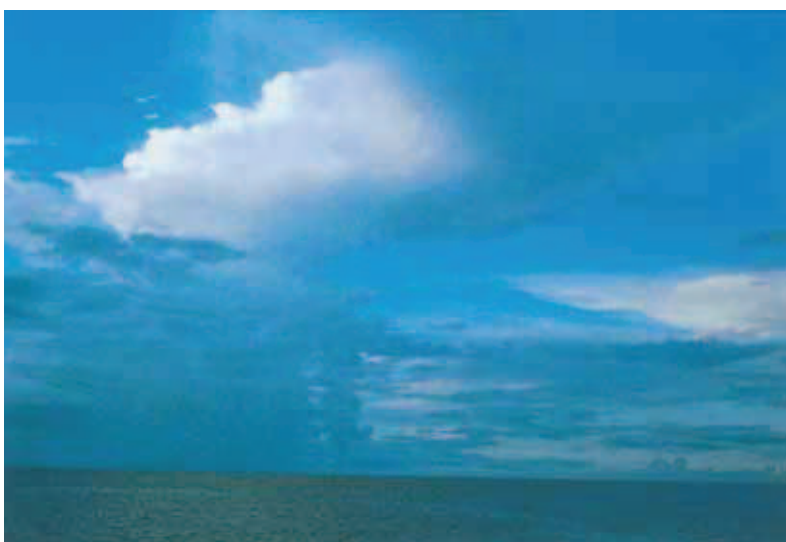
St in a more or less continuous sheet or layer, or in ragged shreds, or both, but no St fractus of bad weather.

**C_L:7**

St fractus of bad weather or Cu fractus of bad weather, or both (pannus), usually below As or Ns.

**C_L:8**

Cu and Sc other than that formed from the spreading out of Cu; the base of the Cu is at a different level from that of the Sc.

**C_L:9**

Cb, the upper part of which is clearly fibrous (cirriform), often in the form of an anvil; either accompanied or not by Cb without anvil or fibrous upper part, by Cu, Sc, St or pannus.

**C_M : 1**

As, the greater part of which is semi-transparent; through this part the sun or moon may be weakly visible, as through ground glass.

**C_M : 2**

As, the greater part of which is sufficiently dense to hide the sun or moon, or Ns.

**C_M : 3**

Ac, the greater part of which is semi-transparent; the various elements of the cloud change only slowly and are all at a single level.

**C_M : 4**

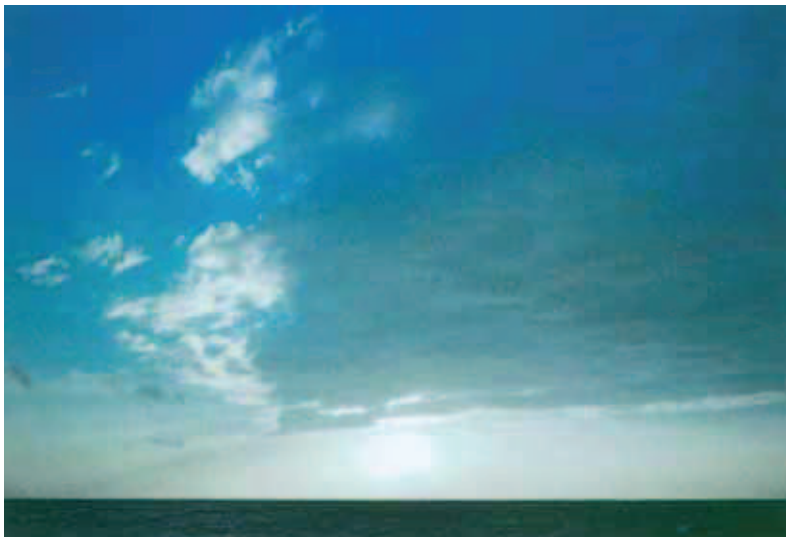
Patches (often in the form of almonds or fishes) of Ac, the greater part of which is semi-transparent; the clouds occur at one or more levels and the elements are continually changing in appearance.

**C_M : 5**

Semi-transparent Ac in bands, or Ac in one or more fairly continuous layers (semi-transparent or opaque), progressively invading the sky; these Ac clouds generally thicken as a whole.

**C_M : 6**

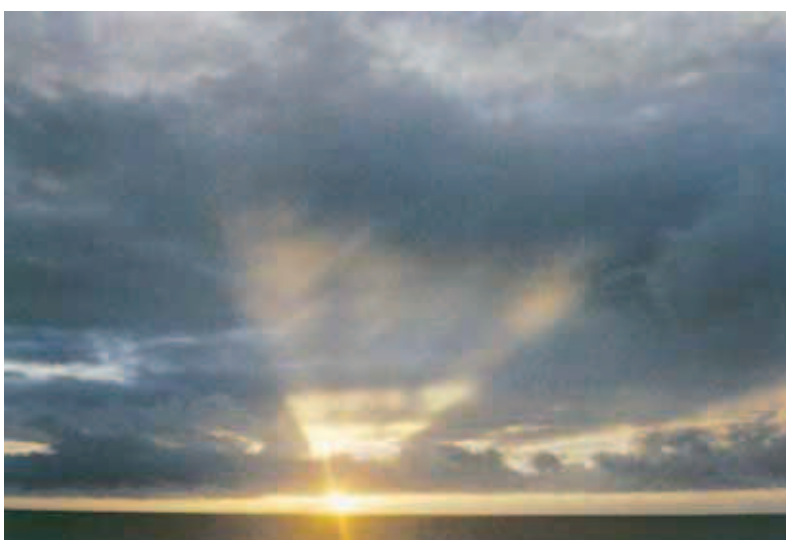
Ac resulting from the spreading out of Cu (or Cb).

**C_M : 7**

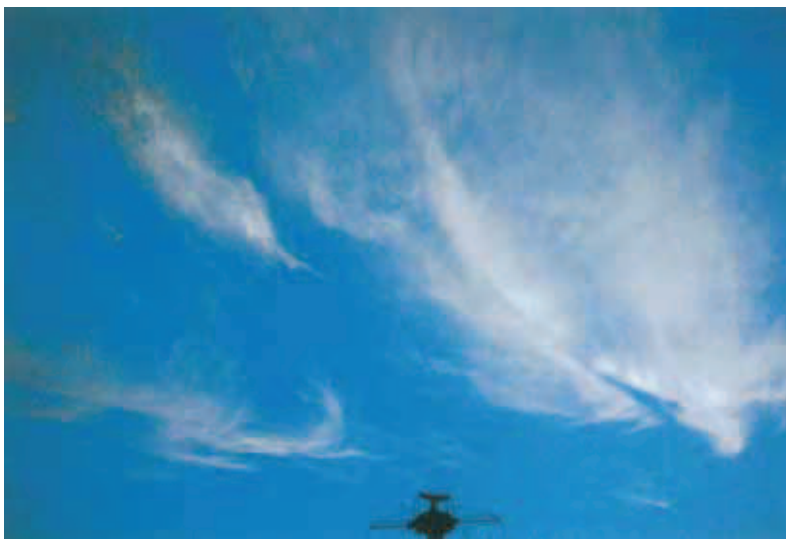
Ac in two or more layers, usually opaque in places, and not progressively invading the sky; or opaque layer of Ac, not progressively invading the sky; or Ac together with As or Ns.

**C_M : 8**

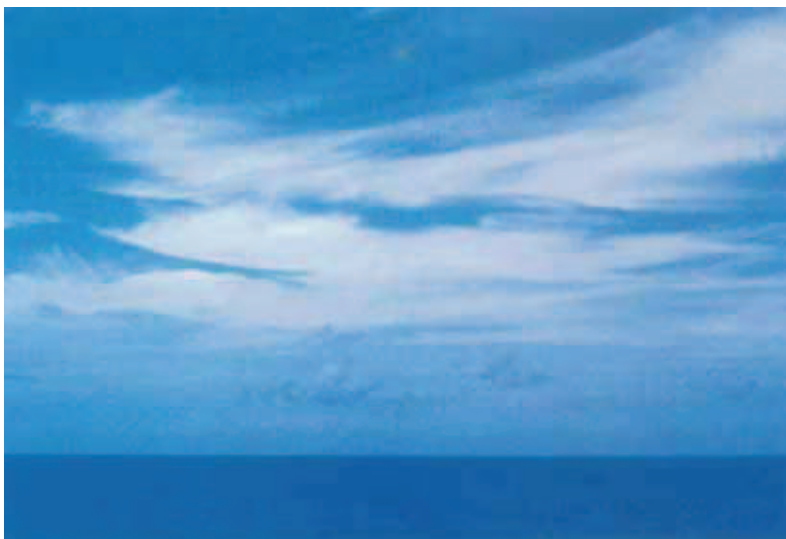
Ac with sprouting in the form of small towers or battlements, or Ac having the appearance of cumuliform tufts.

**C_M : 9**

Ac of a chaotic sky, generally at several levels.

**C_H : 1**

Ci in the form of filaments, strands or hooks, not progressively invading the sky.

**C_H : 2**

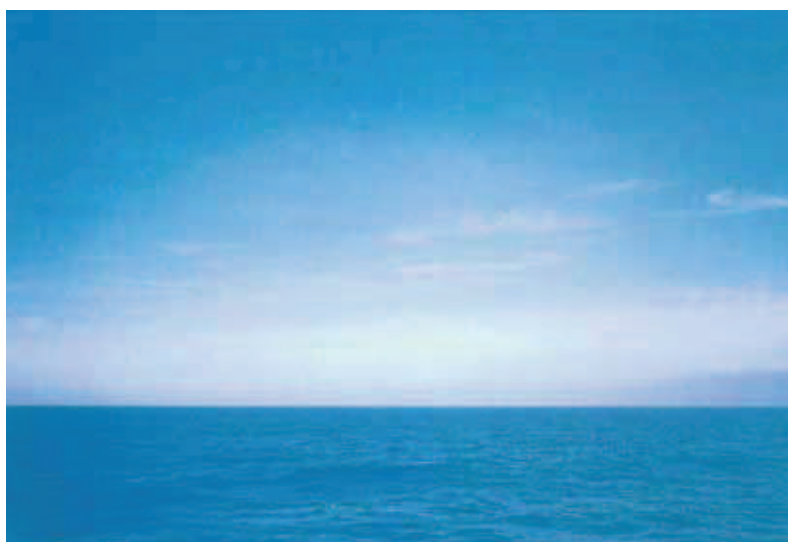
Dense Ci, in patches or entangled sheaves, which usually do not increase and sometimes seem to be the remains of the upper part of a Cb; or Ci with sprouting in the form of small turrets or battlements, or Ci having the appearance of cumuliform tufts.

**C_H : 3**

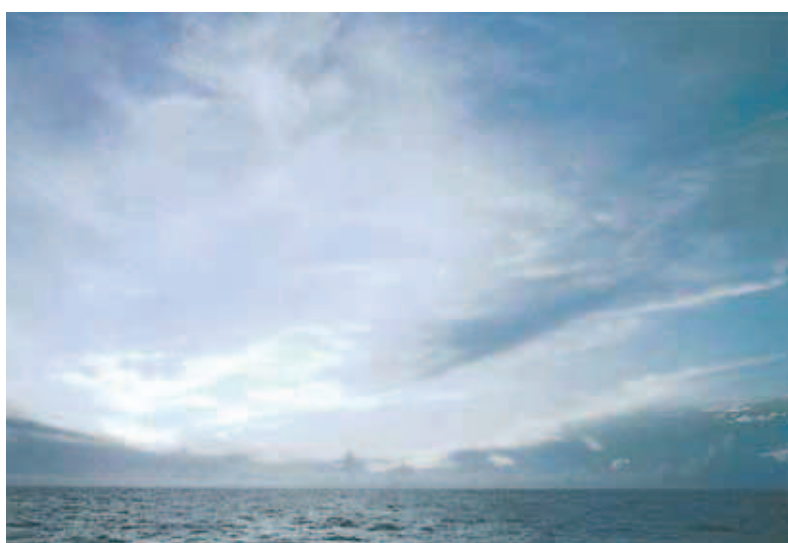
Dense Ci, often in the form of an anvil, being the remains of the upper parts of Cb.

**C_H : 4**

Ci in the form of hooks or of filaments, or both, progressively invading the sky; they generally become denser as a whole.

**C_H : 5**

Ci (often in bands converging towards one point or two opposite points of the horizon) and Cs, or Cs alone; in either case, they are progressively invading the sky, and generally growing denser as a whole, but the continuous veil does not reach 45 degrees above the horizon.

**C_H : 6**

Ci (often in bands converging towards one point or two opposite points of the horizon) and Cs, or Cs alone; in either case, they are progressively invading the sky, and generally growing denser as a whole; the continuous veil extends more than 45 degrees above the horizon, without the sky being totally covered.



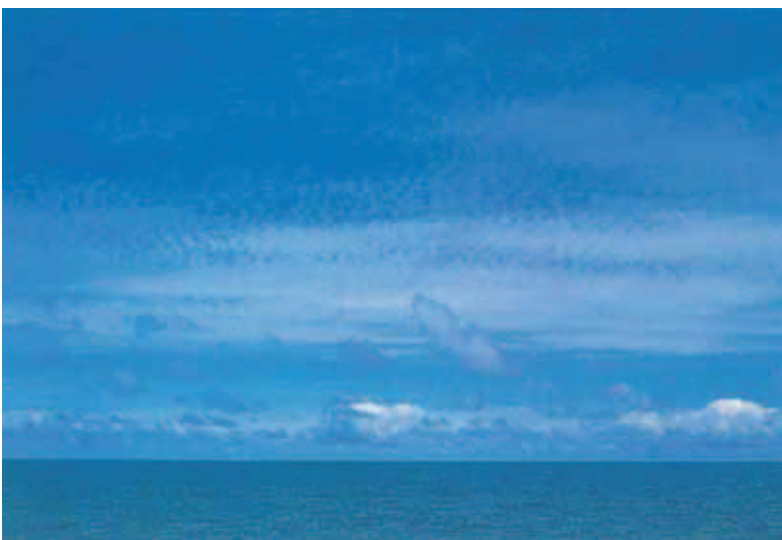
C_H : 7

Veil of Cs covering the celestial dome.



C_H : 8

Cs not progressively invading the sky and not completely covering the celestial dome.



C_H : 9

Cc alone, or Cc accompanied by Ci or Cs, or both, but Cc is predominant.

CHAPTER 6 Observation of Visibility

Visibility is not only to what extent an object can be seen by the observer but a simple indicator of atmospheric stability. Visibility is decreased by material in the atmosphere including water droplets in the form of fog, rain or snow and solid particles in the form of sand dust, smoke or crystallized salt from sea water spray. Visibility is affected by refraction and diffusion of light due to differences in air density. Visibility observations are utilized not only for meteorological analysis but marine traffic and management of atmospheric pollution.

6.1 Definition of visibility

Visibility (horizontal visibility) is determined as the greatest distance at which a black object of suitable dimensions can be seen and identified against the sky at the horizon during daylight or at night if as bright as daytime, meaning visibility is constant regardless of observation time if the atmospheric condition is unchanged.

If visibility differs by direction, adopt the shortest distance. Visibility should be observed with the naked eye or with best corrected vision, not with a telescope, binoculars or a sextant.

See "Guide to Ships' Weather Reports" to code observations.

6.2 Daytime observation

If a ship, island or buoy can be seen at the limit of visibility, the bestmost precise way is to use radar to measure visibility. However, this seldom occurs so training and experience is required for visibility observation. One simple method is to use the relationship between height (h) of observation above the sea surface in meters and distance (L) to the horizon in kilometers.

$$L = 3.6\sqrt{h}$$

as shown in Table 6.1.

Table 6.1 Height of observation above sea surface and distance to the horizon

Height of observer eyes above sea level (m)	2	4	6	8	10	15	20	25	30	40
Distance of object on the horizon at sea (km)	5	7	9	10	11	14	16	18	20	23

For example, if the horizon cannot be seen clearly from a bridge 15 m above the sea surface but can from the deck 8 m above the sea surface, visibility is about 12 km (between 14 km and 10 km in the Table).

6.3 Night-time observation

Estimation of visibility at night is not easy and requires time (from 5 to 15 minutes) to adapt the eyes to the dark. Lights of other vessels, buildings on land and stars around the horizon may be used to estimate visibility.

CHAPTER 7 Observation of Atmospheric Phenomena and Weather

Weather is a manifestation of the atmosphere at a particular time described by atmospheric phenomena. Atmospheric phenomena are generally classified into hydrometeors, lithometeors, electrometeors, and photometeors. This chapter describes these atmospheric phenomena except for photometeors, which are luminous phenomena in the atmosphere including halos, rainbows, mirages, which are unrelated to weather reports.

7.1 Atmospheric phenomena to be reported

7.1.1 Hydrometeor

Hydrometeor is a meteor comprising liquid and/or solid water particles falling through or suspended in the atmosphere.

In the case of precipitation, report whether it is uniform (intermittent or continuous) or shower type and whether it is rain, drizzle, snow, or hail. Shower is characterized by its sudden beginning and ending, and generally by large and rapid changes of intensity. It is often short-lived and heavy, falling from convective clouds such as cumulus (Cu) and cumulonimbus (Cb). Uniform precipitation falls from stratiform clouds including altostratus (As) and nimbostratus (Ns).

Various hydrometeors and their definitions are as follows:

Rain ●, Rain Shower ⚡: Precipitation of liquid water particles, either in the form of drops of more than 0.5 mm in diameter, or of smaller widely scattered drops.

Freezing Rain ❄️: Rain drops freezing on impact with the ground or ship.

Drizzle 🌧️: Fairly uniform precipitation in very fine drops of water (diameter less than 0.5 mm) very close to one another, falling from stratiform clouds.

Freezing Drizzle ❄️: Drizzle drops freezing on impact with the ground or ship.

Snow ❄️, Snow Shower ⚡: Precipitation of ice crystals, isolated or clustered, falling from clouds.

Snow Pellets ❄️: Precipitation of white and opaque ice particles, which fall from Cu and Cb clouds and are generally conical or spherical, with diameters attaining as much as 5 mm.

Snow Grains ❄️: Precipitation of very small opaque white particles of ice and which are fairly flat or elongated with diameters generally less than 1 mm. They usually fall in small quantities, mostly from stratus (St) or from fog and never in the form of a shower.

Ice Pellets ❄️: Precipitation of transparent particles of ice which are spherical or irregular, rarely conical, and which have a diameter of 5 mm or less.

Small Hail ⚡: Precipitation of translucent ice particles, which falls from Cu and Cb clouds. These particles are almost always spherical and sometimes have conical tips. Their diameter may attain or even exceed 5 mm

Hail ⚡: Precipitation of either transparent, or partially or completely opaque particles of ice (hailstones), usually spheroidal, conical or irregular in form and of diameter generally between 5 and 50 mm, which fall from Cu and Cb clouds either separately or frozen together into irregular lumps and generally accompanied by strong thunder.

Diamond Dust ⚡: Precipitation which falls from a clear sky in very small ice crystals, often so tiny that they appear to be suspended in the air.

Fog ☁: Suspension of very small, usually microscopic water droplets in the air, generally reducing horizontal visibility to less than 1 km.

Ice Fog ❄️: Suspension of numerous minute ice particles in the air, reducing visibility. It appears under air temperatures below -30°C and calm wind conditions.

Mist 🌫️: Suspension in the air of microscopic water droplets or wet hygroscopic particles with visibility of more than 1 km.

Spout 🌪️: A phenomenon consisting of an often violent whirlwind, revealed by the presence of a cloud column or inverted cloud cone (funnel cloud), protruding from the base of a Cb, and of a "bush" composed of water droplets raised from the surface of the sea or of dust, sand or litter, raised from the ground.

Ice Accretion: Process by which a layer of ice builds up on a solid surface which is exposed to freezing precipitation or supercooled droplets.

Spray 🌊: Ensemble of water droplets torn by the wind from the surface of an extensive body of water, generally from the crests of waves, and carried up a short distance into the air.

7.1.2 Lithometeor

Lithometeor is meteor consisting of particles most of which are solid and dry; they are more or less suspended in the air, or lifted by the wind from the ground.

Typical lithometeors and their definitions are as follows:

Haze 🌫️: A suspension in the air of extremely small, dry particles which are invisible to the naked eye but numerous enough to give the sky an opalescent appearance.

Smoke 🌫️: A suspension in the air of small particles produced by combustion.

Dust Storm (Sand Storm) 🌪️: An ensemble of particles of dust or sand energetically lifted to great heights by a strong and turbulent wind.

Dust Haze (Sand Haze) 🌫️: A suspension in the air of small sand or dust particles, raised from the ground prior to the time of observation by a dust storm or sand storm.

7.1.3 Electrometeor

Electrometeor is a visible or audible manifestation of atmospheric electricity.

Main electrometeors and their definitions are as follows:

Thunderstorm ⚡: Sudden electrical discharges manifested by a flash of light (lightning) and a sharp or rumbling sound (thunder). Thunderstorms are associated with convective clouds (Cumulonimbus) and are, most often, accompanied by precipitation in the form of rainshowers or hail, or occasionally snow shower, snow pellets, or small hail.

Lightning ⚡: A luminous manifestation accompanying a sudden electrical discharge which takes place from or inside a cloud or, less often, from high structures on the ground or from mountains.

Thunder T: A sharp or rumbling sound which accompanies lightning. It is emitted by rapidly expanding gases along the channel of a lightning discharge.

7.2 Observation and recording of atmospheric phenomena

For observations of atmospheric phenomenon, record the following:

- 1) Time of appearance
- 2) Name of the phenomenon
- 3) State of the phenomenon
- 4) Time of ending

For state of the phenomenon, record whether the precipitation is shower or not, the level of visibility and intensity of the phenomenon, etc. Intensity is classified into three ranks for each atmospheric phenomenon as described below:

(1) Intensity of rain

Light: Scattered drops that do not completely wet an exposed surface, regardless of duration, to a condition where individual drops are easily seen; slight spray is observed over the decks; puddles form slowly; sound on roofs ranges from slow pattering to gentle swishing; steady small streams may flow in scuppers and deck drains.

Moderate: Individual drops are not clearly identifiable; spray is observable just above deck and other hard surfaces; puddles form rapidly; sound on roofs ranges from swishing to gentle roar.

Heavy: Rain seemingly falls in sheets; individual drops are not identifiable; heavy spray to height of several inches is observed over hard surfaces; visibility is greatly reduced; sound on roofs resembles the roll of drums or distant roar.

(2) Intensity of drizzle

Light: Visibility 1 km or more.

Moderate: Visibility more than 0.5 km but less than 1 km.

Heavy: Visibility less than 0.5 km.

(3) Intensity of snow

Light: Visibility 1 km or more.

Moderate: Visibility more than 0.2 km but less than 1 km.

Heavy: Visibility less than 0.2 km.

(4) Intensity of hail and ice pellets

Light: Few stones or pellets falling with little, if any, accumulation.

Moderate: Slow accumulation.

Heavy: Rapid accumulation.

(5) Intensity of thunder, thunderstorm and lightning

Light thunder: Slightly perceived as distant thunder.

Moderate thunder: Thunder with considerably large sound so as to vibrate a window pane.

Heavy thunder: Thunder with deafening and astonishing sound with the effect of rattling windows.

Light thunderstorm: Light thunder with a flash of light.

Moderate thunderstorm: Moderate thunder with a flash of light.

Heavy thunderstorm: Heavy thunder with a flash of light.

Light lightning: Slightly perceived in the daytime and clearly visible at night.

Moderate lightning: Perceived without confrontation in the daytime and perceived from inside a lighted room.

Heavy lightning: A flash of light brightens the surrounding area in the daytime and at night everything is dazzled by the heavy flash of light.

7.3 Present weather and past weather

Weather should be reported by codes under present weather and past weather as described in "Ships' Weather Code Card" and "Guide to Ship's Weather Reports".

Present weather is defined as the state of the atmosphere at the time of observation or within the hour (60 minutes) preceding it in some cases. Table 7.1 shows the relationship between weather phenomenon and codes of present weather, total cloud amount, and visibility.

Past weather refers to the type(s) of weather which occurred for a certain period of time prior to the observation. Table 7.2 shows the period to be covered by the past weather at each observation time. And Table 7.3 shows the past weather codes.

Table 7.1 Relationship between weather phenomenon and weather report codes

Weather phenomenon		Weather report codes			
		Present weather (ww)	Total cloud amount (N: octas)	Visibility (VV)	Remarks
Clear sky	○	00~16 18~32 36~38 40・41, 76	0, 1	≥94 (≥1 km) (except the cases of ww = 40, 41)	
Fine	⊙		2~6		
Overcast (covered with mostly upper level cloud)	⊕		7, 8		
Overcast (covered with mostly lower or middle level cloud)	⊗				
Haze	∞	04~06	9 (unknown; obscured sky)	< 94 (< 1 km)	The criteria of either N or VV must be met.
Dust/Sand storm	☼	30~35			The criteria VV must be met.
Blowing snow	✎	38・39			
Fog	≡	42~49			
Drizzle	☂	50~57			
Rain	●	58~67, 80~82, 91, 92			ww 93 or 94 is interpreted as hail under warm season and snow under cold season if other information is not available.
Rain and snow mixed	✎	68・69, 83・84, 93・94			
Snow	✎	70~75, 77・78, 85・86 93・94			
Small hail	△	79, 87・88, 93・94			
Hail	▲	89・90, 93・94			
Thunderstorm	⚡	17, 95~99			

Table 7.2 Period to be covered by past weather

Observation time	Period
00,06,12,18 UTC	Preceding 6 hours
03,09,15,21 UTC	Preceding 3 hours
Other	Preceding 1 hour

Table 7.3 Past weather codes

Code (W ₁ W ₂)	Symbols	Description of past weather
0	○ ①	Cloud covering 1/2 or less of the sky throughout the appropriate period
1	○ ① ② ③	Cloud covering more than 1/2 of the sky during part of the appropriate period and covering 1/2 or less during part of the period
2	① ② ③	Cloud covering more than 1/2 of the sky throughout the appropriate period
3	☼	Sand storm, dust storm or blowing snow, visibility less than 1 km
4	≡ ≡ ∞	Fog or ice fog, visibility less than 1 km; or thick haze, visibility less than 2 km
5	●	Drizzle
6	●	Rain
7	× ❄	Snow, or rain and snow mixed
8	⬇ ⬇ ⬇ ▲	Shower(s)
9	⚡	Thunderstorm(s)

CHAPTER 8 Observation of Sea Surface Temperature

Sea surface temperature plays an important role in the interaction between the atmosphere and the ocean. The difference between the air temperature and the sea surface temperature gives a basic measure of the vertical stability of the atmosphere and the heat exchange between the atmosphere and the ocean.

The temperature of well mixed sea water at the depth of 1 to 2 m should be measured and recorded to the nearest 0.1°C.

Sea surface temperature is normally observed by either

- 1) Measuring the temperature of the condenser intake water
- 2) Exposing an electrical thermometer to the sea-water either directly or through the hull
- 3) Measuring the temperature of the sea-water sampled with a sea-bucket

Methods 3) and 1) have been used for many years. Recently, as the speed and dimension of ships have increased, method 2) has been more widely used.

8.1 Intake method

The intake sea-water temperature is measured by a thermometer installed in the intake pipe. If this requires reading in cramped conditions, the observer should guard against parallax error (Fig. 3.7). The observer should be aware that when the ship has a deep draught, or there is a marked temperature gradient in the surface layer, intake temperature may differ from that nearer the sea surface. When the ship is stationary, sea-bucket temperature should be measured for comparison because the cooling water may not be circulating. Also, as temperature of the intake pipe may be influenced by heat of the engine. This method is not the best to observe sea-surface temperature. However, it is frequently used in consideration of safety and convenience.

8.2 Hull-attached thermometer method

The sensor in this method is mounted either externally in direct contact with the sea using a “through-the-hull” connection, or internally (the “limpet” type) attached to the inside of the hull. Such hull-attached thermometers provide a convenient and accurate means of measuring sea-surface temperature. Its readout device is installed in a cabin for observation.

8.3 Sea-bucket method

In this method, the sea-bucket is lowered over the side of the ship to collect sea-water which is hauled on board and measured by thermometer. The bucket should be filled and emptied several times beforehand to control for the bucket temperature. The sample should be taken near the bow, from the leeward side of the ship during navigation, from the windward side while at anchor, and well forward of all outlets. The thermometer should be read as soon as possible after it has attained the temperature of the water sample. The bucket should be stored out of direct sunlight.

CHAPTER 9 Observation of Ocean Waves

Navigation of ships is profoundly affected by winds and waves. Consequently, accurate information on ocean waves is essential for disaster prevention and economical navigation. Recent developments in satellite technology do not diminish the importance of observations of ocean waves by ships. The data of ocean waves reported by ships contribute to the analysis and forecasting of ocean waves and statistical studies of the climatology of ocean waves.

9.1 Classification of ocean waves

There are thousands of waves with different wave heights and periods on the ocean. The sea surface is incessantly moving up and down. Among such waves, those caused by wind over the sea surface are called ocean waves and have periods from about 1 to 30 seconds.

Ocean waves are classified into wind waves (or sea) and swell. Wind waves and/or swell change into surfs in approaching a coast, or tidal races in colliding with tidal or ocean currents.

(1) Wind waves (or Sea)

Waves raised by local wind blowing at the time of observation are usually referred to as “wind waves” or “sea”.

Development of wind waves depends on three characteristics of wind: wind speed, fetch (the distance along which a wind is blowing straight) and duration (the time during which a wind with an almost fixed wind direction and speed is blowing along a fetch).

(2) Swell

Waves not raised by the local wind blowing at the time of observation, but due either to winds blowing a distance away or winds that have ceased to blow, are referred to as “swell”.

Figure 9.1 shows a schematic of wind waves (sea) with sharp crests and swell with gentle ones.

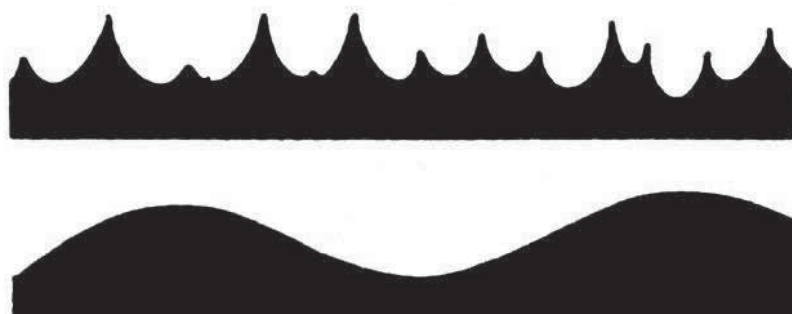


Fig. 9.1 Schematic view of wind wave (upper) and swell (lower)

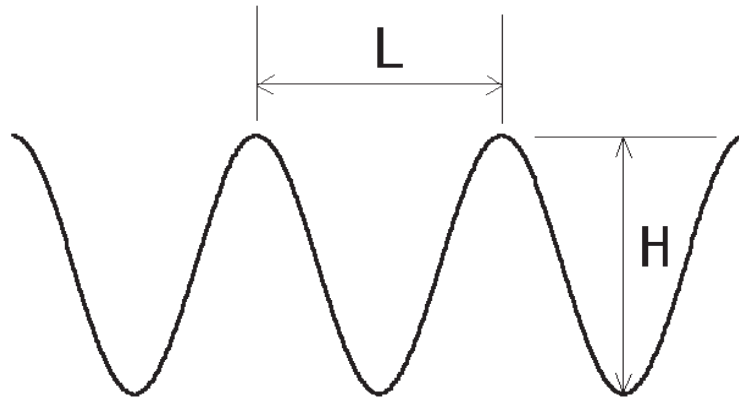


Fig. 9.2 Wave height (H) and wave length (L)

9.2 Characteristics of ocean waves

Major characteristics of ocean wave include,

- 1) Wave direction: the direction from which they come.
- 2) Wave period: the time between the passage of two successive wave crests past a fixed point, which is equal to wave length divided by wave speed.
- 3) Wave height: the vertical distance between trough and crest (see Fig. 9.2).
- 4) Wave length: the horizontal distance between successive crests or troughs, which is equal to wave period multiplied by wave speed (see Fig. 9.2).
- 5) Wave speed: the distance traveled by a wave in a unit of time, which is equal to wave length divided by wave period.

Speed (C; unit: m/s), length (L; unit: m) and period (T; unit: second) of a wave whose height is small compared to the ocean depth are related in theory by the following formulas:

$$C = 1.56T \quad (1)$$

$$L = 0.64C^2 = 1.56T^2 \quad (2)$$

$$T = 0.80L^{1/2} = 0.64C \quad (3)$$

Although the above formulae are not necessarily applicable to all types of waves, they are useful to roughly estimate the value of each element.

9.3 Non-instrument observation

Measures to be observed are wave direction, period and height with respect to each distinguishable wave among wind waves and swells traveling from various directions. Bearing in mind the distinction between wind waves (sea) and swell, observers should differentiate between recognizable waves, on the basis of the direction, appearance and period of the waves. If it is difficult to observe a measure precisely due to, for example, poor light conditions, record that measure as unknown.

(1) Direction

The direction (one of 36) from which waves are coming, is measured from the direction of wave trains traveling a little far from your ship with a gyrocompass. The direction of a wind wave generally coincides with that of the local wind, but keep in mind that swells traveling from different directions are often combined.

(2) Period

Measurement of wave period is made in the unit of second by a stopwatch. The observer notes an object floating on the water at some distance from the ship: if nothing better is available, a distinctive patch of foam can usually be found which remains identifiable for the time required for an observation.

He starts his watch when the object appears at the crest of a wave. As the crest passes on, the object disappears into the trough to reappear on the next crest. The time at which the object appears at the top of each crest is noted. The observations are continued for as long as possible; they will usually terminate when the object becomes too distant to identify, on account of the ship's motion. The longest observation period will be attained by choosing an object initially on the bow as far off as it can be clearly seen.

It is possible to estimate wave period using a formula (3) where wave length is measured based on the length of the ship.

The ratio of wave height to length is less than $1/7$ in theory. For example, if a wave period is 3 seconds, which means its length is about 14 m from the formula (2), its height must be less than 2 m. If observed wave height is larger, the period should be underestimated in most cases.

(3) Height

With experience fairly reliable estimates can be made. For estimating the height of relatively low waves, the observer should take up a position as low down in the ship as possible, preferably amidships where the pitching is least, and on the side of the ship from which the waves are coming. Height is measured by comparing with the known length of the ship.

In case of relatively high wave heights, by climbing up or down some steps when the ship is in a wave trough and vertical observers should position themselves where the wave crest appears to coincide with the horizon (see Fig. 9.3 (a)). The wave height is then equal to the height of the observer's eyes above the level of the water. If the ship is rolling, care should be taken in the estimation as shown in Fig. 9.3 (b).

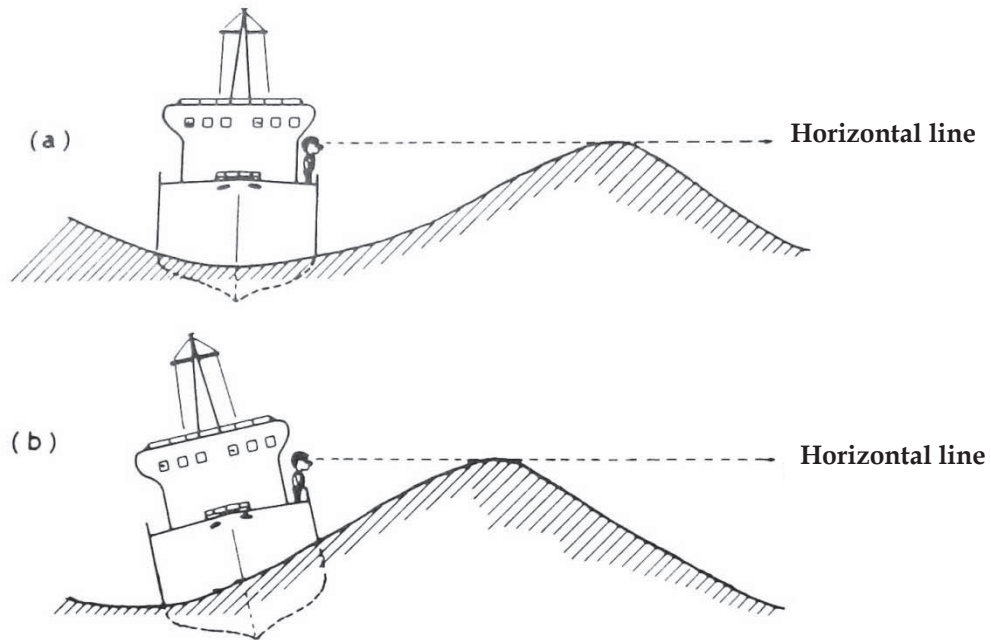


Fig. 9.3 Estimation of wave height at sea
(a) Good example and (b) bad example

CHAPTER 10 Observation of Sea Ice

Several forms of floating ice may be encountered at sea, including sea ice, which results from freezing of the sea surface, and icebergs which are large pieces that have detached from a glacier or an ice shelf. Other forms of ice include river ice which is encountered in harbors and estuaries where it is kept in motion by tidal streams and normally presents only a temporary hindrance to ships, and lake ice. Both icebergs and sea ice can be dangerous to ships and affect navigation. The extent of sea-ice cover may vary significantly from year to year affecting adjacent ocean areas and weather over large areas of the world. Consequently, its distribution is of considerable interest to meteorologists and oceanographers. Although knowledge of the extent of sea-ice cover has been revolutionized by satellite photography, observations from shore stations, ships and aircraft are of great importance in corroborating satellite observations.

10.1 Observation items

Non-instrumental observation of sea ice consists of the following items:

- Concentration or arrangement of sea ice
- Stage of development of sea ice
- Ice of land origin
- Bearing of principal ice edge
- Present ice situation and trend of conditions during past 3 hours

Observed results should be reported according to the format shown in “Guide to Ships’ Weather Reports”. To follow the Guide, refer to the definitions of technical terms in 10.2.

10.1.1 Concentration or arrangement of sea ice

Concentration or arrangement of sea ice (referred to as “*ci*” in the Marine Meteorological Logbook) is expressed by code figures 0 to 9 as shown in Table 10.1. Code figures 2 to 9 are divided into two sections depending on whether sea ice concentration within the area of observation is more or less uniform (code figures 2 to 5) or not (6 to 9). Concentration is the ratio of the amount of sea surface covered by ice to the whole area and expressed in tenths or phrases such as “open ice” and “close ice” (see 10.2.2 (1) for details).

Table 10.1 Concentration or arrangement of sea ice

<i>ci</i>	Concentration or arrangement of sea ice	
0	No sea ice in sight	
1	Ship in open lead more than 1.0 nautical mile wide, or ship in fast ice with boundary beyond limit of visibility	
2	Sea ice present in concentrations less than 3/10 concentration, open water or very open pack ice	Sea ice concentration is uniform in the observation area
3	4/10 to 6/10, open pack ice	
4	7/10 to 8/10, close pack ice	
5	9/10 or more but not 10/10, very close pack ice	Ship in ice or within 0.5 nautical mile of ice edge
6	Strips and patches of pack ice with open water between	
7	Strips and patches of close or very close pack ice with areas of lesser concentration between	
8	Fast ice with open water, very open or open pack ice to seaward of the ice boundary	
9	Fast ice with close or very close pack ice to seaward of the ice boundary	Sea ice concentration is not uniform in the observation area
×	Unable to report, because of darkness, lack of visibility, or because ship is more than 0.5 nautical mile away from ice edge	

10.1.2 Stage of development of sea ice

Code figures for this item (referred to as “*Si*”) are determined based on the stage of development of sea ice and its thickness as shown in Table 10.2. The ice surface color is helpful to distinguish its stage of development such as Nilas, Young ice or First-year ice (see 10.2.1 (1) for details).

Table 10.2 Stage of development

<i>Si</i>	Stage of development
0	New ice only (frazil ice, grease ice, slush, shuga)
1	Nilas or ice rind, less than 10 cm thick
2	Young ice (grey ice, grey-white ice), 10-30 cm thick
3	Predominantly new and/or young ice with some first-year ice
4	Predominantly thin first-year ice with some new and/or young ice
5	All thin first-year ice (30-70 cm thick)
6	Predominantly medium first-year ice (70-120 cm thick) and thick first-year ice (>120 cm thick) with some thinner (younger) first-year ice
7	All medium first-year ice and thick first-year ice
8	Predominantly medium first-year ice and thick first-year ice with some old ice (usually more than 2 m thick)
9	Predominantly old ice
×	Unable to report, because of darkness, lack of visibility or because only ice of land origin is visible or because ship is more than 0.5 nautical mile away from ice edge

10.1.3 Ice of land origin

The number of types of visible ice formed over land such as growlers, bergy bits and icebergs (see 10.2.1 (5)) for definition) are reported for this item (referred to as “*bi*”) and corresponding code figures are shown in Table 10.3.

Table 10.3 Ice of land origin

<i>bi</i>	Ice of land origin
0	No ice of land origin
1	1-5 icebergs, no growlers or bergy bits
2	6-10 icebergs, no growlers or bergy bits
3	11-20 icebergs, no growlers or bergy bits
4	Up to and including 10 growlers and bergy bits -- no icebergs
5	More than 10 growlers and bergy bits -- no icebergs
6	1-5 icebergs, with growlers and bergy bits
7	6-10 icebergs, with growlers and bergy bits
8	11-20 icebergs, with growlers and bergy bits
9	More than 20 icebergs, with growlers and bergy bits -- a major hazard to navigation
×	Unable to report, because of darkness, lack of visibility or because only sea ice is visible

10.1.4 Bearing of closest part of the principal ice edge

This item (referred to as “*Di*”) reports the direction (eight points of compass) of the closest part of the ice edge from the ship as shown in Table 10.4.

Table 10.4 True bearing of principal ice edge

<i>Di</i>	True Bearing of principal ice edge
0	Ship in shore or flaw lead
1	Principal ice edge towards North-East
2	Principal ice edge towards East
3	Principal ice edge towards South-East
4	Principal ice edge towards South
5	Principal ice edge towards South-West
6	Principal ice edge towards West
7	Principal ice edge towards North-West
8	Principal ice edge towards North
9	Not determined (ship in ice)
×	Unable to report, because of darkness, lack of visibility or because only ice of land origin is visible

10.1.5 Present ice situation and trend of conditions over preceding 3 hours

This item (referred to as “*zi*”) represents how sea ice is affecting navigation of the reporting ship. The present status of sea ice (e.g. penetrability) and its change over the preceding 3 hours before the observation should be reported based on Table 10.5.

Table 10.5 Present ice situation and trend of conditions over preceding 3 hours

<i>zi</i>	Present ice situation and trend of conditions over preceding 3 hours
0	Ship in open water with floating ice in sight
1	Ship in easily penetrable ice; conditions improving
2	Ship in easily penetrable ice; conditions not changing
3	Ship in easily penetrable ice; conditions worsening
4	Ship in ice difficult to penetrate; conditions improving
5	Ship in ice difficult to penetrate; conditions not changing
6	Ice forming and floes freezing together
7	Ice under slight pressure
8	Ice under moderate or severe pressure
9	Ship beset
×	Unable to report, because of darkness or lack of visibility

} Ship in ice

} Ship in ice difficult to penetrate and conditions worsening

10.2 Terms of sea ice forms

The definitions of terms in this section are from WMO Meteorological codes “WMO Sea-ice Nomenclature (WMO-No. 259 Edition 1970-2014).”

10.2.1 Classification of sea ice forms

Sea ice form can be classified by its developing or melting stage, and as *fast ice* or *drift ice*. *Ice of land* origin is also distinguished from others.

(1) Development stage

- (a) **New ice:** A general term for recently formed ice which includes *frazil ice*, *grease ice*, *slush* and *shuga*. These types of ice are composed of ice crystals which are only weakly frozen together (if at all) and have a definite form only while they are afloat.

Frazil ice: Fine spicules or plates of ice, suspended in water.

Grease ice: A later stage of freezing than *frazil ice* when the crystals have coagulated to form a soupy layer on the surface. *Grease ice* reflects little light, giving the sea a matt appearance.

Slush: Snow which is saturated and mixed with water on land or ice surfaces, or as a viscous floating mass in water after a heavy snowfall.

Shuga: An accumulation of spongy white ice lumps, a few centimeters across; they are formed from *grease ice* or *slush* and sometimes from *anchor ice* rising to the surface.

- (b) **Nilas:** A thin elastic crust of ice, easily bending on waves and swell and under pressure, thrusting in a pattern of interlocking “fingers” (finger rafting). Has a matt surface and is up to 10 cm in thickness. May be subdivided into *dark nilas* and *light nilas*.

Dark nilas: *Nilas* which is under 5 cm in thickness and is very dark in color.

Light nilas: *Nilas* which is more than 5 cm in thickness and rather lighter in color than *dark nilas*.

Ice rind: A brittle shiny crust of ice formed on a quiet surface by direct freezing or from *grease ice*, usually in water of low salinity. Thickness to about 5 cm. Easily broken by wind or swell, commonly breaking in rectangular pieces.

- (c) **Pancake ice (see drift ice)**

- (d) **Young ice:** Ice in the transition stage between *nilas* and *first-year ice*, 10-30 cm in thickness. May be subdivided into *grey ice* and *grey-white ice*.

Grey ice: *Young ice* 10-15 cm thick. Less elastic than *nilas* and breaks on swell. Usually rafts under pressure.

Grey-white ice: *Young ice* 15-30 cm thick. Under pressure more likely to ridge than to raft.

- (e) **First-year ice:** Sea ice of not more than one winter’s growth, developing from *young ice*; thickness 30 cm - 2 m. May be subdivided into *thin first-year ice (white ice)*, *medium first-year ice (white ice first stage)* and *thick first-year ice (white ice second stage)*.

Thin first-year ice (white ice): *First-year ice* 30-70 cm thick.

Medium first-year ice (white ice first stage): *First-year ice* 70-120 cm thick.

Thick first-year ice (white ice second stage): *First-year ice* over 120 cm thick.

- (f) **Old ice:** Sea ice which has survived at least one summer’s melt; typical thickness up to 3 m or more. Most topographic features are smoother than those of *first-year ice*. May be subdivided into residual, second-year ice and multi-year ice.

(2) Melting stage

- (a) **Puddle:** Accumulation on ice of melt-water, mainly due to melting snow, but in the advanced stages due to melting ice. The initial stage consists of patches of melted snow.

- (b) **Thaw holes:** Vertical holes in sea ice formed when surface *puddles* melt through to the underlying water.
- (c) **Dried ice:** Sea ice on the surface where melt-water has disappeared by draining through cracks and *thaw holes*. During the period of drying, the surface whitens.
- (d) **Rotten ice:** Sea ice which has become honeycombed and is in an advanced stage of disintegration.
- (e) **Flooded ice:** Sea ice, which has been flooded by melt-water or river water and is heavily loaded by water and wet snow.

(3) Fast ice

Sea ice which forms and remains fast along the coast, where it is attached to the shore, to an ice wall, to an ice front, between shoals or grounded/*icebergs*. Vertical fluctuations may be observed during changes of sea-level. *Fast ice* may be formed *in situ* from sea water or by freezing of *floating ice* of any age to the shore which may extend from a few meters to several hundred kilometers from the coast. *Fast ice* may be more than one year old and may then be prefixed with the appropriate age category (*old*, second-year, or multi-year). If it is thicker than about 2 m above sea-level it is called an *ice shelf*.

- (a) **Young coastal ice:** The initial stage of *fast ice* formation consisting of *nilas* or *young ice*, with a width varying from a few meters up to 100-200 m from the shorelines.
- (b) **Icefoot:** A narrow fringe of ice attached to the coast, unmoved by tides and remaining after the *fast ice* has moved away.
- (c) **Anchor ice:** Submerged ice attached or anchored to the bottom, irrespective of the nature of its formation.

(4) Floating ice

- (a) **Drift ice/Pack ice:** Term used in a wide sense to include any area of sea ice other than *fast ice* no matter what form it takes or how it is disposed. When *concentrations* are high, i.e. 7/10 or more, *drift ice* may be replaced by the term *pack ice*.
- (b) **Pancake ice:** Predominantly circular pieces of ice from 30 cm to 3 m in diameter, and up to about 10 cm thick, with raised rims due to the pieces striking against one another. It may be formed on a slight swell from *grease ice*, *shuga* or *slush* or as a result of the breaking of *ice rind*, *nilas* or, under severe conditions of swell or waves, of *grey ice*. It also sometimes forms at some depth at an interface between water bodies of different physical characteristics, from where it floats to the surface; it may rapidly cover wide areas of water.
- (c) **Floe:** Any contiguous piece of sea ice. *Floes* are subdivided according to horizontal extent as follows:

Floe giant: Over 10 km across.

Floe vast: 2-10 km across.

Floe big: 500-2000 m across.

Floe medium: 100-500 m across.

Floe small: 20-100 m across.

Ice cake: Less than 20 m across.

- (d) **Floeberg:** A massive piece of sea ice composed of a hummock, or a group of hummocks frozen together, and separated from any ice surroundings. It may typically protrude up to 5 m above sea-level.
- (e) **Ice breccia:** Ice of different stages of development frozen together.
- (f) **Brash ice:** Accumulations of *floating ice* made up of fragments not more than 2 m across, the wreckage of other forms of ice.

(5) Ice of land origin

- (a) **Glacier ice:** Ice in, or originating from, a glacier, whether on land or floating on the sea as *icebergs*, *bergy bits* or *growlers*.
- (b) **Ice shelf:** A *floating ice* sheet of considerable thickness showing 2-50 m or more above sea-level, attached to the coast. Usually of great horizontal extent and with a level or gently undulating surface, nourished by annual snow accumulation and often also by the seaward extension of land glaciers. Limited areas may be aground. The seaward edge is termed an ice front.
- (c) **Calved ice of land origin:**

Iceberg: A massive piece of ice of greatly varying shape, protruding more than 5 m above sea-level, which has broken away from a glacier or ice shelf, and which may be afloat or aground. *Icebergs* may be described as tabular, dome-shaped, sloping, pinnacled, weathered or glacier bergs.

Bergy bit: A large piece of floating *glacier ice*, generally showing less than 5 m above sea-level but more than 1 m and normally about 100-300 m² in area.

Growler: Piece of ice smaller than a *bergy bit* and floating less than 1 m above the sea surface, a *growler* generally appears white but sometimes transparent or blue-green in color. Extending less than 1 m above sea surface and normally occupying an area of about 20 m², *growlers* are difficult to distinguish when surrounded by sea ice or in high sea state.

10.2.2 Terms related to occurrence of sea ice

(1) Concentration

The ratio expressed in tenths describing the amount of the sea surface covered by ice as a fraction of the whole area being considered. Total *concentration* includes all stages of development that are present, partial *concentration* may refer to the amount of a particular stage or of a particular form of ice and represents only a part of the total.

- (a) **Compact ice:** *Floating ice* in which the *concentration* is 10/10 and no water is visible.
- (b) **Very close ice:** *Floating ice* in which the *concentration* is 9/10 to less than 10/10.
- (c) **Close ice:** *Floating ice* in which the *concentration* is 7/10 to 8/10, composed of *floes* mostly in contact.
- (d) **Open ice:** *Floating ice* in which the *concentration* is 4/10 to 6/10, with many *leads* and

polynyas, and the *floes* are generally not in contact with one another.

- (e) **Very open ice:** *Floating ice* in which the *concentration* is 1/10 to 3/10, and water preponderates over ice.
- (f) **Open water:** A large area of freely navigable water in which sea ice is present in *concentrations* less than 1/10. No *ice of land origin* is present.

(2) Arrangement

- (a) **Ice field:** Area of *floating ice* consisting of any size of *floes*, which is greater than 10 km across.

Ice patch: An area of *floating ice* less than 10 km across.

- (b) **Strip:** Long narrow area of *floating ice*, about 1 km or less in width, usually composed of small fragments detached from the main mass of ice, and run together under the influence of wind, swell or current.
- (c) **Ice edge:** The demarcation at any given time between the open sea and sea ice of any kind, whether fast or drifting. It may be termed compacted or diffuse.
- (d) **Ice boundary:** The demarcation at any given time between *fast ice* and *drift ice* or between areas of *drift ice* of different *concentrations*.

(3) Openings in the ice

- (a) **Fracture:** Any break or rupture through *very close ice*, *compact ice*, consolidated ice, *fast ice* or a single *floe* resulting from deformation processes. *Fractures* may contain *brash ice* and/or be covered with *nilas* and/or *young ice*. Length may vary from a few meters to many kilometers.
- (b) **Lead:** Any *fracture* or passage-way through sea ice navigable by surface vessels.
- (c) **Polynya:** Any non-linear shaped opening enclosed in ice. *Polynyas* may contain *brash ice* and/or be covered with *new ice*, *nilas* or *young ice*.

Shore polynya: A *polynya* between *drift ice* and the coast or *drift ice* and an ice front.

Flaw polynya: A *polynya* between *drift ice* and *fast ice*.

Recurring polynya: A *polynya*, which recurs in the same position every year.

CHAPTER 11 Observation of Ice Accretion

Ice accretion (icing) is growth in size, particularly by accumulation, of ice formed on the ship's exposed surfaces. It can cause radio and radar failures due to the icing of aerials and sometimes cause a rollover due to the weight of ice. Observation of ice accretion is important for safe navigation.

11.1 Ice accretion on ship

Three main causes of ice accretion include

- 1) Spray and sea water thrown up by interaction between the ship and waves, and/or spray blown from the crests of waves
- 2) Freezing rain, drizzle or fog
- 3) Wet snow followed by a drop in temperature

Of the above, 1) poses the greatest concern for ships.

Studies on the meteorological effects on ice accretion in the western North Pacific have revealed conditions to consider as warning signs:

In sea surface temperature below 4°C, ice accretion starts with air temperature below - 3°C and wind speed over 8 m/s. Strong ice accretion (over 2 cm/hour) occurs with air temperature below - 6°C and wind speed over 10m/s. In sea surface temperature below 2°C, ice accretion starts with air temperature below - 2°C. The relation of air temperature and wind speed to ice accretion is shown in Fig. 11.1. With air temperature below - 17°C, spray freezes before it is thrown at the ship so the rate of ice accretion reduces. If navigating in sea surface temperature below 4°C and low air temperature and strong wind are expected, be careful of ice accretion on ship.

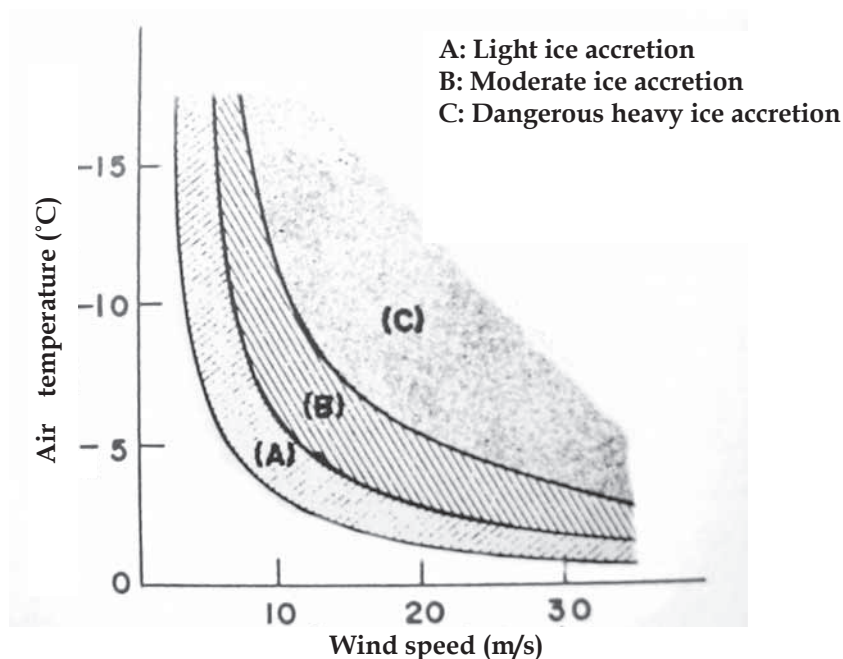


Fig. 11.1 General relation among air temperature, wind speed, and ice accretion
Based on Figure 3 (b) of Sawada (1979)*

11.2 Coding of observation

11.2.1 Causes of ice accretion on ships

Causes of ice accretion (referred to as “Is” in the Marine Meteorological Logbook) should be coded by one of five code figures (see Table 11.1 or “Ships’ Weather Code Card” for details).

11.2.2 Thickness of ice accretion

Thickness of ice accretion (referred to as “EsEs”) should be reported in centimeters. If there are different values of thickness on a ship, the maximum value should be reported.

11.2.3 Rate of ice accretion on ships

Find the description that best applies to the rate of ice accretion at observation time (referred to as “Rs”) in Table 11.2 or “Ships’ Weather Code Card”.

Table 11.1 Ice accretion on ships code

Is	Ice accretion on ships
1	Icing from ocean spray
2	Icing from fog
3	Icing from ocean spray and fog
4	Icing from rain
5	Icing from ocean spray and rain

Table 11.2 Rate of ice accretion code

Rs	Rate of ice accretion
0	Ice not building up
1	Ice building up slowly
2	Ice building up rapidly
3	Ice melting or breaking up slowly
4	Ice melting or breaking up rapidly

* T. Sawada (1975): Relation between the Rate of Ice Accretion on Ship and Meteorological Conditions. Journal of Meteorological Research, Vol.27, No.6, 229-236

CHAPTER 12 Port Meteorological Officer (PMO)

The Port Meteorological Officer (PMO) is defined by WMO as the official of the Meteorological Service of a WMO Member who is stationed at a main seaport with the tasks of maintaining liaison with weather observers on board ships, checking instruments, providing advice, and contacting shipping authorities to enlist their cooperation in operating mobile ship stations (weather station aboard a moving ship). The PMO visits ships to encourage them to report weather and offers the following services free of charge:

- To check and calibrate instruments equipped on ships including barometers and give necessary advice.
- To provide instruction or assistance with regard to questions or inquiries on meteorology or oceanography, specifically on marine meteorological observation and its reporting.
- To explain such materials published by JMA as Marine Meteorological Logbook, Guide to Weather Observation for Ships, Ship's Weather Code Card, etc. If requested, the PMO will supply necessary copies.
- To inform the schedule of radio facsimile transmission from the meteorological services for ships and explain how to receive and utilize it.

There are three PMOs in Japan as shown below. They are in Yokohama, Nagoya and Kobe. Similar services are also available from Sapporo, Sendai, Osaka, Fukuoka and Okinawa Regional Headquarters of the Japan Meteorological Agency. The following E-mail address is common to all officers/offices.

Port Meteorological Officers

Port Meteorological Officer, Yokohama Local Meteorological Office

99, Yamate-cho, Naka-ku, Yokohama 231 -0862, JAPAN

fax: +81-45-622-3520, E-mail: pmo@climar.kishou.go.jp

Port Meteorological Officer, Nagoya Local Meteorological Office

2-18, Hiyori-cho, Chikusa-ku, Nagoya 464 -0039, JAPAN

fax: +81-52-762-1242, E-mail: pmo@climar.kishou.go.jp

Port Meteorological Officer, Kobe Local Meteorological Office

1-4-3 Wakinohamakaigan-Dori, Chuo-ku, Kobe 651-0073, JAPAN

fax: +81-78-222-8946, E-mail: pmo@climar.kishou.go.jp

Other Port Meteorological Service Offices

Climate and Marine Division, Sapporo Regional Headquarters, Japan Meteorological Agency

18-2 Kitanijo-nishi, Chuo-ku, Sapporo 060-0002, JAPAN

fax: +81-11-611-3206, E-mail: pmo@climar.kishou.go.jp

Climate and Marine Division, Sendai Regional Headquarters, Japan Meteorological Agency

1-3-15 Gorin, Miyagino-ku, Sendai 983-0842, JAPAN

fax: +81-22-291-8110, E-mail: pmo@climar.kishou.go.jp

Climate and Marine Division, Osaka Regional Headquarters, Japan Meteorological Agency

4-1-76 Otemae, Chuo-ku, Osaka 540-0008, JAPAN

fax: +81-6-6949-6160, E-mail: pmo@climar.kishou.go.jp

Climate and Marine Division, Fukuoka Regional Headquarters, Japan Meteorological Agency

1-2-36 Ohori, Chuo-ku, Fukuoka 810-0052 JAPAN

fax: +81-92-761-1726, E-mail: pmo@climar.kishou.go.jp

Climate and Marine Division, Okinawa Regional Headquarters, Japan Meteorological Agency

1-15-15 Higawa, Naha 900-8517, JAPAN

fax: +81-98-833-4292, E-mail: pmo@climar.kishou.go.jp

Headquarters

Marine Division, Global Environment and Marine Department, Japan Meteorological Agency

1-3-4, Otemachi, Chiyoda-ku, Tokyo 100 -8122, JAPAN

fax: +81-3-3211-6908, E-mail: vos@climar.kishou.go.jp

To maintain the accuracy of barometers for meteorological observations, they should be checked every six months. If it is not possible for a ship to visit any of the above Japanese ports for a long time, barometers may be checked as follows:

- 1) Visit any foreign port in which a PMO is stationed to receive PMO service regardless of flag.
- 2) In Japanese ports other than above, barometers may be checked using email or facsimile. Please contact any Japanese PMO for details.

Appendix 1

List of supplies for ship weather observations and reports

JMA provides VOSs with the following materials free of charge:

Guide and tables for weather observation

Guide to Weather Observations for Ships
Guide to Ships' Weather Reports
Ships' Weather Code Card
Table for Finding the Dew-point
JMA Cloud Plate
Beaufort Scale of Wind Force

Materials for making weather observation reports

OBSJMA (Software on CD-ROM) and writeable disks for data storage
OBSJMA Operation Manual
Ship's Weather Observation Field Note for OBSJMA
Marine Meteorological Logbook
Envelope to send logbooks, floppy disks or CD-Rs (postage free within Japan)

Brochures

Marine Meteorological Observations and Port Meteorological Services
Marine Meteorological Information Services for Shipping and Fishing

Bulletin

The Ship and Maritime Meteorology

Contact

Marine Division
Global Environment and Marine Department
Japan Meteorological Agency (JMA)
1-3-4, Otemachi, Chiyoda-ku, Tokyo 100-8122 Japan
Facsimile No. +81 3 3211 6908
E-mail vos@climar.kishou.go.jp

Appendix 2

Table for saturated vapor pressure

Table for saturated vapor pressure of water

(°C)	1/10 °C of temperature									
	0	1	2	3	4	5	6	7	8	9
	hPa	hPa	hPa	hPa	hPa	hPa	hPa	hPa	hPa	hPa
0	6.11	6.15	6.20	6.24	6.29	6.33	6.38	6.43	6.47	6.52
1	6.57	6.61	6.66	6.71	6.76	6.81	6.86	6.90	6.95	7.00
2	7.05	7.10	7.16	7.21	7.26	7.31	7.36	7.42	7.47	7.52
3	7.57	7.63	7.68	7.74	7.79	7.85	7.90	7.96	8.02	8.07
4	8.13	8.19	8.24	8.30	8.36	8.42	8.48	8.54	8.60	8.66
5	8.72	8.78	8.84	8.90	8.96	9.03	9.09	9.15	9.22	9.28
6	9.35	9.41	9.48	9.54	9.61	9.67	9.74	9.81	9.88	9.94
7	10.01	10.08	10.15	10.22	10.29	10.36	10.43	10.50	10.58	10.65
8	10.72	10.79	10.87	10.94	11.02	11.09	11.17	11.24	11.32	11.40
9	11.47	11.55	11.63	11.71	11.79	11.87	11.95	12.03	12.11	12.19
10	12.27	12.35	12.44	12.52	12.60	12.69	12.77	12.86	12.94	13.03
11	13.12	13.21	13.29	13.38	13.47	13.56	13.65	13.74	13.83	13.92
12	14.02	14.11	14.20	14.30	14.39	14.49	14.58	14.68	14.77	14.87
13	14.97	15.07	15.16	15.26	15.36	15.46	15.57	15.67	15.77	15.87
14	15.98	16.08	16.18	16.29	16.40	16.50	16.61	16.72	16.82	16.93
15	17.04	17.15	17.26	17.37	17.49	17.60	17.71	17.83	17.94	18.06
16	18.17	18.29	18.41	18.52	18.64	18.76	18.88	19.00	19.12	19.24
17	19.37	19.49	19.61	19.74	19.86	19.99	20.11	20.24	20.37	20.50
18	20.63	20.76	20.89	21.02	21.15	21.29	21.42	21.55	21.69	21.83
19	21.96	22.10	22.24	22.38	22.52	22.66	22.80	22.94	23.08	23.23
20	23.37	23.52	23.66	23.81	23.96	24.10	24.25	24.40	24.55	24.71
21	24.86	25.01	25.17	25.32	25.48	25.63	25.79	25.95	26.11	26.27
22	26.43	26.59	26.75	26.92	27.08	27.25	27.41	27.58	27.75	27.91
23	28.08	28.25	28.43	28.60	28.77	28.95	29.12	29.30	29.47	29.65
24	29.83	30.01	30.19	30.37	30.55	30.74	30.92	31.11	31.29	31.48
25	31.67	31.86	32.05	32.24	32.43	32.62	32.82	33.01	33.21	33.41
26	33.61	33.81	34.01	34.21	34.41	34.61	34.82	35.02	35.23	35.44
27	35.65	35.86	36.07	36.28	36.49	36.71	36.92	37.14	37.36	37.57
28	37.79	38.01	38.24	38.46	38.68	38.91	39.14	39.36	39.59	39.82
29	40.05	40.28	40.52	40.75	40.99	41.23	41.46	41.70	41.94	42.18
30	42.43	42.67	42.92	43.16	43.41	43.66	43.91	44.16	44.42	44.67
31	44.92	45.18	45.44	45.70	45.96	46.22	46.48	46.75	47.01	47.28
32	47.55	47.82	48.09	48.36	48.63	48.91	49.19	49.46	49.74	50.02
33	50.30	50.59	50.87	51.16	51.44	51.73	52.02	52.31	52.61	52.90
34	53.20	53.49	53.79	54.09	54.39	54.70	55.00	55.31	55.61	55.92
35	56.23	56.55	56.86	57.17	57.49	57.81	58.13	58.45	58.77	59.09
36	59.42	59.75	60.07	60.40	60.74	61.07	61.40	61.74	62.08	62.42
37	62.76	63.10	63.45	63.79	64.14	64.49	64.84	65.19	65.55	65.90
38	66.26	66.62	66.98	67.34	67.71	68.07	68.44	68.81	69.18	69.56
39	69.93	70.31	70.68	71.06	71.45	71.83	72.22	72.60	72.99	73.38
40	73.77	74.17	74.56	74.96	75.36	75.76	76.17	76.57	76.98	77.39
41	77.80	78.21	78.63	79.04	79.46	79.88	80.30	80.73	81.15	81.58
42	82.01	82.44	82.88	83.31	83.75	84.19	84.63	85.08	85.52	85.97
43	86.42	86.87	87.32	87.78	88.24	88.70	89.16	89.62	90.09	90.56
44	91.03	91.50	91.98	92.45	92.93	93.41	93.90	94.38	94.87	95.36
45	95.85	96.34	96.84	97.34	97.84	98.34	98.85	99.35	99.86	100.38
46	100.89	101.41	101.92	102.45	102.97	103.49	104.02	104.55	105.08	105.62
47	106.15	106.69	107.24	107.78	108.33	108.87	109.43	109.98	110.54	111.09
48	111.65	112.22	112.78	113.35	113.92	114.49	115.07	115.65	116.23	116.81
49	117.40	117.98	118.57	119.17	119.76	120.36	120.96	121.57	122.17	122.78
50	123.39	124.00	124.62	125.24	125.86	126.48	127.11	127.74	128.37	129.01

Table for saturated vapor pressure of supercooling water

(°C)	1/10 °C of temperature									
	0	1	2	3	4	5	6	7	8	9
	hPa	hPa	hPa	hPa	hPa	hPa	hPa	hPa	hPa	hPa
-50	0.06	0.06	0.06	0.06	0.06	0.06	0.06	0.06	0.06	0.06
-49	0.07	0.07	0.07	0.07	0.07	0.07	0.07	0.07	0.07	0.06
-48	0.08	0.08	0.08	0.08	0.08	0.08	0.08	0.07	0.07	0.07
-47	0.09	0.09	0.09	0.09	0.09	0.09	0.08	0.08	0.08	0.08
-46	0.10	0.10	0.10	0.10	0.10	0.09	0.09	0.09	0.09	0.09
-45	0.11	0.11	0.11	0.11	0.11	0.11	0.10	0.10	0.10	0.10
-44	0.12	0.12	0.12	0.12	0.12	0.12	0.12	0.12	0.11	0.11
-43	0.14	0.14	0.14	0.13	0.13	0.13	0.13	0.13	0.13	0.13
-42	0.15	0.15	0.15	0.15	0.15	0.15	0.14	0.14	0.14	0.14
-41	0.17	0.17	0.17	0.17	0.16	0.16	0.16	0.16	0.16	0.16
-40	0.19	0.19	0.19	0.18	0.18	0.18	0.18	0.18	0.17	0.17
-39	0.21	0.21	0.21	0.20	0.20	0.20	0.20	0.20	0.19	0.19
-38	0.23	0.23	0.23	0.23	0.22	0.22	0.22	0.22	0.21	0.21
-37	0.26	0.25	0.25	0.25	0.25	0.24	0.24	0.24	0.24	0.24
-36	0.28	0.28	0.28	0.28	0.27	0.27	0.27	0.27	0.26	0.26
-35	0.31	0.31	0.31	0.31	0.30	0.30	0.30	0.29	0.29	0.29
-34	0.35	0.34	0.34	0.34	0.33	0.33	0.33	0.32	0.32	0.32
-33	0.38	0.38	0.37	0.37	0.37	0.36	0.36	0.36	0.35	0.35
-32	0.42	0.42	0.41	0.41	0.41	0.40	0.40	0.39	0.39	0.39
-31	0.46	0.46	0.45	0.45	0.45	0.44	0.44	0.43	0.43	0.42
-30	0.51	0.50	0.50	0.49	0.49	0.49	0.48	0.48	0.47	0.47
-29	0.56	0.55	0.55	0.54	0.54	0.53	0.53	0.52	0.52	0.51
-28	0.61	0.61	0.60	0.60	0.59	0.59	0.58	0.58	0.57	0.56
-27	0.67	0.67	0.66	0.65	0.65	0.64	0.64	0.63	0.63	0.62
-26	0.74	0.73	0.72	0.72	0.71	0.70	0.70	0.69	0.69	0.68
-25	0.81	0.80	0.79	0.79	0.78	0.77	0.76	0.76	0.75	0.74
-24	0.88	0.88	0.87	0.86	0.85	0.84	0.84	0.83	0.82	0.81
-23	0.97	0.96	0.95	0.94	0.93	0.92	0.92	0.91	0.90	0.89
-22	1.05	1.04	1.04	1.03	1.02	1.01	1.00	0.99	0.98	0.97
-21	1.15	1.14	1.13	1.12	1.11	1.10	1.09	1.08	1.07	1.06
-20	1.25	1.24	1.23	1.22	1.21	1.20	1.19	1.18	1.17	1.16
-19	1.37	1.35	1.34	1.33	1.32	1.31	1.30	1.29	1.28	1.27
-18	1.49	1.48	1.46	1.45	1.44	1.43	1.41	1.40	1.39	1.38
-17	1.62	1.61	1.59	1.58	1.57	1.55	1.54	1.53	1.51	1.50
-16	1.76	1.75	1.73	1.72	1.70	1.69	1.67	1.66	1.65	1.63
-15	1.91	1.90	1.88	1.87	1.85	1.83	1.82	1.80	1.79	1.77
-14	2.08	2.06	2.04	2.03	2.01	1.99	1.98	1.96	1.94	1.93
-13	2.25	2.23	2.22	2.20	2.18	2.16	2.14	2.13	2.11	2.09
-12	2.44	2.42	2.40	2.38	2.36	2.34	2.33	2.31	2.29	2.27
-11	2.64	2.62	2.60	2.58	2.56	2.54	2.52	2.50	2.48	2.46
-10	2.86	2.84	2.82	2.80	2.77	2.75	2.73	2.71	2.69	2.67
-9	3.10	3.07	3.05	3.03	3.00	2.98	2.95	2.93	2.91	2.89
-8	3.35	3.32	3.30	3.27	3.25	3.22	3.20	3.17	3.15	3.12
-7	3.62	3.59	3.56	3.53	3.51	3.48	3.45	3.43	3.40	3.37
-6	3.91	3.88	3.85	3.82	3.79	3.76	3.73	3.70	3.67	3.65
-5	4.21	4.18	4.15	4.12	4.09	4.06	4.03	4.00	3.97	3.94
-4	4.54	4.51	4.48	4.44	4.41	4.38	4.34	4.31	4.28	4.25
-3	4.90	4.86	4.83	4.79	4.75	4.72	4.68	4.65	4.61	4.58
-2	5.28	5.24	5.20	5.16	5.12	5.08	5.05	5.01	4.97	4.93
-1	5.68	5.64	5.60	5.55	5.51	5.47	5.43	5.39	5.35	5.31
-0	6.11	6.06	6.02	5.98	5.93	5.89	5.85	5.80	5.76	5.72

Table for saturated vapor pressure of ice

(°C)	1/10 °C of temperature									
	0	1	2	3	4	5	6	7	8	9
	hPa	hPa	hPa	hPa	hPa	hPa	hPa	hPa	hPa	hPa
- 0	6.11	6.06	6.01	5.96	5.91	5.86	5.81	5.76	5.72	5.67
- 1	5.62	5.58	5.53	5.48	5.44	5.39	5.35	5.30	5.26	5.22
- 2	5.17	5.13	5.09	5.04	5.00	4.96	4.92	4.88	4.84	4.80
- 3	4.76	4.72	4.68	4.64	4.60	4.56	4.52	4.48	4.45	4.41
- 4	4.37	4.33	4.30	4.26	4.23	4.19	4.15	4.12	4.08	4.05
- 5	4.01	3.98	3.95	3.91	3.88	3.85	3.81	3.78	3.75	3.72
- 6	3.68	3.65	3.62	3.59	3.56	3.53	3.50	3.47	3.44	3.41
- 7	3.38	3.35	3.32	3.29	3.26	3.24	3.21	3.18	3.15	3.12
- 8	3.10	3.07	3.04	3.02	2.99	2.96	2.94	2.91	2.89	2.86
- 9	2.84	2.81	2.79	2.76	2.74	2.71	2.69	2.67	2.64	2.62
-10	2.60	2.57	2.55	2.53	2.51	2.48	2.46	2.44	2.42	2.40
-11	2.38	2.35	2.33	2.31	2.29	2.27	2.25	2.23	2.21	2.19
-12	2.17	2.15	2.13	2.11	2.09	2.08	2.06	2.04	2.02	2.00
-13	1.98	1.97	1.95	1.93	1.91	1.90	1.88	1.86	1.84	1.83
-14	1.81	1.79	1.78	1.76	1.75	1.73	1.71	1.70	1.68	1.67
-15	1.65	1.64	1.62	1.61	1.59	1.58	1.56	1.55	1.53	1.52
-16	1.51	1.49	1.48	1.46	1.45	1.44	1.42	1.41	1.40	1.38
-17	1.37	1.36	1.35	1.33	1.32	1.31	1.30	1.28	1.27	1.26
-18	1.25	1.24	1.23	1.21	1.20	1.19	1.18	1.17	1.16	1.15
-19	1.14	1.12	1.11	1.10	1.09	1.08	1.07	1.06	1.05	1.04
-20	1.03	1.02	1.01	1.00	0.99	0.98	0.97	0.96	0.96	0.95
-21	0.94	0.93	0.92	0.91	0.90	0.89	0.88	0.88	0.87	0.86
-22	0.85	0.84	0.83	0.83	0.82	0.81	0.80	0.79	0.79	0.78
-23	0.77	0.76	0.76	0.75	0.74	0.73	0.73	0.72	0.71	0.71
-24	0.70	0.69	0.69	0.68	0.67	0.67	0.66	0.65	0.65	0.64
-25	0.63	0.63	0.62	0.61	0.61	0.60	0.60	0.59	0.58	0.58
-26	0.57	0.57	0.56	0.56	0.55	0.54	0.54	0.53	0.53	0.52
-27	0.52	0.51	0.51	0.50	0.50	0.49	0.49	0.48	0.48	0.47
-28	0.47	0.46	0.46	0.45	0.45	0.44	0.44	0.43	0.43	0.43
-29	0.42	0.42	0.41	0.41	0.40	0.40	0.40	0.39	0.39	0.38
-30	0.38	0.38	0.37	0.37	0.36	0.36	0.36	0.35	0.35	0.35
-31	0.34	0.34	0.34	0.33	0.33	0.33	0.32	0.32	0.31	0.31
-32	0.31	0.31	0.30	0.30	0.30	0.29	0.29	0.29	0.28	0.28
-33	0.28	0.27	0.27	0.27	0.27	0.26	0.26	0.26	0.25	0.25
-34	0.25	0.25	0.24	0.24	0.24	0.24	0.23	0.23	0.23	0.23
-35	0.22	0.22	0.22	0.22	0.21	0.21	0.21	0.21	0.20	0.20
-36	0.20	0.20	0.20	0.19	0.19	0.19	0.19	0.19	0.18	0.18
-37	0.18	0.18	0.18	0.17	0.17	0.17	0.17	0.17	0.16	0.16
-38	0.16	0.16	0.16	0.16	0.15	0.15	0.15	0.15	0.15	0.15
-39	0.14	0.14	0.14	0.14	0.14	0.14	0.13	0.13	0.13	0.13
-40	0.13	0.13	0.13	0.12	0.12	0.12	0.12	0.12	0.12	0.12
-41	0.12	0.11	0.11	0.11	0.11	0.11	0.11	0.11	0.10	0.10
-42	0.10	0.10	0.10	0.10	0.10	0.10	0.10	0.09	0.09	0.09
-43	0.09	0.09	0.09	0.09	0.09	0.09	0.09	0.08	0.08	0.08
-44	0.08	0.08	0.08	0.08	0.08	0.08	0.08	0.08	0.07	0.07
-45	0.07	0.07	0.07	0.07	0.07	0.07	0.07	0.07	0.07	0.07
-46	0.06	0.06	0.06	0.06	0.06	0.06	0.06	0.06	0.06	0.06
-47	0.06	0.06	0.06	0.06	0.05	0.05	0.05	0.05	0.05	0.05
-48	0.05	0.05	0.05	0.05	0.05	0.05	0.05	0.05	0.05	0.05
-49	0.04	0.04	0.04	0.04	0.04	0.04	0.04	0.04	0.04	0.04
-50	0.04	0.04	0.04	0.04	0.04	0.04	0.04	0.04	0.04	0.04

Third edition March, 2015

Edited and published by:

Japan Meteorological Agency

1-3-4, Otemachi, Chiyoda-ku, Tokyo 100-8122, Japan

This page left intentionally blank.

Sea ice

○Takenobu Toyota (Hokkaido University)

1. Introduction

Sea ice is any form of ice floating at sea which has originated from the freezing of seawater. Ice found at sea may also contain ice of land origin, such as icebergs, lake ice which has formed on a lake, and river ice which has formed on a river. All these kinds of ice floating in water are called floating ice. Almost all the floating ice found in the vicinity of Japan is sea ice. The ice existing in the sea ice area is divided into fast ice (which is attached to the shore or an ice wall) and the remaining drift ice. Since sea ice reflects a higher fraction of solar radiation than the surrounding seawater and significantly reduces the exchange of heat and materials between the atmosphere and ocean, it plays an important role in shaping the polar climate. Therefore, the long-term standardized observation of sea ice provides important information on climate change in polar regions.

Sea ice observations can be conducted from the seashore on land, navigating ships, aircrafts, or satellite remote sensing. In this chapter we will describe the method and style of ship-based observations, focusing on the internationally standardized ship-based visual observation in section 5-2. The description includes an observation protocol designed for the Antarctic sea ice in sections 5-2-2 and 5-2-3, and one for Arctic sea ice in section 5-2-4. Nowadays, the data observed according to these protocols in various sea ice regions on the earth are being archived in Australia. Some results obtained from this observation method will be shown in section 5-2-5. In addition, visual observations from the seashore observatories on land have been continued for more than a century, and this dataset provides an important baseline for studies of climate change. Therefore, we also describe the present style of observation conducted by meteorological observatories by citing the observation guidelines of the Japan Meteorological Agency in section 5-3.

The classification of sea ice used in the standardized observation protocol is based on the sea ice nomenclature published by the World Meteorological Organization (WMO) in 1970 (revised in 2014). Therefore, all the nomenclature of WMO will be listed in section 5-4.

2. Ship based observation

2-1 General description

The ship-based sea ice observation is conducted from the ship by observers with a good knowledge of sea ice nomenclature, at fixed time intervals, to record the ice conditions around the ship while the ship is navigating in the sea ice area. Ice conditions such as ice concentration, floe size, and thicknesses of sea ice and snow are recorded according to the internationally standardized observation protocol. These data not only contribute to the safe navigation by providing an overview

of the ice conditions along the ship, but also can be used as a validation tool for satellite remote sensing data. Besides, the statistics of the observational records for a long-term period provides useful information both for the intercomparison of the ice conditions between different sea ice regions and as a basic dataset of climate change.

For Antarctic sea ice, the standardized ship-based observation protocol was defined by the ASPeCt (Antarctic Sea Ice Processes and Climate) program established by SCAR (Scientific Committee on Antarctic Research) in 1997 (<http://aspect.antarctica.gov.au/>). One of the important purposes of this program is to compile past records of the ice conditions observed in different formats in various Antarctic sea ice regions as well as to provide a guideline for ship-based ice observation. The observation protocol is based on the sea ice nomenclature published in 1970 (revised in 2014) by WMO (World Meteorological Organization) (see section 5-4), and requires the observers to record the ice thickness, floe size, surface topography, and the type and thickness of snow for the individual ice types classified. The observation manual is described by Worby and Allison (1999), and the relevant part of this manual which is essential to the observation is cited here in sections 5-2-2 and 5-2-3.

In this protocol, much attention is paid to the estimation of mean ice thickness including ridged ice. The observer is basically required to observe the thickness for level ice, and the thickness of ridged ice is estimated with the level ice thickness and the areal fraction and sail height of the ridge using a simple ridge model. The mean ice thickness is calculated by areally-weighted thicknesses of level ice and ridged ice (section 5-2-3-3). Another way to apply the results to climate research is to estimate the integrated albedo of the total sea ice region containing various types of sea ice by summing up the albedo prescribed for each ice type (section 5-2-3-4). Since first-year ice often takes common features in form and arrangement irrespective of the regions, it is expected that this observation protocol is applicable in other seasonal ice zones as well as in the Southern Ocean. The simplified version of the ASPeCt protocol for the Japanese Antarctic Research Expedition (JARE) is proposed by Ohshima et al. (2006).

On the other hand, for Arctic sea ice, as may be expected with a longer history of sea ice observation compared with Antarctic sea ice, ice conditions have been recorded in different formats by different organizations so far. Therefore, it was not easy to set the internationally standardized observation protocol (Worby and Eicken, 2009). However, recently with the rapid change of the ice conditions in the Arctic Ocean, the expectation for establishing a network of the in-situ observation and the interest in standardizing the observation method have been increasing. Taking this opportunity, the Climate and Cryosphere (CliC) Arctic Sea Ice Working Group was implemented in 2008 under the auspices of the World Climate Research Programme (WCRP), and has been making every effort to define an internationally standardized observation protocol for Arctic sea ice. While this protocol is based on the ASPeCt protocol designed for Antarctic sea ice, some observation

parameters are added to apply to Arctic sea ice.

The major differences between Arctic and Antarctic sea ice are the surface conditions during the melting season and the concentration of inclusions such as sediments and ice algae within sea ice. In the Arctic, surface melting dominates (unlike the Antarctic sea ice), and a number of melt ponds develop on the surface in the melting season. Since melt ponds evolve with time and affect the surface heat budget significantly, additional codes are set for the observation of melt ponds. Reflecting the fact that sea ice often grows on widespread shallow continental shelves in the Arctic Ocean, it sometimes contains highly concentrated sediments. To record such conditions, observation codes relevant to sediments are also added for Arctic sea ice. Another feature for the Arctic protocol is that it includes observation items relevant to marine creatures. Refer to the Website (<http://www.iarc.uaf.edu/icewatch>) for more details of the observation codes.

As supplemental information for ship-based sea ice observations, ship-borne electromagnetic induction sounding has been used by many icebreakers to monitor the ice thickness distribution along the ship track since the late 1990's. This device is composed of transmitter and receiver coils, which are set apart by a few meters, and is suspended at a distance of few meters from the ship during the navigation to avoid the effect of the ship (Fig.5-1). The transmitter generates a primary electromagnetic field which induces eddy currents just below the ice bottom, because the conductivity of sea ice ($0\text{--}50\text{ mS m}^{-1}$) is negligible compared to that of seawater (2500 mS m^{-1}). In turn the induced currents generate a secondary electromagnetic field. Then the distance to the ice bottom is calculated from the strength of the secondary electromagnetic field sensed by the receiver coil. If we mount a laser profilometer on the instrument and measure the height of the instrument above the combined snow and ice surface, ice thickness can be obtained by subtracting it from the EM results. The merit of this method is that ice thickness data can be obtained irrespective of level ice or ridged ice. Although the observational bias caused by taking the thinner route should sometimes be taken into account, this method has allowed us to obtain the ice thickness distribution quantitatively in a wide region while navigating. Refer to Haas (1998) and Uto et al. (2006) for details of this technique applied to the Southern Ocean and the Sea of Okhotsk, respectively. If the ice thickness monitoring by this method is continued along regular shipping routes, it is expected that these data will form a useful dataset for monitoring climate change.

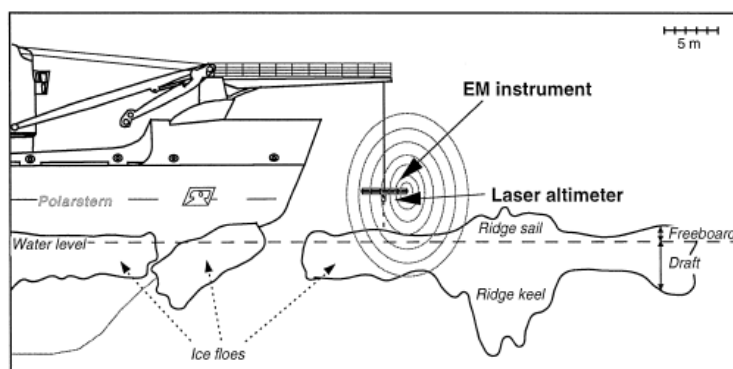


Fig. 5-1. Schematic picture showing the EM sensor suspended from the German ice breaker "Polarstern" (cited from Haas (1998))

2-2 Observational technique for Antarctic sea ice (cited from Worby and Allison (1999))

(Remarks by the author are shown in *Italics*.)

A standard set of observations are made hourly by an observer on the ship's bridge. These include the ship's position and total ice concentration, and an estimate of the areal coverage, thickness, floe size, topography and snow cover of the three dominant ice thickness categories within a radius of approximately 1 km of the ship. The three dominant ice categories are defined as those with the greatest areal concentration, and the thickest of these is defined as the primary ice type. There may be times when only one or two different ice categories are present in which case only the primary, or primary and secondary, classifications are defined. The observations are entered on log sheets using a standard set of codes based on the WMO (1970) nomenclature and designed exclusively for Antarctic sea ice. A set of blank proformas is located in Table 5-1 and observation codes are shown in Table 5-2.

2-2-1 Ice Concentration (c)

Total ice concentration is an estimate of the total area covered by all types of ice, expressed in tenths, and entered as an integer between 0 and 10. In regions of very high ice concentration (95-99%) where only very small cracks are present, the recorded value should be 10 and the open water classification should be 1 (small cracks). Regions of complete ice cover (100%) will be distinguished by recording an open water classification of 0 (no openings). An estimate of the concentration of each of the three dominant ice thickness categories is also made. These values are also expressed in tenths and should sum to the value of the total ice concentration. It is sometimes difficult to divide the pack into three distinct categories, and it may be necessary to group some categories together to ensure their representation.

2-2-2 Ice Type (ty)

The different ice categories, together with the codes used to record the observations, are shown in Table 2.1. The ice categories are based on the [WMO, 1970] sea ice classifications. First year ice greater than approximately 0.1 m thick is classified by its thickness (e.g., young grey ice 0.1-0.15 m; first year ice 0.7-1.2 m), while thinner ice is generally classified by type (e.g., frazil, shuga, grease and nilas). A single category is defined for multi-year ice. There is also a category for brash, which is common between floes in areas affected by swell and where pressure ridging has collapsed.

2-2-3 Ice Thickness (z)

Ice thickness is estimated for each of the three dominant ice types. It is helpful to the observer to suspend an inflatable buoy of known diameter (or other gauge) over the side of the ship, approximately 1 m above the ice, to provide a scaled reference against which floe thickness can be estimated. The ice thickness can then be determined quite accurately as floes turn sideways along the

ship's hull (Fig.5-2). Only the thickness of level floes, or the level ice between ridges, is estimated. This is because ridges tend to break apart into their component blocks when hit by the ship, making it impossible to estimate their thickness. In order to determine the thickness of ridged floes, observations of the areal extent and mean sail height of the ridges are made (see Section 5-2-2-5) and combined with the level ice thickness data into a simple model (see Section 5-2-3-3).



Fig. 5-2. A sample of floes turning sideways along the ship's hull.

Thinner, snow-free ice categories, which are particularly important for ocean-atmosphere heat exchange, can be reliably classified by a trained observer from their apparent albedo, while the thickness of very thick floes may be estimated by their freeboard. The accuracy of careful observations will be within 10-20% of the actual thickness, and a large sample of observations can be expected to provide a good statistical description of the characteristics of the pack. This is particularly true at the thin end of the thickness distribution where changes are most important for both radiant and turbulent heat transfer (e.g., Worby and Allison, 1991).

On dedicated scientific voyages, it is usually possible to make regular *in situ* measurements of ice and snow thickness, both on level ice and across ridges, to “calibrate” the ship-based observations. Worby et al. (1996) demonstrated a technique for combining *in situ* and ship-based observations to estimate the ice thickness distribution in the Bellingshausen Sea. Dedicated scientific voyages also usually provide the opportunity to follow specific routes to optimise data quality, which may be compromised if the ship follows the most easily navigable routes. It is the observer's responsibility to clearly indicate on the observation sheet when the ship is preferentially following leads so that this may be considered during data processing.

2-2-4 Floe size (*f*)

Floe size can be difficult to determine because it is not always clear where the boundary of a floe is located. Cracks and leads delineate floe boundaries whereas ridges do not. Where smaller floes have been cemented together to form larger floes, the larger dimension is recorded, but usually with a comment to indicate that smaller floes are visible. Where two floes have converged and ridged, the floe size is taken as the combined size of the two. A good rule of thumb is : if you could walk from point A to point B, then both points are on the same floe. This guide can be helpful when trying to

determine floe size. The length of the ship (about 100 m for most ice breakers) can act as a good guide for estimating floe size. The ship's radar can be useful for determining the size of very large floes.

Floe size is recorded using a code between 100 and 700. New sheet ice (code 200) is normally used for nilas. This code does not specify a floe size, but is a descriptor for refrozen leads and polynyas. It is often used in conjunction with topography codes 100 (level ice) and 400 (finger rafting).

2-2-5 Topography (t)

As discussed above, the ice thickness estimates are only made of the level ice in a floe. This is because the thickness of ridges can not reliably be estimated from a ship, since they tend to break up in to their component blocks when hit by the ship, rather than turning sideways so that their thickness can be estimated. However, drilled transects across ridged ice floes indicate that the mass of ice in ridges is a major contributor to the total ice mass of the pack, hence it is important to quantify the extent of ridging within the pack. To do this, the areal extent and mean sail height of ridges is recorded for each ice type within the pack. The extent of surface ridging is estimated to the nearest 10%. It is important that observers not look too far from the ship when estimating the areal extent of ridges, otherwise only the ridge peaks are seen and not the level ice between them. This gives a false impression of more heavily deformed ice than is actually present. The mean sail height is estimated to the nearest half metre below 2 m, and to the nearest metre above 2 m. It is important to remember that it is the *mean* sail height that is recorded. This can be difficult to estimate, particularly in flat light when the sky is overcast. our experience has shown that ridge height is generally underestimated due to the vertical perspective from the bridge.

Ridges are classified using a three digit code between 500 and 897. The first digit (5-8) is a description of the type of ridge, which may be unconsolidated, consolidated or weathered. This is determined from the appearance of the ridge and is useful for estimating ridge sail density. The second digit (0-9) describes the areal coverage of ridges, and the third digit (0-7) records the mean sail height to the nearest 0.5 m. These observations are probably the most subjective of those made from the ship, and it is particularly important to standardise them between observers.

The observations of surface ridging are input to a model formulation as described in section 2-3-3, to estimate the mass of ice in ridges.

2-2-6 Snow type (s)

This is a descriptor for the state of the snow cover on sea ice floes. It is important for estimating the area-averaged albedo of the pack as discussed in Section 5-2-3-4. The snow classification is an integer between 0 and 10. For accurate surface albedo calculations, the snow cover classification describes the surface snow. Hence, in a case where fresh snow has fallen over older wind-packed

snow, the classification code should describe the freshly fallen snow cover. However, it is very important that the total snow cover thickness is still recorded.

2-2-7 Snow thickness (sz)

An estimate of the snow cover thickness is made for each of the three dominant ice thickness categories. Snow thickness is relatively straight forward to estimate for floes turned sideways along the ship's hull, although at times the ice/snow interface is difficult to distinguish, particularly when the base of the snow layer has been flooded and snow-ice has formed.

2-2-8 Open water (o/w)

The codes for open water are descriptors for the size of the cracks or leads between floes, not a concentration value (in tenths). As discussed above, the length and breadth of the ship can act as a useful guide when estimating lead dimensions. The ship's radar can also be useful, particularly at night.

2-2-9 Meteorological Observations

Instantaneous conditions are usually recorded hourly, but this may be reduced to three hourly. The standard set of observations include water temperature, air temperature, true wind speed and direction, total cloud cover, visibility, and current weather. On most research vessels, water temperature, air temperature and wind speed and direction will be displayed on the bridge, and may even be logged for the duration of the voyage. Cloud cover can be estimated by the observer in eighths, and visibility is estimated in kilometres from the ship. Wind speed is recorded in ms^{-1} and wind direction relative to north ($^{\circ}\text{T}$). The current weather is recorded using the Australian meteorological observer's two digit codes that are provided in Table 5-4.

2-2-10 Photographic Records

During daylight hours a photographic record of ice conditions can be kept. Slides are usually taken from the bridge at the time of each observation, and the log book has a column for recording film and frame numbers. There is also scope for recording the frame number for a time lapse video recorder which the authors have mounted on the ship's rail. This captures a single video frame every 8 seconds, providing a comprehensive visual record of ice conditions on a single video tape for each 30 day period. This photographic archive is not generally used for quantitative analyses, but provides an excellent reference that can be used in conjunction with the ship-based observations. At night the camera is angled closer to the ship to view an area that can be adequately lit by flood lights mounted on the ship's rail.

**Note: Taking three photos at the fixed observation time from the bridge or the upper bridge of the ship is recommended to record ice conditions, as shown in Fig.5-3.*



Fig. 5-3 Sample photos taken from the upper bridge of P/V “Soya”
in the southern Sea of Okhotsk (From left to right, portside, front, and starboard)

2-2-11 Comments

In addition to the hourly observations entered by code, there is scope for additional comments to be recorded. These usually include a brief description of the characteristics of the pack, in particular features which are not covered by the observation codes, such as frost flowers on dark nilas or swell penetrating the pack. Brief details of sampling sites, buoy deployments or other ‘on ice’ activities may also be recorded and, if necessary, a comment on how typical the ice along the ship’s route is of the surrounding region.

Table 5-1. An observation sheet for ASPeCt (1)

Day/Date (Z):		SEA ICE OBSERVATIONS																		
POSITION		SEA ICE OBSERVATIONS																		
hr (Z)	Lat (°S) dd mm	Long (°E/W) ddd mm	Conc. (tenths)	PRIMARY			SECONDARY			TERTIARY			O/W (Z)	hr (Z)						
				c	ly	z	f	t	s	sz	c	ly	z	f	t	s	sz			
0																				0
1																				1
2																				2
3																				3
4																				4
5																				5
6																				6
7																				7
8																				8
9																				9
10																				10
11																				11
12																				12
13																				13
14																				14
15																				15
16																				16
17																				17
18																				18
19																				19
20																				20
21																				21
22																				22
23																				23

NOTES:
 * PRIMARY SEA ICE IS OF GREATEST THICKNESS. HENCE $t_1 > t_2 > t_3$

Table 5-1. An observation sheet for ASPeCt (2)

Day/Date (Z):												
METEOROLOGICAL OBSERVATIONS							PHOTO	VIDEO	COMMENTS			OBSERVER
hr (Z)	Twater (°C)	Tair (°C)	Wind (sp/d)	Cloud (oktas)	Visib (v)	Weath (ww)	Film/Frame	Tape No./Reading	Text	Ref. no.	Name	hr (Z)
0												0
1												1
2												2
3												3
4												4
5												5
6												6
7												7
8												8
9												9
10												10
11												11
12												12
13												13
14												14
15												15
16												16
17												17
18												18
19												19
20												20
21												21
22												22
23												23

NOTES:
 * ADDITIONAL COMMENTS MAY BE MADE ON THE FOLLOWING PAGE. PROVIDING DUE REFERENCE IS GIVEN

Table 5-2. Observation codes for ASPeCt

ICE TYPE (y)	FLOE SIZE (f)	TOPOGRAPHY (t)	SNOW TYPE (s)
10 Frazil	100 Pancakes	100 Level ice	0 No snow observation
11 Shuga	200 New sheet ice	200 Raftered pancakes	1 No snow, no ice or brash
12 Grease	300 Brash/broken ice	300 Cemented pancakes	2 Cold new snow, <1 day old
20 Nilas	400 Cake ice, <20 m	400 Finger rafting	3 Cold old snow
30 Pancakes	500 Small floes, 20-100 m	5xy New, unconsolidated ridges (no snow)	4 Cold wind-packed snow
40 Young grey ice, 0.1-0.15 m	600 Medium floes, 100-500 m	6xy New ridges filled with snow or a snow cover	5 New melting snow (wet new snow)
50 Young grey-white ice, 0.15-0.3 m	700 Large floes, 500-2000 m	7xy Consolidated ridges (no weathering)	6 Old melting snow
60 First year, 0.3-0.7 m	800 Vast floes, >2000 m	8xy Older, weathered ridges	7 Glaze
70 First year, 0.7-1.2 m		x values: 0 0-10% areal coverage	8 Melt slush
80 First year, >1.2 m		1 10-20%	9 Melt puddles
85 Multiyear floes		2 20-30%	10 Saturated snow (waves)
90 Brash		3 30-40%	11 Sastrugi
95 Fast ice		4 40-50%	
		5 50-60%	
		6 60-70%	
		7 70-80%	
		8 80-90%	
		9 90-100%	
		y values: 1 0.5 m av. sail height	
		2 1.0 m	
		3 1.5 m	
		4 2.0 m	
		5 3.0 m	
		6 4.0 m	
		7 5.0 m	
ICE CONCN^a (c) to be expressed in tenths			OPEN WATER
			0 No openings
			1 Small cracks
			2 Very narrow breaks, <50m
			3 Narrow breaks, 50-200 m
			4 Wide breaks, 200-500 m
			5 Very wide breaks, >500 m
			6 Lead/coastal lead
			7 Polyynal/coastal polyynal
			8 Water broken only by small scattered floes
			9 Open sea
SEA ICE (z) AND SNOW THICKNESS (sz) to be expressed in centimetres			

2-3 Data entry and processing for Antarctic sea ice

(cited from Worby and Allison (1999))

2-3-1 Quality control

Checks are made to identify errors and inconsistencies in the data. These include, but are not limited to:

- snow thicker than ice
- thin ice types greater than 0.1 m thick
- total concentration greater than 10/10, or not adding up to the sum of the concentrations of the three dominant categories
- ice thickness categories not matching assigned thickness values
- topography or floe size codes incompatible with ice type (e.g., consolidated ridges on nilas)
- primary ice category thinner than secondary or tertiary categories
- distance between consecutive hourly observations greater than 20 km.

2-3-2 Editing data

The data set may be edited to exclude observations within a prescribed distance of the previous observation. This is to prevent biasing in areas of heavy ice where the ship's speed is reduced. The distance is usually set to 6 nautical miles, corresponding to a straight line speed of 6 knots which most ice breakers are capable of maintaining in moderate pack ice. The processing software enables the user to specify this distance, or to use all observations regardless of spacing.

Observations are also removed when there is obvious biasing caused by the ship following easily navigable routes. The most common example of this is near the ice edge, when the ship may constantly pick its way through leads. This is usually avoidable on voyages dedicated to sea ice research, but may otherwise prove to be a problem. It is at the discretion of the observer to either note that the data may be biased, or not record data under such circumstances.

2-3-3 Estimating the area-averaged ice and snow thicknesses

Estimates of the area-averaged ice and snow thicknesses may be made over the ice covered region of the pack only, or for the total pack ice zone including the open water fraction. Each observation is equally weighted unless eliminated by the minimum distance rule described above. For each hourly observation, the estimated ice thickness values for each of the three dominant ice thickness categories are weighted by the ice concentration. This provides a mean thickness of the level ice within the pack.

To account for the mass of ice in ridges, the observations described in section 5-2-2-5 are used in conjunction with a simple model to calculate a corrected mean floe thickness (Z_r). The model takes the undeformed floe thickness (Z_u), average sail height (S) and an estimate of the areal extent of

surface ridging (R) as input parameters, and calculates the mean thickness of the floe (Zr), assuming a triangular sail, isostasy and a ratio of ice and snow above sea level to ice below sea level as 5:1. The assumption of a triangular sail cross section is consistent with the formulation of Hibler et al. (1974) for calculating the effective thickness of ridged ice. Their formulation used a fixed slope angle of 26° ; however the present study uses an implied variable slope angle which is dependent upon the areal coverage of ridges and the average sail height. In this way broader ridges are flatter which is consistent with the theory that ridges should build laterally once the limiting height is reached (Tucker and Govoni, 1981). The assumption of a triangular ridge is therefore not likely to induce large errors. Published literature on sea ice density is sparse; however Buynitskiy (1967) presented mean densities from East Antarctic sea ice for summer and winter ice of 875 kg m^{-3} and 920 kg m^{-3} respectively, and these are consistent with the value of 900 kg m^{-3} used in the model formulation. The assumption of hydrostatic equilibrium must also hold on the large scale; however the effect of snow drifts around ridges may induce errors in both the observations and the model. In particular, observers may not be able to differentiate ridge sails from adjoining snow drifts, hence the observations of the areal coverage (and to a lesser extent, height) or ridging will include the fraction covered by snow. This will affect the value r defined as the ratio of ice thickness below sea level to the combined thickness of ice and snow above sea level. Hence, the assumption that ridge sails are solid ice with a density of 900 kg m^{-3} is incorrect, and this is accounted for in the model.

To determine r in the vicinity of ridges, data from drilled thickness transects that intersected ridges were examined. Only transects, or parts thereof, with peaks in freeboard (the height of the snow/ice interface above the sea level) $>0.5 \text{ m}$ were considered, and the mean ice and snow thicknesses were calculated. A total of 339 drill holes from 9 thickness transects had mean ice and snow thicknesses of 1.18 m and 0.16 m respectively. By assuming densities of 900 kg m^{-3} and 360 kg m^{-3} for ice and snow respectively the mean draft was calculated to be 1.12 m . Hence, $r = 5$ in areas of ridged ice. The snow density value was derived from data collected on two voyages to the East Antarctic pack (V9 92/93 and V1 95/96), with a mean value of $360 \pm 110 \text{ kg m}^{-3}$ over the range $120\text{-}760 \text{ kg m}^{-3}$.

In order to calculate only the thickness of ice in ridges it is necessary to remove the snow from the calculation. The ratio of ice below sea level : ice above, r' , is defined as :

$$r' = [1 - (0.16/1.18)] r = 4.3$$

based on the mean ice and snow thickness given above. The value $r' = 4.3$ compares well with the value of 4 used by Dierking (1995), which was based on drilled transect measurements by Lange and Eicken (1991) and Wadhams et al. (1987).

The model formulation to calculate the average thickness of ridged floes (Z_r) can now be written as :

$$Z_r = (r' + 1)(0.5RS) + Z_u$$

where R is the areal extent of surface ridging, S is the average sail height of ridges, and Z_u is the thickness of level (undeformed) ice in the floe (Fig.5-4).

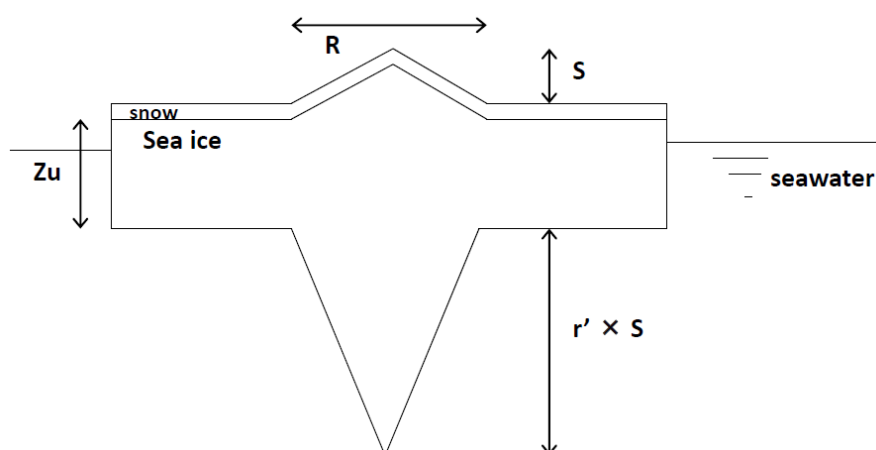


Fig. 5-4 A simple ridge model for estimating the thickness of ridged ice

2-3-4 Calculating area-averaged albedo

The area-averaged albedo is computed from the ice concentration and allwave albedo for each ice type. The allwave albedo values for different ice and snow thickness categories were originally taken from Allison et al. (1993); however these have recently been updated (Brandt et al., 2005; Table 5-3). The average albedo is calculated over the entire pack, including the open water fraction. A value is calculated at each hourly observation site, from which zonal averages may also be calculated.

Table 5-3. Representative all-wave solar albedos of surface types in the East Antarctic sea ice zone in spring and summer. Values in bold are derived from measurements; all others were estimates by interpolation or extrapolation. SON: September to November, DJF: December to February.

(cited from Brandt et al. (2005))

Ice type	Ice thickness (cm)	No snow		Thin snow (<3 cm)				Thick snow (>3 cm)			
				Clear		Cloudy		Clear		Cloudy	
		Clear	Cloudy	SON	DJF	SON	DJF	SON	DJF	SON	DJF
Open water	0	0.07	0.07	—	—	—	—	—	—	—	—
Grease	<1	0.09	0.09	—	—	—	—	—	—	—	—
Nilas	<10	0.14	0.16	0.42	0.39	0.45	0.42	—	—	—	—
Young grey ice	10–15	0.25	0.27	0.55	0.51	0.59	0.56	0.72	0.67	0.76	0.72
Young grey-white ice	15–30	0.32	0.34	0.64	0.59	0.68	0.64	0.76	0.70	0.81	0.76
First-year ice <0.7 m	30–70	0.41	0.45	0.74	0.69	0.79	0.74	0.81	0.75	0.87	0.82
First-year ice >0.7 m	>70	0.49	0.54	0.81	0.75	0.87	0.82	0.81	0.75	0.87	0.82

2-4 Observational technique for Arctic sea ice

Arctic sea ice observations are normally conducted at hourly intervals from the ship's bridge, as with Antarctic sea ice. The standardization of the ship-based sea ice observation protocol for Arctic sea ice is now being made by the Arctic Ice Watch program, with the aim to establish a PC software called ASSIST (Arctic Shipborne Sea Ice Standardization Tool) for operational management. Since the observation protocol is based on ASPeCt, the observations added for Arctic sea ice are listed here. (For details, refer to <http://www.iarc.uaf.edu/icewatch/assist>)





*Melt pond (Puddle)

Melt pond concentration	tenths
Melt pond pattern	1. linked 2. discrete
Melt pond surface type	1. Frozen (dry or wet snow) 2. Open 3. Bottom up
Melt pond freeboard	centimeters
Melt pond depth	centimeters
Melt pond bottom type	1. Solid 2. Some have thaw holes 3. All have thaw holes
Melt dried ice	logical
Melt rotten ice	logical

*Ice algae and Sediments

Algae concentration	0. 0 1. <30 2. <60 3. >60%
Algae density	-1. Not visible 0. Trace 1. Light 2. Medium 3. Strong
Algae location	10. Top 20. Middle 30. bottom
Sediment concentration	0. 0 1. <30 2. <60 3. >60%

As for algae concentration, select from the color menu below:

 0 <3 mg chl a m ⁻²	 2 ~10 mg chl a m ⁻² [Pantone 110e]
 1 ~4.5 mg chl a m ⁻² [Pantone 100C]	 3 ~30 mg chl a m ⁻² [Trumatch 49b]

Additional observation items include the type and amount of cloud for upper, medium, and low cloud. The observation codes are listed in Table 5-4.

2-5 Some achievements

In this section, some results obtained from the ASPeCt protocol will be shown. One of the most important achievements is that this method was the first to reveal a circumpolar map of ice thickness distribution around the Antarctica. Worby et al. (2008) showed the mean annual ice thickness distribution (including ridged ice) for the whole Antarctic region, from a compilation of 21,710 individual ship-based observations collected from 81 voyages to Antarctica for the period of 1981 to 2005, following the ASPeCt protocol (Fig.5-5). This figure clearly shows that the sea ice near the Antarctic Peninsula in the western Weddell Sea and around the coastal area of the eastern Ross Sea is comparatively thicker, and the maximum thickness exceeds 2 m in these regions. In other regions, ice thickness is about 0.3-0.5 m in the marginal ice zone and about 1 m near the coast. These characteristics almost coincide with the results predicted with numerical sea ice models (e.g. Timmermann et al., 2002), providing a valuable ground truth data. However, the observational data and period still does not appear to be sufficient to analyze the interannual variability of ice conditions in the Southern Ocean. For discussion of climate change, further continuous observations are strongly encouraged.

On the other hand, in the southern Sea of Okhotsk, cooperative sea ice observations have been conducted by Hokkaido University and the Japan Coast Guard onboard P/V “Soya” in February every winter since 1996. In particular, after 2001, the ship-based visual observation has been conducted according to the ASPeCt protocol (Toyota et al., 2007). Since the Sea of Okhotsk is a seasonal sea ice zone like most of the Southern Ocean, and since the sea ice there has many common properties with the Antarctic sea ice, the ASPeCt protocol is considered to be useful to obtain the properties of the ice conditions there. Fig. 5-6 shows the histograms of floe size and thickness obtained by compiling 546 ship-based observations collected in the southern Sea of Okhotsk for the period of 2001 to 2015. It is found from this figure that the dominant floe size category is ice cake (2 m to 20 m) and nilas even though vast floes which comprise a few percents of the floe size distribution. The dominant thickness category is thin first-year ice (30 cm to 70 cm) and nilas, which contrasts to the result obtained along the ship track of JARE off East Antarctica (Ohshima et al., 2006) where a small floe (20 m to 100 m) and medium first-year ice (70 cm to 120 cm) are dominant. The mean ice thicknesses of level ice, ridged ice, and total ice floes are estimated to be 0.29 m, 1.58 m, and 0.63 m, which is somewhat thinner than those of winter Antarctic sea ice (level ice: 0.38 – 0.49 m, total thickness: 0.54 – 0.72 m; Worby et al., 2008).

Thus standardized ship-based observations are not only useful to find the properties of the ice conditions in the individual sea ice area, but they also enable us to compare properties between different ice areas. One of the advantages seems to be the feasibility at only a small cost. It is hoped that the continuity of ship-based observations will contribute to the understanding of climate change.

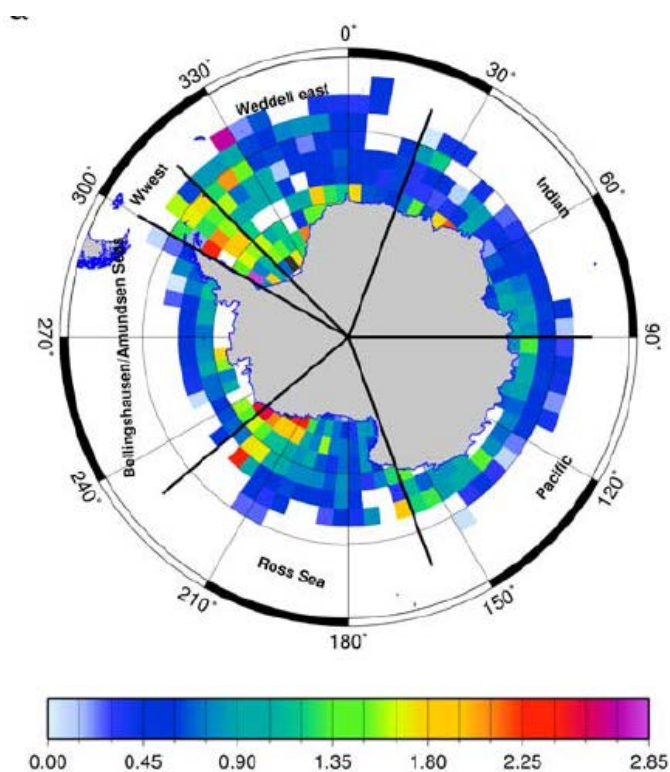


Fig. 5-5 Circumpolar map of mean annual ice thickness distribution, including ridged ice, obtained by compiling ASPeCt data on $2.5^\circ \text{ lat} \times 5.0^\circ \text{ lon}$ grid (cited from Worby et al., 2008).

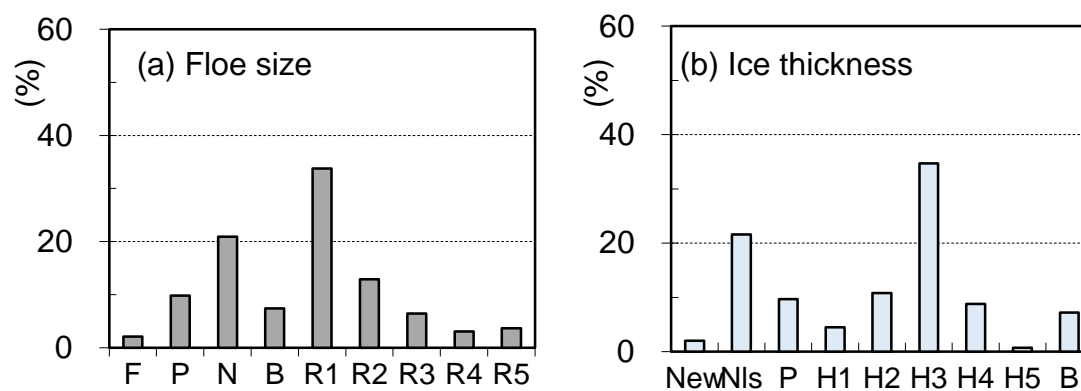


Fig. 5-6 Mean histograms obtained from ASPeCt observations conducted in the southern Sea of Okhotsk for the period of 2001 to 2015 for

(a) floe size (F: Frazil ice, P: Pancake ice, N: Nilas, B: Brash ice, R1: 2-20m, R2: 20-100m, R3: 100-500m, R4: 500m-2km, R5: >2km)

(b) thickness category (New: New ice, NIs: Nilas, P: Pancake ice, B: Brash ice, H1: 10-15cm, H2: 15-30cm, H3: 30-70cm, H4: 70-120cm, H5: >120cm)

3. Coastal observation#

(#Translation of “Guideline for oceanographical observations” published by the Japan Meteorological Agency in 2004)

Coastal sea ice observations are conducted by observers with a good knowledge of sea ice nomenclature at a fixed time of the day at a fixed coastal site. By transmitting the observed ice conditions immediately via a telecommunications network, the data can be used for disaster prevention (e.g., safe ship navigation) as well as ground truth data for sea ice observations conducted by satellite remote sensing. Furthermore, the long-term collection of sea ice observations serves as important baseline dataset for the monitoring of climate.

3-1 Observation site

The observation site should be a relatively high place such as the roof of a building so that observers can view a wide area including the coastline and large sea of the sea surface.

3-2 Observation parameters

Observation parameters include total ice amount, ice conditions around the coastal region, and the first and last dates of sea ice coverage.

3-3 Observation time

Coastal observations are conducted at 09:00 am (LST). If the first or last sea ice phenomena are observed at another time, the observation time should be recorded in the column for remarks on the observation sheet.

3-4 Observation period

In principle, the observation period is from the date when sea ice first appears in sight until the date when sea ice disappears completely out of sight.

3-5 Observation of total ice amount

Ice amount is defined as the areal fraction covered with all types of sea ice within the observation area. Ice amount is classified into *true ice amount*, defined as the fraction of real sea ice area to the real total observation area, and *apparent ice amount* defined as the fraction of apparent sea ice area seen from the slant view to the apparent total observation area. Observers observe the *apparent ice amount*, and record the total ice amount, which is defined as the *apparent ice amount* for the whole sea surface in sight (including the port area), at the fixed observation time.

Ice amount is recorded according to the grade shown in Table 5-5. This expression is analogous to the total cloud amount (in tenths) in surface meteorological observations. Ice amount is determined solely by the area covered with sea ice, independent of ice types. Some matters which require more attention are listed below:

1. As for the sea ice near the horizon, observers should avoid unreasonable judgments and determine ice amount simply from the appearance because the precise conditions such as a space between floes are often hard to see.
2. Observers should take care to notice relatively dark new sheet ice when present.
3. When only part of the sea surface can be seen due to bad visibility caused by blowing snow or fog, ice amount should be observed within the visible range. In this case, observers should write down the data in parenthesis and put remarks about the reason for the bad visibility in the observation sheet.

Table 5-5 Grade of total ice amount

Code	Ice amount	Fraction of sea ice to the total sea surface in sight
0	0	No sea ice
1	0+	Sea ice is present in sight but the fraction is < 10%.
1	1	Sea ice occupies 10% of the total sea surface in sight.
2	2	Sea ice occupies 20% of the total sea surface in sight.
2	3	Sea ice occupies 30% of the total sea surface in sight.
3	4	Sea ice occupies 40% of the total sea surface in sight.
4	5	Sea ice occupies 50% of the total sea surface in sight.
5	6	Sea ice occupies 60% of the total sea surface in sight.
6	7	Sea ice occupies 70% of the total sea surface in sight.
6	8	Sea ice occupies 80% of the total sea surface in sight.
7	9	Sea ice occupies 90% of the total sea surface in sight.
7	10-	Total sea surface in sight is mostly covered with sea ice except for small open area.
8	10	The sea surface is covered completely with sea ice.
/	/	Unknown

3-6 Observation of ice conditions around the coastline

Ice conditions around the coastline are observed, to report the presence of fast ice or drift ice, and

the state of open water such as fractures, leads, and whatever in the sea ice area. The observed data are recorded with the 11 grades listed in Table 5-6, according to the format of coastal sea ice observation report: JM305.

Although in general sea ice is classified into *fast ice* and *drift ice*, it is hard to judge the classification in some cases. Since this matter is relevant to the definition of the first and last dates of sea ice phenomena, however, some standardization is required.

Fast ice is defined by the sea ice which forms and remains fast along the coast, where it is attached to the shore. *Fast ice* may be formed *in situ* from sea water or by freezing of pack ice of any age to the shore.

On the other hand, *drift ice* is the term used in a wide sense to include any area of sea ice, other than *fast ice*, no matter what form it takes. Therefore, *drift ice* includes not only sea ice which has been advected from the northern or central Sea of Okhotsk, far away from the observation site along the Hokkaido coast, but also *new ice* which has formed off shore, and also sea ice which was once originated from *fast ice* but is now drifting after becoming detached from the shore. Although the judgment between *fast ice* and *drift ice* is often difficult from coastal observation, sea ice extending from the shore should be recorded as *fast ice* even if coastal leads covered with new sheet ice may intervene between the shore and the off-shore ice. In the case where the sea ice is not contiguous with the coast, it should be recorded as *drift ice*.

The most important thing in the coastal sea ice observation is the judgment of the presence of coastal leads, or whether *drift ice* is attached to the shore. While it is relatively easy to discriminate *fast ice* from *drift ice* at the beginning of the ice season, the judgment becomes difficult when *drift ice* gets stuck after becoming attached to the shore or when leads form offshore after becoming attached to the shore. In such cases, the offshore ice should be recorded as *drift ice* though the origin is unknown. However, sea ice which is grounded on the shore or remaining in the port after the ice pack retreats should be recorded as *fast ice*, not *drift ice*.

Table 5-6 Ice conditions along the coast (Report format: JM305)

Report code	Ice condition along the coast
0	No sea ice
1	Drift ice on the horizon.
2	Fast ice around the shore, while drift ice offshore separated by leads.
3	Leads along the shore and drift ice offshore.
4	Drift ice along the shore and no ice offshore.
5	Drift ice along the shore and another drift ice offshore separated by leads.
6	Drift ice attached to fast ice along the shore.

7	Drift ice mostly covering all the sea surface in sight.
8	Drift ice mostly approaching the port.
9	Drift ice entering the inside of the port.
/	Unknown
Remarks	(1) If more than two codes are fitting, the larger number should be selected. (2) Ice conditions are independent of ice amount and concentration. However, note that code 7 should be used for ice amount greater than 9.

3-7 Observation of the first and last dates of sea ice coverage

The observation of the first and last dates indicates the duration of ice coverage for the year. The definitions of the first and last dates of sea ice phenomena are as follows:

1. The first date of drift ice in sight

This is defined by the date when *drift ice* advected from offshore beyond the observation area first appears in sight in the ice season. This observation is not for when sea ice first forms in the observation area, or the first formation of *fast ice*.

2. The last date of drift ice in sight

This is defined by the last date when *drift ice* is found in sight within the observation area. *Drift ice* which remains offshore after the retreat of the ice pack should be taken into account, irrespective of ice amount. A small amount of ice floes remaining around the port or near the coast should be excluded.

3. The first date of drift ice attached to the shore

This is defined by the date when *drift ice* first becomes attached to the shore in the ice season, resulting in the closure of coastal lead for the ship navigation.

4. The first date of reopening of the coastal lead (“*Umiake*” in Japanese)

This is defined by the date when reopening of the sea along the coast allows a ship navigation along the shore, with total ice amount less than 5. In the case when *drift ice* gets attached to the shore again after the first formation of coastal lead and this state continues for more than 3 days, the next reopening date should be recorded as “*Umiake*”. In the case when the short-term (< 2 days) attachments of *drift ice* to the shore are repeated and the interval between attachments is less than 15 days, the reopening date after the final attachment period should be recorded as “*Umiake*”. On the other hand, in the case where there is no opening along the shore even if total ice amount is less than 5, the date should not be recorded as “*Umiake*”.

Since the sight range and the distance to the horizon are determined by the observation height, the observational results about the first and last dates of sea ice phenomena should not be recorded except when the observation is conducted at a fixed site. Furthermore, to determine the last date, the observation should be continued for several days even after sea ice coverage appears to end because sea ice coverage may occur again later in the ice season. Particularly when the last date is earlier than normal, monitoring should be continued until around the normal date.

3-8 Monthly observation sheet

In the monthly observation sheet, the following matters should be filled in, compiled and archived as the original data sources. A sample of the records is shown in Table 5-7. In the case where there is no sea ice, total ice amount should be recorded as “0” and the ice conditions as “-“.

1. Total ice amount is filled in according to the grades in Table 5-5. In the case of bad visibility, apparent ice amount should be filled in with parenthesis. When observation is difficult, “×” should be filled in.

2. The coastal ice condition section is filled in according to the transmitting codes listed in Table 5-6 (JM305). When observation is difficult due to bad visibility or other reasons, “×” should be filled in.

3. Remarks should be written when the first date of drift ice in sight or drift ice attached to the shore is observed or in the case where total ice amount is recorded as “×” or in parentheses.

4. The first and last dates of sea ice phenomena and the difference from the dates of the normal year and the previous year should be filled in.

5. General conditions are described briefly about the sea ice conditions during the month. In addition, when disasters related to sea ice have occurred, these should be described in the observation sheet.

Table 5-7. Monthly observation sheet for coastal sea ice observation

2004年2月

沿岸海水観測月表

定時観測 (09時)

○×地方気象台

日	全氷量	沿岸海水の分布状況	記 事
1	×	×	雪のため不明
2	5	3	
3	3	2	
4	10-	6	流水接岸初日
5	10-	7	
6	10-	7	
7	10-	7	
8	9	6	
9	10-	7	
10	6	3	
11	4	3	
12	5	3	
13	3	3	
14	10-	6	
15	×	×	雪のため不明
16	7	2	
17	10-	6	
18	10-	6	
19	10-	6	
20	10-	6	
21	10-	6	
22	7	2	
23	8	2	
24	10-	7	
25	10-	7	
26	(10)	(9)	雪のため視界内海面での観測
27	3	3	
28	0	—	
29	0	—	
30			
31			

海水現象初終日	平年差	昨年差
流水初日	1月23日	3日遅い
流水接岸初日	2月4日	12日早い
海明け	月 日	
流水終日	月 日	

概 況

月を通して流水に覆われた日が続いたが、月末には沖合いへ後退して流水は視界外へいった。

4. Sea ice nomenclature (cited from WMO (2014))

WMO SEA-ICE NOMENCLANTURE

TERMINOLOGY – VOLUME I

WMO/OMM/BMO - No.259 • Edition 1970 – 2014 note:English only

4-1. FLOATING ICE

Any form of ice found floating in water. The principal kinds of floating ice are *lake ice*, *river ice*, and *sea ice* which form by the freezing of water at the surface, and *glacier ice (ice of land origin)* formed on land or in an *ice shelf*. The concept includes ice that is stranded or grounded.

Sea ice:

Any form of ice found at sea which has originated from the freezing of sea water.

Fast ice:

Sea ice which forms and remains fast along the coast, where it is attached to the shore, to an *ice wall*, to an *ice front*, between shoals or grounded *icebergs*. Vertical fluctuations may be observed during changes of sea-level. *Fast ice* may be formed *in situ* from sea water or by freezing of *floating ice* of any age to the shore, and it may extend a few metres or several hundred kilometres from the coast. *Fast ice* may be more than one year old and may then be prefixed with the appropriate age category (*old*, *second-year*, or *multi-year*). If it is thicker than about 2 m above sea-level it is called an *ice shelf*.

Drift ice / pack ice:

Term used in a wide sense to include any area of *sea ice* other than *fast ice* no matter what form it takes or how it is disposed. When *concentrations* are high, i.e. 7/10 or more, *drift ice* may be replaced by the term *pack ice**

*Note: Previously the term pack ice was used for all ranges of concentration.

Ice of land origin:

Ice formed on land or in an *ice shelf*, found floating in water. The concept includes ice that is stranded or grounded.

Lake ice:

Ice formed on a lake, regardless of observed location.

River ice:

Ice formed on a river, regardless of observed location.

4-2. DEVELOPMENT

New ice:

A general term for recently formed ice which includes *frazil ice*, *grease ice*, *slush* and *shuga*. These types of ice are composed of ice crystals which are only weakly frozen together (if at all) and have a definite form only while they are afloat.

Frazil ice:

Fine spicules or plates of ice, suspended in water.

Grease ice:

A later stage of freezing than *frazil ice* when the crystals have coagulated to form a soupy layer on the surface. Grease ice reflects little light, giving the sea a matt appearance.

Slush:

Snow which is saturated and mixed with water on land or ice surfaces, or as a viscous floating mass in water after a heavy snowfall.

Shuga:

An accumulation of spongy white ice lumps, a few centimetres across; they are formed from *grease ice* or *slush* and sometimes from *anchor ice* rising to the surface.

Nilas:

A thin elastic crust of ice, easily bending on waves and swell and under pressure, thrusting in a pattern of interlocking “fingers” (*finger rafting*). Has a matt surface and is up to 10 cm in thickness. May be subdivided into *dark nilas* and *light nilas*.

Dark nilas: *Nilas* which is under 5 cm in thickness and is very dark in colour.

Light nilas:

Nilas which is more than 5 cm in thickness and rather lighter in colour than *dark nilas*.

Ice rind:

A brittle shiny crust of ice formed on a quiet surface by direct freezing or from *grease ice*, usually in water of low salinity. Thickness to about 5 cm. Easily broken by wind or swell, commonly breaking in rectangular pieces.

Pancake ice:

Predominantly circular pieces of ice from 30 cm - 3 m in diameter, and up to about 10 cm in thickness, with raised rims due to the pieces striking against one another. It may be formed on a slight swell from *grease ice*, *shuga* or *slush* or as a result of the breaking of *ice rind*, *nilas* or, under severe conditions of swell or waves, of *grey ice*. It also sometimes forms at some depth at an interface between water bodies of different physical characteristics, from where it floats to the surface; its appearance may rapidly cover wide areas of water.

Young ice:

Ice in the transition stage between *nilas* and *first-year ice*, 10-30 cm in thickness. May be subdivided into *grey ice* and *grey-white ice*.

Grey ice:

Young ice 10-15 cm thick. Less elastic than *nilas* and breaks on swell. Usually rafts under pressure.

Grey-white ice:

Young ice 15-30 cm thick. Under pressure more likely to ridge than to raft.

First-year ice:

Sea ice of not more than one winter's growth, developing from *young ice*; thickness 30 cm – 2 m. May be subdivided into *thin first-year ice* / white ice, *medium first-year ice* and *thick first-year ice*.

Thin first-year ice / white ice: *First-year ice* 30-70 cm thick.

Thin first-year ice / white ice first stage: 30-50 cm thick.

Thin first-year ice / white ice second stage: 50-70 cm thick.

Medium first-year ice: *First-year ice* 70-120 cm thick.

Thick first-year ice: *First-year ice* over 120 cm thick.

Old ice:

Sea ice which has survived at least one summer's melt; typical thickness up to 3m or more. Most topographic features are smoother than on *first-year ice*. May be subdivided into *residual*, *second-year ice* and *multi-year ice*.

Residual ice:

First-year ice that has survived the summer's melt and is now in the new cycle of growth. It is 30 to 180 cm thick depending on the region where it was in summer. After 1 January (in the Southern hemisphere after 1 July), this ice is called *second-year ice*.

Second-year ice:

Old ice which has survived only one summer's melt; typical thickness up to 2.5 m and sometimes more. Because it is thicker than *first-year ice*, it stands higher out of the water. In contrast to *multi-year ice*, summer melting produces a regular pattern of numerous small *puddles*. Bare patches and puddles are usually greenish-blue.

Multi-year ice:

Old ice up to 3 m or more thick which has survived at least two summers' melt. *Hummocks* even smoother than in *second-year ice*, and the ice is almost salt-free. Colour, where bare, is usually blue. Melt pattern consists of large interconnecting irregular *puddles* and a well-developed drainage system.

Development of lake ice:

Because of the absence of salt in the water, the freezing and growth processes of *lake ice* are considerably different from those of *sea ice*. Generally, *lake ice* forms and is destroyed more quickly than *sea ice*, is more brittle and harder than *sea ice*.

New lake ice: Recently formed *lake ice* less than 5 cm thick.

Thin lake ice: *Lake ice* that is 5-15 cm in thickness.

Medium lake ice: *Lake ice* that is 15-30 cm in thickness.

Thick lake ice: *Lake ice* that is 30-70 cm in thickness.

Very thick lake ice: *Lake ice* that is greater than 70 cm in thickness.

Snow Ice:

Ice formed by refreezing flooded snow creating an ice layer that bonds firmly to the top surface of a floe.

4-3. FORMS OF FAST ICE

Fast ice:

Sea ice which forms and remains fast along the coast, where it is attached to the shore, to an *ice wall*, to an ice front, between shoals or grounded *icebergs*. Vertical fluctuations may be observed during changes of sea-level. Fast ice may be formed *in situ* from sea water or by freezing of *floating ice* of any age to the shore, and it may extend a few metres or several hundred kilometres from the coast. Fast ice may be more than one year old and may then be prefixed with the appropriate age category (*old*, *second-year*, or *multi-year*). If it is thicker than about 2 m above sea-level it is called an *ice shelf*.

Young Coastal ice:

The initial stage of *fast ice* formation consisting of *nilas* or *young ice*, its width varying from a few metres up to 100-200 m from the shoreline.

Icefoot:

A narrow fringe of ice attached to the coast, unmoved by tides and remaining after the *fast ice* has moved away.

Anchor ice:

Submerged ice attached or anchored to the bottom, irrespective of the nature of its formation.

Grounded ice:

Floating ice which is aground in shoal water.

Stranded ice:

Ice which has been floating and has been deposited on the shore by retreating high water.

Grounded Hummock:

Hummocked *grounded ice* formation. There are single grounded *hummocks* and lines (or chains) of grounded *hummocks*.

4-4. OCCURRENCE OF FLOATING ICE**Ice cover:**

The ratio of an area of ice of any concentration to the total area of sea surface within some large geographic local; this local may be global, hemispheric, or prescribed by a specific oceanographic entity such as Baffin Bay or the Barents Sea.

Concentration:

The ratio expressed in tenths* describing the amount of the sea surface covered by ice as a fraction of the whole area being considered. Total *concentration* includes all stages of development that are present, partial *concentration* may refer to the amount of a particular stage or of a particular form of ice and represents only a part of the total.

*Note: In historical sea-ice data octas have been used by some countries.

Compact ice:

Floating ice in which the *concentration* is 10/10 and no water is visible.

Consolidated ice:

Floating ice in which the *concentration* is 10/10 and the *floes* are frozen together.

Very Close Ice:

Floating ice in which the *concentration* is 9/10 to less than 10/10.

Close ice:

Floating ice in which the *concentration* is 7/10 to 8/10, composed of *floes* mostly in contact.

Open ice:

Floating ice in which the ice *concentration* is 4/10 to 6/10, with many *leads* and *polynyas*, and the *floes* are generally not in contact with one another.

Very open ice:

Floating ice in which the *concentration* is 1/10 to 3/10 and water preponderates over ice.

Open water:

A large area of freely navigable water in which *sea ice* is present in *concentrations* less than 1/10. No *ice of land origin* is present.

Bergy water:

An area of freely navigable water in which *ice of land origin* is present in *concentrations* less than 1/10. There may be *sea ice* present, although the total *concentration* of all ice shall not exceed 1/10.

Ice-free:

No *sea ice* present. If ice of any kind is present this term should not be used.

Forms of floating ice**Pancake ice:**

Predominantly circular pieces of ice from 30 cm – 3 m in diameter, and up to about 10 cm in thickness, with raised rims due to the pieces striking against one another. It may be formed on a slight swell from *grease ice*, *shuga* or *slush* or as a result of the breaking of *ice rind*, *nilas* or, under severe conditions of swell or waves, of *grey ice*. It also sometimes forms at some depth, at an interface between water bodies of different physical characteristics, from where it floats to the surface; its appearance may rapidly cover wide areas of water.

Floe:

Any contiguous piece of *sea ice*. Floes are subdivided according to horizontal extent as follows:

Floe giant: Over 10 km across.

Floe vast: 2-10 km across.

Floe big: 500-2000 m across.

Floe medium: 100-500 m across.

Floe small: 20-100 m across.

Ice cake: Less than 20 m across.

Small ice cake: Less than 2 m across.

Cake ice:

Cake Ice is commonly used in Antarctica to refer to a collection of ice cakes. This should not be confused with *pancake ice*. Cake ice is older and thicker than *pancake ice*.

Floeberg:

A massive piece of *sea ice* composed of a *hummock*, or a group of *hummocks* frozen together, and separated from any ice surroundings. It may typically protrude up to 5 m above sea-level.

Floe-bit:

A relatively small piece of *sea ice*, normally not more than 10 m across composed of (a) *hummock(s)* or part of (a) *ridge(s)* frozen together and separated from any surroundings. It

typically protrudes up to 2 m above sea-level.

Ice breccia: Ice of different stages of development frozen together.

Brash ice:

Accumulations of *floating ice* made up of fragments not more than 2 m across, the wreckage of other forms of ice.

Iceberg:

A massive piece of ice of greatly varying shape, protruding more than 5 m above sea-level, which has broken away from a *glacier*, and which may be afloat or aground. Icebergs may be described as *tabular, dome-shaped, sloping, pinnacled, dry-docked, blocky, weathered* or *glacier bergs* in addition to having a size qualifier.

Glacier berg: An irregularly shaped *iceberg*

Tabular berg: A flat-topped *iceberg*. Most *tabular bergs* form by *calving* from an *ice shelf* and show horizontal banding (cf. *ice island*).

Domed iceberg: An iceberg which is smooth and rounded on top.

Sloping iceberg: An iceberg which is rather flat on top and with steep vertical sides on one end, sloping to lesser sides on the other end.

Pinnacled iceberg: An iceberg with a central spire or pyramid, with one or more spires.

Dry-docked iceberg: An iceberg which is eroded such that a U-shaped slot is formed near or at water level, with twin columns or pinnacles. This is also referred to as a twinned iceberg.

Blocky iceberg: A flat-topped iceberg with steep vertical sides.

Weathered iceberg: An iceberg that shows marked signs of deterioration from the effects of atmosphere and ocean.

Ice island: A large piece of floating ice protruding about 5 m above sea-level, which has broken away from an Arctic ice shelf, having a thickness of 30-50 m and an area of from a few thousand sq.m to 500 km² or more, and usually characterized by a regularly undulating surface which gives it a ribbed appearance from the air.

Ice island Fragment: Piece of an ice island that has broken away from the main mass.

Very large iceberg: A piece of glacier ice extending more than 75 m above sea level and with a length of more than 200 m.

Large iceberg: A piece of glacier ice extending 46 to 75 m above sea level and with a length of 121 to 200 m.

Medium iceberg: A piece of glacier ice extending 16 to 45 m above sea level and with a length of 61 to 120 m.

Small iceberg: A piece of glacier ice extending 5 to 15 m above sea level and with a length of 15 to 60 m.

Bergy bit: A large piece of floating *glacier ice*, generally showing less than 5 m above sea-level but more than 1 m and normally about 100-300 m² in area.

Growler: Piece of ice smaller than a *bergy bit* and *floating* less than 1 m above the sea surface, a growler generally appears white but sometimes transparent or blue-green in colour. Extending less than 1 m above the sea surface and normally occupying an area of about 20 m², growlers are difficult to distinguish when surrounded by sea ice or in high sea state.

Arrangement

Ice field: Area of *floating ice* consisting of any size of *floes*, which is greater than 10 km across (cf. *patch*).

Large ice field: An *ice field* over 20 km across.

Medium ice field: An *ice field* 15-20 km across.

Small ice field: An *ice field* 10-15 km across.

Ice patch: An area of *floating ice* less than 10 km across.

Ice massif: A variable accumulation of *close* or *very close ice* covering hundreds of square kilometers which is found in the same region every summer.

Belt: A large feature of *drift ice* arrangement; longer than it is wide; from 1 km to more than 100 km in width.

Tongue: A projection of the *ice edge* up to several kilometers in length, caused by wind or current.

Strip: Long narrow area of *floating ice*, about 1 km or less in width, usually composed of small fragments detached from the main mass of ice, and run together under the influence of wind, swell or current.

Ice isthmus: A narrow connection between two ice areas of *very close* or *compact ice*. It may be difficult to pass, whilst sometimes being part of a recommended route.

Bight: An extensive crescent-shaped indentation in the *ice edge*, formed by either wind or current.

Ice jam: An accumulation of broken *river ice* or *sea ice* not moving due to some physical restriction and resisting to pressure.

Ice edge: The demarcation at any given time between the open sea and *sea ice* of any kind, whether fast or drifting. It may be termed *compacted* or *diffuse* (cf. *ice boundary*).

Compacted ice edge: Close, clear-cut *ice edge* compacted by wind or current; usually on the windward side of an area of *drift ice*.

Jammed brash barrier:

A strip or narrow belt of *new, young* or *brash ice* (usually 100-5000 m wide) formed at the edge of either *drift* or *fast ice* or at the shore. It is heavily compacted mostly due to wind action and may extend 2 to 20 m below the surface but does not normally have appreciable topography. *Jammed brash barrier* may disperse with changing winds but can also consolidate

to form a strip of unusually thick ice in comparison with the surrounding *drift ice*. This is also known as a windrow in the Baltic Sea.

Diffuse ice edge: Poorly defined *ice edge* limiting an area of dispersed ice; usually on the leeward side of an area of *drift ice*.

Ice limit: Climatological term referring to the extreme minimum or extreme maximum extent of the *ice edge* in any given month or period based on observations over a number of years. Term should be preceded by minimum or maximum (cf. *mean ice edge*).

Mean ice edge: Average position of the *ice edge* in any given month or period based on observations over a number of years. Other terms which may be used are mean maximum *ice edge* and mean minimum *ice edge* (cf. *ice limit* and *median ice edge*).

Median ice edge: Median (50% occurrence) position of the *ice edge* in any period based on a sufficient number of observations (cf. *ice limit* and *mean ice edge*)

Fast-ice edge:

The demarcation at any given time between *fast ice* and *open water*.

Ice boundary: The demarcation at any given time between *fast ice* and *drift ice* or between areas of *drift ice* of different *concentrations* (cf. *ice edge*).

Fast ice boundary:

The ice boundary at any given time between *fast ice* and *drift ice*.

Concentration boundary:

A line approximating the transition between two areas of *drift ice* with distinctly different *concentrations*.

Iceberg tongue: A major accumulation of *icebergs* projecting from the coast, held in place by grounding and joined together by *fast ice*.

Marginal Ice Zone: The region of an ice cover which is affected by waves and swell penetrating into the ice from the open ocean.

4-5. FLOATING-ICE MOTION PROCESSES

Diverging:

Ice fields or *floes* in an area are subjected to diverging or dispersive motion, thus reducing ice concentration and/or relieving stresses in the ice.

Compacting:

Pieces of *floating ice* are said to be compacting when they are subjected to a converging motion, which increases ice *concentration* and/or produces stresses which may result in ice deformation.

Shearing:

An area of *drift ice* is subject to shear when the ice motion varies significantly in the direction normal

to the motion, subjecting the ice to rotational forces. These forces may result in phenomena similar to a *flaw* (q.v.).

4-6. DEFORMATION PROCESSES

Fracturing:

Pressure process whereby ice is permanently deformed, and rupture occurs. Most commonly used to describe breaking across *very close ice*, *compact ice* and *consolidated ice*.

Hummocking:

The pressure process by which *sea ice* is forced into *hummocks*. When the *floes* rotate in the process it is termed screwing.

Ridging:

The pressure process by which *sea ice* is forced into *ridges*.

Rafting:

Pressure processes whereby one piece of ice overrides another. Most common in *new* and *young ice* (cf. *finger rafting*).

Finger rafting: Type of rafting whereby interlocking thrusts are formed like “fingers” alternately over and under the other. This is commonly found in *nilas* and in *grey ice*. (It was noted that finger rafting in *grey ice* is common in Antarctica).

Shore ice ride-up: A process by which ice is pushed ashore as a slab.

Weathering:

Processes of ablation and accumulation which gradually eliminate irregularities in an ice surface.

4-7. OPENINGS IN THE ICE

Fracture:

Any break or rupture through *very close ice*, *compact ice*, *consolidated ice*, *fast ice*, or a single *floe* resulting from deformation processes. Fractures may contain *brash ice* and/or be covered with *nilas* and/or *young ice*. Length may vary from a few meters to many kilometers.

Crack: Any *fracture of fast ice*, *consolidated ice* or a single *floe* which may have been followed by separation ranging from a few centimeters to 1 m.

Tide crack: Crack at the line of junction between an immovable *ice foot* or *ice wall* and *fast ice*, the latter subject to rise and fall of the tide.

Flaw: A narrow separation zone between *drift ice* and *fast ice*, where the pieces of ice are in chaotic state; it forms when *drift ice* shears under the effect of a strong wind or current along the *fast ice boundary* (cf. *shearing*).

Very small fracture: 1 to 50 m wide.

Small fracture: 50 to 200 m wide.

Medium fracture: 200 to 500 m wide.

Large fracture: More than 500 m wide.

Fracture zone:

An area which has a great number of *fractures*.

Fractures concentration: Degree of disunity in an ice area.

Lead:

Any *fracture* or passage-way through *sea ice* which is navigable by surface vessels.

Shore lead:

A lead between *drift ice* and the shore or between *drift ice* and an *ice front*.

Flaw lead:

A passage-way between *drift ice* and *fast ice* which is navigable by surface vessels.

Polynya:

Any non-linear shaped opening enclosed in ice. *Polynyas* may contain *brash ice* and/or be covered with *new ice*, *nilas* or *young ice*.

Shore polynya:

A *polynya* between *drift ice* and the coast or between *drift ice* and an *ice front*.

Flaw polynya: A *polynya* between *drift ice* and *fast ice*.

Recurring polynya: A *polynya*, which recurs in the same position every year.

4-8. ICE-SURFACE FEATURES

Level ice: *Sea ice* which has not been affected by deformation.

Deformed ice:

A general term for ice which has been squeezed together and in places forced upwards (and downwards). Subdivisions are *rafted ice*, *ridged ice* and *hummocked ice*.

Rafted ice:

Type of *deformed ice* formed by one piece of ice overriding another (cf. *finger rafting*).

Ice rafting concentration:

Concentration (aerial coverage) of ice rafting in an ice area in tenths.

Finger rafted ice:

Type of *rafted ice* in which *floes* thrust 'fingers' alternately over and under the other.

Ridge:

A line or wall of broken ice forced up by *pressure*. May be fresh or weathered. The submerged volume of broken ice under a *ridge*, forced downwards by pressure, is termed an *ice keel*.

New ridge:

Ridge newly formed with sharp peaks and slope of sides usually 40°. Fragments are visible from the air at low altitude.

Weathered ridge:

Ridge with peaks slightly rounded and slope of sides usually 30° to 40°.

Individual fragments are not discernible.

Very weathered ridge:

Ridge with tops very rounded, slope of sides usually 20°-30°.

Aged ridge:

Ridge which has undergone considerable weathering. These *ridges* are best described as undulations.

Consolidated ridge: A *ridge* in which the base has frozen together.

Ridged ice:

Ice piled haphazardly one piece over another in the form of ridges or walls. Usually found in *first-year ice* (cf. *ridging*).

Ridged ice zone:

An area in which much *ridged ice* with similar characteristics has formed.

Shear ridge:

An *ice ridge* formation which develops when one ice feature is grinding past another. This type of *ridge* is more linear than those caused by pressure alone.

Shear ridge field: Many *shear ridges* side by side.

Hummock:

A hillock of broken ice which has been forced upwards by pressure. May be fresh or weathered. The submerged volume of broken ice under the *hummock*, forced downwards by pressure, is termed a *bummock*.

Ice ridge concentration:

Concentration (aerial coverage) of hummocked ice of all kinds in an ice area in tenths. Up to three

values may be given to correspond to the partial concentrations.

Hummocked ice:

Sea ice piled haphazardly one piece over another to form an uneven surface. When weathered, has the appearance of smooth hillocks.

Rubble field:

An area of extremely deformed sea ice of unusual thickness formed during the winter by the motion of drift ice against, or around a protruding rock, islet or other obstruction.

Standing floe: A separate *floe* standing vertically or inclined and enclosed by rather smooth ice.

Ram:

An underwater ice projection from an *ice wall*, *ice front*, *iceberg* or *floe*. Its formation is usually due to a more intensive melting and erosion of the unsubmerged part.

Bare ice: Ice without snow cover.

Snow-covered ice: Ice covered with snow.

Snow cover concentration:

Concentration (aerial coverage) of snow-covered ice in an ice area in tenths.

Sastrugi:

Sharp, irregular *ridges* formed on a snow surface by wind erosion and deposition. On *drift ice* the *ridges* are parallel to the direction of the prevailing wind at the time they were formed.

Snowdrift:

An accumulation of wind-blown snow deposited in the lee of obstructions or heaped by wind eddies. A crescent-shaped *snowdrift*, with ends pointing down-wind, is known as a snow barchan.

Dirty ice:

Ice that has a mineral or organic content of natural or anthropogenic origin on the surface or in its strata.

Frost flowers:

A growth of ice crystals by condensation from the atmosphere at points on the surface of *young ice*. After formation, sea water may be drawn through the ice into the flowers. These delicate, highly saline crystals effectively roughen the surface, often dramatically altering the appearance of sea ice in microwave remote sensing imagery.

4-9. STAGES OF MELTING

Puddle:

An accumulation on ice of melt-water, mainly due to melting snow, but in the more advanced stages also to the melting of ice. Initial stage consists of patches of melted snow.

Thaw holes:

Vertical holes in *sea ice* formed when surface *puddles* melt through to the underlying water.

Dried ice:

Sea ice from the surface of which melt-water has disappeared after the formation of *cracks* and *thaw holes*. During the period of drying, the surface whitens.

Rotten ice:

Sea ice which has become honeycombed and which is in an advanced state of disintegration.

Flooded ice:

Sea ice which has been flooded by melt-water or river water and is heavily loaded by water and wet snow.

Shore melt:

Open water between the shore and the *fast ice*, formed by melting and/or as a result of river discharge.

4-10. ICE OF LAND ORIGIN

Firn:

Old snow which has recrystallized into a dense material. Unlike ordinary snow, the particles are to some extent joined together; but, unlike ice, the air spaces in it still connect with each other.

Glacier ice:

Ice in, or originating from, a *glacier*, whether on land or floating on the sea as *icebergs*, *bergy bits* or *growlers*.

Glacier:

A mass of snow and ice continuously moving from higher to lower ground or, if afloat, continuously spreading. The principal forms of glacier are: inland ice sheets, *ice shelves*, *ice streams*, ice caps, ice piedmonts, cirque glaciers and various types of mountain (valley) glaciers.

Ice wall:

An ice cliff forming the seaward margin of a *glacier* which is not afloat. An ice wall is aground, the rock basement being at or below *sea-level* (cf. *ice front*).

Ice stream:

Part of an inland ice sheet in which the ice flows more rapidly and not necessarily in the same direction as the surrounding ice. The margins are sometimes clearly marked by a change in direction of the surface slope but may be indistinct.

Glacier tongue:

Projecting seaward extension of a *glacier*, usually afloat. In the Antarctic, *glacier tongues* may extend over many tens of kilometers.

Ice shelf:

A floating ice sheet of considerable thickness showing 2-50 m or more above sea-level, attached to the coast. Usually of great horizontal extent and with a level or gently undulating surface. Nourished by annual snow accumulation and often also by the seaward extension of land *glaciers*. Limited areas may be aground. The seaward edge is termed an *ice front*.

Ice front:

The vertical cliff forming the seaward face of an *ice shelf* or other floating *glacier* varying in height from 2-50 m or more above sea-level (cf. *ice wall*).

Calved ice of land origin

Calving: The breaking away of a mass of ice from an *ice wall*, *ice front* or *iceberg*.

Iceberg: A massive piece of ice of greatly varying shape, protruding more than 5 m above sea-level, which has broken away from a *glacier*, and which may be afloat or aground. Icebergs may be described as *tabular*, dome-shaped, sloping, pinnacled, weathered or *glacier bergs*.

Glacier berg: An irregularly shaped *iceberg*.

Tabular berg: A flat-topped *iceberg*. Most *tabular bergs* form by *calving* from an *ice shelf* and show horizontal banding (cf. *ice island*).

Iceberg tongue: A major accumulation of *icebergs* projecting from the coast, held in place by grounding and joined together by *fast ice*.

Ice island:

A large piece of floating ice protruding about 5 m above sea-level, which has broken away from an Arctic ice shelf, having a thickness of 30-50 m and an area of from a few thousand sq.m to 500 km² or more, and usually characterized by a regularly undulating surface which gives it a ribbed appearance from the air.

Bergy bit:

A large piece of floating *glacier ice*, generally showing less than 5 m above sea-level but more than 1 m and normally about 100-300 m² in area.

Growler:

Piece of ice smaller than a *bergy bit* and floating less than 1 m above the sea surface, a growler generally appears white but sometimes transparent or blue-green in colour. Extending less than 1 m above the sea surface and normally occupying an area of about 20 m², growlers are difficult to distinguish when surrounded by sea ice or in high sea state.

4-11. SKY AND AIR INDICATIONS

Water sky:

Dark streaks on the underside of low clouds, indicating the presence of water features in the vicinity of *sea ice*.

Ice blink:

A whitish glare on low clouds above an accumulation of distant ice.

Frost smoke:

Fog-like clouds due to contact of cold air with relatively warm water, which can appear over openings in the ice, or leeward of the *ice edge*, and which may persist while ice is forming.

4-12. TERMS RELATING TO SURFACE SHIPPING

Beset: Situation of a vessel surrounded by ice and unable to move.

Ice-bound:

A harbour, inlet, etc. is said to be *ice-bound* when navigation by ships is prevented on account of ice, except possibly with the assistance of an icebreaker.

Nip:

Ice is said to *nip* when it forcibly presses against a ship. A vessel so caught, though undamaged, is said to have been nipped.

Ice under pressure:

Ice in which deformation processes are actively occurring and hence a potential impediment or danger to shipping.

Difficult area:

A general qualitative expression to indicate, in a relative manner, that the severity of ice conditions prevailing in an area is such that navigation in it is difficult.

Easy area:

A general qualitative expression to indicate in a relative manner, that ice conditions prevailing in an area are such that navigation in it is not difficult.

Area of weakness:

A satellite-observed area in which either the ice *concentration* or the ice thickness is significantly less than that in the surrounding areas. Because the condition is satellite observed, a precise quantitative analysis is not always possible, but navigation conditions are significantly easier than in surrounding areas.

Ice port:

An embayment in an *ice front*, often of a temporary nature, where ships can moor alongside and unload directly onto the *ice shelf*.

4-13. TERMS RELATING TO SUBMARINE NAVIGATION

Ice canopy: *Drift ice* from the point of view of the submariner.

Friendly ice:

From the point of view of the submariner, an *ice canopy* containing many large *skylights* or other features which permit a submarine to surface. There must be more than ten such features per 30 nautical miles (56 km) along the submarine's track.

Hostile ice:

From the point of view of the submariner, an *ice canopy* containing no large *skylights* or other features which permit a submarine to surface.

Bummock:

From the point of view of the submariner, a downward projection from the underside of the *ice canopy*; the counterpart of a *hummock*.

Ice keel:

From the point of view of the submariner, a downward-projecting *ridge* on the underside of the *ice canopy*; the counterpart of a *ridge*. *Ice keels* may extend as much as 50 m below sea-level.

Skylight:

From the point of view of the submariner, thin places in the *ice canopy*, usually less than 1 m thick and appearing from below as relatively light, translucent patches in dark surroundings. The undersurface of a *skylight* is normally flat. *Skylights* are called large if big enough for a submarine to attempt to surface through them (120 m), or small if not.

Acknowledgements:

The author thanks Dr. Anthony Worby (ACE CRC, Australia) for permitting citation of the ASPeCt manual, Dr. Jennifer Hutchings (Oregon State Univ., USA) for providing valuable information on the ASSIST protocol for Arctic sea ice, Dr. Motoyo Itoh (JAMSTEC) and Dr. Kazutaka Tateyama (Kitami Institute of Technology) for information on sea ice observation in the Arctic Ocean, Prof. Christian Haas (Alfred Wegener Institute) for information on the electromagnetic induction method, Mr. Hiroki Kodama and Mr. Masato Ichikawa (Sapporo District Meteorological Observatory, JMA) for offering the manuals for observation of coastal ice conditions published by the Japan Meteorological Agency, Dr. Alexander Fraser (Univ. of Tasmania) for proof reading, and Ms. Eriko Ishikawa (Hokkaido Univ.) for typing the text. The author would like to take this opportunity to express his sincere thanks to the aforementioned people.

Reference

- Allison, I., R.E. Brandt, and S.G. Warren (1993): East Antarctic sea ice: albedo, thickness, distribution, and snow cover. *Journal of Geophysical Research*, 98(C7), 12,417-12,429.
- Brandt, R.E., S.G. Warren, A.P. Worby, T.C. Grenfell (2005): Surface albedo of the Antarctic sea ice zone. *Journal of Climate*, 18, 3606-3622.
- Buynitskiy, V.K. (1967): Structure, principal properties, and strength of Antarctic sea ice. *Sov. Antarct. Exped. Inform. Bull.*, 65, 504-510.
- Dierking, W. (1995): Laser profiling of the ice surface topography during the Winter Weddell Gyre Study 1992. *Journal of Geophysical Research*, 100(C3), 4807-4820.
- Haas, C. (1998). Evaluation of ship-based electromagnetic-inductive thickness measurements of summer sea-ice in the Bellingshausen and Amundsen Seas, Antarctica. *Cold Regions Science and Technology*, 27, 1-16.
- Hibler, W.D., III, S.J. Mock, and W.B. Tucker, III (1974): Classification and variation of sea ice ridging in the western Arctic Basin, *Journal of Geophysical Research*, 79(18), 2735-2743.
- Japan Meteorological Agency (2004): Coastal sea ice observation. In “Guideline for the oceanographical observation”, 21-26. (in Japanese)
- Lange, M.A., and H. Eicken (1991): The sea ice thickness distribution in the Northwestern Weddell Sea. *Journal of Geophysical Research*. 96(C3), 4821-4837.
- Ohshima, K.I., S. Ushio, and A. Otsuki (2006): Sea-ice monitoring by ship-based visual observation during JARE –Simplification of observation method based on the ASPeCt protocol-. *The Nankyoku Shiryo (Antarctic Record)*, 50(3), 304-316. (in Japanese with English summary)
- Timmermann, R., A. Beckmann, and H.H. Hellmer (2002): Simulations of ice-ocean dynamics in the Weddell Sea. I: Model configuration and validation. *Journal of Geophysical Research*, 107(C3), 3024, DOI: 10.1029/2000JC000741.
- Toyota, T., S. Takatsuji, K. Tateyama, K. Naoki, K.I. Ohshima (2007): Properties of sea ice and overlying snow in the southern Sea of Okhotsk. *Journal of Oceanography*, 63, 393-411.
- Tucker, W.B., III, and J.W. Govoni (1981): Morphological investigations of first-year sea ice pressure ridge sails. *Cold Regions Science and Technology*, 5, 1-12.
- Uto, S., T. Toyota, H. Shimoda, K. Tateyama, and K. Shirasawa (2006). Ship-borne electromagnetic induction sounding of sea-ice thickness in the southern Sea of Okhotsk. *Annals of Glaciology*, 44, 253-260.
- Wadhams, P., M.A. Lange, and S.F. Ackley (1987): The ice thickness distribution across the Atlantic sector of the Antarctic Ocean in midwinter. *Journal of Geophysical Research*, 92(C13), 14,535-14,552.
- World Meteorological Organization (1970): Sea-ice nomenclature: Terminology, Codes, and Illustrated Glossary, WMO/OMM/BMO 259, TP 145, World Meteorological Organization, Geneva, Switzerland.
- World Meteorological Organization (2014): Sea-ice nomenclature: Terminology, WMO No.259, Volume 1, World Meteorological Organization, Geneva, Switzerland.

- Worby, A.P., and I. Allison (1991): Ocean-atmosphere energy exchange over thin, variable concentration Antarctic pack-ice, *Annals of Glaciology*, 15, 184-190.
- Worby, A.P., and H. Eicken (2009): Ship-based ice observation programs. In “Field techniques for sea ice research” edited by H. Eicken, R. Gradinger, M. Salganek, K. Shirasawa, D. Perovich, and M. Lepparanta, 565 pp., University of Alaska Press, Fairbanks, USA.
- Worby, A.P., M.O. Jeffries, W.F. Weeks, K. Morris, and R. Jana (1996): The thickness distribution of sea ice and snow cover during late winter in the Bellingshausen and Amundsen Seas, Antarctica. *Journal of Geophysical Research*, 101(C12), 28,441-28,455.
- Worby, A.P., and I. Allison, A technique for making ship-based observations of Antarctic sea ice thickness and characteristics: Part I. Observational technique and results, Res. Rep. 14, pp. 1-23, *Antarct. Coop. Res. Cent.*, Univ. of Tasmania, Australia.
- Worby, A.P., C.A. Geiger, M.J. Paget, M.L. Van Woert, S.F. Ackley, and T.L. DeLiberty (2008): Thickness distribution of Antarctic sea ice. *Journal of Geophysical Research*, 113, C05S92, doi:10.1029/2007JC004254.

Appendix: sea ice photo samples

Frazil ice



(Sea of Okhotsk)

Nilas



(Sea of Okhotsk)

Grease ice



(Sea of Okhotsk)

Shuga



(Sea of Okhotsk)

Pancake ice



(Sea of Okhotsk)



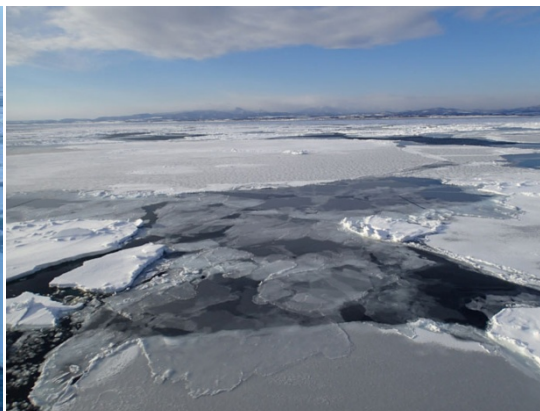
(off East Antarctica)

Snow covered first-year ice



(Sea of Okhotsk)

Nilas & Young ice



(Sea of Okhotsk)

Small floe



(Sea of Okhotsk)

Vast floe



(Weddell Sea)

Ridge



(Weddell Sea)



(Sea of Okhotsk)

Puddle



(Arctic Ocean)

Thaw holes



(Arctic Ocean)

Iceberg



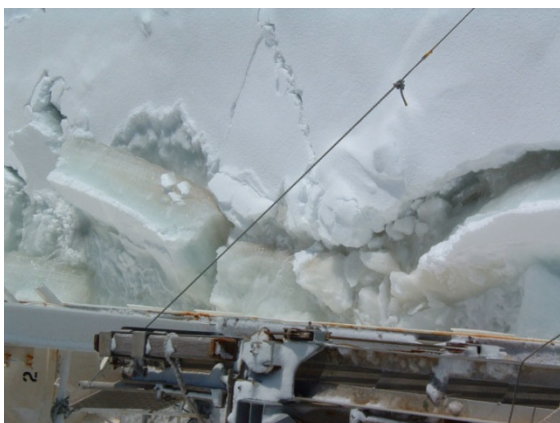
(Weddell Sea)

Characteristic surface snow pattern (Dune)



(Off East Antarctica)

Ice algae



(Sea of Okhotsk)

Frost flowers



(Off East Antarctica)

The photos in the Sea of Okhotsk were taken with the support of P/V “Soya”.

This page left intentionally blank.

Indirect radiation and aerosol optical thickness

○Mitsuhiko TORATANI (Tokai University), Hiroshi KOBAYASHI (University of Yamanashi)

1. Photosynthetically active radiation (PAR) and Solar radiation

1.1 Photosynthetically active radiation

Photosynthetically active radiation (PAR or E_{PAR}) was defined by Mobley (1994).

$$PAR \equiv \int_{350\text{nm}}^{700\text{nm}} \frac{\lambda}{hc} E_0(\lambda) d\lambda \quad (1)$$

where

$E_0(\lambda)$: scalar irradiance

λ : wavelength

h : Planck's constant (6.626×10^{-34} Js)

c : light velocity (2.99×10^8 m s⁻¹).

The unit of PAR is photons s⁻¹ m⁻² or Ein s⁻¹ m⁻². 1 Ein is 1 mol photons (6.023×10^{23} photons). In some cases, “photons” was described as “quanta”, and those are same.

Shipboard observation of PAR generally uses quantum meter such as LI-190. PAR is often estimated using only the visible wavelengths, 400-700 nm. Omission of the near-UV band is usually permissible since wavelengths less than 400 nm are rapidly absorbed near the water surface, except in very clear waters (Mobley, 1994).

-Observation

The instrument should be set on the deck to prevent shadow from some structures.

In order to adhere sea salt, soot of flue gas etc., the sensor surface should be cleaned regularly.

-Data averaging

Before the time averaging, spike noises of the data should be removed, and fluctuations of the baseline voltage of the quantum meter caused by the power supply and the sensor itself should be checked and corrected.

The daily PAR can be obtained by the time integration for one day.

For the data of JAMSTEC (Japan Agency for Marine-earth Science and Technology), ten minutes average of PAR is conducted because it is easier to integrate with other meteorological data. The time is not thirty or one hour in order to avoid missing of the small time and space scale weather phenomenon during the ship move.

-Sensor calibration

Calibration of the sensor should be conducted at the proper intervals.

1.2 *Global solar radiation*

Solar radiation is energy that reaches the ground while solar radiation is absorbed and scattered in the atmosphere, and is observed at wavelengths from 0.29 to 3.0 μm . Between these wavelengths, it accounts for about 97% of the total energy of solar energy. The total solar radiation amount is the sum of solar radiation that reaches the ground surface directly from the sun and solar radiation that reaches the ground surface from various directions due to scattering.

Global solar radiation is observed as the irradiance received by the horizontal plane by the pyrheliometer. Unit of the amount of solar radiation is W m^{-2} .

Details of the amount of solar radiation, the pyranometer, and the observation error of the pyranometer are described in the “Meteorological Observation Guide (in Japanese)” published on the web (Japan Meteorological Agency, 1998).

-Observation

The instrument should be set on the deck to prevent shadow from some structures.

In order to adhere sea salt, soot of flue gas etc., the sensor surface should be cleaned regularly.

-Data averaging

Before the time averaging, spike noises of the data should be removed, and fluctuations of the baseline voltage of the quantum meter caused by the power supply and the sensor itself should be checked and corrected.

The weak current corresponding to about 5~10 W m^{-2} can be recorded over a few days, even the solar radiation should be 0 W m^{-2} at night. The solar radiation at night, before the sunrise and after the sunset, should be corrected to check the occurrence and the magnitude of the night noise.

For the observation of JAMSTEC R/V Mirai, a 10-minute average value is created. To create a 10-minute average, first calculate the 2-minute average. The reason for setting the minimum time to a 2-minute average value is to earn a sample number of 10 samples or more. Since the recording interval is over 6 seconds, that is, less than 10 samples per minute because of recording in synchronization with other instruments, the average is 2 minutes. However, since the short-time fluctuation still remains in the 2-minute average value, the 10-minute average value is created. If the average time is set to 30 minutes or 1 hour, there is a possibility that a weather phenomenon with a short time and space scale may be missed when the ship is moving.

-Sensor calibration

Calibration of the sensor should be conducted at the proper intervals.

1.3 Conversion from global solar radiation to PAR

In order to estimate photosynthetically active radiation (PAR) from the optical observations, it requires the integration for wavelength. However, the pyranometer data does not contain the information for each wavelength. Therefore, conversion from global solar radiation to PAR has been proposed.

$$\text{PAR in water} = \text{global solar radiation} \times \text{wavelength correction coefficient} \\ \times \text{sea surface correction factor}$$

The wavelength correction coefficient corrects the difference in the wavelength range (PAR: 400 to 700 nm with respect to the global solar radiation: about 0.3 to 3.0 μm). Akitsu et al. (2015) reported that the ratio of global solar radiation to 400-700 nm solar radiation on the ground surface varies with weather conditions and is 0.4-0.5. It is also reported as 0.45 by Meek et al. (1984). Therefore, 0.45 is considered appropriate for simple conversion.

The correction factor for sea surface effect (photosynthesis effective radiation amount reaching the water from the sea surface) is the following value according to Morel and Smith (1974).

$$2.5 \times 10^{18} \text{ photons s}^{-1} \text{ W}^{-1} \quad (\text{Unit: photons s}^{-1} \text{ m}^{-2})$$

This value is divided by the Avogadro number (6.023×10^{23}), it can be converted to Ein.

$$4.2 \mu\text{Ein s}^{-1} \text{ W}^{-1} \quad (\text{Unit: Ein s}^{-1} \text{ m}^{-2})$$

Morel and Smith (1974) found that over a wide variety of water types from very clear to turbid, the conversion factor for energy to photons varies by only $\pm 10\%$ about the value

2. Sunphotometer observation

The sunphotometer is used to observe the sky condition on the ship. Sunphotometer data is used to estimate the amount of ozone concentration, optical thickness of the aerosol and water vapor from the difference between the extraterrestrial solar irradiance and the solar irradiance on the sea.

The Sunphotometer and its characteristics are described in detail in the “Technical Report on Calibration of Radiological Observation Instruments (in Japanese)” (Working Group on Calibration of Radiological Observation Instruments, 2015).

Sunphotometer is a compact measuring device on the handheld. We describe Microtops II sunphotometer. It can be measured five wavelengths. Thus, depending on what you want to measure (ozone, aerosols, water vapor), wavelength set is different.

Table 1 Observed object and wavelength set

Observed object	Wavelength set (nm)
Ozone (DOBSON UNIT)	305.5, 312.5, 320
Water vapor	870, 936, 1020
Optical thickness of the aerosol	340, 380, 440, 500, 675, 870, 936, 1020

2.1. Measurement of the optical thickness of aerosol by Sunphotometer

The direct solar light penetrates through the atmosphere to the ground surface while it attenuates to be absorbed and scatters by air molecules and aerosols. The spectral direct solar light intensity at the surface $I(\lambda)$ is expressed as follows,

$$I(\lambda) = I_0(\lambda) \exp(-(\tau_a(\lambda) + \tau_o(\lambda) + \tau_r(\lambda))m) \quad (2)$$

where $I_0(\lambda)$: Spectral extraterrestrial solar irradiance in average distance between Sun and the Earth
(It is pre-set in the device.)

$\tau_a(\lambda)$: Aerosol optical thickness,

$\tau_o(\lambda)$: Optical thickness of ozone absorption

$\tau_r(\lambda)$: Rayleigh scattering optical thickness of air molecules

m : airmass

The $\tau_a(\lambda)$ is calculated from $I(\lambda)$ of under way observation.

The optical thickness is a value obtained by integrating the extinction coefficient, which is the sum of the scattering coefficient and the absorption coefficient, in the vertical direction. In other words, the aerosol optical thickness is the total amount of aerosol in a column expressed by the degree to light attenuation. Therefore, it depends on the aerosol amount itself, but it varies depending on its scattering and absorption characteristics, which is different from mass concentration and number concentration.

2.2. Observation procedure of aerosol optical thickness with sun photometer

The observation procedure is explained based on the NASA protocol for Microtop2 (Knobelspiess et al., 2003).

Preparation for observation

1. Turn on the main unit and warm up.
2. Start up GPS and check reception. When you can receive with good accuracy (Accuracy is less than 5 m), connect GPS to the main unit with a cable. The connection is completed when you hear a beep. When the ship is moving, keep the GPS connection.

Observation

3. Turn off the power once and turn it on immediately. (Dark current is measured only just after the power is turned on.)
Record the temperature at the start of the observation.
4. Open the cover and track the sun. When the sun is catch, press Scan / Escape button to start measurement. Immediately after the measurement is completed, press Scan / Escape button to start the next measurement. Repeat four times for a total of five measurements.
5. Since the optical axes of each sensor may not be aligned, it is recommended to slightly shake the instrument.

6. After the measurement is completed five times, turn off the power and turn it on immediately. (Dark current measurement)
7. Repeat at least 20 measurements per observation. This means four sets of five sequential measurements.
8. If the window is dirty or dusty, blow air and gently wipe it with a Kimwipe®.
9. Record the ship's barometer value.

The photo sensor inside the Sun Photometer is affected by temperature fluctuation. In order to reduce the influence of temperature fluctuation during observation, turn on the power every five times and measure the dark current. In the default setting of the Sun Photometer, one measurement (press Scan / Escape button) is recorded 15 raw signals, and the maximum value is stored (Scan length: 15, Number of averaged samples: 1). It is not necessary to change the initial setting.

It is necessary to change the internal filter setting according to the power frequency of the ship. Change “Line frequency” to 60 or 50 Hz according to the power frequency of the ship. This is to prevent the noise of the ship power from the A / D converter.

The aerosol optical thickness is calculated by subtracting the optical thickness of the air molecules and ozone absorption from the total optical thickness. The optical thickness of the air molecules is calculated by obtaining the atmospheric pressure from a sensor inside the sun photometer, however the ship's barometer is more accurate for the atmospheric pressure. Therefore, a method for calculating the aerosol optical thickness by calculating the optical thickness of the air molecule based on the barometric pressure of the ship's barometer will be described.

2.3. Calculation of aerosol optical thickness

- 1) The optical thickness of the aerosol is derived from Eq. (3).

$$\tau_a(\lambda) = \frac{\ln\left(\frac{I_0(\lambda)}{I_r(\lambda)}\right)}{m} - (\tau_o(\lambda) + \tau_r(\lambda)) \quad (3)$$

Where the extraterrestrial solar irradiance $I_0(\lambda)$ (W m^{-2}) is obtained by multiplying the extraterrestrial solar irradiance of mean distance between solar and earth ($F_0(\lambda)$) and coefficient of distance between solar and earth (S). S is the function of the distance the day of year (DOY).

$$I_0(\lambda) = F_0(\lambda) \cdot S \quad (4)$$

$$S = 1 + 0.034 \cos\left(2\pi \frac{\text{DOY}}{365}\right) \quad (5)$$

- 2) The airmass m is calculated from Eq. (6). θ_0 is the solar zenith angle which is the angle between the zenith and the sun, and is determined by 90° -solar altitude ($^\circ$). The solar altitude of the measurement date and time can be obtained from the National Astronomical Observatory of Japan (NAOJ) web

(<http://eco.mtk.nao.ac.jp/cgi-bin/koyomi/koyomix.cgi>) or NOAA Solar Position Calculator (<https://www.esrl.noaa.gov/gmd/grad/solcalc/azel.html>).

$$m = \frac{1}{\cos\left(\frac{\pi}{180}\theta_0\right) + 0.15(93.885 - \theta_0)^{-1.253}} \quad (6)$$

- 3) The optical thickness of ozone $\tau_o(\lambda)$ is calculated from Eq. (7). DU (Dobson Unit) is the total amount of ozone column. The ozone amount (DU) at the observation point and date is obtained from the NASA web site (<http://ozoneaq.gsfc.nasa.gov/>). $k(\lambda)$ is an ozone absorption coefficient for each wavelength. It is recorded in the sunphotometer.

$$\tau_o(\lambda) = k(\lambda) \frac{DU}{1000} \quad (7)$$

- 4) Molecular optical thickness $\tau_r(\lambda)$ is calculated from Eq. (8). P is the local atmospheric pressure measured with a meteorological instrument at the sunphotometer observation point. Note that unit of λ is μm , not nm.

$$\tau_r(\lambda) = \frac{P}{1013.25} 0.00838\lambda^{-(3.916 + 0.074\lambda + \frac{0.050}{\lambda})} \quad (8)$$

2.4. Calibration of sun photometer

Calibrate the sun photometer at appropriate intervals. If you do not request a contractor, refer to “Technical report on calibration of radiation observation equipment (in Japanese)” (Working Group on calibration of radiation observation equipment, 2015) or .Pietras et al. (2000).

References

- Akitsu T., A. Kume, Y. Hirose, O. Ijima, K. N. Nasahara (2015), On the stability of radiometric ratios of photosynthetically active radiation to global solar radiation in Tsukuba, Japan, *Agricultural and Forest Meteorology*, 209–210, pp.59–68.
http://www.jma.go.jp/jma/kishou/now/kansoku_guide/tebiki.pdf.
- Japan Meteorological Agency (1998), *Meteorological Observation Guide*, Section 7 Global solar radiation, pp.40-42, https://www.jma.go.jp/jma/kishou/now/kansoku_guide/tebiki.pdf, (in Japanese).
- Knobelspiess K. D., C. Pietras, G. S. Fargion (2003), Sun-Pointing-Error Correction for Sea Deployment of the MICROTOPS II Handheld Sun Photometer, *J. Atmospheric and Oceanic Technology*, Vol.20, pp.767-771.
- Meek D. W., J. L. Hatfield, T. A. Howell, S. B. Idso, and R. J. Reginato (1984), A Generalized Relationship Between Photosynthetically Active Radiation and Solar Radiation, *Agronomy Journal*, Vol.76, pp.939-945.
- Morel A. and R. C. Smith (1974), Relation between total quanta and total energy for aquatic photosynthesis, *Limnology and Oceanography*, Vol.19, No.4, pp.591-600.
- Mobley C. D. (1994), *Light and Water: Radiative Transfer in Natural Waters*, Academic Press, <http://www.curtismobley.com/LightandWater.zip>.

Pietras C., M. Miller, E. Ainsworth, R. Frouin, B. Holben and K. Voss (2000), Calibration of Sun Photometers and Sky Radiance Sensors, NASA-Technical Memo.2000-209966, Ocean Optics Protocols for Satellite Ocean Color Sensor Validation Revision 2, Chapter 6, pp.45-56.

Working Group on calibration of radiation observation equipment (Ministry of the Environment and Japan Meteorological Agency) (2015), Technical report on calibration of radiation observation equipment, CGER-REPORT, ISSN 1341-4356, CGER-I124-2015, <http://www.cger.nies.go.jp/publications/report/i124/i124.pdf>, (in Japanese).

This page left intentionally blank.

Notes on CTD/O₂ Data Acquisition and Processing Using Seabird Hardware and Software

A manual of “Notes on CTD/O₂ Data Acquisition and Processing Using Seabird Hardware and Software” can be obtained from a GO-SHIP web site as below.

http://www.go-ship.org/Manual/McTaggart_et_al_CTD.pdf

This page left intentionally blank.

CTD Oxygen Sensor Calibration Procedures

A manual of “CTD Oxygen Sensor Calibration Procedures” can be obtained from a GO-SHIP web site as below.

http://www.go-ship.org/Manual/Uchida_CTDO2proc.pdf

This page left intentionally blank.

Lowered Acoustic Doppler Current Profiler (LADCP)

○ Shinya KOUKETSU (JAMSTEC)

An acoustic Doppler current profiler (ADCP) attached to the frame of a Rosette water sampling system (CTD frame hereafter) is known as a lowered ADCP (LADCP) and can be used to measure velocity profiles in deep layers during water sampling and measurement of water conductivity, temperature, and depth. Because the current velocities are measured relative to the instrument, it is important to know the velocity of the CTD frame at all times. Two methods that are commonly used to obtain current velocities from LADCP measurements are by integration of vertical velocity shears (Fischer and Visbeck, 1993) and by using an inverse method to infer the velocities of both the CTD frame and the currents (Visbeck, 2002). Data processing programs for both of these methods are publicly available (Thurnherr, 2004). The Global Ocean Ship-Based Hydrographic Investigations Program (GO-SHIP) manual (Thurnherr et al., 2010) provides detailed technical information about the LADCP but only summarizes data processing principles.

Despite recent improvements in instrument design and data processing methods, it is often difficult to extract accurate velocity profiles from the surface to the ocean floor from LADCP observations (ex. due to weak echo intensities). For this reason, the data processing methods that are summarized in the GO-SHIP manual are described here in more detail, but excluding instrument- and region-specific technical information.

The two available methods of velocity estimation are presented in section 1 and the data requirements and processing procedures are described in section 2. Section 3 provides an example of an instrument system and its configuration, and section 4 describes onboard observation procedures.

1 Methods for calculation of current velocity profiles

1-a Vertical shear of water velocity and current estimation by integration

Although LADCP data can be obtained for up to ten layers for each ping, the instrument (CTD frame) velocity is unknown, so (unlike the data from shipboard ADCPs; see Kouketsu, 2015) current velocities cannot be measured directly. However, the vertical differences between the data measured for each layer for a particular ping represent vertical shears of water velocity. Absolute ocean currents velocities can then be estimated by integrating the vertical shear profiles from the available reference velocities (Fischer and Visbeck, 1993), as described below.

A downward-looking LADCP measures current velocity relative to the CTD frame ($u_{i,n}^m, v_{i,n}^m, w_{i,n}^m$) for the i -th ping in the n -th layer (Fig. 1). These measurements are strongly influenced by any movement of the CTD frame.

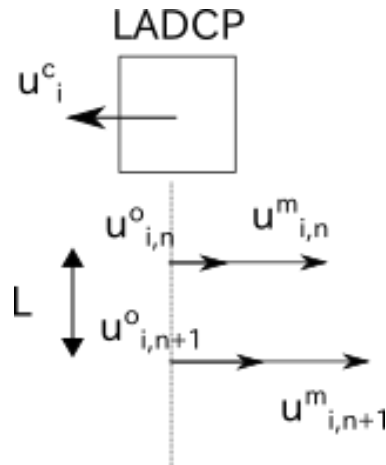


Figure 1 Measured velocity (u^m) for each LADCP ping. $u_{i,n}^m$ is the velocity measured by the i -th ping in the n -th layer. $u_{i,n}^o$ is the ocean current corresponding to $u_{i,n}^m$. Note that $u_{i,n}^m$ includes the CTD frame velocity u_i^c .

Ocean currents ($u_{i,n}^o, v_{i,n}^o, w_{i,n}^o$) are the sum of the measured velocities and the CTD frame velocities (u_i^c, v_i^c, w_i^c):

$$\begin{aligned} u_{i,n}^o &= u_i^c + u_{i,n}^m \\ v_{i,n}^o &= v_i^c + v_{i,n}^m \\ w_{i,n}^o &= w_i^c + w_{i,n}^m. \end{aligned}$$

The vertical velocity shear ($u_{i,n}^L, v_{i,n}^L, w_{i,n}^L$) between the n -th and $(n+1)$ -th layers is calculated for a layer of thickness L , which is initially set equal to the vertical dimension of the observation cell (Fig. 1). These vertical velocity shears are not strongly influenced by movements of the CTD frame and are defined as follows:

$$\begin{aligned} u_{i,n}^L &= \frac{u_{i,n}^o - u_{i,n+1}^o}{L} = \frac{u_{i,n}^m - u_{i,n+1}^m}{L} \\ v_{i,n}^L &= \frac{v_{i,n}^o - v_{i,n+1}^o}{L} = \frac{v_{i,n}^m - v_{i,n+1}^m}{L} \\ w_{i,n}^L &= \frac{w_{i,n}^o - w_{i,n+1}^o}{L} = \frac{w_{i,n}^m - w_{i,n+1}^m}{L}. \end{aligned}$$

By integration of the continuously measured vertical velocity in a layer, the vertical location of the shear measurement ($z_{i,n}$) is determined as a function of time. For this calculation, data from the first or second layer ($w_{i,1}^m$ or $w_{i,2}^m$) or their average are generally used.

$$z_{i,n} = \int_{t=0}^{t=t_i} w \, dt + L(n-1) + L_0$$

Here, the distance between LADCP and the first layer is L_0 , and the i -th ping is emitted at time $t = t_i$. Note that the vertical position of the LADCP that corresponds to the first term of the right-hand side of

the above equation can also be determined from CTD pressure data. To calculate the vertical shear (u_z^L) of the velocities at depth z , the ensemble average of the shear measurements in a layer of thickness h is used.

$$u_z^L = \sum_{i,n \in |z_{i,n} - z| < \frac{h}{2}} u_{i,n}^L / N$$

Here, N is the number of shear measurements in the layer centered at depth z . The vertical velocity profile is obtained by vertical integration of the averaged shears with the reference velocities ($u_{ref}(z_{ref})$) for each level:

$$u(z) = \int_{z'=z_{ref}}^{z'=z} u_{z'}^L dz' + u_{ref}(z_{ref}).$$

If the LADCP is used to obtain bottom-track data, the velocity of the deepest layer is used as the reference velocity. Without bottom-track data, the reference velocity is assumed to be the average ship velocity calculated from GPS locations at the start ($x_s, t = t_s$) and end ($x_e, t = t_e$) of the cast. The measured velocity ($u^m(t)$) is the difference between the velocities of the LADCP and the ocean current, and the temporal integration of the LADCP velocity during the cast is equal to the distance travelled by the ship. The current velocity is the sum of the temporal integration of the velocities ($u(z(t))$) obtained from the first term of the right-hand side of the above equation and the reference velocity. The reference velocity (u_{ref}) can be calculated as follows.

$$\int_{t=t_s}^{t=t_e} u^m(t) dt = u_{ref} (t_e - t_s) + \int_{t=t_s}^{t=t_e} u(z(t)) dt - (x_e - x_s).$$

Note that $u(z(t))$ is obtained from the right-hand side of above equation with z as the temporal function.

1-b Inverse estimation of current and CTD frame velocities

The measured velocities from a single ping for each layer include the same CTD frame velocity (Fig. 1). Assuming that high-frequency disturbances of ocean currents during the cast were negligible, the current profiles are a function of depth and individual ocean currents are measured by successive LADCP pings, thus providing linear equations that represent the unknown ocean current and CTD frame velocities during the cast. The unknown ocean current velocities can be obtained by solving those linear equations (Visbeck, 2002).

In this method, it is assumed that the CTD frame velocity and the ocean current velocity are functions of time and depth, respectively. If the vertical and temporal resolutions of the estimated ocean current velocity profile and CTD frame velocity time series are h and τ , the measured horizontal velocity ($u_{i,n}^m, v_{i,n}^m$) can be determined as the current (u_k, v_k) averaged over the depths from $z_k = kh$ to $(k + 1)h$ and CTD frame velocity (u^c, v^c) averaged over the period from $t_1 = l\tau$ to $(l + 1)\tau$ as follows:

$$u_{i,n}^m = -u_l^c + u_k + \varepsilon_{u_{i,n}^m}$$

$$v_{i,n}^m = -v_l^c + v_k + \varepsilon_{v_{i,n}^m},$$

where $\varepsilon_{u_{i,n}^m}$ and $\varepsilon_{v_{i,n}^m}$ are residuals.

If for a particular ping the measured velocity in another vertical bin (n') is observed at a different level z_k , $u_{i,n'}^m$ can be obtained by the equation

$$u_{i,n'}^m = -u_l^c + u_{k'} + \varepsilon_{u_{i,n'}^m}.$$

In this case the frame velocity is the same as in the other bin because $u_{i,n'}^m$ is obtained from the same ping as $u_{i,n}^m$.

If the measured velocity $u_{i',n''}^m$ for a different (i' -th) ping is the sum of the CTD frame velocity at $t_{i'}$ and the ocean current at z_k , $u_{i',n''}^m$ is defined as

$$u_{i',n''}^m = -u_{l'}^c + u_k + \varepsilon.$$

In this case, the CTD frame velocity is different from u_l^c , but the ocean current is the same as u_k .

As shown above, equations can be obtained for all observed layers. For sufficiently large h (generally 5–20 m) and τ (e.g., during three pings), the unknown CTD frame and ocean current velocities can be estimated by solving the equations so as to minimize residuals. In this method, additional variable conditions can easily be included. For example, if known velocity data u^K are available, the following equation can be added.

$$u^K = u_k + \varepsilon.$$

Furthermore, the equation indicating that the integration of the CTD frame velocity for the cast period is equal to the distance the ship has moved during the cast can also be used.

2 Data processing

Before doing the calculations described in the previous section, corrections are necessary for both the difference between magnetic and true north (Thébaud et al., 2015) and the velocity of sound in water (see Kouketsu, 2015). Furthermore, it is preferable to calculate observation depths from CTD pressure observations rather than by the integration of vertical velocities. This preprocessing can be done with publicly available software (Thurnherr, 2004).

The following data are needed.

- LADCP raw data
- CTD time series data (the average time bin of 1 second)
- Start and end locations of casts (from GPS data)

- Shipboard ADCP profiles
- Local deviation of magnetic north from true north

3 Instrument configurations for LADCP observations

In addition to the ADCP, the essential equipment for an LADCP survey is a battery and PCs for operational data recording and subsequent processing. The battery provides power to the onboard PC (Windows operating system) and to the submerged LADCP. For a single LADCP operation, the LADCP is attached to the CTD frame in a downward-looking orientation. For a dual LADCP operation, one LADCP usually looks down and the other up. RS232C or USB cables are used to connect the onboard PC to the ADCP and battery.

At present, a 300 kHz ADCP provided by Teledyne RD Instruments is available to members of the Oceanographic Society of Japan; previously, a 150 kHz ADCP was provided. Higher frequency instruments are conveniently small, but larger instruments with lower operating frequencies can measure currents more distant from the instrument, albeit with lower vertical resolution. Because reflection amplitudes for deep layers in the subtropics tend to be weak, lower frequency instruments may provide better results there.

Maintenance by the manufacturer are required every few years, during which the magnetometer should be re-calibrated.

The configuration for the LADCP is set by commands sent from the onboard PC to the instrument. For 300 kHz instruments, an 8 m cell size (and 16 observation layers per ping) is recommended. Although smaller cell sizes increase noise levels, a smaller cell size (e.g., 4 m with 25 observation layers) is worth considering for observations of deep layers, as reflections from greater depths tend to be too weak to obtain multi-bin observations per ping. Table 1 lists the commands that control the configuration of an LADCP and the recommended settings. More detailed information about settings is provided in the manufacturer's manuals.

4 Onboard observation processes

To optimize data processing and obtain accurate current velocities, the onboard ADCP observations should be recorded during lowering of the apparatus to within about 100 m of the seafloor and for about 2 minutes at maximum depth to ensure capture of bottom-track data. To ensure that bottom-track data can be obtained, the LADCP should remain about 30 m above the seafloor. Concurrent collection of CTD data is recommended. Both ship travel distance and CTD frame rotations should be kept to a minimum during each cast. Frame rotations can be minimized by a fin attached to the frame and by ensuring that instruments mounted on the frame are evenly balanced. Short-term movements of the CTD frame and ship can be inferred from CTD pressure data and GPS data, respectively. If the variance of these short-term movements is large, the uncertainty of LADCP data may also be large. To

avoid inaccuracies due to deviations of the orientation of the LADCP from the vertical, directional data from the inner gyro sensor should be used. Under normal operational conditions, standard deviations of current velocity data are typically about 10 cm/s.

Onboard observation processes can be summarized as follows.

1. Connect LADCP and PC to battery case.
2. Transfer initial settings from PC to LADCP and start LADCP observations.
3. Detach cable between battery and PC and begin CTD cast.
4. After completion of cast, with CTD frame on deck, re-connect PC to battery case.
5. Transfer data to PC by using the recovery command. Transfer generally takes over 20-30 minutes for a 6000 m cast.
6. After completion of data recovery, activate sleep command.

Table 1 LADCP configuration

Command	Configuration
CR1	Reset to default values
WM15	Use ADCP as LADCP
CF11101	Output settings
EA0	Instrument attachment angle (0 for LADCP)
EB0	Alignment adjustment (0 for LADCP)
ED0	Instrument depth (0 for LADCP)
ES35	Salinity for calculation of sound velocity
EX11111	Coordinate system for output. This setting means geographic coordinates.
EZ0111101	Available sensors to output. This setting means that sound velocity is constant, and that pressure, gyro, inclinometer, and temperature sensors are available.
LW1	Set Narrow band mode (noisy but longer range)
LD111000000	Velocity, correlation, and echo intensity data are stored
LF176	Distance from instrument to first bin (1.76 m)
LN16	Number of observation layers (16)
LS800	Observation layer thickness (8 m)
LV175	Maximum velocity (measurements above this value are discarded)
TE00:00:01.00	Ensemble period
TP00:01.00	Time between pings
CK	Save above configurations
CS	Start pinging

References

- Fischer, J. and M. Visbeck (1993): Deep velocity profiling with self-contained ADCPs, *J. Atmos. Oceanogr. Tech.* 10, 764–77.
- Kouketsu, S. (2015): Acoustic Doppler Current Profilers. *Guideline of ocean observations*, Vol. 7, Chap. 2.
- Thurnherr, A. M. (2004): How to process LADCP data with LDEO software version IX. [Available online at <http://ldeo.columbia.edu/~ant/LADCP.html>]
- Thurnherr, A. M., M. Visbeck, E. Firing, B. A. King J. M. Hummon, G. Krahnemann, and B. Huber (2010): A Manual for Acquiring Lowered Doppler Current Profiler Data, In the GO-SHIP Repeat Hydrography Manual: A Collection of Expert Reports and Guidelines, IOCP Report (14), ICPO Publication Series (134).
- Visbeck, M. (2002): Deep velocity profiling using Lowered Acoustic Doppler Current profilers: Bottom track and inverse solutions, *J. Atmos. Oceanogr. Tech.*, 19. 794–807.
- Thébault et al. (2015): International geomagnetic reference field: the 12th generation. [Available online at <http://www.ngdc.noaa.gov/IAGA/vmod/igrf.html>]

This page left intentionally blank.

Radiometric determination of anthropogenic radionuclides in seawater samples

○Michio Aoyama (Institute of Environmental Radioactivity, Fukushima University)

Abstract

Anthropogenic radionuclides in seawater have been concerned with their ecological effects and oceanographically used as a tracer. Current concentrations of anthropogenic radionuclides in the oceanic waters are generally extremely low except areas affected by Fukushima Dai-ichi Nuclear Power plants accident in 11 March 2011. Determination of anthropogenic radionuclides in seawater has been traditionally performed with radiometric method such as γ -spectrometry, β -counting and α -spectrometry. The radiometric method is still a useful tool to determine concentrations of anthropogenic radionuclides, although recently mass spectrometric methods have been developed extensively. In this paper, the radiometric methods to determine typical anthropogenic radionuclides, ^{137}Cs and ^{90}Sr in seawater, which includes recent development of the radiometric methods such as extremely low background γ -spectrometry are presented.

Keywords: Anthropogenic radionuclides; ^{137}Cs ; ^{90}Sr , Radioanalytical method

1. Introduction

Huge amounts of anthropogenic radionuclides have been introduced in marine environments as global fallout of the large-scale atmospheric nuclear-weapon testing, discharge from nuclear facilities and ocean dumping of nuclear wastes (UNSCEAR, 2000) and Fukushima Dai-ichi Nuclear Power plants accident. The radiological and ecological effects of anthropogenic radionuclides are still world concern. To assess the marine environmental effects of anthropogenic radionuclides, it is significant to clarify their behavior and fate in the marine environments. Therefore, concentrations of anthropogenic radionuclides in seawater are an important tool to evaluate the ecological effect of anthropogenic radionuclides.

^{137}Cs is one of the most important anthropogenic radionuclides in the field of environmental radioactivity because of a long physical half-life of 30.2 years. It is a major fission product (fission yield: 6-7 %) from both plutonium and uranium (UNSCEAR, 2000). ^{137}Cs in the ocean has been mainly derived from global fallout (Reiter, 1978; Bowen et al., 1980; UNSCEAR, 2000; Livingston and Povinec, 2001; Aoyama et al., 2006), together with close-in fallout from the Pacific Proving Ground nuclear explosions (Bowen et al., 1980; Livingston et al., 2001), discharge of radioactive wastes from nuclear facilities and others (Sigiura et al., 1976; Pentreath, 1988; Hirose et al., 1999). ^{137}Cs in seawater has been determined since 1957 to elucidate radioecological effects of anthropogenic radioactivity in the marine environment (Miyake & Sugiura, 1955; Rocco & Broecker, 1963; Shirasawa & Schuert, 1968; Bowen et al., 1980; Folsom, 1980; Nagaya & Nakamura, 1987a; 1987b; Miyake et al., 1988; Hirose et al., 1992; Aoyama & Hirose, 1995; Hirose et al., 1999; Aoyama et al.,

2000; Aoyama et al., 2001; Aoyama & Hirose, 2003; Hirose & Aoyama, 2003a; Hirose & Aoyama, 2003b; Ito et al., 2003; Povinec et al., 2003; 2004; Hirose et al., 2005, Aoyama et al., 2008a; 2009; 2012a; 2012b; 2013, 2016). Additionally, ^{137}Cs in seawater is a powerful chemical tracer of water mass motion at the time scale of several decades (Bowen et al., 1980; Folsom, 1980; Miyake et al., 1988; Miyao et al., 2000; Tsumune et al., 2001; Tsumune et al., 2003a; 2003b; Aoyama et al., 2008a, Tsumune et al., 2011) because most of the ^{137}Cs in water columns is present as a dissolved form. Another advantage of the use of ^{137}Cs as an oceanographic tracer is the quantity and accessibility of marine radioactivity during the past four decades in contrast with other chemical tracers such as CFCs (Warner et al., 1996).

Another important fission product is ^{90}Sr , which is β -emitter with a half-life of 28.8 years. It has been believed that the oceanic behavior of ^{90}Sr is very similar to that of ^{137}Cs because both ^{137}Cs and ^{90}Sr , a typical no particle-reactive element, exist as an ionic form in seawater. In contrast of ^{137}Cs , measurements of ^{90}Sr in seawater are generally inconvenient because of complicated radioanalytical processes. For this reason, it has been performed to estimate ^{90}Sr activity from ^{137}Cs activity using a certain radioactivity ratio (eg 1.6) without measuring ^{90}Sr . However, the behavior of ^{90}Sr in the ocean differs from that of ^{137}Cs ; for example, a significant amount of ^{90}Sr has been introduced to the ocean via river discharge in contrast of ^{137}Cs (Livingston, 1988), which is tightly retained in soil mineral surface. In fact, the $^{90}\text{Sr}/^{137}\text{Cs}$ ratios in oceanic waters varied spatially and temporally. ^{90}Sr may be considered to be a tracer of effect of river discharge to the ocean. These findings suggest that there is a need independently to determine ^{90}Sr in seawater.

In this paper, improved radiometric methods of ^{137}Cs and traditional radiometric method ^{90}Sr in seawater are presented.

2. Analytical method of ^{137}Cs in seawater

2-1 Background

^{137}Cs decays to stable ^{137}Ba to emit β -ray (188 keV) and γ -ray (661.7 keV). Cs, which exists ionic form in the natural water, is one of the alkali metals and chemically shows less affinity with other chemicals. The concentration of stable Cs in the ocean is only 3 nM. Known adsorbents to collect Cs in seawater are limited; ex., ammonium phosphomolybdate (AMP) and hexacyanoferrate compounds (Folsom & Sreekumaran, 1966; La Rosa, et al., 2001). The AMP has been an effective ion exchanger of alkali metals (Van R. Smit, et al., 1959). It has been known that AMP forms insoluble compound with Cs. AMP, therefore, has been used to separate other ions and concentrate Cs in environmental samples. In the late 1950s, determination of ^{137}Cs in seawater was carried out with β -counting because of underdevelopment of γ -spectrometry. Two to several ten mg of Cs carrier is usually added when the radiocaesium is determined by β -counting because of formation of precipitate of Cs_2PtCl_4 and calculation of chemical yields of caesium throughout the procedure (Yamagata & Yamagata, 1958; Rocco & Broecker, 1963). After the development of γ -spectrometry using Ge detectors, the AMP procedure with γ -spectrometry became a convenient concentration procedure for the determination in

the environmental samples.

Traditionally (AMP) method was believed as adsorption method (Wong et al., 1994), therefore a receipt of AMP method was very simple that pH should be adjusted between 1 and 4 by nitric acid and AMP of 0.2 g per 1 liter sample was added without stable caesium carrier. In a modified method (Baskaran et al., 2009), they recommended to add 20 mg of stable Cs carrier to the sample, however, they did not care about stoichiometry between AMP and Cs.

In Japan, the AMP method is recommended for radiocaesium measurements in seawaters, in which Cs carrier is stated to be unnecessary (Science and Technology Agency, 1982). It, however, must be noted that large volumes of seawater samples (more than 100 liters) were required to determine ^{137}Cs because of relatively low efficiency of Ge-detectors (around 10 %).

In the previous literatures, the weight yield of AMP has not been use because the chemical yield of Cs could be obtained and the loss of small amount of AMP during the treatment did not cause serious problems. Actually, the use of AMP reagent produced in the 1960s and in the mid 1980s gave the range from 70% to 90 % as weight yields of AMP without Cs carrier in the laboratory experiment in 1996. These weight yields are in good agreement with the records of weight yields of AMP in our laboratory during the 1970s and 1980s. However, the weight yield of AMP without Cs carrier had been decreasing from the end of the 1980s and it sometimes became very low, less than 10%, in the mid 1990s. To improve ^{137}Cs determination in seawater, Aoyama et al. (2000) and Aoyama and Hirose (2008b) re-examined the ammonium phosphomolybdate (AMP) procedure. Their experiments revealed that the stable Cs carrier of the same equivalent amount as AMP, 1 mol of Cs and 1 mol of AMP, is required to form insoluble the Cs-AMP compound in an acidic solution (pH = 1.2 to 2.2). Therefore, it can be said that the AMP extraction method is by generation of insoluble compounds by chemical reaction, not adsorption method. The improved method has been achieved to have high chemical yields of more than 95% for sample volumes of less than 100 liters. Another improvement is to succeed to reduce the amount of AMP from several ten grams to 4 grams to adsorb ^{137}Cs from seawater samples. As a result, it has been reduced the sample volume from around 100 liters to less than 20 liters to be able to use high-efficiency well-type Ge-detectors. This improvement of ^{137}Cs is favorable to use the chemical tracer of ^{137}Cs in the oceanographic field.

However, there was another serious problem regarding the ^{137}Cs measurement; i.e., large-volume sampling of more than 100 liters has been required to determine ^{137}Cs concentrations in deep waters because of very low concentrations of ^{137}Cs (less than 0.1 Bq m^{-3}). A major problem not to improve sensitivity of high-efficiency well-type Ge-detectors results in higher background accompanied with γ -spectrometry in ground-level laboratories. Especially, it is difficult to determine accurate ^{137}Cs concentrations in deep waters (>1000 m) because of the difficulty acquiring large, non-contaminated samples. However, recently, Komura (Komura, 2004; Komura & Hamajima, 2004) has established an underground facility (Ogoya Underground Laboratory: OUL) to achieve extremely low background γ -spectrometry using Ge detectors with high efficiency and low background materials.

The OUL has been constructed in the tunnel of former Ogoya copper mine (235m height from sea

level, Ishikawa prefecture) in 1995 by Low Level Radioactivity Laboratory, Kanazawa University. Depth of the OUL is 270 meters water equivalent and contributions of muon and neutron are more than two orders of magnitude lower than those at ground level. In order to achieve extremely low background γ -spectrometry, high efficiency well type Ge detectors specially designed for low level counting were shielded with extremely low background lead prepared from the very old roof tile of the Kanazawa Castle. As a result, background of γ -ray corresponding to an energy range of ^{137}Cs is two orders of magnitude lower than that in ground-level facilities. A detection limit of ^{137}Cs at the OUL is 0.18 mBq for a counting time of 10000 minutes (Hirose et al., 2005). And an underground laboratory at Mol, Belgium, a detection limit of ^{137}Cs is 0.1 mBq as measured for 2 weeks (Lutter et al., 2015).

There is a residual problem of underground γ -spectrometry for ^{137}Cs measurements. AMP adsorbs trace amounts of potassium when Cs is extracted from seawater because K is a major component in seawater and radioactive potassium (^{40}K) contains 0.0118 % of total in the natural materials. Trace amounts of ^{40}K cause elevation of background corresponding to energy range of ^{137}Cs due to Compton scattering of ^{40}K . If ^{40}K can be removed in AMP/Cs compound samples, the full performance of underground γ -spectrometry for ^{137}Cs measurements is established. To remove ^{40}K from the AMP/Cs compound, a precipitation method including insoluble platinate salt of Cs was applied for purification of Cs. This method performed to be able to trace amounts of ^{40}K from the AMP/Cs compound with a chemical yield of around 90 % for ^{137}Cs (Hirose et al., 2008).

2-2 Sampling and materials

Seawater samples should be collected without contamination. When using a CTD-rosette sampler, which collected seawater of each 12 liters at 24 -36 different depth layers, before sample seawater collection outside of the sampler bottles should be washed by clean water. When use a bucket, the bucket should be rinsed a few time before sample seawater collection.

In general, sample seawater should be filtered using a filter with pore size of 0.45 micrometer.

All reagents used for ^{137}Cs , ^{90}Sr and Pu assay are special (G.R.) grade for analytical use. All experiments and sample treatments are carried out at ambient temperatures. It is very important to know background γ activity of reagents. For example (Aoyama and Hirose, 2008b), the ^{137}Cs activity in CsCl was less than 0.03 mBq g^{-1} by using extremely low background γ -spectrometry and the ^{137}Cs activity in AMP was less than 0.00₈ mBq g^{-1} , respectively. There is no serious contamination of ^{137}Cs from other reagents before the Fukushima accident in march 2011. It is however that in some of the commercially available AMP reagent which were produced after the Fukushima accident, a clear peak of ^{137}Cs was observed which indicated contamination due to the accident. Therefore specila attention is required for use them..

2-3 Recommended AMP procedure

Proposed improved AMP procedure with the ground-level γ -spectrometer is as follows:

- 1) Measure the seawater volume (5-100 liters) and put into a tank with appropriate size.

- 2) pH should be adjusted to be 1.6-2.0 by adding concentrated HNO₃ (addition of 40 ml conc.HNO₃ for 20 litre seawater sample makes pH of sample seawater about 1.6).
- 3) Add CsCl of 0.26g and stir at a rate of 25 litre per minute or alternative method for one hour.
- 4) Weigh AMP of 4g and pour it into a tank to disperse the AMP with seawater.
- 5) 1 hour stirring at the rate of 25 litre air per minute or alternative method.
- 6) Settle until the supernate becomes clear. A settling time is usually 6 hours to overnight, but no longer than 24 hours.
- 7) Take an aliquot of 50 ml supernate to calculate the amount of the residual caesium in the supernate.
- 8) Loosen the AMP/Cs compound from the bottom of the tank and transfer into a 1-2 litre of beaker, if it is necessary do additional step of decantation.
- 9) Collect the AMP/Cs compound onto 5B filter by filtration and wash the compound with 1M HNO₃
- 10) Dry up the AMP/Cs compound for several days in room temperature
- 11) Weigh the AMP/Cs compound and determine weight yield. This weight yield should be consistent within uncertainty with a chemical yield obtained by measured stable Cs concentration in the supernat collected as step 7)
- 12) Transfer the AMP/Cs compound into a Teflon tube of 4ml volume and subject to γ -ray spectrometry

2-4 Underground γ -spectrometry procedure

- 13) the same procedure from step 1) to step 12)
- 14) Dissolve AMP/Cs compound by adding alkali solution, NaOH
- 15) Adjust the volume of solution ca. 70 ml and boiling to form Mo₂O₃ precipitate for 30 min.
- 16) pH should be adjusted to be ca. 8.1 by adding 2M HCl and adjust the volume of solution ca. 40 ml. Then keep room temperature 30 min. This solution should be kept one night in the refrigerator. Remove formed Mo₂O₃ precipitate by filtration using 5C
- 17) Adjust the volume of solution ca. 70 ml and pH should be adjusted to be ca. 8.1
- 18) Perform precipitation of Cs₂Pt(Cl)₄ to add chloroplatinic acid (1g/5ml D.W) at pH = 8.1 and keep in refrigerator during a half-day.
- 19) Collect the Cs₂Pt(Cl)₄ precipitate onto filter by filtration and wash the compound with solution (pH = 8.1)
- 20) Dry up the Cs₂Pt(Cl)₄ precipitate for several days in room temperature
- 21) Weigh the Cs₂Pt(Cl)₄ precipitate and determine weight yield
- 22) Transfer the Cs₂Pt(Cl)₄ precipitate into a Teflon tube of 4ml volume and subject to underground γ -spectrometry

2-5 Images of recommended AMP procedure and underground γ -spectrometry procedure at selected step



Figure 1 Formed AMP/Cs compound at step 3

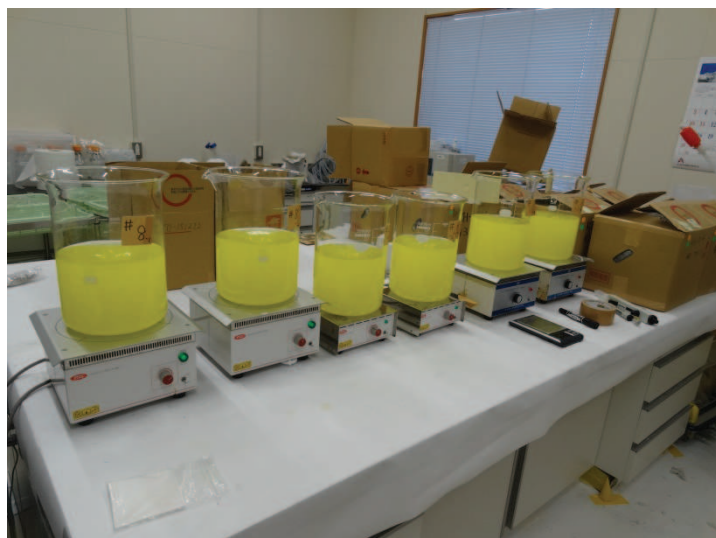


Figure 2 Formed AMP/Cs compound at step 5

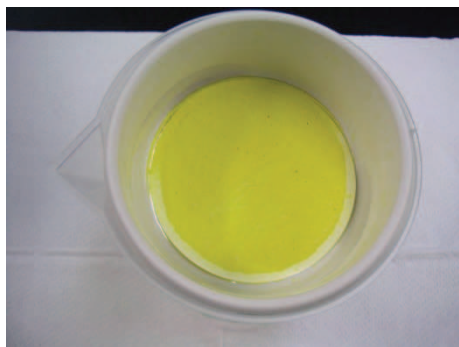


Figure 3 Formed AMP/Cs compound at step 10



Figure 4 Dissolve AMP/Cs compound by adding alkali solution at step 14

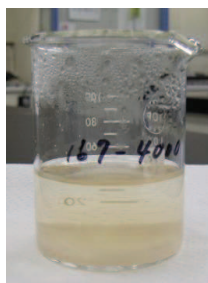


Figure 5 Formed Mo_2O_3 precipitate at step 16



Figure 6 The $\text{Cs}_2\text{Pt}(\text{Cl})_4$ precipitate at step 18



Figure 7 Dry upped $Cs_2Pt(Cl)_4$ precipitate at step 20

3. Analytical method of ^{90}Sr

3-1 Background

^{90}Sr decays to stable ^{90}Zr via ^{90}Y (half life: 2.67 day) with β emitter (934 keV) to emit β -ray (196 keV). Strontium comprises about 0.025 percent of the Earth's crust and the concentration of stable Sr in the ocean is 8.7×10^{-5} M. It is widely distributed with calcium. The chemistry of strontium is quite similar to that of calcium, of which concentration in the ocean is 10^{-2} M. The biological behaviors of strontium in the ocean are also very close to those of calcium, and then the behavior of Sr in the ocean can be considered to be different from that of Cs.

The radiometric method of ^{90}Sr is only β -counting. Therefore, radiochemical separation is required for determination of ^{90}Sr . An essential step in ^{90}Sr analytical methodologies is the separation and purification of the strontium, both to remove radionuclides which may interfere with subsequent β -counting and to free it from the large quantities of inactive substances typically present, i.e., calcium in seawater. In the 1950s, oxalate technique was used to separate Sr and Ca (Miyake & Sugiura, 1955). They applied the fuming HNO_3 method for purification of Sr. On the other hand, carbonate techniques (Sugihara et al., 1959) was used for ^{90}Sr determination for the Atlantic sample in the 1950s. Shirasawa et al. (Shirasawa & Schuert, 1968) used similar procedures to those developed by Rocco and Broecker (1966) in which the oxalate technique was adapted. During the GEOSECS period, the oxalate technique was applied for ^{90}Sr determination for the world ocean (Bowen et al, 1980). Classical methods for the separation of strontium from calcium rely upon the greater solubility of calcium nitrate in fuming nitric acid. Those procedures require numerous steps including repeated precipitation in strong nitric acid. Therefore, various alternative methods for separation have been proposed; precipitation methods of strontium sulfate and strontium rhodizonate (Weiss and Shipman, 1957), sorption of strontium on an ion-exchange resin from a solution of chelating agent such as CyDTA and EDTA (Noshkin & Mott, 1967). These methods, however, had not improved to shorter analytical steps because the precipitation and extraction methods yield strontium fractions containing significant amounts of calcium. In the late 1970s, Kimura et al. (1979) proposed the use of macrocyclic

polyethers for the separation of strontium and calcium. In the 1990s, extraction chromatography, using a solution of 4,4'(5')-bis (tert-butylcyclohexano)-18-crown-6 in 1-octanol sorbed on an inert substrate, has been developed for the separation of strontium and calcium (Horwitz et al., 1990). Recently membrane filter coating crown ether was developed for separation of strontium from others (Lee et al., 2000; Miró et al., 2002). These modern techniques have contributed for down sizing small volumes of samples. On the other hand, large volumes of seawater have been used for determination of ^{90}Sr in seawater due to low concentrations of ^{90}Sr . Therefore, the current practical method for separation and purification of ^{90}Sr in seawater still contains preparing precipitation at the first step.

There are some problems in the current practical methods using the carbonate technique; one is a lower recovery of Sr with a range from 30-60% and another is along radiochemical separation. Since the radioactivity of ^{90}Sr in seawater was lower even in the surface water in present days, improvement of the Sr recovery is one of the key issues for determination of ^{90}Sr activity in seawater. Another key point is that Ca/Sr ratio in the carbonate precipitates is remarkably reduced from that in seawater. To improve ^{90}Sr determination in seawater, we re-examined the Sr separation technique for seawater samples (Aoyama et al., 2006).

3-2 Method

3-2-1 Sampling and materials

Seawater samples should be collected without contamination. When using a CTD-rosette sampler, which collected seawater of each 12 liters at 24 -36 different depth layers, before sample seawater collection outside of the sampler bottles should be washed by clean water. When use a bucket, the bucket should be rinsed a few time before sample seawater collection.

In general, sample seawater should be filtered using a filter with pore size of 0.45 micrometer.

^{90}Sr were assayed as ^{90}Y using β -counting following radiochemical separation described in detail as follows:

3-2-2 Preconcentration of ^{90}Sr

Coprecipitation method has been practically used for extracting Sr from large volumes of seawater. Both oxalate technique and carbonate technique has been carried out for preconcentration of Sr from large volume water samples. The preconcentration of ^{90}Sr due to carbonate was performed 500g NH_4Cl and 500g Na_2CO_3 in 100 liter seawater. To improve the lower recovery of ^{90}Sr using carbonate technique, it is essential to remove Mg as hydroxide at pH=12 from the sample seawater before performing the carbonate precipitation.

3-2-3 Radiochemical separation

At the first step of radiochemical separation of Sr from Ca, Sr is separated from calcium as oxalate precipitation at pH=4. After dissolution of oxidate precipitation, Ra and Ba are removed with Ba chromate. After Ra and Ba are removed as precipitates, Sr is recovered as carbonate precipitation. Further purification of Sr is carried out by using fuming nitric acid to remove Ca. After the ^{90}Sr - ^{90}Y

equilibrium has been attained, coprecipitation of ^{90}Y with ferric hydroxide was formed and mounted on a disk for counting.

3-2-4 β -counting

β -counting of ^{90}Y were carried out by gas proportional counters for external solid samples. A typical efficiency of ^{90}Y counting by gas proportional counters with window is ca. 40 percent. The detection limit of ^{90}Y is several mBq when counting time is 360 minutes.

References

- Aoyama, M., & Hirose, K. (1995). The Temporal and spatial variation of ^{137}Cs concentrations in the western North Pacific and marginal seas during the period from 1979 to 1988. *J. Environ. Radioact.*, 29, 57-74.
- Aoyama, M., Hirose, K., Miyao, T. & Igarashi, Y. (2000). Low level ^{137}Cs measurements in deep seawater samples. *Appl. Radiat. Isot.*, 53, 159-162.
- Aoyama, M., Hirose, K., Miyao, T., Igarashi, Y., & Povinec, P.P. (2001). ^{137}Cs activity in surface water in the western North Pacific. *J. Radioanal. Nucl. Chem.*, 248, 789-793.
- Aoyama, M. & Hirose, K. (2003). Temporal variation of ^{137}Cs inventory in the Pacific Ocean. *J. Environ. Radioact.*, 69, 107-117.
- Aoyama, M., K. Hirose, Y. Igarashi. (2006) Re-construction and updating our understanding on the global weapons tests ^{137}Cs fallout. *Journal of Environmental Monitoring*, 8, 431-438.
- Aoyama, M., K. Hirose, K. Nemoto, Y. Takatsuki, D. Tsumune. (2008a) Water masses labeled with global fallout ^{137}Cs formed by subduction in the North Pacific. *Geophysical Research Letters*, 35, L01604-.
- Aoyama, M., Hirose, K., (2008b) Radiometric determination of anthropogenic radionuclides in seawater, in: Pavel, P.P. (Ed.), *Radioactivity in the Environment*. Elsevier, pp. 137-162.
doi:10.1016/S1569-4860(07)11004-4
- M. Aoyama, Y. Hamajima, M. Fukasawa, T. Kawano and S. Watanabe. (2009) Ultra low level deep water ^{137}Cs activity in the South Pacific Ocean. *Journal of Radioanalytical and Nuclear Chemistry*, 283, 781-785.
- Aoyama, M., Tsumune, D., and Hamajima, Y. (2012a) Distribution of ^{137}Cs and ^{134}Cs in the North Pacific Ocean: impacts of the TEPCO Fukushima-Daiichi NPP accident, *Journal of Radioanalytical and Nuclear Chemistry*, 1-5.
- Aoyama, M., Tsumune, D., Uematsu, M., Kondo, F., and Hamajima, Y. (2012b) Temporal variation of ^{134}Cs and ^{137}Cs activities in surface water at stations along the coastline near the Fukushima Dai-ichi Nuclear Power Plant accident site, Japan, *Geochem. J.*, 46, 321-325.
- Aoyama, M., Uematsu, M., Tsumune, D., and Hamajima, Y. (2013) Surface pathway of radioactive plume of TEPCO Fukushima NPP1 released ^{134}Cs and ^{137}Cs , *Biogeosciences*, 10, 3067–3078.
- Aoyama, Michio, Yasunori Hamajima, Mikael Hult, Mitsuo Uematsu, Eitarou Oka, Daisuke Tsumune and Yuichiro Kumamoto. (2016) ^{134}Cs and ^{137}Cs in the North Pacific Ocean derived from the March 2011 TEPCO Fukushima Dai-ichi Nuclear Power Plant accident, Japan. Part one: surface pathway and vertical distributions. *Journal of Oceanography*, Volume 72, Issue 1, pp 53-65

- Baskaran, M., Gi-Hoon Hong and Peter H. Santschi (2009) Radionuclide Analysis in Seawater, In Practical Guidelines for the Analysis of Seawater, Ed. O. Wurl, ISBN 978-1-4200-7306-5, CRC Press, Boca Rotan, FL, USA
- Bowen, V. T., Noshkin, V. E., Livingston, H. D., & Volchok, H. L. (1980). Fallout radionuclides in the Pacific Ocean: vertical and horizontal distributions, largely from GEOSECS stations. *Earth Planet. Sci. Lett.*, 49, 411-434.
- Folsom T. R. & Sreekumaran, C. (1966). Some reference methods for determining radioactive and natural cesium for marine studies. In *Reference methods for marine radioactivity studies*, Annex IV, IAEA, Vienna.
- Folsom, T. R. (1980). Some measurements of global fallout suggesting characteristics the N. Pacific controlling dispersal rates of certain surface pollutants. In *Isotope Marine Chemistry*, Uchida Rokakudo Publ. Co., Tokyo, Japan, 51-114.
- Hirose, K., Sugimura, Y., & Aoyama, M. (1992). Plutonium and ^{137}Cs in the western North Pacific: Estimation or residence time of plutonium in surface waters. *Appl. Radiat. Isot.*, 43, 349-359.
- Hirose, K., Amano, H., Baxter, M. S., Chaykovskaya, E., Chumichev, V. B., Hong, G. H., Isogai, K., Kim, C. K., Kim, S. H., Miyao, T., Morimoto, T., Nikitin, A., Oda, K., Pettersson, H. B. L., Povinec, P. P., Seto, Y., Tkalin, A., Togawa, O., & Veletova, N. K. (1999). Anthropogenic radionuclides in seawater in the East Sea/Japan Sea: Results of the first-stage Japanese-Korean-Russian expedition. *J. Environ. Radioact.*, 43, 1-13.
- Hirose, K. & Aoyama, M. (2003a). Analysis of ^{137}Cs and $^{239,240}\text{Pu}$ concentrations in surface waters of the Pacific Ocean. *Deep-Sea Res. II*, 50, 2675-2700.
- Hirose, K. & Aoyama, M. (2003b). Present background levels of ^{137}Cs and $^{239,240}\text{Pu}$ concentrations in the Pacific. *J. Environ. Radioact.*, 69, 53-60.
- Hirose, K., Aoyama, M., Igarashi, Y. & Komura, K. (2005). Extremely low background measurements of ^{137}Cs in seawater samples using an underground facility (Ogoya). *J. Radioanal. Nucl. Chem.*, 263, 349-353.
- Hirose, K., Aoyama, M., Igarashi, Y. & Komura, K. (2008). Improvement of ^{137}Cs analysis in small volume seawater samples using the Ogoya underground facility, *Journal of Radioanalytical and Nuclear Chemistry*, 276, 3, 795-798.
- Horwitz, E. P., Dietz, M. L., Diamond, H., LaRosa, J. J. & Fairman, W. D. (1990). Concentration and separation of actinides from urine using a supported bifunctional organophosphorus extractant. *Anal. Chim. Acta*, 238, 263-271.
- Ito, T., Povinec, P. P. Togawa, O. & Hirose, K. (2003). Temporal and spatial variations of anthropogenic radionuclides in the Japan Sea water. *Deep-Sea Res. II*, 50, 2701-2711.
- Kimura, T. K. Iwashima, T. Ishimori, and T. Hamada (1979). Separation of strontium-89 and -90 from calcium in milk with a macrocyclic ether, *Anal. Chem.*, 51 (8), 113-1116
- Komura, K. & Hamajima, Y. (2004). Ogoya Underground Laboratory for the measurement of extremely low levels of environmental radioactivity: Review of recent projects carried out at OUL, *Appl. Radiat. Isot.*, 61, 164-189.

- Komura, K. (2004). Background components of Ge detectors in Ogoya underground laboratory, *Appl. Radiat. Isot.*, 61, 179-183.
- La Rosa, J. J., Burnett, W., Lee, S. H., Levy, I., Gastaud, J. & Povinec, P. P. (2001). Separation of actinides, cesium and strontium from marine samples using extraction chromatography and sorbents. *J. Radioanal. Nucl. Chem.*, 248, No. 3, 765-770.
- Lee, C. W., Hong, K. H., Lee, M. H., Cho, Y. H., Choi, G. S., Choi Y. W. & Moon, S. H (2000). Separation and preconcentration of strontium from calcium in aqueous samples by supported liquid membrane containing crown ether. *J. Radioanal. Nucl. Chem.*, 243, 767-773.
- Livingston, H. D. (1988). The use of Cs and Sr isotopes as tracers in the Arctic Mediterranean Seas. In H. Charnock, J. E. Lovelock, P. S. Liss & M. Ehitfield (Eds), *TRACERS IN THE OCEAN*, (pp. 161-176). Princeton University Press, Princeton, New Jersey.
- Livingston, H. D., Povinec P. P. (2001). A millennium perspective on the contribution of global fallout radionuclides to ocean science. *Health Phys.*, 82 (5), 656-668.
- Livingston, H. D., Povinec P. P., Ito, T., & Togawa, O. (2001). The behavior of plutonium in the Pacific Ocean. In A. Kudo (Ed.), *Plutonium in the Environment*, (pp. 267-292). Elsevier Science.
- Lutter, G., Faidra Tzika, Mikael Hult, Michio Aoyama, Yasunori Hamajima, Gerd Marissens, Heiko Stroh (2015). Measurement of anthropogenic radionuclides in post-Fukushima Pacific seawater samples, *NUKLEONIKA* 2015;60(3):545-550, doi: 10.1515/nuka-2015-0112
- Miró, M., Gómez, E., Estela, J.M., Casas, M., & Cerdà, V. (2002). Sequential injection ^{90}Sr determination in environmental samples using a wetting-film extraction method. *Anal. Chem.*, 74, 826-833.
- Miyake, Y. and Y. Sugiura, (1955). Radiochemical analysis of radio-nuclides in sea water collected near BIKINI atoll, *Pap. Met. Geophys.*, 6, 90-92.
- Miyake, Y., Saruhashi, K., Sugimura, Y., Kanazawa, T., & Hirose, K. (1988). Contents of ^{137}Cs , plutonium and americium isotopes in the Southern Ocean waters. *Papers in Meteorology and Geophysics*, 39, 95-113.
- Miyao, T., K. Hirose, Aoyama, M. & Igarashi, Y. (2000). Trace of the recent deep water formation in the Japan Sea deduced from historical ^{137}Cs data. *Geophys. Res.Let.*, 27, 3731-3734.
- Nagaya, Y & Nakamura, K. (1987a). Artificial radionuclides in the western North Pacific, *J. Oceanogr. Soc. Jpn*, 32, 416-424.
- Nagaya, Y. & Nakamura, K. (1987b). Artificial radionuclides in the western Northwest Pacific (II): ^{137}Cs and $^{239,240}\text{Pu}$ inventories in water and sediment columns observed from 1980 to 1986. *J. Oceanogr. Soc. Jpn*, 43, 345-355.
- Noshkin, V. E. & Mott, N.S. (1967). Separation of strontium from large amounts of calcium, with application to radiostromium analysis. *Talanta*, 14, 45-51.
- Pentreath, R. J. (1988). Sources of artificial radionuclides in the marine environment. In: J. C. Guary, P. Guegueniat & R. J. Pentreath (Eds.), *Radionuclides: A Tool for Oceanography*, (pp.12-34). Elsevier Applied Science, London and New York.
- Povinec, P. P., Livingston, H. D., Shima, S., Aoyama, M., Gastaud, J., Goroncy, I., Hirose, K., Hynh-Ngoc, L., Ikeuchi, Y., Ito, T., LaRosa, J., Kwong, L. L. W., Lee, S.-H., Moriya, H., Mulsow, S., Oregioni, B.,

- Pettersson H. & Togawa, O. (2003). IAEA '97 expedition to the NW Pacific Ocean-results of oceanographic and radionuclide investigations of the water column. *Deep-Sea Res. II*, 50, 2607-2637.
- Povinec, P.P., Hirose, K., Honda, T., Ito, T., Scott, E. M. & Togawa, O. (2004). Spatial distribution of ^3H , ^{90}Sr , ^{137}Cs and $^{239,240}\text{Pu}$ in surface waters of the Pacific and Indian Ocean-GLOMARD database. *J. Environ. Radioact.*, 76, 113-137.
- Reiter, E. R. (1978). Atmospheric Transport Processes Part 4: Radioactive tracers. Technical Information Center, US Department of Energy, 1-605.
- Rocco, G. G. & Broecker, W. S. (1963) The vertical distribution of cesium 137 and strontium 90 in the oceans. *J. Geophys. Res.*, 68, 4501-4512.
- Science and Technology Agency (1982). Procedures of sample treatment for germanium spectrometry, 20 (in Japanese).
- Shirasawa T. H. & Schuert, E. A. (1968). Fallout radioactivity in the north Pacific Ocean: Data compilation of Sr-90 and Cs-137 concentrations in seawater. In E. P. Hardy & J. Rivera (Eds.), *Fallout Program Quarterly Summary Report HASL-197*, (pp. I-66-I-94). Health and Safety Laboratory U. S. Energy Research and Development Administration.
- Sugihara, T. T., James, H. I., Troianello, E. J. & Bowen, V. T. (1959). Radiochemical separations of fission products from large volumes of sea water. *Anal. Chem.*, 31, 44-49.
- Sugiura, Y., Saruhashi, K. & Miyake, Y. (1976). Evaluation on the disposal of radioactive wastes into the North Pacific, *Pap. Met. Geophys.*, 27, 81-87.
- Tsumune, D., Aoyama, M., Hirose, K., Maruyama, K. & Nakashiki, N. (2001). Calculation of artificial radionuclides in the ocean by an ocean general circulation model. *J. Radioanal. Nucl. Chem.*, 248, 777-783.
- Tsumune, D., Aoyama, M. & Hirose, K. (2003a). Behavior of ^{137}Cs concentrations in North Pacific in an ocean general circulation model. *J. Geophys. Res.*, 108(C8), 3262.
- Tsumune, D., Aoyama, M. & Hirose, K. (2003b). Numerical simulation of ^{137}Cs and $^{239,240}\text{Pu}$ concentrations by an ocean general circulation model. *J. Environ. Radioact.*, 69, 61-84.
- Tsumune, D., Tsubono, T., Aoyama, M., and Hirose, K. (2011) Distribution of oceanic ^{137}Cs from the Fukushima Dai-ichi Nuclear Power Plant simulated numerically by a regional ocean model, *Journal of environmental radioactivity*, 111, 100-108.
- UNSCEAR (2000). Sources and effects of ionizing radiation. United Nation, New York.
- Van R. Smit, J., Robb, W., & Jacobs, J. J. (1959). AMP-Effective ion exchanger for treating fission waste. *Nucleonics*, 17, 116-123.
- Warner, M.J., Bullister, J.L., Wisegarver, D.P., Gammon, R.H. & Weiss, R.F. (1996). Basin-wide distributions of chlorofluorocarbons CFC-11 and CFC-12 in the North Pacific: 1985-1989. *J. Geophys. Res. C: Oceans* 101 (C9), 20525-20542.
- Weiss, H. V. and Shipman, W. H. (1957). Separation of strontium from calcium with potassium rhodizonate. Application to radiochemistry. *Anal. Chem.*, 29, 1764-1766.

Wong, Kai M., Terry A. Jokela and Victor E. Noshkin (1994). RADIOCHEMICAL PROCEDURES FOR ANALYSIS OF Pu, Am, Cs, AND Sr IN WATER, SOIL, SEDIMENTS AND BIOTA SAMPLES.

Technical Report UCRL-ID-116497, Lawrence Livermore National Laboratory, Livermore, CA, USA

Yamagata, N. & Yamagata, T. (1958). Separation of radioactive caesium in Biological Materials. *Bull. Chem. Soc. Japan*, 31, 1063-1068.

Seabed sediment

○Shigeyoshi OTOSAKA (Japan Atomic Energy Agency), Hisashi NARITA (Tokai University)

1. Introduction

In the marine environment, anthropogenic radionuclides (e.g., cesium-137) are released by atmospheric nuclear weapon tests, nuclear accident, and operation of nuclear facilities. It is known that some part of the radionuclides is accumulated in the seabed. Accurate analysis of the anthropogenic radionuclides in sediment is crucial to understand their activity concentration levels as well as deposition history to the study area. Natural radionuclides (e.g., uranium/thorium series nuclides, carbon-14) in sediment are helpful to trace the history of sedimentation in the study area and estimate sedimentation rates of the sediment. This chapter aims to provide information for successful observation of distribution of the radionuclides in seabed sediment. Procedures and important points for sediment analysis are also described in Vol. 5 of this Guideline of Ocean Observations or previous protocols (e.g., IAEA, 1993).

2. Planning for sediment collection

2-1 Selection of sampling station

In observing radionuclides in the sediments, sampling stations should be carefully selected so that the samples properly preserve the bottom environment. Especially in coastal areas, it is important to grasp approximate submarine topography and sediment characteristics in advance of the sampling, and nautical charts provide useful information for this purpose. Locations of where sediment consists of sand (symbol *S*) and mud (symbol *M*) are recommended for sediment collection, and those where the sediment consists of stone (symbol *St*) or rock (symbol *R*) should be avoided. In the case of sediments consist of gravel (symbol *G*) and coarse sand (symbol *cS*), caution is required because the sediment characteristics may change every several meters. In coastal areas, influx of material from the land should also be considered using information such as topography and land usage patterns. It is also effective to create equally spaced grids in the target area and comprehensively set sampling points along the grid. In the case of periodic surveys such as monitoring programs, even on a small scale, the use of GPS is strongly recommended from a viewpoint of continuity of the observed data.

2-2 Uncertainties due to sediment sampling

Most radionuclides in marine sediment was originally dissolved in seawater. The dissolved radionuclides adsorb onto the surface of suspended and/or settling particles and incorporated to the seabed. Unlike natural radionuclides, artificial radionuclides are supplied heterogeneously to the marine environment by nuclear incidents, nuclear weapons testing or regular operation of nuclear facilities. Considering that the removal of dissolved radionuclides associates with adsorption to suspended particles, contribution of sand/gravel and the heterogeneity of the geological characteristics affect distribution of the radionuclides in the sediment. Therefore, appropriate samplers and

procedures should carefully be selected according to the situation.

Especially in coastal regions, heterogeneity of the grain size may alter the distribution of radionuclides in sediment. The state of preservation of sediment-water interface during and after the sediment coring would also affect distribution of radionuclides in the core samples. If an observation is the first trial of sample collection in the area/region or a sampling equipment, multiplied sampling at a representative station, and assessment of the uncertainty (reproducibility) due to operation of new equipment are recommended. In order to overcome such heterogeneity problems, increasing of the sample size or use of composite samples would also be effective.

3. Sediment samplers

In this section, representative sediment samplers for measurement of radionuclides are introduced. For a monitoring of pollutants, such as artificial radionuclides, sediment samplers must collect surface sediment as well as suspended particles in the water-sediment interface without loss or disturbance. In order to assess the most recent contributions of contaminants to the surface sediment, the upper section of the sample (0–1 or 0–3 cm) should be carefully taken with the highest priority. If the primary purpose of sampling is to investigate the vertical distribution or sedimentation rates, core sampling without disturbance of the sedimentary layers must be applied. Researcher should select appropriate equipment, and combine several devices as necessary.

3-1 Grab sampler

Grab samplers are commonly used for sediment sampling in brackish and estuarine waters because of its larger sampling area and successful collection of sandy sediment that is difficult to collect by a core sampler. Although the grab sampling is not the ideal way to observe the sediment profile, it gives us some idea of distribution in the top 10 cm of sediment with careful sub-coring.

3-1-1 Ekman-Burge sampler

Ekman-Burge samplers are light weighted equipment (5–10 kg) with a sampling area of about 15 cm × 15 cm. It can collect a sample up to 3 L in volume. After arriving at the bottom, a drop messenger triggers to release shovel blades for sediment collection. It is designed to collect soft surface sediments manually in the absence of strong currents. The lack of sample disturbance, square cross section and moderate penetration make it suitable for collection of the surface sediments. Because of its lightweight and easy handling, it is well-suited for small boat operations.

3-1-2 Smith-McIntyre sampler

Smith-McIntyre sampler can collect samples of up to 20 L of fine-grained and sandy sediments. Unlike the Ekman-Burge sampler, Smith-Macintyre sampler is designed to release the shovel blades at a time when the sampler touches the seafloor.

3-2 Core sampler

Sediment cores provide helpful information for estimating the sedimentation rate, the history of

contaminant discharge to the water system, and the inventories of pollutants. In collection of a core sample, it is important to preserve the original layers of the sediment without disturbance and to avoid losing the surface layer which may hold the most recent pollutants.

The diameter of coring tube should be as large as possible to provide sufficient material for analysis. Coring tubes with a diameter of about 5–12 cm are commonly used. When the coring tube penetrates into the sediment, deformation of the sediment layers may occur by friction between the inner wall of the tube and sediment (a dome-like structure in which the sediment layer becomes convex shaped in the coring tube). Especially when the penetration speed is fast and the contact area of the inner wall of the tube per unit mass of the sediment is large, the extent of deformation becomes large. Generally, when the diameter of the coring tube is 70 mm, the extent of deformation is about 5 mm outside the sediment core, and contamination of the sample (contamination of the upper layer sediment in the lower layer) occurs in this range. In the case of sediments containing sand or larger grain sizes, or sediments with brittlestars (e.g. *Ophiura ophiura*) on the surface, they are dragged along the inner wall of the tube, and the sediment particles near the surface may move downward. Such contamination can be prevented by removing about 5 mm of the outer peripheral part of the sediment column.

3-2-1 Gravity corer

A gravity corer is an open tube fitted with a weight so that gravity can force it sufficiently deep into the sediment to isolate a sediment sample. The simplest possible corer used in shallow environments consists of a piece of plastic tubing and a weight. After this type of sampler is penetrated into the sediment, the top of the coring tube is sealed and retrieved to the boat.

3-2-2 Multiple corer

In a multiple corer, seawater in a cylinder installed at the upper center of the sampler works as a damper, and a multiple polycarbonate coring tubes attached to the lower frame are inserted into the sediment without disturbing the sediment-water interface at a very low speed (1 cm/sec or less). A guide frame surrounding coring tubes helps to maintain the tubes in a vertical position. The frame also permits installation of a mechanism that seals the bottom of the coring tube immediately after the tube is extracted from the sediment. A bottom core seal improves the success of capturing sediment in the coring tube without an internal core catcher. The core seal also enables to collect overlying water as well as sediment core.

2-3-2-3 Box corer

Box corer has a box with surface area up to 2,500 cm² (50 × 50 cm) and a maximum penetration depth of about 50 cm, and is suitable to collect large volumes of sediment. As the winch begins to retrieve the corer after the corer penetrated into the sediment, a single spade or two opposing jaws with rubber sealing surfaces are pulled through the sediment to a position in contact with the cutting edges of the box. By the larger surface area of sediment collection, compared to a tube coring, box corer is able to minimize the change in the thickness of the sediment during the coring. The box core sample is often subsampled by pushing clean coring tubes into the sediment for a further analysis. In order

to avoid shortening during the penetration of sub-coring tube, it is preferable to use a tube with a diameter at least 50 mm of which side wall is as thin as possible. When penetrating the sub-corer into the sediment, do so when overlying water is on the sediment sample in the box. Although a box corer can collect an excellent sample in muddy sediments, it is difficult to collect sandy sediment because the sealing spade is not sufficiently tight to trap water. If a box corer is retrieved with the absence of overlying water on the sediment sample, there is a possibility that the surface sediment was disturbed or partly lost. In such a case, it is recommended to collect the sample again.

3-2-4 Piston corer

In general, conventional piston cores are used when long cores (2–30 m) in fine-grained unconsolidated sediments are required for analysis of sedimentary processes in several thousands to millions of years. Ships need to be equipped with hydraulic cranes, winches and enough space for core handling. After the bottom of the piston, the barrel surrounding the piston (coring tube) penetrates into the sediment while keeping the piston on the bottom surface. When the barrel penetrates the sediment, a negative pressure occurs in a small space between the piston and the sediment, and the friction between the inner wall of the barrel and the sediment is reduced. By the negative pressure, the barrel is more likely to penetrate into the sediment. Since the piston functions as a "plug" when the barrel is pulling out, the core sample can be recovered without falling while keeping the sedimentary layers. However, for the successful sampling, the piston must be held on the seabed surface when the barrel is penetrating into the sediment.

4. Collection of sediment samples

4-1 Sampling record

As general information of sediment sampling, following items should be recorded for every collection of sediment.

Sampling date and time

Researcher/Operator

Location

Bottom depth

Wave and heave heights

Size classification (granule, sand, silt, clay etc.: e.g., ISO, 2002)

If available, detailed cruise data and tension record of the winch would also be helpful for replicate collection at the same location.

4-2 Subsampling from grab sampler/Box corer

After retrieving a sampler, confirm that the sediment sample was successfully collected in the bucket/box. If the sample is not sampled horizontally, if the sample overflows, or if the overlying water is not retained, it should be sampled again because a part of the sediments may be lost during the sampling.

Retrieved sampler is tightly lashed on deck to avoid slipping.

When sub-coring is performed, a sub corer with 40 ~ 80 mm in diameter is slowly penetrated into the sediment. See section 4-3 for processing after subsampling.

Drain overlying water by pumping or siphoning with silicone tube (ID: 5–10 mm). It is recommended to use a pump to prevent water from flowing back and disturb the sediment surface.

After removing the overlying water, measure the thickness of sediment and recorded. Considering the shape of the sediment box, measure the thickness at multiple points as necessary so that the approximate volume of the collected sediment can be estimated.

Place a stainless (or plastic if necessary) container (50 mm height) under the sampler. Open the jaws and scrape the sample in the bucket.

Homogenate sample with a stainless hand shovel, packed into plastic bag and sealed.

As necessary, it is possible to penetrate a clean acrylic tube into the sediment and obtain a sub-core (see section 4-3 to process the core samples). This step must be carried out before draining the overlying water.

4-3 Subsampling from core sampler

Carefully seal the bottom of coring tube with a spatula (the width of spatula must be larger than diameter of coring tube) and remove the coring tube from the corer.

Immediately seal the both ends of corer with rubber plugs, and allowed to settle suspended particles in the overlying water of the sediment surface. Care should be taken not to give shock so that sediments will not be disturbed. As necessary, the rubber plugs are sealed with plastic seal tape (c.a. 50 mm width).

Before starting the core slicing, prepare water (surface seawater or tap water will be acceptable if there is no significant contamination of target radionuclide) in a bucket. Prepare bags or bottles for storage of subsamples and note sampling date, station ID, sampling layer in advance to process samples. Plastic seal bags or plastic bottles with seal top are useful for subsampling.

After at suspended particles in the bottom water is settled, set the coring tube on a cutting piston and release the top plug. Carefully release the bottom plug, immediately slide spatula between the coring tube and bottom plug, and remove the bottom plug.

Carefully slide out the spatula and insert the core into the piston from the bottom of the coring tube.

As necessary, drain the overlying water by a pump or siphon with silicone tube (ID <5 mm). Use of a pump is recommended to prevent disturbing the surface sediment by water from flowing back to the coring tube. The piston should be kept pushing up (core is pushed down when using a fixed height) during the collection of overlying water. Weaken the flow rate of the pump at the end, fix the tip of the tube on the water surface, and suction the water and air.

When it is not necessary to sample the overlying water, push the piston up to allow the overlying water overflow. When the sediment-water interface approaches to 1~2 cm below the top end, set water absorbent material (Kimwipes are useful) on the overlying water and slowly push up the piston. The absorbent should not be contact with sediment surface as much as possible.

Push up the piston until the demanded thickness of sediment comes out. If the sediment has high water content and it is expected to overflow by the uplifting, scoop the sediment for given thickness of sediment layer and stored in a subsample bag/bottle.

Using a spatula, chip off the smearing sediment along the inner wall of coring tube. It is efficient to make a hexagon-shaped core.

Slide a spatula along the line of the top of the coring tube and cut the sediment. During this process, do not move the spatula vertically to prevent disturbing sedimentary layers in the core.

Store the cut subsample in a bag/bottle.

Before cutting the subsequent layer, spatula is washed with water and wiped.

5. Transport and storage

After the collection of the sediments using grabs or corers at the field site, the samples must be transported to the laboratory without altering properties of the original material. This involves special steps to reduce potential contamination and to minimize mixing for biological, chemical, and physical analyses.

When carrying core samples to laboratory on land, it should be secured in a vertical position so as not to disturb the sedimentary layer. For such cores, it is often advantageous to completely fill the space from the water sediment interface to the top of the coring tube with local water and to remove any air bubbles that may be trapped under the core cap.

When carrying the core by a vehicle, an enough cushioning material should be used to suppress vibration.

If the core cannot be held in a vertical position during cutting and transport, the surface of the core is covered with a Teflon sheet (about 1mm thick and cut to the interval diameter of the coring tube) followed by a PVC well plug.

Cryopreservation of core sample is not recommended. When it is necessary to store cores in a freezer, take notice of the change in core length due to expansion and the vertical movement of pore water in the sediment column. Additionally, when frozen core samples are cut, they should be processed without thawing.

6. Analysis of sediment properties

In the analysis of distribution of radionuclides in seabed sediment, the following sediment properties are especially important.

Percentage of water content (see also Vol. 5, Chap. 2 of this Guideline of Ocean Observations).

Loss on ignition, organic matter or total organic carbon (TOC) content (Vol 5, Chap. 3) .

Grain size distribution (Vol. 5, Chap. 4).

Dry bulk density (Vol. 5, Chap. 2)

7. Processing sediment samples for analysis

7-1 Drying

Drying step is required because concentrations of contaminants in sediments are usually reported on a dry-weight basis. The drying step also provides an opportunity to calculate water content by simply weighing the sample before and after drying. Water content is a fundamental parameter of the sedimentary environment. The water content is also applied in calculation of the salt separated from the seawater by the drying. The drying procedures are as follows. Throughout the drying process, attention should be paid not to make cross contamination between subsamples.

Gently mix the wet sediment subsample by stainless spoon and reassemble aggregation.

Put the sample into a pre-weighed container, and measure total weight. The balance should be chosen so that the number of effective digits is 4 or more.

Place the sample in an oven at 60~105 °C (depends on element/isotope of interest).

Allow the sample at room temperature and measure the total weight.

Crush aggregates in a ceramic mortar, remove pebbles and remove stone, shell and organisms (fish, benthos, seaweeds etc.) and organisms with 2 mm sieve. In this procedure, care should be taken not to “grind” the sediment particles.

As necessary, reduce the sample size and store the dried sample in appropriate sealed vessel (see section 7-3).

7-2 Homogenization

Artificial radionuclides are often adsorbed heterogeneously onto the surface of sediment particles. In case a large amount of samples must be handled, an automatic homogenizer (mixer consists of a V- or cylindrical-shaped rotating vessel) is helpful for homogenization. When such a homogenizer is used, all sediment samples, including fine particles and “dust” (which may have a relatively high content of radionuclides), in the vessel must be recovered.

7-3 Reduction of sample size

If large amount of sample for analysis was collected, the size of sample is reduced by the following procedures. Theoretically, it can be estimated that satisfactory homogeneity (less than 3 % of uncertainty due to processing sample) is obtained by subsample sizes larger than 100 mg with particle sizes <0.08 mm (IAEA, 1993).

Incremental method: Spread powdered sample on a clean and smooth board or sheet, let the sample square or rectangle with 15–25 mm in thickness, and divide equally into 9 blocks. Scoop samples from each block with an increment spoon, and repeat until the required amount of sample is obtained. In this method, subsamples should be taken from bottom of each block. In addition, the same number of times must be taken for all blocks.

Dividing method: Repeat dividing the sample size by a riffle sampler.

Automated method: Use a specialized device such as cascade and rotary splitter.

Detailed procedures and instruments are described in JIS (1992).

7-4 Preparation for determination of radionuclides

7-4-1 Nondestructive analysis

Gamma-ray spectrometry is the representative nondestructive technique for the determination of activity concentration of radionuclides from natural or anthropogenic origin. In the gamma-ray spectrometry, a dried and powdered sample is sealed in a pre-weighed plastic bottle for measurement. The bottles must have the same dimension of that of a certified reference material used for calibration of high-purity Germanium (HPGe) detector.

When measuring activity of radium-226 indirectly from activities of lead-214 or bismuth-214, it is necessary to prevent escape of Rn-222 (a daughter nuclide of Ra-226 and a gas component). This process helps to establish the radioactive equilibrium between Ra-226 and Pb-214 or Bi-214. For this purpose, the surface of sample in the container is covered with an acrylic disk and sealed with epoxide resin.

7-4-2 Analysis that requires decomposition, separation and purification of sample

For radioanalytical techniques by alpha-/beta- counting or a high-resolution mass spectrometry, sediment samples must be decomposed by an appropriate method, followed by separation and purification of the target elements/radionuclides. When handling radionuclides as yield tracers, care must be taken so that they do not contaminate other samples by diffusing into the working environment and equipment. On the other hand, especially for mass spectrometry, it is necessary to prevent contamination of the working solution by environmental material (i.e. dust, gas etc.). When selecting the appropriate method for measurement of the target radionuclides, they also should understand correctly about the precautions for the analysis.

References

- ISO (2002): Geotechnical investigation and testing – Identification and classification of soil – Part 1: Identification and description. ISO 14688-1:2002. International Organization for Standardization, Geneva, 12 pp.
- JIS (1992): Particulate materials –General rules for methods of sampling. Japan Industrial Standards Committee, Tokyo, 86 pp. (in Japanese)
- IAEA (1993): Collection and preparation of bottom sediment samples for analysis of radionuclides and trace elements. IAEA-TECDOC-1360. International Atomic Energy Agency, Vienna, 130 pp.
- MEXT (1983): Collection of environmental sample. Ministry of Education, Culture, Sports, Science and Technology, Tokyo, 135 pp. (in Japanese)

Chapter 3 in this volume left intentionally blank.

This page left intentionally blank.

Plankton and Benthos

○Hideki KAERIYAMA (Japan Fisheries Research and Education Agency)

1. Sample Collection and Storage

1-1 Plankton

Phytoplankton and zooplankton play an important role in marine ecosystems as a primary producer and secondary producer, especially zooplankton act as a vital link between primary production (phytoplankton) and higher trophic production through food webs. These organisms also play an important role in understanding the radionuclides cycling within the ocean, and the transfer of radionuclides from seawater to marine organisms. However, the activity concentration of radionuclides found within zooplankton and phytoplankton is low. In particular, the activity concentration of anthropogenic radionuclides is considerably low for long lived radionuclides in general. Analyze the activity concentration of artificial radionuclides in zooplankton and phytoplankton, it is necessary to collect a large sample volume. To collect zooplankton samples, it is recommended to use large mouth-opening plankton net (for example, an Ocean Research Institute (ORI) net or Bongo net). The oblique hauling to collect plankton several times is also recommended through the water to a depth that is approximately equivalent to the depth of the mixed layer or to the depth directly below the thermocline. Because we can expect large biomass of zooplankton existed within that layer. Furthermore, when collecting samples of large crustacean plankton such as euphausiids and micronekton, which are large and have strong swimming abilities, it is best to use larger nets or trawls allowing high speed tow such as Isaacs-Kidd Midwater Trawl Net (IKMT) or Matsuda, Oozeki and Hu Midwater Trawl (MOHT) (cf. Oozeki et al., 2004, Wiebe and Benfield, 2003). Once the net has been pulled up onto the board, the outer surface of the mesh should be thoroughly washed in seawater, and the plankton sample that has accumulated in the cod end of the net should be recovered. To aid in the data interpretation, a portion of the sample should be used to determine ecological information of zooplankton community such as the biomass, species composition, and numerical density (Kaeriyama et al., 2008, Kitamura et al., 2013, Takata et al., 2015). For this, a flow meter should be attached to the plankton net and quantify the amount of water that has been filtered. The remaining portion of the sample should be drained, placed in a Ziploc bag, frozen, and stored. Additionally, it is recommended to obtain the activity concentration of the radionuclide of interest in the seawater (dissolved matter) at the depth at which the plankton net is hauled, to calculate the concentration factor (IAEA, 2004), which is a useful value for data interpretation (Tateda, 1998; Kaeriyama et al., 2015). Furthermore, in cases when the radionuclide activity concentrations are compared among different types of zooplankton, using the concentration of stable isotopes in each type of zooplankton is an effective method for the analysis because it is difficult to collect a large quantity of a single species of plankton. When using the stable isotope concentration as an indicator of the radionuclide activity concentration, it is assumed that isotopic fractionation seen in hydrogen, carbon, nitrogen, oxygen, and sulfur does not occur (Hidaka and Akagi, 2002). The sample collected

through the plankton net should be transferred to a large Petri dish, and individual organisms of the plankton type of interest should be selected one by one using tweezers or a pipette on the board. For large crustacean plankton such as euphausiids, and copepods, several tens of organisms should be collected. The water on the surface of the organisms should be removed, and the organisms should be frozen. The stable isotope concentration can be analyzed by drying the sample, dissolving it in acid, and analyzing the dissolved sample using ICP-AES or ICP-MS (Masuzawa et al., 1988, Marumo et al., 1998). Because exclusively collecting a large amount of phytoplankton is extremely difficult, the use of a large volume *in-situ* filtration system (Bishop and Edmond, 1976, Aono et al., 2008), or a cartridge filter using a seawater collection system on the board may be considered (The Oceanographic Society of Japan, the Great East Japan Earthquake WG /Analysis SWG, 2011). In such a case, the sample obtained is a suspended solid consisting mainly of phytoplankton. When using a large volume *in-situ* filtration system, one recommended method to collect the samples efficiently is to check the vertical profile of the chlorophyll fluorescence beforehand and perform the observation at the depth where the peak is found. The filter paper that is used for collection should be marked with its weight beforehand so that the weight of the dried sample can be calculated afterwards. The amount of filtered water measured by the flow meter should also be recorded. The filter paper with the suspension sample obtained through the cartridge filter should be frozen and carried back to the lab. When filtering the seawater, a flow meter should be installed on the outlet of the housing of the cartridge filter, and the amount of filtered water should be recorded. If it is expected that the seawater contains a high activity concentration of radionuclides, the seawater collection system, hose, and housing of cartridge should be thoroughly rinsed with field seawater, the seawater inside the system should be replaced, and the housing should be thoroughly washed with distilled water.

1-2 Benthos

Benthos collection is performed with the general collection equipment (sledge nets, dredge nets, and trawl nets. Refer to the chapter on benthos, Volume 6 Chapter 2 in this Guideline of Ocean Observations). Afterwards, the organisms should be placed in a Petri dish filled with seawater filtered on-site, and organisms were sorted as possible as in details. During this step, it is important to remove the sediment particles stuck to the benthos as much as possible, using the filtered seawater. For the radioisotopes of conservative elements, such as radiocesium, the sample should be washed with seawater containing the same level of activity concentration of radionuclides as the on-site seawater, to avoid artificial changes in the radionuclide activity concentration of the samples. After being sorted, the samples should be frozen and stored. Depending on the purpose of the investigation, the researchers should consider processing the sample, such as incubating the sample for a certain period in the filtered seawater to empty the digestive systems of the organisms, to eliminate the effect of the gastrointestinal content. For organisms such as mollusks and crustaceans for which it is possible to separate their molluscan part from the exoskeleton, it is desirable to dissect the organism and analyze these parts separately (Sohtome et al., 2014). When collecting benthos, it is recommended to also collect a sample of the sediment on the ocean floor, which is the habitat of the benthos, by using a bottom sampler and to measure the activity concentration of radionuclides in the sample of sediment.

2. Measurement Preprocessing

The best preprocessing and measurement methods depend on the radionuclide of the interest. For general preprocessing methods and radionuclide measurement methods, please refer to the radiation measurement method series published by the Ministry of Education, Culture, Sports, Science and Technology, Japan (Nos. 2, 7, 9, 12 and 16). Also, please refer to gamma ray spectral analysis techniques for emergency situations (Nos. 24 and 29). Here, we describe several points to be cautious about when preprocessing samples for measurements using germanium semiconductor detectors for gamma ray emitting isotopes including radiocesium. When the activity concentration of radionuclides is expected to be high, the raw sample of the frozen zooplankton and benthos can be directly used for the measurement. When defrosting the sample at room temperature, to prevent the loss of the cellular fluid, the sample should be divided into small portions of an amount that can fit inside the measurement container, and defrosted in a container. If the measurement container is not disposable, the sample should be placed in a plastic bag before being placed into the measurement container. To prevent contamination of the detector, the measurement container containing the sample should also be placed in a plastic bag. When the activity concentration of anthropogenic radionuclides is expected to be low, it may be difficult to conduct the measurement using the fresh sample directly. In this case, the water should be removed from the sample to reduce its volume. For this, the sample should be freeze-dried or dried using a dryer. The dried sample should be homogenized by grinding in a mortar. The sample should be filled into the container and measured using a germanium semiconductor detector. If further volume reduction is needed, the sample can be incinerated at an appropriate temperature (please refer to Volume 9 Chapter 3 in this Guideline of Ocean Observations (under review) for incineration methods). In cases where a large amount of phytoplankton suspended matter sample has been collected with a large volume *in-situ* filtration system, the sample can be dried, removed from the filter, ground in a mortar, placed in a pre-weighed measurement container, and measured using a germanium semiconductor detector. In cases where the sample is small, the sample can be dried, cut along with the filter, ground in a mortar, and used to fill the measurement container. The cartridge filter should be cut and should have the center part and core separated from the filter. The filter part should be incinerated to reduce its volume and used to fill the measurement container.

For samples such as radioactive strontium and plutonium isotopes that require chemical separation or extraction, procedures such as acidic cleavage and solvent extraction should be performed for the dried or incinerated sample in the same manner as for the sediment, to use it as an analysis sample (refer to Volume 9 Chapter 2: Marine sediment in this Guideline of Ocean Observations). When analyzing certain types of phytoplankton in which the cell wall contains silica, such as diatoms, it is necessary to select the appropriate method for completely dissolving the sample as per the sample characteristics, such as using hydrochloric acid for dissolving silica. When analyzing tritium, the water in the freeze dryer's cold trap should be recovered after the sample is freeze-dried and used as the sample for analysis as free water tritium (FWT). Organically bound tritium (OBT) can be analyzed in the same manner as large organisms by freeze-drying the sample, placing the dried sample in a quartz tube, and completely burning the sample using a combustion device while running oxygen over the

sample. The generated water vapor should be collected in a cold trap and used as the sample for analysis. For both FWT and OBT, the sample should be distilled and measured using a low background liquid scintillation counter to remove the organic material. For detailed methods of analysis, please refer to No. 9 of the radiation measurement method series published by the Ministry of Education, Culture, Sports, Science and Technology (Ministry of Education, Culture, Sports, Science and Technology, 2002).

References

- Aono, T., M. Kusakabe, T. Nakanishi, M. Yamada, S. Kaneko, T. Nakamura, K. Hori, and J. K. B. Bishop (2008): Large Volume *in-situ* filtration and concentration system for measurements of low-level radioactivity in seawater. *J. Advanced Mar. Sci. Technol. Soc.*, 14-2, 39-50.
- Bishop, J. K. B., and J. M. Edmond (1976): A new large volume filtration system for the sampling of oceanic particle matter. *J. Mar. Res.*, 34, 181–198.
- Hidaka, H., and Akagi, T. (2002): Introduction of Isotopic ratio analysis—Definitions and standard materials for isotopic ratios (in Japanese), *Bunseki*, 2002, Vol. 1. 2-9.
- IAEA (2004): Sediment distribution coefficients and concentration factors for biota in the marine environment. *Technical Reports Series* No. 422. IAEA, Vienna.
- Kaeriyama, H. T. Watabe, and M. Kusakabe (2008): ^{137}Cs concentration in zooplankton and its relation to taxonomic composition in the western North Pacific Ocean. *J. Environ. Radioact.*, 99, 1838–1845.
- Kaeriyama, H. K. Fujimoto, D. Ambe, Y. Shigenobu, T. Ono, K. Tadokoro, Y. Okazaki, S. Takehi, S. Ito, Y. Narimatsu, K. Nakata, T. Morita, and T. Watanabe (2015): Fukushima-derived radionuclides ^{134}Cs and ^{137}Cs in zooplankton and seawater samples collected off the Joban-Sanriku coast, in Sendai Bay, and in the Oyashio region. *Fish. Sci.*, 81, 139–153.
- Kitamura, M., Y. Kumamoto, H. Kawakami, E. C. Cruz, and K. Fujioka (2013): Horizontal distribution of Fukushima-derived radiocesium in zooplankton in the northwestern Pacific Ocean. *Biogeosciences*, 10, 5729–5738.
- Marumo K., T. Ishii, Y. Ishikawa, and T. Ueda (1998): Concentration of elements in marine zooplankton from coastal waters of Boso Peninsula, Japan. *Fish. Sci.*, 64, 185–190.
- Masuzawa, T., M. Koyama, and M. Terazaki (1988): A regularity in trace element contents of marine zooplankton species. *Mar. Biol.*, 97, 587–591.
- Ministry of Education, Culture, Sports, Science and Technology (1990) Radiation measurement methods series No. 12: Plutonium analysis method (in Japanese)
<http://www.kankyo-hoshano.go.jp/series/lib/No12.pdf>
- Ministry of Education, Culture, Sports, Science and Technology (1992) Radiation measurement methods series No. 7: Gamma ray spectrometry using germanium semiconductor detector (in Japanese)
<http://www.kankyo-hoshano.go.jp/series/lib/No7.pdf>
- Ministry of Education, Culture, Sports, Science and Technology (1992) Radiation measurement methods series No. 24: Sample preprocessing methods for gamma ray spectrometry for emergencies (in Japanese)

- <http://www.kankyo-hoshano.go.jp/series/lib/No24.pdf>
 Ministry of Education, Culture, Sports, Science and Technology (2002) Radiation measurement methods series
 No. 9: Tritium analysis method (in Japanese)
- <http://www.kankyo-hoshano.go.jp/series/lib/No9.pdf>
 Ministry of Education, Culture, Sports, Science and Technology (2003) Radiation measurement methods series
 No. 2: Radioactive strontium analysis method (in Japanese)
- <http://www.kankyo-hoshano.go.jp/series/lib/No2.pdf>
 Ministry of Education, Culture, Sports, Science and Technology (2003) Radiation measurement methods series
 No. 16: Environmental sample collection methods (in Japanese)
- <http://www.kankyo-hoshano.go.jp/series/lib/No16.pdf>
 Ministry of Education, Culture, Sports, Science and Technology (2004) Radiation measurement methods series
 No. 29: Gamma ray spectral analysis method for emergencies (in Japanese)
- <http://www.kankyo-hoshano.go.jp/series/lib/No29.pdf>
 The Oceanographic Society of Japan, the Great East Japan Earthquake Working group/Analysis and Sampling
 Subgroup (2011): Collection of marine samples for measuring radiation/Basic recommended method for
 measurement (in Japanese)
- http://kaiyo-gakkai.jp/jos/wp-content/uploads/2013/01/Manual_22May2011.pdf (2017/8/21 accessed)
- Oozeki, Y., Hu, F, Kubota, H., Sugisaki, H., Kimura, R. 2004. Newly designed quantitative frame trawl for
 sampling larval and juvenile pelagic fish. *Fish. Sci.*, 70, 223–232.
- Sohtome T., T. Wada, T. Mizuno, Y. Nemoto, S. Igarashi, A. Nishimune, T. Aono, Y. Ito, J. Kanda, and T.
 Ishimaru (2014): Radiological impact of TEPCO's Fukushima Dai-ichi nuclear power plant accident on
 invertebrates in the coastal benthic food web. *J. Environ. Radioact.*, 138, 106–115.
- Takata, H., M. Kusakabe, and S. Oikawa (2015): Radiocesiums (^{134}Cs , ^{137}Cs) in zooplankton in the waters of
 Miyagi, Fukushima and Ibaraki Prefectures. *J. Radioanal. Nucl. Chem.*, 303, 1265–1271.
- Tateda, Y. (1998): Concentration factor of ^{137}Cs for zooplankton collected from the Misaki coastal water. *Fish.
 Sci.*, 64, 176–177.
- Wiebe, P.H. and Benfield, M.C. (2003): From the Hensen net toward four-dimensional biological oceanography.
Prog. Oceanogr., 56, 7–136.

This page left intentionally blank.

Chapter 1 in this volume left intentionally blank.

This page left intentionally blank.

Petroleum and Hydrocarbons

Hideaki MAKI, National Institute for Environmental Studies

1. Introduction

Analytical methods for the qualification and quantification of hydrocarbons in marine environments are needed for identifying the sources of oil spills, for monitoring pollution status after oil spills, for examining the pyrogenic and terrigenous hydrocarbon content of sediment, and for studying the production of aliphatic hydrocarbons produced by marine organisms and plants.

Polycyclic aromatic hydrocarbons (PAHs) can be classified as being of either petrogenic or pyrogenic origin. The majority of petrogenic PAHs are low-molecular-weight compounds with 2 or 3 rings and their alkylated derivatives (e.g., naphthalene, fluorene, phenanthrene, dibenzothiophene, and anthracene), but includes smaller amount of anthracene and PAHs 4 or more rings (e.g., pyrene, fluoranthene and benzopyrenes). In contrast, the majority of pyrogenic PAHs are high-molecular-weight compounds with 4 or more rings. One exception to this general rule is heavy fuel oil, obtained as a residue from the petroleum refining process, which contains a relatively high amount of high-molecular-weight PAHs.

In Japan, although there are currently no environmental standards or criteria for the regulation of standing stocks of PAHs in any environmental media, some PAHs, such as naphthalene, methylnaphthalenes, and benzo[*a*]pyrene, are designated by the Ministry of the Environment as “compounds to be monitored” (2012) because of their adverse effects in aquatic organisms and humans. Similarly, the US Environmental Protection Agency has designated 16 PAHs as priority compounds to be monitored, seven of which are classified as carcinogenic compounds (benzo[*a*]anthracene, benzo[*a*]pyrene, benzo[*b*]fluoranthene, benzo[*k*]fluoranthene, chrysene, dibenzo[*a,h*]anthracene, and indeno[1,2,3-*cd*]pyrene). In addition, 9 of the PAHs are also regarded as potential mutagenic and teratogenic compounds (benzo[*b*]fluoranthene, benzo[*a*]anthracene, benzo[*a*]pyrene, benzo[*b*]fluoranthene, benzo[*j*]fluoranthene, benzo[*k*]fluoranthene, chrysene, dibenzo[*a,h*]anthracene, and benzo[*ghi*]perylene).

Since some PAHs, such as benzo[*a*]pyrene, are both carcinogenic and mutagenic, and their concentrations are occasionally high in sediment environments, the US National Oceanic and Atmospheric Administration has set sediment quality guidelines for PAHs by using effects range low (ERL) and effects range median (ERM) as indices of toxicity (Table 1). ERL and ERM mean the concentrations of each PAH which can potentially give biologically adverse effect on aquatic biota at 10 and 50% of possibilities, respectively.

Table 1. Effects range low (ERL) and effects range medium (ERM) of polycyclic aromatic hydrocarbons (PAHs) in marine sediment (ng/g-dry sediment), NOAA (1999)

	ERL	ERM
Acenaphthylene	44	640
Acenaphthene	16	500
Naphthalene	160	2100
2-Methylnaphthalene	70	670
Anthracene	85.3	1100
Phenanthrene	240	1500
Fluorene	19	540
Fluoranthene	600	5100
Pyrene	665	2600
Benzo[<i>a</i>]anthracene	261	1600
Chrysene	384	2800
Benzo[<i>a</i>]pyrene	430	1600
Dibenzo[<i>a,h</i>]anthracene	63.4	260
Total PAH	4022	44792

Since there are no environmental criteria for PAHs in Japan, no regulatory monitoring for PAHs has been conducted, as it has for dioxin and polychlorinated biphenyl. Thus, PAH monitoring data have been collected only occasionally through governmental or academic monitoring activities (Horinouchi et al., 1999) and the only systematic data available are from fixed monitoring stations in harbor areas known to be polluted with terrigenous PAHs.

The present manuscript describes the analytical methods used by the Ministry of the Environment of Japan, the Japan Coast Guard, and local environmental organizations in Japan for the determination of total hydrocarbon content and the amounts of individual PAHs and their alkylated derivatives in seawater and sediment.

2. Methods for the analysis of hydrocarbons in seawater and sediment

2-1. Analysis of hydrocarbons in seawater (Integrated Global Ocean Services System; Report of marine pollution surveys, Japan Coast Guard)

A simple, widely employed method for analyzing the hydrocarbon content in seawater is the method developed by the Integrated Global Ocean Services System (Figure 1). Briefly, 100 mL of analytical grade *n*-hexane is added to 2 L of sea water in a glass separatory funnel or bottle, and the mixture is vigorously agitated by using a shaker or magnetic stirrer for 15 min. After agitation, the mixture is left to stand until the seawater and hexane layers are distinctly separated. The upper hexane layer is recovered; 80 mL of *n*-hexane is added to the residual seawater layer; and the agitation, partitioning, and recovery process is repeated. The recovered hexane extracts are combined, dehydrated with sufficient sodium sulfate anhydrous, and concentrated by using a rotary evaporator or Kuderna–Danish concentrator. The volume of the concentrated hexane extract is adjusted to 10 mL and then subjected to fluorescence spectrometry (emission wavelength, 360 nm; excitation wavelength, 310 nm). For quantification of any hydrocarbons in the hexane extract, a known concentration of chrysene in *n*-hexane is used as the standard. The calculated values of samples as chrysene-equivalent concentration should be multiplied by a factor of 6.7, if the calculated value is to be expressed as petroleum-equivalent concentration.

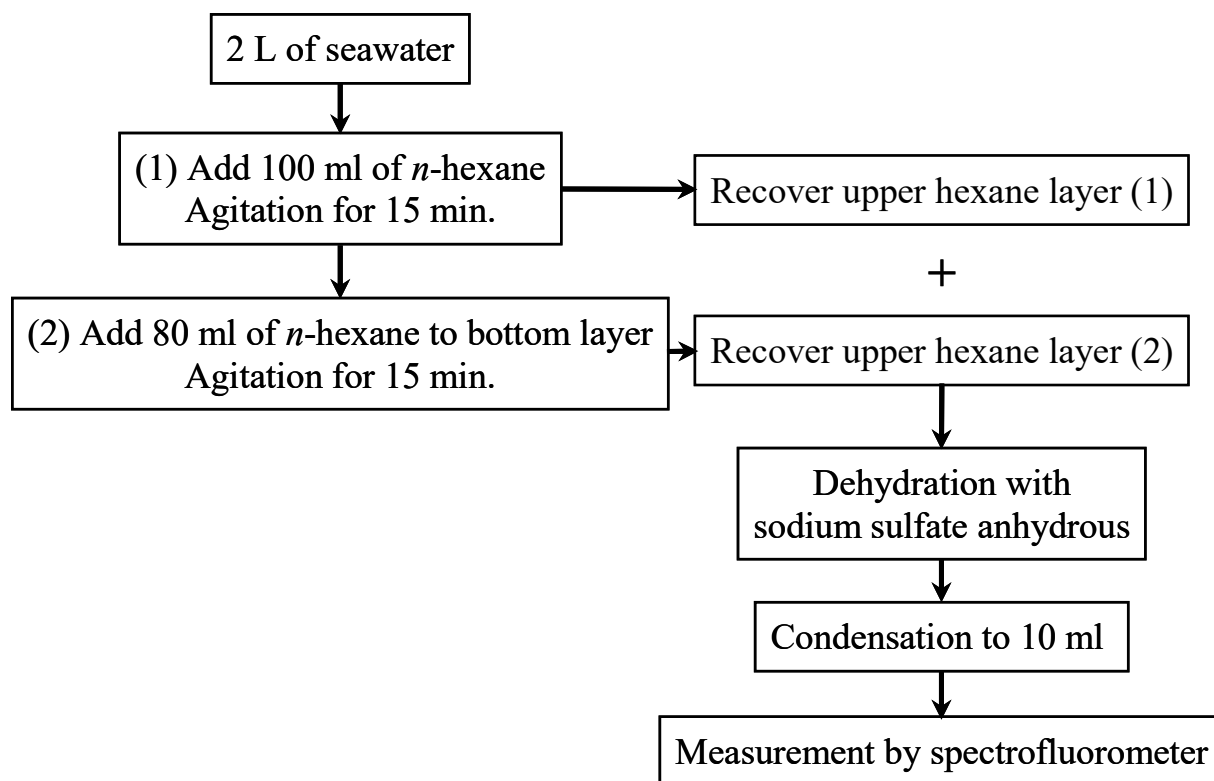


Fig. 1 Flowchart of the Integrated Global Ocean Services System method for the analysis of hydrocarbons in seawater samples.

2-2. Solvent extraction of sediment samples using n-hexane (Ministry of the Environment of Japan, Analytical method for sediments, 2012)

n-Hexane extraction with gravimetric analysis is a method for determining the total hydrocarbon content in sediment. This method is often used to determine the oil content in contaminated soils by subjecting the obtained hexane extract to column chromatography using a column filled with Florisil® powder, a synthetic magnesium silicate, to remove lipids and pigments such as chlorophyll produced by phytoplankton so that only the mineral oil content is analyzed. For marine environments used for commercial fishing, the *n*-hexane extract should be less than 0.1% (weight/weight) (Water quality criteria for fisheries (2018)).

In this method, 20 to 30 g of dried sediment is put into a glass-fiber extraction thimble and subjected to Soxhlet extraction for 5 to 6 h with *n*-hexane as the extraction solvent. The hexane extract is dehydrated with sufficient sodium sulfate anhydrous, and then the hexane is evaporated by heating to 80°C to obtain a residue. The residue is weighed, and the weight is normalized to the dry weight of the sediment sample.

Note that if the sample contains more sulfur particles than mineral oil, the sulfur particles can be co-extracted under reductive conditions, which can markedly influence the gravimetric measurement. In that case, the sulfur can be removed by adding reduced copper granules to the hexane extract and allowing the mixture to stand overnight.

This extraction method can also be used to analyze seawater samples, and the resulting gravimetric concentration is set as the water quality environmental standard in which “non-detectable” is considered as being compliant with the criteria (Ministry of the Environment, Japan).

2-3. Analysis of aliphatic hydrocarbons in sediment by using *n*-hexane extraction (Report of marine pollution survey, Japan Coast Guard)

Figure 2 shows a flowchart of the quantitative analysis of aliphatic hydrocarbons in sediment by *n*-hexane extraction. First, visible coarse materials such as gravel, shell, and pieces of animals and plants are removed from the sediment prior to analysis. Then, 40 to 50 g of wet sediment and 50 mL of ethanol containing 1 N potassium hydroxide are put into a glass centrifuge tube and heated under reflux for 1 h. After cooling, 30 mL of *n*-hexane is added to the centrifuge tube, and the mixture is vigorously agitated and then centrifuged. After centrifugation, the mixture is allowed to stand until the hexane and ethanol layers have separated, and then the upper hexane layer is recovered into a separatory funnel. The hexane extraction is repeated twice more times by adding 10 mL of *n*-hexane to the remaining sediment each time, and the 3 recovered hexane layers are combined. Next, 50 mL of pure water is added to the combined hexane extract, and the mixture is vigorously agitated and then left to stand until the hexane and water layers have separated. After partitioning, the hexane layer is recovered and dehydrated with sufficient sodium sulfate anhydrous. The dehydrated hexane extract is concentrated to approximately 1 mL and loaded onto a chromatography column filled with 3 g of silica gel (Wakogel S-1), 1 g of activated alumina, and 5 g of sodium sulfate anhydrous as the upper, middle, and bottom layers of the column bed, respectively. The sample is eluted from the column with 100 mL of *n*-hexane; the first 20 mL of eluent is collected, and the hexane is completely evaporated to obtain a residue. The residue is dissolved in 5 to 20 mL of carbon tetrachloride and subjected to Fourier transform infrared spectroscopy at 2930 cm^{-1} . A known concentration of eicosane in carbon tetrachloride is used as the standard for the quantification of aliphatic hydrocarbons in the sample.

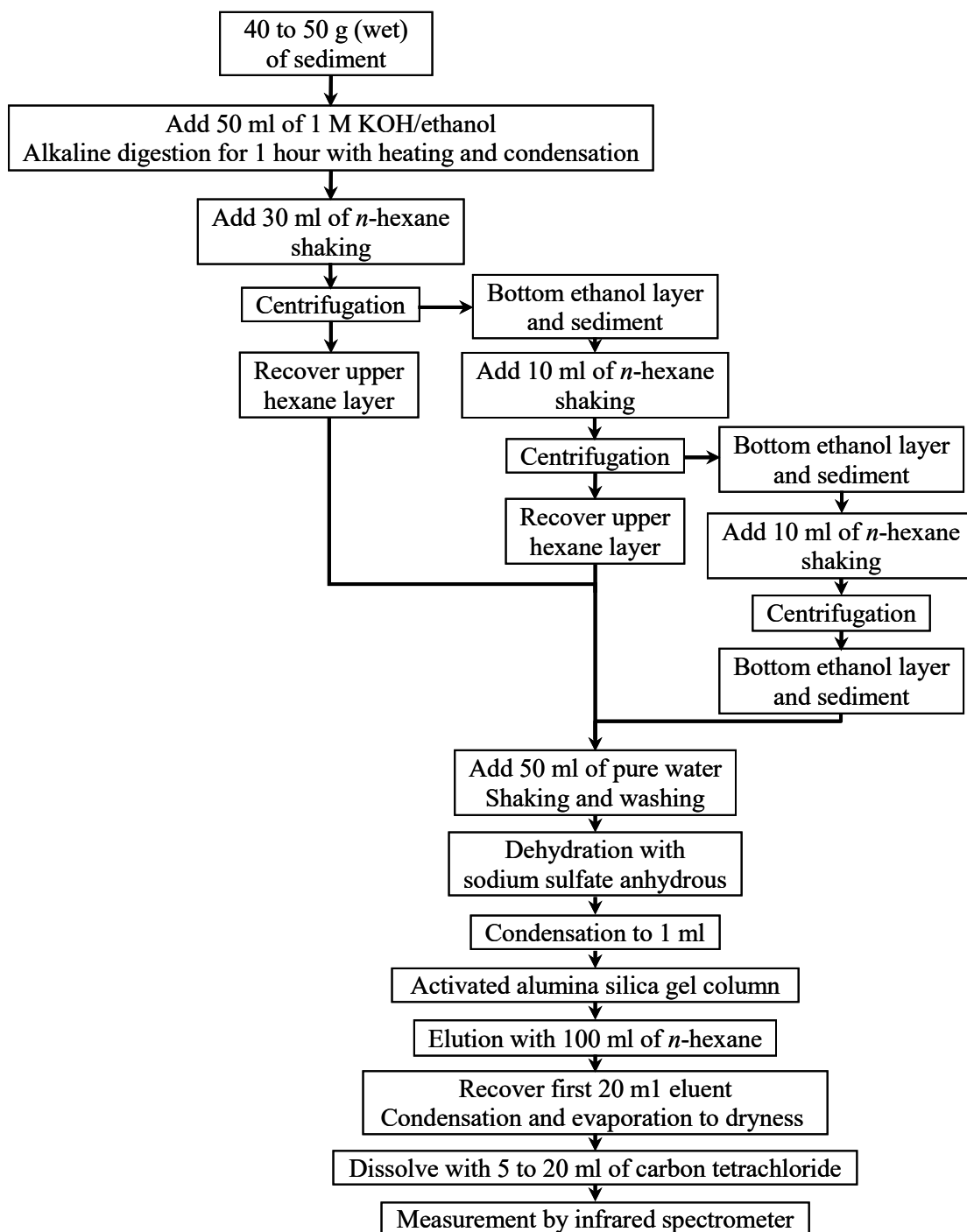


Fig. 2 Flowchart of the analysis of aliphatic hydrocarbons in sediment by *n*-hexane extraction.

2-4. Analysis of individual aliphatic and aromatic hydrocarbons in sediment or biological tissue

Figure 3 shows a flowchart of the procedure for analyzing individual aliphatic and aromatic hydrocarbons in sediment and biological samples.

2-4a. Extraction and pretreatment

Extraction and pretreatment are conducted to extract aromatic and aliphatic hydrocarbons from sediments and biological samples, to extract semi-volatile hydrocarbons directly from wet samples without the need for drying, and to enable the simultaneous extraction of as many samples as possible. This method minimizes the volume of organic solvents and the number of vessels used.

- a. **Sediment sample:** The inside of a glass centrifuge tube is rinsed with 50 mL of acetone, and the tube is left to dry. After drying, the tube is weighed before and after the addition of approximately 3 g of wet sediment (with bulky material removed), and the exact weight of the sediment is calculated. Analytical grade acetone (7 mL) is added to the centrifuge tube, which is then agitated vigorously with a vortex mixer, sonicated for 5 min, and centrifuged at 2500 rpm for 5 min. After centrifugation, the clear acetone extract is transferred to a 50-mL glass centrifuge tube by using a Pasteur pipette. Acetone (5 mL) is added to the remaining sediment, the extraction is repeated, and the acetone extracts are combined.
Biological sample: 20 mL of 1 M potassium hydroxide in ethanol is added to homogenized tissue in a 100-mL stoppered conical flask, and the resulting mixture is stirred for 15 h with a magnetic stirrer for alkaline digestion. After digestion, the mixture is transferred to a 50-mL brown glass centrifuge tube.
- b. Analytical grade dichloromethane (DCM, 10 mL) is added to the sediment or biological tissue remaining after extraction, and the mixture is agitated vigorously, sonicated for 5 min, and centrifuged at 2500 rpm for 5 min. For a sediment sample, the DCM extract is combined with the previous acetone extracts. For a biological sample, the DCM/ethanol extract is transferred to a 50-mL glass centrifuge tube.
- c. Ultrapure water (20 mL) is added to the combined extract, the mixture is agitated vigorously with a vortex mixer and centrifuged at 2500 rpm for 5 min, and the bottom organic solvent layer is recovered and added to a glass funnel or syringe filled with 8 to 10 mL of sodium sulfate anhydrous powder for dehydration; the dehydrated extract is received into a glass test tube.
- d. Steps **b** and **c** are repeated, but with the addition of only 7 mL of DCM in step **b** and without the addition of water in step **c**. After recovery, step **c** is repeated once more with the addition of only 5 mL of DCM but without the addition of water.
- e. After 0.5 mL of *n*-decane and a predetermined volume (e.g., 10 μ L) of analytical grade *n*-hexane containing fixed concentrations (e.g., 50 μ g/mL) of deuterated target PAHs (Table 2) are added to the extract, the acetone and DCM are evaporated under a nitrogen stream with heating by a block heater.

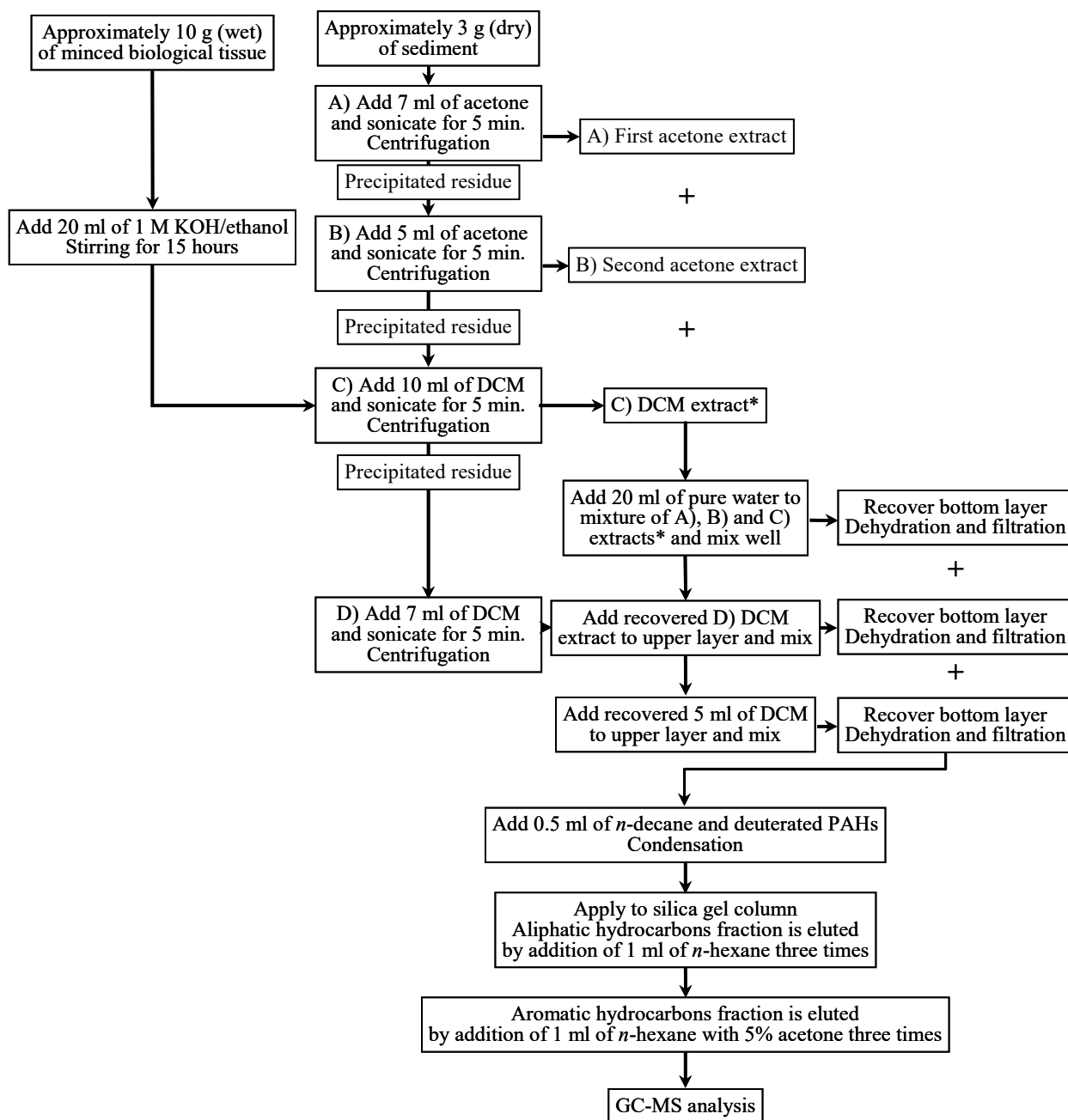


Fig. 3 Flowchart of the procedure for the analysis of individual aliphatic and aromatic hydrocarbons in sediment and biological samples (*mixed ethanol extracts in the case of a biological sample).

2-4b. Fractionation of aliphatic and aromatic hydrocarbons by silica gel column chromatography

- a. A chromatography column (volume, 3 mL) is filled with 0.5 g dry weight of activated silica gel (pre-packed columns are also commercially available) and connected to the vacuum manifold for solid phase extraction via a stopcock. The column bed is washed with 3 mL of *n*-hexane with the cock under the column closed to keep the column bed submerged in the hexane.

- b. Fractionation of aliphatic hydrocarbons: The *n*-decane extract produced in **2-4a** is passed through the column and received into a glass tube with scale marks. The tube originally containing the *n*-decane extract is rinsed with 1 mL of *n*-hexane, and the rinse is passed through the column and into the glass tube with scale marks. The rinsing procedure is repeated 2 more times or until the surface of the *n*-hexane reaches the top of the silica gel bed. The *n*-hexane eluent is obtained as the aliphatic hydrocarbon fraction.

Fractionation of aromatic hydrocarbons: After elution of the aliphatic hydrocarbon fraction, the inside of the glass tube that originally contained the *n*-decane extract is rinsed with 3 mL of *n*-hexane containing 5% (volume/volume) acetone, and the resulting rinse is passed through the silica gel column bed into a brown 10-mL glass tube with scale marks; the rinsing process is repeated 2 more times. The *n*-hexane eluent is obtained as the aromatic hydrocarbon fraction.

2-4c. Sampling and pretreatment of spilled oils and fuels

For the analysis of tarballs or oil paste washed up on beaches, samples are collected using a stainless spatula and stored until analysis in a glass or metal container under dark, cool conditions to avoid microbial and photo-degradation. If the tarball or oil paste cannot be sampled directly, contaminated samples of sediments such as silt-clay, sand, and gravel are collected.

For batch extraction, the collected samples are transferred into individual glass beakers and dissolved in an appropriate volume of DCM. The DCM solutions are dehydrated with sufficient sodium sulfate anhydrous. To remove bulky, non-oily particles, the DCM solutions are filtered through a glass funnel plugged with defatted cotton soaked with DCM or are subjected to Soxhlet extraction. The cleaned-up DCM solutions are then filtered through a polytetrafluoroethylene membrane filter-cartridge (mesh size, 0.45 μm) connected to a glass syringe into pre-weighed glass test tubes or flasks that can be connected to a rotary evaporator. Excess DCM is evaporated by using a centrifugal vacuum concentrator and a rotary evaporator, or by using a stream of nitrogen gas. After removal of the DCM, the glass container containing the residue is weighed, and the net weight of the residue is calculated by subtracting the weight of the empty glass container. The net weight of residue is considered the 'total solvent-extractable material' weight, if all extracting processes described above are quantitatively conducted.

For fine hydrocarbon analysis using a gas chromatograph, extracted oil samples are subjected to silica gel column chromatography to remove non-volatile polar residues, which deteriorate the capillary column, and to separate the aliphatic and aromatic hydrocarbon fractions. Extracted oil samples are dissolved (suspended) in *n*-hexane, adjusted to 30 mg-oil paste/mL-hexane, and 5 mL of the resulting solution is applied to the silica gel column (i.e., 15 mg of oil paste is loaded onto 1 g of silica gel column). The aliphatic and aromatic hydrocarbons are fractionated according to the procedure described in **2-4b**.

2-4d. Target analytes (Wang et al., 1999)

- Target analytes in the aliphatic hydrocarbon fraction
 - a. Normal alkanes (*n*-alkanes) with a carbon number of 12 to 40
Note: In many cases, only alkanes with a carbon number greater than 12 are detected from weathered oil samples.
 - b. Branched alkanes: Pristane and phytane
Biomarkers: 17 α H, 21 β H-hopane, 17 β H, 21 α H-hopane

Hopane is a triterpene contained in petroleum that is persistent to microbial and photo-degradation, unlike aliphatic hydrocarbons and PAHs. Hopane is therefore used as a normalizer to evaluate the biodegradation of petrogenic aliphatic hydrocarbons and PAHs in marine environments (Prince et al., 1994).

- Target analytes in the aromatic hydrocarbon fraction
 - a. 2-ring PAHs: Naphthalene and its alkylated derivatives (carbon number: 1–4)
 - b. 3-ring PAHs: Fluorene and its alkylated derivatives (carbon number: 1–2), dibenzothiophene and its alkylated derivatives (carbon number: 1–3), phenanthrene and its alkylated derivatives (carbon number: 1–3), acenaphthylene, acenaphthene, anthracene
 - c. 4-ring PAHs: Pyrene, fluoranthene, chrysene, benzo[*a*]anthracene
 - d. 5-ring PAHs: Benzo[*e*]pyrene, benzo[*a*]pyrene, benzo[*b*]fluoranthene, benzo[*k*]fluoranthene, dibenzo[*a,h*]anthracene
 - e. 6-ring PAHs: Benzo[*ghi*]perylene, indeno[1,2,3-*cd*]perylene

2-4e. Analytical conditions for gas chromatography (Ministry of the Environment of Japan, Analytical method for sediments, 2012)

Gas chromatography equipped with mass spectrometry (GC-MS) is suitable for the analysis of every semi-volatile aliphatic and aromatic hydrocarbons. For the analysis of linear and branched alkanes, gas chromatography with flame ionization detector (GC-FID) is also available.

- Column (capillary type): Semi-polar type, such as HP-5, DB-5, Ultra-2, and SPB-5, with liquid phase thickness 0.25 μ m, inner diameter 0.25 mm, and length 30 m
- Sample injection: Splitless mode, sampling time 30 to 90 s until purge, temperature 280 to 300 °C, sample injection volume 1 μ L
- Temperature program
 - a. Alkanes and biomarkers: 50 °C for 2 min, increase to 300 °C at 6 °C/min, hold at 300 °C for 15 min
 - b. PAHs: 50 °C for 2 min, increase to 120 °C at 20 °C/min, increase to 270 °C at 7 °C/min, increase to 320 °C at 20 °C/min, hold at 300 °C for 15 min
- Carrier gas: High-purity helium gas is used for both GC-FID and GC-MS. High-purity

nitrogen gas can be also used for GC-FID but not for GC-MS.

- Carrier gas flow rate: 1 to 2 mL/min
- Detector temperature: 300 °C for FID; 230 to 300 °C for the interface between GC and MS
- Detection mode for GC-MS: Selected ion monitoring mode

- Qualification and quantification

Figure 4a shows representative mass chromatograms of alkylated PAHs in extracts of seabed sediment, demonstrating that petrogenic PAHs exist as a complex mixture of isomers and homologues, which means that standard reagents for these PAHs are not commercially available. Therefore, pre-analysis of the aromatic hydrocarbon fraction of oil samples by GC-MS in scan mode is needed to verify the retention time of each alkylated PAH isomer and homologue for setting the selected ion monitoring mode time program. For undetected and/or unidentified PAH peaks in the aromatic hydrocarbon fraction, commercial standard compounds should be pre-analyzed by GC-MS in scan mode to verify the retention time of each of their peaks.

Table 2. Monitor and reference ions for select hydrocarbons analyzed by gas chromatography with mass spectrometry

Analytes and surrogates	Monitor ion (<i>m/z</i>)	Reference ion (<i>m/z</i>)
Linear <i>n</i> -alkanes	71	85
Branched alkanes	71	85
Biomarkers	191	
Acenaphthene	153	154
Acenaphthene-d ₁₀	164	
Acenaphthylene	152	76
Acenaphthylene-d ₁₀	160	
Naphthalene	128	102
Naphthalene-d ₈	136	
C1-Naphthalene	142	115
C2-Naphthalene	156	141
C3-Naphthalene	170	
C4-Naphthalene	184	
Fluorene	166	165
Fluorene-d ₁₀	176	
C1-Fluorene	180	
C2-Fluorene	194	

Dibenzothiophene	184	139
C1-Dibenzothiophene	198	
C2-Dibenzothiophene	212	
C3-Dibenzothiophene	226	
Anthracene, phenanthrene	178	152
Phenanthrene-d ₁₀ , anthracene-d ₁₀	188	
C1-Phenanthrene	192	
C2-Phenanthrene	206	
C3-Phenanthrene	220	
Pyrene, fluoranthene	202	101
Pyrene-d ₁₀ , fluoranthene-d ₁₀	212	
Chrysene, benzo[<i>a</i>]anthracene	228	114
Chrysene-d ₁₂	240	
Benzo[<i>e</i>]pyrene, benzo[<i>a</i>]pyrene, benzo[<i>b</i>]fluoranthene, benzo[<i>k</i>]fluoranthene	252	126
Benzo[<i>k</i>]fluoranthene-d ₁₂ , benzo[<i>a</i>]pyrene-d ₁₂ , benzo[<i>e</i>]pyrene-d ₁₂	264	
Dibenzo[<i>a,h</i>]anthracene	278	139
Dibenzo[<i>a,h</i>]anthracene-d ₁₄	292	

Benzo[ghi]perylene, Indeno[1,2,3-cd]perylene	276	138
Benzo[ghi]perylene-d ₁₂	288	
Terphenyl-d ₁₄	244	

Alkanes and biomarkers are quantified by using deuterated *p*-terphenyl (*p*-terphenyl-d₁₄) as the internal standard. The ratio of the alkane or biomarker peak area (A_x) to that of *p*-terphenyl-d₁₄ (A_{is}) is calculated by co-injecting a mixture with known concentrations of each alkane or biomarker and *p*-terphenyl-d₁₄ into the GC-MS system. Standard curves are created by plotting A_x/A_{is} versus the ratio of a stepwise increase in the concentration of each alkane or biomarker (C_x) to a constant concentration of *p*-terphenyl-d₁₄ (C_{is}) as the vertical and horizontal axes, respectively. The concentration of each alkane or biomarker in the sample is then calculated by multiplying C_{is} by the C_x/C_{is} corresponding to the A_x/A_{is} in the previously created standard curve. A_x/A_{is} is obtained by co-injecting a known concentration of *p*-terphenyl-d₁₄ into the GC-MS system.

For the quantification of PAHs, standard curves are created by plotting the ratio of peak area versus the ratio of the concentration of each non-deuterated PAH to its corresponding deuterated PAH (Table 2), instead of *p*-terphenyl-d₁₄, as the internal standard. For the quantification of alkylated PAHs, standard curves are created by plotting the ratio of peak area versus the ratio of the concentration of the non-deuterated alkylated PAH to that of the corresponding deuterated non-alkylated PAH (Table 3) because deuterated alkylated PAHs are rarely commercially available. The concentration of each non-alkylated and alkylated PAH is calculated as described for alkanes and biomarkers, except the compounds are used as the internal standard instead of *p*-terphenyl-d₁₄. The recovery efficiency for each PAH is calculated by spiking the sample with a known concentration of the corresponding deuterated PAH before extraction and is checked to confirm that it is within the allowable range (70%–130%).

Finally, the concentration of each hydrocarbon is evaluated as a value normalized by dry weight of sediment, dry or wet weight of biological sample, or the total solvent-extractable material of oil sample.

Table 3. Commercially available standards and substitutes of alkylated polycyclic aromatic hydrocarbons (PAHs)

Target alkylated PAH	Corresponding standard or substitute
C1-Naphthalene	1-Methylnaphthalene, 2-methylnaphthalene
C2-Naphthalene	2,6-Dimethylnaphthalene
C3-Naphthalene	2,3,5-Trimethylnaphthalene
C4-Naphthalene	2,3,5-Trimethylnaphthalene
C1-Fluorene	1-Methylfluorene
C2-Fluorene	1-Methylfluorene
C1-Dibenzothiophene	4-Methyldibenzothiophene
C2-Dibenzothiophene	4,6-Dimethyldibenzothiophene
C3-Dibenzothiophene	4,6-Dimethyldibenzothiophene
C1-Phenanthrene	1-Methylphenanthrene, 2-Methylphenanthrene, 3-Methylphenanthrene, 9-Methylphenanthrene
C2-Phenanthrene	3,6-Dimethylphenanthrene
C3-Phenanthrene	3,6-Dimethylphenanthrene

2-4f. Example analysis of real-world samples and accompanying remarks

Figure 4a shows mass chromatograms of alkylated PAHs in extract obtained from the seabed in a bay in the Tohoku region of Japan that was contaminated with spilled oil. The mass chromatograms

contain many vicinal peaks with the same m/z and very similar peak patterns, showing that the extract contained many isomers of alkylated PAHs. Petrogenic alkylated PAHs are more easily biodegraded than petrogenic high-molecular-weight PAHs such as pyrene, fluoranthene, and chrysene; therefore, alkylated PAHs are less persistent in the environment than PAHs with 4 or more rings (Maki et al., 2003).

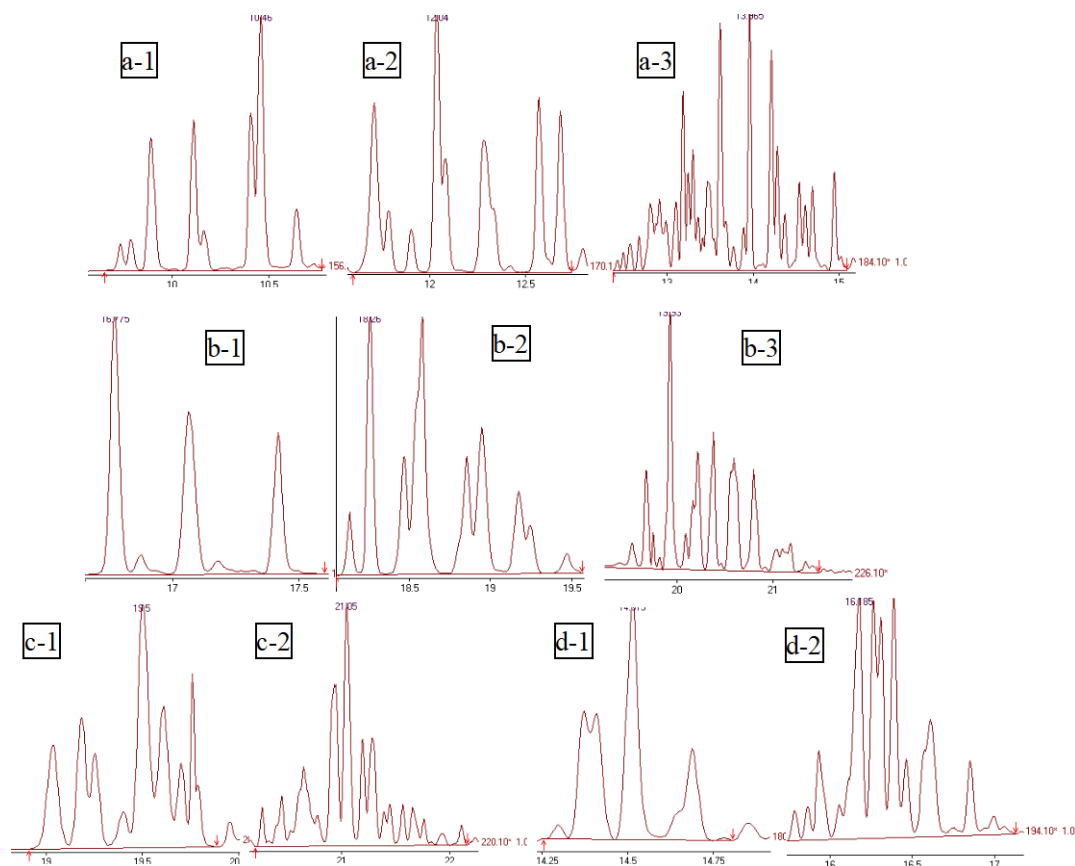


Fig. 4a Mass chromatograms of alkylated polycyclic aromatic hydrocarbons in extract obtained from a contaminated seabed.

a-1: C2-naphthalenes (m/z 156); a-2: C3-naphthalenes (m/z 170); a-3: C4-naphthalenes (m/z 184); b-1: C1-dibenzothiophenes (m/z 198); b-2: C2-dibenzothiophenes (m/z 212); b-3: C3-dibenzothiophenes (m/z 226); c-1: C2-phenanthrenes (m/z 206); c-2: C3-phenanthrenes (m/z 220); d-1: C1-fluorenes (m/z 180); d-2: C2-fluorenes (m/z 194).

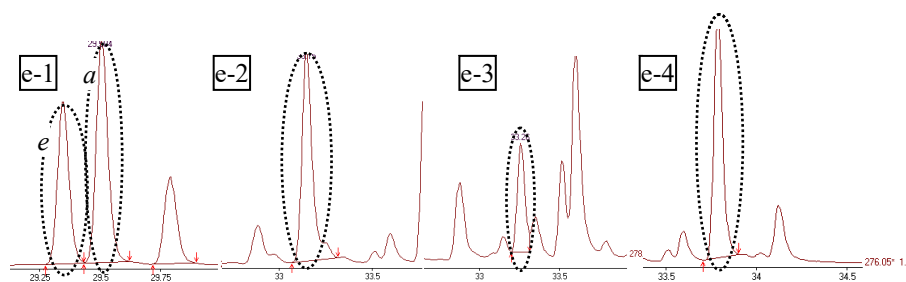


Fig. 4b Mass chromatograms of 5- and 6-rings polycyclic aromatic hydrocarbons in the extract shown in Fig. 4a.

e-1: Benzo[*e*]pyrene (dotted ellipse *e*) (m/z 252), benzo[*a*]pyrene (*a*) (m/z 252); e-2: indeno[1,2,3-*cd*]perylene (dotted ellipse) (m/z 276); e-3: dibenzo[*a,h*]anthracene (dotted ellipse) (m/z 292); e-4: benzo[*ghi*]perylene (dotted ellipse) (m/z 276).

Figure 4b shows mass chromatograms of the high-molecular-weight PAHs with 5 or 6 rings detected in the extract shown in Figure 4a. The presence of fake peaks next to the peak of the target PAH with the same m/z means that the retention time of each peak must be verified by referencing those of PAH standards. Note that the peaks corresponding to benzo[*e*]pyrene, benzo[*a*]pyrene, and benzo[*ghi*]perylene should be carefully identified because they sequentially emerge on the mass chromatogram with a m/z of 252 and a relatively short retention time. Similarly, the peaks of benzo[*b*]fluoranthene and benzo[*k*]fluoranthene cannot be easily resolved on mass chromatogram as they also have an m/z of 252.

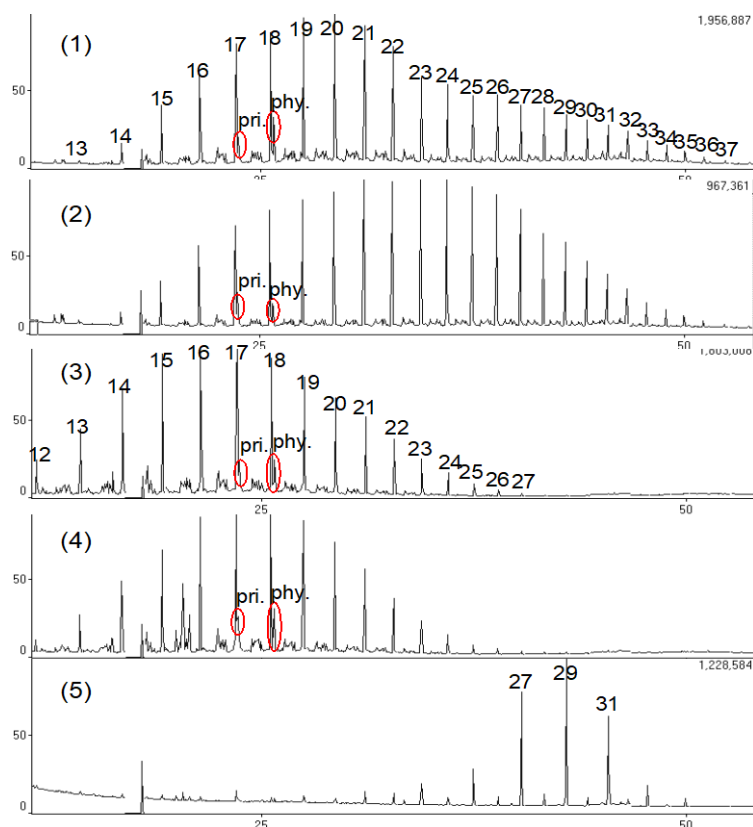


Fig. 5 Mass chromatograms at m/z 71 showing the alkanes in various oils and sediments.

(1) Crude oil spilled by the 2011 Tohoku earthquake and tsunami; (2) heavy fuel used in thermal power stations; (3) heavy fuel used by ships; (4) sediment collected from a bay polluted with heavy fuel spilled by the 2011 Tohoku earthquake and tsunami; (5) sediment collected from a bay not polluted by the 2011 Tohoku earthquake and tsunami. The number above each peak indicates the number of carbon atoms in the alkane; “pri” and “phy” indicate the peak of the branched alkanes pristane and phytane, respectively.

As described above, trace levels of high-molecular-weight PAHs with more than 5 or more rings are detected in Arabic crude oil. However, some heavy fuels, such as that spilled from the wrecked Russian tanker *Nakhodka* in the Sea of Japan in 1997, contain high amounts of high-molecular-weight PAHs (Horinouchi et al., 1999; Maki et al., 2003). GC-detectable hydrocarbons constitute less than 10% of the total compounds in any crude oil sample (Wang et al., 1999). The major compounds in crude oil remain to be identified.

Since low-molecular-weight *n*-alkanes with a carbon number less than 12 are volatile and high-molecular-weight *n*-alkanes with a carbon number of more than 12 are subject to microbial degradation in a short period of time, *n*-alkanes are usually not abundantly detected in environmental samples. However, since unweathered oils and fuels contain abundant amounts of semi- and non-volatile *n*-alkanes, the gas chromatograms of unweathered oils and fuels are characterized by a regular array of peaks for a series of *n*-alkanes that increases by one carbon number for each peak (Fig. 5 (1)–(3)). The peaks immediately after C17 (heptadecane) and C18 (octadecane) represent the

branched alkanes pristane and phytane, respectively, and are characteristic peaks in mass chromatograms of petroleum samples. Since these branched alkanes degrade more slowly than *n*-alkanes, the pristane or phytane to *n*-alkane ratio increases as oil is more weathered.

Figure 5 (5) shows the mass chromatogram of the alkanes in the extract obtained from a sample of non-polluted seabed. The high amounts of alkanes with a high, odd carbon number indicate that the alkanes originated from the wax of terrestrial plants (Wang et al., 1999).

References

- Analytical method for sediments <http://www.env.go.jp/water/teishitsu-chousa/> (2012): Ministry of the Environment, Japan. (in Japanese).
- Horinouchi A., S. Tsutsumi, E. Kouno, H. Takada, P. M. Zakaria and S. Noriki (1999): Chemical characterization of petroleum using GC-MS and behaviors and effects of hydrocarbons in the environments (Symposium: present status and future subjects of researches on petroleum pollution) Bulletin on Coastal Oceanography, 37, 23–34. (in Japanese).
- Maki, H., M. Utsumi, H. Koshikawa, T. Hiwatari, K. Kohata, H. Uchiyama, M. Suzuki, T. Noguchi, T. Yamasaki, M. Furuki, and M. Watanabe (2003): Intrinsic biodegradation of heavy oil from Nakhodka and the effect of exogenous fertilization at a coastal area of the Sea of Japan. Water Air Soil Pollut., 145, 123–138.
- Prince, R. C., D. L. Eimendorf, J. R. Lute, C. S. Hsu, C. E. Haith, J. D. Senius, G. J. Dechert, G. S. Douglas, and E. L. Butler (1994): $17\alpha(H),21\beta(H)$ -hopane as a conserved internal marker for estimating the biodegradation of crude oil. Environ. Sci. Technol., 28, 142–145.
- Report of marine pollution surveys, Hydrographic and Oceanographic Department, Japan Coast Guard. (in Japanese).
- Sediment quality guidelines developed for the national status and trends program <http://ccma.nos.noaa.gov/publications/sqg.pdf> (1999): NOAA, USA.
- Wang, Z., M. Fingas, and D. Page (1999): Oil spill identification. J. Chromatogr. A., 843, 369–411.
- Water quality criteria for fisheries (2018): Japan Fisheries Resource Conservation Association. (in Japanese).

This page left intentionally blank.

Microplastics (Surface Water Trawl Surveys for Small Debris Items)

○Takashi MIYAO (Japan Meteorological Agency)

1. Introduction

Plastic debris in the marine environment has significant impacts on marine ecosystem, and is one of the major global issues. Although small plastic debris is generally undetectable with shipboard sighting survey, there is no doubt that they have been steadily increasing within marine environment in spite of efforts to control the problem (UNEP, 2014). Moreover, it has been revealed that marine plastics carry toxic chemicals of smaller molecular size ($MW < 1000$), which can penetrate through the cell membrane (Takada et al., 2009; Teuten et al., 2009). There is evidence that plastics are fragmenting in the marine environment (Barnes et al., 2009), as a consequence, small fragments of plastics are distributed throughout the ocean, occurring on shorelines, in surface waters, seabed sediments from Arctic to Antarctic and in a wide variety of biota such as invertebrates, fish, seabirds, mammals etc. (Ryan et al., 2009; Reisser et al., 2014).

The term “microplastics” was introduced in mid-2000s, and are used pragmatically to describe plastic particles “smaller than 5mm” (Arthur et al., 2009; GESAMP, 2015). Microplastics are often classified into two main categories: (i) “primary” microplastics are originally manufactured to be of a microscopic size for particular industrial or domestic applications, and (ii) “secondary” microplastics are tiny plastic fragments derived from the breakdown of larger plastic debris, both at sea and on land (Cole et al., 2011).

In this chapter, the methodology of the surface water trawl surveys for small size debris, mainly microplastics, is described. Trawl surveys are less subjective than direct sighting survey (Ryan et al, 2009), but currently no universally accepted standard method is available for observations of microplastics. Therefore, the following is only suggested procedures derived from many previous reports.

Incidentally, examinations of stomach contents of seabirds and sea turtles can also bring information about microplastics; however, they need quite another technique and equipment.

2. Objectives and Setting of Surveys

2-1 Objectives

Shipboard surface water trawl surveys obtain samples of floating microplastics and collect information on their distribution, types and amounts. Typical objectives for open-water trawling surveys are, for example, as follows:

- to obtain samples of microplastics;
- to identify types of microplastics;
- to estimate concentration of microplastics;
- to detect temporal and spatial variation in the occurrence of microplastics.

It is desirable that trawl surveys are accompanied with direct sighting survey for floating pollutants

(see Chapter 4) in order to interpret the connection with the distribution of larger debris. While field sampling and sample processing, avoid wearing clothes made of polymer or synthetic fibers, because they may contaminate plastic samples. Woodall et al. (2015) gave more strict information on the contamination of the samples.

2-2 Site Selection

There has been little information about abundance and types of floating microplastics, as well as about larger pollutants, in the open-ocean. The survey sites should be selected in consideration of the following matters:

- to deliberate on sources and transportation process affected by the wind system and the major currents;
- to focus on areas that are known to accumulate pollutants;
- not to impact on marine ecosystems by the navigation of the observation ship.

For example, the area of concentrated small debris, known as “Great Pacific Garbage Patch”, lies off the Japan Archipelago and between Hawaii and California, almost coincident with the Subtropical Convergence Zone, affected by Ekman dynamics (Dautel, 2009; EPA, 2011). Isobe et al. (2014) described that they sought oceanic fronts before trawl survey, because floating plastic debris is likely to be trapped there. Needless to say, sampling site should not be located close to shore and considered to be shallow, taking the dimension of observation ship into account.

2-3 Frequency and Timing of Surveys

For long-standing monitoring in fixed region, the minimum sampling frequency should be annually. Ideally quarterly sampling is recommended, allowing an interpretation on seasonal changes.

It is well known that depth profiles of microplastics are mainly affected by turbulence in the surface layer; especially smaller particles are more susceptible to vertical transport (Kukulka et al., 2012; Reisser et al., 2015). Therefore, it is desirable that trawl surveys for microplastics floating within thin surface layer are conducted under calm sea state as far as possible.

3. Shipboard Trawl Survey

3-1 Outline of Sampling Method

Surface water trawl surveys are conducted in the daytime, so that the state of sampling net can be seen clearly. Sampling net attached to the end of the towrope is deployed while the ship is moving at constant speed, and trawled for preset time duration (details will be described later). During the trawl, towrope length may be adjusted to ensure approximately half of net mouth is under water, so that sampling net skims the sea surface. In order to stabilize sampling net posture, weights can be attached at the bottom of net mouth frame, or floats can be put on both sides of the net mouth. Sampling net should be placed on a boom, if possible, in order to avoid the wake behind the ship.

After sampling net is recovered, filtered surface water sample is collected in small net bag in the end bucket (traditionally called “cod-end”), washing gently with natural seawater from the outside of

the sampling net. Next, the end bucket is detached and entire contents of small net bag are transferred into another container, rinsing with natural seawater or fresh water. Extra care must be taken because small items are easily lost under rainy or windy condition.

The sample may be consequently processed on shipboard or stored in labeled container for laboratory processing (see 3-4). In the latter case, sample should be frozen or chemically preserved (add formalin etc.) as soon as possible not to turn putrid. Note that the chemically preserved samples generally cannot be submitted for persistent organic pollutants (POPs: such as PCBs, DDTs etc.) analysis.

3-2 Equipment

The observation ship should equip GPS unit for determination of ship position and speed continuously. Appropriate trawling system (crane, winch, capstan etc.) and sampling net with supplies (cable/rope, shackles, swivels etc.) are required for net-based surveys.

Although many kinds of sampling nets are available for trawl surveys, among them neuston net and manta net, shown in Figure 3-1, seem to have been most frequently used (Ribic et al., 1992; Lattin et al., 2004; Ryan et al., 2009; Lippiatt et al., 2013; Reisser et al., 2013; Isobe et al., 2014). Both of them are implements for sea surface sampling, the latter is supposed to resemble a manta ray, with metal wings and broad rectangular mouth.

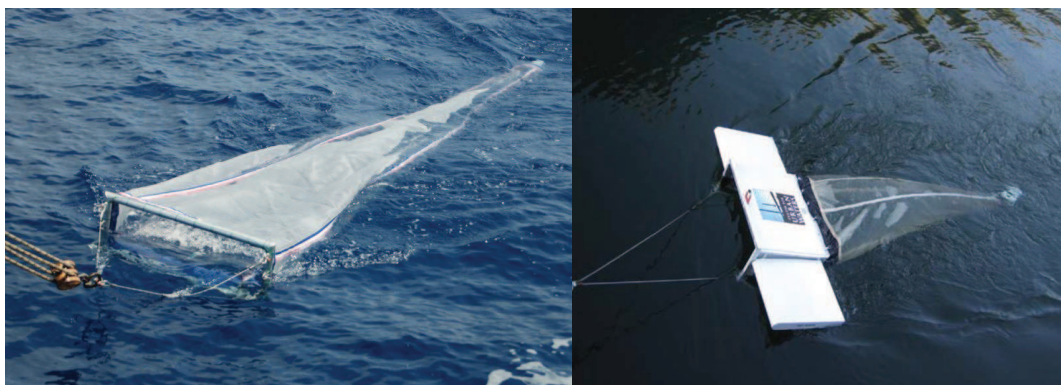


Figure 3-1 Neuston net (left; [http://www.aoml.noaa.gov/ocd/ocdweb/waltonsmith_photos.html]) and manta net (right; Masura et al., 2015).

Desforges et al. (2014) collected subsurface water sample (4.5m below the water line) using the saltwater intake system of the vessel. Although their sampling method is independent on sea state and needs no trawling system on the vessel, the plastic concentration in subsurface water is generally lower than the surface water. Consequently, it is likely that total amount of microplastics in the water column may be underestimated.

4. Sample Processing

Microplastics in surface water samples are often classified by their size, external characteristics (function of the original product) and polymer types. Efforts of classification are important as obtained information can be used to pinpoint sources of plastic debris and target reduction measures.

4-1 Sieving and Visual Separation

First, any obvious large debris items, larger than centimeter-sizes, are manually removed from surface water samples. Consequently, samples are filtered through double-stacked sieves, which have equivalent mesh size of upper and lower limit size of target microplastics (Masura et al. (2015) used 5.6-mm (No. 3.5) and 0.3-mm (No. 50)), to separate debris into two size fractions, and rinsed with distilled water. Material retained on the upper limit size sieve can be discarded or archived for another studies. The sample collected on the lower limit size sieve is transferred into some other container.

Next, plastic fragments are visually (by naked eye or with the aid of magnifier/microscope) identified and picked up and placed in a graduated petri dish with forceps or some adequate instrument from the sample. This is an almost obligatory step to separate plastics from other materials, such as organic debris, small pieces of hull-originated paint, metal, glass, etc., and, if possible, should be confirmed by more than one people for quality assurance (Lippiatt, et al., 2013). Plastic fragments on the petri dish can be counted for every different size categories, and can be weighed after drying process. Pre-weighed vials or dishes are useful for the procedures described here.

4-2 Classification by External Characteristics

Microplastics can be classified by external characteristics into several types. For example, Erikson (2005) introduced seven types: i) Pellet, ii) Fragment, iii) Film – plastic debris of bags or wrappers, iv) Foam, v) Filament, vi) Cigarette parts and vii) Other debris (including glass, rubber, metal, etc.). Lattin et al. (2004) sorted plastics into six categories – i) fragments, ii) styrofoam, iii) pellets, iv) polypropylene/monofilament line, v) thin plastic films and vi) resins. UNEP/IOC (2009) also showed the detail “standard categories” for remote benthic and floating observation, including seven classes; i) Containers, ii) Fishing & Boating, iii) Food and Beverage, iv) Packing, v) Sanitary, vi) Smoking and vii) Other.

4-3 Density Separation

Although many different types of plastics are produced globally, 6 classes are dominant in the market (GESAMP, 2015) and given “SPI Resin Identification Code” (see American Chemistry Council, 2007) as follows: i) polyethylene terephthalate (PET), ii) high-density polyethylene (HDPE), iii) polyvinyl chloride (PVC), iv) low-density polyethylene (LDPE), v) polypropylene (PP), vi) polystyrene (PS, including expanded polystyrene EPS) and vii) others. Their code and density data for typical virgin resins are summarized in Table 3-1.

Table 3-1. SPI Resin Identification Code and Plastic Classes (American Chemistry Council, 2007) with density data (Eriksen, 2005).

Code	Plastic Class		Density [#] [g · cm ⁻³]
1	PET	Polyethylene terephthalate	1.38 – 1.39
2	HDPE	High-density Polyethylene	0.95 – 0.97
3	PVC	Polyvinyl Chloride	1.16 – 1.35
4	LDPE	Low-density Polyethylene	0.92 – 0.94
5	PP	Polypropylene	0.90 – 0.91
6	PS	Polystyrene	1.05 – 1.07
7	(Others)	Cellulose Acetate etc.	-

Densities given here are approximate value for typical virgin resins. Note that plastic products are often mixed with fillers and additives that may alter their density.

The plastic fragments can be separated based on the difference of densities among plastic classes (Corcoran, 2009). Plastics that float in seawater and fresh water are EPS, high and low density PE, and PP. Solid form PS also floats in a saturated NaCl solution ($\rho \cong 1.2$ [g·cm⁻³]). Plastics that finally float in sodium polytungstate solution include flexible/rigid PVCs and PETs. As the density of 30% CaCl₂ solution is approximately equal to 1.3 [g·cm⁻³], it can be used to separate PET and PVC. Ethanol-water mixtures of various densities, including $\rho = 1.0, 0.9408$ and 0.911 [g·cm⁻³], can be used to separate PS, high and low density PE and PP. Cooking oils, their densities are approximately equal to ethanol-water mixtures, may also be used for plastic separation (Eriksen, 2005).

4-4 Spectroscopic Identification

There are some concern that density separation method may make misidentification, because the density of plastic fragments may vary considerably depending not only on the polymer type, but also on the manufacturing process, fillers and additives. For that reason, use of spectroscopic method (FT-IR spectroscopy, near-infrared spectroscopy, Raman spectroscopy etc.) is recommended, because it may bring certain determination of the polymer types of plastic samples (Hidalgo-Ruz et al., 2012).

If plastic samples are not submitted for chemical analysis of PCBs, DDTs etc., they should be disposed appropriately.

5. Variables to Consider

5-1 Weather Condition and Sea State

As mentioned above, depth profiles of microplastics are mainly affected by turbulence in the surface layer. If the sea surface is choppy, net mouth might be submerged and/or be out of the water, and sampling net will not collect “surface water sample”. Trawl surveys should not be conducted in strong wind and rough sea surface condition. It is also recommended to avoid the area where tide and/or current may be strong.

5-2 Ship Speed and Time Duration

Trawl surveys should be conducted at a ship speed of 1-3 knots, if there is interest to size distribution of microplastics. In recent studies, trawling speed are usually 2-4 knots (Lattin et al., 2004; UNEP/IOC, 2009; Reisser et al., 2013; Isobe et al., 2014) , if the ship speed is too fast, objects collected in sampling net may be increasingly susceptible to fragmentation resulting from abrasion, wave-action and turbulence (Cole et al., 2011).

Time duration of the trawl shot depends on the ship speed, and should be set supposing the amount of floating objects; however, as often conducted in neuston study, every trawl shot should be made for at least 10 minutes.

5-3 Mesh Size of Sampling Net

It is a natural consequence that the minimum size of debris collected by sampling net depends on its mesh size. The majority of sampling nets used in recent studies have a mesh size of around 333 μm . For example, Ribic et al. (1992) recommended 333 μm -mesh net. In “NOAA Marine Debris Program”, Lipiatt et al. (2013) and Masura et al. (2015) introduced the 330 μm -mesh and 335 μm -mesh net, respectively. Isobe et al. (2014) used neuston net with mesh size of 0.35mm. Therefore, recommended mesh size of sampling nets is around 333 μm , in this guidance. All the particles smaller than the mesh size go through sampling net.

5-4 Personnel

Required personnel include technical experts, who are experienced in or trained in the use of sampling net and visual separation.

6. Data and Metadata

6-1 Classification of Microplastics

As mentioned in 3-4-2, microplastics can be classified by external characteristics. Their color, shape, dimension (length/width), wear etc. may be close observed and recorded. Microplastics can be counted and weighed for every different size categories or polymer types. Although there is no universally authorized classification of microplastics has, it should be decided based upon previous works, depending on observation purpose.

6-2 Concentration of Microplastics

For quantitative comparisons of different surveys, it is strongly recommended that concentration of microplastics should be reported in either unit among next ones: [$\text{items}\cdot\text{km}^{-2}$], [$\text{items}\cdot\text{m}^{-3}$] and [$\text{mg}\cdot\text{m}^{-3}$].

Sea surface area skimmed by sampling net can be calculated multiplying net mouth width by trawl shot length. Consequently, water volume passed through the sampling net can be estimated from the area found above and net mouth height under water. To measure water volume directly and more

exactly, sampling net should be equipped with a flowmeter, calibrated under the calm sea surface condition, at the net mouth (e.g. Lippiatt et al., 2013; Isobe et al., 2014).

6-3 Metadata

Metadata should include following information:

- Survey name, date, time, location
- Ship characteristics: Name, type (e.g. research, fishing, regular ferry etc.), tonnage, length, width etc.
- Detail of trawl shot: latitude/longitude of start/end point, trawl shot length, ship speed, time duration
- Detail of sampling net: Type, dimension (net mouth width and height), mesh size
- Environmental conditions: wind speed/direction, wave and swell (direction/height/period), surface current etc.

7. Concluding Remarks

Surface water trawling survey can provide valuable information on the concentration and types of microplastics. From results of previous trawl surveys, however, variability in amounts of microplastics may be considerably large. Therefore, increase of sample water volume or number of trawl surveys will be expected for a given level of confidence. Careful consideration to survey design and standardization should be paid in order to develop robust estimates of concentration of microplastics.

References

- American Chemistry Council (2007): Plastic Packaging Resins (SPI Resin Identification Code). Retrieved from [<http://plastics.americanchemistry.com/Education-Resources/Plastics-101/Plastics-Resin-Codes-PDF.pdf>] (2015/07/22).
- Arthur, C., J. Baker, H. Bamford, N. Barnea, R. Lohmann, K. McElwee, C. Morishige and R. Thompson (2009): Summary of the International Research Workshop on the Occurrence, Effects, and Fate of Microplastic Marine Debris. In *Proceedings of the International Research Workshop on the Occurrence, Effects, and Fate of Microplastic Marine Debris*. Sept 9-11, 2008. NOAA Technical Memorandum NOS-OR&R-30.
- Barnes, D. K. A., F. Galgani, R. C. Thompson and M. Barlaz (2009): Accumulation and fragmentation of plastic debris in global environments. *Philosophical Transactions of the Royal Society*. B364, 1985–1998.
- Cole, M., P. Lindeque, C. Halsband, and T. S. Galloway (2011): Microplastics as contaminants in the marine environment: A review. *Marine Pollution Bulletin*, 62, 2588–2597.
- Corcoran, P. L., M. C. Biesinger and M. Grifi (2009): Plastics and beaches: A degrading relationship. *Marine Pollution Bulletin*, 58, 80–84.
- Dautel, S. L. (2009): Transoceanic Trash: International and United States Strategies For the Great Pacific Garbage Patch, *Golden Gate University Environmental Law Journal*, 3, 181-208.
- Desforges, J-P. W., M. Galbraith, N. Dangerfield and P. S. Ross (2014): Widespread distribution of microplastics in subsurface seawater in the NE Pacific Ocean. *Marine Pollution Bulletin*, 79, 94-99.

- EPA (2011): Marine Debris in the North Pacific: A Summary of Existing Information and Identification of Data Gaps. United States Environmental Protection Agency. 23pp.
- Eriksen, M. (2005): Watershed Wonders: Standard Based Activities and Information about Water and Watersheds for Middle and High School Classrooms. Algalita Marine Research Foundation, 91pp. Retrieved from [[http://people.oregonstate.edu/~rochefow/K-12 Outreach Activities/SKIES curriculum/SKIES Ecology and Environmental Engineering/WatershedWonders-curr.pdf](http://people.oregonstate.edu/~rochefow/K-12%20Outreach%20Activities/SKIES%20curriculum/SKIES%20Ecology%20and%20Environmental%20Engineering/WatershedWonders-curr.pdf)] (2015/07/22).
- GESAMP (2015): Sources, Fate and Effects of Microplastics in the Marine Environment: A Global Assessment (Kershaw, P. J., ed). IMO/FAO/UNESCO-IOC/UNIDO/WMO/IAEA/UN/UNEP/UNDP Joint Group of Experts on the Scientific Aspects of Marine Environmental Protection. GESAMP Reports & Studies Series, No. 90, 96pp.
- Hidalgo-Ruz, V., L. Gutow, R. C. Thompson, M. Thiel (2012): Microplastics in the Marine Environment: A review of the Methods Used for Identification and Quantification. *Environmental Science & Technology*, 46, 3060–3075.
- Isobe, A., K. Kubo, Y. Tamura, S. Kako, E. Nakashima and N. Fujii (2014): Selective transport of microplastics and mesoplastics by drifting in coastal waters. *Marine Pollution Bulletin*, 89, 324-330.
- Kukulka, T., G. Proskurowski, S. Morét-Ferguson, D. W. Meyer and K. L. Law (2012): The effect of wind mixing on the vertical distribution of buoyant plastic debris. *Geophys. Res. Lett.*, 39, L07601, doi:10.1029/2012GL051116.
- Lattin, G. L., C. J. Moore, A. F. Zellers, S. L. Moore and S. B. Weisberg (2004): A comparison of neustonic plastic and zooplankton at different depths near the southern California shore. *Marine Pollution Bulletin*, 49, 291-294.
- Lippiatt, S., S. Opfer, and C. Arthur (2013): Marine Debris Monitoring and Assessment. NOAA Technical Memorandum NOS-OR&R-46.
- Masura, J., J. Baker, G. Foster and C. Arthur (2015): Laboratory methods for the analysis of microplastics in the marine environment: recommendations for quantifying synthetic particles in waters and sediments. NOAA Technical Memorandum NOS-OR&R-48.
- Reisser, J., J. Shaw, C. Wilcox, B. D. Hardesty, M. Proietti, M. Thums and C. Pattiaratchi (2013): Marine Plastic Pollution in Waters around Australia: Characteristics, Concentrations, and Pathways. *PLoS ONE* 8, e80466, doi:10.1371/journal.pone.0080466.
- Reisser J., J. Shaw, G. Hallegraeff, M. Proietti, D. K. A. Barnes, M. Thums, C. Wilcox, B. D. Hardesty and C. Pattiaratchi (2014): Millimeter-Sized Marine Plastics: A New Pelagic Habitat for Microorganisms and Invertebrates. *PloS ONE* 9, e100289, doi:10.1371/journal.pone.0100289.
- Reisser, J., B. Slat, K. Noble, K. du Plessis, M. Epp, M. Proietti, J. de Sonnevile, T. Becker and C. Pattiaratchi (2015): The vertical distribution of buoyant plastics at sea: an observational study in the North Atlantic Gyre. *Biogeosciences*, 12, 1249–1256, www.biogeosciences.net/12/1249/2015/, doi:10.5194/bg-12-1249-2015
- Ribic, C. A., T. R. Dixon, and I. Vining (1992): Marine Debris Survey Manual. NOAA Technical Report NMFS 108.

- Ryan, P. G., C. J. Moore, J.A. van Franeker and C. L. Moloney (2009): Monitoring the abundance of plastic debris in the marine environment. *Philosophical Transactions of the Royal Society B: Biological Sciences* 364, 1999–2012.
- Takada, H., Y. Mato, S. Endo, R. Yamashita and M. P. Zakaria (2009): Pellet Watch: Global Monitoring of Persistent Organic Pollutants (POPs) using Beached Plastic Resin Pellets. In *Proceedings of the International Research Workshop on the Occurrence, Effects, and Fate of Microplastic Marine Debris*. Sept 9-11, 2008. NOAA Technical Memorandum NOS-OR&R-30.
- Teuten, E. L., J. M. Saquing, D. R. U. Knappe, M. A. Barlaz, S. Jonsson, A. Björn, S. J. Rowland, R. C. Thompson, T. S. Galloway, R. Yamashita, D. Ochi, Y. Watanuki, C. Moore, P. H. Viet, T. S. Tana, M. Prudente, R. Boonyatumanond, M. P. Zakaria, K. Akkhavong, Y. Ogata, H. Hirai, S. Iwasa, K. Mizukawa, Y. Hagino, A. Imamura, M. Saha and H. Takada (2009): Transport and release of chemicals from plastics to the environment and to wildlife. *Philosophical Transactions of the Royal Society*. B364, 2027–2045.
- UNEP/IOC (2009): Guidelines on Survey and Monitoring of Marine Litter. *Regional Seas Reports and Studies*, No. 186, IOC Technical Series, No. 83. 131pp.
- UNEP (2014): Valuing Plastics: The Business Case for Measuring, Managing and Disclosing Plastic Use in the Consumer Goods Industry. 116pp.
- Woodall, L. C., C. Gwinnett, M. Packer, R. C. Thompson, L. F. Robinson and G. L. J. Paterson (2015): Using a forensic science approach to minimize environmental contamination and to identify microfibres in marine sediments. *Marine Pollution Bulletin*, 95, 40-46.

This page left intentionally blank.

Floating Marine Pollutants (Shipboard Sighting Surveys for Macro-Debris Items)

○Takashi MIYAO (Japan Meteorological Agency)

1. Introduction

Floating marine pollutants (debris) are widely distributed in the world's oceans. They can comprise anything from cigarette butts and plastic bags to discarded or lost fishing nets, endangering marine and coastal wildlife by their ingestion and entanglement; interfere with navigation; cause economic losses; and threaten human health and safety. Above all, plastics are the most prevalent of marine pollutants, and remain in the environment for a long time and have a negative impact upon marine ecosystems. Moreover, with time they break down into small fragments becoming difficult to remove. The source of these pollutants source is human activities, especially improper waste disposal and mismanagement of trash and industrial products.

In this chapter, the dedicated shipboard sighting surveys for visible size debris from an elevated platform on a moving ship are mainly described. Other possible platforms are airplanes, with the disadvantage that only large debris items could be determined. In fact, shipboard sighting surveys do not necessarily need to occur as a stand-alone activity, and are relatively easy method for crowd-sourcing marine debris sighting (i.e. from ships of opportunity). In spite of their differences in environmental factors, they can provide useful information on the spatial and temporal variability of floating debris. Nonetheless, it should be noted that results of sighting survey will be skewed toward larger debris items.

2. Objectives and Setting of Surveys

2-1 Objectives

Sighting surveys collect information on the distribution and amounts of visible floating debris during specific time periods. The most common variables of interest for open-ocean sighting surveys are density and types of pollutants. Therefore, typical objectives for open-water sighting surveys are, for example, as follows:

- to identify types of floating marine pollutants;
- to estimate densities of floating marine pollutants;
- to detect temporal and spatial variation in the occurrence of floating marine pollutants.

2-2 Site Selection

There have been many studies on macro-debris in beaches and coastal waters, but little information about abundance and types of floating marine debris in the open-ocean. The survey sites should be chosen in consideration of the following matters:

- to deliberate on sources and transportation process affected by the wind system and the major currents;
- to focus on areas that are known to accumulate pollutants;
- not to impact on marine ecosystems by the navigation of the observation ship.

2-3 Frequency and Timing of Surveys

For long-standing monitoring in fixed region, the minimum sampling frequency should be annually. Ideally quarterly sampling is recommended, allowing an interpretation on seasonal changes.

Bearing in mind that the sighting survey for floating debris is affected by environmental factors, in particular, sea state and wind speed. Thus the sighting survey should be conducted after a minimum duration of calm sea, so that there is no bias by floating debris which has been mixed into the water column by recent storms. In addition, it is desirable that the wind speed should be less than 2 in Beaufort scale (i.e. $3.3 \text{ [m s}^{-1}\text{]})$ (DeFishGear, 2013).

3. Field Measurement

3-1 General Information

Sighting surveys must be conducted in the daytime, from the sunrise to the sunset. Observer(s) on a moving ship stand on the bridge or other elevated section, and continuously focused on the port or starboard side of the ship. Observer heights above the water line vary according to the type of ship. The cruising track does not need to be straight, although it is easier to handle the data. Observer(s) will record type, size, number and other information on the provided data sheet, as well as ancillary data (date, time, latitude, longitude etc.), whenever floating pollutant is found (it may be convenient to use tablet computer instead of the data sheet). If the line transect sampling (see Figure 4-2) is adopted, perpendicular distance from the cruising track (or sighting distance and angle from the bow) must be also recorded.

It is desirable that observer(s) use only glare-free side of the ship, especially in dedicated surveys. Debris object should be detected with the naked eye, and binoculars can be used only for the purpose to confirm the identity or to estimate sizes of objects. The number of observers on a survey varies, but it is recommended that a minimum of two observers be employed in any survey (Ribic, 1990).

3-2 Equipment

The observation ship must equip GPS unit for determination of ship position and speed. It is desirable that some system for visually marking the observation area also can be used.

As mentioned above, debris object should be detected with the naked eye, polarizing glasses may be useful for protecting eyes from strong sunrays and glare of sea-surface. Binoculars (8 to 10-power might be adequate) are indispensable to sighting survey. Range finder and/or inclinometer can be used to measure the distance to detected debris. Digital cameras are also useful to re-confirm the identity of

debris, to re-estimate sizes of objects, and to record detailed images of floating debris with the complicated appearance.

3-3 Variables to Consider

(1) Weather Condition

It is desirable to avoid making sighting surveys under poor visibility. For example, Yoshida and Baba (1985) made no surveys when visibility fell below 200m. Unfavorable sea state, that is high wave and swell, also affect detectability.

(2) Characteristics of Debris

It is well known that color, size, shape, and buoyancy of floating objects affect their detectability. Large and fine-colored debris are found with ease. Especially, buoyancy has a large effect; light plastic bottles appeared from the sea surface can be much easily detected than fishing nets floating just beneath the sea surface. If the line transect approach is taken, the detection function should be configured for each category of debris.

(3) Vessel Variability

Ship speed and observer heights above the water line affect detectability of floating debris. On large vessels, observers are typically stand higher above the water line and farther from the bow, which causes objects close to the bow to become undetected. It is considerable fact that ship body shape might also make undetectable area.

(4) Personnel

Sighting survey of floating marine pollutants should be made by dedicated observer(s) who do not have other duties at the same time (Ribic et al., 1992; DeFishGear, 2013). Required personnel include at least two observers experienced or trained in sighting objects floating at sea, who can measure distances and angle or who can use measuring equipment (range finder, inclinometer, binoculars with reticles etc.). Experienced observers often detect more debris items and estimate distance more accurate than inexperienced observers. Novice observers should be trained pairing with skilled observers.

4. Data and Metadata

4-1 Pollutant Density

It is strongly recommended that density of debris should be reported in unit of [*items km⁻²*]; not in [*items km⁻¹*] etc., for quantitative comparisons of different survey. Scanned area can be calculated based on the transect length and width. The transect length will determined from the latitude and longitude of transect start and end points. Therefore, the ship position should be recorded whenever a course-change occurred.

Calculating formulas of the pollutant density are given, dividing the number of detected objects by

scanned area. The method of scanning area estimation should be selected from following two approaches, depending on the actual situation of the survey.

(1) Strip Transect Approach

When a strip transect approach is adopted, only debris within a specific distance from the side of the ship are detected (Figure 1). It is assumed that all objects within the strip transect are counted and any objects seen outside the strip transect are not recorded.

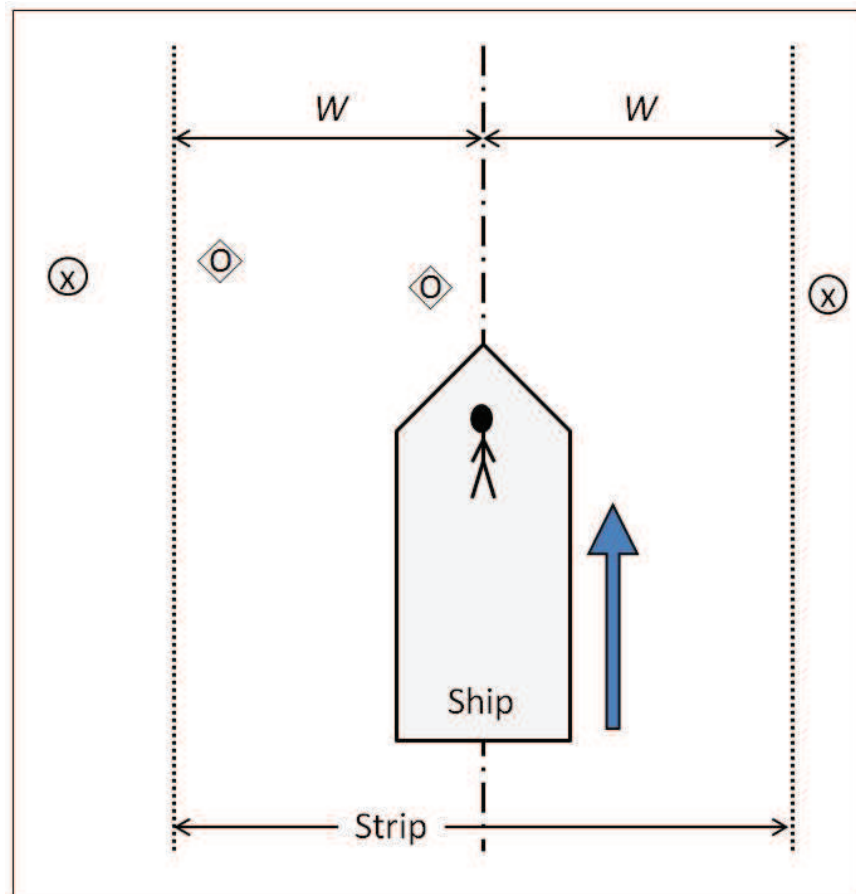


Figure 1 Schematic diagram of a strip transect [after Ribic et al., 1992].

W is strip width. Objects labelled "O" are inside of the strip and can be recorded, while object labelled "x" are outside of the strip and not recorded (even if detected).

The practical strip transect width will depend on the debris size and ship speed. In case that surveys ensure the detection of debris at 2.5cm size, the preliminary strip transect widths based on observation height and ship speed are given in Table 4-1. The strip widths most commonly used are 50m and 100m (Ribic et al., 1992), or maximum perpendicular distance from the transect center to detected debris (Thiel et al. 2003; Shiimoto and Kameda, 2005), for larger debris sighting. Generally, however, these suggested strip widths need to be tested (Lippiatt et al., 2013) and should be determined taking into account survey objectives.

Table 1. Preliminary strip transect widths from different observer height above the water line and the ship speed (MSFD Technical Subgroup on Marine Litter, 2013).

Observer height above the water line	Ship speed		
	2 knots	6 knots	10 knots
1 m	6 m	4 m	3 m
3 m	8 m	6 m	4 m
6 m	10 m	8 m	6 m
10 m	15 m	10 m	5 m

Finally, the density of floating debris is given by

$$D = \frac{N}{A} = \frac{N}{2 \cdot W \cdot L} \quad [items \ km^{-2}]$$

where

N : number of object counted,

A : scanned area [km^2],

W : width of strip transect [km],

L : length of transect [km].

(2) Line Transect Approach

When a line transect approach is adopted, all objects are assumed to be counted regardless the distance from the observer, and perpendicular distance from the ship to the object is measured (Figure 2). However, probability of detection equal 1 on the transect center line, and will decreases according to “detection function” with perpendicular distance. For example, commonly employed detection functions are:

i) The half-normal: $g(x) = \exp\left(-\frac{x^2}{2\sigma^2}\right)$,

ii) The exponential: $g(x) = \exp\left(-\frac{x}{\sigma}\right)$,

iii) The hazard-rate: $g(x) = 1 - \exp\left[-\left(\frac{x}{\sigma}\right)^{-b}\right]$,

where, x is perpendicular distance, $\sigma(> 0)$ and $b(> 1)$ are, respectively, the scale and shape parameters to be estimated based on survey data.

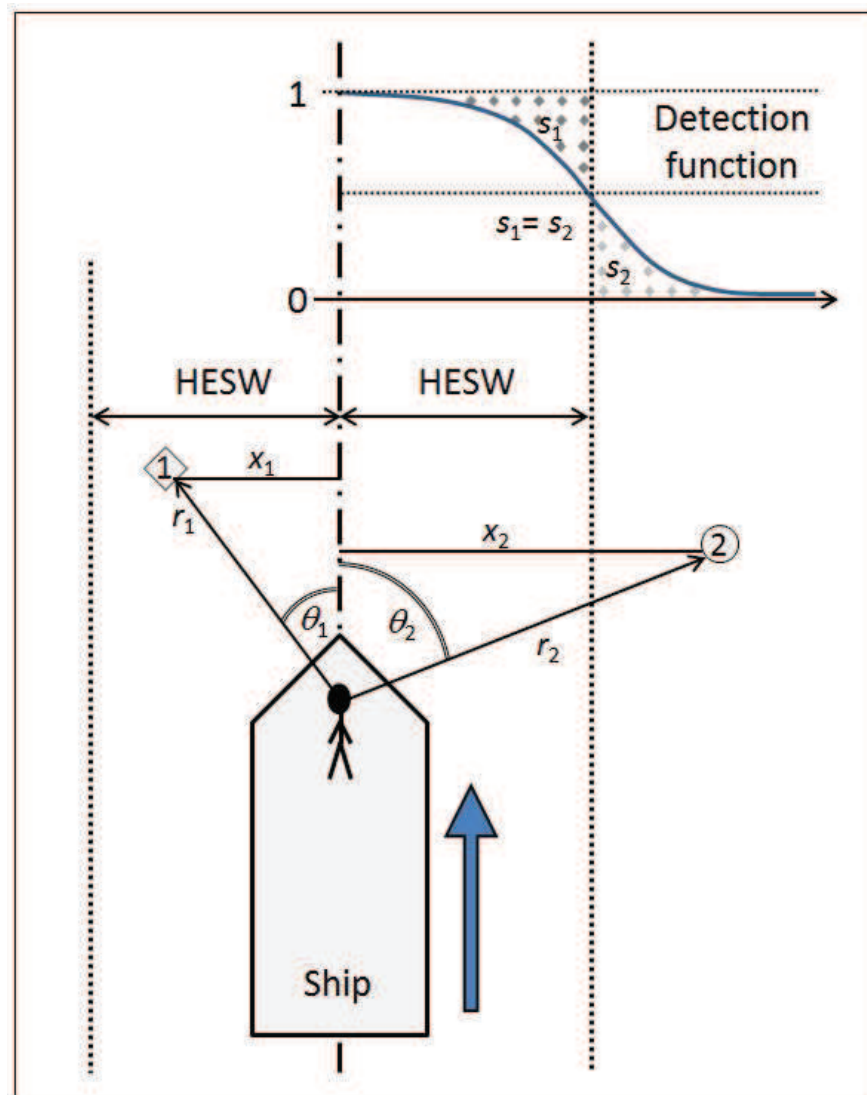


Figure 2 Schematic diagram of a line transect [after Ribic et al., 1992].

All objects are assumed to be recorded regardless the distance from the observer. Perpendicular distances to the object i (X_i) can be estimated directly when they pass just beside observer, or can be calculated from sighting distance (r_i) and angle from the bow (θ_i). Using “detection function”, HESW, within which theoretically all floating debris are detected (meaning in upper part of the figure, $s_1 = s_2$), can be estimated.

Using an adequate detection function, “Half the effective strip width: HESW”, within which theoretically all floating debris are detected, is estimated. Finally, the density of floating debris is given by

$$D = \frac{N}{A} = \frac{N}{2 \cdot HESW \cdot L} \quad [items \ km^{-2}]$$

where

N : number of object counted,

A : scanned area [km^2],

W : Half the effective strip width($HESW$) [km],

L : length of transect [km].

More precisely, detection function should be configured for each category of debris, as mentioned above.

For further detail of line transect sampling method, see Buckland et al. (2001).

4-2 Classification of Floating Marine Pollutants

(1) Size Classes

Floating marine pollutants in the size of a 2.5cm to 1m (in the longest dimension), so-called “macro-debris” (GESAMP, 2015), should be monitored. However, sighting survey will not permit the correct measuring of object sizes, the following size classification, introduced by DeFishGear (2013) and MSFD Technical Subgroup on Marine Litter (2013), are suggested as an example (L denotes the longest dimension of the pollutants):

- i) $2.5cm \leq L < 5cm$
- ii) $5cm \leq L < 10cm$
- iii) $10cm \leq L < 20cm$
- iv) $20cm \leq L < 30cm$
- v) $30cm \leq L < 50cm$
- vi) $50cm \leq L$

These classes can be merged appropriately at statistical processing. When small debris cannot be detected owing to observer heights, the lower limit size should be changed.

(2) Identification of Debris

The categories of items for floating debris are desirable to be consistent with the categories selected for beach litter, seafloor litter and others. For example, UNEP/IOC (2009) introduced seven large classes based on their appearances as follows: i) Containers, ii) Fishing & Boating, iii) Food & Beverage, iv) Packaging, v) Sanitary, vi) Smoking and vii) Other. The Master List of items (MSFD Technical Subgroup on Marine Litter, 2013) include eight large groups; i) Artificial polymer materials, ii) Rubber, iii) Cloth/textile, iv) Paper/Cardboard, v) Processed/worked wood, vi) Metal, vii) Glass/ceramics, viii) Others (chemicals, food waste, unidentified).

However, the world common classification does not yet exist. For the practical use during the monitoring, the categories of items can be arranged by object occurrence frequency so that the data acquisition can be easily done in short time.

4-3 Metadata

Metadata should include following information:

- Survey name, date, time, location
- Ship characteristics: Name, type (e.g. research, fishing, regular ferry etc.), tonnage, length, width etc.
- Detail of transect: latitude/longitude of start/end point, ship speed, observer height above the surface line, total distance covered by transect, scanned area
- Environmental conditions: wind speed/direction, visibility, wave and swell (direction/height/period)

5. Concluding Remarks

Shipboard sighting survey for floating marine pollutants can provide valuable information on the density and types of marine debris. However, uncertainty in categories of items for floating debris stays as an unsettled problem yet. Careful consideration to survey design and standardization should be paid in order to develop robust estimates of floating marine pollutants density.

Reference

- Buckland, S. T., D. R. Anderson, K. P. Burnham, J. L. Laake, D. L. Borchers, and L. Thomas (2001): Introduction to distance sampling: estimating abundance of biological population. Oxford University Press, New York.
- DeFishGear (2013): Methodology for Monitoring Marine Litter on the Sea Surface. Visual Observation. Derelict Fishing Gear management system in the Adriatic Region, 10pp.
Retrieved from [http://issuu.com/defishgear/docs/floating_litter_monitoring_methodol/10?e=0]
- GESAMP (2015): Sources, Fate and Effects of Microplastics in the Marine Environment: A Global Assessment (Kershaw, P. J., ed). IMO/FAO/UNESCO-IOC/UNIDO/WMO/IAEA/UN/UNEP/UNDP Joint Group of Experts on the Scientific Aspects of Marine Environmental Protection. GESAMP Reports & Studies Series, No. 90, 96pp.
- Lippiatt, S., S. Opfer and C. Arthur (2013): Marine Debris Monitoring and Assessment. NOAA Technical Memorandum NOS-OR&R-46.
- MSFD Technical Subgroup on Marine Litter (2013): Guidance on Monitoring of Marine Litter in European Seas. A guidance document within the Common Implementation Strategy for the Marine Strategy Framework Directive. 128pp.
- Ribic, C. A. (Chair) (1990): Report of the working group on methods to assess the amount and types of marine debris. *In* Proceedings of the second international conference on marine debris; 2-7 April 1989, Honolulu, HI (R. S. Shomura and M. L. Godfrey, eds.), 1201-1206. NOAA Technical Memorandum. NMFS, NOAA-TM-NMFS-SWFSC-154.
- Ribic, C. A., T. R. Dixon and I. Vining (1992): Marine Debris Survey Manual. NOAA Technical Report NMFS 108.

- Siomoto, A. and T. Kameda (2005): Distribution of Manufactured Floating Marine Debris in Near-Shore Areas around Japan. *Marine Pollution Bulletin*, 50, 1430-1432.
- Thiel, M., I. Hinojosa, N. Vásquez and E. Macaya (2003): Floating marine debris in coastal waters of the SE Pacific (Chile). *Marine Pollution Bulletin*, 46, 224–231.
- UNEP/IOC (2009): Guidelines on Survey and Monitoring of Marine Litter. Regional Seas Reports and Studies No. 186, IOC Technical Series No. 83. 131pp.
- Yoshida, K. and N. Baba (1985): A survey of drifting stray fishing net fragments in the northern Sea of Japan (Western Pacific Ocean). Document submitted to the 28th Meeting of the Standing Scientific Committee of the North Pacific Fur Seal Commission, Tokyo, 4-12 April 1985, 13pp.

This page left intentionally blank.

List of the editors

Editor in chief, Shigeyoshi OTOSAKA

Vol.1 Editor	Iwao UEKI
Vol.2 Editors	Daisuke SASANO Yuichiro KUMAMOTO
Vol.3 Editors	Yuichiro KUMAMOTO Daisuke SASANO Hajime OBATA
Vol.4 Editors	Hideki FUKUDA Yuichiro NISHIBE
Vol.5 Editors	Shigeyoshi OTOSAKA Hideki FUKUDA
Vol.6 Editor	Yuichiro NISHIBE
Vol.7 Editors	Daisuke SASANO Yuichiro KUMAMOTO
Vol.8 Editors	Iwao UEKI Daisuke SASANO
Vol.9 Editor	Shigeyoshi OTOSAKA
Vol.10 Editors	Hideaki MAKI Koichi GOTO
Technical Editors	Michio AOYAMA Tsuneo ONO

Assistants of the editorial board

Michiyo SUWADA, a current staff of Aoyama Laboratory, Center for Research in Isotopes and Environmental Dynamics, Univ. of Tsukuba, Japan

This page left intentionally blank.

Title: Guideline of Ocean Observations

Volumes 1 - 10

Editor: Committee of Guide of Ocean Observations,
the Oceanographic Society of Japan

Publisher: The Oceanographic Society of Japan

Publication date: December 2016, First Edition

February 2018, Second Edition

April 2018, Third Edition

April 2020, Fourth Edition

ISBN 978-4-908553-67-7

ISBN 978-4-908553-67-7

ISBN: 9784908553677



9 784908 553677